CH-TRU Payload Appendices
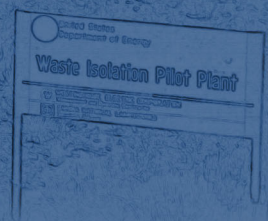
Revision 1
February 2005

This page intentionally left blank to facilitate duplex printing.

TABLE OF CONTENTS

TABLE OF CONTENTS (Continued)

1.0 INTRODUCTION

This document, the CH-TRU Payload Appendices, accompanies the Contact-Handled Transuranic Waste Authorized Methods for Payload Control (CH-TRAMPAC) and is provided as supplemental information pertaining to issues related to the transportation of contact-handled transuranic (CH-TRU) waste in the TRUPACT-II or HalfPACT. The CH-TRAMPAC contains all information, including requirements and methods of compliance, required for the qualification of a payload for transport in the TRUPACT-II or HalfPACT. The methodology and logic for the requirements are provided in this document, along with previously performed assessments and evaluations.

The information contained in this document is separated into specific sections, as follows:

- Payload Qualification Methodology (Section 2.0)
- Gas Generation Methodology (Section 3.0)
- Payload Container Design Basis Evaluations (Section 4.0)
- Assessment Methods (Section 5.0)
- Supporting Evaluations (Section 6.0).

This document supports both the TRUPACT-II and HalfPACT SARs, as well as the CH-TRAMPAC document.

This page intentionally left blank

APPENDIX 2.1

LOGIC FOR PAYLOAD SHIPPING CATEGORIES

This page intentionally left blank.

2.1   Logic for Payload Shipping Categories

The contact-handled transuranic (CH-TRU) waste at the U.S. Department of Energy (DOE) sites has been classified into "payload shipping categories" to evaluate and ensure compliance with the gas generation requirements contained in the Contact-Handled Transuranic Waste Authorized Methods for Payload Control (CH-TRAMPAC). As shown in Appendices 6.1, 6.5, and 6.6 of the CH-TRU Payload Appendices, gas generation due to chemical, biological, and thermal mechanisms is insignificant during transport, and radiolysis is the primary mechanism for potential flammable gas generation.

A shipping category is defined by the following parameters:

- Chemical composition of the waste (waste type)

- Gas generation potential of the waste material type (quantified by the "G value" for hydrogen, which is the number of molecules of hydrogen generated per 100 electron volts (eV) of energy absorbed)

- Gas release resistance (type of payload container and type and maximum number of confinement layers used).

For any given payload container, the shipping category provides a basis to determine the gas generation potential of the contents and the resistance to gas release of the packaging configuration. This enables evaluation of compliance with the gas generation requirements.

Two payload shipping category notations are available. A shipping site may use either notation. Descriptions of the two notations are presented in the following sections.

2.1.1 Numeric Shipping Category Notation

The numeric shipping category notation is a ten-digit code:

$$XX\ YYYY\ ZZZZ$$

where,

XX	=	The waste type, which indicates the chemical composition of the waste
YYYY	=	The G value, or gas generation potential, of the waste material type multiplied by 10^2
ZZZZ	=	The resistance to hydrogen release of the packaging configuration multiplied by 10^{-4}.

A description of each of the parameters follows.

Waste Type
Payloads are subdivided into four (4) waste types based on physical and chemical form as shown in Table 2.1-1. Table 2.1-1 also shows the shipping category notation denoting each waste type.

Table 2.1-1 — Summary of Payload Waste Types

Waste Type[a]	Waste Type[b] (XX)	Description and Examples

I	10	Solidified Aqueous or Homogeneous Inorganic Solids (<1 percent organics - not including packaging)
		   - absorbed, adsorbed or solidified inorganic liquid
		   - soils, solidified particulates, or sludges formed from precipitates
		   - concreted inorganic particulate waste

II	20	Solid Inorganics
		   - glass, metal, crucibles
		   - other solid inorganics

III	30	Solid Organics
		   - plastics (e.g., polyethylene, polyvinyl chloride)
		   - cellulose (e.g., paper, cloth, wood)
		   - cemented organic solids
		   - other solid organics

IV	40	Solidified Organics - cemented or immobilized organic liquids and solids

[a]Payload shipping category notation used until June 1999.
[b]Payload shipping category notation initiated in June 1999.

Waste Material Type
The four waste types may be further subdivided into waste material types. The waste material types define the gas generation potential of the waste, and a listing of the chemicals/materials allowed in each waste material type is presented in Tables 4.3-1 through 4.3-8 of the CH-TRAMPAC. An effective bounding G value quantifying the gas generation potential of each waste material type is assigned based on the chemicals allowed. Dose-dependent G values are applicable to containers of CH-TRU waste materials of Waste Material Type II.1 and Waste Type III that meet a watt*year criteria of greater than 0.012. The determination of bounding G values for each waste material type is described in Appendices 3.2 and 3.3 of the CH-TRU Payload Appendices. Table 2.1-2 presents the waste material types and their respective bounding G values, along with the shipping category notation denoting the bounding G value.

Table 2.1-2 — CH-TRU Waste Material Types and G Values

Waste Material Type	Typical Material Description[a]	G Value[b]	Numeric Shipping Category Notation (G Value x 10^2) (YYYY)
I.1	Absorbed, adsorbed, or solidified inorganic liquid	1.6	0160
I.2	Soils, solidified particulates, or sludges formed from precipitation	1.3	0130
I.3	Concreted inorganic particulate waste	0.4	0040
II.1	Solid inorganic materials in plastic bags (watt*year ≤0.012)	1.7	0170
II.1	Solid inorganic materials in plastic bags (watt*year >0.012)	0.32	0032
II.2	Solid inorganic materials in metal cans	0	0000
II.3	Homogeneous solid inorganic materials with unbound absorbed ambient moisture (≤6% by weight) in metal cans	0.08	0008
III.1	Solid organic materials (watt*year ≤0.012)	3.4	0340
III.1	Solid organic materials (watt*year >0.012)	1.09	0109
III.2	Homogeneous mixed organic (10% by weight) and inorganic (90% by weight) materials in metal cans (watt*year ≤0.012)	0.34	0034
III.2	Homogeneous mixed organic (10% by weight) and inorganic (90% by weight) materials in metal cans (watt*year >0.012)	0.11	0011
III.3	Homogeneous mixed organic (10% by weight) and inorganic (90% by weight) materials in plastic bags (watt*year ≤0.012)	1.85	0185
III.3	Homogeneous mixed organic (10% by weight) and inorganic (90% by weight) materials in plastic bags (watt*year >0.012)	0.4	0040
IV.1	Solidified organics	Unknown (test)	9999

[a]Appendix 3.3 of the CH-TRU Payload Appendices provides a complete discussion of watt*year criteria.

[b]Dose-dependent G values meeting the watt*year criteria (watt*year >0.012) cannot be used if absorbed, adsorbed, or solidified aqueous materials are present in the waste (see Appendix 3.3 of the CH-TRU Payload Appendices). Appendices 3.1 and 3.2 of the CH-TRU Payload Appendices provide a complete discussion of G values.

Total Resistance

The determination of the total resistance to gas release of a payload container requires a knowledge of the type and maximum number of layers of confinement used to package the waste. CH-TRU materials are typically placed in a payload container within multiple layers of plastic and/or metal cans that act as layers of confinement for radionuclides during waste handling operations. The payload safety analysis considers the layers of confinement as barriers that impede, but do not preclude, the release of gases from inside the layers of confinement (e.g., plastic bags or metal cans) to the outside of the payload container. Allowable closure methods for confinement layers are specified in Appendix 3.8 of the CH-TRU Payload Appendices. The plastic layers of confinement in payload containers are of three types—liner bags, inner bags, and filtered inner and liner bags. As described in Appendices 3.8, 6.7, and 6.13 of the CH-TRU Payload Appendices, the release rates for confinement layers have been quantified or presented as specifications. Any other type of confinement layer used at the sites shall be shown to be equivalent to one of these for purposes of minimum hydrogen release.

The numeric payload shipping category notation used to denote the total resistance to hydrogen release of the packaging configuration of a payload container is the sum of the resistances from all confinement layers (seconds/mole) multiplied by 10^{-4}, rounded up, and reported as four digits (ZZZZ). For example, the shipping category notation for a total resistance of 1,395,163 seconds/ mole is "0140."

The shipping category assignment for a 55-gallon drum containing solid inorganic waste packaged within two filtered, plastic liner bag layers is:

<div align="center">

20 0170 0140

</div>

where,

20	=	Waste Type II
0170	=	G value (1.7) of Waste Material Type II.1 (x 10^2)
0140	=	Total resistance to hydrogen release (x 10^{-4}) of two filtered liner bags, 55-gallon drum filter, rigid drum liner, and payload shipping configuration.

2.1.2 Alpha-numeric Shipping Category Notation

The alpha-numeric shipping category notation was based on the same parameters as the numeric notation, but conveyed the information through a different set of parameters. The alpha-numeric shipping category notation was based on the waste material type, the payload container type, and the type and number of confinement layers within a payload container. An example of the alpha-numeric shipping category notation is:

II.1A2af

where,

II.1	=	The waste material type (solid inorganics in plastic bags, see Table 2.1-2)
A	=	The type of payload container (55-gallon drum, see Table 2.1-3)
2	=	The number of confinement layers (2 bag layers, see Table 2.1-4)
af	=	The type of confinement layers (filtered drum liner bags, see Table 2.1-4).

Table 2.1-3 — Alpha-numeric Shipping Category Notation for Payload Container Configurations

Notation	Description
A	55-gallon drums with materials in additional layers of confinement [such as rigid liner(s), bag(s), and can(s)] (includes 55-gallon drums overpacked in a TDOP)
B	Overpack of four 55-gallon drums in an SWB (SWB overpack)
C	SWB with materials in additional layers of confinement [such as bags(s) and can(s)]
D	Overpack of one experimental bin in an SWB
E	Overpack of one pipe component in a 55-gallon drum (standard pipe overpack)

Table 2.1-4 —Alpha-numeric Shipping Category Notation for Layers of Confinement in Payload Containers

Notation	Description
0	No closed bags around waste
1	Up to a maximum of 1 closed bag around waste
2	Up to a maximum of 2 closed layers of bags around waste
3	Up to a maximum of 3 closed layers of bags around waste
4	Up to a maximum of 4 closed layers of bags around waste
5	Up to a maximum of 5 closed layers of bags around waste
6	Up to a maximum of 6 closed layers of bags around waste
M	Metal container(s) as the innermost layer of confinement
a	For Waste Types II and III packaged in drums, denotes a minimum of 2 liner bags
b	For all waste types packaged in SWBs, denotes a minimum of 1 SWB liner bag
f	All layers of bags around waste are vented with a minimum of one filter vent
T	Payload container qualified for shipment under the test category (see Section 5.2 of the CH-TRAMPAC)

This page intentionally left blank.

APPENDIX 2.2

PROCEDURE FOR DETERMINING NUMERIC
PAYLOAD SHIPPING CATEGORY

This page intentionally left blank.

2.2   Procedure for Determining Numeric Payload Shipping Category

Completion of Tables 2.2-1 through 2.2-4, at the end of this appendix, constitutes the determination of the numeric payload shipping category.

2.2.1   Instructions for Completing Table 2.2-1: Numeric Payload Shipping Category Worksheet

For all of the tables, only the blank (unshaded) boxes need to be completed. Note that there are two separate columns for determining total resistance based on waste material type. Column 1 is used to calculate resistance factors for waste material types with G values based on water [waste material types with six-digit notations (XX YYYY) 10 0160, 10 0130, 10 0040, and 20 0008]. Column 2 is used to calculate resistance factors for all other waste material types. (Appendix 6.9 of the CH-TRU Payload Appendices describes the logic for using different resistances based on waste material type.)

Container ID
Record the container ID number in the space provided.

Waste Type
Record the two-digit waste type notation (XX) of the container from Table 2.1-1 of Appendix 2.1 of the CH-TRU Payload Appendices.

G Value

- From Table 2.1-2 of Appendix 2.1 of the CH-TRU Payload Appendices, determine the waste material type to which the container belongs.

- Record the G value for this waste material type from Table 2.1-2 of Appendix 2.1 of the CH-TRU Payload Appendices.

- Record the corresponding four-digit G value notation (YYYY) from Table 2.1-2 of Appendix 2.1 of the CH-TRU Payload Appendices.

Note: If the notation entered under Waste Type (XX) and G Value (YYYY) is 20 0000, the "Total Resistance Notation" to be entered at the bottom of Table 2.2-1 (ZZZZ) is always 0000, and the payload shipping category to be entered in the last row of Table 2.2-1 (XX YYYY ZZZZ) is 20 0000 0000. For Waste Material Type II.2 (20 0000), this completes the determination of the numeric payload shipping category, and the remainder of the instructions do not apply.

Total Resistance
For each packaging configuration, a unique resistance factor exists and is determined by totaling the individual resistance factors for the confinement layers, the payload container, and the load type. Instructions for completing this portion of the worksheet are as follows:

- Confinement Layers:

  Packaging: Choose the layers of confinement that are applicable to the payload container. As specified in Appendix 3.8 of the CH-TRU Payload Appendices, if a confinement layer used for the payload container is not listed, but has been shown by testing or analysis to be equivalent to (i.e., hydrogen release rate equal to or greater than) one of the entries, choose the equivalent entry.

  Type: Within each applicable layer of confinement, choose the closure type and calculate the "Total Resistance Factor" as shown below. If the confinement layer is filtered or if it is a rigid drum liner, the "Total Resistance Factor" for the layer is calculated using Table 2.2-2.

  Number of Layers: Enter the number of layers of confinement for each type of internal packaging that is applicable to the payload container. Leave the space blank or enter zero (0) if it is not applicable.

  Resistance Factor: Choose the "Resistance Factor" from either Column 1 or Column 2 that corresponds to the six-digit notation (XX YYYY) recorded above (see footnote "a" of Table 2.2-1). This is a numeric value associated with the resistance to hydrogen diffusion for each layer of confinement (resistance to hydrogen diffusion in seconds/mole divided by 100). The "Resistance Factor" for filtered or punctured confinement layers is calculated using Table 2.2-2.

  Total Resistance Factor: Multiply the "Resistance Factor" by the "Number of Layers" of confinement for each applicable type of internal packaging. The total resistance factor for each confinement layer type is equal to the number of layers of confinement times the resistance factor (e.g., 2 twist-and-tape drum liner bags would have a total resistance factor of 2 x 2,142 = 4,284). Enter the "Total Resistance Factor" for each confinement layer type in the designated column on Table 2.2-1. Enter zero (0) or leave the space blank for confinement layers that are not applicable.

- Payload Container: The "Total Resistance Factor" for this section is calculated using Table 2.2-3.

- Load Type: The "Total Resistance Factor" for this section is calculated using Table 2.2-4.

- Total Resistance Factor Sum: Sum all the values in the "Total Resistance Factor" column and record on this line.

- Total Resistance Notation: Divide the "Total Resistance Factor Sum" by 100 and round up to the nearest whole number. Record "Total Resistance Notation" as four digits (ZZZZ) (e.g., for a total resistance factor sum of 13,954, 13,954 / 100 = 139.54, rounded up to nearest whole number is 140, and reported as four digits, the total resistance notation is 0140).

The "Payload Shipping Category" on the worksheet is determined by combining the three components of the shipping category determined above. The shipping category is recorded as XX YYYY ZZZZ.

2.2.2 Instructions for Completing Table 2.2-2: Filtered/Punctured Confinement Layers Resistance Worksheet

Packaging/Type: Choose the layers of confinement that are applicable to the payload container.

Minimum Filter Hydrogen Diffusivity/Minimum Puncture Diameter: Choose the appropriate filter based on the minimum hydrogen diffusivity applicable to the filter. Section 2.5 of the Contact-Handled Transuranic Waste Authorized Methods for Payload Control (CH-TRAMPAC) lists the venting requirements for the payload container and confinement layers. Sites shall verify and document the use of filters with greater hydrogen diffusivity values in order to take credit for the associated decrease in total resistance per packaging configuration.

For the rigid drum liner, choose the value that matches the puncture diameter or filter diffusivity in the liner.

If the hydrogen diffusivity or puncture diameter of the confinement layer falls in between the numbers listed, select the lower value. For example, if a container has a rigid liner with a puncture diameter of 0.5 inch, select "0.375" Diameter Hole."

Number of Layers: Enter the number of layers of confinement for each type of internal packaging that is applicable to the payload container. Leave the space blank or enter zero (0) if it is not applicable.

Resistance Factor: Choose the "Resistance Factor" from either Column 1 or Column 2 that corresponds to the six-digit notation (XX YYYY) recorded on Table 2.2-1 (see footnote "a" of Table 2.2-2). This is a numeric value associated with the resistance to hydrogen diffusion for each layer of confinement.

Number of Filters/Punctures per Layer: Enter the number of filters in each confinement layer or the number of punctures in the rigid liner. If the number of filters on a given type of confinement layer varies from layer to layer, enter the minimum number of filter(s) that applies to all layers of that type. For example, if a payload container holds waste packaged in two filtered inner bag layers, one bag fitted with one filter, and one bag fitted with two filters, enter "1" for the "Number of Filters/Punctures."

Total Resistance Factor: The Total Resistance Factor for each layer is obtained as follows:

$$\frac{\text{Resistance Factor} * \text{Number of Layers}}{\text{Number of Filters/Punctures per Layer}}$$

If the calculated "Total Resistance Factor" is not a whole number, round up to the nearest whole number. Enter this number in the appropriate column in Table 2.2-2 and Table 2.2-1. Enter zero (0) or leave the space blank if it is not applicable.

2.2.3   Instructions for Completing Table 2.2-3: Payload Container Resistance Worksheet

Payload Container: Choose the payload container packaging configuration components that are applicable to the payload container (e.g., for a 55-gallon drum overpacked in a standard waste box (SWB), both 55-gallon drum and SWB overpack would be selected). For some overpacked configurations, overpacking does not impact the selection of the appropriate payload container. For example, for 55-gallon drums, the total resistance is not affected by overpacking in an SWB with filters having a total hydrogen diffusivity of 1.48×10^{-5} moles per second per mole fraction (m/s/mf) (equivalent to four filters each with a diffusivity of 3.7×10^{-6} m/s/mf) or greater or in a ten-drum overpack (TDOP). Therefore, only the Resistance Factor for the 55-gallon drum applies, and the resistance of the overpacking container is assigned a value of zero. See Appendix 6.10 of the CH-TRU Payload Appendices regarding the selection of Payload Containers for overpacked configurations.

Filter Type: Choose the filter type on the payload container (see Section 2.5 of the CH-TRAMPAC for minimum filter specifications). Choose the appropriate filter based on the minimum hydrogen diffusivity applicable to the filter. Section 2.5 of the CH-TRAMPAC lists the venting requirements for payload containers. Sites shall verify and document the use of filters with greater hydrogen diffusivity values in order to take credit for the associated decrease in total resistance per packaging configuration. If the minimum hydrogen diffusivity applicable to the filter falls in between the numbers listed, select the lower value. For example, if a 55-gallon drum filter has a minimum hydrogen diffusivity of 3.0×10^{-6} m/s/mf, select "1.9×10^{-6} m/s/mf Filter."

Number of Filters on Payload Container: Enter the number of filters on each container. Section 2.5 of the CH-TRAMPAC specifies the minimum total hydrogen diffusivity required per container. The combination of filter diffusivity and number of filters must meet or exceed the minimum requirements of Section 2.5 of the CH-TRAMPAC. Leave the space blank or enter zero (0) if it is not applicable.

Resistance Factor: Choose the "Resistance Factor" from either Column 1 or Column 2 that corresponds to the six-digit notation (XX YYYY) recorded on Table 2.2-1 (see footnote "b" of Table 2.2-3). This is the numeric value associated with the resistance to hydrogen diffusion for each container.

Total Resistance Factor: Divide the "Resistance Factor" by the "Number of Filters on the Container" to obtain the "Total Resistance Factor." If the calculated "Total Resistance Factor" is not a whole number, round up to the nearest whole number. Enter this number in the designated column on Tables 2.2-3 and 2.2-1. Enter zero (0) or leave the space blank if it is not applicable.

2.2.4 Instructions for Completing Table 2.2-4: Load Type Resistance Worksheet

Shipping Period: Choose the appropriate shipping period for the payload, as follows:

- 60 Days (General Case): All shipments that do not meet the criteria for the other shipping periods.

- 20 Days (Close-Proximity Shipment): For shipments to destinations within a radius of approximately 1,000 miles or less. For example, all shipments from the Los Alamos National Laboratory, the Rocky Flats Environmental Technology Site, and the Nevada Test Site to the Waste Isolation Pilot Plant meet this criterion, and a 20-day shipping period is applicable.

- 10 Days (Controlled Shipment): For all shipments that satisfy the administrative control requirements set forth in Appendix 3.6 of the CH-TRU Payload Appendices and Section 6.2.3 of the CH-TRAMPAC.

Payload Container: Choose the appropriate payload container for the load type. The load type describes how the payload container will be shipped with other payload containers in the TRUPACT-II or HalfPACT inner containment vessel; therefore, select only one load type. For some overpacked configurations, overpacking does not impact the selection of the appropriate Load Type. If a zero was entered in Table 2.2-3 for the overpacking payload container total resistance factor, select the load type for the container that is overpacked. For example, for 55-gallon drums, the total resistance and payload shipping category are not affected by overpacking in an SWB with filters having a total hydrogen diffusivity of 1.48×10^{-5} m/s/mf (equivalent to four filters each with a diffusivity of 3.7×10^{-6} m/s/mf) or greater. A zero should have been entered in Table 2.2-3 for the SWB in this configuration. Therefore, for this overpacked configuration, select the Load Type resistance for a payload of 55-gallon drums (Resistance Factor of 7,147). See Appendix 6.10 of the CH-TRU Payload Appendices regarding the use of equivalent Load Type resistance factors for overpacked configurations.

Resistance Factor: Choose the "Resistance Factor" for the load type.

Total Resistance Factor: Enter the chosen value in the "Total Resistance Factor" column. Enter zero (0) or leave the space blank for load types that are not applicable. Note: Only one value for Total Resistance Factor is entered in Table 2.2-4.

Table 2.2-1 — Numeric Payload Shipping Category Worksheet

Container ID Number:						
Two Digit **Waste Type** Notation (**XX**) from Table 2.1-1 of the CH-TRU Payload Appendices						
G Value for Waste Material Type from Table 2.1-2		Four Digit G Value Notation (**YYYY**) from Table 2.1-2				

	Packaging	Type	Number of Layers	Resistance Factor (Use One Column Only)[a]		Total Resistance Factor[b]
				Column 1	Column 2	
Confinement Layers	Inner Bag Layers	Filtered		From Table 2.2-2		
		Twist and Tape		23,989	17,922	
	Confinement Layers (e.g., Metal Can)	Slip-Top/Unsealed		0	0	
		Filtered		From Table 2.2-2		
	Liner Bag Layers	Filtered Drum Liner Bag		From Table 2.2-2		
		Twist and Tape Drum Liner Bag		2,142	2,142	
		Filtered SWB/Bin/TDOP Liner Bag		From Table 2.2-2		
		Fold and Tape SWB/ Bin/TDOP Liner Bag		1,257	1,257	
	Rigid Drum Liner	Rigid Liner		From Table 2.2-2		

Choose Those That Apply	Payload Container	Pipe Component	From Table 2.2-3	
		55-Gallon Drum or Pipe Overpack	From Table 2.2-3	
		85-Gallon Drum – Direct Load	From Table 2.2-3	
		100-Gallon Drum	From Table 2.2-3	
		Bin	From Table 2.2-3	
		85-Gallon Drum Overpack – One 55-Gallon Drum	From Table 2.2-3	
		SWB – Direct Load or Overpacking Bin	From Table 2.2-3	
		SWB Overpack - Four 55-Gallon Drums	From Table 2.2-3	
		TDOP – Direct Load	From Table 2.2-3	
	Load Type	55-Gallon Drums or Pipe Overpacks	From Table 2.2-4	
		85-Gallon Drums – Direct Load	From Table 2.2-4	
		100-Gallon Drums	From Table 2.2-4	
		SWBs – Direct Load or Overpacking Bin	From Table 2.2-4	
		SWB Overpacks Containing Up To Four 55-Gallon Drums per SWB; or 85-Gallon Drum Overpacks of 55-Gallon Drums	From Table 2.2-4	
		TDOP – Direct Load	From Table 2.2-4	

Total Resistance Factor Sum	
Divide Total Resistance Factor Sum by 100 and Round Up to Whole Number	÷ 100
Total Resistance Notation (**ZZZZ**) Report as Four Digits If Waste Material Type II.2 (20 0000), enter 0000.	
Payload Shipping Category (XX YYYY ZZZZ)	__ __ __ __ __ __ __ __

a   Use Column 1 for the following six-digit notations (XX YYYY): 10 0160, 10 0130, 10 0040, and 20 0008. Use Column 2 for all other six-digit notations.
b   Multiply the "Number of Layers" by the appropriate "Resistance Factor" to obtain the "Total Resistance Factor."

Table 2.2-2 — Filtered/Punctured Confinement Layers Resistance Worksheet

Packaging/Type	Minimum Filter Hydrogen Diffusivity/Minimum Puncture Diameter	Number of Layers	Resistance Factor[a] (Use One Column Only) Column 1	Resistance Factor[a] (Use One Column Only) Column 2	Number of Filters/ Punctures per Layer	Total Resistance Factor[b]
Inner Bag Layers: Filtered[c]	1.075×10^{-5} m/s/mf Filter		1,290	931		
	2.150×10^{-5} m/s/mf Filter		645	466		
	5.375×10^{-5} m/s/mf Filter		258	187		
	2.688×10^{-4} m/s/mf Filter		52	38		
	1.075×10^{-3} m/s/mf Filter		13	10		
Confinement Layer (e.g., Metal Can or Rigid Liner): Filtered	1.9×10^{-6} m/s/mf Filter		7,294	5,264		
	3.7×10^{-6} m/s/mf Filter		3,746	2,703		
	7.4×10^{-6} m/s/mf Filter		1,873	1,352		
	1.85×10^{-5} m/s/mf Filter		750	541		
	9.25×10^{-5} m/s/mf Filter		150	109		
	3.7×10^{-4} m/s/mf Filter		38	28		
Liner Bag Layers: Filtered Drum Liner Bag[c]	1.075×10^{-5} m/s/mf Filter		933	673		
	2.150×10^{-5} m/s/mf Filter		542	391		
	5.375×10^{-5} m/s/mf Filter		240	173		
	2.688×10^{-4} m/s/mf Filter		51	37		
	1.075×10^{-3} m/s/mf Filter		13	10		
Liner Bag Layers: Filtered SWB/Bin/TDOP Liner Bag[c]	1.075×10^{-5} m/s/mf Filter		764	551		
	2.150×10^{-5} m/s/mf Filter		480	347		
	5.375×10^{-5} m/s/mf Filter		227	164		
	2.688×10^{-4} m/s/mf Filter		51	37		
	1.075×10^{-3} m/s/mf Filter		13	10		
Rigid Drum Liner:	0.3" Diameter Hole		197	197		
	0.375" Diameter Hole		126	126		
	0.75" Diameter Hole		32	32		
	1" Diameter Hole		18	18		
	2" Diameter Hole		5	5		

a   Use Column 1 for the following six-digit notations (XX YYYY): 10 0160, 10 0130, 10 0040, and 20 0008. Use Column 2 for all other six-digit notations.
b   Multiply the "Number of Layers" by the appropriate "Resistance Factor" and divide by the "Number of Filters/Punctures per Layer" to obtain the "Total Resistance Factor."
c   No credit allowed for filter if waste is directly packaged in a filtered bag and there is potential for contact of the filter with water (see Appendix 3.11 of the CH-TRU Payload Appendices).
m/s/mf = Moles/second/mole fraction.

Table 2.2-3 — Payload Container Resistance Worksheet[a]

Payload Container	Filter Type	Number of Filters on Payload Container	Resistance Factor[b] (Use One Column Only)		Total Resistance Factor[c]
			Column 1	Column 2	
Pipe Component (Must also select Pipe Overpack)	1.9×10^{-6} m/s/mf Filter	1	7,294	5,264	
	3.7×10^{-6} m/s/mf Filter	1	3,746	2,703	
	7.4×10^{-6} m/s/mf Filter	1	1,873	1,352	
	1.85×10^{-5} m/s/mf Filter	1	750	541	
	9.25×10^{-5} m/s/mf Filter	1	150	109	
	3.7×10^{-4} m/s/mf Filter	1	38	28	
55-Gallon Drum or Pipe Overpack	1.9×10^{-6} m/s/mf Filter		7,294	5,264	
	3.7×10^{-6} m/s/mf Filter		3,746	2,703	
	7.4×10^{-6} m/s/mf Filter		1,873	1,352	
	1.85×10^{-5} m/s/mf Filter		750	541	
	9.25×10^{-5} m/s/mf Filter		150	109	
	3.7×10^{-4} m/s/mf Filter		38	28	
85-Gallon Drum Direct load	3.7×10^{-6} m/s/mf Filter		3,746	2,703	
	7.4×10^{-6} m/s/mf Filter		1,873	1,352	
	1.85×10^{-5} m/s/mf Filter		750	541	
	9.25×10^{-5} m/s/mf Filter		150	109	
	3.7×10^{-4} m/s/mf Filter		38	28	
100-Gallon Drum	3.7×10^{-6} m/s/mf Filter		3,746	2,703	
	7.4×10^{-6} m/s/mf Filter		1,873	1,352	
	1.85×10^{-5} m/s/mf Filter		750	541	
	9.25×10^{-5} m/s/mf Filter		150	109	
	3.7×10^{-4} m/s/mf Filter		38	28	
Bin (Must also select SWB)	3.7×10^{-6} m/s/mf Filter		3,746	2,703	
	7.4×10^{-6} m/s/mf Filter		1,873	1,352	
	1.85×10^{-5} m/s/mf Filter		750	541	
	9.25×10^{-5} m/s/mf Filter		150	109	
	3.7×10^{-4} m/s/mf Filter		38	28	

Table 2.2-3 — Payload Container Resistance Worksheet[a] (Concluded)

Payload Container	Filter Type	Number of Filters on Payload Container	Resistance Factor[b] (Use One Column Only)		Total Resistance Factor[c]
			Column 1	Column 2	
85-Gallon Drum Overpack Containing One 55-Gallon Drum (Must also select 55-Gallon Drum)	3.7×10^{-6} m/s/mf Filter		7,490	5,406	
	7.4×10^{-6} m/s/mf Filter		3,746	2,703	
	1.85×10^{-5} m/s/mf Filter		1,499	1,082	
	9.25×10^{-5} m/s/mf Filter		300	217	
	3.7×10^{-4} m/s/mf Filter		75	55	
SWB Direct load or overpacking one bin	3.7×10^{-6} m/s/mf Filter		3,746	2,703	
	7.4×10^{-6} m/s/mf Filter		1,873	1,352	
	1.85×10^{-5} m/s/mf Filter		750	541	
	9.25×10^{-5} m/s/mf Filter		150	109	
	3.7×10^{-4} m/s/mf Filter		38	28	
SWB Overpack Containing Up to Four 55-Gallon Drums (Must also select 55-Gallon Drum)[d]	3.7×10^{-6} m/s/mf Filter		14,980	10,812	
	7.4×10^{-6} m/s/mf Filter		7,490	5,406	
	1.85×10^{-5} m/s/mf Filter		2,998	2,164	0
	9.25×10^{-5} m/s/mf Filter		600	434	0
	3.7×10^{-4} m/s/mf Filter		150	110	0
TDOP Direct load	3.7×10^{-6} m/s/mf Filter		3,746	2,703	
	7.4×10^{-6} m/s/mf Filter		1,873	1,352	
	1.85×10^{-5} m/s/mf Filter		750	541	
	9.25×10^{-5} m/s/mf Filter		150	109	
	3.7×10^{-4} m/s/mf Filter		38	28	

a   See Appendix 6.10 of the CH-TRU Payload Appendices regarding the selection of payload containers for overpacked configurations.

b   Use Column 1 for the following six-digit notations (XX YYYY): 10 0160, 10 0130, 10 0040, and 20 0008. Use Column 2 for all other six-digit notations.

c   Divide the appropriate "Resistance Factor" by the "Number of Filters on Payload Container" to obtain the "Total Resistance Factor."

d   If total resistance factor of an SWB overpacking up to four 55-gallon drums is ≤3745 (if using Column 1) or ≤2703 (if using Column 2), the total resistance of the SWB layer can be assigned a value of zero pursuant to Appendix 6.10 of the CH-TRU Payload Appendices.

m/s/mf = Moles/second/mole fraction.

Table 2.2-4 — Load Type Resistance Worksheet[a]

Shipping Period[a]	Payload Container[b]	Resistance Factor	Total Resistance Factor
60 Days (General Case)	55-Gallon Drum	7,147	
	85-Gallon Drum	4,795	
	100-Gallon Drum	2,764	
	SWB – Direct Load	1,430	
	SWB Overpack	5,718	
	TDOP – Direct Load	980	
20 Days (Close-Proximity Shipment)	55-Gallon Drum	2,383	
	85-Gallon Drum	1,599	
	100-Gallon Drum	922	
	SWB – Direct Load	477	
	SWB Overpack	1,906	
	TDOP – Direct Load	327	
10 Days (Controlled Shipment)[c]	55-Gallon Drum	1,192	
	85-Gallon Drum	800	
	100-Gallon Drum	461	
	SWB – Direct Load	239	
	SWB Overpack	953	
	TDOP – Direct Load	164	

[a]See Appendices 3.4, 3.5, and 3.6 of the CH-TRU Payload Appendices regarding the selection of a shipping period.
[b]See Appendix 6.10 of the CH-TRU Payload Appendices regarding the use of equivalent Load Type factors for overpacked configurations.
[c]The 10-day shipping period may be used only if the requirements for controlled shipment are met as described in Appendix 3.6 of the CH-TRU Payload Appendices and Section 6.2.3 of the CH-TRAMPAC.

APPENDIX 2.3

DERIVATION OF DECAY HEAT LIMITS

This page intentionally left blank.

2.3   Derivation of Decay Heat Limits

The purpose of this appendix is to provide the logic and mathematical analysis used to arrive at the maximum decay heats for each payload shipping category when all payload containers in a payload belong to the same shipping category and a complete payload is shipped.
Appendix 6.12 of the CH-TRU Payload Appendices describes the derivation of decay heat limits for Content Code LA 154 and establishes associated conditions for compliance. Due to the similarities of the TRUPACT-II and HalfPACT packagings (with respect to void volume per payload container and all other variables such as shipment time), decay heat limits per payload container are determined using conservative values and are independent of the packaging (e.g., void volumes per payload container are slightly higher for the HalfPACT, but decay heat limits are calculated using the TRUPACT-II void volumes). Appendix 2.4 of the CH-TRU Payload Appendices presents the methodology for arriving at allowable flammable gas generation limits when dunnage containers are used and/or mixing of shipping categories is used in a payload.

When the logic and mathematical analysis requires the variable of shipment time, the conservative value of 60 days is utilized. For close-proximity shipments and controlled shipments, conservative values of 20 days and 10 days may be assumed, as described in Appendices 3.5 and 3.6, respectively, of the CH-TRU Payload Appendices.

At steady state, the flow rate of hydrogen across each of the confinement layers is equal to the same value and to the hydrogen generation rate. The maximum hydrogen concentration in a payload container vented per Section 2.5 of the Contact-Handled Transuranic Waste Authorized Methods for Payload Control (CH-TRAMPAC) is reached at steady state. That is, a filter vented container with a hydrogen generation source has increasing concentrations of hydrogen with time until steady state conditions are reached. For the purpose of these calculations, it has been assumed that all payload containers are at steady state at the start of transport. As described in Section 5.3 of the CH-TRAMPAC, all payload containers generated in an unvented condition are required to be aspirated to ensure steady-state conditions prior to transport.

The temperature dependence of decay heat limits is discussed in Appendix 6.9 of the CH-TRU Payload Appendices. As shown in that appendix, for Waste Material Type II.1 and Waste Type III, minimum values for the decay heat limits are obtained by using the hydrogen generation and release rates at an ambient temperature of 70°F. For Waste Type I and Waste Material Type II.3, the lowest values for the decay heat limits are obtained by using the hydrogen generation and release rates at the minimum operating temperature of -20°F.

Once the payload containers are sealed inside the TRUPACT-II or HalfPACT inner containment vessel (ICV), concentrations of hydrogen in the different layers increase due to the accumulation of hydrogen in the ICV cavity. Some of the hydrogen generated during the transport period would accumulate in the payload containers, with the remainder being released into the cavity. For the purpose of these calculations, the mole fraction of hydrogen in a bag layer is set equal to the steady state value plus the mole fraction of hydrogen that has accumulated in the cavity. The ICV cavity mole fraction of hydrogen is obtained by assuming that all of the hydrogen generated is released into the ICV cavity. The maximum hydrogen concentration in the innermost layer is then limited to less than or equal to five (5) volume percent at the end of the shipping period by

suitably choosing the gas generation rates. The maximum number of moles of hydrogen that can accumulate in the ICV cavity is:

$$N_{gen} = (CG)(n_{gen})(t) \tag{1}$$

Where:

N_{gen} = total moles of hydrogen generated

CG = hydrogen gas generation rate per innermost layer of confinement (moles/sec)

n_{gen} = number of hydrogen generators (55-gallon drums, standard pipe overpacks, S100 pipe overpacks, S200 pipe overpacks, S300 pipe overpacks, 85-gallon drums, 100-gallon drums, SWBs, TDOPs) (see Table 2.4-1 of Appendix 2.4 of the CH-TRU Payload Appendices)

t = shipping period duration (e.g., 60 days).

The maximum mole fraction of hydrogen in the TRUPACT-II or HalfPACT ICV cavity is then equal to:

$$X_{fh} = (N_{gen}/N_{tg}) = \{N_{gen}/[P(V_{void})/RT]\} \tag{2}$$

Where:

X_{fh} = maximum mole fraction of hydrogen in the ICV cavity

N_{tg} = total moles of gas inside the ICV cavity

P = pressure inside the TRUPACT-II or HalfPACT, assumed to be constant at 1 atm (760 mm Hg), because the amount of gas generated is much less than the total amount of air originally in the cavity

V_{void} = void volume inside the ICV cavity (liters)

R = gas constant = 62.361 mm Hg-liter/mole-K

T = absolute temperature of air in the ICV cavity at the time of closure = 70°F = 294K.

The gas generation rate per innermost confinement layer that will yield a maximum hydrogen concentration of five (5) volume percent is then computed as the following:

$$X_{inner} = X_{fh} + (CG)(R_{eff}) \tag{3}$$

Where:

> X_{inner} =   mole fraction of hydrogen in innermost confinement layer (a value of 0.05 has been used for this parameter since this is the maximum permissible concentration)

> R_{eff} =   the effective resistance to the release of hydrogen (sec/mole).

The effective resistance is computed by summing the individual confinement layer resistances. The resistance of a layer is equal to the reciprocal of the release rate from that layer. After substituting equations (1) and (2) into (3) and solving for the gas generation rate the following results:

$$CG \; = \; (X_{inner})/\{R_{eff} + [(t)(n_{gen})/N_{tg}]\} \tag{4}$$

where all terms are as defined previously. The decay heat per innermost confinement layer is then computed as:

$$Q_i \; = \; [(CG)(N_A)/(G \text{ molecules}/100eV)][1.602(10)^{-19} \text{ watt-sec/eV}] \tag{5}$$

Where:

> Q_i =   decay heat per innermost confinement layer (watts)

> N_A =   Avogadro's number = $6.023(10)^{23}$ molecules/mole

> G = G_{eff} (flam gas) = effective G value for flammable gas (molecules of hydrogen formed/100 electron volts [eV] emitted energy).

The logic for arriving at the input parameters is detailed in Appendix 6.7 of the CH-TRU Payload Appendices.

As an example, the decay heat limit per innermost confinement layer will be computed for shipping category I.1A2 (or 10 0160 0190).

The effective resistance is the sum of the following resistances (see Appendix 6.8 of the CH-TRU Payload Appendices for a derivation of the resistances):

- There are two liner bags, thus the combined resistance is twice the resistance of one liner bag, 2 x 214,133 sec/mole or 428,266 sec/mole.

- Resistance of the drum liner, which is 19,646 sec/mole, and

- Resistance of the drum filter, which is 729,327 sec/mole.

The effective resistance, R_{eff}, is therefore 1,177,239 sec/mole.

Assuming an atmospheric pressure of 760 mm Hg, a TRUPACT-II ICV cavity void volume of 2,450 liters (for 14 drums/TRUPACT-II) and a temperature of 70°F (294K), the total moles of gas inside the TRUPACT-II Package ICV cavity is computed using the ideal gas law,

$$N_{tg} \quad = \quad (P)(V_{void})/RT = (760 \text{ mm Hg}) (2,450 \text{ liters}) / [(62.361 \text{ mm Hg - liter/mole-K})(294K)]$$
$$= \quad 101.56 \text{ moles}$$

There will be 14 drums of shipping category I.1A2 (10 0160 0190) inside a TRUPACT-II package so that the number of gas generators, $n_{gen} = 14$.

The hydrogen gas generation rate per the innermost confinement layer may then be computed using equation (4) assuming a maximum five (5) volume percent concentration at the end of sixty days.

$$CG \quad = \quad (0.05)/\{1,177,239 \text{ sec/mole} + [(60 \text{ days})(86,400 \text{ sec/day})(14)/(101.56 \text{ moles})]\}$$

$$= \quad 2.643(10)^{-8} \text{ mole/sec}$$

[Note: The ratio of number of generators to total moles for a HalfPACT is 7/76.52 moles, which results in a slightly higher CG. Therefore, use of the TRUPACT-II CG value for the HalfPACT is conservative.]

For shipping category I.1A2 (10 0160 0190), the effective G (flam gas) value is 1.60. Therefore, the decay heat limit per innermost confinement layer, Q_i, through equation (5) is:

$$Q_i \quad = \quad [2.643(10)^{-8} \text{ mole/sec}][6.023(10)^{23} \text{ molecules/mole}]$$
$$x \; [1.602(10)^{-19} \text{ watt-sec/eV}]/[1.6 \text{ molecules/100 eV}]$$

$$= \quad 0.1594 \text{ watt}$$

The methodology used for deriving the decay heat limit described above applies to the derivation of decay heat limits for all shipping categories under the alpha-numeric notation system (see Appendix 2.1 of the CH-TRU Payload Appendices). The methodology used for calculating the decay heat limits for numeric shipping categories is simplified and conservative to provide a direct correlation between shipping category and decay heat limits. Both methodologies produce decay heat limits that limit the concentration of hydrogen gas within any layer of confinement to less than or equal to 5% by volume.

For numeric shipping categories that do not have a corresponding alpha-numeric shipping category notation, the decay heat limit calculation methodology follows. As described in Appendix 2.1 of the CH-TRU Payload Appendices, the last four digits of the numeric shipping category is a notation for the total resistance to hydrogen release. From equation (4) above, the total resistance (R_T) can be defined as the combination of the effective resistance (R_{eff}), the

resistance provided by the moles of gas in the void volume within the packaging (N_{tg}), the number of generators (n_{gen}), and the shipping period (t).

$$R_T = R_{eff} + [(t) (n_{gen}) / N_{tg}] \tag{6}$$

Substituting equation (6) into equation (4) yields:

$$CG = \frac{X_{inner}}{R_T}$$

Combining equations (4), (5), and (6), and solving for Q_i yields:

$$Q_i = \frac{(0.05 * 6.023 (10)^{23} \text{ molecules/mole} * 1.602 (10)^{-19} \text{ watt-sec/eV})}{(R_T \text{ sec/mole} * G \text{ value} / 100 \text{ eV})} \tag{7}$$

Simplifying and using the shipping category notation form of XX YYYY ZZZZ (described in Appendix 2.1 of the CH-TRU Payload Appendices) where YYYY represents the G value (multiplied by 100) and ZZZZ represents the total resistance, R_T, (divided by 10,000 and rounded up) yields:

$$CG = \frac{0.05}{(ZZZZ * 10,000) \text{ sec/mole}} \tag{8}$$

and

$$Qi = \frac{(4824.42 \text{ molecules/mole} * \text{watt-sec/eV})}{(ZZZZ * YYYY) \text{ sec-molecules/mole-eV}} \tag{9}$$

For shipping category 10 0040 0160, substituting 0040 for YYYY and 0160 for ZZZZ yields:

$$CG = \frac{0.05}{(0160 * 10,000) \text{ sec/mole}} = 3.125E\text{-}08 \text{ mole/sec}$$

$$Q_i = \frac{4824.42 \text{ molecules/mole} * \text{watt-sec/eV}}{(0160 * 0040) \text{ sec-molecules/mole-eV}} = 0.7538 \text{ watts}$$

Because the total resistance, R_T, is rounded up to the nearest 10,000 sec/mole, the calculated decay heat limit using this simplified method is conservative. Decay heat limits for all other numeric shipping categories that do not have a corresponding alpha-numeric shipping category are calculated from the shipping category notation using this simplified equation.

Because the decay heat limit cannot be directly calculated from the alpha-numeric payload shipping category notation, Table 2.3-1 presents the hydrogen gas generation rate limit and the decay heat limit for each alpha-numeric payload shipping category.

The parameters that are used in the calculations are described below.

Parameter	Description
Alpha-numeric Payload Shipping Category	Identifies payload shipping category using the alpha-numeric shipping category notation (form of the waste).
G Value (H_2)	G_{eff} (flam gas)—Number of molecules of hydrogen produced per 100 eV of emitted energy. There is a characteristic effective G (flam gas) value associated with each waste material type as described in Appendix 3.2 of the CH-TRU Payload Appendices.
Number of Generators in ICV	n_{gen}—The number of generators inside the packaging ICV, e.g., in the case of SWB overpack in a TRUPACT-II, the number of generators is 8 (4 55-gallon drums per SWB) x (2 SWBs per TRUPACT-II ICV).
Number of Inner Bags	These are the small bags, such as those used to bag-out solid inorganics and organics. Only the leakage from the closure or filter has been used as the hydrogen release rate.
Number of Liner Bags	These are the large bags, such as those used to contain the solidified aqueous or homogeneous inorganic solids or that serve as drum liners for Waste Types II or III. Hydrogen release from both permeation through the bag material and diffusion through the closure or filter has been used in computing hydrogen release rates.
Total Number of Bags	Sum of the number of inner and liner bags.
Number of Containers in ICV	Number of payload containers inside the packaging ICV cavity.
Void Vol. in ICV Effective Resistance	Void volume inside the packaging ICV cavity (liters). Effective resistance to the release of hydrogen computed by summing the individual confinement layer resistances.
Number of Moles in ICV	Number of moles in the packaging ICV cavity computed via the ideal gas law equation.

Parameter	Description
Gas Generation Rate	Gas generation rate per generator (CG), which is computed from input parameters via equation (4) for alpha-numeric shipping categories and equation (8) for numeric shipping categories.
Decay Heat Limit Per Generator (watts)	Decay heat limit per generator (watts), which is computed using equation (9) for numeric shipping categories and equation (5) for alpha-numeric shipping categories.
Numeric Payload Shipping Category	Identifies payload shipping category using the numeric shipping category notation (form of the waste).

Table 2.3-1 - List of Approved Alpha-numeric Shipping Categories, Maximum Allowable Hydrogen Gas Generation Rates, and Maximum Allowable Wattages

Numeric Payload Shipping Category	Alpha-numeric Payload Shipping Category	Maximum Allowable Hydrogen Gas Generation Rate (moles/sec)	Maximum Allowable Wattage (watts)
10 0040 0034	I.3C0	1.514E-07	3.6528
10 0040 0147	I.3A0	3.416E-08	0.8241
10 0040 0168	I.3A1	2.980E-08	0.7189
10 0040 0190	I.3A2	2.643E-08	0.6375
10 0040 0207	I.3B0	2.416E-08	0.5827
10 0040 0229	I.3B1	2.189E-08	0.5281
10 0040 0250	I.3B2	2.002E-08	0.4828
10 0040 0648	I.3A3	7.721E-09	0.1863
10 0040 0709	I.3B3	7.061E-09	0.1703
10 0040 0888	I.3A4	5.634E-09	0.1359
10 0040 0949	I.3B4	5.274E-09	0.1272
10 0130 0034	I.2C0	1.514E-07	1.1240
10 0130 0147	I.2A0	3.416E-08	0.2536
10 0130 0168	I.2A1	2.980E-08	0.2212
10 0130 0190	I.2A2	2.643E-08	0.1962
10 0130 0207	I.2B0	2.416E-08	0.1793
10 0130 0229	I.2B1	2.189E-08	0.1625
10 0130 0250	I.2B2	2.002E-08	0.1486
10 0130 0648	I.2A3	7.721E-09	0.0573
10 0130 0709	I.2B3	7.061E-09	0.0524
10 0130 0888	I.2A4	5.634E-09	0.0418
10 0130 0949	I.2B4	5.274E-09	0.0391
10 0160 0034	I.1C0	1.514E-07	0.9132
10 0160 0059	I.1C2	8.598E-08	0.5185
10 0160 0147	I.1A0	3.416E-08	0.2060
10 0160 0168	I.1A1	2.980E-08	0.1797
10 0160 0190	I.1A2	2.643E-08	0.1594
10 0160 0207	I.1B0	2.416E-08	0.1457

Table 2.3-1 - List of Approved Alpha-numeric Shipping Categories, Maximum Allowable Hydrogen Gas Generation Rates, and Maximum Allowable Wattages (Continued)

Numeric Payload Shipping Category	Alpha-numeric Payload Shipping Category	Maximum Allowable Hydrogen Gas Generation Rate (moles/sec)	Maximum Allowable Wattage (watts)
10 0160 0229	I.1B1	2.189E-08	0.1320
10 0160 0250	I.1B2	2.002E-08	0.1207
10 0160 0286	I.1C2b	1.751E-08	0.1056
10 0160 0648	I.1A3	7.721E-09	0.0466
10 0160 0709	I.1B3	7.061E-09	0.0426
20 0000 0000	II.2AM	NA	40.0000
20 0000 0000	II.2BM	NA	40.0000
20 0000 0000	II.2CM	NA	40.0000
20 0000 0000	II.2E0	NA	40.0000
20 0170 0028	II.1C0	1.798E-07	1.0206
20 0170 0034	II.1C1f	1.501E-07	0.8518
20 0170 0039	II.1C2f	1.288E-07	0.7309
20 0170 0041	II.1C1	1.238E-07	0.7029
20 0170 0043	II.1C2bf	1.173E-07	0.6659
20 0170 0049	II.1C3f	1.039E-07	0.5897
20 0170 0053	II.1C2	9.445E-08	0.5361
20 0170 0067	II.1D2	7.524E-08	0.4271
20 0170 0127	II.1A0	3.966E-08	0.2251
20 0170 0133	II.1A1f	3.765E-08	0.2137
20 0170 0140	II.1A2af	3.584E-08	0.2034
20 0170 0143	II.1A2f	3.519E-08	0.1997
20 0170 0148	II.1A1	3.391E-08	0.1924
20 0170 0152	II.1A3f	3.303E-08	0.1875
20 0170 0166	II.1B0	3.015E-08	0.1711
20 0170 0169	II.1A2a	2.961E-08	0.1680
20 0170 0188	II.1B1	2.670E-08	0.1516
20 0170 0209	II.1B2a	2.396E-08	0.1360
20 0170 0220	II.1C2b	2.277E-08	0.1292

Table 2.3-1 - List of Approved Alpha-numeric Shipping Categories, Maximum Allowable Hydrogen Gas Generation Rates, and Maximum Allowable Wattages (Continued)

Numeric Payload Shipping Category	Alpha-numeric Payload Shipping Category	Maximum Allowable Hydrogen Gas Generation Rate (moles/sec)	Maximum Allowable Wattage (watts)
20 0170 0233	II.1C3	2.154E-08	0.1222
20 0170 0327	II.1A2	1.531E-08	0.0869
20 0170 0367	II.1B2	1.364E-08	0.0774
20 0170 0412	II.1C4	1.215E-08	0.0690
20 0170 0506	II.1A3	9.883E-09	0.0561
20 0170 0546	II.1B3	9.163E-09	0.0520
20 0170 0686	II.1A4	7.298E-09	0.0414
20 0170 0725	II.1B4	6.898E-09	0.0392
20 0170 0865	II.1A5	5.785E-09	0.0328
20 0170 0905	II.1B5	5.530E-09	0.0314
20 0170 1044	II.1A6	4.791E-09	0.0272
20 0170 1084	II.1B6	4.616E-09	0.0262
30 0340 0028	III.1C0	1.798E-07	0.5103
30 0340 0034	III.1C1f	1.501E-07	0.4259
30 0340 0039	III.1C2f	1.288E-07	0.3655
30 0340 0041	III.1C1	1.238E-07	0.3515
30 0340 0043	III.1C2bf	1.173E-07	0.3329
30 0340 0049	III.1C3f	1.039E-07	0.2948
30 0340 0053	III.1C2	9.445E-08	0.2680
30 0340 0067	III.1D2	7.524E-08	0.2135
30 0340 0127	III.1A0	3.966E-08	0.1126
30 0340 0133	III.1A1f	3.765E-08	0.1069
30 0340 0140	III.1A2af	3.584E-08	0.1017
30 0340 0143	III.1A2f	3.519E-08	0.0999
30 0340 0148	III.1A1	3.391E-08	0.0962
30 0340 0152	III.1A3f	3.303E-08	0.0937
30 0340 0166	III.1B0	3.015E-08	0.0856
30 0340 0169	III.1A2a	2.961E-08	0.0840
30 0340 0188	III.1B1	2.670E-08	0.0758

Table 2.3-1 - List of Approved Alpha-numeric Shipping Categories, Maximum Allowable Hydrogen Gas Generation Rates, and Maximum Allowable Wattages (Concluded)

Numeric Payload Shipping Category	Alpha-numeric Payload Shipping Category	Maximum Allowable Hydrogen Gas Generation Rate (moles/sec)	Maximum Allowable Wattage (watts)
30 0340 0209	III.1B2a	2.396E-08	0.0680
30 0340 0220	III.1C2b	2.277E-08	0.0646
30 0340 0233	III.1C3	2.154E-08	0.0611
30 0340 0327	III.1A2	1.531E-08	0.0434
30 0340 0367	III.1B2	1.364E-08	0.0387
30 0340 0412	III.1C4	1.215E-08	0.0345
30 0340 0506	III.1A3	9.883E-09	0.0280
30 0340 0546	III.1B3	9.163E-09	0.0260
30 0340 0686	III.1A4	7.298E-09	0.0207
30 0340 0725	III.1B4	6.898E-09	0.0196
30 0340 0865	III.1A5	5.785E-09	0.0164
30 0340 0905	III.1B5	5.530E-09	0.0157
30 0340 1044	III.1A6	4.791E-09	0.0136
30 0340 1084	III.1B6	4.616E-09	0.0131
40 9999 0127	IV.1A0T	3.937E-08	7.0000
40 9999 0148	IV.1A1T	3.378E-08	7.0000
40 9999 0169	IV.1A2T	2.959E-08	7.0000
40 9999 0188	IV.1B1T	2.660E-08	7.0000
40 9999 0209	IV.1B2T	2.392E-08	7.0000
40 9999 0506	IV.1A3T	9.881E-09	7.0000
40 9999 0546	IV.1B3T	9.158E-09	7.0000

This page intentionally left blank.

APPENDIX 2.4

MIXING OF SHIPPING CATEGORIES AND DETERMINATION OF THE FLAMMABILITY INDEX

This page intentionally left blank.

2.4 Mixing of Shipping Categories and Determination of the Flammability Index

The purpose of this appendix is to provide the logic and mathematical analysis for assembling a payload of containers with different shipping categories. An assembly of payload containers with different shipping categories is approved by ensuring that each payload container does not contain a flammable mixture of gases, while accounting for the properties of each of the other payload containers in the assembly, which may include dunnage containers. Each payload container is assessed through the calculation of the flammability index (FI) for the container, which accounts for the flammable properties of each container in the assembly. For each payload container, the FI is calculated as the ratio of the actual flammable gas generation rate to the allowable flammable gas generation rate limit multiplied by 50,000. Thus, the FI must be a non-negative number less than or equal to 50,000 for each payload container. The determination of allowable flammable gas generation rates takes into account the concentrations of flammable volatile organic compounds (VOCs) within the innermost layer of confinement, if present, and the void volume of dunnage containers. Unlimited mixing of shipping categories is allowed for direct loaded payload configurations, with the FIs calculated based on each payload container in the configuration. For overpacked payload configurations documented in this appendix, unlimited mixing of shipping categories is allowed pursuant to implementation of the methodology described in this appendix. For Content Code LA 154, mixing is only allowed within the content code as presented in Appendix 6.12 of the CH-TRU Payload Appendices.

At steady state, the flow of flammable gas across each of the confinement layers is equal to the flammable gas generation rate. The maximum flammable gas concentration in a payload container vented per Section 2.5 of the Contact-Handled Transuranic Waste Authorized Methods for Payload Control (CH-TRAMPAC) is reached at steady state. That is, a filtered container with a flammable gas generation source has increasing concentrations of hydrogen with time until steady-state conditions are reached. For the purpose of these calculations, it has been conservatively assumed that all payload containers are at steady state at the start of transport. As described in Section 5.3 of the CH-TRAMPAC, all payload containers generated in an unvented condition are required to be aspirated to ensure steady-state conditions prior to transport.

Once payload containers are sealed inside the packaging inner containment vessel (ICV), concentrations of flammable gas in the different layers increase due to the accumulation of flammable gas in the packaging ICV cavity. Some of the flammable gas generated during the transport period would accumulate in the innermost container and in the overpacking container (if present), with the remainder being released into the cavity. The packaging ICV cavity mole fraction of flammable gas is obtained by assuming that all of the flammable gas generated is instantaneously released into the packaging ICV cavity. The maximum concentration of flammable gas and flammable VOCs in the innermost layer is then limited to the mixture lower explosive limit (MLEL). The allowable flammable gas concentration (AFGC) is then calculated as the difference between the MLEL and the sum of the flammable VOC concentrations.

For analytical category payload containers or test category payload containers that have headspace concentrations of flammable VOCs less than or equal to 500 parts per million (ppm),

the AFGC is equal to the MLEL of 0.05 mole fraction (i.e., 5 volume percent). For test category containers with headspace flammable VOC concentrations in excess of 500 ppm, the AFGC is calculated as the difference between the MLEL at the end of the 60-day shipping period and the innermost confinement layer sum of flammable VOC concentrations. For close-proximity shipments and controlled shipments, conservative values of 20 days and 10 days may be assumed, as described in Appendices 3.5 and 3.6, respectively, of the CH-TRU Payload Appendices.

The maximum number of moles of flammable gas that can accumulate in the packaging ICV cavity is:

$$N_{gen} = \sum_{i=1}^{n_{containers}} CG_i\, t \tag{1}$$

where,

N_{gen} =   Total moles of flammable gas generated (mole).

CG_i =   Flammable gas generation rate per innermost confinement layer of payload container "i" (mole/sec). When shipping categories are mixed in a single payload, this rate will be different for each payload container.

t   =   Shipping period duration (60 days or 5,184,000 seconds).

$n_{containers}$ =   Number of generators in the payload (Table 2.4-1 lists the maximum number of generators based on the payload assembly configuration).

The maximum flammable gas mole fraction in the packaging ICV cavity is then equal to:

$$X_{fg} = \frac{N_{gen}}{N_{tg}} = \sum_{i=1}^{n_{containers}} \frac{CG_i\, t}{N_{tg}} \tag{2}$$

where,

X_{fg} =   Maximum mole fraction of flammable gas in the packaging ICV cavity

N_{tg} =   Total moles of gas inside the packaging ICV cavity that are equal to:

$$N_{tg} = \sum_{i=1}^{n_{containers}} CG_i\, t + \frac{PV_{void}}{RT} \tag{3}$$

Table 2.4-1 Parameter Values for Payload Assembly Configurations

Payload Assembly Configuration	Maximum Number of Flammable Gas Generators	Void Volume of Dunnage Payload Containers (liters)	V_{void} (liters)
Fourteen 55-Gallon Drums in TRUPACT-II Fourteen Standard Pipe Overpacks in TRUPACT-II Fourteen S100 Pipe Overpacks in TRUPACT-II Fourteen S200 Pipe Overpacks in TRUPACT-II Fourteen S300 Pipe Overpacks in TRUAPCT-II	14	208	$2{,}450 + n_{dunnage}*208$
Seven 55-Gallon Drums in HalfPACT Seven Standard Pipe Overpacks in HalfPACT Seven S100 Pipe Overpacks in HalfPACT Seven S200 Pipe Overpacks in HalfPACT Seven S300 Pipe Overpacks in HalfPACT	7	208	$1{,}225 + n_{dunnage}*208$
Eight 85-Gallon Drums in TRUPACT-II	8	321	$2{,}087 + n_{dunnage}*321$
Four 85-Gallon Drums in HalfPACT Four 85-Gallon Drum Overpacks in HalfPACT	4	321	$1{,}043 + n_{dunnage}*321$
Six 100-Gallon Drums in TRUPACT-II	6	378	$2{,}715 + n_{dunnage}*378$
Three 100-Gallon Drums in HalfPACT	3	378	$1{,}357 + n_{dunnage}*378$
TDOP With Ten 55-Gallon Drums in TRUPACT-II	10 Actual + 4 assumed with most restrictive properties	208	$2{,}450 + n_{dunnage}*208$
TDOP With Six 85-Gallon Drums in TRUPACT-II	6 Actual + 2 assumed with most restrictive properties	321	$2{,}087 + n_{dunnage}*321$
TDOP With Six 85-Gallon Drum Overpacks in TRUPACT-II	See Two SWB Overpacks in TRUPACT-II		
Two SWBs in TRUPACT-II	2	1,750	1,750 or 3,500 with dunnage SWB
Two SWB Overpacks in TRUPACT-II	8	208	1,750 or 3,500 with dunnage SWB + $n_{dunnage}*208$

Table 2.4-1 Parameter Values for Payload Assembly Configurations (Continued)

Payload Assembly Configuration	Maximum Number of Flammable Gas Generators	Void Volume of Dunnage Payload Containers (liters)	V_{void} (liters)
One SWB in HalfPACT	1	No dunnage available	875
One SWB Overpack in HalfPACT	4	208	$875 + n_{dunnage}*208$
One TDOP direct load in TRUPACT-II	1	No dunnage available	1,277

SWB = Standard waste box
TDOP = Ten-drum overpack

where,

P = Pressure inside the package, conservatively assumed to be constant at 1 atmosphere (atm), because the amount of gas generated is much less than the total amount of air originally in the cavity

V_{void} = Void volume inside the packaging ICV cavity, which includes the void volume of appropriate dunnage containers (Table 2.4-1 lists appropriate values based on the payload assembly configuration)

R = Gas constant (0.082056 atm-liter/mole-K)

T = Absolute temperature of air originally in the cavity (294K).

It is assumed that the moles of flammable gas generated is much less than the moles of gas in the packaging ICV cavity at the time of package sealing:

$$\sum_{i=1}^{n_{containers}} CG_t\ t << \frac{PV_{void}}{RT} \tag{4}$$

Therefore, from equation (3),

$$N_{tg} \approx \frac{PV_{void}}{RT} \tag{5}$$

2.4-4

2.4.1   Derivation of Mass Balances for Payload Assembly Configurations

2.4.1.1   Drums, Drum Overpacks, or Pipe Overpacks Loaded in ICV

The flammable gas generation rate per innermost confinement layer that will yield a maximum flammable gas concentration equivalent to the AFGC, is then calculated for each payload container "i" as the following:

$$CG_i \, r_{eff\,i} = AFGC_i - X_{fg} \tag{6}$$

where,

AFGC$_i$ =   Allowable flammable gas concentration in innermost confinement layer of payload container "i"

$r_{eff,i}$ =   The effective resistance to the release of hydrogen of payload container "i" (sec/mole).

The effective resistance is computed by summing the individual confinement layer resistances. The resistance of a layer is equal to the reciprocal of the release rate from that layer. Substituting X$_{fg}$ from equation (2) into equation (6) and rearranging terms yields the following system of equations:

$$\left(r_{eff,1} + \frac{t}{N_{tg}} \right) CG_1 + \frac{t}{N_{tg}} CG_2 + \ldots + \frac{t}{N_{tg}} CG_{n_{containers}} = AFGC_1$$

$$\frac{t}{N_{tg}} CG_1 + \left(r_{eff,2} + \frac{t}{N_{tg}} \right) CG_2 + \ldots + \frac{t}{N_{tg}} CG_{n_{containers}} = AFGC_2$$

$$\begin{array}{ccc} \bullet & \bullet & \bullet \\ \bullet & \bullet & \bullet \\ \bullet & \bullet & \bullet \end{array}$$

$$\frac{t}{N_{tg}} CG_1 + \frac{t}{N_{tg}} CG_2 + \ldots + \left(r_{eff,n_{containers}} + \frac{t}{N_{tg}} \right) CG_{n_{containers}} = AFGC_{n_{containers}} \tag{7}$$

2.4.1.2   Ten-Drum Overpack With 55-Gallon Drums

The analyses presented in Appendix 6.10 of the CH-TRU Payload Appendices show that overpacking payload containers in a ten-drum overpack (TDOP) will not decrease the allowable decay heat limits, even when payload containers are allowed to remain overpacked in a TDOP

for indefinite periods of time before transport inside a TRUPACT-II. For example, a 55-gallon drum that meets the decay heat limit for a 14-drum payload in a TRUPACT-II can also be shipped in a 10-drum configuration in a TDOP inside a TRUPACT-II. The overpacked configurations can be conservatively assigned the same decay heat limits as the equivalent configurations not using the TDOP. If 55-gallon drums or 85-gallon drum overpacks of different shipping categories are mixed within a TDOP, the mixing of shipping categories methodology for 14 55-gallon drums directly loaded in the ICV shall apply. For purposes of establishing allowable flammable gas generation rates, the payload will be assumed to consist of four additional drums that will be assigned the same packaging configuration as the most restrictive waste drum. These four drums will each be assigned the minimum AFGC value of the actual waste drums.

2.4.1.3 TDOP With 85-Gallon Drums/85-Gallon Drum Overpacks

As indicated above, the analyses presented in Appendix 6.10 of the CH-TRU Payload Appendices show that overpacking payload containers in a TDOP will not decrease the allowable decay heat limits, even when payload containers are allowed to remain overpacked in a TDOP for indefinite periods of time before transport inside a TRUPACT-II. The overpacked configurations can be conservatively assigned the same decay heat limits as the equivalent configurations not using the TDOP. If 85-gallon drums of different shipping categories are mixed within a TDOP, the mixing of shipping categories methodology for eight 85-gallon drums directly loaded in the ICV shall apply. As shown in Appendix 6.10, 85-gallon drum overpacks will be evaluated as eight 55-gallon drums overpacked in two SWBs with two filters using the methodology of Section 2.4.1.4. For purposes of establishing allowable flammable gas generation rates, the payload will be assumed to consist of two additional drums that will be assigned the same packaging configuration as the most restrictive waste drum. These two drums will each be assigned the minimum AFGC value of the actual waste drums.

2.4.1.4 Standard Waste Box Overpacks Loaded in ICV

The mass balances on hydrogen within a drum "i" and within the standard waste box (SWB) overpacking the n_{drums} number of waste drums may be expressed as:

Transient Mass Balance of Hydrogen in Drum "i"

$$\frac{PV_{ij}}{RT}\frac{dX_{ij}}{dt} = CG_{ij} - \frac{(X_{ij} - X_{SWB\,j})}{r_{eff\,ij}} \tag{8}$$

Transient Mass Balance on Hydrogen in SWB Overpack "j" Void

$$\frac{PV_{SWB\,j}}{RT}\frac{dX_{SWB\,j}}{dt} = \sum_{i=1}^{n_j}\frac{(X_{ij} - X_{SWB\,j})}{r_{eff\,ij}} - \frac{(X_{SWB\,j} - X_{fg})}{r_{SWB\,j}} \tag{9}$$

where,

V_{ij} =   Void volume within the innermost confinement layer of drum "i" overpacked in SWB "j" (liters)

$V_{SWB\,j}$ =   Void volume within an SWB overpack containing n_j drums of waste (liters)

n_j =   Number of waste drums inside SWB "j"

X_{ij} =   Mole fraction of flammable gas within innermost confinement layer of drum "i" overpacked in SWB "j" (dimensionless)

$X_{SWB\,j}$ =   Mole fraction of flammable gas within SWB "j" void volume (dimensionless)

X_{fg} =   Mole fraction of flammable gas in the packaging ICV cavity (dimensionless)

t   =   time (sec)

CG_{ij} =   Flammable gas generation rate per innermost confinement layer of drum "i" overpacked in SWB "j" (mole/sec)

$r_{eff,ij}$ =   The effective resistance to the release of hydrogen of drum "i" overpacked in SWB "j" (sec/mole)

$r_{SWB,j}$ =   The effective resistance to the release of hydrogen of the filters on SWB "j" (sec/mole).

Based on the pseudo steady-state assumption, the mass balance equations (equations (8) and (9)) are set to zero. The maximum concentration of flammable gas within the innermost confinement layer at the end of the transport period is set equal to the AFGC value:

$$X_{ij} = AFGC_{ij} \tag{10}$$

$AFGC_{ij}$ =   Allowable flammable gas concentration in innermost confinement layer of drum "i" in SWB "j".

Substitution of equation (10) into equations (8) and (9), which are both set to zero, and rearrangement of terms yields:

Pseudo Steady-State Mass Balance of Hydrogen in Drum "i"

$$CG_{ij} = \frac{AFGC_{ij} - X_{SWB\,j}}{r_{eff\,ij}} \tag{11}$$

Pseudo Steady-State Mass Balance on Hydrogen in SWB Overpack "j" Void

$$\sum_{i=1}^{n_j} \frac{AFGC_{ij} - X_{SWB\,j}}{r_{eff\,ij}} = \frac{X_{SWB\,j} - X_{fg}}{r_{SWB\,j}} \tag{12}$$

Rearranging equation (11) to express the SWB mole fraction in terms of drum "i" variables results in:

$$X_{SWB\,j} = AFGC_{ij} - CG_{ij} r_{eff\,ij} \tag{13}$$

Substitution of equation (13) in the left-hand side of equation (12) and substitution of equations (2) and (13) in the right-hand side of equation (12) results in the following system:

For j = 1 to n_{SWB}

For k = 1 to n_j

$$\sum_{i=1}^{n_j} CG_{ij} = \frac{AFGC_{kj} - CG_{kj} r_{eff\,kj} - \sum_{j=1}^{n_{SWB}} \sum_{i=1}^{n_j} \frac{CG_{ij} t}{N_{tg}}}{r_{SWB,j}} \tag{14}$$

Rearranging equation (14) results in the following system of equations that must be solved to obtain the allowable flammable gas generation rate limit for each drum "kj" (CG_{kj}):

For j = 1 to n_{SWB}

For k = 1 to n_j

$$r_{eff\,kj} CG_{kj} + r_{SWB,j} \sum_{i=1}^{n_j} CG_{ij} + \frac{t}{N_{tg}} \sum_{j=1}^{n_{SWB}} \sum_{i=1}^{n_j} CG_{ij} = AFGC_{kj} \tag{15}$$

2.4.2   Calculation of Allowable Flammable Gas Generation Rates

The systems of equations represented by equations (7) and (15) may be written in matrix form as:

$$A\,CG = b \tag{16}$$

where

A   =   Matrix of gas generation rate coefficients (i.e., $r_{eff\,i}$, $r_{eff\,kj}$, $r_{SWB\,j}$, and t/N_{tg} terms)

CG   =   Column vector of allowable gas generation rates

b   =   Column vector of AFGCs within the innermost confinement layers. Thus, the elements of this vector are equal to the individual payload container AFGC values.

The solution for the unknown allowable flammable gas generation rate for each payload container is given as:

$$CG = A^{-1}\ b \tag{17}$$

where

A^{-1} =   Inverse of matrix A.

Dunnage containers and payload containers that have no flammable gas generation rate are excluded from the system of linear equations.

2.4.3 Calculation of the Flammability Index

The FI of each container is then calculated as:

$$FI_i = \frac{CG_{i,actual}}{CG_{i,allowable}} \times 50,000 \tag{18}$$

where

FI_i =   Flammability index of payload container "i"

$CG_{i,actual}$ =   Actual flammable gas generation of payload container "i" (mole/sec)

$CG_{i,allowable}$ =   Allowable flammable gas generation rate of payload container "i" (mole/sec).

For analytical category payload containers, the actual flammable gas generation rate is calculated as:

$$CG_{i,actual} = \frac{Q_i \left(G\ molecules\ /\ 100\ eV \right)}{N_A \left(1.602 (10)^{-19}\ watt - second\ /\ eV \right)} \tag{19}$$

where

Q_i =   Decay heat of payload container (watts)

N_A =   Avogadro's number = $6.0225(10)^{23}$ molecules/mole

G   = G_{eff} (flam gas) = effective G value for flammable gas (molecules of flammable gas formed/100 eV emitted energy).

For test category containers, the actual gas generation rate is obtained either through measurement of the flammable gas concentration and calculation of the rate through the AltMeth methodology (Appendix 3.10 of the CH-TRU Payload Appendices), or through testing pursuant to Section 5.2.5 of the CH-TRAMPAC. A payload is qualified for shipment only if the FI of each payload container is a non-negative number less than or equal to 50,000. If one or more containers fail the FI requirement, the payload shall be reconfigured until all containers satisfy this requirement. The FI determination can be performed either manually or by the use of a validated software package.

APPENDIX 3.1

RADIOLYTIC G VALUES FOR WASTE MATERIALS

This page intentionally left blank.

Table of Contents

Table of Contents (Concluded)

List of Tables

List of Tables (Concluded)

Figures

Attachments

A   Chemical Properties and Commercial Uses of Organic Materials
B   Absorption of Alpha Decay Energy Inside Particles of PuO_2

Glossary

adsorption   The adhesion in an extremely thin layer of molecules (such as gases, solutes, or liquids) to the surfaces of solid bodies or liquids with which they are in contact.

absorbed dose   The amount of energy absorbed from the radiation field per unit of mass of irradiated material.

activation energy   The energy, in excess over the ground state, that must be added to an atomic or molecular system to allow a particular process to take place.

adiabatic   Any change or process resulting in no heat loss or gain.

alcohol   A class of organic compounds derived from hydrocarbons, containing the hydroxyl group OH (general formula ROH). Phenols, a subgroup of alcohols, are derived from aromatic hydrocarbons.

aldehyde   Compounds of the general formula RCHO, where R is any aliphatic or aromatic group and the oxygen is attached via a double bond to the carbon chain.

aliphatic   Any of a class of organic compounds characterized by straight or branched chain structures. Aliphatic compounds may contain single, double, and/or triple carbon-carbon bonds.

alkane   Any of a class of aliphatic hydrocarbon compounds characterized by single carbon-carbon bonds.

alkene   Any of a class of unsaturated aliphatic hydrocarbon compounds characterized by at least one double carbon-carbon bond.

alkyd   A thermoplastic or thermoset synthetic resin used especially for protective coatings.

alkyl   An aliphatic hydrocarbon group that may be derived from an alkane by dropping one hydrogen from the formula, such as "methyl" (CH_3).

alkyne   Any of a class of organic compounds containing at least one triple carbon-carbon bond.

alpha particle   A massive, positively charged particle (He^{++}) emitted by certain radioactive materials; particle energy depends on the parent material, and penetrating ability is limited.

amine   Any of a class of organic compounds that can be considered to be derived from ammonia by replacement of one or more hydrogen atoms with alkyl or aryl groups.

anaerobic   In the absence of oxygen.

antioxidant   An inhibitor, such as ascorbic acid, effective in preventing replacement of other elements by molecular oxygen.

aqueous solution   A solution that contains water as the dominant solvent.

aromatic   Any of a class of organic compounds characterized by closed ring structure and resonance stabilized (shifting/shared) unsaturation.

Arrhenius Equation   An equation relating the rate constant of a chemical reaction and the temperature at which the reaction is taking place:

$$k = A \exp(-E/RT)$$

where A is a constant, k the rate constant, T the temperature in degrees Kelvin, R the gas constant, and E the activation energy of the reaction.

aryl   A compound whose molecules have the ring structure characterized by benzene; that is, six carbon atoms condensed into a planar ring.

beta particle   A particle emitted by certain radioactive materials. A negatively charged beta particle has the characteristics of an electron; a positively charged beta particle is called a positron.

bond dissociation energy   The required energy for complete separation of two atoms within a molecule.

carbonyl compound   A compound containing the carbonyl group, (C=O), such as aldehydes, carboxylic acids, esters, etc.

carboxyl   A univalent group (-COOH) typical of organic acids.

cellulosic   Any of the derivatives of cellulose, such as cellulose acetate.

chain reaction | A reaction that involves a series of steps, each of which generates a reactive substance that brings about the next step.

chemical reaction rate | The speed at which a change occurs when a substance (or substances) is (are) changed into one or more new substances.

contact-handled | Radioactively contaminated materials having a container surface dose rate of no more than 200 mrem/hr, which may be handled manually.

crosslink | A chemical bond formed between separate polymer elements; crosslinking may be intermolecular (between molecules) or intramolecular (between parts of the same molecule).

Curie | The basic unit of radioactivity; equal to 3.7×10^{10} disintegrations per second.

depolymerization | The decomposition of macromolecular compounds into relatively simple compounds.

diffusion | The spontaneous movement and scattering of atomic and molecular particles of liquids, gases, and solids.

diluent | An inert substance added to a material so that the concentration per unit volume of the material is decreased.

dose | See "absorbed dose."

dose rate | The rate at which energy is deposited in a material.

dose rate effect | An effect depending on the rate at which a material is irradiated.

elastomer | A natural or synthetic rubber that stretches to at least twice its original length and retracts rapidly to near its original length when released.

emulsifier | A surface-active agent (like a soap) that promotes the formation and stabilization of a solid-in-liquid or liquid-in-liquid suspension.

Envirostone® | A licensed (U. S. Gypsum) gypsum-based process used for the solidification of organic and low pH aqueous sludges.

ester | A compound formed from the bonding of an alcohol (including phenols) with an organic acid or organic acid derivative by the elimination of water.

ether   A compound formed by attaching two groups to an oxygen atom, of the form R-O-R'.

excitation   The process by which energy is supplied to electrons, atoms, or radicals, usually rendering them chemically more reactive.

free radical   An atom or group of atoms having at least one unpaired electron not involved in bond formation. Free radicals are highly reactive.

gamma rays   Electromagnetic radiation (photons) emitted from the nucleus of certain radioactive materials; gamma rays are more penetrating than particle radiation of comparable energy.

Gray (Gy)   The SI recommended unit of absorbed dose that represents an absorption by a specified material of 1×10^4 ergs/gram; 1 Gray = 100 rads.

G value   The number of molecules, radicals, crosslinks, etc., of a specified type formed or consumed per 100 electron volts (eV) of energy absorbed by a system; this value is also used to specify the number of reactions that occur per 100 eV absorbed.

half-life   The time required for a quantity of a specific radionuclide to decay to one-half of its original amount.

halogenated compound   A compound that contains a member of the halogen family (for example, fluorine, chlorine, bromine).

halogenation   A chemical process or reaction in which a halogen atom (F, Cl, Br, I, At) is introduced into a substance.

hydrocarbon   One of a very large group of chemical compounds composed only of carbon and hydrogen.

hydrolysis   Decomposition or alteration of a chemical substance by water. In aqueous solutions of electrolytes, the reaction of cations with water to produce a weak base or of anions with water to produce a weak acid.

inelastic collision   An encounter in which the total kinetic energy of the colliding particles is lower after the collision than before it.

inhibitor   A substance that slows down or stops a reaction.

ion	An electrically charged atom, radical, or molecule resulting from the addition or removal of electrons by any of a number of possible processes.
ionization	The process of ion formation.
ionizing radiation	Particles or photons that have sufficient energy to produce ionization directly by their passage through a substance.
irradiation	Exposure to radiation.
isomer	One of two or more chemical substances having the same elementary percentage composition and molecular weight but differing in structure and, therefore, usually differing in properties.
isotactic	Refers to crystalline polymers in which groups in the asymmetric carbon atoms have the same (rather than random) configuration in relation to the main chain.
ketone	Any of a class of organic compounds characterized by the presence of the carbonyl group, C=O, attached to two alkyl groups.
LET (Linear Energy Transfer)	The radiation energy lost per unit length of path through a material, usually expressed in kilo-electron volts (keV) per micron of path (or eV/nm). A higher value of LET indicates more effective ionization of the absorber.
monomer	A simple molecule that is a repeating structural unit within a polymer. It is capable of combining with a number of like or unlike molecules to form a polymer.
neutron	An uncharged elementary particle present in the nucleus of every atom heavier than hydrogen; neutrons are released during fission.
nitration	Introduction of an NO_3^- group into an organic compound.
olefin	An alkene.
organic acid	A chemical compound with one or more carboxyl radicals (-COOH) in its structure.
outgas	The release of adsorbed or occluded gases or water vapor, usually as the result of heating or differences in vapor pressure.
oxidation	A chemical reaction in which a compound or radical loses electrons.

paraffin   An alkane.

permeation   The movement of atoms, molecules, or ions into or through a
                        porous or permeable substance (such as a membrane).

pi orbital   A region in a molecule, formed by the overlap of atomic orbitals,
                        in which there is a high probability of finding a "p" or "d" electron;
                        two atomic p or d orbitals overlapping at right angles to the axis
                        between the atoms' nuclei form a pi orbital with electron regions
                        above and below the axis.

polyamide   The product of polymerization of an amino acid or the
                        condensation of a polyamine with a polycarboxylic acid.

polymer   Any of a class of organic compounds characterized by repeating
                        structural units (monomers).

polymerization   The process of bonding two or more monomers to produce a
                        polymer.

rad   The traditional unit of absorbed radiation dose representing the
                        absorption by a specified material of 100 ergs per gram of that
                        material; 1 rad = 1.0E-2 Gray; 1 rad = 6.24E13 eV/g.

radiation   The emission and propagation of energy through matter or space;
                        also, the energy so propagated; the term has been extended to
                        particles, as well as electromagnetic radiation.

radical   A molecular fragment having one or more unpaired electrons (e.g.,
                        $^-$H or $^-$CH$_3$). It may be charged or uncharged.

radical scavenger   A substance that readily combines with a radical.

radiolysis   Alteration of materials caused by irradiation.

range   The distance a given ionizing particle can penetrate into a given
                        material before its energy drops to the point that the particle no
                        longer ionizes the material.

repeat unit   See "monomer."

resin   Any of a class of solid or semisolid organic products of natural or
                        synthetic origin with no definite melting point, generally of high
                        molecular weight; most resins are polymers.

saturated hydrocarbon   A carbon-hydrogen compound containing no double or triple bonds.

saturated vapor pressure   The vapor pressure of a substance at its boiling point.

scission   The process by which chemical bonds are broken; also, the number of bonds broken by the process. Usually refers to breaks in the backbone of a polymer macromolecule.

spur   A small group of excited and ionized species associated with the track caused by passage of ionizing radiation. Consists of the molecules ionized directly, radicals, and secondary ionizations produced by electrons released in the primary ionization. A spur usually forms a side track from the path of the particle or ray.

steric hindrance   The prevention or retardation of chemical reaction caused by geometrical restrictions of neighboring groups on the same molecule.

synergistic effect   The effect on a material of two or more stresses applied simultaneously that is greater in magnitude than that resulting from the same stresses applied separately.

track   The path of gamma rays, x-rays, or charged particles through matter.

TRU nuclide   A nuclide with an atomic number greater than that of uranium (92). All transuranic nuclides are produced artificially and are radioactive.

TRU waste   Waste materials contaminated with alpha-emitting TRU nuclides with half-lives >20 years, in concentration >100 nCi/g of waste at the time of assay.

unsaturated hydrocarbon   One of a class of hydrocarbons that have at least one double or triple carbon-carbon bond. Such compounds are different from aromatic hydrocarbons.

vapor   A gas that exists at a temperature below the critical temperature and that can be liquefied by compression without lowering its temperature.

viscous   Having relatively high resistance to flow.

x-rays   Penetrating electromagnetic radiation, usually generated by decelerating high-velocity electrons through collision with a solid body or by inner-shell electron transitions for atoms with atomic number greater than 10.

Acronyms and Abbreviations

CH-TRU (wastes)	contact-handled transuranic wastes
e	accelerated electrons
E_a	activation energy
EPRI	Electric Power Research Institute
F	fraction of energy absorbed
FDA	Food and Drug Administration
HC	hydrocarbon
HDPE	high-density polyethylene
INEEL	Idaho National Engineering and Environmental Laboratory
LANL	Los Alamos National Laboratory
LDPE	low-density polyethylene
LET	linear energy transfer
ORNL	Oak Ridge National Laboratory
PET	polyethylene terephthalate
PMMA	polymethyl methacrylate
PTFE	polytetrafluoroethylene (Teflon)
PVC	polyvinyl chloride
RFETS	Rocky Flats Environmental Technology Site
SAR	Safety Analysis Report
SRS	Savannah River Site

Chemical Notation

$CaCl_2$	calcium chloride
CaO	calcium oxide
Ca	calcium
$C\text{-}C$	carbon-carbon bond
$C\text{-}Cl$	carbon-chlorine bond
CCl_3F	trichlorofluoromethane
CCl_4	carbon tetrachloride
$C\text{-}F$	carbon-fluorine bond
CF_4	carbon tetrafluoride
C_4H_8	butene
C_4H_{10}	butane
$C\text{-}H$	carbon-hydrogen bond
$CHCl_3$	chloroform
CH_3	methyl group
CH_4	methane
Cl_2	chlorine
$Cm\text{-}244$	curium isotope with atomic mass of 244
CO	carbon monoxide
CO_2	carbon dioxide
C_3H_6	cyclopropane or propylene
C_3H_8	propane
C_2H_2	acetylene (or ethyne)
C_2H_4	ethylene (or ethene)
C_2H_6	ethane
Fe_2O_3	iron (III) oxide (ferric oxide)
HCl	hydrogen chloride
He^{++}	doubly charged helium ion. An alpha particle.
H_2	Hydrogen
KCl	potassium chloride
$MgCl_2$	magnesium chloride
MgO	magnesium oxide
$NaCl$	sodium chloride
Na_2O	sodium oxide
OH	hydroxyl group
O_2	oxygen
Po	polonium
$Pu\text{-}238$	plutonium isotope with atomic mass of 238
$Pu\text{-}239$	plutonium isotope with atomic mass of 239
$Pu(NO_3)_x$	plutonium nitrate
PuO_2	plutonium dioxide
R, R'	any alkyl or aromatic group
SiO_2	silicon dioxide
SO_2	sulfur dioxide
Z	atomic number
Zn	zinc

G Value Notation

Notation   Interpretation - G Value for

$G(C_2)$ all hydrocarbons with two carbon atoms
$G(C_3)$ all hydrocarbons with three carbon atoms
$G(C_4)$ all hydrocarbons with four carbon atoms
$G(CH_4)$ methane
$G(C_2H_6)$ ethane
$G(H_2)$ hydrogen
$G(S)$ scission
$G(gas)$ all gas generated
$G(water\ vapor)$ water vapor
$G(X)$ crosslinking

Executive Summary

This document presents radiolytic G values for solids, liquids, vapors, and gases obtained from the technical literature. Experimental data are evaluated, and applicable maximum G values are determined for use in calculations of flammable gas concentration and total pressure for transport of contact-handled transuranic (CH-TRU) wastes. G values for organic solids are related to G values for structurally-related liquids. It is demonstrated that G values (for hydrogen and other flammable gases) for organic materials can be ranked according to the functional groups that determine most other chemical properties. This relationship allows G values for other organic solids to be estimated. Maximum G values obtained from laboratory-scale experiments are compared to effective G values measured for actual drums of CH-TRU wastes. For materials that are commonly present in the CH-TRU wastes, polyethylene has the highest value of $G(H_2)$ of 4.0. The maximum $G(H_2)$ value for water is 1.6.

This document is not meant to be a comprehensive summary of all radiolysis experiments that have measured gas generation. Instead, the literature has been searched for typical and upper bound G values, and for general characteristics that allow extrapolation to other materials for which no radiolysis experiments have been reported. Where possible, data obtained by various authors are discussed and compared. When authors disagree, an effort has been made to determine which data are valid and the reasons for the differences.

Factors affecting gas generation from the reactions of alpha, beta, neutron, or gamma radiation with matter are discussed. These factors include the linear energy transfer (LET) and range of the incident radiation; irradiation environment, including temperature, pressure, and gases present; absorbed dose and dose rate; specific composition of the material; and particle size and distribution of radioactive contaminants.

The controlling factor in the behavior of materials under irradiation, as under most other environmental influences, is the chemical structure. Chemical bonds are not broken randomly even though the excitation energy may exceed the bond dissociation energy. Energy may be transferred from the location on a molecule where it is absorbed to another chemical bond that is broken. Additives to improve physical or aging properties may affect changes produced by radiation.

For this reason, radiolysis can be discussed in terms of functional groups as can other chemical reactions. The functional group is the atom or group of atoms that defines the structure of a particular family of organic compounds, and, at the same time, determines their properties. A particular set of properties can be associated with a particular group wherever it is found.

G values for a given material may depend on the type of radiation absorbed by the material (LET effect). For several liquids, such as cyclohexane, benzene, water, and acetone, alpha radiolysis experiments yield higher G values than gamma radiolysis experiments. Similar effects may also occur in solids, such as polymers, but very few experiments have been conducted to determine LET effects in gas generation in solids. This is possibly due to the difficulty in measuring the absorbed dose in alpha radiolysis, where self-absorption of some of the alpha radiation emitted from particulate contamination occurs. G values measured using nonalpha radiation are the best

data available for many materials. These data are included in establishing maximum G values in a best faith effort to establish upper bound gas generation calculations for CH-TRU wastes.

Liquids that have G values for flammable gas greater than 4.0 are saturated hydrocarbons, alcohols, ethers, ketones, and organic acids. Liquids that have G values for flammable gases less than 4.0 include unsaturated hydrocarbons, aromatic hydrocarbons, water, esters, halogenated hydrocarbons, aromatic halides, and commercial lubricant oils. G values for liquid organic nitrogen compounds are low for those having aromatic characteristics or C-N triple bonds.

Common plastics and papers are composed of one or more base polymers and additives designed to increase flexibility, stability, or other properties. Organic functional groups found in common polymers include saturated C-C bonds, unsaturated C-C bonds, and alcohol, ether, and ester groups. Aromatic characteristics (resonant structures containing carbon and hydrogen or carbon and nitrogen atoms) greatly increase the stability of many polymers, and are commonly found in additives.

Saturated hydrocarbons produce hydrogen as the principal radiolysis gas. Small amounts of other hydrocarbons are formed. The maximum $G(H_2)$ value is 4.0 for polyethylene.

Polymers having ether functional groups generate gases that contain oxygen, even when irradiated in a vacuum. G values for cellulose and urea formaldehyde have been shown to be strongly dependent on the absorbed dose. For absorbed doses greater than 10 Mrad, the maximum value of $G(H_2)$ is 3.2 for cellulose. One of the polymers in this family (polyoxymethylene) generates other flammable gases that cause the G(flam gas) value to exceed 4.1, and another (polyvinyl formal) has a measured G(gas) that is 1.4 times the G(gas) value for polyethylene. For this reason, polyoxymethylene and polyvinyl formal are permitted in CH-TRU wastes only in trace amounts.

Polymers containing chlorine are stabilized to reduce the catalytic effect of HCl generated by radiolysis or thermal degradation. The strong effect of the plasticizers and stabilizers on the radiolysis of PVC is demonstrated by the differences in the composition of the radiolysis gas, which vary from 85% H_2 to 83% HCl to 70% CO_2, depending on the specific polymer formulation and whether oxygen is present.

Radiolysis of adsorbed or absorbed liquids indicates that the sorbing medium can either be inert to radiation or can transfer energy to the sorbed liquid. Unless experimental data demonstrate that the binding medium is radiolytically inert (e.g., vermiculite), all of the radiation energy should be assumed to interact with the sorbed liquid. Nitrates present in solidified aqueous wastes significantly reduce $G(H_2)$ from the value for water, while increasing $G(O_2)$.

Very low G values have been observed from irradiation of water present as the hydrate in crystals. Water in the hydrates appears to exhibit the property of an "energy sink."

Gas generation experiments conducted on actual CH-TRU wastes are summarized. Typically, several different contaminated materials were present inside a given waste container. The results

are presented in terms of effective G values that include the effects of the different materials and self-absorption of some alpha decay energy by particulate contamination.

On the whole, the effective hydrogen G values for actual CH-TRU wastes are much lower than the maximum hydrogen G values for the waste forms that would be estimated based on the worst-case material. For drums of combustible wastes, the maximum $G(H_2)$ value determined in controlled experiments was 2.1 versus a possible value of 4.0 based on laboratory experiments. For drums of sludge, the maximum $G(H_2)$ value measured was 0.3 versus a possible value of 1.6 based on laboratory experiments. No explanation currently exists for high $G(H_2)$ values calculated from experiments conducted on solidified organic waste forms.

Gas pressure and composition data for retrieved drums of stored wastes are also discussed. Calculated G values for sealed retrieved drums provide only lower limits, because of uncertainties in the rates at which gases can permeate through the drum gaskets or diffuse through gaps between the gasket and the sealing surfaces. Typically, only the drum head space was sampled, and the concentrations of generated gases could have been higher inside the rigid liner and waste bags. Most of the lower limit G values were very low.

This page intentionally left blank

3.1   Radiolytic G Values for Waste Materials

3.1.1   Introduction

The purpose of this document is to establish maximum G values from the technical literature for production of gas (particularly hydrogen) from the radiolysis of materials in contact-handled transuranic (CH-TRU) wastes. These maximum G values are used in calculations of flammable gas concentrations and total pressure in safety analyses for transport of the wastes. In Section 3.1, the maximum G values obtained from laboratory-scale experiments are compared to G values calculated from gas generation experiments conducted on drums of actual CH-TRU wastes. The maximum G values typically are much larger than those obtained from actual wastes.

This document reports radiolysis data (including temperature dependence) for many types of materials, including the chemical families of organic compounds that are liquids (e.g., alcohols, aldehydes, and ketones); organic solvents; water; polymers; and commercial plastics, cellulosics, and rubbers. Inorganic materials and commercial plastics, cellulosics, and rubbers are the major constituents in CH-TRU wastes and packaging materials. Liquids may be major constituents (> 10 wt%) of solidified liquid wastes or minor or trace (< 1 wt%) constituents when they are absorbed on paper tissues or used as plasticizers in plastics and rubbers. For solid materials for which the G values are unknown, related organic solids or liquids are used to estimate bounding values. In order to provide a thorough discussion of this subject, G values are reported for some materials that are not known to be present in the CH-TRU wastes.

This document is not meant to be a comprehensive summary of all radiolysis experiments that have measured gas generation. Instead, the literature has been searched for typical and upper bound G values, and for general characteristics that allow extrapolation to other materials for which no radiolysis experiments have been reported. Where possible, data obtained by various authors are discussed and compared. When authors disagree, an effort has been made to determine which data are valid and the reasons for the differences. For example, discrepant data in the case of PVC appear to be largely caused by variations in material composition and not by experimental error.

Radiolysis data used in this report result from irradiation of materials by gamma, alpha, or other particles; accelerated electrons; or x-rays. For the CH-TRU wastes, alpha irradiation is the only signficant contributor to gas generation. Chemists and materials scientists for many years have used gamma radiolysis as a tool to explore the stability of materials. As a result, many more materials have been studied by gamma than by alpha radiolysis. Many alpha radiolysis experiments were performed during the 1970s at the Los Alamos National Laboratory (LANL), the Savannah River Site (SRS), and the Rocky Flats Environmental Technology Site (RFETS) to measure radiolytic gas generation from common materials that appear in CH-TRU wastes [see Molecke (1979[1]) and Blauvelt (1986[2]) for discussions of these experiments]. Some of these data have been reanalyzed in this report, and different conclusions are now drawn from these data.

---

[1] Molecke 1979. M. A. Molecke, "Gas Generation from Transuranic Waste Degradation: Data Summary and Interpretation," Sandia National Laboratories, SAND79-1245, December 1979.

[2] Blauvelt 1986. R. K. Blauvelt and R. J. Janowiecki, "General Strategy for Evaluating the Radiolytic Gas Generation Potential in Newly-Generated CH-TRU Waste," Monsanto Research Corporation, Mound Laboratory, MLM-MU-86-61-0013, January 1986.

G values for a given material may depend on the type of radiation absorbed by the material (known as an LET effect). For several liquids, such as cyclohexane, benzene, water, and acetone, alpha radiolysis experiments yield higher G values than gamma radiolysis experiments. Similar effects may also occur in solids, such as polymers, but very few experiments have been conducted to determine LET effects in gas generation in solids. This is possibly due to the difficulty in measuring the absorbed dose in alpha radiolysis, where self-absorption of some of the alpha radiation emitted from particulate contamination occurs. G values measured using nonalpha radiation are the best data available for many materials. These data are included in establishing maximum G values in a best-faith effort to establish upper bound gas generation calculations for CH-TRU wastes.

Section 3.1.2 of this document introduces basic concepts of radiation chemistry and factors that affect radiolytic gas generation or consumption. This forms the basis for discussions of the experimental data on radiolysis of liquids and vapors in Section 3.1.3, the radiolysis of polymers in Section 3.1.4, and the radiolysis of non-polymer solids in Section 3.1.5. Section 3.1.6 compares the laboratory G values measured for specific materials with rates of gas generation measured for actual drums of CH-TRU wastes. Attachment A describes the families of organic liquids and polymers, and shows the structures of many common polymers. Attachment B calculates the fraction of alpha decay energy escaping from a particle of PuO_2 as a function of particle radius. A glossary is provided that includes acronyms, abbreviations, chemical notation, and G value notation.

Major reviews of the radiation chemistry literature, such as An Introduction to Radiation Chemistry by J.W.T. Spinks; The Radiation Chemistry of Macromolecules edited by M. Dole; and Radiation Effects on Organic Materials edited by R.O. Bolt and J.G. Carroll, have been used extensively. When these references are cited, the original reports were not reviewed by this author.

3.1.2 Radiation Chemistry

Radiation chemistry is the study of the chemical effects produced in a system by the absorption of ionizing radiation. Included in this definition are the chemical effects produced by radiation (alpha and beta particles and gamma rays) and by electromagnetic radiation of short wavelength (x-rays). Photochemistry, on the other hand, deals with reactions of excited species unaccompanied by ionization.

This chapter discusses the factors affecting gas generation from the reactions of alpha, beta, gamma, or neutron radiation with matter. These factors include linear energy transfer (LET) and range of the incident radiation; irradiation environment including temperature, pressure, and atmosphere present; absorbed dose and dose rate; specific composition of the irradiated material; and particle size and distribution of radioactive contaminants.

3.1.2.1 Reactions of Radiation with Matter

The discussion that follows is based primarily on Spinks (1976[3]).

Absorption of energy from ionizing radiation results in the formation of tracks of excited and ionized species in matter. The incident radiation is not selective and may react with electrons of any atom or molecule lying along its track. Free radicals are produced by the dissociation of excited molecules and by ion reactions in or near the tracks of ionizing particles. Free radicals have one or more unpaired electrons available to form chemical bonds, but free radicals are generally uncharged. These free radicals are often more important in the chemical reactions that follow than are the primary species. Back reactions can combine two radicals to form a stable molecule. Radicals that do not undergo radical-radical reactions in the tracks diffuse into the bulk of the material and generally react there. Some of the more reactive radicals are H^+, ^-OH, Cl^+, and $^-CH_3$. Stable radicals include NO, NO_2, and O_2. Nitric oxide and nitrogen dioxide both have a single unpaired electron. Oxygen has a triplet ground state and behaves in radical reactions as a diradical.[3] Oxygen readily reacts with other free radicals and, if it is present, will almost invariably affect the radiation-induced reactions. Free radicals can also be produced by other processes, such as thermal degradation.

The species produced by ionizing radiation will, in general, be the same in a particular material regardless of the type or energy of the ionizing radiation. All ionizing radiation will, therefore, give rise to qualitatively similar chemical effects. With respect to gas generation, different types of ionizing radiation will generally produce the same gas species, though possibly in different amounts.

Alpha particles consist of two protons and two neutrons and, therefore, are the same as the nuclei of helium atoms and have a double positive charge. On passing through matter, alpha particles lose energy principally by inelastic collisions with electrons lying in their paths, leading to excitation and ionization (if the energy transmitted is high enough) of the atoms and molecules to which those electrons belong. Electrons liberated in the process also interact with other atoms and molecules of the material. An alpha particle loses only a small fraction of its energy per collision. As a consequence, alpha particles slow down gradually as the result of a large number of small energy losses and travel in a nearly straight path. The energy of an alpha particle decreases as the distance traveled increases. Because each of the alpha particles from a given radionuclide has the same initial energy, each will have about the same range in a given material. Alpha particles can also be produced in situ in a material by combining it with a compound of boron or lithium and irradiating the mixture with slow neutrons. Some radiolysis experiments have used this technique for producing alpha particles.

Beta particles are fast electrons emitted by radioactive nuclei. In contrast to alpha particles, the beta particles from a particular radioactive element are not all emitted with the same energy.[3] Instead, the energies range from zero up to a maximum value that is characteristic of the element. On passing through matter, beta particles lose energy predominantly through inelastic collisions

---

[3] Spinks 1976. J. W. T. Spinks and R. J. Woods, <u>An Introduction to Radiation Chemistry</u>, John Wiley & Sons, New York, 1976.

with electrons, in a similar manner to alpha particles. However, because the beta particle and the electron with which it collides have the same mass, the beta particle can lose up to half of its energy in a single collision and may be deflected through a large angle. As a result, even beta particles that start with the same energy may come to rest at widely separated points.

Gamma rays are electromagnetic radiation with wavelengths in the region of 3E-9 to 3E-11 cm. The gamma rays emitted by radionuclides are monoenergetic, but each decay may be to one of a small number of discrete energies. Low-energy gamma rays tend to lose most of their energy through a single interaction with an electron (the photoelectric effect). The entire energy is transferred to a single electron, which is then ejected from the atom. Photoelectric interactions are most probable for high-atomic-number materials and for low gamma energies. A fraction of the incident gamma rays is completely absorbed by the material, but the remainder are transmitted through the material with up to their full initial energy. For example, the number of low-energy-gamma photons transmitted through a sheet of absorbing material decreases exponentially as the thickness of the absorber increases.

For low-atomic-number materials and for gamma energies between 1 and 5 MeV in high-atomic-number materials, the Compton effect predominates. In the Compton effect, a gamma ray interacts with an electron, which may be loosely bound or free, so that the electron is accelerated and the gamma ray deflected with reduced energy. For example, Compton interactions in water predominate for gamma rays with energy from about 30 keV to 20 MeV.

Neutrons are uncharged nuclear particles with a mass of one mass unit (Spinks 1976[3]). Because they are uncharged, neutrons do not produce ionization directly in matter. However, the products of neutron interactions can produce ionization and give rise to radiation-induced chemical changes. The main ionizing species are protons or heavier positive ions, and the chemical effects of neutron irradiation are similar to those produced by beams of these positively charged particles.

3.1.2.2 Energy Transfer

Sometimes energy absorbed at one location on a large molecule appears to damage a more susceptible site elsewhere on the molecule. Thus, one type of bond may be broken more frequently than would be calculated from the statistical distribution of electrons.[4] Another way of looking at this phenomenon is to compare the likelihood of a recombination reaction when a given kind of bond is broken. For example, by comparing the C-C and C-H bond energies in hydrocarbon polymers, one would think that cleavage of the main polymer chain is more probable than the splitting off of the hydrogen atoms. However, during irradiation of most polymers, processes caused by the cleavage of the C-H bonds predominate. A model used to explain this apparent contradiction is that simultaneous cleavages of the C-C and C-H bonds occur. In the case of polymers that primarily crosslink, a considerable fraction of the broken C-C

---

[4] O'Donnell 1970. J. H. O'Donnell and D. F. Sangster, Principles of Radiation Chemistry, American Elsevier Publishing Company, Inc., New York, 1970.

bonds recombine, and as a result, the C-H bond cleavage processes predominate. In degradable polymers, a rapid recombination of the split ends of the chain is sterically hindered[5].

The concept of energy transfer from the location on a molecule where energy is absorbed to the chemical bond that is broken is a key concept for understanding the effects of radiolysis. The major products of radiolysis are influenced by molecular structure[6]. Chemical bonds are not broken randomly even though the excitation energy may exceed the bond dissociation energy.

For this reason, radiolysis can be discussed in terms of functional groups as can other chemical reactions. The functional group is the atom or group of atoms that defines the structure of a particular family of organic compounds, and, at the same time, determines their properties[7]. A particular set of properties can be associated with a particular group wherever it is found. Functional groups in macromolecules also determine their chemical reactions. Sections 3.1.3 and 3.1.4 contain more detailed discussions of the functional groups.

Certain structures, such as aromatic rings (e.g., a benzene ring), seem to absorb ionizing energy and dissipate it as heat in the form of molecular vibrations. In this way, systems containing these structures undergo less decomposition than would be expected.[4]

When a homogeneous mixture of two compounds is irradiated, the yields of the different products often are generally directly proportional to the yields from the pure components and their relative proportions (by electron density) in the mixture. This behavior is found when each component degrades independently of another. However, some components of a mixture may transfer absorbed energy to other components. In a two-component mixture, the second component may be decomposed more readily, and the result is a higher product yield. On the other hand, if the second component is less readily decomposed, as with an aromatic compound, there may be correspondingly less decomposition and a lower product yield.[4]

During gamma irradiation of polymers filled with finely dispersed metals, the absorbed energy can distribute itself nonuniformly between the two components of the system. In rubbers containing heavy metals ($Z \geq 40$) in a free state or in the form of chemical compounds, the rate of radiation cross-linking has been observed to double. The energy absorbed by the polymeric component increases because of secondary electrons generated by gamma interactions with the metal.[5] This effect is not expected to be significant for surface alpha irradiation of leaded rubber gloves because the lead is dispersed throughout the rubber material.

---

[5] Makhlis 1975. F. A. Makhlis, Radiation Physics and Chemistry of Polymers, John Wiley & Sons, New York, 1975, translated from the Russian.

[6] Hall 1963. K. L. Hall, et al., "Radiation Chemistry of Pure Compounds," in Radiation Effects on Organic Materials, Academic Press, New York, 1963, eds. R. O. Bolt and J. G. Carroll.

[7] Morrison 1973. R. T. Morrison and R. N. Boyd, Organic Chemistry, Allyn and Bacon, Inc., Boston, 1973, 3rd edition.

3.1.2.3 Factors Affecting the Rate of Radiolytic Gas Generation
(or Consumption) from a Material

The rate of radiolytic gas generation (or consumption) from a material depends on: (1) the
G value for gas production (or consumption) for the given material and type of radiation, (2) the
energy emitted from radioactive decay, and (3) the fraction of emitted energy absorbed by the
material (F). G values also appear in the radiation chemistry literature for other products, such as
the number of crosslinks or scissions, or the production of a non-gas substance. A G value may
be positive (as in the generation of hydrogen or carbon dioxide) or negative (as in the depletion
of oxygen). F depends on the nature of the emitted energy and the materials being irradiated. In
the case of short-range radiation. F also will depend on the spatial distribution of radioactivity,
especially when several different materials are present, such as in wastes.

The rate of radiolytic gas generation (n) in moles per second from a material is given by:

$$n = W \times \Sigma_i(F_i \times G_i) \times C$$

where

$\quad$ W $\;=\;$ total decay heat (watts),

$\quad$ F_i $\;=\;$ fraction of energy emitted that is of radiation type i and is absorbed by the material
$\qquad\quad$ (range 0 to 1),

$\quad$ G_i $\;=\;$ number of molecules of gas produced (or consumed) per 100 eV of energy absorbed
$\qquad\quad$ from radiation type i, and

$\quad$ C $\;=\;$ conversion constant

$\qquad\;=\;$ (1 joule/W-sec) x (1E7 erg/joule) x (1 eV/1.6E-12 erg)
$\qquad\qquad\qquad$ x (1 g-mole/6.02E23 molecules)

$\qquad\;=\;$ 1.04E-5 (g-mole)(eV)/(molecule)(W-s)

$\qquad\;=\;$ 1.04E-7 (g-mole)(100 eV)/(molecule)(W-s).

3.1.2.3.1 Factors Affecting the G Value

A number of factors influence the G value measured in an experiment. They include LET of the
radiation, temperature, pressure, atmosphere in which irradiation occurs, total absorbed dose, and
specific composition of the material.

3.1.2.3.1.1   <u>Linear Energy Transfer (LET) Effect</u>

Differences in G values for a material when irradiated by different types of radiation are ascribed
to differences in the ways in which energy is lost in matter. Linear energy transfer (LET) is the
linear rate of energy loss by an ionizing particle traveling through a material. An average LET

value is calculated by dividing the initial energy of a particle by its range in the material. Expressions that reflect the changing density of active species in particle tracks, such as specific ionization and LET, are useful in evaluating the overall chemical effect. Track effects of this sort have been thought to be more important in the case of liquids or solids, where the active species are hindered from moving apart by the proximity of other molecules, than in gases, where species can move apart with relative ease. In gases, the different types of radiation do not give the different yields of products that may be found in liquids or solids.

The linear energy transfer from alpha particles to irradiated materials follows the Bragg curve, which rises sharply from low energies to reach a peak at about 1 MeV, then falls off gradually at higher alpha particle energies. This behavior leads to an "end of track" effect, with higher LET than at the beginning of the track.[8] Table 3.1-1 lists average LET values for irradiation of water.

Radiation-chemistry studies on LET effects in low-molecular-weight compounds have shown that the molecular product yields increase with increasing LET. Molecular products are generated in the spurs, before the reactive species can diffuse into the bulk of the system.[9] The result is that $G(H_2)$ appears to increase with increasing LET, at least in liquids such as benzene, acetone, cyclohexane, and water (see Section 3.1.3 for details). These effects could also occur in solids. Unfortunately, similar experiments have not been uncovered in the radiation chemistry literature that measure G values of a solid material using different LET radiation at the same absorbed dose.

A characteristic feature of radiation with high LET is the sharp decrease in the effectiveness of protective additives (such as antioxidants) in the material being irradiated, particularly those that react with free radicals. The reason for this is the intense reactions of the radicals in the track.[5]

Table 3.1-1 — Average Values of LET in Water Irradiated with Various Types of Radiation

Radiation	Average LET (eV/nm)
Co-60 γ-rays	0.2
2-MeV electrons	0.2
200-kV x-rays	1.7
H-3 ß-rays	4.7
50-kV x-rays	6.3
10 MeV H-1	8.3
10 MeV He-4	92
5.3 MeV α-particles (Po-210)	136
3 MeV He-4	180
65.7-MeV N-14 ions	553

Refs.:   Spinks 1976[3], Chapter 2 and Table 8.19.

---

[8] Cember 1978. H. Cember, Introduction to Health Physics, Pergamon Press, New York, 1978.

[9] Schnabel 1981. W. Schnabel, Polymer Degradation--Principles and Practical Applications, Macmillan Publishing Company, Inc., New York, 1981.

3.1.2.3.1.2   **Temperature**

Chemical reaction rates depend on temperature. The rate (k) of a chemical reaction can be expressed by: $k = A \exp(-B/T)$ where T is the absolute temperature, and A and B are constants. The equation can be written in the form $k = A \exp(-E_a/RT)$, generally known as the Arrhenius law. E_a is an activation energy, which will have different values for different chemical reactions. This law holds for elementary reactions but does not necessarily hold for successive reactions that may have different E_as.[3] Also, the E_a can change when the reactions change, as at the melting point for crystalline materials.

In an Arrhenius plot, the log of the reaction rate versus the reciprocal temperature (degrees Kelvin), ln k vs. 1/T, has a slope equal to $-E_a/R$. Arrhenius plots of G values versus 1/T for several materials are shown in Chapiro 1962[10] and Jellinek 1978[11].

The activation energy (E_a) for G values for gas generation from most materials appears to be less than or equal to 3 kcal/g-mole, giving a weak temperature dependence compared to many other chemical reactions. E_a for PVC is about 3 kcal/g-mole, and E_a for polyethylene is about 0.8 kcal/g-mole (see Section 3.1.3.1.4). Alpha radiolysis data for cellulosics are consistent with an E_a of 1-2 kcal/g-mole [12,13] (see Section 3.1.3.1.4). The temperature dependence of $G(H_2)$ in liquid n-hexane and neopentane corresponds to an activation energy of about 3 kcal/g-mole.[14]

The relationship between the rate constants k_2 and k_1 at two different temperatures T_2 and T_1 is given by:

$$\ln (k_2/k_1) = (E_a/R)[(T_2-T_1)/(T_2 \times T_1)]$$

where R = ideal gas constant (1.99 cal/g-mole-K) and temperatures are in degrees Kelvin. For example, if the activation energy for gas produced by a material is equal to 1 kcal/g-mole, then the ratio of the G(gas) value at 55°C to the G(gas) value at 25°C would be:

$$G(55\ °C)/G(25\ °C) \ = \ \exp \{(1E3/1.99)[(328\ K - 298\ K)/(328\ K \times 298\ K)]\}$$

$$= \ \exp \{(5.03E2)[30/(328)(298)]\}$$

---

[10] Chapiro 1962. A. Chapiro, <u>Radiation Chemistry of Polymeric Systems</u>, Interscience Publishers, New York, 1962.

[11] Jellinek 1978. H. H. G. Jellinek, <u>Aspects of Degradation and Stabilization of Polymers</u>, Elsevier Scientific Publishing Company, New York, 1978.

[12] Kosiewicz 1981. S. T. Kosiewicz, "Gas Generation from Organic Transuranic Wastes. I. Alpha Radiolysis at Atmospheric Pressure," <u>Nuclear Technology 54</u>, pp. 92-99, 1981.

[13] Zerwekh 1979. A. Zerwekh, "Gas Generation from Radiolytic Attack of TRU-Contaminated Hydrogeneous Waste," Los Alamos National Laboratory, LA-7674-MS, June 1979.

[14] Bolt 1963. R. O. Bolt and J. G. Carroll, <u>Radiation Effects on Organic Materials</u>, Academic Press, New York, 1963.

$$= \exp(0.154)$$

$$= 1.17.$$

At -29 °C, the ratio $G(-29\,°C)/G(25\,°C)$ would be 0.69 for $E_a = 1$ kcal/g-mole. An activation energy of $E_a = 3$ kcal/g-mole, considered as the maximum value of E_a for materials present in the CH-TRU wastes, results in the following:

$$G(55\,°C)/G(25\,°C) \;=\; \exp(3 \times 0.154) = \exp(0.462)$$

$$= 1.59.$$

For most polymers then, the radiolytic gas generation rate at 55°C should be no greater than approximately 1.6 times the gas generation rate at room temperature (25°C).

Rates and product yields from radiation-induced chemical reactions in many polymers are influenced by molecular mobility.[9, 15] This explains why increases in temperature, leading to phase transitions or allowing specific intramolecular motions (such as rotations of side groups), frequently influence the G values. Increasing the temperature generally reduces the probability of radical recombinations[9] and increases the diffusion rates of gas molecules, such as H_2.

For polymers containing crystalline areas, the molecular mobility increases drastically above the crystalline melting temperature, with consequent changes radiation chemical yields.[11] For example, an abrupt increase in the activation energy occurs for both G(X) (crosslinking between polymer molecules) and G(S) (scission - breaking of the polymer molecule backbone) near the melting temperature. Large changes in the ratio G(X)/G(S) are often observed at higher temperatures, which suggests changes in reaction mechanisms. For example, a ten-fold increase in G(S) is observed in radiolysis of polystyrene when the temperature is increased from 30 to 150°C.[15]

There is no general correlation between thermal stability and radiation resistance. For instance, irradiated polytetrafluoroethylene (Teflon[R]) readily undergoes main-chain scission while polysiloxanes are efficiently crosslinked, although both polymers are heat resistant.[9] At elevated temperatures, radiation may accelerate the usual thermal degradation reactions because thermal initiation characterized by a high activation energy (about 20 to 80 kcal/g-mole[16]) is replaced by radiation initiation, which has a much lower activation energy.[5] The threshold temperature for thermal degradation can be decreased significantly if the material is irradiated before (or during) heating.

---

[15] Jellinek 1983. H. H. G. Jellinek, ed., <u>Degradation and Stabilization of Polymers</u>, Vol. 1, Elsevier, New York, 1983.

[16] Madorsky 1964. S. L. Madorsky, <u>Thermal Degradation of Organic Polymers</u>, Interscience Publishers, John Wiley & Sons, New York, 1964.

3.1.2.3.1.3   **Pressure**

Pressure up to 50 psig may slightly lower G values as a result of back reactions. Experiments conducted in a vacuum measure more of the gas generated than do experiments conducted at ambient pressure, in which some of the gases can remain dissolved in thematerial being irradiated.

The decrease in segmental motions in polybutadiene with increasing pressure led to a corresponding decrease in G values for chain scission in polybutadiene[17] and an increase in G values for crosslinking.

3.1.2.3.1.4   **Atmosphere in Which Irradiation Occurs**

Measured total gas G values depend on the atmosphere in which the irradiation occurs, especially whether or not any oxygen is present. In most polymers, oxygen retards or completely eliminates formation of a cross-linked network. Even polymers that otherwise would crosslink will degrade in the presence of oxygen.[5] Radiation-induced oxidation initially consumes dissolved oxygen that has diffused into the material from the surrounding oxygen-containing atmosphere.[5] The efficiency of radiolytic oxidation of polymers under otherwise equal conditions depends on the dose rate and on other factors determining the rate at which oxygen can permeate the sample (e.g., oxygen pressure, sample thickness, oxygen solubility and ability to penetrate through the material, irradiation temperature, and polymer phase state).[5]

Organic solvents can change the net effect of radiolysis by permeating the material and reacting chemically. Reactions of trapped radicals may occur with chemically active molecules (such as oxygen or solvents) that have diffused into the sample after irradiation ceases.[5] These effects are most pronounced in materials that have been irradiated in the absence of oxygen. Intense degradation of polymers that have been pre-irradiated in the absence of oxygen has been observed when the polymers are exposed to oxygen.[5]

Most G values are measured in a vacuum, in air, or in pure oxygen. In the vacuum experiments, a larger amount of evolved gas may be measured because gas molecules will be pulled out of the materials rather than remain dissolved in the materials. A few experiments have been conducted in atmospheres different from air or pure oxygen, such as oxygen plus carbon tetrachloride, chloroform vapor, or nitrous oxide; or air saturated with water vapor. (The results of these experiments are discussed in later chapters.)

Various thermal, chemical, and radiolytic oxidation processes occurring in the CH-TRU waste materials, the packaging materials, and the waste containers themselves will react with the oxygen initally present inside the innermost waste bags. Eventually, these processes could deplete the oxygen inside the transport package cavity.

The gases that could be present inside the transport package include the following: (1) air; (2) nitrogen, argon, or helium used to inert the cavity; (3) nitrogen plus hydrogen and carbon

---

[17] Sasuga 1975. T. Sasuga and M. Takehisa, "Effect of High Pressure on Radiation-Induced Cross-Linking of Synthetic Rubbers," <u>J. Macromol, Sci.-Phys. B11</u>, pp. 389-401, 1975.

dioxide, with trace amounts of carbon monoxide, oxygen, and methane; (4) any of the above plus vapor from absorbed water or other liquids. These liquids may include various oils and solvents. For example, some of the solvents that could be present in the wastes include: 1,1,1-trichloroethane, carbon tetrachloride, 1,1,2-trichloro-1,2,2 trifluoroethane (Freon), methylene chloride, methanol, xylene, and butanol.

3.1.2.3.1.5 <u>Total Absorbed Dose</u>

As irradiation of a material proceeds, the end products of radiolysis (called primary products) may increase to such a concentration in the material that they are irradiated or react with some of the free radicals or other species to form secondary products. It follows that the G value (slope of the yield of a product versus dose curve) may decrease as the absorbed dose increases (assuming that the products are more stable under irradiation than the parent material), and the concentration of the product may ultimately reach a steady-state limit.[4] Many of the common plastics contain saturated carbon-carbon bonds. Radiolysis of these materials results in release of hydrogen and an increase in unsaturation. Unsaturated hydrocarbon liquids have much lower $G(H_2)$ values than do related saturated hydrocarbon liquids. Therefore, the degraded material in the plastics should be more stable than the parent material with respect to gas formation, leading to lower $G(H_2)$ values with absorbed dose. Eventually, all of the available hydrogen will have been released from the material. The decrease in G values with absorbed dose has also been called a "matrix-depletion" effect. To avoid this complication, G values are often expressed as initial G values or as the G values extrapolated to zero absorbed dose.

On the other hand, radiolysis of plastics where additives are used to acheive stabilty, such as PVC, could result in higher G values with increasing absorbed dose as the additives are consumed.

Absorbed dose effects can disappear at higher temperatures. For example, for irradiation of crystalline polyethylene at 25°C, the value of $G(H_2)$ decreased from about 3.7 to 3.2 as the absorbed dose increased from near zero to 15 Mrad (0.15 MGy).[18] For the same sample, irradiated at 120°C, virtually no change in $G(H_2)$ with increasing radiation dose was reported.

Several reports discuss absorbed dose effects for alpha radiolysis. For Cm-244 irradiation of paper tissue, Bibler observed a decrease in G(gas) from an initial value of 1.9 to about 0.8 after 17 days.[19] Zerwekh's data show decreases in G(gas) values by about 50% in 250 days of irradiation from Pu-238.[13]

For alpha irradiation, the absorbed dose for waste materials is applicable only to the mass of the waste reached by the alpha particles. The range of alpha particles in low density materials for $4 < E < 8$ MeV is given by (see Section 3.1.2.3.2.1):

---

[18] Mandelkern 1972. L. Mandelkern, "Radiation Chemistry of Linear Polyethylene," in <u>The Radiation Chemistry of Macromolecules</u>, Vol. I, Academic Press, New York, 1972, ed. M. Dole.

[19] Bibler 1976. N. E. Bibler, "Radiolytic Gas Production During Long-Term Storage of Nuclear Wastes," E. I. DuPont de Nemours and Company, Savannah River Laboratory, DP-MS-76-51, American Chemical Society Meeting (preprint), October 27-29, 1976.

Range(cm) = [1.24 x E(MeV) - 2.62] x [1.2E-3 g/cm^3/(density of material)].

The density of plastics and paper is approximately 1 g/cm^3. The range of a 5.14 MeV alpha particle (Pu-239 alpha) in plastics or paper would be 4.6E-3 cm, while the range of 5.59 MeV alpha particle (Pu-238 alpha) would be 5.2E-3 cm.

The alpha particle track is cylindrical, with 90% of the ions present within a diameter of 1E-2 microns. The remaining 10% are recoil electrons with sufficient energy to produce their own ionization(s). Such ions are present out to about 0.2 microns from the center of the track.[20]

The volume of material most affected by an alpha particle can, therefore, be approximated by a cylinder of diameter 0.01E^{-4} cm and length equal to the range of the alpha particle. For 5.59-MeV alpha particles, the estimated volume of irradiated material is 4.1E-15 cm^3. For 5.14-MeV alpha particles, the estimated volume of irradiated material is 3.6E-15 cm^3. The corresponding dose absorbed by that material from one alpha particle is given by:

$$Dose\,(rad) = \frac{Decay\,energy\,(eV) \times 1rad \big/ \big[6.24E13 \quad eV/g\big]}{Volume\,(cm^3) \times density\,(g/cm^3)}$$

Therefore, the dose absorbed by material irradiated by a Pu-238 or Pu-239 alpha particle is 22-23 Mrad. With time, the particle tracks will begin to overlap, and the dose absorbed by the material will increase. For a given particle size of PuO$_2$, for example, absorbed dose effects should be observed much more quickly during Pu-238 irradiation, which produces a factor of about 200 times the disintegrations per second of Pu-239 irradiation.

Several conclusions may be reached from this discussion:

(1)   The gas-generation rates from materials irradiated to absorbed doses much less than 22 Mrad are expected to be greater than expected for alpha radiolysis of these materials in CH-TRU wastes.

(2)   A particle of Pu-238 oxide will have an activity over 200 times the activity of the same size Pu-239 oxide particle. Absorbed dose effects should occur much sooner with Pu-238 contamination than with Pu-239 contamination.

(3)   G values measured using Pu-238 contamination should be extrapolated to initial G values before the results are applied to Pu-239 contamination to minimize the difference in absorbed dose effects.

---

[20] NAS 1976. National Academy of Sciences, "Health Effects of Alpha-Emitting Particles in the Respiratory Tract," EPA 520/4-76-013, October 1976.

3.1.2.3.1.6   Dose Rate

Some radicals are fairly stable and may build up to quite high concentrations. Under these conditions they may react with other radicals, rather than with the material being irradiated. If this occurs, the G values may exhibit a nonlinear dependence on the dose rate.   For example, a radiation-initiated chain reaction can result in a G value for products that is inversely proportional to the square root of the dose rate.[4] In a number of experiments, however, the G values for molecular gas products for specific materials were independent of dose rate for the ranges studied [e.g., Bibler 1976[19], Chapiro 1962[10] (p. 415)].

Some apparent dose rate effects are caused by an increase in the material's temperature. Since the major portion of the absorbed radiation energy is converted to heat, at high dose rates the rate of heat release to the environment can be insufficient, resulting in an increase in temperature. Many chemical reactions have activation energies in the range of 20-50 kcal/mole. Consequently, it is feasible that at high absorbed dose rates (i.e., at high localized material temperatures), reaction pathways different from those occurring at low dose rates may dominate.[9]

Gillen and co-workers have documented evidence of physical and chemical dose-rate effects in gamma radiolysis of polymers in oxygen-containing environments as part of their efforts to perform accelerated aging simulations. Much of this work is summarized in Bonzon (1986)[21].

Physical dose-rate effects appear to be a common occurrence for gamma radiation aging of polymeric materials. Evidence for dose-rate effects was observed for polyolefins and ethylene-propylene rubber, while no noticeable dose-rate effects were noted for a chloroprene rubber, silicone, and two chlorosulfonated polyethylene materials. The dose-rate effects ranged from insignificant to very large, depending on such factors as polymer type, aging conditions, sample geometry, and the degradation parameter being monitored. (Change in tensile elongation was commonly used in these studies to detect radiation damage.) More mechanical degradation was produced for a given total dose as the dose rate was lowered. Diffusion-limited oxidation processes were shown to be the cause of such effects. When the oxidation processes in a material use up dissolved oxygen faster than it can be replenished from the atmosphere surrounding the material (through diffusion), a heavily oxidized layer of material is formed near the sample surfaces, and oxygen depletion occurs in the sample interior. As the dose rate is reduced, oxidation of the sample increases due to the longer times available for the diffusion processes.

Oxidation-controlled dose-rate effects are less likely to occur for alpha irradiation of polymers from surface contamination. In order for the reactions to be dose-rate independent, oxygen must diffuse only to a depth equal to the range of the alpha particles. Physical dose-rate effects are minimized in gamma irradiation experiments by using thin films.[21]

---

[21] Bonzon 1986. L. L. Bonzon, et al., "Status Report on Equipment Qualification Issues -- Research and Resolution," Sandia National Laboratories, NUREG/CR-4301, SAND85-1309, November 1986.

Other chemical dose-rate effects were observed in the interactions between radiation and thermal degradation. Deterioration in polyethylene and polyvinyl chloride cable materials was found in the containment building of the Savannah River nuclear reactor.[22] The degradation in material properties was much higher than expected for the maximum dose [2 Mrad (0.02 MGy)] experienced by the cable materials at the relatively low operating temperature of 43°C. Experiments performed to model this behavior showed that the most severe mechanical degradation was found when irradiation occurred at elevated temperature. The observed degradation was much greater than the sum of the damage caused by separate exposure to radiation and to the elevated temperature. This effect was also attributed to an oxidation mechanism, in which peroxides initially formed by the radiation are then thermally decomposed.

Chemical dose-rate effects caused by synergistic behavior of radiation and elevated temperature would also occur for alpha irradiation when oxygen is present. The magnitude of these effects could be reduced by removing any remaining oxygen before the irradiated materials are heated.

3.1.2.3.1.7 <u>Specific Material Composition</u>

Many of the radiolysis experiments reported in the radiation chemistry literature were performed to examine the chemical reactions occurring in the pure material. However, commercial plastics differ from the pure polymers because they contain large fractions of various additives, such as stabilizers and plasticizers. These materials can significantly influence the amount and species of gases generated by thermal degradation and radiolysis. See Attachment A of this appendix and Section 3.1.4 for more detailed discussions.

3.1.2.3.1.8 <u>Extreme Upper Bound Estimate for Gas Generation G Values in Most Organic Liquids and Polymers</u>

For most materials, bond dissociation energies can be used to estimate an extreme upper bound to the number of gas molecules produced by radiolysis per unit energy absorbed. Dissociation energies of chemical bonds in common polymers range from about 65 kcal/g-mol (C-Cl) to 108 kcal/g-mol (C-F), with carbon-carbon bonds in the middle of the range (75-85 kcal/g-mol)[3]. The carbon-hydrogen bond dissociation energy is about 90-100 kcal/g-mole (3.9-4.4 eV/molecule).

Hydrogen is the major gaseous product from radiolysis of most organic liquids and polymers that contain hydrogen. In the simplest case, a hydrogen molecule conceptually could be formed by breaking two C-H bonds and recombining the two hydrogen atoms. If all the radiation energy went into breaking bonds, then the energy needed to form one hydrogen molecule is given by twice the bond dissociation energy, or 2 x (3.9-4.4 eV)/molecule. This required energy results in an extreme upper bound G value estimated to be about 12 molecules generated per 100 eV of energy absorbed. This is an extreme upper bound because it ignores the H atoms that recombine with the parent molecule and the energy that is dissipated as heat.

---

[22] Gillen 1982. K. T. Gillen, R. L. Clough, and L. H. Jones, "Investigation of Cable Deterioration in the Containment Building of the Savannah River Nuclear Reactor," NUREG CR-2877, SAND81-2613, August 1982.

Most measured G values lie between 0.1 and 10.[4] Higher G values usually indicate a chain reaction has occurred. For example, the radiolysis products may chemically degrade the parent material, as occurs from HCl generated in pure PVC.

3.1.2.3.2 Factors Affecting the Fraction of Energy Absorbed by a Material

Factors affecting the fraction of energy absorbed by a material include the range of effectiveness of the radiation in the material, distribution of radioactive contaminants, and (in the case of alpha radiolysis) particle size of the radioactive contaminant (such as PuO_2 particles).

3.1.2.3.2.1   Range of Effectiveness of the Radiation

The range of alpha particles in gases, liquids, and solids must be considered both when comparing alpha with gamma radiolysis experiments on specific materials, and when evaluating the gas generation rates expected from actual waste drums. For example, the range of alpha particles in air at 0°C and 760 mm Hg pressure is approximated by Cember (1978)[8]:

$$Range(cm) = [1.24 \text{ x } E(MeV)] - 2.62, \text{ for } 4 < E < 8 \text{ MeV.}$$

For 5.5 MeV alpha particles, the range in air would be 4.2 cm. The presence of water vapor or other vapors would decrease that distance. The range of alpha particles in biological tissue, or other materials of low density, is given by Cember (1978)[8]:

$$Range = Range(air) \text{ x } (density \text{ of air})/(density \text{ of material})$$

$$= 4 \text{ cm x } (1.2E\text{-}3 \text{ g/cm}^3)/(density \text{ of material}).$$

Plastics and cellulosics (or liquid water) have densities of about 1 g/cm^3. Therefore the range of alpha particles in typical combustible wastes or absorbed aqueous solutions is estimated to be about 5E-3 cm [(5E-3 cm x 1E4 microns/cm = 50 microns; 5E-3 cm/(2.54 cm/in) x 1E3 mils/in = 2 mils)].

Several conclusions that can be reached from the above calculations are:

(1)   For low-density materials less than about 2 mils thick, both alpha particles and gamma rays can penetrate completely through the material.

(2)   Materials more than about 4 cm away from all alpha-emitting radionuclides should not experience any alpha radiolysis.

(3)   Radiolysis of gases or vapors within 4 cm of alpha-emitting radionuclides will occur unless the alpha particles are first absorbed by other materials.

3.1.2.3.2.2   Distribution of Radioactive Contaminants

The distribution of radioactive contaminants can affect the rate of gas generation. This is especially important when the materials being irradiated are heterogeneous. For example, consider a drum containing mixed combustible and dry metal waste, where the thick metal pieces

are individually wrapped with plastic, and the activity all results from alpha decay. Several possible distributions of the alpha activity include the following:

(1)   All the activity is located in the interior of the metal pieces.

(2)   All of the activity is located on the exterior of the metal pieces, in contact with both the plastic wrapping and the metal pieces.

(3)   All of the activity is uniformly distributed in the mixed combustible waste.

The rate of gas production will be different for each of the three cases. In Case 1, no radiolytic gas will be generated. In Case 2, gas could be generated at a rate up to one-half the rate characteristic of plastic (no radiolytic gas is generated by metal). In Case 3, gas will be generated at a rate equal to the weighted average G value for the mixed combustibles. An upper-bound estimate of the quantity of radiolytic gas generated from a mixture of materials can be calculated by assuming that all of the emitted alpha energy is absorbed by the material having the highest G value.

If a plutonium dioxide particle is located on a surface, up to half the alpha particles may interact with gases or vapors above the contaminated surface, unless another surface is in contact with the first. The quantity of gas generated may be greater than calculated based only on the surface-contaminated material if a significant fraction of the atmosphere above the surface consists of organic vapors.

3.1.2.3.2.3   Particle Size of the Contaminant

The plutonium contaminants in CH-TRU wastes are usually in particle form as PuO_2 or hydroxides but may also be in the form of plutonium nitrate from solution in nitric acid. If the plutonium is in particle form, some of the alpha particles will interact with plutonium or oxygen atoms (in the process known as self-absorption), rather than with the waste material. Attachment B of this document presents a calculation of the fraction of alpha decay energy escaping from a particle of PuO_2 as a function of the PuO_2 particle radius.

The gas generation rate reported from particulate contamination could then be less than the rate predicted using maximum G values and all of the activity measured in the waste using segmented gamma scan, passive/active neutron interrogation, or other assay methods. For example, the $G(H_2)$ value for Pu-238 dissolved in nitric acid was observed to be about 2.5 times the $G(H_2)$ value for 2-micron particles of the oxide.[23] (These particles had probably agglomerated to larger particles.)

---

[23] Bibler 1979. N. E. Bibler, "Gas Production from Alpha Radiolysis of Concrete Containing TRU Incinerator Ash, Progress Report 2, August 1, 1978 - November 30, 1978," E. I. DuPont de Nemours and Company, Savannah River Laboratory, DPST-78-150-2, April 1979.

3.1.2.3.3 Use of G Values Measured by Non-Alpha Irradiation

Alpha radiolysis predominates in the CH-TRU wastes. However, many radiolysis experiments have been performed using gamma (or other) radiation. Some differences are found in the gases produced in alpha radiolysis versus gamma radiolysis, but the results in most cases are very similar, as shown in Sections 3.1.3, 3.1.4, and 3.1.5. The quantities and compositions of the evolved gases should be comparable when:

(1)   The total absorbed dose for the gamma radiolysis experiment is similar to the total absorbed dose for the alpha radiolysis experiment.

(2)   The dose rate for the gamma radiolysis experiment is similar to the dose rate for the alpha radiolysis experiment.

(3)   For materials that are surface contaminated in an alpha radiolysis experiment, the gamma radiolysis experiment is performed on powders or thin films, to minimize diffusion effects in bulk materials.

3.1.3   Radiolysis of Liquids, Vapors, and Gases

G values for liquids are applicable to the following three waste forms: liquids absorbed onto various waste materials, liquids incorporated into a matrix such as concrete, and liquids used as plasticizers in plastics and rubbers. Radiolysis of vapors near contaminated surfaces may occur. The organic liquids are grouped into families based on their functional groups.[7] The functional group is the atom or group of atoms that defines the structure of a particular family of organic compounds, and, at the same time, determines their properties. For example, the functional group in alcohols is the -OH group, while in alkenes the functional group is the carbon-carbon double bond. A large part of organic chemistry is the chemistry of the various functional groups. A particular set of properties can be associated with a particular group wherever it is found. When a molecule contains a number of different functional groups, the properties of the molecule are expected to be roughly a composite of the properties of the various functional groups. (The properties of a particular group may be modified by the presence of another group, however.) Functional groups in macromolecules also determine their chemical reactions.

The major products of radiolysis are also influenced by molecular structure.[6] Chemical bonds are not broken randomly even though the excitation energy may exceed the bond dissociation energy. For solid materials for which the G values are unknown, structurally related organic liquids can provide estimates of maximum G values.

The radiolysis data are organized by families of liquids, which are based on functional groups (see Attachment A of this document for more details). Where data are available, G values at different LETs are shown.

Liquids that have G values for flammable gas greater than 4.1 are: saturated hydrocarbons, alcohols, ethers, ketones, and organic acids. Liquids that have G values for flammable gases less than 4.1 include unsaturated hydrocarbons, aromatic hydrocarbons, water, esters, halogenated hydrocarbons, aromatic halides, and commercial lubricant oils. G values for flammable gases for

organic nitrogen compounds are low for those having aromatic characteristics or C-N triple bonds.

3.1.3.1 Radiolysis of Saturated Hydrocarbons

Saturated hydrocarbons contain only hydrogen and carbon atoms and single carbon-carbon bonds. They include most of the common petroleum fuels. An example of a saturated hydrocarbon is hexane, with the following structure:
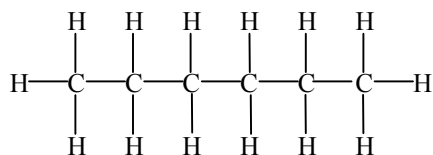
Table 3.1-2 presents G values for saturated hydrocarbons for irradiation at room temperature in vacuum. G(gas) is the G value for all gas produced.

From Table 3.1-2, the bounding $G(H_2)$ value is 5.6 for saturated hydrocarbons in the liquid phase at room temperature. In addition to hydrogen, other flammable gases may be generated. Newton[24] has observed some general characteristics of gas generation from saturated hydrocarbons. Normal saturated hydrocarbons yield principally hydrogen, with methane being produced only from the end groups. Therefore, the ratio of hydrogen to methane increases with increasing molecular weight. With branched-chain hydrocarbons (such as isobutane or neopentane), relatively more methane is produced, and the yield of methane increases with the number of methyl groups on the hydrocarbon chain.

Hall[6] reports an activation energy of about 3 kcal/mole for the $G(H_2)$ value for the liquid phase of neopentane and n-hexane. (See Section 3.1.3.4.1.1 for the use of activation energies in calculating the temperature dependence of G values.)

Table 3.1-2 — G Values for Saturated Hydrocarbons

Material	$G(H_2)$	$G(CH_4)$	$G(gas)^a$	Comments	Reference
Vapor phase					
propane	8.2	0.4		alpha; vacuum	(1)
butane	9.0	1.2		alpha; vacuum	(1)
pentane	7.3	0.8		alpha; vacuum	(1)
hexane	5.6	0.8		alpha; vacuum	(1)
isobutane	7.4	2.7		alpha; vacuum	(1)
neopentane	2.0	2.0		alpha; vacuum	(1)

---

[24] Newton 1963. A. S. Newton, "Chemical Effects of Ionizing Radiation," in Radiation Effects on Organic Materials, Academic Press, New York, 1963, eds. R. O. Bolt and J. G. Carroll.

Table 3.1-2 — G Values for Saturated Hydrocarbons (Concluded)

Material	G(H₂)	G(CH₄)	G(gas)[a]	Comments	Reference
Liquid phase					
pentane	4.2	0.4		electron; vacuum	(1)
	4.2	0.2	5.4	electron; vacuum	(2)
hexane	5.0	0.2	5.2	electron; vacuum	(1)
	5.0	0.1	7.2	electron; vacuum	(2)
cyclohexane	5.6	0.1	5.7	electron; vacuum	(1)
	5.3	0	5.3	alpha; vacuum	(1)
	7.7	--		fission fragments; vacuum	(3)
heptane	4.7	0.1		electron; vacuum	(1)
octane	4.8	0.1		electron; vacuum	(1)
	4.6	0.1		gamma; air	(4)
	4.2	--		alpha; air	(4)
nonane	5.0	0.1		electron; vacuum	(1)
decane	5.2	0.1		electron; vacuum	(1)
dodecane	4.9	0.1		electron; vacuum	(1)
hexadecane	4.8	0		electron; vacuum	(1)
2-methylpentane	4.0	0.5		electron; vacuum	(1)
2,2-dimethyl-butane	2.0	1.2		electron; vacuum	(1)
neopentane	1.6	3.7	5.6	gamma; vacuum	(2)

Refs.: (1) Spinks 1976[3], p. 365; (2) Hall 1963[6], p. 71; (3) Gaumann 1968[25]; (4) Bibler 1977[26].

Note: [a]G(gas) includes miscellaneous gaseous hydrocarbons C_2-C_4.

3.1.3.2 Radiolysis of Unsaturated Hydrocarbons

Unsaturated hydrocarbons are hydrocarbons that have at least one double or triple carbon-carbon bond. Examples include acetylene, ethylene, 1-hexene, and cyclohexene. The compound 1-hexene has the following structure.
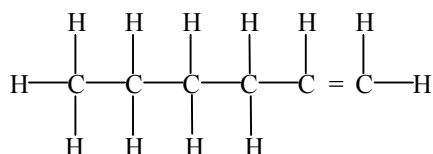
G(H₂) values for unsaturated hydrocarbons are generally much smaller than for saturated hydrocarbons, even when the only structural difference occurs in a small area of a long molecule (e.g., hexane compared to 1-hexene). Table 3.1-3 gives G values for three unsaturated hydrocarbons.

---

[25] Gauman, 1968.

[26] Bibler 1977. N. E. Bibler and E. G. Orebaugh, "Radiolytic Gas Production from Tritiated Waste Forms, Gamma and Alpha Radiolysis Studies," E. I. DuPont de Nemours and Company, Savannah River Laboratory, DP-1459, July 1977.

Radiolysis products of liquid cyclohexene and their G values are listed in Table 3.1-4 for both gamma and alpha (1.5 MeV) radiation.[3]

Table 3.1-3 — G Values for Three Unsaturated Hydrocarbons

Material	$G(H_2)$	$G(CH_4)$	$G(gas)^a$	Comments	Reference
ethylene[b]	1.2	0.1	2.8	electron; vacuum	(1)
cyclohexene	1.3	0	1.3	gamma; vacuum	(2)
	3.0	0	3.0	alpha; vacuum	(2)
1-hexene	0.8	0	0.8	electron; vacuum	(1)

Refs.:   (1) Hall 1963[6], p.78; (2) Spinks 1976[3], p. 384.

Notes: [a]$G(gas)$ includes C_2H_2.
                    [b]Gas phase.

Table 3.1-4 — Radiolysis Products and G Values for Liquid Cyclohexene

Product	G (Product)	
	^{60}Co γ-Ray	1.5 MeV α
H_2	1.3	3.0
cyclohexane	1.0	0.3
2,2'-bicyclohexenyl (II)	1.8-1.9	0.4
3-cyclohexylcyclohexene (III)	0.5-0.6	0.5
bicyclohexyl (IV)	0.2	0.1
polymer, unidentified dimer (as C_6 units)	8.9-9.8	6.1

Ref.:   Spinks 1976[3], Table 8.6.

3.1.3.3 Radiolysis of Aromatic Hydrocarbons

An aromatic hydrocarbon has a closed ring structure and resonance-stabilized unsaturation. The stability of aromatic compounds is attributed to the presence in the aromatic ring system of electrons in pi orbitals, which can dissipate energy throughout the ring system. This reduces the probability that excited or ionized aromatic molecules will dissociate. Alternative modes of energy dissipation are favored that do not result in dissociation of the molecule.[3] Examples include benzene, xylene, and discrete-ring polyphenyls. All of the aromatic hydrocarbons have very low G values for hydrogen and total gas, as shown in Table 3.1-5.

Aromatic hydrocarbons are good protective agents for a large number of chemicals because they have many low-lying excited states, have low ionization potentials, and are themselves radiation resistant.[24] The transfer of energy from higher excited states or charge exchange with the ion of the primary compound results in dissipation of energy in the aromatic hydrocarbon. For example, cyclohexane is protected from radiolytic decomposition by small amounts of added benzene. Internal protective agents can be built into molecules by adding aromatic groups.

Table 3.1-5 — G Values for Several Aromatic Hydrocarbons

Material	$G(H_2)$	$G(CH_4)$	G(gas)	Comments	Reference
benzene	0.6	0	0.8	alpha; vacuum	(1)
	~0	~0	~0	gamma; vacuum	(1)
	~0	~0	~0	electron; vacuum	(3)
toluene	0.6	0	0.6	alpha; vacuum	(1)
	0.1	~0	0.1	gamma; vacuum	(1)
	0.1	~0	0.1	electron; vacuum	(2)
p-xylene	0.2	0	0.2	gamma; vacuum	(1)
ethyl benzene	0.2	~0	0.2	electron; vacuum	(2), (3)
	0.2	~0	0.2	gamma; vacuum	(1)
	0.2	~0	0.2	reactor; vacuum	(2)
isopropyl benzene	0.2	0.1	0.3	gamma; vacuum	(1)
	0.2	0.1	0.3	electron; vacuum	(2), (3)
	0.3	0.1	0.4	alpha; vacuum	(3)
	0.2	0.1	0.3	reactor; vacuum	(2)
tert-butyl benzene	0.1	0.1	0.2	electron; vacuum	(2), (3)
	0.2	~0	0.2	reactor; vacuum	(2)
mesitylene	0.2	~0	0.2	electron; vacuum	(3)
biphenyl	a	a	~0	electron; vacuum	(2)
	a	a	0.1	reactor; vacuum	(2)
p-terphenyl	~0	~0	~0	electron; vacuum	(2)
	~0	~0	~0	reactor; vacuum	(2)

Refs.:   (1) Spinks 1976[3], p. 388; (2) Hall 1963[6], p. 91; (3) Rad. Effects 1963[27], p. 63.

Notes: [a]not listed;

~0 denotes a value <0.1.

3.1.3.4 Radiolysis of Water

Table 3.1-6 presents G values for radiolysis of water. $G(H_2)$ strongly depends on LET, increasing by a factor of 3-4 from gamma radiolysis to alpha radiolysis. (Note that LET for alpha particles decreases for increasing alpha particle energy that is greater than 1.5 MeV.)

---

[27] Rad. Effects 1963. "Radiation Effects Handbook," S-146, Institute of Electrical and Electronics Engineers, Inc., June 1963.

The maximum $G(H_2)$ value for water is 1.6 for alpha radiation. The maximum $G(O_2)$ value for water would be 0.8. Addition of nitrates to water lowers the production of hydrogen, but can increase the production of oxygen.

Bibler[28] measured gas evolution from aerated nitric acid or sodium nitrate-0.4-M H_2SO_4 irradiated by Cm-244 and Pu(IV)-239 alpha particles. The nitrate ions scavenged the precursors of hydrogen and reduced $G(H_2)$ as observed in gamma radiolysis experiments. Above 1-M NO_3^- concentration, oxygen and nitrite ions were produced as a result of direct energy absorption by nitrate ions.

Table 3.1-6 — G Values for Water[a,b]

Radiation Type	pH	$G(H_2)$	Reference
Vapor phase gamma, e	not given	0.5	(1)
Liquid phase gamma, e	0.5	0.4	(1),(2)
	3 to 13	0.45	(1),(2)
6.4 MeV He^{++}	not stated	1.1^d	(2)
^{244}Cm alpha (5.8 MeV)	not stated	1.3	(3)
5.3 MeV alpha (Po)^c	0.5	1.6	(1)
^{252}Cf alpha, beta, and fission fragments	0.4M- H_2SO_4	1.7	(4)

Refs.:   (1) Spinks 1976[3], p. 258; (2) Burns 1981[29]; (3) Bibler 1974[27]; (4) Bibler 1975[30].
Notes: [a]"e" means accelerated electrons.
          [b]$G(O_2)$ values not reported; maximum $G(O_2)$ would be 1/2 $G(H_2)$.
          [c]Po = polonium.
          [d]G(H2) value from curve fit to data from seven authors at a wide range of LET values.

The $G(H_2)$ value in alpha radiolysis experiments was found to decrease sharply from about 1.3 for zero concentration of NO_3^-, to 0.7 at 1-M NO_3^-, to about 0.25 at 2.5-M NO_3^-. The decrease

---

[28] Bibler 1974. N. E. Bibler, "Curium-244 Radiolysis of Nitric Acid. Oxygen Production from Direct Radiolysis of Nitrate Ions," J. Phys. Chem. 78, pp. 211-215, 1974.

[29] Burns 1981. W. G. Burns and H. E. Sims, "Effect of Radiation Type in Water Radiolysis," J. Chem. Soc., Faraday Trans. I 77, pp. 2803-2813, 1981.

[30] Bibler 1975. N. E. Bibler, "Radiolysis of 0.4 M Sulfuric Acid Solutions with Fission Fragments from Dissolved Californium-252. Estimated Yields of Radical and Molecular Products that Escape Reactions in Fission Fragment Tracks," J. Phys. Chem. 79, pp. 1991-1995, 1975.

in $G(H_2)$ was more pronounced for Co-60 gamma irradiation than for alpha irradiation. This effect has been attributed by Bibler and others to nitrate ions being more efficient hydrogen scavengers for gamma irradiation than for alpha irradiation. The $G(O_2)$ variation with NO_3^- concentration was approximately linear, from about $G(O_2)=0.25$ at zero concentration NO_3^- to $G(O_2)=0.75$ at 5.6-M NO_3^-. Agitation of the samples was necessary to release all of the generated O_2, much of which otherwise stayed in solution.

Bibler[29] reports measurements of gas produced from irradiation of 0.4-M sulfuric acid by Cf-252, which is a transuranic isotope that decays by alpha emission as well as spontaneous fission. The total absorbed dose from Cf-252 is due to alpha particles, fission fragments, and beta particles from decay of the fission fragments. The net $G(H_2)$ value reported from all contributions was 1.7. The fission fragment contribution (LET of 400 eV/A) was calculated to have $G(H_2)=2.1$.

$G(H_2)$ values and equilibrium concentrations of H_2 for irradiated water are controlled by a back reaction of H_2 with the OH^- radical to form water.[31,25] This back reaction is much more efficient for gamma radiation than for alpha radiation, resulting in a $G(H_2)$ value for gamma radiolysis 3-4 times lower than that for alpha radiolysis. The gas pressure above the water also was found to reach an equilibrium value at a much lower pressure for gamma radiolysis than for alpha radiolysis.

Another scavenger species that could compete with H_2 for OH^- is Cl^-, present in salt brines. The results of an experimental program to measure gas generation from radiolysis of salt brines are reported by Gray (Gray 1984[30]). The brine was prepared by dissolving Permian Basin salt, consisting primarily of NaCl with a small amount of calcium sulfate, in deionized water. The irradiations were conducted in pressure vessels. The alpha radiolysis tests were terminated as the pressure approached the capacity of the pressure transducers. Gas compositions for both gamma and alpha radiolysis were roughly two parts H_2 to one part O_2 in most cases. The gamma radiolysis experiments reached an equilibrium pressure of about 100 atm, while the alpha radiolysis experiments were extrapolated to reach an equilibrium pressure of about 275 atm.

Alpha radiolysis experiments conducted by Bibler (Bibler 1981[32]) on the free water in concrete demonstrated that below 100°C, the H_2 production rate is independent of temperature and radiation dose rate.

---

[31] Gray 1984. W. J. Gray and S. A. Simonson, "Gamma and Alpha Radiolysis of Salt Brines," PNL-SA-12746, 1984 Fall Meeting of the Materials Research Society in Boston, Mass., November 1984.

[32] Bibler 1981. N. E. Bibler, "Gas Production from Alpha Radiolysis of Concrete Containing TRU Incinerator Ash, Progress Report 4, September 1, 1979 - August 31, 1980," E. I. DuPont de Nemours and Company, Savannah River Laboratory, DPST-80-150-2, March 1981.

3.1.3.5 Radiolysis of Alcohols

Alcohols are compounds of the general formula ROH, where R is any alkyl or substituted alkyl group.[7] The group may be open-chain or cyclic; it may contain a double bond, a halogen atom, or an aromatic ring. All alcohols contain the hydroxyl (-OH) group, which determines the properties characteristic of this family. Compounds in which the hydroxyl group is attached directly to an aromatic ring are called phenols, and differ markedly from the alcohols. A glycol is a dihydroxy alcohol, containing two hydroxyl groups. For example, ethylene glycol has the structure

$$CH_2 \text{---} CH_2$$
$$OH \quad\quad OH$$
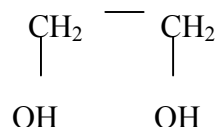
Table 3.1-7 presents G values for many alcohols.

3.1.3.6 Radiolysis of Ethers

Ethers are compounds of the general formula R-O-R, Ar-O-R, or Ar-O-Ar.[7]

Table 3.1-8 presents G values for many ethers. The maximum reported value of $G(H_2)$ is 3.6. Almost all of the other radiolysis gases or vapors are also flammable. Branching in the alkyl group decreases hydrogen evolution but increases hydrocarbon yields.[6]

3.1.3.7 Radiolysis of Aldehydes and Ketones

Aldehydes are compounds of the general formula RCHO; ketones are compounds of the general formula RR'CO.[7] The groups R and R' may be aliphatic or aromatic. Both aldehydes and ketones contain the carbonyl group, C=O, and are often referred to collectively as carbonyl compounds. It is the carbonyl group that largely determines the chemistry of aldehydes and ketones. For example, the structure of acetone is

$$CH_3 \text{---} C=0$$
$$|$$
$$CH_3$$
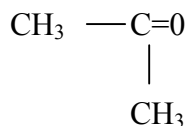
Table 3.1-9 presents G values for propionaldehyde. Table 3.1-10 illustrates the effect of LET on the gaseous products of acetone. Table 3.1-11 presents G values for several ketones, including acetone. The maximum total G value for flammable gas production from gamma or alpha radiolysis of these aldehydes or ketones is 3.1.

The series consisting of formaldehyde, acetaldehyde, and acetone was irradiated in the gas phase with electrons.[6] Hydrogen, CO, and CO_2 were the principal products from formaldehyde. Replacing one or both hydrogen atoms of the formaldehyde molecule with CH_3 groups (giving acetaldehyde or acetone) resulted in lower radiolytic production of CO_2 and H_2, but gave substantial yields of alkanes and alkenes. This result was considered by those authors to be as expected on the basis of a group-to-product correlation.

Table 3.1-7 — G Values for Alcohols

Material	$G(H_2)$	$G(CO)$	$G(CH_4)$	$G(gas)^{a,b}$	Comments	Reference
Vapor phase						
ethanol	10.8	1.2	0.9	12.9	electron; vacuum	(1)
methanol	10.8	1.0	0.3	12.1	gamma; vacuum	(1)
Liquid phase						
ethanol	5.0	0.1	0.6	5.7	gamma; vacuum	(1)
	3.5	0.1	0.4	4.5	alpha; vacuum	(2)
	4.1	0.1	0.4	4.6	alpha; vacuum	(3)
methanol	5.4	0.1	0.7	6.2	gamma; vacuum	(1)
	3.5	0.2	0.4	4.5	alpha; vacuum	(2)
	4.0	0.2	0.2	4.4	gamma; vacuum	(3)
methanol	major product is formaldehyde				gamma; oxygen	(1)
1-propanol	4.4	--	--	4.4^c	gamma; vacuum	(1)
	2.8	0.1	0.1	3.0	alpha; vacuum	(3)
2-propanol	3.7	--	1.5	5.2^c	gamma; vacuum	(1)
n-propanol	2.8	--	0.1	3.9	alpha; vacuum	(2)
1-butanol	4.6	--	--	4.6^c	gamma; vacuum	(1)
	3.6	0.1	0.1	4.3	alpha; vacuum	(3)
t-butanol	1.0	--	3.6	4.6^c	gamma; vacuum	(1)
n-butanol	3.6	--	0.1	4.3	alpha; vacuum	(2)
1-octanol	3.5	0.1	~0	3.7	alpha; vacuum	(3)
1-decanol	3.5	~0	~0	3.6	alpha; vacuum	(3)

Refs.:   (1) Spinks 1976[3], pp. 410, 417, 420; (2) <u>Rad Effects</u>, 1963[26], pp. 59-61; (3) Hall 1963[6], p. 92.

Notes: [a]Water vapor is generated but is not included.

[b]Other highly volatile products, such as formaldehyde, acetylene, ethylene, ethane, acetaldehyde, ethyl ether, and others, are also generated. G(gas) values greater than the sum of $G(H_2)$, $G(CO)$, and $G(CH_4)$ have included these vapors.

[c]Only major products were listed.

Table 3.1-8 — G Values for Ethers in the Liquid Phase

Material	$G(H_2)$	$G(CO)$	$G(CH_4)$	$G(gas)$[a]	Comments	Reference
ethyl ether	3.4	--	0.4	3.8	gamma; vacuum	(1)
	3.6	0.1	0.2	3.9	alpha; vacuum	(2)
ethyl n-butyl ether	3.3	0.1	0.1	3.5	alpha; vacuum	(2)
dibutyl ether	2.9	--	0.1	3.0	gamma; vacuum	(1)
n-butyl ether	2.7	0.1	0.1	2.9	alpha; vacuum	(2)
ethyl tertbutyl ether	2.0	0.1	0.8	2.9	alpha; vacuum	(2)
isopropyl ether	2.2	~0	1.5	8.4	gamma; vacuum	(3)
	2.4	0.1	0.9	5.8	alpha; vacuum	(3)
di-isopropyl ether	2.4	--	1.7	4.1	gamma; vacuum	(1)
dioxan	2.1	0.3	--	2.4	gamma; vacuum	(1)
tetrahydrofuran	2.6	--	--	2.6	gamma; vacuum	(1)

Refs.:   (1) Spinks 1976[3], pp. 421-423; (2) Hall 1963[6], p. 98; (3) Newton 1963[24], p. 55.

Note: [a]Other gases or highly volatile products, such as formaldehyde, acetylene, ethylene, ethane, acetaldehyde, alcohols, and others, are also generated. G(gas) values greater than the sum of $G(H_2)$, $G(C_O)$, and $G(CH_4)$ have included these other gases or vapors.

Table 3.1-9 — G Values for Propionaldehyde

Material	$G(H_2)$	$G(CO)$	$G(CH_4)$	$G(gas)$[a]	Comments
propionaldehyde	1.2	1.6	0.1	4.4	electron; vacuum

Refs.:   Hall 1963[6], p. 102.

Note: [a]G(gas) includes C_2-C_4 hydrocarbons.

Table 3.1-10 — Effect of LET on the Gaseous Products of Acetone

Radiation -dE/dx(eV/nm)	^{60}Co-γ 0.2	6.9-MeV He-ions 131	67-MeV C-ions 390	65.7-MeV N-ions 553
$G(H_2)$	0.96	1.47	2.36	2.71
$G(CO)$	0.56	0.80	1.05	1.22
$G(CH_4)$	1.76	0.97	0.99	0.96
$G(C_2H_4)$	0.04	0.12	0.21	0.24
$G(C_2H_6)$	0.30	0.50	0.56	0.64
$G(gas)$	3.62	3.86	5.17	5.77

Ref.:   Spinks 1976[3], Table 8.19.

Table 3.1-11 — G Values for Three Ketones

Material	G(H$_2$)	G(CO)	G(CH$_4$)	G(gas)[a]	Comments	Reference
acetone	1.0	0.6	1.8	3.6	gamma; vacuum	(1)
	1.5	0.8	1.0	3.9	alpha; vacuum	(1)
	0.9	0.8	2.6	4.8	gamma; vacuum	(2)
methyl ethyl ketone	1.2	0.8	0.9	6.8	gamma; vacuum	(2)
diethyl ketone	1.2	1.5	0.1	7.7	gamma; vacuum	(2)

Refs.:   (1) Spinks 1976[3], p. 427; (2) Hall 1963[6], p. 102.
Note: [a]G(gas) includes C$_2$-C$_4$ hydrocarbons.

3.1.3.8 Radiolysis of Carboxylic Acids

Carboxylic acids contain the carboxyl group

$$\begin{array}{c} O \\ \parallel \\ -C \\ \diagdown \\ OH \end{array}$$
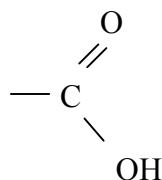
attached to either an alkyl group (RCOOH) or an aryl group (ArCOOH).[7] For example, acetic acid, CH$_3$COOH, has the structure

$$CH_3 - \underset{\underset{OH}{|}}{C}=O$$
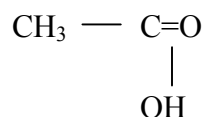
Whether the group is aliphatic or aromatic, saturated or unsaturated, substituted or unsubstituted, the properties of the carboxyl group are essentially the same.

Table 3.1-12 gives G values for two carboxylic acids that are liquids at room temperature. G values for some carboxylic acids that are solids at room temperature are given in Section 3.1.5.

Table 3.1-12 — G Values for Carboxylic Acids (Liquids at Room Temperature)

Material	$G(H_2)$	$G(CO)$	$G(CO_2)$	$G(CH_4)$	$G(gas)$	Comments	Reference
acetic acid	0.5	0.2	5.4	3.9	10.5	gamma; vacuum	(1)
	0.5	0.4	4.0	1.4	7.2	alpha; vacuum	(1)
propionic acid	0.8	0.3	3.9	0.5	5.5	alpha; vacuum	(2)

Refs.:   (1) Spinks 1976[3], pp. 428-429; (2) Hall 1963[6], p. 108.

Note: [a]$G(gas)$ may include C_2; water vapor is also generated but is not included.

3.1.3.9 Radiolysis of Esters

Esters are functional derivatives of carboxylic acids in which the -OH of the carboxyl group has been replaced by -OR'.[7] Phosphate esters are discussed separately. For example, the structure of methyl acetate is

$$CH_3 — C=O$$
$$|$$
$$O—CH_3$$
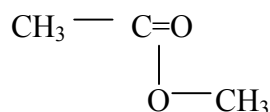
The emulsifier for Envirostone[R], a gypsum-based material used to solidify organic and low pH aqueous sludges and liquid waste, has been identified as a polyethyl glycol ester. Many plasticizers added to polymers to form commercial plastics are esters, such as dioctyl phthalate. Table 3.1-13 gives G values for many esters. Note that benzyl acetate, which includes a benzene ring in its structure, has a much lower $G(H_2)$ value than the other esters.

Table 3.1-13 — G Values for Esters

Material	$G(H_2)$	$G(CO)$	$G(CO_2)$	$G(CH_4)$	$G(gas)$[a]	Comments	Reference
methyl acetate	0.8	1.6	1.0	2.0	5.7	gamma; vacuum	(1)
	0.9	1.6	0.8	2.1	5.6	gamma; vacuum	(2)
	0.6	1.2	0.4	0.8	3.4	electron; vacuum	(2)
ethyl acetate	0.9	1.1	--	1.6	3.6	gamma; vacuum	(2)
isopropyl acetate	0.9	1.2	0.8	0.9	5.6	alpha; vacuum	(2)
	0.5	0.8	0.6	1.0	3.6	electron; vacuum	(2)
n-propyl acetate	0.8	1.1	0.6	0.4	4.0	electron; vacuum	(2)
benzyl acetate	0.1	0.2	1.6	0.8	2.7	electron; vacuum; aromatic character	(2)

Table 3.1-13 — G Values for Esters (Concluded)

Material	G(H$_2$)	G(CO)	G(CO$_2$)	G(CH$_4$)	G(gas)[a]	Comments	Reference
di (2-ethyl) hexyl sebacate	1.0	0.3	0.2	~0	1.8	electron; vacuum	(3)
	1.0	0.3	0.2	~0	1.5	gamma; vacuum	(4)
di (2-ethyl) hexyl adipate	0.9	0.5	0.2	~0	1.7	gamma; vacuum	(4)
pentaerythritol ester	0.8	0.8	0.3	~0[b]	1.9	gamma; vacuum	(4)

Refs.: (1) Spinks 1976[3], p. 430; (2) Hall 1963[6], p. 104; (3) Rad. Effects 1963[26], p. 62; (4) Arakawa 1983a.[33]

Note: [a]G(gas) may include C$_2$ hydrocarbons or vapors from volatile liquids, such as aldehydes, alcohols, or ethers.

[b]The value of 0.3 in the reference appears to be in error (0.03 vs. 0.3).

3.1.3.10 Radiolysis of Phosphate Esters

Phosphate esters have one of the following structures[7]:

$$
\text{HO—P(=O)(OR)—OH,} \quad \text{RO—P(=O)(OR)—OH,} \quad \text{or RO—P(=O)(OR)—OR}
$$
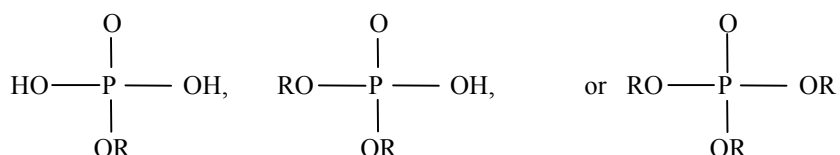
Table 3.1-14 gives G values for phosphate esters. Tricresyl phosphate contains three benzene rings and has a much lower G(H$_2$) value than either trioctyl or tributyl phosphate.

Table 3.1-14 — G Values for Phosphate Esters

Material	G(H$_2$)	G(CO)	G(CO$_2$)	G(CH$_4$)	G(gas)[a]	Comments	Reference
tricresyl phosphate	0.05	~0	~0	~0	0.06	gamma; vacuum; aromatic character	(1)
tributyl phosphate	2.0	--	--	0.3	2.3	gamma	(2)
trioctyl phosphate	2.3	~0	~0	0.1	2.6	gamma; vacuum	(1)

Refs.: (1) Arakawa 1983a[32]; (2) Holland 1978[34].

Note: [a]G(gas) may include C2 hydrocarbons

---

[33] Arakawa 1983a. K. Arakawa, et al., "Radiation-Induced Gas Evolution from Commercial Lubricant Base Oil," Nuclear Technology 61, pp. 533-539, 1983.

[34] Holland 1978. J. P. Holland, et al., "The Radiolysis of Dodecane-Tributylphosphate Solutions," Nuclear Instruments and Methods 153, pp. 589-593, 1978.

Tri-n-butyl phosphate (TBP), an organic ester of phosphoric acid, is used as an extractant in the reprocessing of nuclear fuel. Radiolysis experiments have been conducted to determine the decomposition of TBP in different phases of the extraction system. The Purex process uses solution of TBP in dodecane.[35]

Ladrielle[34] conducted both gamma and alpha radiolysis experiments in solutions of TBP in dodecane at room temperature. The average alpha particle energy from the cyclotron beam interacting with the solution was estimated to be 10.5 MeV. Pure TBP and dodecane were also irradiated. Radiolysis of pure TBP resulted in the formation of mono and dibutylphosphate, butanol, and saturated hydrocarbons (C_5 to C_8). Radiolysis of pure dodecane yielded hydrocarbons (C_5 to C_{11}). Lower molecular weight hydrocarbons (C_4 and below) were neglected in this study.

Holland[33] performed gamma radiolysis experiments on TBP, dodecane, and mixtures of TBP and dodecane. All samples were treated with dry clean helium for a period of four to eight hours. The number of moles of gas volatile at 161 K was determined by PVT analysis. A sample of the gas extracted was analyzed at 40 C by gas chromatography. Values of $G(H_2)$=6.7 and $G(CH_4)$=0.05 were determined for dodecane. Corresponding G values for pure TBP were $G(H_2)$=2.0 and $G(CH_4)$=0.3. Mixtures of TBP and dodecane were also irradiated, with dodecane electron fractions of 40%, 70%, 80%, 90%, and 95%. Plots of $G(H_2)$ versus TBP electron fraction were nonlinear. The yield of hydrogen was less than would be predicted by the mixture law (the yield of acid was greater).

Aromatic hydrocarbons, such as benzene, toluene, and cyclohexene protect TBP, while saturated hydrocarbons such as hexane, cyclohexane, and dodecane sensitize TBP to radiolytic degradation.[36] Carbon tetrachloride also sensitizes TBP radiolysis. Barney found that chlorinated aromatic hydrocarbons also provided more protection to TBP for alpha radiolysis than did the chlorinated unsaturated hydrocarbons. The rate of chloride ion formation in 20% TBP mixtures with various chlorinated hydrocarbon diluents was also measured. The relative rates were in the ratio 1/0.7/0.5 for carbon tetrachloride/trichloroethylene/ tetrachloroethylene. No detectable chloride ion formation was found for 1,2,4-trichlorobenzene or o-dichlorobenzene.

3.1.3.11 Radiolysis of Halogenated Hydrocarbons

Halogenated hydrocarbons are hydrocarbons in which at least one and possibly all of the hydrogen atoms have been replaced by halogen atoms (the major functional group for these materials). Radiolysis of halogenated hydrocarbons can be strongly affected by the presence of oxygen or moisture, and chain reactions can occur involving HCl for chlorinated hydrocarbons.

---

[35] Ladrielle 1983. Ladrielle, et al., "Alpha and Gamma Induced Radiolysis of Tributyl-Phosphate," Radiochem. Radioanal. Letters 59, pp. 355-364, 1983.

[36] Barney 1977. G. S. Barney and D. G. Bouse, "Alpha Radiolysis of Tributyl Phosphate - Effect of Diluents," Atlantic Richfield Hanford Company, ARH-ST-153, April 1977.

3.1.3.11.1   Radiolysis of Carbon Tetrachloride

Radiolysis of carbon tetrachloride, CCl_4, represents a simple example of radiolysis of an organic halogen compound because the radicals produced have limited possible reactions. Only two products are found: chlorine and hexachloroethane (not a gas). The observed G values for both products are 0.65 to 0.75 for gamma radiation.[3] When carbon tetrachloride is irradiated in the presence of oxygen, phosgene gas and chlorine are formed, each with a G value for gamma radiation of 4.3.[3]

Kazanjian[37] measured gas generation from carbon tetrachloride contaminated with plutonium dioxide and mixed with calcium silicate to form a paste. The initial atmosphere was air. The only gaseous product found was carbon dioxide, with a G value of 0.6. After the oxygen was completely depleted in about 40 days, the gas production rate became essentially nil. Kazanjian remarked that finding only carbon dioxide was puzzling because previous studies had shown that chlorine and phosgene were the only gaseous products. He hypothesized that chlorine was not detected because of its high reactivity. Phosgene can react with water to form HCl and CO_2[38]. Another possibility is that the calcium silicate, while radiolytically inert, could sorb radiolysis products, such as chlorine. Table 3.1-15 gives G values for carbon tetrachloride.

Table 3.1-15 — G Values for Carbon Tetrachloride

Radiation Type	G(Products)	Comments	Reference
gamma	G(gas)=0.7-0.8 $G(Cl_2)$=0.7-0.8	vacuum	(1),(2)
gamma	G(gas)=8.6	oxygen	(1)
alpha	G(gas)=0.6 $G(CO_2)$=0.6	air; CCl_4 mixed with calcium silicate to form a paste	(3)

Refs.:   (1) Spinks 1976[3], pp. 401-403; (2) Rad. Effects 1963[26], p. 62; (3) Kazanjian 1976[36].

3.1.3.11.2   Radiolysis of Aromatic Halides

The aromatic halides chlorobenzene, bromobenzene, and iodobenzene consist of a benzene ring with one hydrogen atom replaced by a chlorine, bromine, or iodine atom, respectively.

Table 3.1-16 lists G values for several aromatic halides. Very low $G(H_2)$ values are found, as for the aromatic hydrocarbons.

---

[37] Kazanjian 1976. A. R. Kazanjian, "Radiolytic Gas Generation in Plutonium Contaminated Waste Materials," Rockwell International, Rocky Flats Plant, RFP-2469, October 1976.

[38] Kazanjian 1969. A. R. Kazanjian and A. K. Brown, "Radiation Chemistry of Materials Used in Plutonium Processing," The Dow Chemical Company, Rocky Flats Division, RFP-1376, December 1969.

Table 3.1-16 — G Values for Aromatic Halides

Material	G(Products)	G(gas)[a]
chlorobenzene	$G(H_2)\sim0$; $G(HCl)=1.4$; $G(Cl_2)\sim0$	1.4
bromobenzene	$G(H_2)\sim0$; $G(HBr)=2.3$; $G(Br_2)=0.2$	2.5
iodobenzene	$G(H_2)\sim0$; $G(HI)\sim0$; $G(I_2)=2.0$	2.0

Ref.:   Spinks 1976[3], p. 407.

Note: [a]Gamma irradiation in a vacuum.

3.1.3.11.3   Radiolysis of Miscellaneous Halogenated Hydrocarbons

Some of the halogenated hydrocarbons that may be present in CH-TRU wastes are chloroform, methylene chloride, 1,1,1-trichloroethane, and 1,1,2-trichloro-1,2,2-trifluoroethane (Freon-113).

The amounts and species of gases generated from gamma radiolysis of liquid chloroform are dependent on temperature and dose rate and, in particular, on traces of oxygen and moisture that induce chain reactions. Aqueous solutions of chloroform do not decompose by a chain reaction.[3] Measured values of G(HCl) from about 5 up to 11 have been reported at 22-25°C (Ottolenghi 1961[39], Chen 1960[40]) for pure chloroform.

In the presence of oxygen, chloroform takes part in a radiation-initiated chain reaction. Nearly 100 chloroform molecules are decomposed per 100 eV of energy absorbed[41]. Most of the radiolysis products are hydrolyzed by water to produce hydrochloric acid.

Kazanjian[36] measured gas generation from the alpha radiolysis of Chlorothene-VG solvent, which is a trade name for 1,1,1-trichloroethane. The samples were mixed with calcium silicate to form a paste. The total pressure decreased for the first 30 days because of oxygen depletion; then it increased because of evolved gases. The main products measured were hydrogen, carbon dioxide, and dichloroethylene. Kazanjian remarked that formation of dichloroethylene inferred the production of hydrogen chloride, and that the hydrogen chloride probably was not detected because of its high reactivity. Calculations using Kazanjian's data show average G values for

---

[39] Ottolenghi 1961. M. Ottolenghi and G. Stein, "The Radiation Chemistry of Chloroform," Radiation Research 14, pp. 281-290, 1961.

[40] Chen 1960. T. H. Chen, et al., "Radiolysis of Chloroform and Carbon Tetrachloride," J. Phys. Chem. 64, pp. 1023-1025, 1960.

[41] Schulte 1953. J. W. Schulte, et al., "Chemical Effects Produced in Chloroform by Gamma-Rays," J. Am. Chem. Soc. 75, pp. 2222-2227, 1953.

CO_2 and H_2 of 0.3 and 0.2, respectively; and G(gas)=0.7. The G values did not decrease with increasing dose.

Getoff [42] performed gamma irradiation of oxygenated waste water containing 1,1,1-trichloroethane and found G(Cl⁻)=0.4.

Kazanjian[37,43] performed gamma radiolysis experiments on Baker reagent-grade trichloroethylene. Trichloroethylene is a highly sensitive compound, and very little energy input is necessary to initiate decomposition. In the absence of air, there were only two major products: hydrochloric acid and chloroacetylene, each with a G value of 0.25. A chain reaction was observed to occur when trichloroethylene was irradiated in the presence of oxygen. Extremely high yields were obtained, but the products were difficult to analyze because of their high reactivity. The major products were determined to be dichloroacetyl chloride, phosgene, and trichloroethylene oxide. There was no HCl or Cl_2 measured. Rapid reaction of the products with water to form HCl made it possible to analyze for total acidity. The total acid yield was measured by shaking the irradiated solvent with water and titrating the mixture with standardized NaOH solution. The $G(H^+)$ obtained was 4600 at room temperature[42] and increased with increasing temperature with an activation energy value of 2.2 kcal/mole.

Kazanjian[37] also measured the products from gamma irradiation of Alk-Tri^R, a commercial brand of trichloroethylene, which contains diisopropylamine for light stabilization. $G(H^+)$ was found to be 1600. Acid yields for this material would be expected to increase to the yields obtained for the reagent grade chemical as the additives were depleted through continued irradiation.

Perchloroethylene is expected to have a radiation chemistry similar to that of trichloroethylene and to produce an extremely high yield of acidic products in the presence of oxygen[37].

Alfassi and co-workers have performed gamma radiolysis experiments on two Freons, $CFCl_3$ and CF_2Cl_2, in the liquid phase.[44,45] A variety of C-F-Cl compounds were found with maximum measured G value for products of 2.6 in the presence of oxygen. All of the products were gases or highly volatile liquids.

Table 3.1-17 gives G values for miscellaneous organic halogen compounds.

---

[42] Getoff 1985. N. Getoff and W. Lutz, "Radiation Induced Decomposition of Hydrocarbons in Water Resources," Radiat. Phys. Chem. 25, pp. 21-26, 1985.

[43] Kazanjian 1970. A. R. Kazanjian and D. R. Horrell, "The Radiation-Induced Oxidation of Trichloroethylene," J. Phys. Chem. 75, pp. 613-616, 1971.

[44] Alfassi 1982. Z. B. Alfassi, "The Radiation Chemistry of CFCl3 in the Liquid Phase," Radiochem. Radioanal. Letters 56, pp. 333-342, 1982.

[45] Alfassi 1983. Z. B. Alfassi and H. Heusinger, "The Radiation Chemistry of CF2Cl2 in the Liquid Phase," Radiat. Phys. Chem. 22, pp. 995-1000, 1983.

3.1.3.12 Radiolysis of Organic Nitrogen Compounds

Organic nitrogen compounds are basically hydrocarbons where a functional group has been replaced by an NO_2, NH_2, or other group containing one or more nitrogen atoms. Amides (such as propionamide) are functional derivatives of carboxylic acids in which the -OH of the carboxyl group has been replaced by $-NH_2$[7]. Amines have the general formula RNH_2, R_2NH, or R_3N, where R is any alkyl or aryl group. In many of their reactions, the final products depend on the number of hydrogen atoms attached to the nitrogen atom. Two examples of amines are methylamine (CH_3NH_2) and analine, which has the NH_2 group attached to a benzene ring. Some of the heterocyclic compounds containing nitrogen (such as pyrrole, pyrazole, pyridine, and pyrimidine) have aromatic properties, while others, including 3-pyrroline and pyrrolidiene, do not.

G values for radiolysis of organic nitrogen compounds that have aromatic characteristics are low, as were the G values for radiolysis of aromatic hydrocarbons. Table 3.1-18 lists the G values for the products generated by the gamma radiolysis of many liquid organic nitrogen compounds. Ammonia is one of the products formed for a few of the compounds.

Table 3.1-17 — G Values for Miscellaneous Organic Halogen Compounds

Material	G(Products)	Comments	Reference
chloroform[a]	G(HCl)=5.3	gamma; vacuum	(1)
methylene chloride	G(HC1)=4.9	gamma; vacuum	(2)
1,1,1-trichloroethane	G(gas)=0.7; G(H_2)=0.2; G(CO_2)=0.3; G(dichloroethylene)=0.2	alpha; with or without O_2 present	(3)[b]
	G(Cl^-)=0.4	gamma; O_2 present in aqueous solution	(4)
trichloroethylene	G(H^+)=4600[a] G(HCl)=0.25	gamma; oxygen present gamma; vacuum	(5) (5),(6)
Freons	G(gas)=2.6(max); G(C-F-Cl compounds)=1.6; G(CO_2)=0-1.1	gamma; with or without O_2 present	(7),(8)

Refs.: (1) Spinks 1976[3], p. 403; (2) <u>Rad. Effects</u> 1963[26], p. 62; (3) Kazanjian 1976[36]; (4) Getoff 1985[41]; (5) Kazanjian 1970[42]; (6) Kazanjian 1969[37]; (7) Alfassi 1982[43]; (8) Alfassi 1983[44].

Notes: [a]G(H^+) is large for irradiation in oxygen. A chain reaction occurs in the liquid.
[b]Average G values calculated using author's data.

Table 3.1-18 — G Values for Liquid Organic Nitrogen Compounds[a]

Material	G(Products)	Comments
nitromethane	G(HCHO)=2.0	
nitrobenzene	G(N$_2$)=0.16	
acetonitrile	G(H$_2$)=0.67; G(CH$_4$)=0.65; G(HCN)=0.2	C N bond
methylamine	G(H$_2$)=5.4; G(CH$_4$)=0.18	
aniline	G(H$_2$)=0.12; G(NH$_3$)=0.25; G(C$_6$H$_6$)=0.04	contains benzene ring
propionamide	G(H$_2$)=0.14; G(CO)=2.6; G(CH$_4$)=0.93	
pyrrole	G(H$_2$)=0.20	aromatic N-C bonds
3-pyrroline	G(H$_2$)=2.34	
pyrollidine	G(H$_2$)=6.35	
pyrazole	G(H$_2$)=0.04; G(N$_2$)=0.12	aromatic N-C bonds
tetrazole	G(H$_2$)=trace; G(N$_2$)=0.96	aromatic N-C bonds
pyridine	G(H$_2$)=0.025	aromatic N-C bonds
pyrimidine	G(H$_2$)=0.030	aromatic N-C bonds

Ref.:   Spinks 1976[3], Table 8.22.

Note: [a]Gamma irradiation in vacuum. Other liquid products are also formed.

A value of G(gas)=10.1 was reported for gamma irradiation at room temperature of mono-n-butylamine (Mirchi 1981[46]). Major gas constituents were hydrogen [G(H$_2$)=5.6] and ammonia [G(NH$_3$)=4.0]. For dibutylamine and tri-n-butylamine, measurements of G(H$_2$) values at room temperature were 3.6 and 2.7, respectively. In all three cases, the total G value for hydrocarbon gases was 0.5.

Diethylenetriaminepentaacetic acid (DTPA) is a polyamino-carboxylic acid used as an eluting agent for the purification of Cm-244 by cation exchange chromatography. DTPA has been irradiated in aqueous solution by alpha and gamma radiation sources (Bibler 1972[47]). In some experiments, the solutions were degassed before irradiation, and the amounts of radiolytically produced gases that were noncondensible at -196°C and at -78°C were determined. The products were identified by mass spectrometry. Gamma radiolysis of solutions of DTPA in 4-M HNO$_3$ or 0.4-M H$_2$SO$_4$ produced CO$_2$ and H$_2$, with measured G values of 6.5 and 4.2, respectively. Gases produced in the alpha radiolysis experiments were not reported. However, measured G values for the destruction of DTPA were much lower for the alpha radiolysis experiments than for the gamma radiolysis experiments, indicating that gas production for alpha radiolysis should also be much lower than for gamma radiolysis.

[46] Mirichi 1981. R. Mirichi, et al., "Selected Problems of Radiation Stability of Some Solvents and Amines Used in the Reprocessing of Nuclear Fuel," Nukleonika 26, pp. 827–848, 1981.

[47] Bibler 1972. N. E. Bibler, "Gamma and Alpha Radiolysis of Aqueous Solutions of Diethylenetriaminepentaacetic Acid," J. Inorg. Nucl. Chem. 34, pp. 1417-1425, 1972.

3.1.3.13 Radiolysis of Commercial Lubricants

Commercial lubricants consist of paraffinic, naphthenic, and aromatic hydrocarbons. The aromatics have much lower G values than the paraffins but are largely removed from the oils by refining because of their poor viscosity-temperature properties (Carroll 1963[48]).

G values have been measured for many different commercial lubricants using gamma irradiation at room temperature at a dose rate of 1 Mrad/h and absorbed doses ranging from 100 to 3000 Mrad (Arakawa 1983a[32]). Graphs of the amount of evolved gas versus dose were nearly linear even at high absorbed dose, indicating nearly constant G values.

G values for Texaco Regal A motor oil, used in machining operations at the RFETS, were measured by Kazanjian using Co-60 gamma irradiation (Kazanjian 1969[37]) and alpha irradiation from Pu-239 (Kazanjian 1976[36]). In the gamma irradiation experiment, samples of the oil were irradiated under vacuum or sealed under 500 torr air. Values of $G(H_2)$ at 8.4 Mrad absorbed dose were 2.3 for the vacuum experiment and 1.8 for the experiment in air. The author did not consider this difference significant. At 8.4 Mrad absorbed dose, $G(-O_2)=1.6$, decreased from a value of 3.0 at 1.4 Mrad.

In the alpha radiolysis experiment, the Texaco oil was contaminated with plutonium dioxide and mixed with calcium silicate to form a paste. About 15% of the alpha energy could have been absorbed by the calcium silicate, which was considered to be radiation stable. In the first experiment the materials were contained in an initial air atmosphere in a valved stainless steel vessel. The oxygen concentration decreased from 21% to 5% over the course of the 100-day experiment. For the second experiment the vessel was evacuated and backfilled with helium. Calculations using Kazanjian's data show that as the absorbed dose increased, the G values for H_2 and total gas increased from about 1.6 to 2.8-2.9 for the first experiment. During the second experiment in vacuum, the G values decreased from about 2.3 to 1.9-2.1. The cause for thes changes in G values is unknown. Maximum values for these experiments are listed in Table 3.1-18.

Zerwekh (Zerwekh 1979[13]) measured gas generated from the alpha radiolysis of vacuum pump oil (DuoSeal) absorbed on vermiculite. Two experimental cylinders were prepared. One cylinder contained 62 mg of Pu-238 in the oxide form dispersed in 35 g of oil, which was then absorbed on 17.5 g of vermiculite. The other cylinder contained the same amounts of oil and vermiculite but only half as much PuO_2. The gases in the cylinders were sampled each time the pressure reached 15-17 psig, and then the pressure was reduced to 1 psig. The O_2 concentration was less than 0.1% at the first sampling. The gas generated was predominantly hydrogen, with a small amount of methane. Concentrations of CO and CO_2 did not exceed 0.7% (each) at any time during the experiment. The maximum G(gas) value observed was about 1.7. The initial G(gas) value observed for the sample contaminated with 32 mg of PuO_2 was about 10% higher than for the sample contaminated with 62 mg of PuO_2.

---

[48] Carroll 1963. J. G. Carroll and R. O. Bolt, "Lubricants," in <u>Radiation Effects on Organic Materials,</u> Academic Press, New York, 1963, eds. R. O. Bolt and J. G. Carroll.

G values for Cm-244 alpha and Co-60 gamma radiolysis of DuoSeal vacuum pump oil absorbed on vermiculite were measured by Bibler (Bibler 1977[25]) at various dose rates, absorbed doses, and mass fraction of oil. (Vermiculite is a hydrated magnesium-aluminum-iron silicate, and produced no H_2 when irradiated.) Usually, 2.5 ml of the oil was absorbed onto each gram of vermiculite. At low gamma dose rates (1.5-4.8E5 rad/hr), a $G(H_2)$ of 2.0 was calculated based on energy absorbed only by the organic material. The composition of the evolved gas was about 96% H_2, 3% CO_2, and 1% CH_4. Experiments conducted at a dose rate of 1.4E7 rad/hr (gamma) showed that $G(H_2)$ was directly proportional to the amount of organic material present, indicating that the energy absorbed by the vermiculite was not transferred to the organic material.

The corresponding alpha radiolysis experiment using vacuum pump oil absorbed on vermiculite contaminated with 7.2 mg Cm-244 (dose rate 1.4E6 rads/hr) resulted in a $G(H_2)$ value of 2.7. No decrease in G values with increasing absorbed dose was observed for the alpha radiolysis experiment.

Rykon lubricating grease was irradiated under vacuum and in air using a Co-60 gamma source (Kazanjian 1969[37]). The gas yield was low and consisted mostly of hydrogen, with an approximate value of $G(H_2)=1$.

Table 3.1-19 gives G values for many commercial lubricants. The maximum G values for commercial lubricants are $G(gas)=2.9$ and $G(H_2) = 2.8$.

3.1.3.14 Radiolysis of Gases

Radiolysis of the nitrogen/oxygen mixture found in air produces a small amount of ozone, as well as oxides of nitrogen (Spinks 1976[3]). Back reactions lead to an equilibrium concentration of these gases of a few ppm for ozone to a few percent for NO_2 and N_2O. The NO yields are much smaller (Kazanjian 1969[37]). When moisture is present, the main product is nitric acid, which is formed until the water vapor is exhausted (Spinks 1976[3], Kazanjian 1969[37]). G values are around 1 for nitric acid formation but vary with water concentration (Kazanjian 1969[37]).

Gaseous carbon dioxide is almost unaffected by ionizing radiation (Spinks 1976[3]), possibly due to a back reaction between CO and ozone to form CO_2 plus O_2.

3.1.4 Radiolysis of Polymers

Radiation effects in organic solids are generally similar to those for the same compound in the liquid state when allowance is made for the restricted mobility of the active species in the solid. Polymers, including materials such as polyethylene, PVC, and cellulose, are common organic solids found in CH-TRU wastes. Attachment A of this document describes the families of polymers and their use in commercial plastics. Other solids, such as solidified organic liquids, aqueous sludges, and bitumen, are discussed in Section 3.1.5. Some of the polymers discussed in this chapter occur in the liquid state at room temperature.

Table 3.1-19 — G Values for Many Commercial Lubricants

Material/ Radiation Type	G(Products)	Comments	Reference
Mineral oils			
gamma	G(gas)=2.8; G(H$_2$)=2.7; G(CH$_4$)=0.05	vacuum; highest G values for four paraffin oils	(1)
Naphthenic neutral oil			
gamma	G(gas)=0.9; G(H$_2$)=0.9	vacuum	(1)
Poly-alpha-olefin oil			
gamma	G(gas)=2.4; G(H$_2$)=2.3	vacuum	(1)
Ester lubricants			
gamma	G(gas)=2.6; G(H$_2$)=2.3; G(CH$_4$)=0.1; G(CO)~0	vacuum; highest G values for 5 oils[a]	(1)
Aromatic lubricants			
gamma	G(gas)=0.6; G(H$_2$)=0.5	vacuum; highest G values for 7 aromatic oils	(1)
Silicones			
gamma	G(gas)=2.3; G(H$_2$)=0.6 G(CH$_4$)=1.4; G(C$_2$H$_6$)=0.3	vacuum; highest G values for 2 silicones	(1)
Texaco Regal-A machining oil			
alpha (^{239}Pu)[b]	G(gas)=2.9; G(H$_2$)=2.8; G(HC)[c]=0.1	in air, before or after oxygen depletion; maximum values; mixed with calcium silicate to form a paste	(2)[b]
gamma	G(H$_2$)=2.3	vacuum; 8.4 Mrad	(3)
gamma	G(H$_2$)=1.8	500 torr O$_2$; 8.4 Mrad	(3)
gamma	G(H$_2$)=2.1	500 torr O$_2$; 1.4 Mrad	(3)
DuoSeal vacuum oil			
alpha (^{238}Pu)	G(gas)=1.7; G(H$_2$)~1.6	in air after oxygen depleted; sorbed on vermiculite	(4)
alpha (^{244}Cm)	G(gas)=2.8; G(H$_2$)=2.7; G(CO$_2$)=0.1	in air	(5)
gamma	G(gas)=2.1; G(H$_2$)=2.0; G(CO$_2$)=0.1	in air; extrapolated to zero dose	(5)
Rycon grease			
gamma	G(H$_2$)=1	vacuum or air	(3)

Refs.: (1) Arakawa 1983a[32]; (2) Kazanjian 1976[36]; (3) Kazanjian 1969[37]; (4) Zerwekh 1979[13]; (5) Bibler 1977[25].

Note: [a]Includes oils based on di-2-ethylhexyl sebacate (DOS), di-2-ethylhexyl adipate (DOA), pentaerythritol ester, tricresyl phosphate (TCP), and trioctyl phosphate (TOP).
[b]Calculated using author's data. Assumes all decay energy was absorbed by the oil (85% by weight).
[c]HC = hydrocarbons.

The controlling factor in the behavior of polymers under irradiation, as under most other environmental influences, is the chemical structure (Sisman 1963[49]). Additives to improve physical or aging properties affect changes produced by radiation.

For example, polystyrene demonstrates the stabilizing effect of a regularly recurring phenyl group on the main chain (Sisman 1963[48]). The protective effect appears to depend on closeness to the phenyl group (not more than six carbon atoms away). A part of the stability of polystyrene must be assigned to the low mobility of the molecular segments in the solid.

Radiolysis of polymers generally results in two types of reactions: (a) chain scission and (b) crosslinking. Chain scission (degradation) is the term used for breaking of main-chain bonds in polymer molecules, which results in the formation of species of lower molecular weight. When scission of the polymer is predominant, structural strength and plasticity are rapidly lost. The polymer may actually crumble to a powder. Crosslinking results in network structures that are insoluble and infusible because of increased molecular weight and size. Generally, competition occurs between the two reaction mechanisms.

In the absence of oxygen, polymers can be divided into classes according to their tendency to degrade or crosslink. Tables 3.1-20 through 3.1-22 list common polymers in order of their decreasing resistance when irradiated to net molecular-weight change for polymers that

Table 3.1-20 — Radiation Resistance of Common Polymers that Predominantly Crosslink[a]

Polymer	Characteristics
poly(vinyl carbazole)	aromatic, N in main chain
polystyrene	aromatic
analine-formaldehyde	aromatic, N in main chain
Nylon[R]	N in main chain (amide)
polymethyl acrylate	ester
polyacrylonitrile	C-N triple bond
styrene-butadiene rubber	aromatic, unsaturated
polybutadiene	unsaturated
polyisoprene	unsaturated
nitrile-butadiene rubber	C-N triple bond, unsaturated
polyethylene oxide	ether
polyvinyl acetate	ester
polyvinyl methyl ether	
polyethylene	saturated
silicone	

Ref.:   Sisman 1963[48].
Note: [a]Listed in order of decreasing resistance to net molecular-weight change.

---

[49] Sisman 1963. O. Sisman, et al., "Polymers," in <u>Radiation Effects on Organic Materials</u>, Academic Press, New York, 1963, eds. R. O. Bolt and J. G. Carroll.

Table 3.1-21 — Radiation Resistance of Common Polymers that are Borderline Between Predominant Crosslinking and Scission[a]

Polymer	Characteristics
polysulfide rubber	S in main chain
polyethylene terephthalate	aromatic, ester
polyvinyl chloride	halogen
polyvinylidene chloride	halogen
polypropylene	saturated

Ref.:   Sisman 1963[48].
Note: [a]Listed in order of decreasing resistance to net molecular-weight change.

Table 3.1-22 — Radiation Resistance of Common Polymers that Scission Predominantly[a]

Polymer	Characteristics
phenol-formaldehyde	aromatic
polymethyl methacrylate	ester
polyvinyl alcohol	alcohol
polytetrafluoroethylene	halogen
polyisobutylene	saturated
cellulose	alcohol/ether

Ref.:   Sisman 1963[48].
Note: [a]Listed in order of decreasing resistance to net molecular-weight change.

predominantly crosslink, are borderline between crosslinking and scission, or that predominantly undergo scission, respectively. Oxygen enhances the degradation of most polymers (polymethyl methacrylate is one exception).

Ether-type oxygen linkages occur in the main chain in polyethylene oxide. Cellulose is made up of glucose residues joined through acetal linkages (ether links formed between hydroxyl and carbonyl groups). Cellulose and cellulose esters and ethers undergo scission, probably resulting from a break in the acetal link rather than rupture of the glucose ring (Sisman 1963[48]).

Commercial plastics and papers contain additives that modify the properties of the base polymer in the material. In general, the additives improve the radiation stability of the commercial materials and reduce G values for flammable gases.

Additives and nonpolymer components can be divided into two categories: active and inert materials. The active additives can be subdivided into two classes: the energy-sink materials and the chemical reactants. The aromatic ring acts as an energy sink incorporated intramolecularly in the polymer. Antioxidants are usually complex aromatic amines or phenols, which should have low G values as a result of their aromatic characteristics (Sisman 1963[48]).

Scission of polymethyl methacrylate has been reduced by the addition of aromatic compounds dissolved in the polymer (Bopp 1963[50]). Protection was shown to be concentration dependent. For several of the additives, no dose dependence was found, indicating that the additives were not being radiolytically degraded, but in other cases, a dose dependence was observed. Antioxidants and aromatic stabilizers and plasticizers are frequently used to enhance durability of mechanical properties. Polyethylene and hydrocarbon rubbers normally require a small quantity of antioxidant for stability during hot processing.

From the observed G values for flammable gas [G(flam gas)], the expected relationships between the G(flam gas) values for structurally related polymers are shown in Table 3.1-23.

Table 3.1-23 — Expected Relative G(flam gas) Values for Polymers from G(flam gas) Values in Structurally Related Liquids

High
Hydrocarbon polymers containing only saturated C-C bonds
Polymers containing alcohol functional groups
Polymers containing ether functional groups
Medium
Hydrocarbon polymers containing unsaturated C-C bonds
Polymers containing ester functional groups
Low
Polymers with aromatic characteristics

Notes: High: liquid G(flam gas)=5-7; Medium: liquid G(flam gas)=2-3; Low: liquid G(flam gas)<1.

Radiolysis experiments on polymers that are discussed in this chapter are organized into the following groups, that follow the approximate order of high to low G values for flammable gas expected for synthetic polymers containing only carbon, hydrogen, nitrogen, and oxygen:

(1)   Hydrocarbon polymers containing only saturated C-C bonds (polyethylene, polypropylene, ethylene-propylene rubber, and polyisobutylene)

(2)   Polymers containing alcohol functional groups (polyvinyl alcohol and polyethylene glycol)

(3)   Polymers containing ether functional groups (cellulose, urea formaldehyde, polyoxymethylene, polypropylene oxide, and polyvinyl formal)

(4)   Hydrocarbon polymers containing unsaturated C-C bonds (polybutadiene and polyisoprene)

(5)   Polymers containing ester functional groups (polymethyl methacrylate and polyvinyl acetate)

---

[50] Bopp 1963. C. D. Bopp, et al., "Plastics," in Radiation Effects on Organic Materials, Academic Press, New York, 1963, eds. R. O. Bolt and J. G. Carroll.

(6)   Polymers with aromatic characteristics (polystyrene, polysulfone, polycarbonate, and polyethylene terephthalate and other polyesters)

Additional groupings include halogen-containing polymers and miscellaneous:

(7)   Polymers containing halogens (polyvinyl chloride, polychloroprene, chlorosulfonated polyethylene, polytetrafluoroethylene, polychlorotrifluorethylene, chlorinated polyether, rubber hydrochloride, and polyvinylidene chloride.

(8)   Miscellaneous polymers (polyamides, ion-exchange resins, and others).

The maximum G values are summarized in Table 3.1-24.

3.1.4.1 Radiolysis of Hydrocarbon Polymers Containing Only Saturated C-C Bonds

Polymers included in this section are polyethylene, polypropylene, ethylene-propylene rubber, and polyisobutylene. The polymers in this group produce hydrogen as the principal radiolysis gas. Small amounts of other hydrocarbons are formed. The maximum $G(H_2)$ value is 4.0 for polyethylene; the maximum G(flam gas) value is 4.1 for polyethylene.

3.1.4.1.1 Polyethylene

Polyethylene has the repeat unit:

$$— (CH_2) —$$

Polyethylene materials are generally divided into two classes: low-density polyethylene (LDPE) and high-density polyethylene (HDPE). Polyethylene bags and a 90-mil HDPE rigid drum liner are commonly used polyethylene products that are found in CH-TRU wastes. Unirradiated polyethylene softens in the range of 70 to 90°C, and melts to a viscous liquid at about 115 to 125°C (Spinks 1976[3]). Some of the G values and gas species produced by radiolysis of polyethylene depend on whether or not oxygen is present.

3.1.4.1.1.1   Radiolysis of Polyethylene in the Absence of Oxygen

When irradiated, polyethylene crosslinks in the absence of oxygen and evolves a considerable amount of gas (80-95% hydrogen along with other simple aliphatic hydrocarbons). The amount of volatile hydrocarbons produced by radiolysis of polyethylene increases while the hydrogen yield decreases, as the degree of chain branching increases. The evolution of hydrogen and hydrocarbon gases is accompanied both by an increase in unsaturation in the polymer chain and by an increase in crosslinking density (Chapiro 1962[10]).

Table 3.1-24 — Summary of Maximum G Values for Polymers at Room Temperature[a]

Group[b]	Polymer	$G(H_2)$	G(flam gas)	G(net gas)[c]
S-HC	polyethylene	4.0	4.1	4.1
	polypropylene	3.3	3.4	3.4
	ethylene-propylene	d	d	d
	polyisobutylene	1.6	2.4	2.4
Al	polyvinyl alcohol	3.1	3.1	3.1
	polyethylene glycol	3.5	3.5	3.5
Eth	cellulose	3.2	3.2	10.2
	cellulose nitrate	e	e	6.0[f]
	urea formaldehyde	2.4	2.8	2.8
	polyoxymethylene	2.1	5.6	14.1
	polypropylene oxide	1.1	e	e
	polyvinyl formal	e	e	5.6[f]
U-HC	polybutadiene	0.5	0.5	0.5
	polyisoprene	0.7	0.9	0.9
Est	polymethyl methacrylate	0.4	2.0	4.1
	polyvinyl acetate	0.9	1.4	1.4
Ar	polystyrene	0.2	0.2	0.2
	polysulfone	0.1	0.1	0.1
	polycarbonate	<0.1	<0.1	0.8
	polyesters	0.3	0.3	<0.8
	polyphenyl methacrylate	<0.1	<0.1	1.3
Hal	polyvinyl chloride	0.7	0.7	2.6
	polychloroprene	0.1	0.1	0.7
	chlorosulfonated polyethylene	0.3	0.3	0.6
	polychlorotrifluoro-ethylene	0	0	1.1
	polytetrafluoroethylene	0	0	<0.3
	chlorinated polyether	0.7	0.8	0.8
	rubber hydrochloride	0	0	<2.1
	polyvinylidene chloride	0	0	<2.1
M	polyamides	1.1	1.2	1.5
	ion-exchange resins	1.7	1.7	2.1

Notes: [a]Values listed are those most appropriate for CH-TRU waste, i.e., above 10 Mrad absorbed dose or for commercial rather than for pure materials

[b]S-HC = saturated hydrocarbon, Al = alcohol functional group, Eth = ether functional group, U-HC = unsaturated hydrocarbon, Est = ester functional group, Ar = aromatic character, Hal = halogen functional group, and M = miscellaneous

[c]G(net gas)is the net G value, and includes depletion of oxygen when applicable

[d]Values are intermediate between those for polyethylene and those for polypropylene

[e]Not reported

[f]Calculated on the basis of G(gas) = factor x G(gas) for polyethylene; factor=1.5 for cellulose nitrate, factor=1.4 for polyvinyl formal, and G(gas)=4.1 for polyethylene

Experimental measurements of G values from radiolysis of polyethylene in a vacuum, using reactor, gamma, accelerated electron, and x-ray radiation, are shown in Table 3.1-25 from Chapiro 1962[10]. Chapiro also plotted the data in an Arrhenius plot and found a temperature dependence with an activation energy of about 0.8 kcal/mole. From these data, Chapiro concluded that the G value for hydrogen at room temperature is about 4.1 and about 3.2 near the glass-transition temperature of -120°C. G values for volatile hydrocarbon formation were found to be usually less than 0.1. More recent experiments, discussed later in this section, have measured lower $G(H_2)$ values, and a maximum $G(H_2)$ value is established at $G(H_2)=4.0$.

One set of gamma irradiation experiments examined the effect of molecular weight on the $G(H_2)$ value for crystalline samples of polyethylene in the absence of oxygen (Mandelkern 1972[18]). A maximum value of $G(H_2)=4$ was found for the higher molecular weights studied ($2.5-4.5 \times 10^4$); a $G(H_2)$ value as low as 2.8 was found for the lowest molecular weight studied (2×10^3).

Zerwekh (Zerwekh 1979[13]) contaminated pieces of LDPE bags (0.05 mm thick) with Pu-238 dissolved in 2-M HNO_3. In other experiments, pieces of the HDPE drum liner material (2.3 mm thick, 100% cross-linked) were contaminated with Pu-238 as chloride solution. The materials were allowed to dry, then placed into stainless steel cylinders. Gases were sampled and the pressure reduced to 1 psig when the pressure in a cylinder reached 15-17 psig. Almost all of the oxygen had been depleted by the time of first sampling. Gas compositions were determined using a mass spectrometer. The majority of the gas produced from LDPE in these alpha radiolysis experiments was hydrogen. The maximum G(gas) value measured for LDPE was 1.7.

The HDPE experiment, containing 62 mg of Pu-238, never pressurized to 15 psig (even after 1,300 days). At day 674, a gas sample was taken, and consisted of 5% H_2, 17% CO_2, and 77% N_2, with very small amounts of CH_4, O_2, and CO.

Kosiewicz (Kosiewicz 1981[12]) performed alpha radiolysis experiments on samples of commercial LDPE. The composition of the generated gas was 98% H_2, 1% CH_4, and 1% CO plus CO_2. Kosiewicz has reviewed his experimental data, and has corrected the originally published G values. The measured value of G(gas) was 2.0-2.4. Typically, 50 g of the material was cut into small squares onto which the TRU contaminant (Pu-238 or Pu-239 oxide powder) was distributed. A second piece of the test material was placed over the first to contain the plutonium. The initial atmosphere inside the experimental cylinders was air at local atmospheric pressure at Los Alamos of 77 kPa (11.2 psia). The gases in the cylinders were sampled and the pressures relieved when the pressure had increased to 100 kPa over ambient pressure. The rate of gas generation was calculated from the rate of pressure change. (This method results in an underestimate of the G values for generated gases while oxygen is present inside the experimental cylinder.)

Mitsui (Mitsui 1979[51]) measured gas generation from films made from Hizex 1200P polyethylene powder containing no antioxidant that were gamma irradiated in a vacuum. Values of $G(H_2)$ obtained at different temperatures were 3.0 at 30°C, 3.2 at 50°C, 3.4 at 70°C, and 3.6 at

---

[51] Mitsui 1979. H. Mitsui and Y. Shimizu, "Kinetic Study of the Gamma Radiolysis of Polyethylene," J. Polym. Sci., Polymer Chem. Ed. 17, pp. 2805-2813, 1979.

100°C. From these data the authors calculated an activation energy of 0.6 kcal/g-mole for formation of H_2.

Table 3.1-25 — Summary of G Values for Hydrogen and Methane for Radiolysis of Polyethylene in a Vacuum

Material[a]	Type of Radiation and Irradiation Temperature[b]	$G(H_2)$	$G(CH_4)$
LDPE	reactor (70°C)	4.0	0.08
LDPE	800 keV electrons	5.0	0.9
LDPE	reactor	5.0[c]	--
LDPE	Co^{60} gamma	3.75	--
LDPE and HDPE	2 MeV electrons (-196°C to +80°C)	3.1	--
PE	Co^{60} gamma	4.0	--
PE	reactor (80°C)	7.0	--
HDPE	800 keV electrons		
Marlex-50[R]	(-170 to 34°C)	3.75	0.07
Marlex-50[R]	136°C	5.5	0.13
Marlex-50[R]	240°C	5.8	0.17
LDPE	50 kV x-rays, 13°C	2.5	0.15
LDPE	50 kV x-rays, 80°C	3.0	0.36
HDPE	50 kV x-rays, 10°C	2.8	0.03
HDPE	50 kV x-rays, 80°C	3.0	0.09

Ref.:   Chapiro 1962[10], Table IX.I.

Note: [a]LDPE = low density polyethylene; HDPE = high density polyethylene. "High pressure" = "low density"; "low pressure" = "high density"; (Wiley 1986[52]).
          [b]Liquid above about 130°C.
          [c]G(gas).

Kang (Kang 1966[53]) measured $G(H_2)$ values for polyethylene (Marlex-6002[R] film) as a function of temperature and dose. The room temperature $G(H_2)$ value varied from 3.7 (extrapolated to zero dose) to 3.3 (at an absorbed dose of 13 Mrad or more). A large increase in G value from 3.7 to 5.6 was observed when polyethylene was heated from room temperature to the liquid state at 140°C. The $G(H_2)$ values extrapolated to zero dose for the temperatures studied were: 3.68 at room temperature, 3.73 at 60°C, 3.81 at 80°C, 4.05 at 100°C, and 4.11 at 120°C. (The values at 60 and 120°C yield an activation energy of 0.4 kcal/g-mole.)

---

[52] Wiley 1986. The Wiley Encyclopedia of Packaging Technology, John Wiley & Sons, New York, 1986, ed. M. Bakker.

[53] Kang 1966. H. Y. Kang, et al., "The Radiation Chemistry of Polyethylene. IX. Temperature Coefficient of Cross-Linking and Other Effects," J. Am. Chem. Soc. 89, pp. 1980-1986, 1966.

Krasnansky (Krasnansky 1961[54]) performed gamma radiolysis experiments (6 Mrad absorbed dose) in vacuum on various commercial packaging materials. The measured value of G(gas) was reported to be between 1.6 and 3.2 for samples of both low- and high-density polyethylene. Both LDPE and HDPE generated 90-91% H_2 and 3% CO_2. The major difference in the observed gas composition was that the HDPE sample produced 6.5% CO and 0.5% propane, while the LDPE sample produced 2.5% propane, 2% ethane, and 1.5% ethene. The authors stated that the relatively high proportion of CO and CO_2 could have been a result of oxidation of the polyethylene prior to the irradiation.

Bowmer (Bowmer 1977[55]) measured G values from two types of LDPE and one type of HDPE at 30 and 150°C using gamma irradiation in a vacuum of small (5-35 mg) or large (0.5-2.5 g) samples. For the small samples, the following G values were obtained at 30°C: HDPE, G(H_2)=2.9, G(HC)=0.01; LDPE-1, G(H_2)=3.5, G(HC)=0.09; LDPE-2, G(H_2)=3.1, G(HC)=0.1. Values for G(H_2) increased by about 11% for LDPE and 53% for HDPE when the irradiation temperature was changed from 30°C to 150°C.

G(H_2) values about 25% lower were observed for the large samples, even when they were heated at 150-200°C for 60-90 minutes to allow volatiles to escape from the materials (Bowmer 1977[54]). This effect was attributed to reactions of double bonds and trapped polymer radicals with hydrogen atoms and molecules for the large samples, for which the hydrogen pressure was an order of magnitude higher than in the small samples.

G values for various gases generated from the irradiation of polyethylene when oxygen is absent or has been depleted are listed in Table 3.1-26 for experiments not reported by Chapiro (Chapiro 1962[10]). The highest value of G(H_2) in these experiments at room temperature was 4.0. The data listed in the table for Kosiewicz (Kosiewicz 1981[12]) are values that incorporate a correction for a calculational error in the original data, supplied by that author.

3.1.4.1.1.2   Radiolysis of Polyethylene in the Presence of Oxygen

In an early gamma radiolysis experiment, the change in the total gas pressure was measured for irradiation of high-density polyethylene in pure oxygen. The G value for oxygen consumption [G(-O_2)] was found to be at least twice the sum of the G values for oxygen-containing gas molecules. The rest of the oxygen was assumed to be converted to peroxides and hydroxyl groups in the polyethylene (Dole 1973a[56]).

Relative amounts of gaseous products were measured for gamma irradiation of commercial samples of LDPE and HDPE in air and in vacuum up to 5.6 Mrad absorbed dose.[57] For both

---

[54] Krasnansky 1961. V. J. Krasnansky, et al., "Effect of Gamma Radiation on Chemical Structure of Plastics," SPE (Society of Plastics Eng.) Trans. 1, pp. 133-138, 1961.

[55] Bowmer 1977. T. N. Bowmer and J. H. O'Donnell, "Nature of the Side Chain Branches in Low Density Polyethylene: Volatile Products from Gamma Radiolysis," Polymer 18, pp. 1032-1040, 1977.

[56] Dole 1973a. M. Dole, "Oxidation of Irradiated Polymers," in The Radiation Chemistry of Macromolecules, Vol. II, Academic Press, New York, 1973, ed. M. Dole.

[57] Bersch 1959. C. F. Bersch, et al., "Effect of Radiation on Plastic Films," Modern Packaging 32, pp. 117-168, l959.

low- and high-density polyethylene, greater amounts of products per gram of material were obtained for irradiation in air than in vacuum (a ratio of 2.0 for LDPE and 1.4 for HDPE). The corresponding ratios of hydrogen production in air versus in vacuum were 1.8 for LDPE and 1.2 for HDPE. The LDPE produced 1.6 times the gaseous products of the HDPE in air, and 1.2 times the products of HDPE in vacuum. The second most abundant product for irradiation in air was carbon dioxide. All of the oxygen in the sample tubes was consumed for both types of polyethylene films. The experiments were repeated for an absorbed dose of 0.93 Mrad. Radiolysis of the LDPE exposed to air generated only carbon dioxide, while the $G(H_2)$ value for HDPE was higher than at 5.6 Mrad. These results contradict trends observed in most other radiolysis experiments on polyethylene and lower the credibility of Bersch's data on polyethylene.

Arakawa[58] performed gamma radiolysis of low- and high-density polyethylene in the presence of oxygen to examine the effect of antirad additives. For the pure polymers, hydrogen and carbon dioxide were the primary gases evolved. For LDPE, values of $G(H_2)=3.3$ and $G(CO_2)=1.3$ were obtained; for HDPE, values of $G(H_2)=3.2$ and $G(CO_2)=4.1$ were measured. The addition of propyl-fluoranthene, an antirad additive, reduced the $G(H_2)$ values by 15-30%. Radiolysis of an ethylene-propylene copolymer showed that the $G(H_2)$ value was independent of the amount of oxygen present.

Table 3.1-26 — G Values for Polyethylene (Oxygen Depleted or Absent)

Radiation Type	G(Products)	Comments	Reference
gamma	$G(H_2)=6.2$ (max)	no oxygen, 130°C	(1)
gamma	$G(H_2)=2.8-4.0^a$	no oxygen, room temp	(1)
alpha (^{238}Pu)	$G(gas)=1.7$ (90-98% H_2)	oxygen depleted from initial air atmosphere; room temp	(2)
alpha (^{238}Pu)	$G(gas)=2.0-2.4$ (98% H_2, 1% CH_4, 1% $CO_2 + CO$)	oxygen depleted from initial air atmosphere; 20°C; corrected data	(3)
gamma	$G(H_2)=3.0$	vacuum; 30°C	(4)
gamma	$G(H_2)=3.2$	vacuum; 50°C	(4)
gamma	$G(H_2)=3.4$	vacuum; 70°C	(4)

---

[58] Arakawa 1983b. K. Arakawa, et al., "Radiation-Induced Oxidation of Polymers. Effect of Antioxidant and Antirad Agent on Oxygen Consumption and Gas Evolution," J. Polym. Sci.: Polym. Chem. Ed. 21, 1983 (preprint).

Table 3.1-26 — G Values for Polyethylene (Oxygen Depleted or Absent) (Concluded)

Radiation Type	G(Products)	Comments	Reference
gamma	$G(H_2)=3.6$	vacuum; 100°C	(4)
gamma	$G(H_2)=3.7$	vacuum; 25°C to 60°C	(5)
gamma	$G(H_2)=3.8$	vacuum; 80°C	(5)
gamma	$G(H_2)=4.05$	vacuum; 100°C	(5)
gamma	$G(H_2)=4.11$	vacuum; 120°C	(5)
gamma	1.6 G(gas) 3.2 (92% H_2, 2-8% $CO+CO_2$, 0-6% HC)[b]	vacuum; room temp	(6)
gamma	$G(H_2)=2.9$;$G(HC)=0.01$[b]	HDPE; vacuum; 30°C	(7)
gamma	$G(H_2)=4.5$;$G(HC)=0.03$[b]	HDPE; vacuum; 150°C	(7)
gamma	$G(H_2)=3.5$;$G(HC)=0.09$[b]	LDPE; vacuum; 30°C	(7)
gamma	$G(H_2)=3.9$;$G(HC)=0.18$[b]	LDPE; vacuum; 150°C	(7)
gamma	$G(H_2)=3.1$;$G(HC)=0.11$[b]	LDPE; vacuum; 30°C	(7)
gamma	$G(H_2)=3.5$;$G(HC)=0.36$[b]	LDPE; vacuum; 150°C	(7)

Refs.:   (1) Mandelkern 1972[18]; (2) Zerwekh 1979[13]; (3) Kosiewicz 1981[12] (data corrected by that author); (4) Mitsui 1979[50]; (5) Kang 1966[52]; (6) Krasnansky 1961[53]; (7) Bowmer 1977[54].

Notes: [a]Values were 3.9, 3.4, 3.6, 4.0, 3.9, 3.2, 3.4, and 2.8, depending on the molecular weight and degree of crystallinity.
[b]HC = hydrocarbons.

Fourteen samples of polyethylene sheet used for bags (presumably LDPE) were gamma irradiated in the presence of oxygen (Kazanjian 1969[37]). Hydrogen was the only significant product, and a value of $G(H_2)$=2.2 was obtained. Oxygen consumption occurred; a value of $G(-O_2)$=8.1 was measured.

Kazanjian (Kazanjian 1976[36]) obtained radiolysis data during the time period when oxygen was being depleted for alpha radiolysis of LDPE bags contaminated with Pu-238 oxide powder (9.0 mg of Pu-238 to 3.6 g of material). The experiment was conducted for a total of 267 days, starting with an air atmosphere. The G(gas) and $G(H_2)$ values calculated from these data show sharp decreases with time from G(gas)=1.7 to G(gas)=0.7 and $G(H_2)$=1.3 to $G(H_2)$=0.7 after 36 days of exposure. This decrease in G values could have been caused by (1) a very strong dependence of the G values on absorbed dose, (2) much higher G values in the presence of oxygen, or (3) experimental error. The oxygen initially present had been completely depleted by day 21 (5.8E22 eV absorbed energy). The $G(-O_2)$ value was about 3. Only small quantities of CO or CO_2 were detected, with maximum G values of 0.1 and 0.3, respectively.

Polyethylene and polyethylene oxide were gamma irradiated in oxygen in the presence of carbon tetrachloride (Jellinek 1983[15]). In both cases, chloroform was evolved. The G(scission) values increased for polyethylene from about 10 in oxygen to about 32 in oxygen mixed with carbon tetrachloride.

G values for various gases evolved from the irradiation of polyethylene when oxygen is present are listed in Table 3.1-27. The maximum measured value of $G(H_2)$ at room temperature when oxygen was present was 3.5, with the exception of Bersch's (Bersch 1959[56]) anomalous measurement of $G(H_2)$=5.4.

3.1.4.1.1.3   Hydrogen G Value for Polyethylene

Even at elevated temperature, almost all of the reported $G(H_2)$ values for polyethylene are less than 4.0. All of the $G(H_2)$>4 values that were found in the technical literature are for experiments conducted prior to 1962. The credibility of the experiments is questionable, as noted in the discussion, or the data were obtained using reactor radiation, where calculation of the absorbed dose is questionable. The available $G(H_2)$ data from alpha radiolysis experiments are in the 1.6-2.4 range. It is concluded that $G(H_2)$=4.0 and G(flam gas)=4.1 for polyethylene provide upper bound $G(H_2)$ and G(flam gas) values for commercial polyethylene materials.

Table 3.1-27 — G Values for Polyethylene (Oxygen Present)

| Radiation Type	G(Products)	Comments	Reference
gamma	$G(-O_2)=10.0$, $G(H_2O)=2.5$, $G(CO)=1.0$, $G(CO_2)=0.6$	30°C; only measured gases containing oxygen	(1)
gamma	$G(H_2)=2.2$; $G(-O_2)=8.1$	LDPE bags; room temp	(2)
gamma	$G(gas)=5.3$; $G(H_2)=3.5$; $G(-O_2)=14.0$; $G(CO_2)=1.3$; $G(CO)=0.6$; $G(CH_4)=0.1$	LDPE; room temp; pure material; 20 Mrad	(3)
gamma	$G(gas)=3.9$; $G(H_2)=2.8$ $G(-O_2)=7.4$; $G(CO_2)=0.9$; $G(CO)=0.2$	LDPE; room temp; contained antirad additive; 20 Mrad	(3)
gamma	$G(gas)=8.6$; $G(H_2)=3.2$ $G(-O_2)=29$; $G(CO_2)=4.1$; $G(CO)=1.3$	HDPE; room temp; pure material; 20 Mrad	(3)
gamma	$G(gas)=5.6$; $G(H_2)=2.2$; $G(-O_2)=12.1$; $G(CO_2)=2.8$; $G(CO)=0.6$	HDPE; room temp; contained antirad additive; 20 Mrad	(3)
gamma	$G(gas)=6.4$; $G(H_2)=5.4$; $G(CO_2)=0.6$; $G(CO)=0.1$[a]	LDPE; room temp; commercial material; 5.6 Mrad	(4)
gamma	$G(gas)=3.9$; $G(H_2)=3.1$; $G(CO_2)=0.6$[b]	HDPE; room temp; commercial material; 5.6 Mrad	(4)
gamma	$G(gas)=2.7$; $G(H_2)=0$; $G(CO_2)=2.7$	LDPE; room temp; commercial material; 0.93 Mrad	(4)
gamma	$G(gas)=8.5$; $G(H_2)=4.0$; $G(CO_2)=3.4$; $G(CO)=1.1$	HDPE; room temp; commercial material; 0.93 Mrad	(4)
alpha (Pu-238)	$G(gas)=1.7$; $G(H_2)=1.3$; $G(-O_2)=3$; $G(CO_2)=0.3$; $G(HC)=0.1$[b]	LDPE bags; room temp; water vapor also detected.	(5)

Refs.:   (1) Dole 1973a[55], (2) Kazanjian 1969[37], (3) Arakawa 1983b[57]; (4) Bersch 1959[56]; (5) Kazanjian 1976[36].

Notes: [a]Water vapor, oxygenated hydrocarbons and unsaturated hydrocarbons also were detected.

[b]Calculated from author's data; HC = hydrocarbons; maximum G values are given.

3.1.4.1.2 Polypropylene

Polypropylene has the repeat unit:

$$—— (CH_2\ CH) ——$$
$$|$$
$$CH_3$$
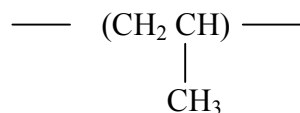
Polypropylene is termed isotactic if the methyl groups are on the same side of the chain, and atactic if the arrangement is random. The isotactic polymer is the more common commercially (Bopp 1963[49]).

Polypropylene may be manufactured into fibers (Herculon[R] is one example) or into molded shapes. Ful-Flo[R] filters used at the RFETS for filtering liquid wastes are made of polypropylene.

The maximum G values for hydrogen and total flammable gas are $G(H_2)=3.3$ and G(flam gas)=3.4.

3.1.4.1.2.1   Radiolysis of Polypropylene in the Absence of Oxygen

Hydrogen is the major gas produced from the gamma irradiation of polypropylene in a vacuum at room temperature, as shown in Table 3.1-28. Traces of methane and carbon monoxide are also found (Schnabel 1963[59]).

Polypropylene and other polymers have been gamma irradiated in the presence of carbon tetrachloride or chloroform in order to modify the polymer (Ramanan 1981[60]). When polypropylene fibers were immersed in carbon tetrachloride, generated HCl gas was collected by cooling the irradiated ampoules to 77 K and then breaking them under distilled water. The HCl released was estimated by following the change in pH. High yields of HCl were measured (Ramanan 1981[60]).

3.1.4.1.2.2   Radiolysis of Polypropylene in the Presence of Oxygen

Hegazy (Hegazy 1981a[61]) measured a G value for oxygen consumption of about 4 for oxidative radiolysis of isotactic polypropylene (PP) film at ambient temperature and 150 torr initial oxygen pressure (which approximates the oxygen partial pressure in ambient air). The sum of the G values for production of oxygen containing gases (CO_2 and CO) was less than 0.3, suggesting that most of the consumed oxygen had combined with polymer chains.

Table 3.1-29 lists G values for radiolysis of polypropylene in the presence of oxygen.

---

[59] Schnabel 1963. W. Schnabel and M. Dole, "Radiation Chemistry of Isotactic and Atactic Polypropylene. I. Gas Evolution and Gel Studies," J. Phys. Chem. 67, pp. 295-299, 1963.

[60] Ramanan 1981. G. Ramanan, et al., "Gamma Irradiation of Polypropylene Fibers in the Presence of Carbon Tetrachloride," J. Appl. Polym. Sci. 26, pp. 1439-1451, 1981.

[61] Hegazy 1981a. E. A. Hegazy, et al., "Radiation-Induced Oxidative Degradation of Isotactic Polypropylene," J. Appl. Polym. Sci. 26, pp. 1361-1372, 1981.

Table 3.1-28 — G Values for Polypropylene (Oxygen Absent)

Radiation Type	G(Products)	Comments	Reference
gamma	G(gas)=2.4-2.9 G(H_2)=2.3-2.8, G(CH_4)=0.1	vacuum; room temp; actactic and isotactic PP	(1)
gamma	G(gas)=3.0; G(H_2)=2.9; G(CH_4)=0.1	vacuum; 10 Mrad; room temp; isotactic PP film	(2)
gamma	G(gas)=3.5; G(H_2)=3.3; G(CH_4)=0.1	vacuum; 10 Mrad; room temp; isotactic PP powder	(2)
gamma	G(gas) 3.2; (95% H_2, 1% CO_2, 1% CO, 3% CH_4)	vacuum; room temp; film	(3)
gamma	G(gas)=3.8; G(H_2)=3.2; G(CH_4)=0.1[a]	vacuum; 0.1 MGy (10 Mrad); room temp; stabi- lized isotactic PP film	(4)
gamma	G(gas)=3.0; G(H_2)=2.8; G(CH_4)=0.1[a]	vacuum; 0.2 MGy (20 Mrad); room temp; stabi- lized isotactic PP film	(4)

Refs.:   (1) Geymer 1973[62]; (2) Hegazy 1981a[61]; (3) Krasnansky 1961[53]; (4) Hegazy 1986[63].

Note: [a]Author's G values for gas constituents do not add up to his G(gas) value.

---

[62] Geymer 1973. D. O. Geymer, "Radiation Chemistry of Substituted Vinyl Polymers. Polypropylene," in The Radiation Chemistry of Macromolecules, Vol. II, Academic Press, New York, 1973, ed. M. Dole.

[63] Hegazy 1986. E. A. Hegazy, et al., "Radiation Effect on Stabilized Polypropylene," Radiat. Phys. Chem. 27, pp. 139-144, 1986.

Table 3.1-29 — G Values for Polypropylene (Oxygen Present)

Radiation Type	G(Products)	Comments	Reference
gamma	G(gas)=3.0; G(H$_2$)=2.5; G(CH$_4$=0.1; G(CO)=0.1; G(CO$_2$)=0.2, G(-O$_2$)=4.2	150 torr O$_2$ initial pressure; 20 Mrad; room temp; isotactic PP film	(1)
gamma	G(gas)=2.9; G(H$_2$)=2.6; G(CH$_4$)=0.1; G(CO)=0.1 G(CO$_2$)=0.2; G(-O$_2$)=5.0[a]	150 torr O$_2$ initial pressure; 0.2 MGy (20 Mrad); stabilized isotactic PP film	(2)

Refs.:   (1) Hegazy 1981a[61]; (2) Hegazy 1986[63].

Note: [a]Author's G values for gas constituents do not add up to his G(gas) value.

G(scission) values increased for polypropylene from about 5 in oxygen to about 33 in oxygen mixed with carbon tetrachloride vapor (Jellinek 1983[15]); chloroform was evolved.

3.1.4.1.3 Ethylene-Propylene Rubber

G values for ethylene-propylene rubbers (EPR, EPDM) are close to G values for polyethylene and polypropylene (Arakawa 1983b[57], Arakawa 1987[64], Decker 1973[65]).

3.1.4.1.4 Polyisobutylene

The repeat unit for polyisobutylene is:

$$
\begin{array}{c}
CH_3 \\
| \\
-\!\!-(CH_2C)-\!\!- \\
| \\
CH_3
\end{array}
$$
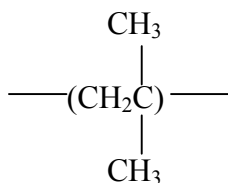
Bohm (Bohm 1982[66]) summarized several radiolysis experiments conducted on polyisobutylene. The composition of the gas evolved from polyisobutylene during gamma radiolysis experiments conducted in vacuum was approximately 95% hydrogen and methane, with the remainder composed of isobutylene and other fragments. Values of G(H$_2$)=1.3-1.6 and G(CH$_4$)=0.5-0.8 have been reported for gamma radiolysis experiments. A G(gas) value of only 0.9 was measured for mixed reactor radiation. Gas production in polyisobutylene is attributed to the fracture of side chains.

---

[64] Arakawa 1987. K. Arakawa, "Oxygen Consumption and Gas Evolution by Radiation-Induced Oxidation in Ethylene-Propylene-Diene Terpolymers," J. Polym. Sci.: Part A: Polym. Chem. 25, pp. 1713-1716, 1987.

[65] Decker 1973. C. Decker, et al., "Aging and Degradation of Polyolefins. III. Polyethylene and Ethylene-Propylene Copolymers," J. Polym. Sci.: Polym. Chem. Ed. 11, pp. 2879-2898, 1973.

[66] Bohm 1982. G. Bohm, "Radiation Chemistry," Rubber Chem. Tech. 55, pp. 575-666, 1982.

3.1.4.2 Radiolysis of Polymers Containing Alcohol Functional Groups

Polymers containing alcohol functional groups include polyvinyl alcohol and polyethylene glycol.

Gas generation from polyvinyl alcohol that was gamma irradiated in a vacuum at 12°C, -78°C, and -196°C was measured by Okada (Okada 1967[67]). Over 99% of the gas evolved was hydrogen. G(gas) values were measured to be 3.1 at 12°C, 2.0 at -78°C, and 1.5 at -196°C (maximum activation energy = 0.6 kcal/g-mole). [The corresponding G(gas) value at 25°C would be unchanged from the value at 12°C because of the low activation energy for gas generation.]

Polyethylene glycol (commercial name, Carbowax), having a molecular weight of 6,000, was irradiated using Co-60 gamma rays in a vacuum at room temperature (Nitta 1959[68]). The maximum G(gas) value measured was 3.5. The gas consisted primarily of hydrogen with some methane, acetylene, and carbon monoxide. Experiments conducted on a 4,000-molecular-weight Carbowax at various temperatures showed only a minor change in the G(gas) value from -196°C to 70°C (2.4 to 2.1) (Nitta 1961b[69]).

3.1.4.3 Radiolysis of Polymers Containing Ether Functional Groups

Polymers containing ether functional groups include cellulose, urea formaldehyde, polyoxymethylene, polypropylene oxide, and polyvinyl formal. The polymers in this group generate gases that contain oxygen, even when irradiated in a vacuum. Another polymer in this group is polyethylene oxide. G values for cellulose and urea formaldehyde have been shown to be strongly dependent on the absorbed dose, at least for gamma radiolysis. For absorbed doses greater than 10 Mrad, the maximum value of $G(H_2)$ is 3.2 for cellulose. One of the polymers in this family (polyoxymethylene) generates other flammable gases that cause the G(flam gas) value to exceed 4.1, and another (polyvinyl formal) has a measured G(gas) that is 1.4 times the G(gas) value for polyethylene. For this reason, polyoxymethylene and polyvinyl formal are permitted in CH-TRU wastes only in trace amounts.

3.1.4.3.1 Cellulose

Cellulose is a linear macromolecule consisting of monomeric units with the empirical formula $C_6H_{10}O_5$. Cellulosic materials commonly present in the CH-TRU wastes include paper, cloth, wood, and Benelex[R], which is composed of wood fiber plus phenolic resin. Other commercial materials that contain cellulosics include cellophane, cellulose acetate (used to manufacture Rayon[R], molded items, paints, coatings), and ethyl cellulose (used to manufacture paints, molded items).

---

[67] Okada, 1967. T. Okada, "Radiolysis of Poly (Vinyl Alcohol)," in Annual Report of the Japanese Assn. for Radiation Research on Polymers, Vol. 8, pp. 33-43, 1967.

[68] Nitta 1959. I. Nitta, et al., "Irradiation Effects of Co-60 Radiation on Polyethylene Glycol," in Annual Report of the Japanese Assn. for Radiation Research on Polymers, Vol 1., pp. 320-328, 1959.

[69] Nitta 1961b. I. Nitta, et al., "Effect of Radiation on Polyethylene Glycol," in Annual Report of the Japanese Assn. for Radiation Research on Polymers, Vol. 3, AEC-tr-6372, pp. 445-453, 1961.

Natural cotton cellulose, having lattice type I, is about 70-80% crystalline and 20-30% amorphous. The other commercially important form of cellulose has lattice Type II, which is commonly referred to as mercerized cotton, and usually consists of regenerated cellulosic materials, paper, and wood products. Cellulose lattice type II is less ordered than cellulose lattice type I and is usually about 60% crystalline.[70] Differences between these types of cellulose may cause differences in the amount and composition of radiolysis gases.

Authors differ as to whether the presence of oxygen affects the radiation chemistry of cellulose. The results of experiments conducted both in the absence and presence of oxygen are summarized at the end of this section.

Sulfite cellulose, dried to a constant weight at 378 K, was irradiated using Co-60 in sealed, evacuated ampules of known volume, as well as in a medium of air and argon (Ershov 1986[71]). The experimental data for each of the media were not reported. The authors stated that the irradiation medium did not appreciably affect the rate at which the products were generated. The dose rate was 20 kGy/h (2 Mrad/h). The volume of gas generated was determined according to the pressure in the ampules. For total absorbed doses from 100-300 kGy (10-30 Mrad) and room temperature, a value of G(gas)=10.2 (31% H_2, 59% CO_2, 9% CO, and 1% CH_4) was observed. At liquid nitrogen temperature of 77 K, a value of G(gas)=6.0 (48% H_2 and 52% CO_2) was observed.

Concentrations of radiolytically generated carboxyl, carbonyl, and aldehyde groups were measured using thin-layer chromatography for samples of powdered native cellulose that were gamma irradiated in air and in a vacuum (Dziedziela 1984[72]). No gases were measured. Some of the samples were outgassed for four days before irradiation. In all cases, yields of functional groups increased linearly with absorbed dose, indicating constant G values. For each functional group, the samples irradiated in a vacuum display two straight-line portions, with the low-dose part of the graph coincident with the straight line found for irradiation in oxygen. The authors attribute this effect to traces of oxygen from air still left in the samples, in spite of outgassing, and conclude that formation of functional groups occurs according to the same mechanism as in air up to the exhaustion of oxygen absorbed on the surface of the cellulose. For each functional group, the slope of the second line is much lower, indicating a lower G value in the absence of oxygen. The ratio of the G value in air to the G value in a vacuum for each of the functional groups was equal to 3:1.

---

[70] Arthur 1970. J. C. Arthur, Jr., "Graft Polymerization onto Polysaccharides," in Advances in Macromolecular Chemistry 2, Academic Press, London, 1970, ed. by W. M. Pasika, pp. 1-87.

[71] Ershov 1986. B. G. Ershov, et al., "Mechanism of the Radiation Chemical Conversions of Cellulose," translated from Khimiya Vysokikh Energii 20, pp. 142-147, 1986.

[72] Dziedziela 1984. W. M. Dziedziela and D. Kotynska, "Functional Groups in Gamma-Irradiated Cellulose," Radiat. Phys. Chem. 23, pp. 723-725, 1984.

Cotton cellulose was irradiated under oxygen or nitrogen atmosphere with Co-60 in the dose range 0-130 kGy (0-13 Mrad) (Bludovsky 1984[73]). The yields of the nongas radiolytic products were measured. The samples were analyzed immediately after irradiation to eliminate any effects of reactions occurring after the irradiation. No differences were observed in the qualitative composition of the products between those produced in nitrogen versus those produced in oxygen atmosphere. In all cases the presence of oxygen increased the yields of radiolytic products. The ratios of the yields varied from nearly 1 up to 1.7. The ratio of the chain scission G value in oxygen to the chain scission G value in nitrogen was 1.3.

Arthur (Arthur 1970[70]) reports the G values for gamma irradiation of cotton cellulose I at absorbed doses of 14E20-42E20 eV/g (22-67 Mrad) in vacuum, oxygen, air, and nitrogen atmospheres. The three measurements in a nitrogen atmosphere at different doses show a total absorbed dose effect, with the G(gas) value reduced from 4.5 at 22E20 eV/g (35 Mrad) to 4.0 at 38E20 eV/g (61 Mrad). All of the difference in G values comes from changes in the G(CO) value with absorbed dose. [The ratio of the G values for carbon-containing gases generated in air or oxygen to the values for gases generated in nitrogen at low dose is about 1.4, which agrees with the data of Bludovsky (Bludovsky 1984[73]). However, significant differences were seen in the gas composition.]

In one experiment (Dalton 1963[74]), samples of purified American cotton weighing 0.1-2 g were outgassed at 60°C, and electron irradiation was conducted in a vacuum at ambient temperature. The evolved gas consisted almost entirely of hydrogen. A G value near 2 was obtained at (relatively) high doses (75-400 Mrad), while the G value near 6 was obtained at 0.1 Mrad. A G value of about 3 was obtained at 5 Mrad. As discussed in Section 2.3.1.5, the dose experienced by plastics or paper irradiated by Pu-238 or Pu-239 alpha particles is at least 22-23 Mrad. Therefore, the G value of 6 measured for 0.1 Mrad absorbed dose is not applicable to CH-TRU wastes.

Purified American cotton samples were also irradiated in a vacuum without outgassing, and a gas mixture of 82% H_2, 5% CO, and 13% CO_2 was obtained. A value for G(gas) was not reported for that experiment (Dalton 1963[74]). The difference in the gas composition was attributed to oxidation processes involving residual oxygen dissolved in the material.

Kazanjian (Kazanjian 1976[36]) measured gas consumption and generation from Pu-238 alpha irradiation of both wet and dry Kimwipes[R] (paper tissues). The Kimwipes[R] were cut up, and the plutonium oxide powder was added to the material in increments and the mixture shaken or stirred in a container. The wet Kimwipes[R] contained 11.9 g of water to 4.8 g of paper tissues. The initial atmosphere was air.

---

[73] Bludovsky 1984. R. Bludovsky, et al., "The Influence of Oxygen on the Radiolytical Products of Cellulose," J. Radioanal. Nucl. Chem. Letters 87, pp. 69-80, 1984.

[74] Dalton 1963. F. L. Dalton, et al., "Gas Yields from Electron-Irradiated Cotton Cellulose," Nature 200, pp. 862-864, 1963.

G values were calculated using Kazanjian's data for both dry and wet Kimwipes[R]. In both cases, the G values decreased as the dose increased. G(gas) decreased from about 1.1 initially to about 0.5 at 6.0E23 eV for dry Kimwipes[R], and from about 0.6 initially to about 0.3 at 4.5E23 eV absorbed dose for wet Kimwipes[R]. All of the G values were significantly lower for wet Kimwipes[R] compared to the values for dry Kimwipes[R]. This is attributed to some of the alpha decay energy being absorbed by water rather than by the cellulose.

The composition of the evolved gas from wet Kimwipes[R] was richer in hydrogen than for dry Kimwipes[R] (73% vs. 55%) with smaller concentrations of hydrocarbons. The graphs of moles of evolved gas versus time remained approximately linear until oxygen was depleted, then began to decrease in slope. This could be caused by an absorbed dose effect or lower G values in the absence of oxygen.

Zerwekh (Zerwekh 1979[13]) performed alpha radiolysis experiments on two different mixtures of cellulosic materials, one dry mixture and one wet mixture. The dry mixture consisted of paper wipes, paper tissues, embossed paper towel with polyethylene backing, cheesecloth, and cotton laboratory smock material. The final composition of the evolved gas from the dry mixture contained about 60% H_2, 25% CO_2, plus a small amount of CH_4 [estimated from Figure 10 of Zerwekh (Zerwekh 1979[13])]. The initial composition of the evolved gas contained higher concentrations of CO_2, up to a maximum of about 50%. The wet mixture consisted of damp cheesecloth contaminated with Pu-238 as chloride solution. The final composition of the evolved gas contained about 55% H_2 and 35% CO_2 [estimated from Figure 13 of Zerwekh (Zerwekh 1979[13])]. The initial composition of the evolved gas contained about 85% H_2 and 5% CO_2. The high initial concentration of H_2 may indicate that radiolysis of the water dominated early in the experiment, but radiolysis of the cheesecloth dominated near the end of the experiment (1,000 days). G(gas) values for dry cellulosic materials fell to about half of their initial values after about 750 days (1.2E25 eV absorbed energy).

In one of Zerwekh's experiments, gas generation from two identical cylinders was compared, where one cylinder was sampled and the pressure relieved at 15 psig, and the other one sampled and the pressure relieved only when the pressure reached 100 psig. From a plot in Zerwekh 1979[13], the rate of gas pressure buildup in the low-pressure cylinder was about twice the rate of gas pressure buildup in the high-pressure cylinder. The evolved gases had the same composition, but water was also found in the high-pressure cylinder.

Bibler (Bibler 1976[19]) conducted alpha radiolysis experiments using Cm-244 solution (5-M nitric acid), which was absorbed by paper tissue that was dried and folded to surround the Cm-244 deposit. The evolved gas collected at constant pressure consisted of 49% H_2, 36% CO_2, and 15% CO. The value of G(gas) decreased to G(gas)=0.6 at 2.5E23 eV absorbed dose. A value of G(gas)=1.9 was measured during the first five hours of one experiment, with the first measurement taken at about 4E19 eV absorbed dose. Three different concentrations of Cm-244, up to a factor of 4 difference, were used in the experiments, and all observations appeared to fit the same curve of G(gas) versus absorbed dose.

Kosiewicz (Kosiewicz 1981[12], corrected) measured G(gas) values of about 1.9 at very low absorbed dose and about 1.5 from paper at a total absorbed dose of about 5E23 eV. The G(gas)

value decreased to half its initial value after an absorbed dose of about 2.5E24 eV. The radiolytic gas composition was about 61% H_2, 26% CO_2, and 13% CO and nearly independent of total absorbed dose. Oxygen was initially present, but was rapidly depleted. Water vapor was not measured. Typically, 50 g of the material was cut into 1.5- to 3.0-cm squares onto which the finely divided plutonium dioxide (either Pu-239 or Pu-238) was distributed. A second piece of the test material was placed over the first to sandwich the plutonium particles. The sample vessel was a stainless steel cylinder instrumented with a pressure gauge or transducer. The gases in the cylinders were sampled and the pressures relieved when the pressure had increased to 100 kPa over the ambient pressure.

One set of experiments on paper was conducted in an argon atmosphere to measure the initial G(gas) value (at low dose) (Kosiewicz 1981[12], corrected). Data points started at absorbed dose as low as about 0.5E23 eV, for 0.016 Ci of Pu-238 per g of waste. A G(gas) value of 1.4 was estimated. A similar experiment with air as the initial atmosphere reached a maximum G(gas)=1.4 at about 4E23 eV. The first measured value of G(gas) was about 30% lower than the maximum value, probably because oxygen depletion was occurring.

Zerwekh (Zerwekh 1979[13]) measured the rate of gas evolution from mixed cellulosic materials at -13°C, 20°C, and 55°C to be 2.59 kPa/day, 3.45 kPa/day, and 4.93 kPa/day, respectively. The composition of the evolved gas was generally independent of temperature (although the experiment at 55°C also generated a gaseous component of molecular weight about 60). After corrections for thermal expansion of the gas, the activation energy calculated from these data by this author ranges from 0.8 kcal/mole (-13°C, 20°C) to 1.3 kcal/g-mole (20°C, 55°C).

Kosiewicz (Kosiewicz 1981[12]) also performed experiments to measure the temperature dependence of radiolysis of cellulosic materials, represented by paper. High dose rates (640E5 nCi/g) were used so that radiolysis would produce the majority of the gas and other potential modes of gas generation, such as thermal degradation, could be neglected. The rate of gas evolution was measured for experiments conducted at both 20 and 70°C. The higher temperature experiment initially had a rate of gas evolution that was 70% greater than for the lower temperature experiment. The difference in the rate of gas evolution was observed to decrease with increasing dose. At 180E23 eV absorbed dose, the difference had decreased to about 30%. (The activation energy for a 70% or 30% increase would be 2.1 kcal/g-mole or 1.0 kcal/g-mole, respectively.) The composition of the evolved gases was not significantly different for the two experiments.

Table 3.1-30 presents a summary of G values for several cellulosic materials when oxygen is absent or has been depleted. Table 3.1-31 presents the results of irradiation experiments conducted when oxygen is present.

Table 3.1-30 — G Values for Cellulosic Materials (Oxygen Absent or Depleted)

Material/Radiation Type	G(Products)	Comments	Reference
Sulfite cellulose			
gamma	G(gas)=10.2; G(H$_2$)=3.2 (31% H$_2$, 59% CO$_2$, 9% CO,1% CH$_4$)	vacuum, air, or oxygen; room temp; 10-30 Mrad	(1)
Cotton cellulose I			
gamma	G(gas)=3.7; G(H$_2$)=1.3 (35% H$_2$, 22% CO, 43% CO$_2$)	vacuum; room temp; 33E20 eV/g (53 Mrad)	(2)
gamma	G(gas)=4.5; G(H$_2$)=1.0 (22% H$_2$, 56% CO, 22% CO$_2$)	nitrogen; room temp; 22E20 eV/g (35 Mrad)	(2)
gamma	G(gas)=4.1; G(H$_2$)=1.0 (24% H$_2$, 51% CO, 24% CO$_2$)	nitrogen; room temp; 32E20 eV/g (51 Mrad)	(2)
gamma	G(gas)=4.0; G(H$_2$)=1.0 (25% H$_2$, 50% CO, 25% CO$_2$)	nitrogen; room temp; 38E20 eV/g (61 Mrad)	(2)
American cotton			
electrons	G(gas) 6; G(H$_2$) 6	vacuum + outgassing; room temp; 0.1 Mrad	(3)
electrons	G(gas)~3; G(H$_2$)~3	vacuum + outgassing; room temp; 5 Mrad	(3)
electrons	G(gas)~2.5; G(H$_2$)~2.5 (98% H$_2$, 1% CO, 0.4% CO$_2$)	vacuum + outgassing; room temp; 25 Mrad	(3)
electrons	G(gas)=2.0	vacuum + outgassing; room temp; 75-100 Mrad	(3)
electrons	G(gas) not reported (82% H$_2$, 5% CO, 13% CO$_2$)	vacuum w/o outgassing; room temp; 48 Mrad	(3)
Mixed cellulosics (dry)			
alpha (Pu-238)	G(gas)~0.5; G(H$_2$)~0.3 (60% H$_2$, 25% CO$_2$, 15% misc)a	oxygen depleted from initial air atmosphere; room temp; after 1,000 days of exposure	(4)
Cheesecloth (wet)			
alpha (Pu-238)	G(gas)~1.3; G(H$_2$)~0.7 (55% H$_2$, 35% CO$_2$, 10% misc)a	oxygen depleted from initial air atmosphere; room temp; after 1,000 days of exposure	(4)
Paper			
alpha (Pu-238, -239)	G(gas) 1.5; G(H$_2$) 0.9 (61% H$_2$, 26% CO$_2$, 13% CO)	oxygen depleted from initial air atmosphere; room temp; 3E23eV for 50 g material; corrected data	(5)
Paper			
alpha (Pu-238, -239),	G(gas)=1.44	argon; room temp; corrected data	(5)

Refs.:   (1) Ershov 1986[71]; (2) Arthur 1970[70]; (3) Dalton 1963[74]; (4) Zerwekh 1979[13]; (5) Kosiewicz 1981[12], corrected.

Note: ^{a}Estimated from author's data.

Table 3.1-31 — G Values for Cellulosic Materials (Oxygen Present)

Radiation Type	G(Products)	Comments	Reference
Cotton cellulose I			
gamma	G(gas)=6.2; G(H$_2$)=1.2 (19% H$_2$, 27% CO, 55% CO$_2$)	oxygen; 42E20 eV/g (67 Mrad); room temp	(1)
gamma	G(gas)=5.5; G(H$_2$)=0.7 (13% H$_2$, 60% CO, 27% CO$_2$)	air; 14E20 eV/g (22 Mrad); room temp	(1)
Mixed cellulosics (dry)			
alpha (Pu-238)	G(gas)~1.6; G(H$_2$)~0.6 (40% H$_2$, 40% CO$_2$; (20% misc)[b]	air; room temp first measurement that was taken	(2)
Cheesecloth (wet)			
alpha (Pu-238)	G(gas)~1.6; G(H$_2$)~1.4 (85% H$_2$, 5% CO$_2$, 10% misc)[b]	air; room temp; first measurement that was taken	(2)
Kimwipes[R] (dry)			
alpha (Pu-238)	G(gas)=1.1; G(H$_2$)=0.6 (55% H$_2$, 9% CO, 32% CO$_2$, 3% HC)[a]	air; room temp	(3)
Kimwipes[R] (wet)			
alpha (Pu-238)	G(gas)=0.6; G(H$_2$)=0.4 (73% H$_2$, 5% CO, 22% CO$_2$)[a]		(3)
Paper tissue			
alpha (Cm-244)	G(gas) 1.9; G(H$_2$) 0.9 (49% H$_2$, 36% CO$_2$, 15% CO)	air; room temp	(4)

Refs.:   (1) Arthur 1970[70]; (2) Zerwekh 1979[13]; (3) Kazanjian 1976[36]; (4) Bibler 1976[19].
Note: [a]Calculated from author's data.
          [b]Estimated from author's data.

3.1.4.3.2 Urea-Formaldehyde

Urea-formaldehyde has been examined as a possible solidification medium for power reactor wastes (Colombo 1977[75]). Gamma radiolysis experiments in vacuum were conducted on a urea-

---

[75] Colombo 1977. P. Colombo and R. M. Neilson, Jr., "Properties of Radioactive Wastes and Waste Containers, Quarterly Progress Report July-September 1976," Brookhaven National Laboratory Associated Universities, Inc., BNL-NUREG-50617, 1977.

formaldehyde formulation using Borden Casco-Resin 2[R] that was catalyzed with a 25 wt% solution of sodium bisulfate in water. Measured values of G(gas) and $G(H_2)$ were strongly dose-dependent: at 0.1 Mrad, G(gas)=21 and $G(H_2)$=4.8; at 1 Mrad, G(gas)=8.6 and $G(H_2)$=6.5; at 10 Mrad, G(gas)=2.8 and $G(H_2)$=2.4, and at 100 Mrad, G(gas)=2.0 and $G(H_2)$=1.3

3.1.4.3.3 Polyoxymethylene

Krasnansky (Krasnansky 1961[53]) measured gas evolution from plastic films exposed to gamma radiation to determine their order of radiation stability. Polyacetyl (polyoxymethane) had a value of G(gas) 8.1 for an absorbed dose of 6 Mrad. For that polymer, the gas consisted of 69% CO_2, 8% H_2, 2% methanol, 15% methane, and 6% dimethyl ether. (The minimum G value for all flammable gases would be about 5.6.)

Dole (Dole 1973d[76]) reported analysis (by gas chromatography) of the gas evolved from electron irradiation of polyoxymethylene at 30°C and 0.1 torr pressure. In addition to hydrogen [$G(H_2)$=1.7], formaldehyde [G(HCHO)=4], methane [$G(CH_4)$=0.1], carbon monoxide [G(CO)=0.1] and various oxygen-containing gases were detected. Gases excluded were oxygen, carbon dioxide, C_2 hydrocarbons, methanol, dimethyl ether, and butyl alcohol.

Sobashima (Sobashima 1959[77]) measured G values for gas generation from polyoxymethylene (Delrin 500X from DuPont) exposed to gamma irradiation in vacuum at room temperature. The G(gas) value measured was 14.1 at low doses. The gas composition was the following: 15% H_2, 67% CO_2, 1% CO, 10% CH_4, 1% methyl formate, 2% methyl ether, and 3% other. The maximum G value for flammable gases or vapors would be 4.4. The G(gas) values measured at different irradiation temperatures were G(gas)=6.1 at -196°C, G(gas)=9.4 at 20°C, and G(gas)=22.7 at 50°C (Nitta 1961a[78]).

3.1.4.3.4 Polypropylene Oxide

Polypropylene oxide is more susceptible to degradation under irradiation than polypropylene, and yields less hydrogen (Geymer 1973[62]). For irradiation in vacuum, measured G values for H_2, CH_4, and CO were 1.0, 0.1, and 0.3 for atactic polypropylene oxide, and 1.1, 0.1, and 0.4 for isotactic polypropylene oxide, respectively. G values for other oxygen-containing gases were not discussed. Measured G(OH) values were 1.8 for atactic polypropylene oxide and 1.7 for isotactic polypropylene oxide, compared to a value of 4.5 for polyoxymethylene.

3.1.4.3.5 Polyvinyl Formal

Polyvinyl formal was one of the many commercial plastics irradiated by Bopp and Sisman using the Oak Ridge National Laboratory (ORNL) Graphite Reactor (see Section 3.1.4.8.4 for more

---

[76] Dole 1973d. M. Dole, "Polyoxymethylene," in <u>The Radiation Chemistry of Macromolecules</u>, Vol. II, Academic Press, New York, 1973, ed. M. Dole.

[77] Sobashima 1959. S. Sobashima, et al., "Irradiation Effects on Polyoxymethylene," in <u>Annual Report of the Japanese Assn. for Radiation Research on Polymers</u>, Vol. 1, AEC-tr-6231, pp. 329-338, 1959.

[78] Nitta 1961a. I. Nitta, et al., "Effect of Radiation on Polyoxymethylene," in <u>Annual Report of the Japanese Assn. for Radiation Research on Polymers</u>, Vol. 3, AEC-tr-6372, pp. 437-443, 1961.

details). The value of G(gas) measured for polyvinyl formal was 1.4 times the value of G(gas) measured for polyethylene.

3.1.4.4 Radiolysis of Hydrocarbon Polymers Containing Unsaturated C-C Bonds

Polybutadiene and polyisoprene (Latex[R]) contain unsaturated C-C bonds. The G values for polybutadiene (and copolymers) and polyisoprene (Latex[R]) are given in Table 3.1-32.

Table 3.1-32 — G Values for Polybutadiene (and Copolymers) and Polyisoprene

Material/Radiation Type	G(Products)	Comments	Reference
Polybutadiene and copolymers			
gamma, electrons, and reactor	G(gas) 0.5; $G(H_2+CH_4)$ 0.5	vacuum or air; room temp	(1)
Latex[R] gloves alpha (Pu-238)	G(gas)=0.4;$G(H_2)$=0.4	oxygen depleted; room temp	(2)
Isoprene[R] gloves alpha (Pu-238)	G(gas)<0.9;$G(H_2)$<0.7[a]	oxygen depleted; room temp	(3)

Refs.:   (1) Bohm 1973[79]; (2) Kazanjian 1976[36]; (3) Zerwekh 1979[13].
Note: [a]Estimated from author's data.

3.1.4.5 Radiolysis of Polymers Containing Ester Functional Groups

Polymers containing ester functional groups include polymethyl methacrylate (PMMA) and polyvinyl acetate. The maximum measured value of G(flam gas) for these two polymers is 2.0.

3.1.4.5.1 Polymethyl Methacrylate (PMMA)

Polymethyl methacrylate has the repeat unit:

$$CH_3$$
$$|$$
$$—— (CH_2C) ——$$
$$|$$
$$O=COCH_3$$
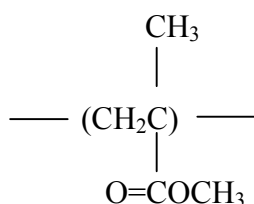
Two common materials made of PMMA are Plexiglas[R] and Lucite[R].

---

[79] Bohm 1973. G. G. A. Bohm, "Radiation Chemistry of Elastomers," in The Radiation Chemistry of Macromolecules, Vol. II, Academic Press, New York, 1973, ed. M. Dole.

Because PMMA has a high glass-transition temperature (about 106°C), free radicals created within the material at lower temperatures are trapped and can persist days after irradiation. Gases generated from the free radicals are also trapped, and the larger molecular components can be released only by heating the sample (near the glass transition temperature) (Dole 1973c[80]). Even in the absence of oxygen, chain scission dominates. The melting temperature decreases as the absorbed dose increases, from about 140°C at zero dose to about 110°C at 100 Mrad absorbed dose (Jellinek 1978[11]).

G values for PMMA measured using nonalpha irradiation (probably in a vacuum) differ among authors. The main volatile products formed are H_2, CO_2, CO, CH_4, propane, and methyl methacrylate monomer. The individual G values vary depending on temperature and the type of ionizing radiation; and G(gas)<2 (Chapiro 1962[10], Bolt 1963[14]).

Busfield (Busfield 1982[81]) summarized measurements of volatile products from PMMA that was gamma irradiated in vacuum at 30°C. The highest G value for volatile products was 4.1, which included gases and highly volatile liquids including methyl alcohol, dimethyl ether, methyl formate, dimethoxymethane, and methyl acetate. The highest G value for all flammable gases or vapors was 2.2.

Kazanjian (Kazanjian 1976[36]) measured gas generated from alpha radiolysis of 12.8 g of shredded Plexiglas[R] contaminated with 1 g of Pu-239 oxide powder, initially in an air atmosphere. After 100 days of exposure, about half of the remaining gas was replaced with helium, and the experiment continued for an additional 347 days. Calculations were made of G values as functions of absorbed dose using Kazanjian's data. G(gas) values appeared to be gradually decreasing with time from about 2 initially to 1.0 at 450 days (5.0E23 eV absorbed dose) with no apparent differences between the two phases of the experiment. The value of $G(H_2)$ fell from 0.4 initially to less than 0.2 in the same time period. The initial G value for oxygen consumption was $G(-O_2) \sim 3.8$. The oxygen was considerably reduced after 19 days but was not completely exhausted.

G values for PMMA are summarized in Table 3.1-33.

---

[80] Dole 1973c. M. Dole, "Radiation Chemistry of Substituted Vinyl Polymers. Polymers that Primarily Degrade on Irradiation," in The Radiation Chemistry of Macromolecules, Vol. II, Academic Press, New York, 1973, ed. M. Dole.

[81] Busfield 1982. W. K. Busfield, et al., "Radiation Degradation of Poly (Styrene-co-Methylmethacrylate). 2. Protective Effects of Styrene on Volatile Products, Chain Scission and Flexural Strength," Polymer 23, pp. 431-434, 1982.

Table 3.1-33 — G Values for PMMA

Radiation Type	G(Products)	Comments	Reference
alpha (Pu-238)	very low	oxygen depleted; room temp; Lucite[R]	(1)
alpha (Pu-239)	G(gas)=2.0 (23% H_2, 42% CO, 23% CO_2, 11% CH_4, 2% HC)[a]	oxygen depleted; room temp; Plexiglas[R]	(2)
gamma	G(gas)=4.1; G(H_2)=0.3; G(CO)=1.3 G(CH_4)=0.6; G(CO_2)=0.8; G(vapors)=1.1[c]	vacuum; 30°C; PMMA; worst case of three experiments	(3)
various	G(gas) < 2	vacuum; room temp; PMMA	(4), (5)

Refs.: (1) Zerwekh 1979[13]; (2) Kazanjian 1976[36]; (3) Busfield 1982[81]; (4) Chapiro 1962[10], (5) Bolt 1963[14].

Note: [a]Calculated from author's data; HC = hydrocarbons.

[c]Vapors include methyl alcohol, dimethyl ether, methyl formate, methyl acetate, and dimethoxymethane.

3.1.4.5.2 Polyvinyl Acetate

Measurements of G values for gas generation from polyvinyl acetate at 20 Mrad absorbed dose from gamma irradiation in a vacuum are reported by Graessley (Graessley 1973[82]). The value of G(gas) obtained was 1.4. The evolved gas consisted of 64% H_2, 34% CH_4, and 2% CO_2 + CO. Small amounts of acetic acid also were evolved but were not detected in the mass spectrometer analysis.

3.1.4.6 Radiolysis of Polymers with Aromatic Characteristics

Polymers having aromatic characteristics include polystyrene, polysulfone, polycarbonate, polyethylene terephthalate and polyesters, and others. These polymers are characteristically low [G(gas) is usually less than 0.8]. Other polymers in this group, for which scant radiolysis data are available, include polyurethane, analine-formaldehyde, styrene-butadiene rubber, phenol-formaldehyde, phenolic resin, epoxy resin, and polyimides.

---

[82] Graessley 1973. W. W. Graessley, "Polyvinyl Acetate," in The Radiation Chemistry of Macromolecules, Vol. II, Academic Press, New York, 1973, ed. M. Dole.

3.1.4.6.1 Polystyrene

The repeat unit for polystyrene is:

$$——(CH_2CH)——$$
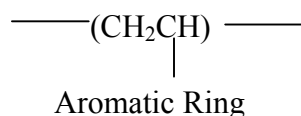
Aromatic Ring

One common material composed of polystyrene is Styrofoam[R]. Polystyrene contains aromatic rings and exhibits the low G values and relatively strong LET effects characteristic of aromatic compounds [$G(H_2)$ is 0.2 or less] (Parkinson 1973[83]). Production of very small amounts of methane and benzene by radiolysis has also been observed. Bersch (Bersch 1959[56]) measured $G(H_2)$=0.1 and G(gas)=0.3 for gamma radiolysis of polystyrene in air and G(gas)<0.1 in a vacuum. Busfield (Busfield 1982[81]) reported an even lower value of $G(H_2)$=0.03.

The values of G(scission) increased for polystyrene from about 10 in oxygen to about 45 in oxygen mixed with carbon tetrachloride (Jellinek 1983[15]).

3.1.4.6.2 Polysulfone

G values for polysulfone have been reported for gamma and electron irradiation of several different materials (Giori 1984[84]). The value of G(gas) ranged from 0.01 to 0.1. Hydrogen, methane, carbon monoxide, and carbon dioxide composed most of the gas generated.

3.1.4.6.3 Polycarbonate

Krasnansky (Krasnansky 1961[53]) measured gas evolution from commercial polycarbonate powder exposed to gamma radiation in vacuum. The value of G(gas) calculated from his data was less than 0.8. Most of the gas was carbon dioxide or carbon monoxide. The value of $G(H_2)$ was less than 0.012.

Samples of polycarbonates were irradiated in vacuum at room temperature using a Co-60 source.[85] The measured value of G(gas) was 0.9, 97% of which was carbon monoxide or carbon dioxide.

3.1.4.6.4 Polyethylene Terephthalate and Other Polyesters

Commercial polyesters include Dacron[R] and Mylar[R]. Polyethylene terephthalate (PET) is the polymer on which these materials are based. Oxygen atoms appear in the backbone of the molecule as well as in side branches. One or more aromatic rings occur in the backbone or side

---

[83] Parkinson 1973. W. W. Parkinson and R. M. Keyser, "Radiation Chemistry of Substituted Vinyl Polymers. Polystyrene and Related Polymers," in The Radiation Chemistry of Macromolecules, Vol. II, Academic Press, New York, 1973, ed. M. Dole.

[84] Giori 1984. C. Giori and T. Yamauchi, "Effects of Ultraviolet and Electron Radiations on Graphite-Reinforced Polysulfone and Epoxy Resins," J. Appl. Polym. Sci. 29, pp. 237-249, 1984.

[85] Amamiya 1959. A. Amamiya and S. Sekigawa, "Irradiation Effects on Polycarbonates," in Annual Report of the Japanese Assn. for Radiation Research on Polymers, Vol 1., pp. 469-476, 1959.

branches; consequently, low G values are expected. Table 3.1-34 lists G values for several polyesters. The hydrogen chloride reported by Krasnansky (Krasnansky 1961[53]) that was evolved from polyester III was believed to have resulted from the breakdown of the coating on that material.

3.1.4.6.5 Other Polymers Containing Aromatic Rings

Polyphenyl methacrylate produced G values for gamma irradiation in vacuum that were determined to vary from 1.3 for a high molecular weight polymer to 0.7 for a low molecular weight polymer (Raghunath 1983[86]). The majority of the gas in each case was CO. The value of $G(H_2)$ was less than 0.1. Scission of the ester group appeared to be the most important degradation process.

Table 3.1-34 — G Values for Polyesters

Material/Radiation Type	G(Products)	Comments	Reference
PET			
gamma, electrons	G(gas)=0.1-0.3; $G(H_2)$=0.01-0.02 ($CO+CO_2$=83-90%)		(1)
gamma	G(gas)=0.3; $G(H_2)$<0.1	air; room temp; 5.6 Mrad	(2)
gamma	G(gas)<0.1	vacuum; room temp; 5.6 Mrad	(2)
Polyester I			
gamma	G(gas) 0.2; $G(H_2)$<0.1 (34% H_2, 56% CO_2, 6% HC, 4% other[a])[b]	vacuum; room temp; 6 Mrad	(3)
Polyester II			
gamma	G(gas) 0.8; $G(H_2)$<0.1 (18% H_2, 82% CO_2)[b]	vacuum; room temp; 6 Mrad	(3)
Polyester III			
gamma	G(gas) 0.2; $G(H_2)$=0.3 (60% H_2, 24% CO_2, 16% CH_4+HCl)	vacuum; room temp; 6 Mrad	(3)

Refs.:   (1) Turner 1973[87]; (2) Bersch 1959[56]; (3) Krasnansky 1961[53].

Notes: [a]Other = methyl chloride.
          [b]Calculated from author's data.

---

[86] Raghunath 1983. S. Raghunath, et al., "Effect of Co-60 Gamma-Rays on Polyphenyl Methacrylate Obtained by Gamma-ray Irradiation," Radiat. Phys. Chem. 22, pp. 1023-1027, 1983.

[87] Turner 1973. D. T. Turner, "Radiation Chemistry of Some Miscellaneous Polymers. Polyethylene Terephthalate," The Radiation Chemistry of Macromolecules, Vol. II, Academic Press, New York, 1973, ed. M. Dole.

3.1.4.7 Radiolysis of Polymers Containing Halogens

Polymers containing halogen atoms include polymers that also contain hydrogen (e.g., polyvinyl chloride, polychloroprene, chlorosulfonated polyethylene, and polyvinylidene chloride) and polymers that contain no hydrogen (i.e., polytetrafluroethylene and polychlorotrifluoroethylene).

For the polymers containing both halogen and hydrogen atoms, the G values for production of possible gas species, such as HCl, H_2, etc., are strongly dependent on the plasticizers and stabilizers added to the base polymers. Where G values for commercial materials have been measured, these are used for the maximum G values applicable to CH-TRU wastes, rather than G values for the pure polymers. Maximum values are $G(H_2)$=0.7-0.8 and $G(gas)$=3.2.

3.1.4.7.1 Polyvinyl Chloride (PVC)

The repeat unit for polyvinyl chloride (PVC) is:

$$\overline{}\ (CH_2CH) \ \overline{}$$
$$|$$
$$Cl$$
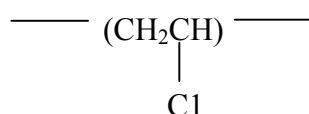
PVC is found in many of the CH-TRU wastes as a packaging material, such as the 10-mil PVC box liner or 10-mil PVC O-ring bag. Various forms of PVC also appear in combustible wastes. PVC and its copolymers are used in electrical components, in Tygon[R] tubing, and in Pylox[R] gloves.

The conventional technique for commercial PVC heat stabilization is the addition of a stabilizer or a combination of stabilizers to the polymer. Most PVC heat stabilizers are organometallic salts containing calcium, zinc, barium, cadmium, or lead. Most traditional stabilizers function as hydrogen chloride acceptors, which reduce the catalytic effect of evolved HCl gas (Kelen 1983[88]).

Brittle polymers such as PVC are usually plasticized to produce flexible films and containers. Tricresyl phosphate, the original plasticizer for commercial PVC, has been replaced by phthalic acid esters, such as dioctyl phthalate (DOP). Plasticizers may be external plasticizers, such as the phthalates, or internal plasticizers that form copolymers with vinyl chloride, such as vinyl acetate, ethylene, or methyl acrylate. Citric acid esters, epoxidized oils, and dioctyl adipate are substituted for DOP for food packaging materials. Low molecular weight polyesters are also used as nonvolatile plasticizers (Wiley 1986[50]).

A typical Ca/Zn-stabilized PVC compound for food packaging films consists of 100 parts PVC, 30-70 parts plasticizer, 2-3 parts Ca/Zn stabilizer, 1-2 parts epoxidized soybean oil, and 0.1-0.2 part stearic acid. Electrical insulation and jacketing for wires and cables are generally made from PVC formulations that are stabilized by lead (Kelen 1983[88]).

---

[88] Kelen 1983. T. Kelen, <u>Polymer Degradation</u>, Van Nostrand Reinhold Company, New York, 1983.

The strong effect of the plasticizers and stabilizers on the radiolysis of PVC is demonstrated by the differences in the composition of the radiolysis gas, which varies from 85% H_2, to 83% HCl, to 70% CO_2 depending on the specific formulation and whether oxygen is present.

3.1.4.7.1.1 <u>Radiolysis of PVC in the Absence of Oxygen</u>

Values of G(HCl) up to 13 at room temperature, increasing to 23 at 70°C, have been reported for electron irradiation in a vacuum of unstabilized Geon 101[R] PVC powder (Miller 1959[89]). The evolved gas was collected in a stainless-steel irradiation cell. The PVC powder was outgassed for several hours while the temperature was raised, then the sample was irradiated to doses of 5-20 Mrad. Following irradiation, the cell was allowed to stand for one hour at room temperature, allowing diffusion of the HCl out of the PVC particles to a constant pressure reading. Cooling of the evolved gas into a liquid nitrogen trap showed that at least 95% was condensable and that little or no hydrogen (noncondensable) was formed. The author assumed all of the condensable product was HCl, which is a reasonable assumption for pure PVC that had been thoroughly outgassed before irradiation. For irradiation at 70°C, the irradiation cell was immediately quenched in liquid nitrogen to cool the sample to room temperature in less than 5 minutes, to avoid collecting gas resulting from purely thermal degradation. G values were also measured at low temperatures, down to -145°C. Very little change in the G value occurred between 0 and -145°C. The minimum value of G(HCl) measured was 5.6.

Lawton (Lawton 1961[90]) performed similar experiments involving electron irradiation of Geon 101[R] PVC powder and measured values of G(H_2)=0.4 and G(HCl)=0.5 for irradiation at -196°C. He reported a chain dehydrochlorination process that occurred at temperatures as low as -70°C and concluded that Miller's value (Miller 1959[89]) of G(HCl)=5.6 at -196°C was not the true radiation yield.

The gas yield from irradiation of samples of commercial PVC depends strongly on the materials added to the PVC resin, and even on the solvent used to dissolve the resin. Szymanski (Szymanski 1976[91]) reports a value of G(HCl)=8-9 for films prepared by dissolving PVC resin in tetrahydrofuran (THF) and a value of G(HCl)=4-5 for films prepared using cyclohexanone as the solvent. The HCl yield was measured by determining the chloride concentration. Films containing various concentrations of three different stabilizers were prepared using THF, and irradiated with Co-60 gamma radiation at room temperature to a dose of about 3 Mrad. (It is unclear whether oxygen was present during the irradiation.) Addition of 2-3% p-terphenyl or Tinuvin P[R] decreased the value of G(HCl) to 5. Addition of 1% Epidian 5[R] (an epoxy resin) decreased the value of G(HCl) to about 0.3.

---

[89] Miller 1959. A. A. Miller, "Radiation Chemistry of Polyvinyl Chloride," <u>J. Phys. Chem. 63</u>, pp. 1755-1759, 1959.

[90] Lawton 1961. E. J. Lawton and J. S. Balwit, "Electron Paramagnetic Resonance Study of Irradiated Polyvinyl Chloride," <u>J. Phys. Chem. 65</u>, pp. 815-822, 1961.

[91] Szymanski 1976. W. Szymanski, et al., "Increase of Poly (Vinyl Chloride) Stability Towards Ionizing Radiation. II. Effects of Epidian Addition in PVC Films. III. Effects of the Addition of Ethylene Glycol Bis-beta-Aminocrotonate in PVC Foils," <u>Nukleonika 21</u>, pp. 277-283, 1976.

Additional experiments were performed using PVC films formulated with 18% DOP (plasticizer) and 1-5% metallic soaps as stabilizers. Values of G(HCl) ranged from 1.7 to nearly 0, with most in the range of 0.3-0.7 (Szymanski 1976[91]). For three of the films, no HCl was detected. The average value of G(HCl) for 19 formulations of plasticized, stabilized PVC was $G(HCl)_{avg}$=0.54. A value of G(HCl) for 18% DOP plasticizer but no stabilizer was G(HCL)=3.1.

Gamma radiolysis of pure PVC powder and plasticized PVC film was studied with and without oxygen present to determine the effects of additives and oxygen on the gases generated (Hegazy 1981b[92]). (His experiments conducted with oxygen present are discussed in Section 3.1.4.7.1.2.) Oxygen consumption and gas evolution were measured by gas chromatography and mass spectrometry. The PVC film contained PVC, DOP, epoxy oil, and Ca-Zn stearate compounds in the ratio of 100/50/5/2. The dose rate was 1 Mrad/hr, and the experiments were conducted at room temperature. In the absence of oxygen, the amount of hydrogen produced as a function of absorbed dose remained linear (constant G value) up to about 80 Mrad absorbed dose. CO_2 and CH_4 production began to decrease at about 30 Mrad absorbed dose.

For pure PVC powder irradiated to 10 Mrad absorbed dose in a vacuum, G values obtained were G(gas)=8.4, $G(H_2)$=0.2, and G(HCl)=8.2. At 60 Mrad absorbed dose, the values were G(gas)=5.2, $G(H_2)$=0.2, and G(HCl)=4.9. The plasticized/stabilized PVC film displayed much lower G values than the pure PVC powder and produced different ratios of gases depending on the absorbed dose. For PVC film irradiated in a vacuum to 10 Mrad absorbed dose, the following G values were obtained: G(gas)=0.3, $G(H_2)$=0.1, and G(HCl)=0.03. At 21 Mrad absorbed dose, the values were G(gas)=0.3, $G(H_2)$=0.2, and G(HCl)=0.03; while at 60 Mrad absorbed dose, the values were G(gas)=1.7, $G(H_2)$=0.2, and G(HCl)=1.4. The increases in G(gas) and G(HCl) with absorbed dose were attributed to degradation of the stabilizers and DOP above 20 Mrad absorbed dose (Hegazy 1981b[92]), probably through reaction with radiolysis products.

Rigid PVC films containing stabilizers and anti-oxidants in the range of 0.2-0.5 wt% were gamma irradiated in a vacuum and at various oxygen pressures (Zahran 1985[93]). For a rigid PVC film in a vacuum irradiated to 10 Mrad absorbed dose, G values obtained were G(gas)=2.9, $G(H_2)$=0.2, and G(HCl)=2.7; while in a vacuum at 20 Mrad absorbed dose, the values were G(gas)=2.6, $G(H_2)$=0.2, and G(HCl)=2.4 (Zahran 1985[93]). Oxygen consumption and gas evolution were analyzed using gas chromatography.

Arakawa[94] measured gas evolution and oxygen consumption of PVC gamma irradiated at room temperature in a vacuum and in an oxygen environment and used gas chromatography to determine the gas composition. Three samples containing various plasticizers and stabilizers

---

[92] Hegazy 1981b. E. A. Hegazy, et al., "Radiation-Induced Oxidative Degradation of Poly (vinyl Chloride)," J. Appl. Polymer Sci. 26, pp. 2947-2957, 1981.

[93] Zahran 1985. A. H. Zahran et al.,"Radiation Effects on Poly (vinyl chloride) -- I. Gas Evolution and Physical Properties of Rigid PVC Films," Radiat. Phys. Chem. 26, pp. 25-32, 1985.

[94] Arakawa 1986. K. Arakawa, et al., "Radiation-Induced Gas Evolution in Chlorine-Containing Polymer. Poly (vinyl chloride), Chloroprene Rubber, and Chlorosulfonated-Polyethylene," Radiat. Phys. Chem. 27, pp. 157-163, 1986.

were tested. One sample (model formulated PVC) contained PVC, DOP, tribasic lead sulfate, stearic acid, and clay #33 in the proportions 100/50/5/1/10. The other two samples were of unknown composition but were considered to be representative of insulating materials used for electric cables. All three samples had G(gas) values of 1.4 or less at 20 Mrad absorbed dose. The gas generated from each of the two unknown samples contained 50% or more CO_2. CO_2 generation has also been noted in the thermal degradation of PVC stabilized using basic lead carbonates (Michell 1986[95]).

From these experiments it appears that the plasticizers added to flexible PVC films, in addition to the stabilizers, have a major effect in reducing the G(HCl) value.

Modified PVC, containing 6.5-15.7 mole % N,N-dimethyl dithiocarbamate or 8.3-17.5 mole% N,N-diethyl dithiocarbamate, was irradiated with gamma rays from Co-60 at room temperature under vacuum (Nakagawa 1976[96]). The evolved gases were measured and analyzed with a mass spectrometer. G values were much lower [G(gas)=0.1-0.3] than those measured for pure PVC, and little (if any) HCl was detected. Major peaks in the mass spectra of the gaseous products were measured at mass 28 (CO_2), mass 32, and mass 60. No peaks were reported at mass 2 (H_2) or mass 16 (CH_4).

Kazanjian (Kazanjian 1969[37]) measured radiolysis products from nine samples of PVC bag material used at the RFETS irradiated using a Co-60 gamma source. The measured hydrogen G value was G(H_2)=0.11. The tubes containing the irradiated PVC were opened under water, shaken, and titrated with 0.04-N NaOH to determine the yield of water soluble acid. The acid yield, most of which was HCl, gave G(HCl)=0.21.

Kazanjian (Kazanjian 1976[36]) measured radiolytic gas generation from PVC O-ring bags attached to glove box ports at the RFETS. The bags were cut into pieces and contaminated with PuO_2 powder. Two samples were prepared, one contaminated with 1 g of Pu-239 oxide, the other contaminated with 13.5 mg of Pu-238 oxide. The initial atmosphere was air in each experiment. In both cases, the primary gas produced was hydrogen. Measurements were continued in the Pu-239 experiment after the vessel was partially evacuated to estimate the void volume. No HCl was detected using a mass spectrometer (possibly due to reactions with the stainless steel test vessel or the inlet of the instrument).

G values for hydrogen were calculated from Kazanjian's data for both the Pu-239 and Pu-238 experiments. Taken as a whole, the data are consistent with a value of G(H_2) of about 0.6. At doses above 3E23 eV (about 100 days of exposure), the Pu-238 G(H_2) value appeared to be decreasing slightly.

---

[95] Michell 1986. E. W. J. Michell, "True Stabilization: A Mechanism for the Behavior of Lead Compounds and Other Primary Stabilizers Against PVC Thermal Dehydrochlorination," J. Vinyl Technology 8, pp. 55-65, 1986.

[96] Nakagawa 1976. T. Nakagawa and Y. Fujiwara, "Radiation Protection of Poly (vinyl chloride) by N,N-Dialkyl Dithiocarbamate Substitution," J. Appl. Polym. Sci. 20, pp. 753-763, 1976.

Kosiewicz (Kosiewicz 1979[97], Kosiewicz 1981[12]) measured gas generated by alpha radiolysis of PVC Pylox[R] gloves. The contaminant, in the form of finely divided powders of PuO_2 (either Pu-239 or Pu-238), was distributed onto squares of the material 2.5-3 cm on a side. A second piece of the test material was placed over the first to sandwich the plutonium. Gases in the cylinders were sampled and the pressures relieved when the pressure had increased to 100 kPa over the ambient pressure of about 77 kPa. The gas composition observed was 85% hydrogen with small amounts of methane, carbon dioxide, and carbon monoxide. No HCl was detected, but it may have been absorbed by the steel cylinder walls or inlet of the measuring instrument. The (Kosiewicz 1981[12], corrected) values of G(gas) were about 0.8 at 20°C for a dose rate of 5E22 eV/day and about 6.3 at 70°C for a dose rate of 3E20 eV/day. The G(gas) value appeared to be increasing with time (Kosiewicz 1979[97]), perhaps indicating depletion of stabilizers or plasticizers was occurring.

Zerwekh (Zerwekh 1979[13]) performed similar experiments using PVC and vinyl Bakelite[R] 0.3-mm thick bag materials used to package wastes removed from glove boxes. The materials were cut into pieces approximately 5 x 5 cm and contaminated with Pu-238 dissolved in 2-M HNO_3. The solution was placed on the materials with a medicine dropper in as uniform a pattern as possible. The solution was allowed to evaporate, and then the test materials were loaded into all-glass systems used to reduce absorption of any HCl generated. Orsat-type gas burets were used to collect the gases produced. The maximum radionuclide contamination level was 62 mg of heat-source grade Pu on 52.5 g of waste (specific activity of about 14 Ci/g). Vinyl Bakelite[R] produced 100 cm^3 of gas in 69 days. The gas contained 4% H_2, 2% CO, 0.9% CO_2, and 0.2% CH_4. No Cl or HCl was detected in the gas using a mass spectrometer, but wet chemical analysis found 0.06% Cl. The PVC bagout material produced only 10 cm^3 of gas in 335 days, containing 0.6% H_2, 0.1% CO, 1.0% CO_2, and 0.1% CH_4. The balance of each sample was oxygen-depleted air. [The final O_2 concentrations were not reported, so the $G(H_2)$ and G(gas) values cannot be calculated from Zerwekh's data.]

G values for pure PVC irradiated in a vacuum are listed in Table 3.1-35. HCl is the primary gas produced. Table 3.1-36 lists G values for plasticized or stabilized PVC irradiated in a vacuum or after oxygen depletion.

In most instances, $G(H_2)$ 0.3 at room temperature. The highest value of $G(H_2)$ reported was 0.7 for alpha irradiation. A bounding value at room temperature, therefore, appears to be $G(H_2)_{max} = 0.7$.

---

[97] Kosiewicz 1979. S. T. Kosiewicz, et al., "Studies of Transuranic Waste Storage Under Conditions Expected in the Waste Isolation Pilot Plant (WIPP), Interim Summary Report October 1, 1977--June 15, 1979," Los Alamos National Laboratory, LA-7931-PR.

Table 3.1-35 — G Values for Pure PVC (in Vacuum)

Radiation Type	G(Products)	Comments	Reference
electrons	G(gas)=G(HCl)=13	30°C	(1)
electrons	G(gas)=G(HCl)=23	70°C	(1)
gamma	G(HCl)=4-9	room temp; 3 Mrad; only HCl detectable by measurement technique	(2)
gamma	G(gas)=8.4; G(H_2)=0.2; G(HCl)=8.2	room temp; 10 Mrad	(3)
gamma	G(gas)=8.8; G(H_2)=0.3; G(HCl)=8.0	room temp; 20 Mrad	(4)

Refs.:   (1) Miller 1959[89]; (2) Szymanski 1976[91]; (3) Hegazy 1981b[92]; (4) Arakawa 1986[94].

Table 3.1-36 — G Values for Plasticized and/or Stabilized PVC (Oxygen Absent or Depleted)

Material/Radiation Type	G(Products)	Comments	Reference
Films w/stabilizers gamma	G(HCl)=0.3-5	vacuum; room temp; 3 Mrad; only HCl detectable by measurement technique	(1)
gamma	G(gas)=2.9; G(H_2)=0.2; G(HCl)=2.7	vacuum; room temp; 10 Mrad	(2)
Films w/stabilizers and plasticizers gamma	G(HCl)=0-1.7 (most 0.3-0.7);G(HCl)$_{avg}$=0.54	vacuum; room temp; 3 Mrad; only HCl detectable by measurement technique	(1)
gamma	G(gas)=0.3; G(H_2)=0.1; G(HCl)=0.03[a]; G(CO)=0.1; G(CO_2)=0.1	vacuum; room temp; 10-20 Mrad	(3)
gamma	G(gas)=1.4; G(H_2)=0.1; G(HCl)=1.2 (8% H_2, 83% HCl, 5% CO, 3% CO_2, 1.2% HC)[b] G(gas)=0.7; G(H_2)=0.2; G(HCl)=0.1 (26% H_2, 14% HCl, 8% CO, 50% CO_2, 1.4% HC)[b] G(gas)=1.1; G(H_2)=0.2; G(HCl)=0.1 (15% H_2, 8% HCl, 9% CO, 66% CO_2, 2% HC)[b]	vacuum; room temp; 10 Mrad; three different materials	(4)
alpha (Pu-238, -239)	G(gas)=0.7; G(H_2)=0.6 (83% H_2, 12% CO + CO_2, 5% HC)[b]	oxygen depleted; room temp; O-ring bags	(5)
alpha (Pu-238)	G(gas)~0.8; G(H_2)=0.7 (85% H_2, 2% CH_4, 6% CO_2, 7% CO)[c]	oxygen depleted; 20°C; Pylox[R] gloves; corrected data	(6)
alpha (Pu-238)	G(gas)~6.3; G(H_2)=5.3 (85% H_2, 2% CH_4, 6% CO_2, 7% CO)[c]	oxygen depleted; 70°C; Pylox[R] gloves; corrected data	(6)

Refs.:   (1) Szymanski 1976[91]; (2) Zahran 1985[93]; (3) Hegazy 1981b[92]; (4) Arakawa 1986[94]; (5) Kazanjian 1976[36]; (6) Kosiewicz 1981[12] (corrected).

Notes: [a]At an absorbed dose of 60 Mrad, G(HCl)=1.4.

[b]HC = hydrocarbons; calculated using author's data.

[c]An increase from G(H2)=0.7 to G(H2)=5.3 between 20°C and 70°C corresponds to an activation energy of 8.1 kcal/mole; see Section 3.1.2.3.1.2.

3.1.4.7.1.2   Radiolysis of PVC in the Presence of Oxygen

Zeppenfeld (Zeppenfeld 1967[98]) irradiated PVC (apparently pure PVC) with Co- gamma rays in the presence of oxygen. The HCl formed was absorbed in water and then titrated. The HCl yield as a function of radiation dose was a straight line through the origin, with a G(HCl) value of 46 at about 95°C (estimated from the author's data). Experiments conducted at several different temperatures between about 84 and 119°C yielded an activation energy of 5 kcal/g-mole. The corresponding value of G(HCl) at 25°C would be 9.4.

Pure PVC powder and PVC film containing PVC, DOP, epoxy oil, and Ca-Zn stearate compounds in the ratio of 100/50/5/2 were irradiated at various oxygen pressures (Hegazy 1981b[92]). The dose rate was 1 Mrad/h, and the experiments were conducted at room temperature. At an absorbed dose of 20 Mrad with an initial oxygen pressure of 150 torr (the oxygen partial pressure in ambient air), plasticized PVC again produced much less gas than pure PVC. For pure PVC powder, G values measured were G(gas)=10, G(H_2)=0.1, G(HCl)=8.0, and G($-O_2$)=11.3. For PVC film, G values measured were G(gas)=2.4, G(H_2)=0.2, G(HCl)=1.7, and G($-O_2$)=6. Corresponding results at an oxygen pressure of 500 torr are: for pure PVC powder, G values measured were G(gas)=20.3, G(H_2)=0.1, G(HCl)=15, and G($-O_2$)=29; for PVC film, G values measured were G(gas)=5.9, G(H_2)=0.2, G(HCl)=5.0, and G($-O_2$)=11 (Hegazy 1981b[92]).

Rigid PVC films containing stabilizers and anti-oxidants in the range of 0.2-0.5 wt% were gamma irradiated in a vacuum and also at various oxygen pressures (Zahran 1985[93]). At an absorbed dose of 20 Mrad with an initial oxygen pressure of 150 torr, G values for rigid PVC film were G(gas)=6.1, G(H_2)=0.1, G(HCl)=5.9, and G($-O_2$)=2.9.

Gas evolution and oxygen consumption were measured for three samples of PVC containing various plasticizers and stabilizers that were gamma irradiated at room temperature with oxygen present (the O_2 concentration was not stated) (Arakawa 1986[94]). The formulations of these samples are discussed in Section 3.1.6.6.1. Pure PVC powder was also studied. G(gas) for the pure PVC powder was much higher (21.6) than G(gas) for any of the plasticized/stabilized samples (1.4-5.0). Radiolysis of the model-formulation PVC produced primarily HCl, while the two commercial samples of unknown composition produced primarily CO_2 (as was the case for irradiation in vacuum). Values of G(H_2), however, were consistently between 0.2 and 0.3 for all four PVC samples studied.

Examination of the efficiency in forming a gel fraction in gamma radiolysis of plasticized PVC samples in air led Krylova (Krylova 1979[99]) to conclude that the plasticizers were functioning as anti-rad additives. The plasticizers, containing esters with long hydrocarbon chains, appeared to break down more readily than the PVC base polymer. Energy transfer from the PVC molecules to the plasticizer molecules seemed to be occurring.

---

[98] Zeppenfeld 1967. G. Zeppenfeld and L. Wuckel, "On the Mechanism of the Radiation Oxidation of Poly (Vinyl Chloride)," in Proceedings of the Second Tihany Symposium, Akademiai Kiado, Budapest, 1967.

[99] Krylova 1979. S. V. Krylova, et al., "Effect of Plasticizers on the Behavior of Polyvinyl Chloride in γ-Irradiation," Polym. Sci. 21, pp. 749-757, 1979.

Table 3.1-37 lists G values for PVC irradiated in the presence of oxygen. The highest value of $G(H_2)$ observed for PVC irradiated at room temperature, with or without oxygen present, is $G(H_2)=0.7$.

3.1.4.7.2 Polychloroprene

Neoprene rubber is composed of polychloroprene. G values for polychloroprene are listed in Table 3.1-38.

3.1.4.7.3 Chlorosulfonated Polyethylene

Hypalon[R] gloves are composed of chlorosulfonated polyethylene. Lead oxide is often incorporated into the glove material to provide gamma shielding. Table 3.1-39 provides G values for chlorosulfonated polyethylene (Hypalon®).

3.1.4.7.4 Polytetrafluoroethylene (PTFE) and Polychlorotrifluoroethylene

Both polytetrafluoroethylene and polychlorotrifluoroethylene contain no hydrogen in their base polymers. Polychlorotrifluoroethylene has the repeat unit:
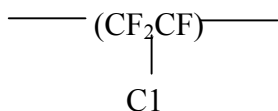
$$—\ (CF_2CF)—$$
$$|$$
$$C1$$

Bersch (Bersch 1959[56]) measured gas evolution in air and in a vacuum from gamma radiolysis of two brands of Kel-F[R], which has polychlorotrifluoroethylene as the base polymer. The maximum value of G(gas) calculated from Bersch's data was 1.1 in air versus 0.1 in vacuum. Almost all of the radiolysis gas produced in air consisted of CO_2.

Polytetrafluoroethylene (PTFE) has the repeat unit:

$$—(CF_2)\ —$$
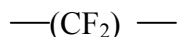
Teflon[R] is a trade name for PTFE. Teflon[R] is similar in structure to polyethylene; however, all of the hydrogen atoms are replaced by fluorine atoms. Differences in the energy relationships between possible chemical reactions lead to the generation of hydrogen gas from polyethylene but no fluorine gas from Teflon[R] (Dole 1973b[100]).

---

[100] Dole 1973b. M. Dole, "Radiation Chemistry of Some Miscellaneous Polymers. Fluoropolymers," in The Radiation Chemistry of Macromolecules, Vol. II, Academic Press, New York, 1973, ed. M. Dole.

Table 3.1-37 — G Values for PVC (Oxygen Present)[a]

Material/ Radiation Type	G(Products)	Comments	Reference
Pure PVC			
gamma	G(gas)=10.3; G(H_2)=0.1; G(HCl)=8.0; G(CO)=1.0; G(CO_2)=1.2; G($-O_2$)=11.3	150 torr O_2; 20 Mrad; room temp	(1)
gamma	G(gas)=21.6[a]; G(H_2)=0.2 (1% H_2, 85% HCl, 4% CO, 10% CO_2)[b] G($-O_2$)=37.7[b]	O_2 pressure not reported[c]; room temp	(2)
Films w/stabilizers			
gamma	G(gas)=6.1; G(H_2)=0.1; G(HCl)=5.9; G($-O_2$)=2.9	150 torr O_2; room temp	(3)
Films w/stabilizers and plasticizers			
gamma	G(gas)=2.4; G(H_2)=0.2; G(HCl)=1.7; G(CO)=0.2; G(CO_2)=0.2; G($-O_2$)=6	150 torr O_2; 20 Mrad; room temp	(1)
gamma	G(gas)=5.0[a]; G(H_2)=0.3 G(HCl)=2.6 (5% H_2, 52% HCl, 6% CO, 37% CO_2)[b] G($-O_2$)=8.1[b]	O_2 pressure not reported; 10 Mrad; room temp	(2)
gamma	G(gas)=1.4[a]; G(H_2)=0.2; G(HCl)=0.2; (15% H_2, 15% HCl, 17% CO, 51% CO_2, 1% HC)[b] G($-O_2$)=6.9[b]		(2)
gamma	G(gas)=1.9[a]; G(H_2)=0.2; G(HCl)=0.2; (10% H_2, 10% HCl, 9% CO, 70% CO_2, 1% HC)[b] G($-O_2$)=6.6[b\]		(2)
gamma	G(H_2)=0.11; G(HCl)=0.21	G(HCl) determined from G(acid)	(4)

Refs.:   (1) Hegazy 1981b[92]; (2) Arakawa 1986[94]; (3) Zahran 1985[93]; (4) Kazanjian 1969[37].
Note: [a]See also Kazanjian 1976[36].
         [b]Calculated using author's data.
         [c]Probably ambient pressure (~760 torr).

Table 3.1-38 — G Values for Polychloroprene

Material/ Radiation Type	G(Products)	Comments	Reference
Pure polychloroprene			
gamma	G(gas)=3.5; G(H_2)=0.2 (5% H_2, 93% HCl,1% CO_2)[a]	vacuum; room temp	(1)
gamma	G(gas)=7.7; G(H_2)=0.3 (4% H_2, 39% HCl, 14% CO, 43% CO_2)[a]	oxygen; room temp	(1)
Commercial Neoprene[R]			
alpha (Pu-238)	G(gas)=0.03; G(H_2)=0.03 (95% H_2, 3% CO_2, 1% CO, 1% CH_4)	oxygen depleted; room temp; corrected data	(2)
alpha (Pu-238)	G(gas)<0.1; G(H_2)<0.1[b]	oxygen depleted; room temp	(3)
gamma	G(gas)=0.2; G(H_2)=0.1 (35% H_2, 16% HCl, 3% CO, 43% CO_2, 3% SO_2)[a]	vacuum; room temp; model compound	(1)
gamma	G(gas)=0.3; G(H_2)=0.1 (29% H_2, 17% HCl, 1% CO, 50% CO_2, 3% SO_2)[a]	vacuum; room temp; special compound	(1)
gamma	G(gas)=0.6; G(H_2)<0.1 (6% H_2, 7% HCl, 8% CO, 79% CO_2)[a]	oxygen; room temp; model compound	(1)
gamma	G(gas)=0.7; G(H_2)=0.1 (17% H_2, 9% HCl, 9% CO, 58% CO_2, 1% CH_4, 6% SO_2)[a]	oxygen; room temp; special compound	(1)

Refs.:   (1) Arakawa 1986[94]; (2) Kosiewicz 1981,[12] corrected (3) Zerwekh 1979[13].
Notes: [a]Calculated from author's data.
          [b]Estimated from author's data.

Table 3.1-39 — G Values for Hypalon[R]

Material/Radiation Type	G(Products)	Comments	Reference
Pure Hypalon[R]			
gamma	G(gas)=5.0; G(H$_2$)=0.6 (12% H$_2$, 42% HCl, 9% CO$_2$, 37% SO$_2$)	vacuum; room temp	(1)
gamma	G(gas)=7.8; G(H$_2$)=0.5 (6% H$_2$, 62% HCl, 2% CO, 20% CO$_2$, 10% SO$_2$)	oxygen; room temp	(1)
Commercial Hypalon[R]			
alpha (Pu-238)	G(gas)=0.15; G(H$_2$)=0.15 (96% H$_2$, 1% CH$_4$, 2% CO$_2$, 1% CO)	oxygen depleted from initial air atmosphere; room temp; temp; corrected data	(2)
alpha (Pu-238)	G(gas)<0.1; G(H$_2$)<0.1[a]	oxygen depleted from initial air atmosphere; room temp; dry box gloves	(3)
alpha (Pu-239)	G(gas)=0.4; G(H$_2$)=0.2; (56% H$_2$, 42% CO$_2$, 2% HC)[b]	oxygen present; room temp; Neoprene-Hypalon glove box gloves	(4)
gamma	G(gas)=0.3; G(H$_2$)=0.3 (90% H$_2$, 8% CO$_2$, 2% CO)	vacuum; room temp; model compound	(1)
gamma	G(gas)=0.4; G(H$_2$)=0.3 (66% H$_2$, 33% CO$_2$, 1% CO)	vacuum; room temp; special compound	(1)
gamma	G(gas)=0.5; G(H$_2$)=0.3 (59% H$_2$, 31% CO$_2$, 10% CO)	oxygen; room temp; model compound	(1)
gamma	G(gas)=0.6; G(H$_2$)=0.3 (52% H$_2$, 44% CO$_2$, 4% CO)	oxygen; room temp; special compound	(1)

Refs.:   (1) Arakawa 1986[94]; (2) Kosiewicz 1981,[12] corrected; (3) Zerwekh 1979[13]; (4) Kazanjian 1976[36].
Note: [a]Estimated from author's data.
          [b]Calculated from author's data.

Teflon[R] is one of the most stable polymers with respect to heat, solvents, and most corrosive chemicals. In contrast, this polymer is extremely sensitive to radiation and incurs marked damage to its mechanical properties after relatively low radiation doses.

3.1.4.7.4.1   Radiolysis of PTFE in the Absence of Oxygen

While authors disagree about the details of PTFE radiolysis in the absence of oxygen, they agree that the total gas generation rate is relatively low. Pure PTFE contains no hydrogen, so

radiolysis of commercial Teflon[R] should yield little or no hydrogen-containing gases. Table 3.1-40 gives G values for PTFE in the absence of oxygen.

Table 3.1-40 — G Values for PTFE (Oxygen Depleted or Absent)

Radiation Type	G(Products)	Comments	Reference
gamma	G(gas)=0.3 for condensable gases	vacuum; room temp	(1)
reactor	(primarily CF_4; no G value given)		(2)
reactor	G(gas)=0.02-0.05 (CO_2 + CO)		(2)
alpha (Pu-238)	G(gas)=0.06 (0% H_2, 0.2% CH_4, 16.8% CO_2, 83% CO)	oxygen depleted from initial air atmosphere; room temp; Teflon[R], corrected data	(3)

Refs.:   (1) Dole 1973b[100]; (2) Chapiro 1962[10], (3) Kosiewicz 1981,[12] corrected.

3.1.4.7.4.2   Radiolysis of PTFE in the Presence of Oxygen

Irradiation of PTFE in the presence of oxygen increases the rate of degradation. Gamma irradiation of powdered PTFE resulted in a G value for oxygen consumption of $G(-O_2)=5$. A G value of 3.5 for condensable gases was measured; a large percentage of the gas was carbonyl fluoride. The G value for condensable gases (0.33) for irradiation in a vacuum was much smaller (Dole 1973b[100]).

G(scission) values for PTFE increased from about 7 in oxygen to about 26 in oxygen mixed with carbon tetrachloride vapor (Jellinek 1983[15]). The evolved gas was CCl_3F.

Table 3.1-41 gives G values for PTFE in the presence of oxygen.

Table 3.1-41 — G Values for PTFE (Oxygen Present)

Radiation Type	G(Products)	Comments
gamma	$G(-O_2)=5$, G(gas)=3.5 for condensable gases	oxygen present; mostly CF_2O produced

Ref.:   Dole 1973b[100].

3.1.4.7.5 Other Polymers Containing Halogens

Krasnansky (Krasnansky 1961[53]) measured gas evolution from commercial chlorinated polyether film exposed to gamma radiation in vacuum. The value of G(gas) calculated from his data was less than 0.8, with hydrogen composing 86% of the gas and butene 1.4%.

Bersch (Bersch 1959[56]) measured gas evolution in air and in a vacuum from gamma radiolysis of rubber hydrochloride (Pliofilm[R]) and two brands of polyvinylidene chloride. For these polymers, measured G values were much smaller than those for polyethylene [G(gas)$_{max}$=2.1 for polyvinylidene chloride in vacuum], and the evolved gas for the polymers when irradiated in air consisted mostly of CO_2.

3.1.4.8 Radiolysis of Miscellaneous Polymers

Radiolysis experiments have been conducted for a variety of additional polymers and commercial plastics.

3.1.4.8.1 Polyamides

Polyamides include materials, such as Nylon[R], which contain H-N bonds as well as H-C and C=O bonds. Nomex[R], used in filters, is an aromatic polyamide (EPRI 1981[101]). G values for polyamides are summarized in Table 3.1-42. Polyacrylonitrile contains C=N bonds and should also have low G values (see Section 3.1.3.12 for a discussion of structurally-related liquids).

3.1.4.8.2 Ion-Exchange Resins

The vast majority of ion-exchange resins used are synthetic organic resins (Pillay 1986[102]). G values vary, depending on the resin and the ionic form. Pillay (Pillay 1986[102]) reports G values for many different ion-exchange resins. The bounding values are G(gas) 2.1, and G(H$_2$) 1.7 for Zeocarb-215[R] resin (wet) (Mohorcic 1968[103]). Most G(gas) and G(H$_2$) values are much lower. Kazanjian (Kazanjian 1976[36]) obtained a value of G(gas)=0.1 for Dowex-1[R] resin.

3.1.4.8.3 Other Miscellaneous Polymers

Some specialty materials have been developed to be highly sensitive to radiation. These include the poly(olefin sulfone)s, which have very high G values for production of SO_2, hydrogen, and olefins. For example, a value of G(gas) of 71 is reported for polyhexene-1-sulfone (Jellinek 1978[11]). These materials are not used in common commercial plastics.

---

[101] EPRI 1981. Georgia Institute of Technology, "Radiation Effects on Organic Materials in Nuclear Plants," Electric Power Research Institute, EPRI NP-2129, November 1981.

[102] Pillay 1986. K. K. S. Pillay, "The Effects of Ionizing Radiations on Synthetic Organic Ion Exchangers," J. Radioanaly. Nuc. Chem., Articles 97/1, pp. 135-210, 1986.

[103] Mohorcic 1968. G. Mohorcic and V. Kramer, "Gasses Evolved by Co-60 Radiation Degradation of Strongly Acidic Ion Exchange Resins," J. Polym. Sci.: Part C, pp. 4185-4195, 1968.

Table 3.1-42 — G Values for Polyamides

Material/ Radiation Type	G(Products)	Comments	Reference
Polymid MXD-6[R]			
gamma	G(gas)=0.1[a];G(H$_2$)<0.1[a] (75% H$_2$, 25% CO$_2$)	vacuum; room temp; 36 Mrad	(1)
Nylon 66[R]			
gamma	G(gas)=0.5[a];G(H$_2$)=0.4[a] (82.5% H$_2$, 16% CO, 1.5% CO$_2$)	vacuum; room temp; 36 Mrad	(1)
Nylon 6-6[R]			
gamma	G(gas) not reported; G(H$_2$)=0.4	vacuum; room temp	(2)
Nylon II[R]			
gamma	G(gas)=1.5[a];G(H$_2$)=1.1[a] (75% H$_2$, 22.5% CO; 0.5% CO$_2$; 2% CH$_4$)	vacuum; room temp; 36 Mrad	(1)
Aromatic polyamide			
not reported	G(gas) not reported; G(H$_2$)=0.01		(3)

Refs.:   (1) Krasnansky 1961[53]; (2) Dole 1983[104]; (3) Zimmerman 1973[105].
Note: [a]Calculated from author's data.

The radiation stability of various commercial plastics was studied in the 1950s by members of the ORNL by irradiating the materials in the ORNL Graphite Reactor (Bopp 1953[106], Bopp 1955[107], Bopp 1963[49]). The radiation exposure was converted to absorbed dose using the chemical composition of the material. The data as reported in Bopp (Bopp 1963[49]) were arbitrarily scaled up to match a higher G value for polyethylene, indicating some uncertainty in the absolute values. Because of inherent dosimetry problems in these early studies, these data are used only in a qualitative sense to establish the gas generation potential of the materials with

[104] Dole 1983. M. Dole, "Effects of Radiation Environments on Plastics," in The Effects of Hostile Environments on Coatings and Plastics, American Chemical Society, Washington, D. C., 1983, ed. D. P. Garner, pp. 17-24.

[105] Zimmerman 1973. J. Zimmerman, "Radiation Chemistry of Some Miscellaneous Polymers. Polyamides," The Radiation Chemistry of Macromolecules, Vol. II, Academic Press, New York, 1973, ed

[106] Bopp 1953. C. D. Bopp and O. Sisman, "Radiation Stability of Plastics and Elastomers," Oak Ridge National Laboratory, ORNL-1373, July 1953.

[107] Bopp 1955. C. D. Bopp and O. Sisman, "Radiation Stability of Plastics and Elastomers," Nucleonics 13, pp. 28-33, 1955.

respect to polyethylene (one of the materials irradiated). G values obtained from these experiments relative to polyethylene are listed in Table 3.1-43.

Table 3.1-43 — G(gas) Values for Miscellaneous Commercial Plastics (Relative to Polyethylene)

Material	G(gas) Value Relative to Polyethylene[a]
cellulose nitrate	1.5
polyvinyl formal	1.4
polyethylene	1.0
allyl diglycol carbonate	0.6
ethyl cellulose	0.5
methyl methacrylate	0.5
cellulose propionate	0.5
cellulose acetate butyrate	0.4
Nylon[R]	0.4
phenolics (no filler, or cellulosic or mineral filler)	<0.3
urea formaldehyde (cellulosic filler)	0.3
Silastic[R]	0.3
cellulose acetate	0.3
butyl rubber	0.3
natural rubber-butyl rubber mixtures	<0.3
melamine formaldehyde (cellulosic filler)	0.2
Selectron 5038[R] polyester	0.2
natural rubber with fillers	<0.2
natural rubber	0.1
Thiokol ST[R]	0.09
Neoprene[R]	<0.06
casein plastic	0.05
Mylar[R] film	0.05
Plaskon[R] alkyd	0.03
triallyl cyanurate	0.02
aniline formaldehyde	0.01
furane resin (asbestos & carbon filler)	<0.01
polystyrene	<0.01
styrene-butadiene copolymer	<0.01

Ref.:   Bopp 1953[106].
Note: [a]Calculated from author's data.

Only two materials, polyvinyl formal and cellulose nitrate, had higher G(gas) values than polyethylene in the ORNL reactor irradiation experiments. The composition of the evolved gas was not reported. The major use of polyvinyl formal is in heat-resistant nonconductive electrical wire enamels and other coatings (Deanin 1972[108]). Because of its thermal instability, cellulose nitrate does not have wide application in commonly used materials in general commerce, except

---

[108] Deanin 1972. R. D. Deanin, <u>Polymer Structure, Properties and Applications</u>, Chaners Books, Boston, 1972.

in photographic film and lacquers (cellulose nitrate commonly is the film remaining after the volatile constituents have evaporated) (Deanin 1972[108]). As a result, polyvinyl formal and cellulose nitrate will be present in the CH-TRU wastes only in trace amounts.

3.1.5   Radiolysis of Non-Polymer Solids

Other common solid materials in the CH-TRU wastes are solidified liquid wastes, solid organic acids, asphalt, and miscellaneous inorganic materials.

3.1.5.1 Radiolysis of Solidified Liquid Wastes

Solidified liquid wastes include sludges, concretes, and gel-like or monolithic structures that bind liquid wastes so that free liquids are minimized.

3.1.5.1.1 Aqueous Sludges

One common sludge is produced at the RFETS by the neutralization of nitric acid solutions in the plutonium recovery process. The sludge consists of hydroxides of calcium, sodium, potassium, silicon, magnesium, aluminum, iron, and other metals at lower concentrations (Kazanjian 1981[109]). The water and nitrate content of the sludge can vary.

Kazanjian (Kazanjian 1981[109]) conducted experiments on this sludge to determine the radiolytic gas yields as a function of water and nitrate content. The nitrate concentration in the material was determined to be 10.2 wt%, and the water content was 52 wt%. The water content was varied either by drying or adding water to the as-received sludge. Mass spectrometric analysis of the gases evolved under drying conditions showed that the weight loss was essentially all due to water evaporation. In order to examine the effect of the nitrates on gas yields, nitrate salts were removed by washing the sludge with water. All of the experiments were conducted at lowered pressure to permit more accurate analysis of the evolved gases using mass spectrometry.

The experiments were conducted using gamma radiation. The dose rate was 4.45E5 rad/h, except for the 75% water sample, which was irradiated at 3.8E5 rad/h.

The results show that decreasing the water content of the sludge decreases the rate of gas generation. Small amounts of CO and NO_x were also observed. Removing nitrates from the sludge changed the amount and composition of the evolved gas. Oxygen generation was virtually eliminated. Hydrogen evolution in these samples, which contained about 65% water, was up to three times greater than hydrogen evolution obtained from sludge containing nitrate. The measured value of $G(H_2)$ varied from 0.23 to 0.43. [The largest $G(H_2)$ value observed (0.43) is very close to the value of 0.45 for $G(H_2)$ measured for gamma irradiation of liquid water at high pH (see Section 3.1.3.4).] A maximum value of $G(O_2)$ of 0.9 was found in the nitrate sludges from the radiolysis of nitrates. These findings are in agreement with other experiments on the radiolysis of nitric acid and solid inorganic nitrates.

---

[109] Kazanjian 1981. A. R. Kazanjian and M. E. Killion, Results of experiments on radiolytic gas generation from sludge, Rockwell International, Rocky Flats Plant, personal communication.

Sludge from waste water processing at Mound Laboratory, composed primarily of carbon, iron, and calcium compounds, is immobilized in Portland cement (Lewis 1983[110]). A sample of the sludge was contaminated with heat-source plutonium dioxide, consisting of particles averaging 20 microns in size, and mixed with cement. The sludge/cement contained 20 wt% water. The G(gas) value measured was 0.21 (for generated gases only), consisting almost entirely of hydrogen; the G(-O_2) value was 0.13. A small amount of nitrogen was also generated.

Gas generation from cemented caustic waste resulting from immobilization at Mound Laboratory of 1-N NaOH contaminated scrubber solution in Portland cement is reported in Lewis (Lewis 1983[110]). The caustic waste was contaminated with heat-source plutonium in the form of PuO_2 particles averaging 20 microns in size. The caustic/cement waste form contained 22 wt% water. The measured G(gas) value was 0.26, consisting of about equal amounts of oxygen and hydrogen [G(O_2)=0.11 and G(H_2)=0.13]. A small amount of nitrogen was also generated.

3.1.5.1.2 Concretes

The cement-based and other hydraulic binders used for immobilization of wastes require water in their curing reactions. Generally, some excess water remains in the materials in a closed-pore system (Dole 1986[111]). Radiolysis of this unbound water contributes most of the gas generation from within these solidified radioactive wastes.

High-level radioactive sludges at the SRS were simulated using Fe_2O_3, MnO_2, or equimolar mixtures of the two compounds, which were solidified in high-alumina cement (Bibler 1976[19], Bibler 1978[112]). For all tests, the simulated wastes were 40 wt% of the dry cement-waste mixtures. Irradiation of this material with Co-60 gamma rays generated a gas consisting predominantly of hydrogen. The hydrogen pressure reached a steady-state value; higher pressures corresponded to higher dose rates. The equilibrium pressure also depended on the specific material being irradiated, with equilibrium pressures in descending order for Fe_2O_3-cement, neat cement, and MnO_2-cement. In all three cases, oxygen was partially consumed to form hydrogen peroxide, as verified by chemical analysis of the irradiated concrete.

In alpha radiolysis experiments conducted on the same concretes, oxygen was a product as well as hydrogen, composing 20 to 50% of the evolved gas. Up to 200 psi, no steady-state pressure was reached. The average value of G(H_2) was 0.21 (Bibler 1978[112]).

---

[110] Lewis 1983. E. L. Lewis, "TRU Waste Certification: Experimental Data and Results," Monsanto Research Corporation, Mound Laboratory, MLM-3096, September 1983.

[111] Dole 1986. L. R. Dole and H. A. Friedman, "Radiolytic Gas Generation from Cement-Based Waste Hosts for DOE Low-Level Radioactive Wastes," preprint of a presentation at the Symposium on the Effects of Radiation on Materials, Seattle, Washington, June 1986.

[112] Bibler 1978. N. E. Bibler, "Radiolytic Gas Production from Concrete Containing Savannah River Plant Waste," E. I DuPont de Nemours and Company, Savannah River Laboratory, DP-1464, January 1978.

The effect of adding NO_3^- or NO_2^- ions was also examined (Bibler 1978[112]). In low-dose-rate (0.09 Mrad/hr) gamma radiolysis tests, added NO_3^- or NO_2^- did not lead to additional pressurization. O_2 was still consumed, and H_2 was still produced. At the high dose rate (28 Mrad/hr), O_2 was a product, indicating that a different radiolytic process dominates at this dose rate. Also, a steady-state pressure was not reached.

Gas generation from a concrete consisting of a mixture of Portland cement and gypsum-perlite plaster mixed with water in the ratio of approximately 1.7:1 was measured by Bibler (Bibler 1977[25]). The value of G(gas) measured in the gamma radiolysis experiment was 0.03. Hydrogen was the only gas produced. As the hydrogen pressure increased, back reactions occurred to reduce the rate of hydrogen formation, resulting in a steady-state pressure that depended on the dose rate. Oxygen in the air was partially consumed, and nitrogen was unaffected. For the alpha radiolysis tests, Cm-244 was dissolved in the water used to make the concrete, ensuring that the Cm-244 was in direct contact with the elements in the concrete. In four tests with varying amounts of Cm-244, $G(H_2)$ was constant and equal to 0.6, a value 20 times greater than measured in the gamma radiolysis experiment. As with gamma radiolysis, oxygen was partially consumed and nitrogen was unaffected. However, a steady-state pressure was not attained even at about 200 psi of hydrogen.

Bibler (Bibler 1980[113]) conducted a series of alpha radiolysis experiments to study radiolysis of CH-TRU wastes immobilized in concrete, especially incinerator ash. Drying the concrete at 200°C reduced the water content from 35 to 7.4% (80% reduction) but greatly reduced the $G(H_2)$ value from 0.38 to 0.0002. The water remaining was thought to be involved in hydration reactions and not as easily degraded as the free water remaining in the concrete after curing.

The similarity in the radiolysis results for concrete and water led Bibler (Bibler 1977[25]) to conclude that the metal oxides of the concrete do not significantly alter the radiation chemistry of the water, even when the water is incorporated in the concrete. In gamma radiolysis tests, O_2 in the air sealed in the container was partially consumed, while N_2 was unaffected. A steady-state H_2 pressure up to 45 psig was attained. Higher equilibrium pressures were seen for the higher dose rates in the experiment. The values of $G(H_2)$ were measured to be 0.03 for all dose rates.

In the alpha radiolysis experiments on concrete, a value of $G(H_2)$=0.6 was measured, independent of the amount of Cm-244. This $G(H_2)$ value was a factor of 20 times higher than the $G(H_2)$ value measured for gamma radiolysis. As with gamma radiolysis, oxygen was partially consumed while N_2 was unaffected. In contrast to gamma radiolysis, a steady-state pressure was not attained even to about 200 psig H_2.

Tests were also performed (Bibler 1979[23]) to determine if self-absorption of alpha energy would occur when plutonium dioxide particles were added to concrete. The amount of energy absorbed by a particle depends on the size of the particle and its density. The value of $G(H_2)$ was decreased by about a factor of 2 for concrete containing PuO_2 particles having an average size of

---

[113] Bibler 1980. N. E. Bibler, "Radiolytic Gas Generation in Concrete Made with Incinerator Ash Containing Transuranium Nuclides," in Scientific Basis for Nuclear Waste Management, Vol. 2, pp. 585-592, 1980.

2 microns and a density about 80% of the maximum density, compared to concrete containing plutonium dissolved in nitric acid. (The particles may have agglomerated to form larger particles.) The calculated range of the Pu-238 alpha particles (in PuO_2 of the maximum theoretical density of 11.4 g/cm^3) is 11 microns (Bibler 1979[23]).

Bibler (Bibler 1979[23], Bibler 1980[114]) reported gas generation experiments on three types of concrete containing simulated TRU incinerator ash: high-alumina cement, Portland Type I cement, and Portland-pozzolanic cement. Simulated incinerator ash containing primarily CaO and TiO_2 was mixed with dry cement (30 wt% ash, 70 wt% cement). Pu-238 solution was added, and the resulting paste was transferred to a mold and cured to allow 30-40% of the free water to evaporate. $G(H_2)$ values ranged from 0.3 to 0.6. $G(H_2)$ values were unaffected by either dose rate or the pH of the water used to make the concrete. $G(H_2)$ could be decreased by reducing the water content of the concrete and by adding an organic acid (EDTA) to the concrete.

Bibler (Bibler 1979[23], Bibler 1980[114]) conducted further experiments on high-alumina and Portland Type I cements. He determined that addition of NO_3^- or NO_2^- ions to the water used to make the concrete lowered the alpha radiolysis $G(H_2)$ values by a factor of 20 for 6-M NO_3^- or a factor of 2.4 for 3-M NO_2^-. Oxygen was also produced from the concrete containing 6-M NO_3^-, while oxygen was consumed in the concrete containing 3-M NO_2^-.

Radiolysis experiments conducted at 70 and 100°C indicated that $G(H_2)$ for concretes does not increase with temperature below 100°C (Bibler 1979[23], Bibler 1980[114]). In fact, decreases in the hydrogen generation rate were noted, caused by evolution of free water from the concretes.

Bibler (Bibler 1979[23]) also compared $G(H_2)$ values measured for dissolved TRU contaminants versus contaminants present as small particles. When Pu-238 was added as PuO_2, $G(H_2)$ for high-alumina concrete was 0.21 compared to 0.55 determined using dissolved Pu-238. $G(H_2)$ for Portland Type I cement was 0.28 compared to 0.65. The PuO_2 particles used had an initial average size of 2 microns initially but could have agglomerated to larger particles.

Radiolysis of simulated radioactive waste immobilized in cement-based grouts was examined by Dole (Dole 1986[111]). All specimens were cured for 28 days before the radiolysis gases were collected. Some dewatered specimens were dried at elevated temperature for seven days in order to establish the role of the porewater in the production of radiolysis gases. Cm-244 was used as the contaminant in the alpha radiolysis experiments. Two waste streams were simulated: current acid waste and double-shell slurry (DSS) waste. Both waste streams were acidic and contained metal sulfates and nitrates. The cement used was low alumina cement. The authors stated that the gas tightness of their containers was unreliable, and seals were broken as the pressure increased. G(gas) values for the current acid waste samples were estimated that ranged from 0.32 to 0.43 for alpha radiolysis. When samples were dried at elevated temperature following cure, no evolved gas was detected. The DSS samples had much lower G(gas) values of 0.04-0.15 for alpha radiolysis and 0.02 for gamma radiolysis. Gas compositions remaining in the vessels at the end of the tests indicated generation of hydrogen in all of the tests; production of oxygen was reported in all six of the alpha radiolysis experiments using current acid waste. Only

the DSS waste was examined by both alpha and gamma radiolysis, and conflicting data were obtained for the two alpha radiolysis experiments.

Very low G values have been reported from irradiation of water present as the hydrate in crystals (Zagorski 1983[114]). Water in the hydrates appears to exhibit the property of an energy sink. This has been attributed to the presence of a hydrated electron that can absorb energy by changing its state. For example, KOH 0.5 H_2O was irradiated up to 1 MGy absorbed dose without generation of any observable H_2, O_2, or H_2O_2. The authors stated that this concept is also applicable to hydrates of organic materials.

3.1.5.1.3 Adsorbed or Absorbed Liquids

Radiolysis of adsorbed or absorbed liquids indicates that the sorbing medium can either be inert to radiation or can transfer energy to the sorbed liquid. Unless experimental data demonstrate that the binding medium is radiolytically inert (e.g., vermiculite), all of the radiation energy should be assumed to interact with the sorbed liquid.

Bibler (Bibler 1977[25]) reported gamma and alpha radiolysis experiments on octane or a commercial vacuum pump oil sorbed onto vermiculite. Hydrogen was evolved, and oxygen was consumed. $G(H_2)$ was found to vary linearly with the mass fraction of organic material. This suggested that the vermiculite absorbed some of the emitted energy, and it acted as an inert diluent (no energy transfer occurred between the vermiculite and the organic liquid). The extrapolated $G(H_2)$ values for 100% liquid were 3 for octane and 1.6 for oil at high dose rate. At lower dose rates, the $G(H_2)$ values reported were 4.5 for octane and 2.0 for oil. Radiolysis gases were produced in the nominal ratio of $H_2/CO_2/CH_4 = 1.0/0.03/0.01$.

Kinetic studies of water radiolysis in the presence of oxide systems have shown that the exposure of an oxide plus adsorbed water system to gamma radiation can result in energy transfer from the oxide to the water molecules (Garibov 1983[115]). Oxides studied included SiO_2, SiO_2-Al, SiO_2-Ca, Er_2O_3, La_2O_3, and Al_2O_3. Values of $G(H_2)$ measured indicate that the energy transferred from the oxide to the adsorbed water molecules can easily be 3-5 times the energy that is originally absorbed by the water. Very little gas generation was observed from irradiation of silica gel that had been evacuated to remove adsorbed water (Krylova 1967). Lower values of $G(H_2)$ were observed when the silica gel was purified. This effect was attributed to recombination of hydrogen precursors by the organic impurities on the surface of the silica gel.

Garibov (Garibov 1983[116]) also examined the effect of temperature on charge transfer in silica gel. Increasing the temperature at which the sample was irradiated decreased the value of $G(H_2)$ measured. This was attributed to a greater desorption rate of water molecules from the oxide surface, which inhibited effective energy transfer to adsorbed molecules, and to thermal annealing of radiation defects in the oxide phase.

---

[114] Zagorski 1983. Z. P. Zagorski, "Applied Aspects of Radiation Chemistry of Hydrates," in Proceedings of the Fifth Tihany Symposium on Radiation Chemistry, Akademiai Kiado, Budapest, 1983, pp. 331-336.

[115] Garibov 1983. A. A. Garibov, "Water Radiolysis in the Presence of Oxides," in Proceedings of the Fifth Tihany Symposium on Radiation Chemistry, Akademiai Kiado, Budapest, 1983, pp. 377-384.

Vereshchinskii (Vereschinskii 1964[116]) summarized radiolysis experiments conducted on pentane adsorbed on zeolites or silica gel. The observed values of $G(H_2)$ were examined as a function of the electron fraction of pentane when the system pentane-solid was irradiated. The total dose absorbed by the system was used in calculating the $G(H_2)$ value. The results depended to a great extent on the identity of the solids studied. In most cases, more hydrogen was generated than would be expected without energy transfer from the adsorbent to the pentane. The charge transfer appeared to affect only one mono-layer of the absorbed liquid. In contrast, radiolysis of water adsorbed on zeolites indicated that there is no energy transfer in that system (Krylova 1967).

3.1.5.2 Radiolysis of Solid Organic Acids

$G(H_2)$ values for some organic acids that are solid at room temperature have been reported in the range from 1.2 to 2.3 (Bolt 1963[14]). G(gas) values for the same materials range from 1.8 to 4.1. The maximum G value for flammable gas was 2.6. A value of $G(CO_2)$ up to 14 has been reported for one of the organic acids (isobutyric acid) (Spinks 1976[3]).

3.1.5.3 Radiolysis of Asphalt

A value of G(gas) for bitumen (asphalt) for low absorbed dose was estimated to be 1.3, with hydrogen being the primary gas evolved (Kosiewicz 1980[117], corrected). No dependence was seen on temperature from 20 to 70°C. Gamma radiolysis experiments reported by Burnay (Burnay 1987[118]) measured lower G values.

3.1.5.4 Radiolysis of Soil

Gas evolution from plutonium-contaminated soil was reported by Pajunen (Pajunen 1977[119]). The soil was removed from the Z-9 Trench, which had been used as a liquid waste disposal site for the Plutonium Finishing Plant at the Hanford site. The waste solutions were acidic and consisted of aluminum, magnesium, calcium, and other metal nitrate salt wastes; degraded solvents (15% tributyl phosphate or dibutylbutyl phosphate in CCl_4); and other organics, such as solvent washings, fabrication oil, and other waste materials from hood and equipment flushes (Ludowise 1978[120]). The top 30 cm of soil in the trench was mined. The soil moisture content ranged between 0.2 and 25.5 wt%, averaging approximately 5 wt%. Organic content averaged 7.1 wt % with a range of 0.2 to 46.4 wt %. The highest value of G(gas) calculated from Pajunen's data was 1.6, for a soil having a combined organic and moisture content of about 15

---

[116] Vereshchinskii 1964. I. V. Vereshchinskii and A. K. Pikaev, Introduction to Radiation Chemistry, Israel Program for Scientific Translations, Ltd., Jerusalem, 1964.

[117] Kosiewicz 1980. S. T. Kosiewicz, "Gas Generation from the Alpha Radiolysis of Bitumen," Nuclear and Chemical Waste Management 1, pp. 139-141, 1980.

[118] Burnay 1987. S. G. Burnay, "Comparative Evaluation of and Radiation Effects in a Bitumenisate," Nuclear and Chemical Waste Management 7, pp. 107-127, 1987.

[119] Pajunen 1977. A. O. Pajunen, "Radiolytic Evolution of Gases from Z-9 Soils," Rockwell Hanford Operations, RHO-CD-13, July 1977.

[120] Ludowise 1978. J. D. Ludowise, "Report on Plutonium Mining Activities at 216-Z-9 Enclosed Trench," Rockwell International, Rockwell Hanford Operations, RHO-ST-21, September 1978.

wt%. The typical composition of the gas generated by the soils was 50% N_2, 14% O_2, 23% H_2, and 13% CO_2.

Soil samples from Mound Laboratory property were contaminated with heat-source plutonium in the form of PuO_2 particles averaging 20 microns in size (Lewis 1983[110]). Gas generation was measured from a soil sample that contained about 5 wt% water. The G(gas) value was 0.22, with $G(H_2)$=0.15 and $G(CO_2)$=0.07. Oxygen was consumed, with $G(-O_2)$=0.10.

3.1.5.5 Radiolysis of Dry, Solid Inorganic Materials

Dry, solid inorganic materials do not generate hydrogen gas but may produce other gases (frequently oxygen).

Some common inorganic chemicals used in processing aqueous wastes include ferric sulfate, calcium chloride, and magnesium sulfate. One treatment process produces a precipitate of the hydrated oxides of iron, magnesium, aluminum, silicon, etc. (Kazanjian 1981[109]). Various nitrates and carbonates can also be present (Clements 1985a[121], Clements 1985b[122]).

The yield of nitrite ions is more frequently measured in gamma radiolysis of solid nitrates than is the oxygen yield. For stoichiometric decomposition, a value of $G(O_2)$ should be one-half of the $G(NO_2^-$ value. A value of $G(O_2)$<1.3 has been determined (Johnson 1970[123]). G values measured for gamma radiolysis of barium, potassium, and sodium chlorates had $G(Cl^-.8$ and $G(O_2)$<4.0.

For alkali and alkaline earth perchlorates, values of $G(Cl^-)$<1.1 and $G(O_2)$<5.3 were measured. Careful tests were conducted to detect the presence of ozone and free chlorine, but neither of those gases was observed (Johnson 1970[124]).

3.1.6 Comparison of Laboratory G Values With Effective G Values Measured for Drums of CH-TRU Wastes

Actual CH-TRU wastes consist of general laboratory waste (glass, crucibles), combustible materials (paper, plastic), organic shielding materials (Benelex[R], Plexiglas[R]), metals, sludges or concreted wastes, and various other materials. The materials are contaminated with TRU radionuclides in solution (such as dilute nitric acid) or in particle form (such as PuO_2). Typically, several different contaminated materials are present in a given waste container. The G value calculated for actual CH-TRU wastes is an effective G value. All of the radioactivity present in the waste container is assumed to be absorbed by the waste materials, when actually some self-absorption of the alpha decay energy occurs inside particulate contamination.

---

[121] Clements 1985a. T. L. Clements, Jr. and D. E. Kudera, "TRU Waste Sampling Program: Volume I--Waste Characterization," EG&G Idaho, Inc., EGG-WM-6503, September 1985.

[122] Clements 1985b. T. L. Clements, Jr. and D. E. Kudera, "TRU Waste Sampling Program: Volume II--Gas Generation Studies," EG&G Idaho, Inc., EGG-WM-6503, September 1985.

[123] Johnson 1970. E. R. Johnson, The Radiation-Induced Decomposition of Inorganic Molecular Ions, Gordon and Breach Science Publishers, New York, 1970.

Effective G values have been measured for drums of actual CH-TRU wastes. On the whole, the effective hydrogen G values are much lower than maximum hydrogen G values for the waste forms based on the material in the waste form with the highest G value. For drums of combustible wastes, the maximum $G(H_2)$ value determined in controlled experiments was 2.1 versus a possible value of 4.0 based on laboratory experiments. For drums of sludge, the maximum $G(H_2)$ value measured was 0.3 versus a possible value of 1.6 based on laboratory experiments.

Sources of information for gas generated from actual CH-TRU wastes include examinations of drums retrieved from storage at the Idaho National Engineering and Environmental Laboratory (INEEL) (Clements 1985a[122]) and at LANL (Warren 1985[124], Clements 1985a[122]), and experiments measuring gas composition and pressure for newly generated drums of wastes at the RFETS (Clements 1985b[123], Kazanjian 1985[125]), at LANL (Clements 1985b[123], Zerwekh 1986[126]) and at the SRS (Ryan 1982[127]).

3.1.6.1 Retrieved Drums of CH-TRU Wastes

G values for radiolytic gas production from unvented retrieved drums can only provide lower limits, because of uncertainties in the rates at which gases can permeate through the drum gaskets or diffuse through gaps between the gaskets and sealing surfaces. [Tests conducted at INEEL indicate that drums will vent when pressurized above 20 psig (Clements 1985a[122]).] Only gas in the drum headspace was sampled, and the concentrations of generated gases could have been higher inside the waste bags.

A total of 209 waste containers (199 drums) of wastes that originated at the RFETS were retrieved from storage at INEEL (Clements 1985a[122]). A sample of the headspace gas in each drum was taken and analyzed. Internal pressure and void volume for gas accumulation were measured, and the containers were opened and the wastes examined. All but seven of the waste drums had been sealed with nonporous styrene-butadiene gaskets.

A lower limit for the hydrogen G value was calculated (by this author) for each of the drums using reported alpha activity, void space, pressure, time since drum closure, and hydrogen concentration in the headspace. Almost all of the drums had minimum $G(H_2)$ values less than 1.0. Those that had minimum $G(H_2)$ values greater than 1.0 and activity greater than 0.1 Ci (the specific activity of Pu-239 is 0.07 Ci/g) are listed in Table 3.1-44.

---

[124] Warren 1985. J. L. Warren and A. Zerwekh, "TRU Waste-Sampling Program," Los Alamos National Laboratory, LA-10479-MS, August 1985.

[125] Kazanjian 1985. A. R. Kazanjian, et al., "Gas Generation Results and Venting Study for Transuranic Waste Drums," Rockwell International, Rocky Flats Plant, RFP-3739, 1985.

[126] Zerwekh 1986. A. Zerwekh and J. L. Warren, "Gas Generation and Migration Studies Involving Recently Generated Pu-238-Contaminated Waste for the TRU Waste Sampling Program," Los Alamos National Laboratory, LA-10732-MS, July 1986.

[127] Ryan 1982. J. P. Ryan, "Radiogenic Gas Accumulation in TRU Waste Storage Drums," E. I. du Pont de Nemours & Co., Savannah River Laboratory, DP-1604, January 1982.

One possible source of a high apparent G value is that the time period for gas generation may have been underestimated. The storage times are based on the dates the drums were sealed, while wastes may have been placed into the drum weeks or months prior to the closure date. Four of the drums had calculated effective G values of 6.0 or higher. These include one drum of combustibles and three drums of cemented sludges and solutions containing organic complexing chemical wastes.

Solidified liquid organic wastes, including cemented sludges and solutions and organic sludges, will not be transported until more information is available on their potential for hydrogen (or other flammable) gas generation.

Combustible waste Drum No. 76-02898 had a calculated $G(H_2)$ value of 6.0, which is above the bounding laboratory value of 4 (at room temperature). The most probable explanation for the high calculated $G(H_2)$ value is that the drum contained a significant amount of Am-241. Drum No 76-02898 was lead-lined, a procedure necessary when Am-241 is present in higher concentration than in usual weapons-grade plutonium. This was the only one of the combustible waste containers that was lead lined. The original assay listed 32 g Pu and no Am. A second assay, conducted on a NaI system using a 100-second count (not long enough to measure americium) listed 29 g Pu and no Am. Reassay records showed a measurement of 29 ± 16.3 g Pu.

Drums of CH-TRU wastes were also retrieved at LANL, but those drums had been closed with a gas-permeable sponge-rubber gasket. All of the LANL drums were at ambient pressure, demonstrating that flow or diffusion of gases through the porous gasket had occurred.

3.1.6.2 Newly Generated Waste Experiments

Experiments on newly generated wastes have been conducted at RFETS, LANL, and SRS.

3.1.6.2.1 Rocky Flats Environmental Technology Site Experiments

The gas generated inside each of 16 drums of newly generated wastes contaminated with weapons-grade plutonium was measured over a 13-week period as the second phase of a two-phase experiment (Clements 1985b[123], Kazanjian 1985[124]). Wastes were assayed as individual packages or by radiochemical analysis to determine total alpha activity. In Phase I, the drums were vented for three months using one of three potential venting devices (a filter, a semi-permeable gasket, or a Hanford vent clip). Drum pressure and gas concentrations in the drum headspaces were measured. At the conclusion of Phase I, the drums were purged with air, and a gas sample was taken to obtain the initial gas composition for the second phase of the study. In all cases the plug in the lid of the rigid liner was left out, so that the rigid liner was not a primary barrier for gas escape.

Table 3.1-44 — Data for RFETS Retrieved Waste Drums with $G(H_2)_{min} > 1.0^{a,b}$

	Waste	Activity	Time	Gauge Pressure	Void Vol.	Gas Composition						Minimum G Values			
ID No.	Form	(Ci)	(days)	(mmHg)	(l)	H₂	O₂	N₂	Ar	CO₂	HC	G(H₂)	G(CO₂)	G(HC)	G(gas)
22-01194	Combustibles	0.30	276	2.0	181	0.4	18.8	79.2	0.9	0.2	0.3	1.0	0.6	0.7	2.3
02-39371	combustibles^c	1.78	245	28.5	182	2.1	0.1	96.5	1.1	0.0	0	1.1	0	0	1.1
02-39465	combustibles	0.74	227	-19.0	179	0.9	17.2	79.4	0.9	1.1	0.3	1.1	1.3	0.3	2.7
02-39195	combustibles	0.15	307	-36.0	168	0.3	12.5	83.3	0.9	2.1	0.3	1.4	8.4	1.2	10.9
744-3829	cmt s&s	0.16	263	13.5	77	0.8	1.7	95.0	1.1	0.8	0.1	1.7	0.2	0.3	2.1
76-01642	spc slud	0.74	880	-43.0	151	7.5	5.6	85.2	1.0	0.0	0.6	1.9	0	0.2	2.1
76-02898	combustibles	2.15	326	87.5	171	18.2	0.0	64.6	0.8	15.2	0.8	6.0	5.0	0.2	11.3
744-3841	cmt s&s	0.15	256	5.4	76	2.7	2.8	91.8	1.1	0.0	0.3	6.3	0	0.6	6.9
744-3837	cmt s&s	0.17	256	5.5	38	6.2	0.2	90.7	1.1	0.0	0	6.4	0	0	6.4
744-2389	cmt s&s	0.20	4439	154.0	162	32.4	0.1	64.2	0.8	0.0	2.3	8.6	0	0.6	9.2

Notes:
[a] cmt s&s = cemented sludges and solutions consisting of organic complexing chemical wastes; spc slud = an uncemented sludge packaged in polyethylene bottles inside a drum; HC = hydrocarbons.

[b] Ambient pressure at RFETS is about 613 mmHg; ambient pressure at INEEL is about 640 mmHg.

[c] Contained Ful-Flo^R (polypropylene) filters coated with grease.

The drum lids were sealed to the drums using Permatex Form-a-Gasket[R]. The drums were pressure tested and considered to be sealed if they held a pressure of 155 torr above atmospheric pressure for 3 hours with a pressure loss of no more than 5 torr. Two of the drums developed leaks of 41 torr and 28 torr. These values were not considered in determining the gas generation rates. The drum pressure and gas composition of samples taken from the drum headspace were recorded weekly. Gas compositions were determined by mass spectrometry.

While no gas samples were taken from inside the waste bags, the gas generation rates calculated from the drum headspace samples should give the gas generation rates inside the waste bags. In these experiments, hydrogen generated inside the inner waste bags had permeated through the layers of plastic in the drum into the drum headspace, and the hydrogen concentration increased linearly with time. When this occurs, the hydrogen concentrations in the inner waste bags, drum liner bags, and drum headspaces are all increasing at the same rate.

The G values for hydrogen, carbon dioxide, hydrocarbons, and total gas were calculated for each of the drums in the cited reports. Plots of hydrogen gas production versus time that are shown in the reports appear linear, indicating that absorbed dose effects were minimal. The G values so obtained are listed in Table 3.1-45. Figure 3.1-1 shows Ar, CO_2, H_2, hydrocarbons, and isopropanol partial pressures as functions of time for a drum containing leaded rubber gloves (Figure #16 in Table 3.1-45). (The isopropanol is attributed to the Permatex Form-a-Gasket[R] material.)

The high values of $G(H_2)$ for the organic setup waste form (solidified organics) are much greater than the $G(H_2)$ values of less than 3 that have been measured for oils. The radionuclide content of the drums was confirmed by reassaying samples of the sludge. The authors (Clements 1985b[123], Kazanjian 1985[126]) suggested that corrosion of the mild steel drum could be responsible for the high rate of hydrogen production. Corrosion can produce hydrogen gas in an anaerobic, wet atmosphere, which were the conditions inside each of the two drums after the first week of the experiment.

The relatively large amounts of CO_2 generated in several of the drums could have been caused by microbial action or chemical reactions. Measured $G(H_2)$ values for combustibles (maximum of 2.1) are all well within the maximum G value of 4 at room temperature established in Section 3.1.4. Measured $G(H_2)$ values for inorganic sludges (maximum of 0.3) are much lower than the maximum $G(H_2)$ value of 1.6 for water.

Table 3.1-45 — Effective G Values for RFETS Newly-Generated Waste Drums

Fig #	Waste Form Description	Effective G values			
		H$_2$	CO$_2$	HC	Total
1	inorganic sludge	0.30	0.01	--	0.31
2	inorganic sludge	0.28	0.01	--	0.29
3	inorganic sludge	0.19	0.01	--	0.92[a]
4	inorganic sludge	0.16	0.01	0.02	0.19
5	organic setup	15.1	0	--	15.1
6	organic setup	22.5	0	--	22.5
7	dry combustibles	2.1	1.6	--	3.7
8	dry combustibles	1.4	1.3	0.9	3.6
9	dry combustibles	0.79	0.47	--	1.26
10	dry combustibles	0.39	5.1	--	5.49
11	wet combustibles	0.74	0.17	--	0.91
12	wet combustibles	0.52	0.28	0.25	1.05
13	plastic & rubber	1.1	2.2	--	3.3
14	plastic & rubber	0.65	0.77	--	1.42
15	leaded rubber	0.32	6.4	--	6.72
16	leaded rubber	0.95	0.49	0.07	1.51

Notes: [a]Includes G(O$_2$)=0.72. All other G(O$_2$)s were negative.

DRUM ATMOSPHERE
D-30175

Partial Pressure (Torr)

Argon ①

Carbon
Dioxide ②

Hydrogen ③

Other
Hydrocarbons ④

Isopropanol ⑤
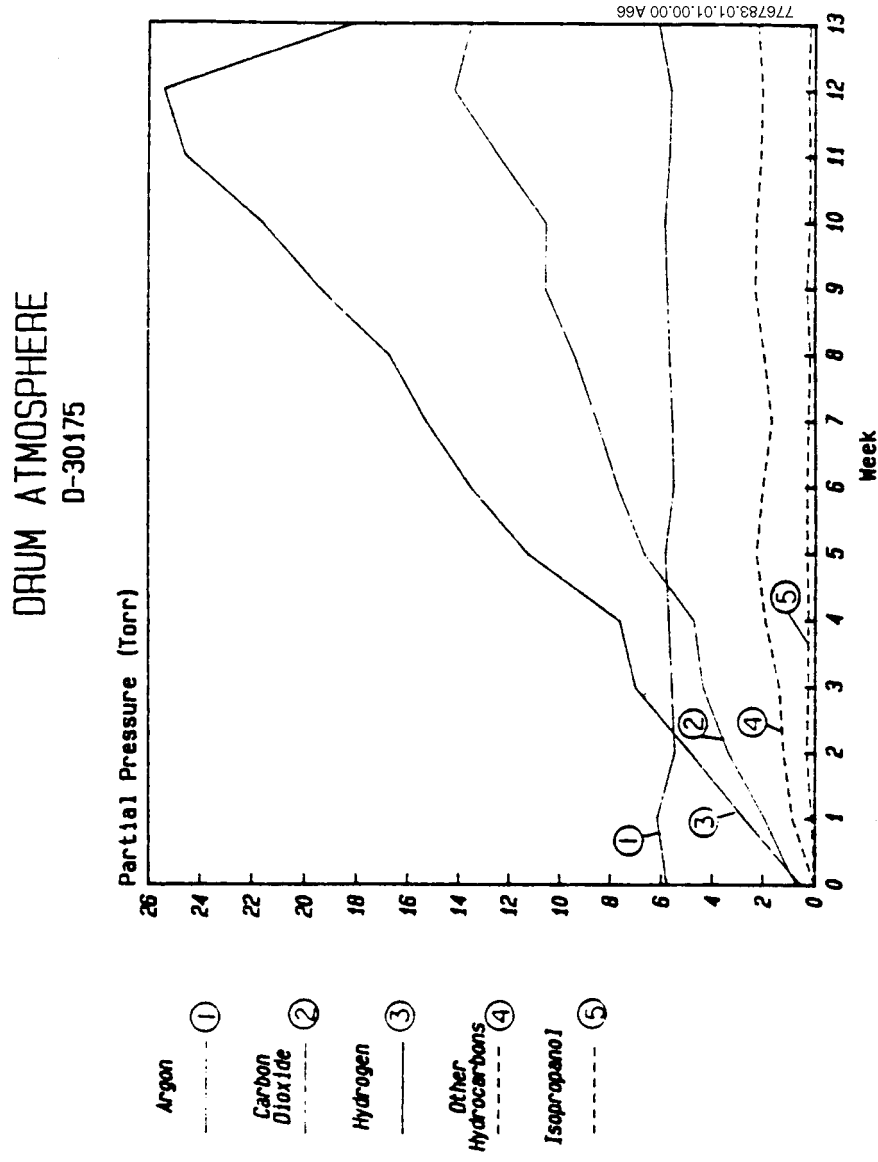
776783.01.01.00.00 A66

Week

Figure 3.1-1 — Partial Pressures of Various Gases in a Drum of Newly-Generated Waste from RFP (Leaded Rubber Gloves)

3.1.6.2.2 Los Alamos National Laboratory Experiments

In the LANL experiments, six high-activity newly generated Pu-238 waste drums were examined to determine gas generation rates and the ability of filters to limit the hydrogen concentration in the drum. Two additional drums of wastes provided information on the permeation of hydrogen through the 90-mil high-density polyethylene rigid liner. The experiments were separated into the same two phases as the RFETS experiments.

All of the drums selected contained combustible materials. Each waste package within the drum was individually assayed using segmented gamma scan techniques, and the assay results for the individual packages were added to obtain the total activity. The wastes had been generated from three to eight months before the gas generation phase of the experiments began.

Gas generation data for five of the six drums of waste for which void volumes could be measured are listed in Table 3.1-46. An ambient atmospheric pressure at Los Alamos of 579 mm Hg was assumed for all cases. (Actual ambient pressures were obtained for sampling dates, but using those pressures did not reduce the scatter of the measurements.)

No observable decrease in G values appeared to occur in these experiments until after about 100 days into the experiment (for wastes that had been generated three to eight months before the experiments began). In another 200 days, the G values had dropped to about one-half of their initial values. A plot of gas yields versus time for drum BFB-116 is shown in Figure 3.1-2. The composition of the generated gas was 46% CO_2, 41% H_2, 12% CO, and 1% CH_4, comparable to the gas composition measured in laboratory radiolysis experiments on Hypalon[R] or Neoprene[R].

3.1.6.2.3 Savannah River Site Experiments

SRS initiated a series of experiments in 1976 to acquire data on drum pressures and gas compositions under actual storage conditions at SRS (Ryan 1982[128]). Four drums were filled with highly contaminated material consisting of typical SRS waste. Data were collected on a monthly basis for over four years. The waste materials were contained in plastic bags that were placed within a 90-mil-thick high-density polyethylene liner. The liner was sealed with an adhesive. The drum lids were locked on over a neoprene-butadiene O-ring gasket (specified to be nonporous), with a galvanized ring bolt. While sealing compound was used to hold the gasket in place on the drum lid, no adhesive was applied to the lower surface of the gasket. Valves and airtight bulkhead fittings were connected to each drum wall before the drums were filled with waste. A detailed inventory and radioactive material assay were conducted of each bag of waste materials. The test drums were placed in concrete culverts. The culverts, 7-ft high by 7-ft dia. cylindrical containers with 6-in. thick walls, were designed to contain 14 drums of waste in two tiers of seven. The culvert lids were grouted in place and sealed with epoxy.

About 100 days after the experimental drums had been filled with waste and sealed, the drums were placed into the culvert. Two thermocouple wires were included in the instrumentation, one attached to the drum that contained the greatest amount of radioactivity (Drum No. 122), the other suspended in the culvert to read the air temperature. Ryan (Ryan 1982[128]) reported most of the temperature data only for outside air. Where data were available, the drum surface

Table 3.1-46 — Effective G Values for LANL Newly-Generated Waste Drums[a]

Drum No.	Waste Form Description	Dates			^{238}Pu		Void Vol.[c]	Effective G Values			
								Initial		Final	
		Pkg.	Start	End	g	Ci	ℓ	H2	Total	H2	Total
BFB-112	plastic, leaded gloves	7/28/83	4/10/84	2/22/85	1.2	16.8	198.1	0.3	0.6[b]	0.1	0.3
BFB-114	plastic, rags	9/23/83	12/29/83	3/30/84	15.6	218.4	201.1	0.4	0.7	0.1	0.6
BFB-116	leaded gloves	10/27/83	4/10/84	2/22/85	2.28	31.9	210.3	0.2	0.5[b]	0.1	0.2
BFB-118	rags, plastics, metals, metal oxides	10/27/83	4/10/84	1/29/85	4.92	68.9	201.3	0.4	0.8[b]	0.2	0.4
BFB-120	leaded gloves	1/03/84	8/10/84	3/06/85	1.6	22.4	215.6	0.2	0.4	0.1	0.3

Notes: [a]Calculated using authors' data; Drum BFB-113 has been omitted because of the scarcity of data in the sealed condition.

[b]Initial G values apply to the first 100 days of the 300-day experiment.

[c]Void volume for drum BFB-114 is the volume inside the rigid liner; other void volumes include the void between the rigid liner and the drum.
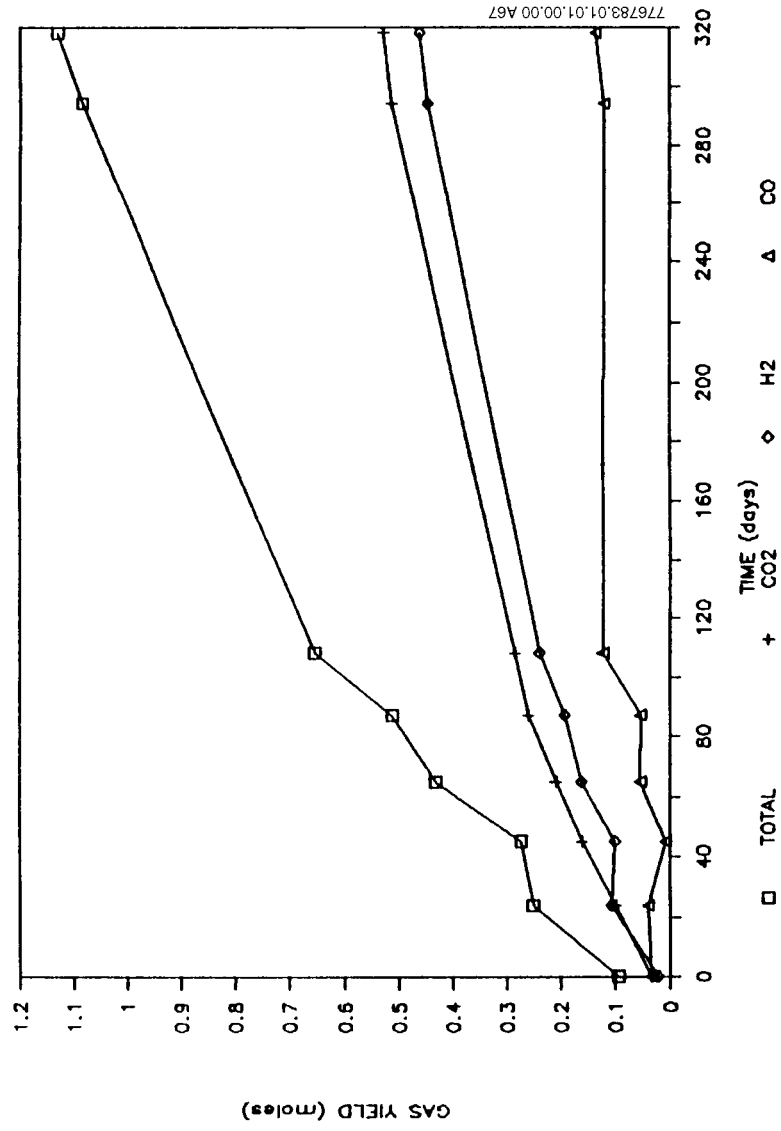
Figure 3.1-2 — Gas Yields vs. Time LANL Drum BFB-116 (Leaded Rubber Gloves)

temperature typically was no more than 5°C different from the outside air temperature, although one measurement showed a difference of 12°C.

The first gas samples were drawn 101 days after the drums were sealed. Subsequent samples were taken about every 30 days. The composition of ambient air was determined as part of the standardization of each gas analysis and was, on the average, 79% N_2, 21% O_2, and 0.1% CO_2. [The 1% Ar that is present in ambient air was not reported.]

Ryan (Ryan 1982[128]) plotted drum gas concentrations versus time and drum gauge pressures versus time. The gas composition of the culvert atmosphere was also measured. The largest hydrogen concentration measured in a culvert air sample was about 0.7 mole %. No appreciable hydrogen concentration was measured inside the culvert until day 993. Ryan stated that a significant quantity of gas was escaping from the drums at all times. This conclusion appears to be based on the maximum G values calculated from the largest (or close to largest) increases in the amounts of gas present, and then extrapolating the pressures from those G values. Ryan concluded that G(gas) appeared to be at least equal to 1.0 and more likely about 2.0.

Ryan's data (concentrations for each gas species, air temperature, gauge pressure, drum void volume, activity, and sampling date) were entered onto a LOTUS spreadsheet that calculates moles of gas and G values as functions of time. Drums 119 and 121 appear to have leaked, while drums 120 and 122 could have been well sealed, at least for most of the four-year period. Plots of gauge pressure and total moles of gas present are shown in Figures 3.1-3 and 3.1-4 for drum 122. The cyclical behavior of the gauge pressure versus time plot corresponds to annual temperature variations.

Figure 3.1-5 shows a plot of $G(H_2)$ versus time, with the points chosen by Ryan checked. The plot illustrates the variability in the experimental data. The greatest slope of the curve (ignoring wide swings in the data) occurs at the beginning of the experiment, with $G(H_2)_{max}$=0.2. Similar evaluations performed for the other three drums show that the G values appear to be much less than 1, in agreement with laboratory data for the radiolysis of rubber.

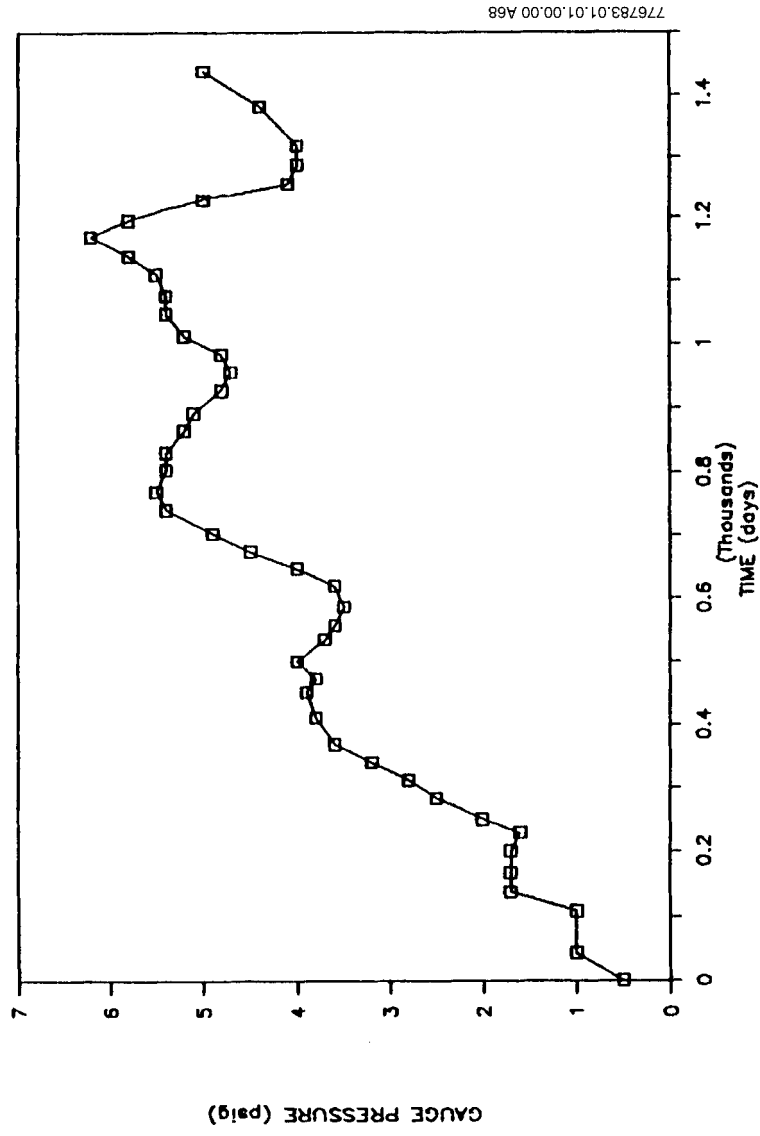776783.01.01.00.00 A68

Figure 3.1-3 — Gauge Pressure in Drum 122 vs. Time

777783.01.01.00.00 A69
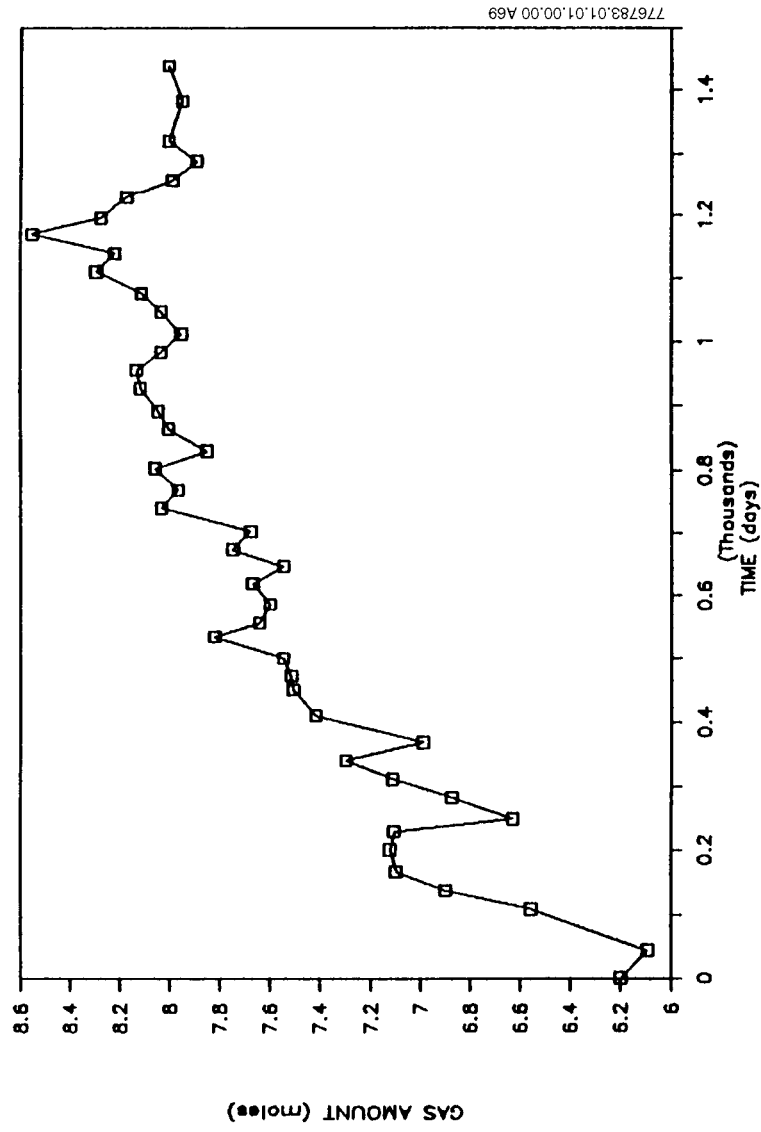
Figure 3.1-4 — Moles of Gas Present in Drum 122 vs. Time
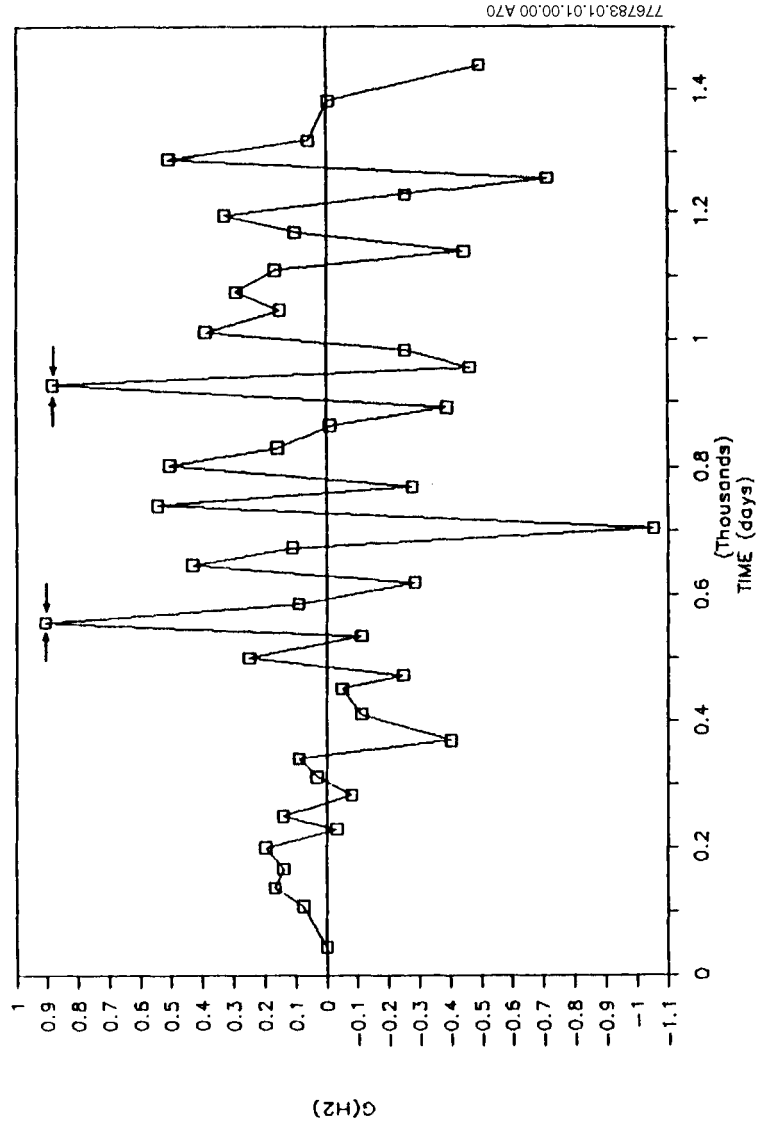
3.1-101

776783.01.01.00.00 A70

Figure 3.1-5 — G(H₂) vs. Time for Drum 122

3.1-102

Attachment A
Chemical Properties and Commercial Uses of Organic Materials

Executive Summary

Almost all of the materials that are potential generators of gas from radiolysis are organic materials (water and inorganic materials containing water being the primary exceptions). These organic materials are hydrocarbons or their derivatives containing oxygen, nitrogen, halogens, or other atoms. Naturally occurring organic materials that are present in the CH-TRU wastes, such as cellulose, also may generate radiolytic gas.

Basic families of organic liquids are described in Section A1.1. Polymers and their use in commercial materials are discussed in Section A1.2. Section A1.3 illustrates structural features of many commercial polymers.

A1.1 Families of Organic Liquids

Common names for families of organic liquids are: the hydrocarbons [alkanes (paraffins), alkenes (olefins), alkynes, cyclic hydrocarbons, and aromatic hydrocarbons]; the oxygenated organic compounds [ethers, esters, alcohols, aldehydes, ketones, and organic acids]; and the organic derivatives of ammonia (called amines). Compounds having the same formula but different structures and properties are called isomers (Pierce 1970[1]). (Higher-molecular-weight members of these families may be solids at room temperature rather than liquids.)

Hydrocarbons, as the name implies, contain only hydrogen and carbon atoms. Except for methane (CH_4), the carbon atoms form chains that consist of two or more atoms. The main chain may also contain side branches of atoms.

The alkanes are saturated hydrocarbons in which only carbon-carbon single bonds occur. All of the alkane names end in "-ane," such as methane, ethane, propane, and butane. In the petroleum industry, a high-temperature process called cracking of the saturated hydrocarbons causes the molecules to separate into fragments that then recombine at random to form other hydrocarbons and hydrogen gas. The alkanes are used as fuels to generate energy by oxidation (combustion). The addition of halogens forms such compounds as carbon tetrachloride, chloroform, trichloroethylene, hydrogen chloride, and other halogenated compounds.

The alkenes (olefins) are unsaturated hydrocarbons that contain double carbon-carbon bonds. All of the names of the alkenes end in "-ene," such as ethene, propene, and butene. Many of the olefins polymerize, forming macromolecules having gram molecular masses on the order of 10^4 to 10^6.

In the alkynes, the double bond of the alkenes is replaced by a triple carbon-carbon bond. Acetylene is one of the common alkynes.

---

[1] Pierce 1970. J. B. Pierce, The Chemistry of Matter, Houghton Mifflin Company, Boston, 1970.

Cyclic hydrocarbons may be alkanes (such as cyclohexane), alkenes, or alkynes. All of the cyclic alkanes have saturated carbon-carbon bonds.

Aromatic hydrocarbons contain a benzene ring and include benzene, toluene, naphthalene, and xylene. Aromatic compounds may be formed by joining benzene rings together through the elimination of hydrogen, for example, biphenyl (two benzene rings). Naphthalene is an example of a condensed-ring structure and is used in the manufacture of alkyd resins. A hydrogen atom on a benzene ring can be replaced by other chemical species through halogenation, sulfonation, or nitration. Toluene is formed by replacing one of the hydrogen atoms in benzene by a methyl (CH_3) group. Xylene is formed by replacing two of the hydrogens by methyl groups. The location of the substituted groups determines the isomer (ortho, meta, para). Phenol is formed by adding a hydroxyl group (OH) to the benzene molecule and is used in the formation of Bakelite® plastics and glues.

Organic compounds may also contain oxygen. The oxygen atoms may be bonded between carbon atoms to form ethers or esters. Oxygen atoms may bond to single carbon atoms to form alcohols (ROH), ketones (RCOR'), aldehydes (RCOH), or carboxylic acids (RCOOH).

Individual alcohols are named by adding the suffix "-ol" to the name of the corresponding alkane, such as "methanol." Several different isomers of alcohols are possible as the number of carbons in the chain increases, such as in propanol and butanol. More than one hydroxyl (OH) group may be present in the molecule, such as for ethylene glycol and glycerol.

Aldehydes are formed by oxidation of alcohols which have an hydroxyl group on a terminal carbon atom. The simplest aldehyde is formaldehyde. It reacts with phenol and urea to form phenol-formaldehyde and urea-formaldehyde resins.

Ketones are formed by oxidation of a secondary alcohol. The simplest ketone is acetone.

The organic (carboxylic) acids contain the group -COOH attached to either an alkyl or an aryl group. Examples of these acids are formic acid, acetic acid, oleic acid, and oxalic acid. Long-chain organic acids are called fatty acids.

The reaction of a carboxylic acid with an alcohol produces an ester (RCOOR') plus water. Common names for esters end in "-ate." When there are no double or triple bonds between the carbon atoms, the materials are solids; otherwise, they are liquids at room temperature. Esters of low molecular mass are used as solvents, artificial flavors, and components in perfumes. Waxes contain esters formed by the reaction of long-chain acids and alcohols. Fatty-acid esters of glycerol are found in vegetable oils and animal fats. The less volatile esters (such as dioctyl phthalate) are commonly used as plasticizers. The reaction of fats with boiling sodium hydroxide solution forms soaps.

Amines are organic derivatives of ammonia. Amines are used in the production of polyamides, such as Nylon®. Proteins are also polyamides.

A1.2 Polymers

Polymers are natural or synthetic materials that are composed of very large molecules containing repeating structural units called monomers. The structural features of many commercial polymers are shown in Section A1.3.

Knowledge of the repeat unit can aid in interpreting or predicting the gases generated by radiolysis (or thermal degradation). Additives also can affect the gas generation potential of commercial materials made from polymers. Polymers composed of more than one kind of repeat unit are termed copolymers.

Various additives are combined with the base polymer or polymers in compounding to produce the final commercial composition and properties of a plastic. Liquid plasticizers are added to polymers such as polyvinyl chloride (PVC) or cellulose esters to increase their flexibility. These compounds are chosen for their relatively low volatility but may be lost from a material that is heated or aged for long periods of time. Plasticizers in PVC commonly compose about 30-40% of the total material. Most of the plasticizers are less solvent- and chemical-resistant than the polymer to which they are added. Many plasticizers may be extracted by oils or dry-cleaning solvents. Most of the plasticizers are combustible, and lower the flame resistance and softening points of the total composition (Deanin 1972[2]).

Stabilizers are added to the polymer to increase resistance to heat, ultraviolet light, or other forms of degradation. Most plastics contain antioxidants, which may be consumed eventually by chemical reactions with oxygen. Polymers that crosslink are often rendered quite sensitive to oxidative degradation by radiation. The use of effective antioxidants can significantly improve their radiation resistance. Materials added to obtain other desirable properties could result in a final product which is less radiation resistant than the base polymer. However, this does not appear to happen often. Inorganic fillers are usually effective in increasing radiation resistance by dilution of the base polymer (EPRI 1981[3]).

Organic phosphates and halogenated compounds are frequently added to polymers to increase their flame resistance. At the same time, these additives may decrease thermal and other types of stability, particularly if they contain organic halogen compounds (Deanin 1972[2]).

The CH-TRU wastes consist of commercial materials, containing plasticizers and stabilizers that can affect radiolytic gas production (both the composition and amount of gas). For this reason, maximum G values measured for commercial materials provide more realistic upper bounds for radiolytic gas generation than do the G values measured for pure polymers.

---

[2] Deanin 1972. R. D. Deanin, Polymer Structure, Properties and Applications, Chaners Books, Boston, 1972.

[3] EPRI 1981. Georgia Institute of Technology, "Radiation Effects on Organic Materials in Nuclear Plants," Electric Power Research Institute, EPRI NP-2129, November 1981.

Chain lengths on the order of a hundred thousand monomer units are not uncommon in polymers (Sisman 1963[4]). Branched or network structures may be present. Most linear commercial polymers have a small amount of branching caused by impurities in the starting material or side reactions during the polymerization process. Polymers may be amorphous, crystalline, or contain regions of each. The linear polymers are used in a wide variety of molded and extruded objects. The solubility of linear polymers in solvents permits their use as paints, coatings, and films. Other applications include fibers, fabrics, tires, hoses, and gaskets.

Polymers are useful as electrical and thermal insulators. The rigidity and hardness of cross-linked polymers have been utilized in molded objects, which can be produced economically by thermally initiating cross-linking reactions within the mold. Polymers having network structures are generally insoluble. They have a strong tendency to retain their shape through rubber-like elasticity in materials with a low density of cross links or through high rigidity and hardness in heavily cross-linked materials (Sisman 1963[4]).

Table A1.2-1 lists the families of plastics (Dean 1987[5]). Cross-references of commercial names with the base polymers are available in Desk-Top Data Bank (1977[6], 1979[7], 1980[8]).

A1.2.1   Acetals

Acetal homopolymers are prepared from formaldehyde and consist of high-molecular-weight linear polymers of formaldehyde. They are among a group of high-performance engineering thermoplastics that resemble Nylon® in appearance (but not in properties). Trade names include Delrin® and Celcon®. Prolonged exposure to elevated temperatures results in the liberation of increasing amounts of formaldehyde. Acetals have relatively low radiation stability (Harper 1975[9]). Major applications for polyoxymethylene (an acetal) are in business machines, automotive gears and bearings, plumbing fittings, such as tub assemblies, and in consumer articles, such as aerosol containers (Deanin 1972[2]).

---

[4] Sisman 1963. O. Sisman, et al., "Polymers," in <u>Radiation Effects on Organic Materials</u>, Academic Press, New York, 1963, eds. R. O. Bolt and J. G. Carroll.

[5] Dean 1987. J. A. Dean, <u>Handbook of Organic Chemistry</u>, McGraw-Hill Book Company, New York, 1987.

[6] Desk-Top Data Bank 1977. Desk-Top Data Bank, <u>Elastomeric Materials</u>, The International Plastics Selector, Inc., San Diego, 1977.

[7] Desk-Top Data Bank 1979. Desk-Top Data Bank, <u>Films, Sheets, and Laminates</u>, The International Plastics Selector, Inc., San Diego, 1979.

[8] Desk-Top Data Bank 1980. Desk-Top Data Bank, <u>Commercial Names and Sources for Plastics and Additives</u>, The International Plastics Selector, Inc., San Diego, 1980.

[9] Harper 1975. C. A. Harper, <u>Handbook of Plastics and Elastomers</u>, McGraw-Hill Book Company, New York, 1975.

Table A1.2-1 — Families of Plastics

Acetals
Acrylics
      Polymethyl methacrylate (PMMA)
      Polyacrylonitrile (PAN)
Alkyds
Alloys
      Acrylic-polyvinyl chloride alloy
      Acrylonitrile-butadiene-styrene-polyvinyl chloride alloy (ABS-PVC)
      Acrylonitrile-butadiene-styrene-polycarbonate (ABS-PC)
Allyls
      Allyl-diglycol-carbonate polymer
      Diallyl phthalate (DAP) polymer
Cellulosics
      Cellulose acetate resin
      Cellulose-acetate-propionate resin
      Cellulose-acetate-butyrate resin
      Cellulose nitrate resin
      Ethyl cellulose resin
      Rayon®
Chlorinated polyether
Epoxy
Fluorocarbons
      Polytetrafluoroethylene (PTFE)
      Polychlorotrifluoroethylene
      Perfluoroalkoxy (PFA) resin
      Fluorinated ethylene-propylene (FEP) resin
      Polyvinylidene fluoride
      Ethylene-chlorotrifluoroethylene copolymer
      Ethylene-tetrafluoroethylene copolymer
Polyvinyl fluoride
Melamine-formaldehyde
Melamine phenolic
Nitrile resins
Phenolics
Polyamides
      Nylon®s
      Aromatic Nylon®s
Polyamide-imide
Polyaryl ether
Polycarbonate
Polyesters
      Polyethylene terephthalate (PET)
      Unsaturated polyesters

Table A1.2-1 — Families of Plastics (Concluded)

Polyimide

Polymethyl pentene
Polyolefins
       Low-density polyethylene (LDPE)
       High-density polyethylene (HDPE)
       Ultrahigh-molecular-weight polyethylene
       Polypropylene
       Polybutylene
       Polyallomers
Polyphenylene oxide
Polyphenylene sulfide
Polyurethanes
Silicones
Styrenics
       Polystyrene
       Acrylonitrile-butadiene-styrene (ABS) copolymer
       Styrene-acrylonitrile (SAN) copolymer
       Styrene-butadiene copolymer
Sulfones
       Polysulfone
       Polyether sulfone
       Polyphenyl sulfone
Thermoplastic elastomers
Urea-formaldehyde
Vinyls
       Polyvinyl chloride (PVC)
       Polyvinyl acetate (PVAC)
       Polyvinylidene chloride
       Polyvinyl butyrate
       Polyvinyl formal
       Polyvinyl alcohol

Ref: Dean 1987[5].

A1.2.2   Acrylics

Polyacrylates are derivatives of acrylic acid. They are frequently used as coatings or paints.
Polyethyl acrylate is used as a component of synthetic rubbers in which resistance to oils and
high temperatures is important (Bopp 1963[10]). Polymethyl methacrylate (PMMA), a related
compound, has common trade names of Plexiglas® and Lucite®. Acrylics are also made into
fibers and fabrics, such as Orlon®, Acrilan®, and Creslan® (Rutherford 1963[11]).

---

[10] Bopp 1963. C —D. Bopp, et al., "Plastics," in <u>Radiation Effects on Organic Materials</u>, Academic Press, New York, 1963, eds. R. O. Bolt and J. G. Carroll.

[11] Rutherford 1963. H. A. Rutherford, "Textiles," in <u>Radiation Effects on Organic Materials</u>, Academic Press, New York, 1963, eds. R. O. Bolt and J. G. Carroll.

Polyacrylonitrile (PAN) is a member of the acrylic family that includes nitrogen atoms in its structure. Its major use is in the production of wool-like fibers used in sweaters, blankets, and carpeting (Deanin 1972[2]).

A1.2.3 Alkyds

Alkyds are thermosetting plastics that are widely used for molded electrical parts. They have high degrees of cross-linking (Deanin 1972[2]) and are chemically similar to polyester resins (Harper 1975[9]).

A1.2.4 Alloys

Polymer alloys are physical mixtures of structurally different homopolymers or copolymers. The mixture is held together by secondary intermolecular forces such as dipole interaction, hydrogen bonding, or van der Waals' forces. The physical properties of these alloys are averages based on composition (Dean 1987[5]). Polymer alloys include acrylic-polyvinyl chloride, acrylonitrile-butadiene-styrene-polyvinyl chloride (ABS-PVC), and acrylonitrile-butadiene-styrene-polycarbonate (ABS-PC). ABS alloyed or blended with polycarbonate results in a thermoplastic that is easier to process, has high heat and impact resistance, and is cheaper than polycarbonate alone.

A1.2.5 Allyls

Allyl polymers are linear thermoplastic structures. Molding compounds with mineral, glass, or synthetic fiber filling are used for electrical components. Allyl polymers include allyl-diglycol-carbonate and diallyl phthalate (DAP). Their benzene rings, a high degree of cross-linking, and the usual glass fiber reinforcement provide high rigidity and strength. Primary applications are in molded structural electrical insulation. Diallyl phthalate resin is also used for surfacing laminates in furniture and paneling (Deanin 1972[2]).

A1.2.6 Cellulosics

Cellulosics are a class of polymers that are prepared by various treatments of purified cotton or special grades of wood cellulose. Trade names include Tenite®, Ethocel®, and Forticel®. Cellulosics are among the toughest of thermoplastics, are generally economical, and are good insulating materials (Harper 1975[9]). The most prominent industrial cellulosics are cellulose acetate, cellulose acetate butyrate, cellulose propionate, and ethyl cellulose.

Cellulose butyrate, propionate, and acetate are tough and rigid, and useful for applications where clarity, outdoor weatherability, and aging characteristics are needed. The materials are fast-molding plastics and can be manufactured to have hard, glossy surfaces (Bopp 1963[10]). Major applications of these cellulose esters include blister packaging, pencils, lighting fixtures, tool handles, and tubing (Deanin 1972[2]). Ethyl cellulose is compatible with many other resins and with most plasticizers. These properties, along with its compatibility with cellulose nitrate, are responsible for its use in paints and as a coating for fabrics (Bopp 1963[10]).

Incompletely nitrated cellulose nitrate is used in molded objects, and as a constituent of lacquers and photographic film. Because of its flammability and tendency to decompose at high

temperatures, cellulose nitrate is not used as a compression or injection molding material (Bopp 1963[10]). The nitrogen content for cellulose nitrate plastics is usually about 11%, for lacquers and cement base it is 12%, and for explosives it is 13% (Dean 1987[5]).

Cotton and cellulose acetate (Rayon[®]) are two cellulosics that are made into fibers. Cellulosics (cotton and wood) are blended in making paper. Cellophane is also based on cellulose (Deanin 1972[2]). Cellulose triacetate is used primarily in motion picture film and magnetic recording tape (Deanin 1972[2]). Cellulose ethers have applications where low temperature impact strength is needed, such as in instrument cases, electrical appliance parts, and tool handles. Different processing produces a polymer that is completely soluble in water and is used primarily as a thickening agent in foods, shampoo, latex paints, paper, and adhesives (Deanin 1972[2]).

A1.2.7   Epoxy

Epoxies and unsaturated polyesters are cross-linking resins that can be cured by chemical agents with little or no application of heat or pressure. They are frequently used in paints and finishes (Bopp 1963[10]).

A1.2.8   Fluorocarbons

Fluorocarbons include polytetrafluoroethylene (PTFE), polychloro-trifluoroethylene, perfluoroalkoxy (PFA) resin, fluorinated ethylene-propylene (FEP) resin, polyvinylidene fluoride, ethylene-chlorotrifluoroethylene copolymer, ethylene-tetrafluoroethylene copolymer, and polyvinyl fluoride.

These polymers have good abrasion and solvent resistance and electrical properties. Polyvinyl fluoride is used only as a film (Dean 1987[5]).

Polytetrafluoroethylene is the base polymer for Teflon[®]. Polychloro-trifluoroethylene resins may be processed by melting and can be molded as extruded. Kel-F[®] is one of the trade names (Harper 1975[9]). PFA resins are used as electrical insulations in flat cables and circuitry and in laminates used in electrical and mechanical applications. Fluorinated ethylene/propylene copolymer has applications in capacitors, cables, flexible belting, textile finishing, and printing (Deanin 1972[2]).

A1.2.9   Nitrile Resins

The principal monomer of nitrile resins is acrylonitrile (see Section B.2.1).

A1.2.10 Polyamides

Polyamides are called nylons, which include hard materials used in mechanical parts as well as soft materials used for fibers and textiles. Aromatic nylons (also called aramids) are high temperature nylons such as Nomex[®]. Nomex[®] is used in sheet, fiber, and paper form for insulation (Harper 1975[9]) and in filters.

A1.2.11 Polyaryl Ether

Polyaryl ether is one of the relatively new thermoplastics that can be used for engineering applications in the automotive, appliance, and electrical industries. One trade name is Arylon[®] (Harper 1975[9]).

A1.2.12 Polycarbonate

Polycarbonates have high performance characteristics in engineering designs, which require very high impact strength. As with most plastics containing aromatic groups, polycarbonates have high radiation stability (Harper 1975[9]).

A1.2.13 Polyesters

Polyesters are used in the production of film and fibers. Glass reinforced polyesters are used in automotive, electrical/electronic, and other industrial applications replacing other plastics or metals. The basic polymer is polyethylene terephthlate (PET). Brand names include Mylar[®] (sheet) and Dacron[®] (fiber). Unsaturated polyesters are discussed under "Epoxies".

A1.2.14 Polyimides

Polyimides can be used at the highest temperatures among the commercially available plastics, and they are the strongest and most rigid (Harper 1975[9]). These materials can be used in various forms, including moldings, laminates, films, coatings, and adhesives.

A1.2.15 Polymethyl Pentene

Polymethyl pentene is another thermoplastic based on the ethylene structure. Applications for this material have been developed in the fields of lighting and in the automotive, appliance, and electrical industries (Harper 1975[9]).

A1.2.16 Polyolefins

The family of polyolefins includes various polyethylenes (low-density polyethylene, high-density polyethylene, ultrahigh-molecular-weight polyethylene), polypropylenes, polyethylene oxide, polypropylene oxide, and polybutylene.

Polypropylenes are chemically similar to polyethylenes (Harper 1975[9]). The material is termed isotactic if the methyl groups are on the same side of the chain and atactic if the arrangement is random. The isotactic polymer is more frequently used commercially (Sisman 1963[4]). The polymer is used to make molded items or fibers (Herculon is one example).

Commercial polyethylene oxide is waxy and fibrous. Because of its water solubility, it is used as a plasticizer and as an additive in non-polymeric materials rather than as a base polymer (Bopp 1963[10]).

Treatment of polyethylene with chlorine and sulfur dioxide decreases the crystallinity of the polyethylene and results in a rubbery material. Applications include wire and cable insulation,

3.1-111

liquid roof coatings, gaskets, floor tile, and shoe soles (Deanin 1972[2]). One trade name is Hypalon[®], which is used in fabricating glovebox gloves.

Polybutylene low-molecular-weight polymers are viscous liquids used in compounding adhesives, caulks, and sealants. High-molecular weight polymers are used in elastomers and sealants, such as butyl rubber (Deanin 1972[2]).

Polyallomers are polyolefin-type thermoplastic polymers produced from two or more different monomers, such as propylene and ethylene. In general, the properties of polyallomers are similar to those of polyethylenes and polypropylenes (Harper 1975[9]).

A1.2.17 Polyphenyl Polymers

Polyphenylene oxide is formulated by the oxidative coupling of phenolic monomers. This material is used for engineering applications. One trade name is Noryl[®]. Polyphenylene sulfide is a crystalline polymer, and is used for coatings and molded materials. One trade name is Ryton[®].

A1.2.18 Polyurethanes

The most common usage of polyurethane is in foams, which may be flexible or rigid (Deanin 1972[2]). These foams have applications as insulation, structural reinforcement, packaging, and gaskets (Harper 1975[9]).

A1.2.19 Silicones

Silicones are also called polysiloxanes. They are characterized by their three-dimensional branched-chain structure. Various organic groups (such as methyl, phenyl, vinyl) introduced within the polysiloxane chain impart certain characteristics and properties. Applications include waterproofing, paper coatings, elastomers, sealants, medical equipment, and transformers (Deanin 1972[2]).

A1.2.20 Styrenics

Polystyrene can be regarded as a substituted polyethylene with phenyl groups on alternate carbon atoms (Sisman 1963[4]). Polystyrene is highly rigid at room temperature, but the rigidity may be decreased and the impact strength increased by the addition of plasticizers. It can be used in moldings or in small electrical components, as well as in containers and other packaging items (Sisman 1963[4]). Common trade names are Lustrex[®] and Styron[®].

Styrene-acrylonitrile (SAN) copolymers are random, amorphous copolymers whose properties vary with molecular weight and copolymer composition. SAN resins are rigid, hard, transparent thermoplastics (Dean 1987[5]). Acrylonitrile-butadiene-styrene (ABS) copolymer is a thermoplastic resin. Trade names include Marbon Cycolac[®], Bason[®], and Lustran[®]. ABS plastics have hardness and rigidity without brittleness, at moderate costs (Harper 1975[9]). Styrene-butadiene copolymers are used in gaskets.

A1.2.21 Sulfones

Polysulfones are rigid, strong thermoplastics, and can be molded, extruded, or thermoformed into a wide variety of shapes. The chemical structure is highly resonating (contains benzene rings), resulting in high stability (Harper 1975[9]). Copolymers with olefins, however, have low radiation stability (Jellinek 1978[12]).

A1.2.22 Thermosetting Plastics

Thermosetting plastics are insoluble and infusible because of their three-dimensional structure. They are used chiefly as molding powders and as binders for laminates. Examples are phenol-formaldehyde, urea-formaldehyde, and melamine-formaldehyde. Common uses are in molded household items. Laminated sheets and tubes are widely used in electrical components or molded components of industrial equipment (Bopp 1963[10]).

A1.2.23 Vinyls

Vinyl polymers are structurally based on the ethylene chain (Harper 1975[9]).

Polyvinyl chloride (PVC) is a material with a wide range of rigidity or flexibility. PVC can be plasticized with a wide variety of materials to produce soft, yielding plastics. Without plasticizers, PVC is a strong, rigid material that can be machined, heat-formed, or welded by solvents or heat. Typical uses include wire and cable insulation and foam applications. PVC can also be made into film and sheet (Harper 1975[9]). Other uses are as a fabric coating, for upholstery and similar household articles, and for hoses and tubular items (Bopp 1963[10]).

Polyvinyl acetate (PVAC) is used in latex paints because of its quick-drying and self-priming properties, and resistance to weathering. It is also used in hot-melt and solution adhesives (Dean 1987[5]). Copolymers of polyvinylidene chloride and PVC are used to make Saran (Bopp 1963[10]).

Polyvinyl alcohol is made by the hydrolysis of polyvinyl acetate. It is soluble in water and resistant to most organic solvents. It is used in solvent-resistant hoses, diaphragms, and gaskets, and in coatings, textile sizing, and as an adhesive (Bopp 1963[10]).

Polyvinyl acetals, consisting of polyvinyl butyral, polyvinyl formal, and polyvinyl acetal, are the most abundantly used plastics related to polyvinyl alcohol. Polyvinyl formal is used in coating electrical wire. Polyvinyl acetal is tough and easy to mold, and is used for bottle caps, combs, and as a binder in heavily filled molded items. Polyvinyl butyral is a very important item of commerce as the interlayer in safety glass (Bopp 1963[10]).

A1.3 Structural Features of Commercial Polymers

The structural features of many commercial polymers are shown in Table A1.3-1.

---

[12] Jellinek 1978. H. H. G. Jellinek, Aspects of Degradation and Stabilization of Polymers, Elsevier Scientific Publishing Company, New York, 1978.

Table A1.3-1 — Structural Features of Commercial Polymers

Acrylonitrile/butaiene/styrene terpolymer (ABS)

$$— (CH_2CH = (CHCH) —$$

Alkyd

$$— (C\ COCH_2CHCH_2O) —$$

Butadiene/acrylonitrile rubber (nitrile rubber or NBR)

$$— (CH_2CH = CHCH_2) — (CH_2CH) —$$

$$(C \equiv N)$$

Butadiene/styrene rubber (SBR or GR-S)

$$— (CH_2CH = CHCH_2) — (CH_2CH) —$$

Cellulose

$$— CH_2OH$$

Table A1.3-1 — Structural Features of Commercial Polymers (Continued)

Cellulose Nitrate

$$CH_2ONO_2$$
$$CH\!-\!O$$
$$-\,(OCH \qquad CH)\!-$$
$$CH\!-\!CH$$
$$OH \qquad ONO_2$$

Cellulose Triacetate

$$O$$
$$\|$$
$$CH_2OCCH_3$$
$$CH\!-\!O$$
$$-\,(OCH \qquad CH)\!-$$
$$O \qquad CH\!-\!CH \quad O$$
$$\|\qquad\qquad\qquad \|$$
$$CH_3C\!-\!O \qquad O\!-\!CCH_3$$

Chlorosulfonated Polyethylene

$$-\,(CH_2CH_2)\!-\!(CH_2CH)\!-\!(CH_2CH)$$
$$Cl \qquad O\!=\!S\!=\!O$$
$$Cl$$

Diallyl Phthalate

$$O\ O$$
$$\|\ \|$$
$$-\,(CH_2CHCH_2O\!-\!C\ \ COCH_2CHCH_2)\!-$$

Epoxy Resin

$$O \qquad\qquad CH_3 \qquad\qquad O$$
$$-\,CH_2\!-\!CHCH_2O\!\!\bigcirc\!\!C\!\!\bigcirc\!\!OCH_2CH\!-\!CH_2$$
$$CH_3$$

Table A1.3-1 — Structural Features of Commercial Polymers (Continued)

Ethyl Cellulose

$$\begin{array}{c} CH_2OC_2H_5 \\ | \\ CH - O \\ \diagup \quad \diagdown \\ -(OCH \quad\quad CH)- \\ | \quad\quad | \\ CH-CH \\ | \quad\quad | \\ OH \quad OC_2H_5 \end{array}$$

Ethylene/Ethyl Acrylate Copolymer

$$-(CH_2CH_2)-(CH_2CH)-$$
$$|$$
$$O{=}C-OC_2H_5$$

Ethylene/Propylene Copolymer

$$-(CH_2CH_2)-(CH_2CH)-$$
$$|$$
$$CH_3$$
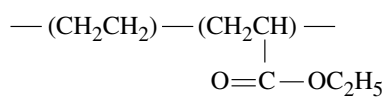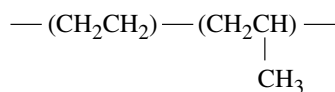
Ethylene/Vinyl Acetate Copolymer
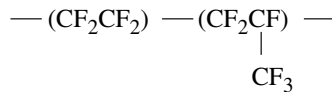
$$-(CH_2CH_2)-(CH_2CH)-$$
$$|$$
$$OCCH_3$$
$$\|$$
$$O$$

Fluorinated Ethylene/Propylen Copolymer

$$-(CF_2CF_2)-(CF_2CF)-$$
$$|$$
$$CF_3$$

Melamine-Formaldehyde

$$\begin{array}{c} N \quad\quad CH_2)- \\ \diagup \quad \diagdown \quad \diagup \\ -(N-C \quad\quad C-N-CH_2)- \\ | \quad \| \quad\quad \| \\ N \quad\quad N \\ \diagdown \quad \diagup \\ C \\ | \\ -(CH_2-N-CH_2)- \end{array}$$

Table A1.3-1 — Structural Features of Commercial Polymers (Continued)

Nylon 6

$$— [(CH_2)_5 \overset{\overset{\displaystyle O}{\|}}{C} — \overset{\overset{\displaystyle H}{|}}{N}] —$$

Nylon 11

$$—[(CH_2)_{10} \overset{\overset{\displaystyle O}{\|}}{C} — \overset{\overset{\displaystyle H}{|}}{N}] —$$

Nylon 12

$$—[(CH_2)_{11} \overset{\overset{\displaystyle O}{\|}}{C} — \overset{\overset{\displaystyle H}{|}}{N}] —$$

Nylon 610

$$—[(CH_2)_6 \overset{\overset{\displaystyle H}{|}}{N} — \overset{\overset{\displaystyle O}{\|}}{C}(CH_2)_8 \overset{\overset{\displaystyle O}{\|}}{C} — \overset{\overset{\displaystyle H}{|}}{N}] —$$

Nylon 66

$$—[(CH_2)_6 \overset{\overset{\displaystyle H}{|}}{N} — \overset{\overset{\displaystyle O}{\|}}{C}(CH_2)_4 \overset{\overset{\displaystyle O}{\|}}{C} — \overset{\overset{\displaystyle H}{|}}{N}] —$$
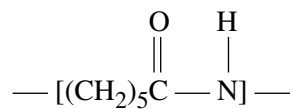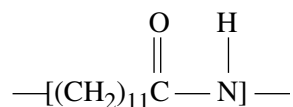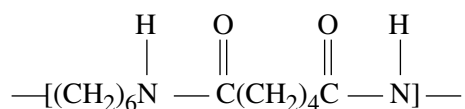
Phenol-formaldehyde
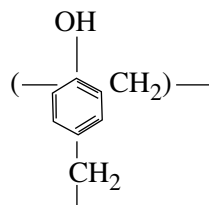
Phenoxy Resin

Table A1.3-1 — **Structural Features of Commercial Polymers (Continued)**

Polyacrylonitrile

$$-(CH_2CH)-$$
$$|$$
$$C\equiv N$$
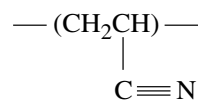
Polybenzimidazole
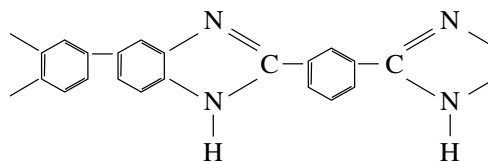
Poly-3,3-bis (chloromethyl) oxetane (Penton)

$$CH_2Cl$$
$$|$$
$$-(OCH_2CCH_2)-$$
$$|$$
$$CH_2Cl$$

Polybutadiene

$$-(CH_2CH=CHCH_2)$$

Poly-1-Butene

$$-(CH_2CH)$$
$$|$$
$$C_2H_5$$
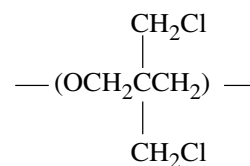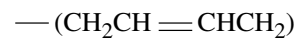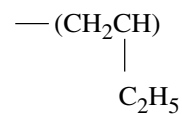
Polycarbonate

Polychloroprene (neoprene)

$$-(CH_2C=CHCH_2)-$$
$$|$$
$$Cl$$
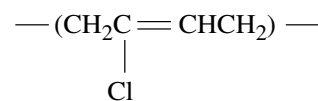
Table A1.3-1 — Structural Features of Commercial Polymers (Continued)

Polychlorotrifluoroethylene

$$— (CF_2CF) —$$
$$| $$
$$Cl$$
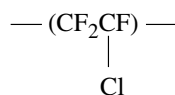
Poly (2,6-dimethylphenylene oxide) (PPO)
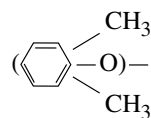
Polyepichlorohydrin

$$— (CH_2CHO) —$$
$$| $$
$$CH_2Cl$$
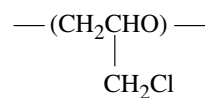
Polyester Polyurethane

$$— [(CH_2CH_2O\overset{O}{\overset{||}{C}}(CH_2)_4\overset{O}{\overset{||}{C}}O]CH_2CH_2O\overset{O}{\overset{||}{C}} — N ...$$
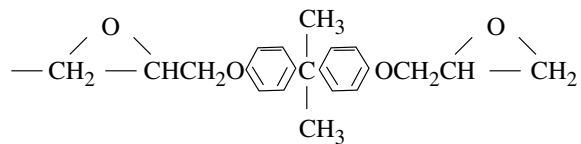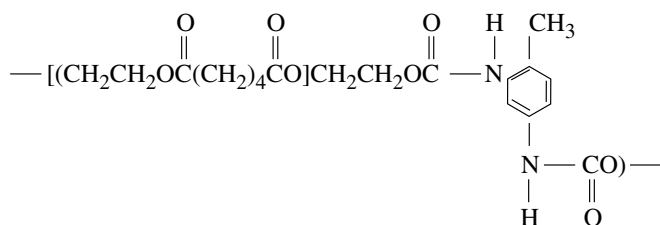
Unsaturated Polyester (cured)
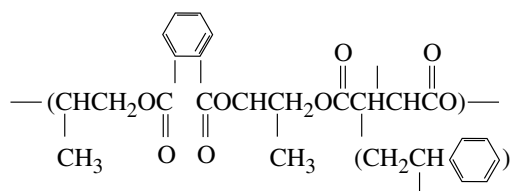
Polyether Polyurethane
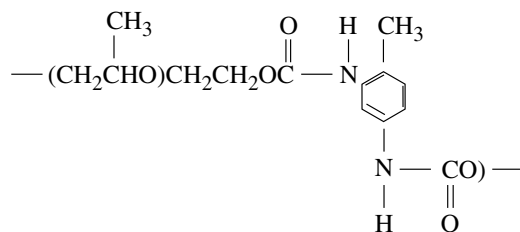
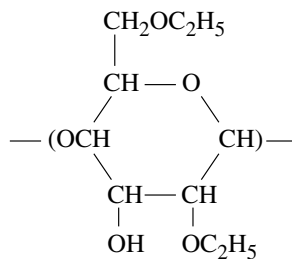## Table A1.3-1 — Structural Features of Commercial Polymers (Continued)

Polyethyl Acrylate

$$-(CH_2CH)-$$
$$| $$
$$O=COC_2H_5$$

High-Density Polyethylene

$$-(CH_2CH_2)-$$

Low-Density Polyethelene

$$-(CH_2CH_2)-(CH_2CH)-(CH_2CH)-(CH_2CH)-$$
$$C_2H_5 \qquad C_4H_9 \qquad C_nH_{2n+1}$$
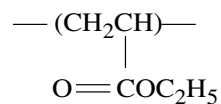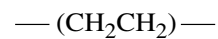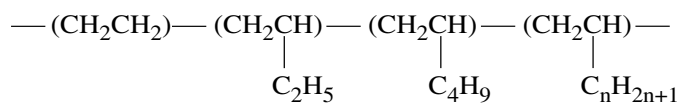
Polyethelene Oxide

$$-(CH_2CH_2O)-$$

Poly(ethelene terephalate)

$$-(CH_2CH_2OC\bigcirc CO)-$$
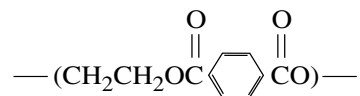
Polyimide

Polyisobutylene

$$CH_3$$
$$|$$
$$-(CH_2C)-$$
$$|$$
$$CH_3$$
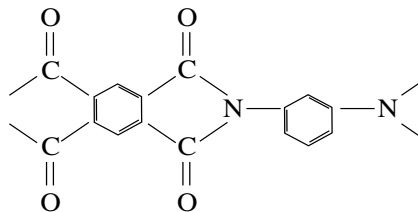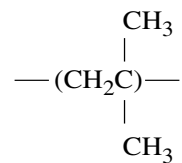
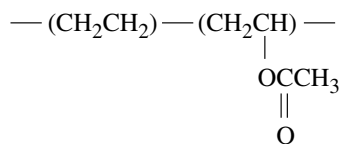## Table A1.3-1 — Structural Features of Commercial Polymers (Continued)

Polyisoprene (Natural Rubber)

$$—(CH_2C\!=\!CHCH_2)—$$
$$\underset{CH_3}{|}$$
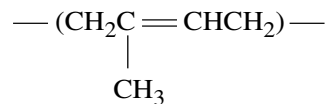
Polymethyl Metacrylate

$$\overset{CH_3}{\underset{|}{}}$$
$$—(CH_2\overset{|}{C})—$$
$$\underset{O\!=\!COCH_3}{|}$$
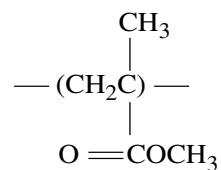
Poly (4-methylpentene-1)
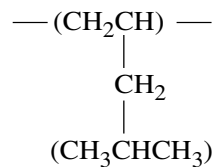
$$—(CH_2CH)—$$
$$\underset{CH_2}{|}$$
$$\underset{(CH_3CHCH_3)}{|}$$

Polyoxymethylene (Acetal)
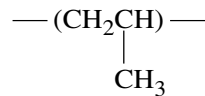
$$—(CH_2O)—$$

Polypropylene

$$—(CH_2CH)—$$
$$\underset{CH_3}{|}$$

Polypropylene-Oxide

$$—(CH_2CHO)—$$
$$\underset{CH_3}{|}$$
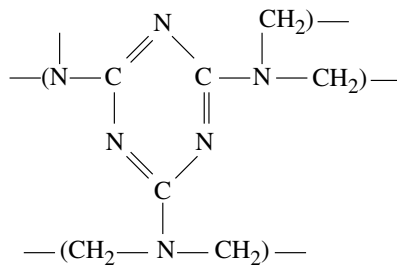
Poly-p-xylylene

$$—(CH_2 \langle \bigcirc \rangle CH_2)—$$
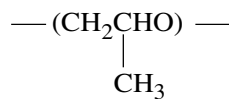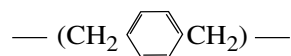
Table A1.3-1 — Structural Features of Commercial Polymers (Continued)

Polysulfide Elastomer

$$— (CH_2CH_2OCH_2OCH_2CH_2SSCH_2CH_2SS)—$$
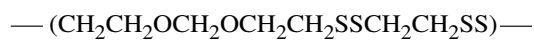
Polysulfone

Polystyrene

$$— (CH_2CH) —$$

Polytetrafluoroethylene

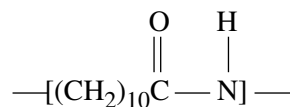$$— (CF_2CF_2) —$$
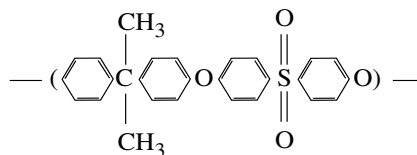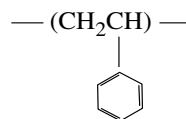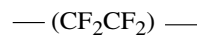
Polyvinyl Acetate
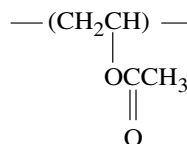
Polyvinyl Alchohol
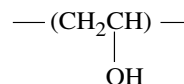
Polyvinyl Butyral
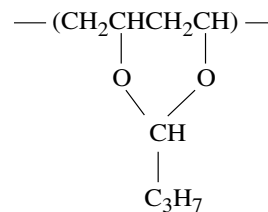
Table A1.3-1 — Structural Features of Commercial Polymers (Continued)

Polyvinyl Chloride
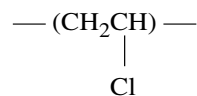
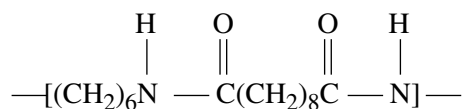$$— (CH_2CH) —$$
$$\vert$$
$$Cl$$

Polyvinyl Ethyl Ether
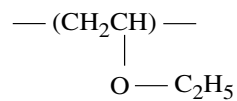
$$— (CH_2CH) —$$
$$\vert$$
$$O — C_2H_5$$

Polyvinyl Fluoride

$$— (CH_2CH) —$$
$$\vert$$
$$F$$

Polyvinyl Formal

$$— (CH_2CHCH_2CH) —$$
$$\vert \qquad \vert$$
$$O \qquad O$$
$$\diagdown \quad \diagup$$
$$CH_2$$

Polyvinylidene Chloride

$$Cl$$
$$\vert$$
$$— (CH_2C) —$$
$$\vert$$
$$Cl$$

Polyvinylidene Fluoride

$$— (CH_2CF_2) —$$
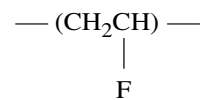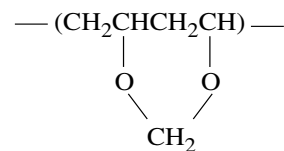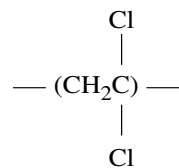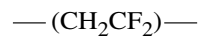
Polyvinyl Pyrrolidone

$$— (CH_2CH) —$$
$$\vert$$
$$N$$
$$\diagup \quad \diagdown$$
$$CH_2 \qquad C = O$$
$$\vert \qquad \vert$$
$$CH_2 — CH_2$$

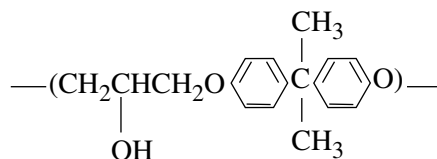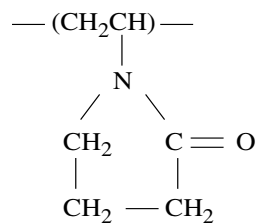## **Table A1.3-1 — Structural Features of Commercial Polymers (Concluded)**

Silicone

$$— (Si—O) —$$

with CH_3 above and CH_3 below Si
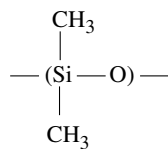
Sodium Carboxymethyl Cellulose (CMC)

$CH_2OCH_2CO^-Na^+$ (with O double bonded)

$CH—O$

$—(OCH \qquad CH)—$

$CH—CH$

$OH \qquad OH$

Styrene/Acrylonitrile Coplolymer

$$— (CH_2CH)—(CH_2CH)—$$

with phenyl ring below first, $C≡N$ below second

Impact Styrene

$$— (CH_2CH=CHCH)—$$

$$—(CH_2CH)—$$

with phenyl ring below

Urea-Formaldehyde

$$—(N—C—N—CH_2)—$$

with O double bonded to C, and $CH_2)—$ below N
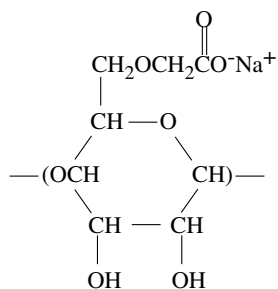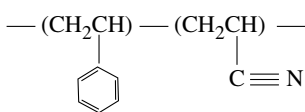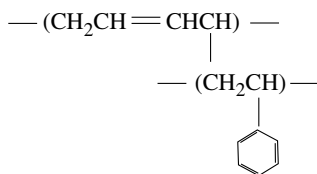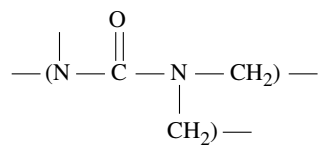
Vinyl Chloride Vinyl Acetate Copolymer

$$—(CH_2CH)—(CH_2CH)—$$

with Cl below first, $OCCH_3$ below second, O double bonded below
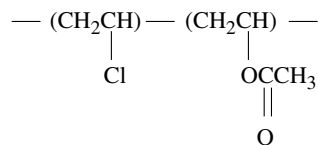
Vinylidene Fluoride/Hexafluoroporylene Copolymer

$$—(CH_2CF_2)—(CF_2CF)—$$

with CF_3 below

3.1-124
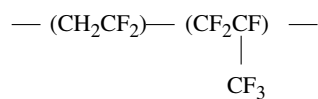
Attachment B
Absorption of Alpha Decay Energy Inside Particles of PuO_2

Executive Summary

This attachment derives the fraction of alpha decay energy escaping from a spherical particle of PuO_2 of radius r. The rate of energy deposition is calculated from an estimated Bragg curve for PuO_2.

B1.1 Introduction

Let

        s = stopping distance of alpha particles in PuO_2,
        a = radius of spherical particles of PuO_2.
        E_0 = energy generated per unit volume.

The solution is separated into three cases: for Case I, the diameter of the particle is less than the stopping distance (2a < s), for Case II, the stopping distance is between the radius and the diameter of the particle (a ≤ s ≤ 2a), and for Case III, the radius of the particle is greater than the stopping distance (s < a).

The rate of alpha particle energy deposition inside the PuO_2 particle is calculated based on the estimated Bragg curve shown in Figure B1-1. This curve was generated by the program TRIM-88 "The Transport of Ions in Matter," copyrighted by J. P. Biersack and J. F. Ziegler (discussed in Ziegler 1985[1]).

The highest atomic number nucleus included in the program is U(92), so UO_2 with the density of PuO_2 (11.4 g/cm^3) was used to simulate PuO_2. Figure B1-2 shows the alpha particle energy in MeV versus distance traveled from its origin for alpha particles having initial energies of 5.15 MeV (Pu-239) and 5.49 MeV (Pu-238). [The total distance along the particle's path is somewhat greater, due to straggling that occurs at low energies when collisions of the alpha particle with nuclei become more important than interactions of the alpha particle with electrons.]

B2.1 Case I, 2a < s

The geometry of Case I is shown in Figure B2-1. The fraction of energy reaching point Q from point P along r' is

$$E_F = f(E_o, r') \tag{B2-1}$$

---

[1] Ziegler 1985. J. F. Ziegler, J. P. Biersack, and U. Littmark, <u>The Stopping and Range of Ions in Solids</u>, Vol. I, Pergamon Press, New York, N.Y., 1985.
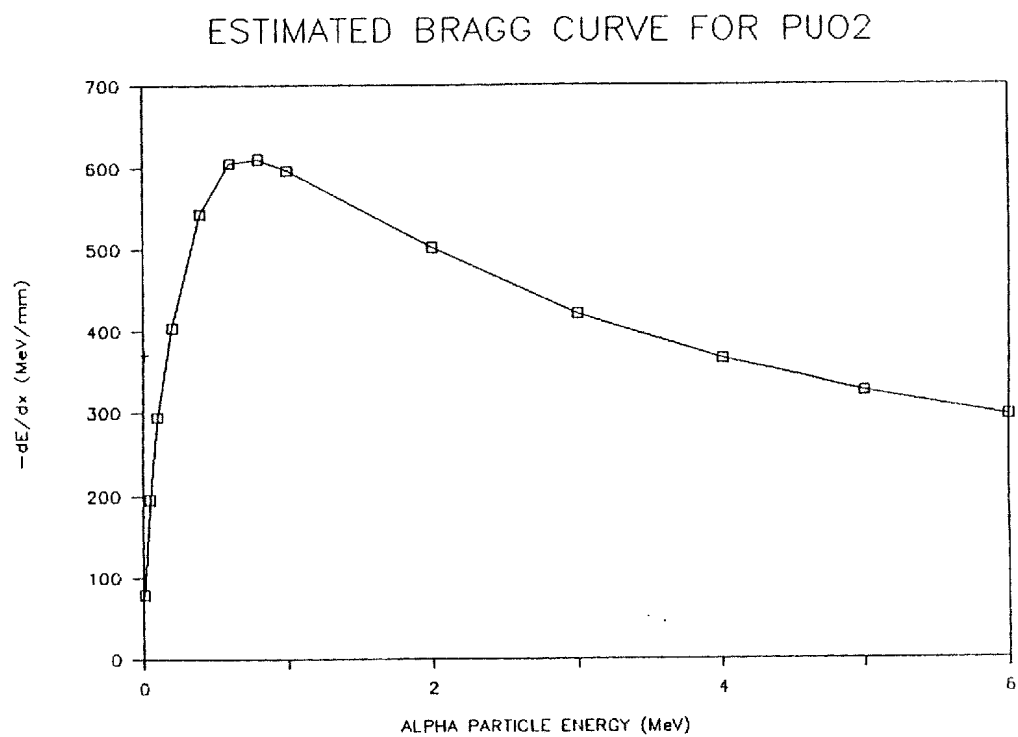
Figure B1-1
Estimated Bragg Curve for PuO$_2$
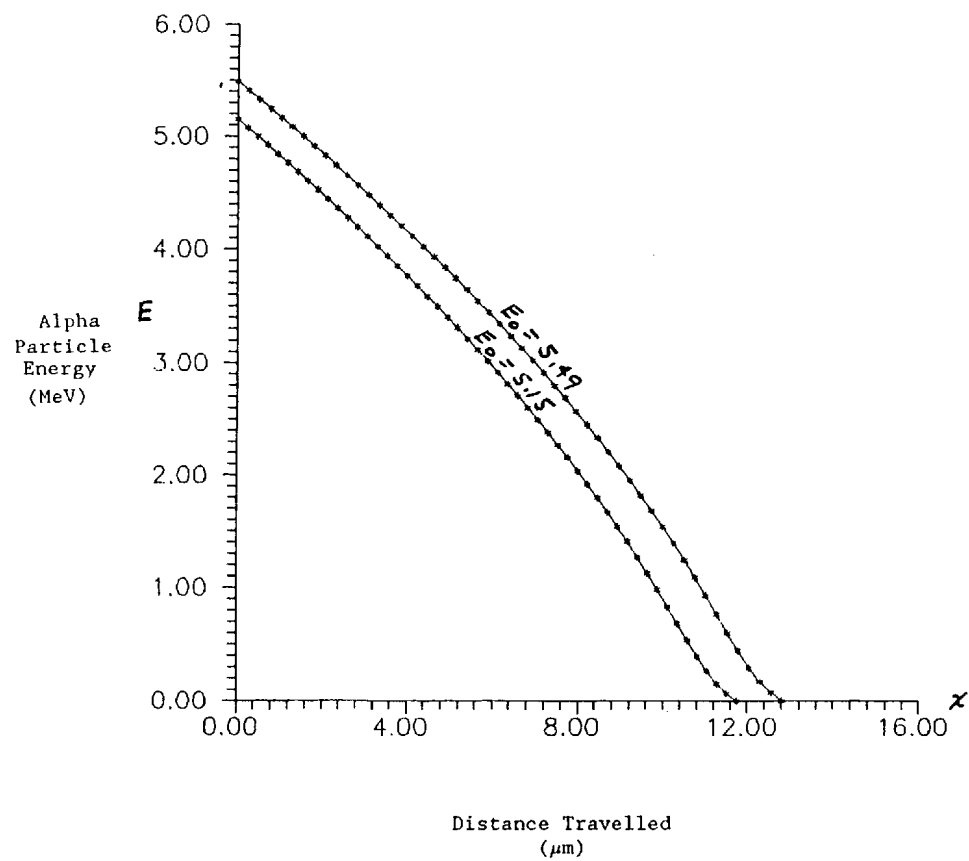
Figure B1-2
Alpha Particle Energy vs. Distance Traveled from Point of Origin

Where:

$$r'^2 = a^2 + r^2 - 2 \; ar \; \cos \; \omega \qquad \text{(B2-2)}$$

since r' < s for this case, and $f(E_0, r')$ is shown graphically in Figure B1-2 for two values of E_0.

The fraction of the area of a sphere centered at P, subtended by dϕ and revolved about the x axis is

$$A = \frac{r' d\phi 2 \; \pi \; r' \; \sin \; \phi}{4\pi \; r'^2} \qquad . \qquad \text{(B2-3)}$$

The total energy reaching the boundary, a, from point P is

$$\rho(r) = 1/2 \int_0^\pi \; f(E_O, r') \sin \phi \; d\phi \qquad . \qquad \text{(B2-4)}$$

The total energy from all points, P, in the sphere is

$$E = \int_0^a \; 4\pi \; r^2 \rho(r) \; dr = 2\pi \; \int_0^a \; r^2 \int_0^\pi \; f(E_O, r') \sin \phi \; d\phi \; dr \qquad . \qquad \text{(B2-5)}$$

The fraction of energy generated in the sphere and escaping from the surface is

$$\frac{E}{E_r} = \frac{2\pi}{4/3 \; \pi \; a^3 E_O} \int_0^a r^2 \int_0^\pi \; f(E_O, r') \; \sin \phi \; d\phi \; dr \qquad \text{(B2-6)}$$

where r' is defined in Eq. (B2-2).

The law of signs allows cos ω to be expressed in terms of ϕ where

$$\frac{r'}{\sin \; \omega} = \frac{a}{\sin \; (\pi - \phi)} = \frac{a}{\sin \; \phi} , \qquad \text{(B2-7)}$$

$$r' = \frac{a \sin \; \omega}{\sin \; \phi} = \sqrt{a^2 + r^2 - 2 \; ra \; \cos \; \omega} , \qquad \text{(B2-8)}$$

$$\frac{a^2 \sin^2 \; \omega}{\sin^2 \; \phi} = a^2 + r^2 - 2 \; ra \; \cos \; \omega , \qquad \text{(B2-9)}$$

$$\frac{a^2}{\sin^2 \; \phi} (1 - \cos^2 \; \omega \;) = a^2 + r^2 - 2 \; ra \; \cos \; \omega , \qquad \text{(B2-10)}$$

3.1-128

$$\frac{a^2}{\sin^2 \phi} \cos^2 \omega - 2\, ra \cos \omega + a^2 + r^2 - \frac{a^2}{\sin^2 \phi} = 0 \,, \qquad (\text{B2-11})$$

$$\frac{a^2}{\sin^2 \phi} \cos^2 \omega - 2\, ra \cos \omega + r^2 - \frac{a^2 \cos^2 \phi}{\sin^2 \phi} = 0 \,, \qquad (\text{B2-12})$$

$$\cos \omega = \frac{2\, ra \, \pm \sqrt{4r^2 a^2 - \dfrac{4a^2}{\sin^2 \phi} \left[r^2 - a^2 \dfrac{\cos^2 \phi}{\sin^2 \phi} \right]}}{\dfrac{2a^2}{\sin^2 \phi}} \qquad (\text{B2-13})$$

$$= \left[r \pm \sqrt{-\frac{r^2 \cos^2 \phi}{\sin^2 \phi} + \frac{a^2 \cos^2 \phi}{\sin^4 \phi}} \right] \frac{\sin^2 \phi}{a} \qquad (\text{B2-14})$$

$$= \frac{r}{a} \sin^2 \phi \pm \frac{|\cos \phi| \, |\sin \phi|}{a} \sqrt{\frac{a^2}{\sin^2 \phi} - r^2} \,, \qquad (\text{B2-15})$$

$$= \frac{r}{a} \sin^2 \phi + \frac{\cos \phi}{a} \sqrt{a^2 - r^2 \sin^2 \phi} \,. \qquad (\text{B2-16})$$

The positive solution is chosen since when $\phi = 0$, $\omega = 0$ and when $\phi = \pi$, $\omega = \pi$, and when $r = 0$, $\omega = \phi$.

Therefore,

$$\cos \omega = \frac{r}{a} \sin^2 \phi + \cos \phi \sqrt{1 - \left(\frac{r}{a}\right)^2 \sin^2 \phi} \,. \qquad (\text{B2-17})$$

B2.2 Case II, a ≤ s ≤ 2a

Case II is divided into two subcases. Figure B2-2 shows the geometry for Case IIa where r ≤ s-a. The geometry for Case IIb is shown in Figure B2-3 where r > s-a.

For Case IIa, tangency occurs when r = s-a. The total energy reaching the boundary, a, is

`

$$\rho(r) = \int_0^\pi f(E_o, r') \frac{r' \, d\phi \; 2\pi \, r' \sin \phi}{4\pi \, r'^2} \qquad (\text{B2-18})$$

since r′ < s.

For Case IIb intersection occurs for r' = s. From Figure B2-3,

$$a^2 = r^2 + s^2 - 2\,rs\,\cos\,(\pi - \phi\,(r,s))\,, \tag{B2-19}$$

$$= r^2 + s^2 + 2\,rs\,\cos\,\phi\,(r,s)\,, \tag{B2-20}$$

$$\phi\,(r,s) = \cos^{-1}\frac{a^2 - r^2 - s^2}{2\,rs} \tag{B2-21}$$

The total energy reaching the boundary, a, is

$$\rho\,(r) = \int_0^{\phi(r,s)} f(E_o, r')\,\sin\,\phi\,\,d\phi\,\,dr \tag{B2-22}$$

Where r' is given in Eq. (B2-2) and cos ω is defined in Eq. (B2-17).

The fraction of energy generated in the sphere and escaping from the surface is

$$\frac{E}{E_T} = \frac{1.5}{a^3 E_0}\left[\int_0^{s-a} r^2 \int_0^{II} f(E_o, r')\sin\,\phi\,\,d\phi\,\,dr\right.$$

$$\left.+ \int_{s-a}^a r^2 \int_0^{\phi(r,s)} f(E_o - r')\,\sin\,\phi\,\,d\phi\,\,dr\,\right] \tag{B2-23}$$

or

$$\frac{E}{E_T} = \frac{3}{2a^3\,E_o}\int_0^a r^2 \int_0^{\phi\,(r,s)} f(E_o, r')\sin\,\phi\,d\phi\,dr \tag{B2-24}$$

where

$$\phi(r,s) = \pi \qquad\qquad\qquad if\ r \leq s - a \tag{B2-25}$$

$$= \cos^{-1}\left[\frac{a^2 - r^2 - s^2}{2\,rs}\right] \quad if\ r > s - a\quad. \tag{B2-26}$$

B2.3 Case III, s < a

In this case, the energy reaching the boundary a from point P is confined to a shell of thickness s as shown in Figure B2-4. The total energy is given by

$$\rho(r) = \int_0^{\phi(r,\,s)} f(E_O, r')\,\frac{r'\,d\phi\,2\pi\,r'\sin\,\phi}{4\pi\,r'^2} \tag{B2-27}$$

where Equation (B2-26) defines ϕ(r, s).

The fraction of energy generated in the sphere and escaping from the surface is

$$\frac{E}{E_T} = \frac{2\pi \, E_O}{4/3 \, \pi \, a^3 \, E_O} \int_{a-s}^{a} r^2 \int_0^{\phi(r,\,s)} f(E_O, r') \sin \phi \, d\phi \, dr \,. \qquad \text{(B2-28)}$$

B2.4 Numerical Solution

The fractional energy equations, E/E_T, were evaluated for particles with radii, a, between 0 and 100 microns and initial energies of 5.15 and 5.49 MeV. Adaptive 8-point Legendre-Gauss integration was performed with GAUS8 (see VanDevender 1984[2] and Cowell 1984[3]). An integration error tolerance of 10^{-4} was used. Figures B2-5 and B2-6 display fractional energy for $0 \geq a \geq 100$ and $0 \leq a \leq 20$, respectively, for $E_o = 5.15$ MeV. Table B2-1 lists the fraction of energy escaping from particles of various radii.

---

[2] VanDevender 1984. W. H. VanDevender, "Slatec Mathematical Subprogram Library Version 2.0," Sandia National Laboratories, SAND84-0281, April 1984.

[3] Cowell 1984. W. R. Cowell, <u>Sources and Development of Mathematical Software</u>. Prentice Hall, New York, N.Y., 1984.
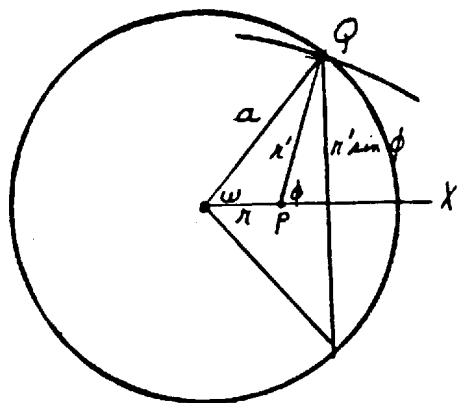
Fig. B2-1 Case I 2a < s
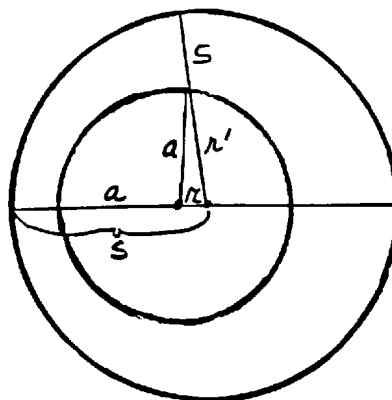
Fig. B2-2 Case IIa r ≤ s-a
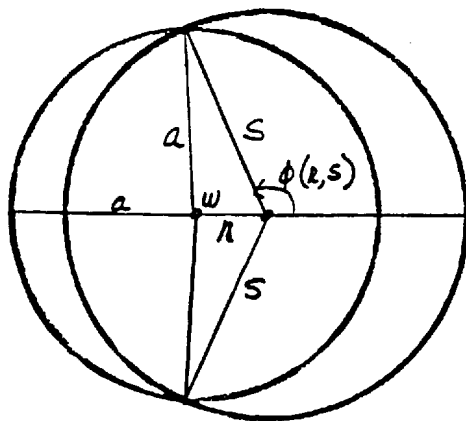
Fig. B2-3 Case IIb r > s-a
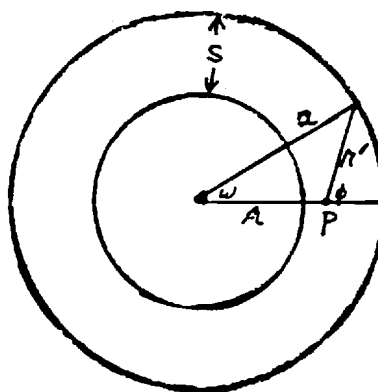
Fig. B2-4 Case III s < a
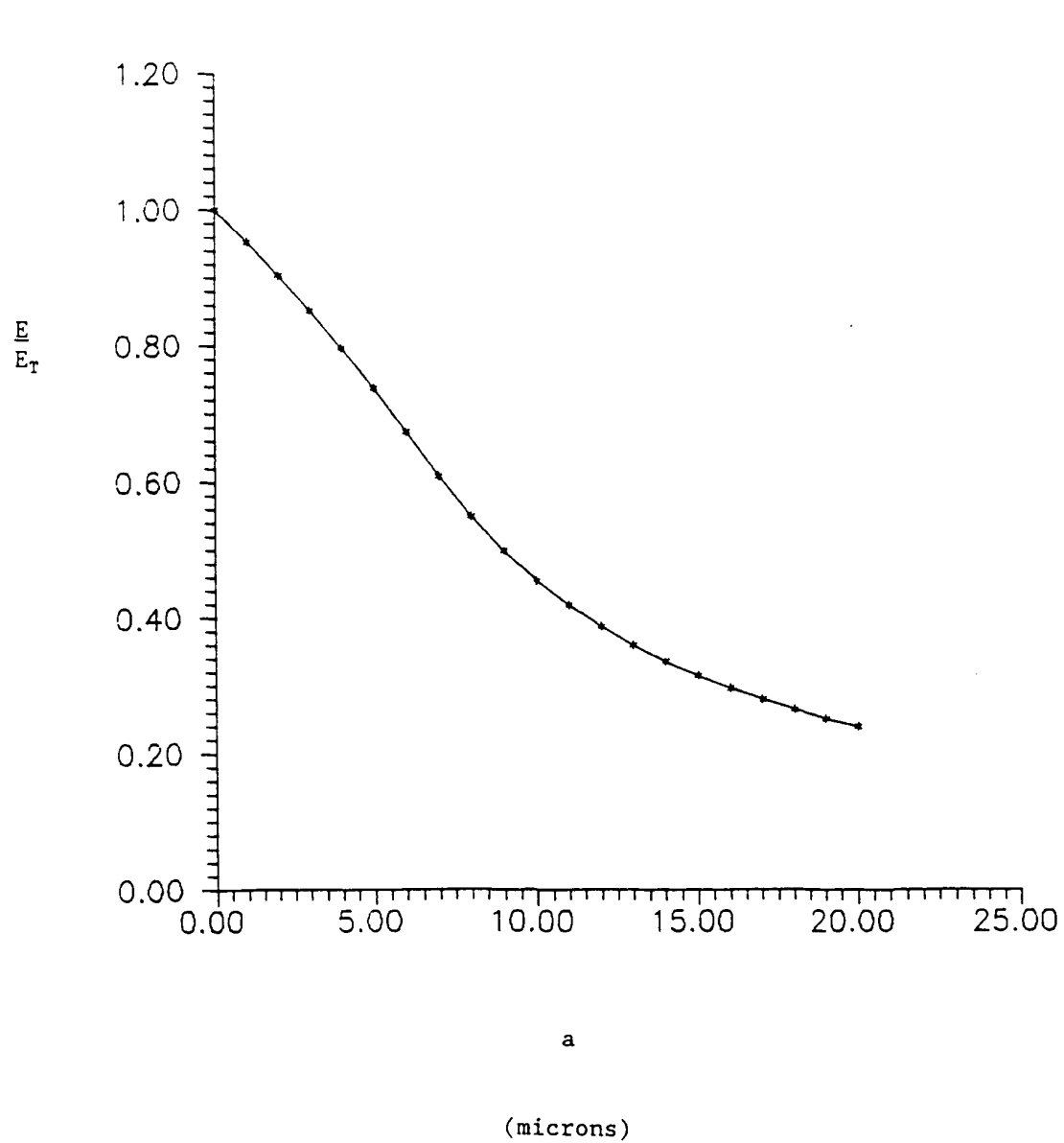
Figure B2-5
PuO₂ Fractional Energy vs. Radius for E₀ = 5.15 MeV

a

(microns)
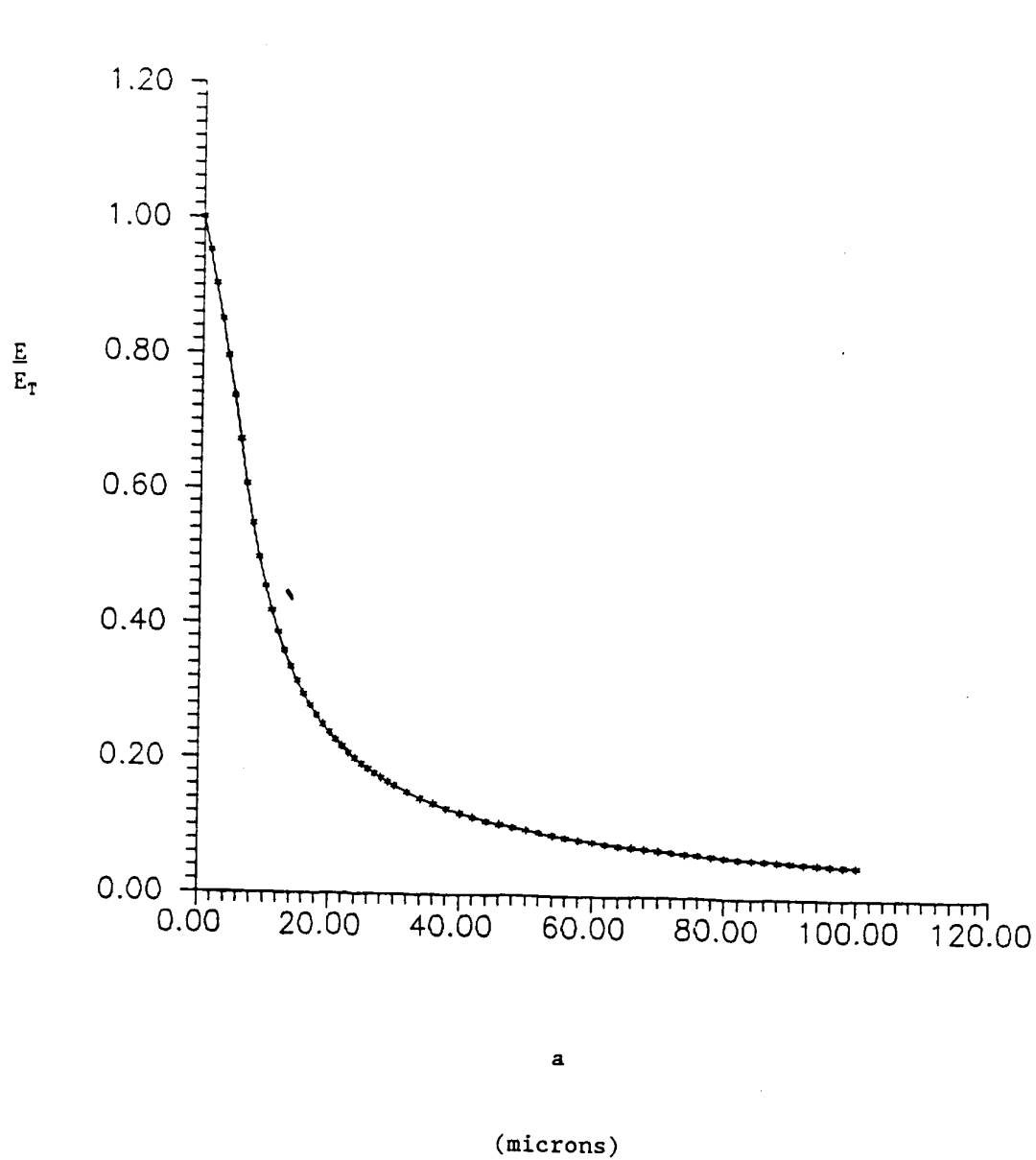
Figure B2-6
PuO$_2$ Fractional Energy vs. Radius E$_o$ = 5.15 MeV

Table B2-1 — Fraction of Alpha Particle Energy Escaping from PuO$_2$ Particles as a Function of Particle Radius and Initial Energy

Particle Radius (μm)	Fraction of Energy Escaping	
	Eo = 5.15 MeV	Eo = 5.49 MeV
9.5	0.476	0.515
7.0	0.607	0.647
4.5	0.766	0.790
3.5	0.823	0.840
2.5	0.877	0.888
1.5	0.927	0.934
0.75	0.964	0.967
0.28	0.987	0.988

This page intentionally left blank.

APPENDIX 3.2

EFFECTIVE G VALUES FOR CH-TRU WASTE MATERIAL TYPES

This page intentionally left blank.

3.2   Effective G Values for CH-TRU Waste Material Types

3.2.1   Summary

This appendix determines the effective G values for payload shipping categories of contact-handled transuranic (CH-TRU) waste materials, based on the radiolytic G values for waste materials that are discussed in detail in Appendix 3.1 of the CH-TRU Payload Appendices. The effective G values take into account self-absorption of alpha decay energy inside particulate contamination, the fraction of energy absorbed by nongas-generating materials, and the dose absorbed by the target matrix material.

Increasing dose (defined as the product of the decay heat and elapsed time from waste generation to date of compliance evaluation and expressed in units of watt*year) decreases the flammable gas generation rate of hydrogenous materials (such as plastics and combustibles) due to depletion of hydrogen in the target material in the vicinity of alpha-emitting sources. This effect has been demonstrated for a variety of materials present in TRU waste by a number of researchers.[1] Extensive radiolytic testing of polyethylene (PE), polyvinyl chloride (PVC), and cellulosics has established a steady-state, dose-dependent G value for each material when a container has attained a dose level of 0.012 watt*year.[1] The applicability of dose-dependent G values for CH-TRU waste types is further described in Appendix 3.3 of the CH-TRU Payload Appendices.

CH-TRU waste materials in payloads for the transportation packaging are described according to the following waste types (I, II, III, or IV) or can be divided into waste material types (I.1, I.2, I.3, II.1, II.2, II.3, III.1, III.2, III.3, and IV.1):

I.   Solidified aqueous or homogeneous inorganic solids (that contain water)

     I.1   Absorbed, adsorbed, or solidified inorganic liquids (nuclides may be in solution and energy transfer may occur between the liquid and the inorganic binder).

     I.2   Soils, solidified particulates, or sludges formed from precipitates.

     I.3   Concreted inorganic particulate waste having a maximum of 30 weight percent unbound water.

II.   Solid inorganic materials

     II.1   Solid inorganic materials packaged in organic materials.

     II.2   Solid inorganic materials packaged in metal cans.

---

[1] Idaho National Engineering and Environmental Laboratory, 1999, "TRUPACT-II Matrix Depletion Program Final Report," INEL/EXT-98-00987, Rev. 1, Idaho National Engineering and Environmental Laboratory, Idaho Falls, Idaho.

II.3   Homogeneous solid inorganic materials with unbound absorbed ambient moisture (≤6 percent by weight) in metal cans.

III.   Solid organic materials

III.1   Solid organic materials (including some absorbed liquids and cemented organics).

III.2   Homogeneous mixed organic (10 percent by weight) and inorganic (90 percent by weight) materials packaged in metal cans.

III.3   Homogeneous mixed organic (10 percent by weight) and inorganic (90 percent by weight) materials packaged in organic materials.

IV.   Solidified organic materials. Waste Type IV (Waste Material Type IV.1) is in the test category since a bounding G value has not been established and is not addressed in this appendix.

Effective G values are determined for use in calculating concentrations of potentially flammable gases, quantities of HCl that could be generated, and for net gas generated (equal to the total amount of gas generated minus the amount of oxygen consumed, if applicable). Factors are also provided that allow G values at room temperature to be corrected for a higher or lower waste temperature. Table 3.2-1 summarizes the effective G values at an assumed room temperature of $70^{\circ}F$.

3.2.2 Introduction

As described in Appendix 3.1 of the CH-TRU Payload Appendices, an effective G value, G_{eff}, is defined by:

$G_{eff} = \sum_M (F_M \times G_M)$
F_M = fraction of energy absorbed by material M
G_M = maximum G value for a material M

where the sum is over all materials present inside a waste container.

The G value itself is determined primarily by the chemical properties of the material and its temperature. The value of F is determined primarily by the size of the particles containing the radionuclides, the distribution of radioactivity on the various materials present inside the waste container, and the stopping distance of alpha particles in air, in the waste materials, or in the waste packaging materials.

Table 3.2-1 — Effective G Values for Waste Material Types at Room Temperature

Waste Material Type	Effective G Values		
	Flammable Gas	HCl	Net Gas[a]
I.1	1.6	~0	2.4
I.2	1.3	~0	2.0
I.3	0.4	~0	0.6
II.1 (watt*year ≤0.012)	1.7	0.3	1.7
II.1 (watt*year >0.012)	0.32	0.3	1.7
II.2	0	0	0
II.3	0.08	0	0.12
III.1 (watt*year ≤0.012)	3.4	0.5	8.4
III.1 (watt*year >0.012)	1.09	0.5	8.4
III.2 (watt*year ≤0.012)	0.34	0.05	0.84
III.2 (watt*year >0.012)	0.11	0.05	0.84
III.3 (watt*year ≤0.012)	1.85	0.29	2.35
III.3 (watt*year >0.012)	0.4	0.29	2.35

a   Net gas is equal to the total amount of gas generated minus the amount of oxygen consumed.

Waste materials have been placed into three general waste types: solidified aqueous or homogeneous inorganic solids (containing bound and unbound water), solid inorganic materials, and solid organic materials. For the purpose of determining bounding G values, a distinction is made between the use of organic (e.g., plastic bags) and inorganic (e.g., metal cans) packaging materials for Waste Types II and III. All three waste types can be packaged using organic packaging materials (e.g., plastic bags or cardboard cartons); solid inorganic materials and homogeneous mixed organic and inorganic materials can also be packaged in metal cans, resulting in different G values. The G values for the organic packaging provide the maximum G values applicable for solid inorganic materials (except for waste in metal cans). PE, PVC, and cellulosics (e.g., paper, cardboard, and wood) are the most common solid organic materials present in the CH-TRU wastes. Radiolytic G values for generation of flammable gases, HCl, and net gas for these materials provide upper bounds for the G values for solid organic waste materials that are present in greater than trace quantities. For pressure calculations, a G value for net gas has been determined that includes the effect of oxygen consumption, if oxygen was present in the experiment.

3.2.3 G Values for Waste Materials

For flammable gas generation or total pressure, the maximum G values for materials are used. For generation of HCl, an average G(HCl) value is used. This average G(HCl) value has been calculated from literature G values for PVC formulations that are most common in general commerce. The G(HCl) values used in determining the average G(HCl) value are included in those discussed in Appendix 3.1 of the CH-TRU Payload Appendices and are shown in Table 3.2-2. An average G(HCl) was used in the calculations because of wide variations in

formulation of PVC film materials and the very low values observed for actual bagging materials used at the waste generator sites (Table 3.2-2).

Table 3.2-2 — G(HCl) Values Measured for Common PVC Formulations at Room Temperature

PVC Formulation	Rad. Type/Dose	Oxygenated Atmosphere	G(HCl)	Contribution to G(HCl)avg
19 types, 18% DOP plasticizer, 1-5% metallic soaps as stabilizers	gamma/ 3 Mrad	no	0-1.7 0.54 (avg)	10.26
1 type, 2 dose extremes, 50 phr DOP plasticizer, 5 phr epoxy oil, 2% Ca-Zn stabilizer	gamma/ 20-60 Mrad	no	0.03-1.4 0.72 (avg)	1.44
50 phr DOP plasticizer, 5 phr tribasic lead sulfate, 1 phr stearic acid, 10 phr clay #33	gamma/ 10 Mrad	no	1.2	1.2
50 phr DOP plasticizer, 5 phr epoxy oil, 2% Ca-Zn stabilizer	gamma/ 20 Mrad	yes	1.7	1.7
50 phr DOP plasticizer, 5 phr tribasic lead sulfate, 1 phr stearic acid, 10 phr clay #33	gamma/ 10 Mrad	yes	2.6	2.6
O-ring bags used at RFETS	gamma	yes	0.2	0.2
O-ring bags used at RFETS	alpha	yes	none detected	0
Bag materials used at Los Alamos National Laboratory	alpha	yes	none detected	0
			$G(HCl)_{avg} = 17.4/27 =$	0.64

Notes: avg   = Average
        DOP   = Dioctyl phthalate
        HCl   = Hydrochloric acid
        Mrad   = Millirad
        phr   = Parts per hundred resin
        PVC   = Polyvinyl chloride
        RFETS   = Rocky Flats Environmental Technology Site

The use of an average value of 0.64 for G(HCl) is considered bounding for the following reasons.

- Gas sampling programs (discussed in Appendices 5.3 and 6.2 of the CH-TRU Payload Appendices) at the Idaho National Engineering and Environmental Laboratory (INEEL) and Rocky Flats Environmental Technology Site (RFETS) did not detect HCl gas in the headspace of any of the 249 drums of CH-TRU waste that were sampled. In addition to drum headspace sampling, twenty-two drums of waste were sampled for gases, within successive layers of confinement up to and including the innermost layer of the waste. In all cases, HCl was never detected in any layer of confinement.

- Experimentally derived G(HCl) values for waste materials frequently found in CH-TRU wastes are listed in Table 6.2-1 of Appendix 6.2 of the CH-TRU Payload Appendices. All the values for G(HCl) are very low for both alpha and gamma radiolysis experiments. These data indicate that the potential for HCl production from radiolysis of commonly used PVC materials in CH-TRU waste is minimal and less than the average G(HCl) value of 0.64 from the literature results.

The temperature dependence of G values is approximated by the Arrhenius equation (see Appendix 3.1 of the CH-TRU Payload Appendices):

$$G(T_2) = G(T_1) \exp[(E_a / R)\{(T_2 - T_1)/(T_2 - T_1)/(T_2 \times T_1)\}]$$

where, E_a is the activation energy in cal/g-mole for a gas species, R is the ideal gas constant (1.99 cal/g-mole-K), and T is the absolute temperature. The value of the activation energy can change when a material melts or otherwise significantly changes its physical properties (such as becoming brittle).

Table 3.2-3 summarizes G values from Appendix 3.1 of the CH-TRU Payload Appendices that provide maximum G values for the waste types and an average G(HCl) value for PVC calculated in Table 3.2-2. The activation energy for calculating G values at temperatures other than room temperature is also given. No temperature dependence has been observed for radiolysis of water (in the liquid state or solidified in concrete) from room temperature to 100°C.

For all waste types, PVC is the bounding material for G(HCl). Water is the bounding material for G(net gas) and G(flammable) in Waste Type I and Waste Material Type II.3. G(net gas) is equal to G(total) minus any measured consumption of oxygen. For Waste Material Type II.1, PE is the bounding material for G(flammable gas) and G(net gas). PE is the bounding material for G(flammable gas), and cellulose is the bounding material for G(net gas) for Waste Type III containers that have not met the 0.012 watt*year dose criteria. Cellulosics are the bounding material for G(flammable gas) for Waste Type III containers that have satisfied the 0.012 watt*year dose criteria. For applicable waste material types satisfying the watt*year criteria and using

Table 3.2-3 — Summary of Maximum G Values for Bounding Materials in Waste Types at Room Temperature

Waste Material	G Value[a]			
	Flammable Gas	HCl	Net Gas	Activation Energy[b]
Water	1.6	0	2.4	0
Polyethylene	4.1[c] 0.64[d]	0	4.1	0.8
Polyvinyl chloride Maximum	0.7[c] 0.54[d]	2.6	2.6	3.0 (HCl) 8.1 (H_2)
Average	N/A	0.64	N/A	3.0 (HCl)
Cellulose	3.2[c] 1.09[d]	0	10.2	2.1

a G values are in units of molecules per 100 eV of energy at 70°F.
b Activation energies are in units of kcal/g-mole.
c Watt*year criteria not satisfied.
d Watt*year criteria satisfied.

dose-dependent G values, only the dose-dependent flammable gas G value is calculated, as HCl and net gas G values are conservatively assumed to be the same as for the corresponding waste material type that has not satisfied the watt*year criteria.

3.2.4 Fraction of Alpha Decay Energy Absorbed in Particles

Most CH-TRU wastes consist of materials that have been contaminated with particles of radioactive material, usually in the oxide form. The solid inorganic materials (e.g., glass and metal) and the solid organic materials (e.g., paper and plastic) meet this description. The solidified aqueous sludges and most other homogeneous solids consist of precipitated solids and radioactivity in particulate form. The major exceptions are liquids containing dissolved radioactivity that may be present as bound liquid within the solid mass, as opposed to water of hydration.

The equation for effective G value can be rewritten as:

$$G_{eff} = \sum_M (F_P \times F_M) \times G_M$$

$$= \sum_M (F_M \times G_M) \times F_P$$

where, F_P = fraction of energy emerging from the particles
      F_M = fraction of energy absorbed by material M
      G_M = maximum G value for material M.

Attachment B of Appendix 3.1 of the CH-TRU Payload Appendices describes a mathematical calculation of the fraction of alpha decay energy that escapes from a spherical particle containing uniformly distributed TRU nuclides. Attachment A of this appendix shows that a maximum of 82 percent of the alpha decay energy escapes from particles of PuO_2 when the particle size distribution is taken into account.

For waste containing contamination in solution (i.e., solidified wastes), a maximum of 100 percent of the alpha decay energy may emerge from the particles. For waste forms using dose-dependent G values, a value of 1.0 is used for the fraction of energy emerging from the particles, because the experimentally determined dose-dependent G values provided in Table 3.2-3 already account for particle size distribution and were conducted with materials representative of TRU waste.

3.2.5   Effective G Values for Waste Types

3.2.5.1   Waste Type I – Solidified Aqueous or Homogeneous Inorganic Solids

This waste type includes soil and concreted or sludge wastes that do not contain more than trace amounts (<1 weight percent) of organic materials (with the exception of organic packaging materials). The materials are well mixed.

For this waste type, the radioactive materials are dispersed throughout the solidified or solid mass, and the fraction of the alpha decay energy absorbed by the plastic bags or high-density polyethylene rigid (HDPE) liner is negligible. The range of alpha particles (t) in water is only about 5E-3 cm. Only a shell at most equal to the surface area of the waste volume and 5E-3 cm thick, will emit alpha particles that can reach the plastic. For a cylindrical waste volume having radius r and height h, the fraction of alpha particles that can reach the plastic packaging materials is given by:

$$P = \frac{t \times 2\pi r(r+h)}{\pi r^2 h} = \frac{2t(r+h)}{rh}$$

For waste with an approximate volume of one gallon (with a radius of three inches and height of eight inches), P = 1.8E-3. This provides an upper bound for the fraction of alpha particles that can interact with the plastic packaging materials for Waste Type I.

Water is the only material present in solidified aqueous or homogeneous inorganic solids in other than trace quantities that could generate potentially flammable gases. The maximum values for water provide the maximum values for solidified inorganic waste containing water.

3.2.5.1.1 Waste Material Type I.1

For Waste Material Type I.1, any inorganic absorbents or solidification agents can be used. Because energy transfer can occur between some inorganic materials and water, the fraction of available energy absorbed by the water is assumed to be 1.0. The activity may be present as particles or in solution encapsulated by the solidification materials.

The effective G value for Waste Material Type I.1 is given by:

$$G_{eff,I.1} = \sum_M (F_M \times G_M) \times F_P$$

$$= [1.8E\text{-}3 \times G(plastic) + 1.0 \times G(water)] \times 1.0$$

Therefore, the effective G values for potentially flammable gas, HCl, and net gas are given respectively by:

G(flam gas)= $[1.8E\text{-}3 \times 4.1 + 1.0 \times 1.6] \times 1.0 = 1.6$

G(HCl) = $[1.8E\text{-}3 \times 0.64] \times 1.0 = {\sim}0$

G(net gas) = $[1.8E\text{-}3 \times 4.1 + 1.0 \times 2.4] \times 1.0 = 2.4.$

3.2.5.1.2 Waste Material Type I.2

For Waste Material Type I.2 (solidified particulates, soil or sludges) data presented in Appendix 3.1 of the CH-TRU Payload Appendices demonstrate that energy transfer can occur between many of the materials and the water. For Waste Material Type I.2, therefore, all of the energy available is assumed to be absorbed by the water. The sludges are formed by precipitating the radionuclides from solution, so the radionuclides should be present in the form of particles.

The effective G value for Waste Material Type I.2 is given by:

$$G_{eff,I.2} = \sum_M (F_M \times G_M) \times F_P$$

$$= [1.8E\text{-}3 \times G(plastic) + 1.0 \times G(water)] \times 0.82$$

Therefore the effective G values for flammable gas, HCl, and net gas are given respectively by:

G(flam gas)= $[1.8E\text{-}3 \times 4.1 + 1.0 \times 1.6] \times 0.82 = 1.3$

G(HCl) = $[1.8E\text{-}3 \times 0.64] \times 0.82 = {\sim}0$

G(net gas) = $[1.8E\text{-}3 \times 4.1 + 1.0 \times 2.4] \times 0.82 = 2.0.$

3.2.5.1.3 Waste Material Type I.3

For Waste Material Type I.3 (concreted inorganic particulate waste), data presented in Appendix 3.1 of the CH-TRU Payload Appendices demonstrate that energy transfer does not occur between the cement and the bound or unbound water, and the G value for the bound water (water of hydration) is close to zero. The unbound water content of the cured concrete is limited to 30 weight percent. For Waste Material Type I.3, therefore, only 30 percent of the energy available is absorbed by the water.

The effective G value for Waste Material Type I.3 is given by:

$$G_{eff,I.3} = \sum_M (F_M \times G_M) \times F_p$$

$$= [1.8E\text{-}3 \times G(plastic) + 0.30 \times G(water)] \times 0.82$$

Therefore the effective G values for flammable gas, HCl, and net gas are given respectively by:

$G(flam\ gas) = [1.8E\text{-}3 \times 4.1 + 0.30 \times 1.6] \times 0.82 = 0.4$

$G(HCl) = [1.8E\text{-}3 \times 0.64] \times 0.82 = 0$

$G(net\ gas) = [1.8E\text{-}3 \times 4.1 + 0.30 \times 2.4] \times 0.82 = 0.6.$

Water within concreted wastes is actually found in two forms. Part of the water is chemically bound during the hydration of the cement phases. The remaining water is unbounded or loosely bound and is part of the excess water added to make the freshly mixed cement paste workable. In an average cemented sludge (e.g., RFETS, RF 114A), the amount of water added to the cement/sludge mixture at the time of mixing, plus the water contained in the sludge totals approximately 37 percent by weight of the mixture. The water content of the sludge is conservatively assumed to be 50 percent by volume. After only 50 percent hydration, attained within 6 to 7 days of mixing,[2] 5.7 percent water by weight of the mixture is bound within the cement phases. This leaves approximately 31 percent unbound water by weight. Some of this water is lost due to evaporation during mixing and curing. Bibler reports that concrete (simulating Savannah River Plant cemented sludge) cured at ambient conditions for two to five days had lost 30 to 40 weight percent of the free water to evaporation.[3] This results in a free water content of 19 to 22 percent by weight.

Calculation of the total porosity of the concrete after 50 percent hydration at the water/cement ratio prescribed by RFETS (0.775) yielded 45 volume percent. If the concrete were 100 percent saturated at the porosity, the maximum unbound (free water) moisture content would be only 32 weight percent. Again, evaporation is expected to remove 30 to 40 percent of the free water during the curing leaving 19 to 22 weight percent free water. Even assuming a high relative humidity during the curing process, 30 percent represents an estimated upper bound for this free water moisture content.

The experiment referred to in Section 3.1.5.1.2 of Appendix 3.1 of the CH-TRU Payload Appendices appears to use initial moisture content of the cement/sludge mixture, before

---

[2] Mindess, S., and J. F. Young, 1981, Concrete, Prentice-Hall, Inc., Englewood Cliffs, NJ.

[3] Bibler, N. E., 1979, "Gas Production From Alpha Radiolysis of Concrete Containing TRU Incinerator Ash, Progress Report 2, August 1 - November 30, 1978," E.I. Du Pont De Nemours and Co., Savannah River Laboratory, Aiken, South Carolina.

hydration occurs.[4] The initial moisture content of the mix was 35 weight percent. After drying at 200°C, it was reported that 7.4 percent moisture content by weight remained. This refers to the water bound by hydration of the cement minerals after approximately 36 days curing time plus water contained in the cement gel pores. Cement gel porosity refers to the pore space within the structure of the hydrated cement phases. The pores measure less than 10 nanometers and water contained in these pores is nonevaporable and can be considered bound within the cement.[2] The gel porosity is small and makes up only ~15 percent of the total porosity. The unbound (free water) content of the sample reported to contain 35 percent water is approximately (35 - 7.4 percent) or 27.6 percent by weight.

Examples of acceptable materials for Waste Material Types I.1, I.2 and I.3 that can be present in quantities greater than or equal to one weight percent are listed in Section 4.0 of the CH-TRAMPAC. Any other inorganic material is also acceptable in Waste Type I.

3.2.5.2 Waste Type II – Solid Inorganic Materials

This waste type includes surface-contaminated inorganic materials, such as glass, metal, ceramics, and fiberglass. The waste materials must be dry (Note: Waste Material Type II.3 may have less than or equal to 6 weight percent unbound absorbed ambient moisture) and free of oil, grease, or other organics except for trace quantities (less than 1 weight percent). The wastes may be packaged first inside plastic bags (II.1) or metal cans (II.2 and II.3), then in drums, which are lined with plastic bags (polyethylene or PVC) and/or the rigid high-density polyethylene liner, or placed directly into payload containers.

Due to the short range of an alpha particle and surface irregularities, the surface-contaminated inorganic wastes will, on the average, absorb half of the alpha decay energy escaping from particulate contamination. (The other half of the alpha decay energy could be absorbed by air, the packaging materials, or other inorganic waste materials.) The assumption is made that the remaining half of the alpha decay energy is absorbed by the packaging materials. The inorganic materials are considered to generate no net gas.

Examples of acceptable materials for Waste Type II are listed in Section 4.0 of the CH-TRAMPAC. Any other dry, solid, inorganic material is acceptable for Waste Type II.

3.2.5.2.1 Waste Material Type II.1—Dose Criteria Not Satisfied (Watt*Year ≤0.012)

The effective G value for Waste Material Type II.1 is given by:

$$G_{eff,II.1} \ = \ \Sigma_M \ (F_M \ x \ G_M) \ x \ F_P$$

$$= \ [0.5 \ x \ G(plastic) + 0.5 \ x \ G(inorganics)] \ x \ 0.82$$

---

[4] Bibler, N. E., 1980, "Radiolytic Gas Generation is Concrete Made with Incinerator Ash Containing TRU Nuclides," Scientific Basis for Nuclear Waste Management, Vol. 2, Plenum Publishing. Corp., New York, NY.

Therefore the effective G values for flammable gas, HCl, and net gas are given respectively by:

G(flam gas)= [0.5 x 4.1 + 0.5 x 0] x 0.82 = 1.7

    G(HCl) = [0.5 x 0.64 + 0.5 x 0] x 0.82 = 0.3

 G(net gas) = [0.5 x 4.1] x 0.82 = 1.7

3.2.5.2.2 Waste Material Type II.1—Dose Criteria Satisfied (Watt*Year >0.012)

The effective G value for Waste Material Type II.1 is given by:

$$G_{eff,II.1} = \sum_M (F_M \times G_M) \times F_P$$

$$= [0.5 \times G(plastic) + 0.5 \times G(inorganics)] \times F_P$$

Therefore the effective G value for flammable gas is:

G(flam gas)= [0.5 x 0.64 + 0.5 x 0] x 1.0 = 0.32

3.2.5.2.3 Waste Material Type II.2

The effective G value for Waste Material Type II.2 is equal to zero, since the inorganic materials and metal containers generate no gas from radiolysis.

3.2.5.2.4 Waste Material Type II.3

Waste Material Type II.3 is a homogeneous solid inorganic waste with ≤6 percent (by weight) unbound absorbed ambient moisture packaged in metal containers. The effective G value for Waste Material Type II.3 with 6 percent water and 94 percent inorganic material and packaging is given by:

$$G_{eff,\ II.3} = \sum_M (F_M \times G_M) \times F_P$$

$$= [0.06 \times G(water) + 0.94 \times G(inorganic)] \times 0.82$$

Therefore, the effective G values for flammable gas, HCl, and net gas are given respectively by:

G(flam gas)= [0.06 x 1.6 + 0.94 x 0] x 0.82 = 0.08

    G(HCl) = [0.06 x 0 + 0.94 x 0] x 0.82 = 0

 G(net gas) = [0.06 x 2.4 + 0.94 x 0] x 0.82 = 0.12

Acceptable materials for Waste Material Type II.3 wastes are listed in the CH-TRAMPAC.

3.2.5.3 Waste Type III – Solid Organic Materials

This waste type includes surface-contaminated solid organic materials, such as plastics, paper, cloth, Plexiglas®, and Benelex®. The materials may contain absorbed water, commercial greases, oils or organic liquids having sufficiently low G values. Cemented organic process solids are included in this category.

3.2.5.3.1 Waste Material Type III.1—Dose Criteria Not Satisfied (Watt*Year ≤0.012)

The surface-contaminated organic wastes or their organic packaging are assumed to absorb 100 percent of the available alpha decay energy. Any gas generated by inorganic materials (which are also permitted in this category) would be oxygen, which will be used in the oxidation of the plastic packaging materials. Therefore, any inorganic materials present are considered to generate no net gas.

The effective G value for Waste Material Type III.1 is given by:

$$G_{eff,III.1} \ = \ \Sigma_M \ (F_M \ x \ G_M) \ x \ F_p$$

$$= \ [1.0 \ x \ G(solid \ organic)] \ x \ 0.82$$

Therefore the effective G values for flammable gas, HCl, and net gas are given respectively by:

G(flam gas)= [1.0 x 4.1] x 0.82 = 3.4

$\quad$ G(HCl) = [1.0 x 0.64] x 0.82 = 0.5

$\quad$ G(net gas) = [1.0 x 10.2] x 0.82 = 8.4

Acceptable materials for Waste Material Type III.1 wastes are listed in Section 4.0 of the CH-TRAMPAC.

Materials for which the G value at room temperature for flammable gas could be greater than 4.1 are limited to trace quantities (<1 weight percent) based on current data. These materials are cellulose nitrate, polyvinyl formal, polyoxymethylene, and poly(olefin sulfone)s, as determined in Appendix 3.1 of the CH-TRU Payload Appendices. Other polymers containing ether functional groups may also have high G (flammable gas) values.

3.2.5.3.2 Waste Material Type III.1—Dose Criteria Satisfied (Watt*Year >0.012)

The surface-contaminated organic wastes or their organic packaging are assumed to absorb 100 percent of the available alpha decay energy. Any gas generated by inorganic materials (which are also permitted in this category) would be oxygen, which will be used in the oxidation of the plastic packaging materials. Therefore, any inorganic materials present are considered to generate no net gas.

The effective G value for Waste Material Type III.1 is given by:

$$G_{eff.,III.1} = \sum_M (F_M \times G_M) \times F_P$$

$$= [1.0 \times G(solid\ organic)] \times F_P.$$

Therefore the effective G value for flammable gas is:

G(flam gas)= $[1.0 \times 1.09] \times 1.0 = 1.09$.

Acceptable materials for Waste Material Type III.1 wastes are listed in Section 4.0 of the CH-TRAMPAC.

Materials for which the G value at room temperature for flammable gas could be greater than for cellulosics are limited to trace quantities (<1 weight percent) based on current data. These materials are cellulose nitrate, polyvinyl formal, polyoxymethylene, and poly(olefin sulfone)s, as determined in Appendix 3.1 of the CH-TRU Payload Appendices. Other polymers containing ether functional groups may also have high G (flammable gas) values.

3.2.5.3.3 Waste Material Type III.2—Dose Criteria Not Satisfied (Watt*Year ≤0.012)

Waste Material Type III.2 is a homogeneous mixture made up of ≤10 percent (by weight) solid organic material and ≥90 percent (by weight) solid inorganic material packaged in metal containers. The effective G value for Waste Material Type III.2 is calculated proportionally from Waste Material Types III.1 (10 percent) and II.2 (90 percent). The effective G value is given by:

$$G_{eff,III.2} = \sum_M (F_M \times G_M) \times F_P$$

$$= [0.1 \times G(solid\ organic) + 0.9 \times G(solid\ inorganic)] \times 0.82$$

Therefore, the effective G values for flammable gas, HCl, and net gas are given respectively by:

G(flam gas)= $[0.1 \times 4.1 + 0.9 \times 0] \times 0.82 = 0.34$

G(HCl) = $[0.1 \times 0.64 + 0.9 \times 0] \times 0.82 = 0.05$

G(net gas) = $[0.1 \times 10.2 + 0.9 \times 0] \times 0.82 = 0.84$

Acceptable materials for Waste Material Type III.2 wastes are listed in Section 4.0 of the CH-TRAMPAC.

3.2.5.3.4 Waste Material Type III.2—Dose Criteria Satisfied (Watt*Year >0.012)

Waste Material Type III.2 is a homogeneous mixture made up of ≤10 percent (by weight) solid organic material and ≥90 percent (by weight) solid inorganic material packaged in metal containers. The effective G value for Waste Material Type III.2 is calculated proportionally from Waste Material Types III.1 (10 percent) and II.2 (90 percent). The effective G value is given by:

$$G_{eff.,III.2} = \sum_M (F_M \times G_M) \times F_P$$

$$= [0.1 \times G(\text{solid organic}) + 0.9 \times G(\text{solid inorganic})] \times F_P.$$

Therefore, the effective G value for flammable gas is:

$$G(\text{flam gas}) = [0.1 \times 1.09 + 0.9 \times 0] \times 1.0 = 0.11$$

Acceptable materials for Waste Material Type III.2 wastes are listed in Section 4.0 of the CH-TRAMPAC.

3.2.5.3.5 Waste Material Type III.3—Dose Criteria Not Satisfied (Watt*Year ≤0.012)

Waste Material Type III.3 is a homogeneous mixture made up of ≤10 percent (by weight) solid organic material and ≥90 percent (by weight) solid inorganic material packaged in plastic. The effective G value for Waste Material Type III.3 is calculated proportionally from Waste Material Types III.1 (10 percent) and II.1 (90 percent). The effective G value is given by:

$$G_{eff,III.3} = \sum_M (F_M \times G_M) \times F_P$$

$$= \{0.1 \times G(\text{solid organic}) + 0.9 \times [0.5 \times G(\text{plastic}) + 0.5 \times G(\text{inorganics})]\} \times 0.82$$

Therefore, the effective G values for flammable gas, HCl, and net gas are given respectively by:

$$G(\text{flam gas}) = \{0.1 \times 4.1 + 0.9 \times [0.5 \times 4.1 + 0.5 \times 0]\} \times 0.82 = 1.85$$

$$G(\text{HCl}) = \{0.1 \times 0.64 + 0.9 \times [0.5 \times 0.64 + 0.5 \times 0]\} \times 0.82 = 0.29$$

$$G(\text{net gas}) = \{0.1 \times 10.2 + 0.9 \times [0.5 \times 4.1 + 0.5 \times 0]\} \times 0.82 = 2.35$$

Acceptable materials for Waste Material Type III.3 wastes are listed in Section 4.0 of the CH-TRAMPAC.

3.2.5.3.6 Waste Material Type III.3—Dose Criteria Satisfied (Watt*Year >0.012)

Waste Material Type III.3 is a homogeneous mixture made up of ≤10 percent (by weight) solid organic material and ≥90 percent (by weight) solid inorganic material packaged in plastic. The effective G value for Waste Material Type III.3 is calculated proportionally from Waste Material Types III.1 (10 percent) and II.1 (90 percent). The effective G value is given by:

$$G_{eff.,III.3} = \sum_M (F_M \times G_M) \times F_P$$

$$= \{0.1 \times G(\text{solid organic}) + 0.9 \times [0.5 \times G(\text{plastic}) + 0.5 \times G(\text{inorganics})]\} \times F_P.$$

Therefore, the effective G value for flammable gas is:

G(flam gas)= {0.1 x 1.09 + 0.9 x [0.5 x 0.64 + 0.5 x 0]} x 1.0 = 0.40

Acceptable materials for Waste Material Type III.3 wastes are listed in Section 4.0 of the CH-TRAMPAC.

Attachment A
Mass-Weighted Fraction of Energy Escaping from PuO$_2$ Particles

A.1 Introduction

This attachment demonstrates that a maximum of 82 percent of the alpha decay energy escapes from particles of PuO$_2$ when the particle size distribution is taken into account.

A.2 Mass-Weighted Fraction of Energy Escaping from PuO$_2$ Particles

Attachment B of Appendix 3.1 of the CH-TRU Payload Appendices describes a mathematical calculation of the fraction of alpha decay energy that escapes from a spherical particle containing uniformly distributed TRU nuclides.

As the PuO$_2$ particle radius exceeds the stopping distance of the alpha particles, some of the alpha particles are completely absorbed within the PuO$_2$ particle. Only the outer shell of the PuO$_2$ particle (11-12 μm thick) contains radionuclides whose alpha particles can escape from the PuO$_2$ particle.

Many different particle-size distributions for PuO$_2$ have been reported in the literature. Mishima[5] in his examination of transport methods for PuO$_2$ powder for fuel considered thirteen different distributions. The PuO$_2$ used for fuel fabrication is required to be finely divided powder or coprecipitate so that it can be intimately blended with UO$_2$ to form a mixed oxide fuel. It is unlikely that the PuO$_2$ found in surface-contaminated waste would be as fine a powder as is used in fuel fabrication. HEPA filters in glovebox exhaust systems will trap the smaller particles, which more easily become airborne. Size distributions for aerosols are applicable only to HEPA filters (which typically have inorganic filtration media). Small particles can also agglomerate, creating larger particles.

The particle size distribution used in this document was chosen by Schwendiman[6] as most appropriate for evaluating leakage from a transportation container for PuO$_2$ powder. The distribution corresponds to 1000°C calcined plutonium oxalate with a 15-minute dispersion prior to measurement. This particle size distribution is listed in Table A-1. The particle size distributions in most wastes are expected to have larger mean particle sizes.

These data were converted to mass fraction of particles having diameters between two values, and the mass fraction was assigned to a diameter corresponding to the range midpoint. The fraction of the alpha decay energy escaping from each size particle was calculated using Table B2-1 of Appendix 3.1 of the CH-TRU Payload Appendices, Attachment B. The results and the mass-weighted total energy escaping from the PuO$_2$ particles are tabulated in Tables A-2 and A-3.

---

[5] Mishima, J., and C. G. Lindsey, "Investigation into the Feasibility of Alternative Plutonium Shipping Forms," Pacific Northwest Laboratory, Battelle Memorial Institute, NUREG/CR-3007, PNL-4507, 1983.

[6] Schwendiman, L. C., "Supporting Information for the Estimation of Plutonium Oxide Leak Rates through Very Small Apertures," Battelle, Pacific Northwest Laboratories, BNWL-2198, NRC-12, 1977.

The conclusion drawn is that at most 82 percent of the alpha decay energy from particulate contamination is available to interact with waste materials.

Table A-1 — PuO$_2$ Particle Size Distribution

Particle Diameter and Smaller (µm)	Cumulative Percent by Weight
20	100
18	99
10	81
8	56
6	39
4	20
2	4
1	1
0.5	0.15
0.1	0.1

Source: Schwendiman, L. C., "Supporting Information for the Estimation of Plutonium Oxide Leak Rates through Very Small Apertures," Battelle, Pacific Northwest Laboratories, BNWL-2198, NRC-12, 1977.

Table A-2 — Mass-Weighted Total Energy Escaping from PuO$_2$ Particles for Pu-239

Midpoint Particle Radius (µm)	Fraction of Alpha Energy Escaping	Mass Fraction in Distribution	Mass-Weighted Fraction of Energy Escaping
9.5	0.48	0.01	0.005
7.0	0.61	0.18	0.110
4.5	0.77	0.25	0.193
3.5	0.82	0.17	0.139
2.5	0.88	0.19	0.167
1.5	0.93	0.16	0.149
0.75	0.96	0.03	0.029
0.28	0.99	0.01	0.010
		TOTAL	0.802

Note: Particles have the size distribution given in Table A-1.

Table A-3 — Mass-Weighted Total Energy Escaping from PuO$_2$ Particles for Pu-238

Midpoint Particle Radius (μm)	Fraction of Alpha Energy Escaping	Mass Fraction in Distribution	Mass-Weighted Fraction of Energy Escaping
9.5	0.52	0.01	0.005
7.0	0.65	0.18	0.117
4.5	0.79	0.25	0.198
3.5	0.84	0.17	0.143
2.5	0.89	0.19	0.169
1.5	0.93	0.16	0.149
0.75	0.97	0.03	0.029
0.28	0.99	0.01	0.010
		TOTAL	0.820

Note: Particles have the size distribution given in Table A-1.

APPENDIX 3.3

USE OF DOSE-DEPENDENT G VALUES FOR CH-TRU WASTES

This page intentionally left blank.

3.3   Use of Dose-Dependent G Values for CH-TRU Wastes

3.3.1   Background

This appendix describes controlled studies and experiments that quantify the reduction in the rate of hydrogen gas generation (G value) over time based on the total dose received by the target matrix. Over time and with constant exposure to radiation, hydrogen is removed from the hydrogenous waste or packaging material (the matrix), thus decreasing the number of hydrogen bonds available for further radiolytic breakdown (the matrix is depleted). Therefore, when the alpha-generating source is dispersed in the target matrix, it will affect only that portion of the target material that is present in a small spherical volume surrounding the source particle. As the amount of available hydrogen is reduced over time, the effective G value decreases with increasing dose to a limit that is defined as the "dose-dependent G value." This phenomenon of matrix depletion has been studied and observed in previous studies (see Appendix 3.1 of the CH-TRU Payload Appendices). A formal study was recently undertaken to quantify dose-dependent G values under strictly controlled conditions and evaluate their applicability to contact-handled transuranic (CH-TRU) wastes.[1] This appendix summarizes the results of this study and derives dose-dependent G values for CH-TRU waste materials, as applicable.

3.3.2   Overview of the Matrix Depletion Program

The Matrix Depletion Program (MDP), established as a joint venture by the U.S. Department of Energy (DOE) National TRU Waste Program and the DOE Mixed Waste Focus Area, is comprised of the following elements:

1. Laboratory experiments for the assessment of effective G values as a function of dose for matrices expected in CH-TRU wastes (polyethylene, polyvinyl chloride, cellulose, etc.), as well as an assessment of the impact of other variables (isotope, temperature, etc.) on the dose-dependent G values.

2. Measurements of effective G values and hydrogen concentrations in real waste and comparisons with dose-dependent G values.

3. Analysis to calculate effective G values from fundamental nuclear and molecular mechanisms.

A total of 60 one-liter test cylinders containing the simulated CH-TRU waste materials were used, with two replicates for each test. Solid waste matrices (plastics and cellulose) were prepared by sprinkling the radioactive isotope powders over the matrix, folding the matrix over the contaminated surfaces, securing them, and placing them in test cylinders. Solidified waste matrices (cement) were mixed with a solution of dissolved plutonium oxide, water, and sodium hydroxide to adjust the pH. The test cylinders were connected to measurement devices that

---

[1] Idaho National Engineering and Environmental Laboratory, "TRUPACT-II Matrix Depletion Program Final Report," *INEL/EXT-98-00987*, Rev. 1, prepared for the U.S. Department of Energy, Idaho Operations Office, Idaho Falls, Idaho (1999).

facilitated sampling of generated gases and quantifying the gas generation over time. The entire test apparatus was controlled by a personal computer through LABVIEW software.

All activities of the MDP were performed under a documented quality assurance (QA) program that specified the performance-based QA/quality control requirements for all aspects of the program.[2] The experiments under the MDP were designed using an U.S. Environmental Protection Agency established procedure to formulate data quality objectives. QA objectives for the MDP were defined in terms of precision, accuracy, representativeness, completeness, and comparability. All data were validated and verified pursuant to the performance objectives of the program. The MDP was run for a duration of approximately three years.

3.3.3 Results and Conclusions from the MDP

Results from the MDP are described in detail in the MDP final report[1] and are summarized in Table 3.3-1 in terms of the dose-dependent G values for each matrix tested.

Table 3.3-1 — Experimental Dose-Dependent G Values

Matrix	Current Waste Material Type G Value	Number of Observations	Mean	Standard Deviation	95% Upper Tolerance Limit
Cement	1.3	202	0.25	0.18	0.58
Dry Cellulose	3.4	302	0.27	0.18	0.59
Polyethylene	3.4	186	0.23	0.22	0.64
Polyvinyl Chloride	3.4	99	0.14	0.19	0.50
Wet Cellulose	3.4	276	0.44	0.36	1.09

Source: Idaho National Engineering and Environmental Laboratory, "TRUPACT-II Matrix Depletion Program Final Report," *INEL/EXT-98-00987*, Rev. 1, prepared for the U.S. Department of Energy, Idaho Operations Office, Idaho Falls, Idaho (1999).

For all matrices, these dose-dependent G values were achieved within a maximum dose of 0.006 watt*year (product of watts times years). For example, for a waste container with a watt loading of 0.1 watt, the dose-dependent G value shown in Table 3.3-1 would be reached after 0.06 years or 22 days. The lower the watt loading, the longer it would take for the watt*year criteria to be satisfied and the dose-dependent G value to be applicable.

The following conclusions can be drawn from the results of the MDP:

- Increasing dose (product of the decay heat loading and elapsed time) decreases the effective G value for hydrogen due to depletion of the matrix in the vicinity of the

---

[2] Connolly, M.J., G.R. Hayes, T.J. Krause, and J.S. Burt, "TRUPACT-II Matrix Depletion Quality Assurance Program Plan," *INEL95/0361*, Rev. 1, Idaho National Engineering and Environmental Laboratory, Idaho Falls, Idaho (1997).

alpha-emitting radioactive source particle. The lower G value, called the "dose-dependent G value," is applicable after a dose of 0.006 watt*years.

- As with initial G values, the dose-dependent G values are a function of the waste matrix.

- Dose-dependent G values for wet cellulosics were higher than those for dry cellulosics because of the presence of water.

- The dose-dependent G values were independent of temperature based on testing performed at room temperature and at 140°F.

- Experiments performed with different particle sizes show that while initial G values could be higher for smaller particle sizes, the dose-dependent G values for all particle sizes tested are bounded by the values shown in Table 3.3-1.

- Previous experiments that included agitation of cylinders similar to those used in the MDP indicated that agitation did not affect dose-dependent G values.[1]

- Isotopic composition did not have a significant impact on the dose-dependent G values based on experiments performed with two different isotopes of Pu (Pu-238 and Pu-239).

Data from actual CH-TRU waste containers at the Rocky Flats Environmental Technology Site and the Idaho National Engineering and Environmental Laboratory show that even when compared to the mean dose-dependent G values from the matrix depletion experiments, G values from real waste containers are lower. Theoretical analysis, using nuclear and molecular level mechanisms, also shows that hydrogen generation from radiolysis and matrix depletion is consistent with the experimental results from the MDP.

3.3.4 Effects of Agitation on Dose-Dependent G Values

The effects of agitation on dose-dependent G values have been evaluated by previous studies at both the laboratory-scale and drum-scale levels, and agitation has been found to have no impact on dose-dependent gas generation rates. Agitation could occur under transportation conditions but, as shown below, does not cause redistribution of the radionuclides to a nondepleted portion of the waste matrix and therefore does not cause an increase in the dose-dependent G values as shown in this section.

The earliest study of the effects of agitation on gas generation rates was performed by Zerwekh at the Los Alamos National Laboratory (LANL) in the late 1970s.[3] Zerwekh prepared an experimental array of 300-cm^3 stainless steel pressure cylinders, each loaded with 52.5 grams of a single or a combination of TRU waste matrix materials. Materials tested included cellulosics,

---

[3] Zerwekh, A., "Gas Generation from Radiolytic Attack of TRU-Contaminated Hydrogenous Waste," *LA-7674-MS*, Los Alamos National Laboratory, Los Alamos, New Mexico (1979).

polyethylene (PE) (low-density) bags, PE (high-density) drum liner material, and other typical TRU waste material. Net gas G values as a function of elapsed time were derived for each of the test cylinders and showed the characteristic decrease in G value with dose. Thorough mechanical shaking of two of the cylinders on two different occasions did not affect the rate of gas generation.[3]

In a second study, researchers at LANL retrieved six drums of [238]Pu contaminated waste from storage to study gas generation.[4] The wastes were contained in 30-gallon drums and consisted of either mixed cellulosic wastes or mixed combustible wastes. The drums ranged in age from four to ten years. Two of the drums containing mixed combustible wastes were tumbled end over end in a drum tumbler for four hours.[4] The researchers also reported G values for three drums of newly generated waste that were previously characterized. All six retrieved drums had measured G values that were lower than those measured for newly generated drums. The researchers concluded that the retrieved drums' effective hydrogen G values corroborate the matrix depletion observed for the laboratory-scale experiments in Zerwekh (1979)[3]. Also, because of the vigorous nature of the agitation experienced by two of the four-year-old drums, the researchers concluded that radionuclide redistribution does not occur under transportation conditions.[3]

More recently, experiments on alpha radiolysis were conducted at LANL by Smith et al.[5] to determine radionuclide loading limits for safe on-site storage of containers at LANL. Simulated TRU waste matrices in the form of cellulose (cheesecloth and computer paper) and PE (bottle and bag material forms) were contaminated with pre-weighed amounts of [238]PuO$_2$ powder. The first PE experiment (referred to as PE test cylinder 1) used a PE bottle to allow any potential later redistribution of the radionuclide particles to fresh matrix surfaces. The radionuclide powder was poured into the bottle, which was sealed and gently rolled to allow contamination of the sides of the bottle. The bottle was returned to an upright position and the lid was punctured with an approximately 0.5-inch diameter hole to allow free movement of generated gas from the bottle to the test canister. It was noted that the [238]PuO$_2$ powder adhered to the walls of the bottle and very little, if any, collected at the bottom. The remaining five test sample matrices were prepared by uniformly sprinkling the powder across a letter-sized sheet of the waste matrix, folding the sheet in toward the center from each end, and finally rolling each sheet into a cylindrical shape of about 2 by 4 inches. The six test matrices were placed inside six cylindrical, 2.06 liter stainless steel sealed canisters. Gas samples were extracted periodically and analyzed by mass spectrometry.

The first test canister for each waste material was subjected to vigorous dropping, rolling several times, and shaking on day 188 to simulate drum handling and transportation that could result in redistribution of the [238]PuO$_2$ to fresh nondepleted portions of the waste matrix. Any agitation effects were expected to be most pronounced for the test canister containing the PE bottle in PE test cylinder 1, because some aggregation of the powder at the bottom of the bottle was expected.

---

[4] Zerwekh, A., J. Warren, and S. Kosiewicz, "The Effect of Vibration on Alpha Radiolysis of Transuranic (TRU) Waste," Proceedings of Symposium on Waste Management, Tucson, Arizona (1993).

[5] Smith, M.C., E.L. Callis, J.H. Cappis, E.M. Foltyn, R.S. Marshall, and J. Espinoza, "Alpha Radiolytic Gas Generation: Determination of Effective G-values," Benchmark Environmental Corporation, Albuquerque, New Mexico (1997).

However, no change in the effective hydrogen G value was observed for either the cellulose or PE test canisters.

In summary, three separate studies have investigated the ability of agitation to redistribute radionuclide particles to nondepleted surfaces of TRU waste matrices. All three studies conclusively showed that the dose-dependent G values are not impacted by agitation during transportation. Application of dose-dependent effective G values is discussed in Section 3.3.5.

3.3.5 Application of Dose-Dependent G Values to CH-TRU Wastes

Dose-dependent G values are applicable to CH-TRU waste materials of Waste Types II and III. Waste Type I, Solidified Inorganic Solids, will be governed by the initial G values under all conditions because the solidified, aqueous nature of these waste forms, in theory, precludes observation of matrix depletion (as the matrix near the Pu is depleted, water can move to replace the depleted matrix). Similarly, if CH-TRU waste materials of Waste Types II and III contain absorbed, adsorbed, or solidified aqueous materials, matrix depleted G values cannot be used. The presence of absorbed, adsorbed, or solidified aqueous materials precludes the observation of matrix depletion and requires the use of initial G values for Waste Types II and III that include such materials although the watt*year criteria (watt*year >0.012) may be met.

The watt*year criteria used to apply dose-dependent G values is twice the highest value recorded in the experiments. The dose-dependent G values chosen for CH-TRU waste materials of Waste Types II and III are the 95% upper tolerance limit values shown in Table 3.3-1. The application of dose-dependent G values to the waste types is as follows:

- Waste Type II: Dose-dependent G value (H_2) for containers meeting a watt*year criteria of 0.012 is governed by assuming polyethylene as the packaging material, with a G value (H_2) of 0.64.

- Waste Type III: Dose-dependent G value (H_2) for containers meeting a watt*year criteria of 0.012 is governed by wet cellulosic materials in the waste, with a G value (H_2) of 1.09.

As can be seen from Table 3.3-1, the above dose-dependent G values represent conservative values that are more than two times the mean value from the experiments.

This page intentionally left blank.

APPENDIX 3.4

SHIPPING PERIOD ─ GENERAL CASE

This page intentionally left blank.

3.4   Shipping Period — General Case

3.4.1   Introduction

The purpose of this appendix is to develop, on a conservative basis, the time for the shipping period from closure until venting that should be considered for the analysis of gas generation in TRUPACT-II and HalfPACT.

3.4.2   Background

A large number of shipments of contact handled transuranic (CH-TRU) waste to the Waste Isolation Pilot Plant (WIPP) from U.S. Department of Energy (DOE) facilities have been planned. These shipments will be made by a fleet of trucks, each capable of transporting up to three packages, or by rail. The analysis in this appendix is presented for the case of shipments by truck. Shipments by rail shall meet the 60-day total maximum shipping period requirement for truck shipments. A 20-day shipping period is applicable to shipments to destinations (WIPP or other DOE site) within a radius of approximately 1,000 miles, as presented in Appendix 3.5 of the CH-TRU Payload Appendices. Using administrative controls, a 10-day shipping period is applicable for shipments to WIPP as presented in Appendix 3.6 of the CH-TRU Payload Appendices. For Content Code LA 154, a shipping period of 5 days is justified, as presented in Appendix 6.12 of the CH-TRU Payload Appendices.

The packages are loaded on specially designed trailers and travel over the routes shown in Figure 3.4-1. The waste transportation activity will span a 25-year period. Because of the large number of trips and because of the agreements for notification to the states through which these shipments will pass on their way to WIPP, a state-of-the-art satellite tracking system will be employed to monitor the progress and position of each shipment. This monitoring capability will be available to authorities in the affected states as well as the transportation management people at the WIPP site and other DOE sites.

3.4.3   Approach

The approach to be taken in establishing the shipping period will be to develop a normal or expected shipment time based on the planned loading, transport, and unloading times. Then a maximum shipment time will be based on adding to the normal shipment time delays caused by a number of factors. This maximum shipment time will assume that each of these delays occurs. The probability of each of these delays occurring is small. The joint probability of all of these delays occurring would be extremely small. Thus the development of a maximum shipment time based on the sum of extended delays for each of the factors is considered to have a large margin of error. In the event that a particular shipment is experiencing delays (for one reason or another) resulting in an abnormal shipment time, close monitoring of the delay by WIPP will ensure minimum delays in the schedule.

Figure 3.4-1—TRU Waste Generator/Storage Site and Potential Shipment Corridor States

3.4.3.1 Normal or Expected Shipment Time

The normal transport time is the sum of the times associated with loading the packages, the normal transit time, and the unloading of the packages. The loading time to be considered as important is the time interval from closing (sealing) the inner containment vessel (ICV) until the truck leaves the waste shipper's facility. The transit time is that time interval beginning with departure from the shipper's facility and ending with the arrival at the WIPP site. The unloading time is that time interval beginning with the arrival at the site and ending with the venting of the ICV. This total time defines the expected shipment time.

3.4.3.2 Off-Normal or Maximum Shipment Time

The maximum shipment time includes those delays that could extend the shipment time. These delays are:

- Delays in loading or releasing the truck at the shipper's facility.

- Delays in transit caused by adverse weather conditions leading to road closures, or road closures due to accidents involving other vehicles.

- Accidents involving the shipment vehicle. These delays would include the time required for notification of appropriate authorities (including the DOE Emergency Response Team), and the time to take corrective action. This corrective action may involve transfer of the packages to a back-up truck, which would require the services of heavy equipment.

- Delays in transit caused by mechanical problems with the truck. This factor would include such things as tire problems, broken belts and hoses, and any other such minor problems.

- Delays caused by one or both of the drivers becoming ill.

- Delays in unloading the packages at the WIPP site. These could potentially be caused by factors such as truck arrival at the start of a long holiday weekend or equipment problems at the WIPP Waste Handling Building.

3.4.4 Discussion

3.4.4.1 Normal or Expected Shipment Time

As stated previously, the normal or expected shipment time is that time interval beginning with the sealing of the ICV at the shipper's facility and ending with the venting of the ICV in the WIPP Waste Handling Building.

3.4.4.1.1 Package Loading

The package is designed so that it can be loaded within one hour. The loading operation is facilitated by design features and contents handling methods aimed at a quick turnaround during either loading or unloading. For example, the closure lids on both the inner and outer containment vessels are fastened with a breech-lock type of mechanism. The contents are handled in vertical sets as a payload assembly, and only one lift is required. All steps in the loading process (from attaching the lifting fixture to the crane until the lift fixture lift links are disconnected from the outer closure following loading) can be accomplished in two hours or less. Thus the time associated with loading the three packages for a single shipment is expected to be less than eight hours. However, to be conservative, one day (24 hours) is allotted for this activity.

3.4.4.1.2 Transit Time

Specific routes have been selected for transport of waste from each of the DOE facilities to the WIPP site. The distances for the primary DOE facilities are given in Table 3.4-1.

These shipments will all be made by trucks having two drivers. Regulations governing maximum driving and on-duty times are given in 49 CFR 395, "Hours of Service of Drivers."[1]

These regulations permit a driver to drive not more than ten (10) hours following eight (8) consecutive hours off duty or, be in the on-duty status not more than fifteen (15) hours. If the fifteen hours on-duty status is reached, a driver must be out of the vehicle in an off-duty status for eight hours. Drivers using sleeper berth equipment may cumulate the eight (8) hours off duty (for the ten hour on-duty status) resting in the sleeper in two separate periods (each period must be at least two hours) totaling eight (8) hours. Drivers cannot be on duty more than seventy (70) hours in eight consecutive days. By using the two drivers and a rotational on-duty/off-duty system of approximately five (5) hours, the vehicle can be maintained operational for twenty-four (24) hours per day for seven days.

Table 3.4-1 — Normal Transit Times

To WIPP From	Distance (Miles)	Transit Time in Hours (Miles per Hour)				Transit Time in Days (Miles per Hour)			
		40	45	50	55	40	45	50	55
RFETS*	666	16.7	14.8	13.3	12.1	0.7	0.6	0.6	0.5
INEEL	1484	37.1	33.0	29.7	27.0	1.5	1.4	1.2	1.1
WHC	1847	46.2	41.0	36.9	33.6	1.9	1.7	1.5	1.4
LANL*	352	8.8	7.8	7.0	6.4	0.4	0.3	0.3	0.3
SRP	1447	36.2	32.2	28.9	26.3	1.5	1.3	1.2	1.1
LLNL	1345	33.6	29.9	26.9	24.5	1.4	1.2	1.1	1.0
NTS*	1017	25.4	22.6	20.3	18.5	1.1	0.9	0.8	0.8
ORNL	1493	37.3	33.2	29.9	27.1	1.6	1.4	1.2	1.1
ML	1460	36.5	32.4	29.2	26.5	1.5	1.4	1.2	1.1
ANL	1404	35.1	31.2	28.1	25.5	1.5	1.3	1.2	1.1

*See Appendix 3.5 of the CH-TRU Payload Appendices for the shipping period determination for these sites, which are within an approximately 1,000 mile radius of WIPP.

Experience at the Idaho National Engineering and Environmental Laboratory (INEEL) has shown that shipments of this type can achieve an average speed of 45 mph. This average speed includes stops for vehicle inspections every two hours, fueling, meals, driver relief and state vehicle inspections.

The normal transit time ranges from 0.6 day for shipments from Rocky Flats Environmental Technology Site to 1.7 days for shipments from Hanford (WHC) as shown in Table 3.4-1. For the purpose of conservatism three days is assumed for a maximum normal transit time.

---

[1] Title 49, Code of Federal Regulations, Section 395 (49 CFR 395), "Hours of Service of Drivers."

3.4.4.1.3 Unloading

Normal loading will be accomplished in less than a day. The whole waste receipt system has been designed to perform the waste unloading in less than a half day since on the average, WIPP will be receiving three to four shipments per day, and the waste handling equipment and procedures have been designed and developed to meet this demand. Once the truck has undergone the health physics survey and security checks, the tractor is disconnected, and a trailer jockey is connected to the trailer. The trailer and packages are cleaned, and the trailer is moved to the unloading area. The packages are removed from the trailer, passed through an air lock into the Waste Handling Building and placed into unloading stands. The outer and inner lids are removed after the containment vessels have been vented through a facility gas-handling system, and other procedural steps are then taken. The Waste Handling Building has unloading capacity for two trailers, each carrying three packages; that is, the WIPP surface facility includes parallel docks and parallel or redundant handling equipment. Thus, the normal unloading of a trailer with three packages will be accomplished in less than a half day. The storage space is adequate to accommodate the contents of every package in the fleet. The unloading time is, thus, conservatively assigned a value of one day.

3.4.4.1.4 Total Normal or Expected Shipment Time

The total normal or expected shipment time is three to five days depending on the origin of the waste. Normal loading time is one day, transit time is one to three days and unloading time is one day.

3.4.4.2   Off-Normal or Maximum Shipping Time

3.4.4.2.1 Loading Delays

There are a number of factors that could extend the time interval between the sealing of the ICV and the truck getting under way:

- Loading could begin on a day preceding a holiday weekend.

- Difficulty testing the ICV or Outer Containment Vessel (OCV) seals.

- Handling equipment failure.

In the most severe sequence, one package of the load would already have been filled and sealed. Loading could begin on a day preceding a long (holiday) weekend. If, for example, loading began on a Friday preceding a three-day weekend, loading would not be completed until the following Tuesday. This would result in a four-day loading period.

The inner or outer seal may fail the leak test, which would generally call for some maintenance. The worst case would probably be a failure in the leak test equipment that could take up to two days to correct.

The crane or the lifting fixture with center of gravity load compensation could also fail, forcing a delay in any further package loading until corrected. This could also take two days.

It would be very unlikely for more than two of these scenarios to happen simultaneously, so a total of six days is deemed to be a reasonable maximum time to account for delays associated with loading. If there were conditions that could cause long, totally unanticipated delays, the packages can be vented at the shipper's facility.

3.4.4.2.2 Transit Time Delays

There are several factors that could extend the normal transit time of three days from the DOE waste sites to the WIPP site. Adverse weather conditions could lead to delays and road closures. A telephone survey of each of the states in the waste shipment corridor states was conducted to ascertain a reasonable time to assume for weather delays. Table 3.4-2 provides the results of this survey. One can conclude from this survey that weather conditions may close a major highway for two to five days. Long-term interruptions in normal traffic caused by bridge outages etc., would result in rerouting traffic to alternate routes. Accidents involving other vehicles could also cause delays and road closures of up to a day. It is concluded that a total transit delay of five (5) days is reasonable to assume for weather delays or road closures.

Accidents involving the shipment vehicle itself could cause lengthy delays. These delays would include the accident response time for notifying appropriate authorities (including Radiological Assistance Teams, if required) and the time to take corrective action or to mitigate the accident. One day is conservatively assumed for the response to the accident. (In addition to normal accident responses, monitoring of the satellite tracking system would also facilitate an early response to accidents). Corrective action may involve retrieving the packages from a damaged trailer (including the possibility that the truck could be over an embankment), and transferring them to a back-up truck. Special equipment such as cranes may be required to carry out these operations. An accident mitigation time of five days will be assumed. This time includes the time for delivery of a back-up truck, and the time to move in special heavy equipment and rig special lifting fixtures to retrieve and transfer the packages to the back-up vehicle.

Table 3.4-2 — Survey of Weather Related Delays on Interstate Highways of the TRU Waste Shipment Corridor Sites

State/City	Office Contacted	Date Contacted	Type of Weather Related Delays	Highway
1. Alabama/Montgomery	State DOT	2/4/88	24 hrs. max.	All
2. Arizona/Phoenix	Dept. of Public Safety	2/4/88	8 hrs. maximum for any type of emergency.	All
3. Arkansas/Little Rock	State DOT Construction of Maintenance	2/17/88	1/2 day maximum.	All
4. California/Sacramento	State DOT Highway Dept.	2/18/88	2 days due to snow every 2 to 3 years. Few minutes to 2 to 3 weeks due to flood. 2 weeks due to earthquake. Detours provided.	I-5 I-15 Route 14
5. Colorado/Denver	State DOT	2/5/88	12 hrs. maximum.	
6. Georgia/Atlanta	State DOT Maintenance	2/2/88	No information available.	
7. Idaho/Boise	State DOT	2/4/88	3 to 4 hrs. due to blizzard.	
8. Illinois/Springfield	State DOT	2/7/88	10 days because a bridge pier slipped. (Trucks were off the road for 14 days). Detours provided.	Northbound I-90, I-94
9. Indiana/Indianapolis	Dept. of Highway Operations	2/5/88	2 days due to snowstorm or blizzard/wind.	I-65
10. Kentucky/Frankfort	State DOT Highway Maintenance	2/5/88	8 hrs. maximum.	
11. Louisiana/Boston Range	State DOT Office of Highway Traffic and Planning	2/3/88	No information available.	
12. Mississippi/Jackson	State DOT Highway Dept.	2/17/88	None.	
13. Missouri/Jefferson City	Highway Patrol	2/4/88	1/2 to 1 day due to flooding. 1 to 1-1/2 days with detours provided.	I-70
14. Nevada/Carson City	State DOT Maintenance Div.	2/4/88	4 to 8 hrs. due to snow.	I-80
15. New Mexico/Santa Fe	State DOT	2/9/88	Closed periodically due to snow and/or wind but for a very short period of time.	Interstate
16. Ohio/Columbus	State DOT	2/5/88	8 hrs. maximum.	All
17. Oklahoma/Oklahoma City	State DOT	2/5/88	1 month due to a bridge was washed out on Cimmaron River.	I-35
18. Oregon/Salem	State DOT	2/4/88	8 hrs. maximum. Generally, usage of highway stopped for trucks/oversized vehicles for up to 8 hours for icy conditions	Interstate
19. South Carolina/ Columbia	State DOT State Dept. of Health and Control	2/3/88	No information but generally 8 hrs. maximum.	

3.4-7

Table 3.4-2 — Survey of Weather Related Delays on Interstate Highways of the TRU Waste Shipment Corridor Sites *(Continued)*

State/City	Office Contacted	Date Contacted	Type of Weather Related Delays	Highway
20. Tennessee/Nashville	State DOT	2/3/88	96 hours due to rain.	State Route 54 N in Haywood County
			72 Hours due to rain/high water level.	State Route 188
21. Texas/Austin	State DOT	2/16/88	2 to 3 hours due to flooding. 8 hours maximum due to snow.	I-20
22. Utah/Salt Lake City	State DOT Traffic Engr.	2/4/88	4 to 5 hours due to blizzard.	I-15
23. Washington/Olympia	State DOT	2/4/88	2 days due to avalanche.	I-90
24. Wyoming/Cheyenne	State DOT Motor Vehicle Safety	2/4/88	4 to 5 days predominantly due to weather.	I-80

Delays in transit could be caused by routine mechanical problems with the truck. These problems could include tire failures, broken belts and hoses, electrical failures and similar minor problems; or more significant problems necessitating bringing a back-up truck into service. It is conservatively assumed that appropriate responses to mechanical failures of the truck can be made in four days.

Lastly, one or both of the drivers could become ill during the trip, necessitating the possibility that one driver must do all the driving or relief drivers would have to be sent to wherever the truck is parked. If one driver has to do all the driving, the transit time would be doubled (i.e., add three days). If relief drivers are required, a two-day delay will occur to allow for travel time of the replacement driver(s).

3.4.4.2.3 Unloading Delays

Delays in unloading the packages at the WIPP site could be caused by a number of factors: A truck could arrive at the WIPP site late on a Friday preceding a three day weekend, and the normal processing and unloading would not be completed until the following Tuesday, causing a delay in unloading of approximately 4-1/2 to 5 days. There could be equipment problems in the Waste Handling Building that could cause delays in unloading the packages. Venting and handling equipment could break down. A total unloading time of four days will be assumed if unloading begins just before a regular weekend or five days for a holiday weekend. This is a reasonable maximum time to account for delays associated with unloading because the packages can be vented at the WIPP site (using workers overtime) if a totally unanticipated chain of delays were to occur.

3.4.4.2.4 Total Off-Normal or Maximum Shipment Time

The total off-normal or maximum shipment time is summarized in Table 3.4-3. A maximum shipment time of 31 days is projected assuming the worst-case scenario of all off-normal occurrences happening in the same shipment.

Table 3.4-3 — Shipment Time Summary

Activity	Time (Days)
Normal Shipment Time	
Loading	1
Transit Time	1-3
Unloading	1
Maximum Normal Shipment Time	3-5
Off-Normal or Maximum Shipment Time[a]	
Loading	6
Transit Time	
• Normal (maximum)	3
• Weather delays and road closures	5
• Accident response	1
• Accident Mitigation	5
• Truck maintenance problems	4
• Driver illness	2
Unloading	5
Maximum Off-Normal Shipment Time	31

[a]Adding all the times for relatively low-probability, independent delays provides a conservative value for the maximum off-normal transit time.

3.4.5 Summary and Conclusions

The total normal or expected shipment time from the DOE facilities to the WIPP site will be three to five days with the longest time associated with the trip from Hanford to WIPP. The maximum or off-normal shipment time that has been postulated to occur as a consequence of a series of accidents or other off-normal events and delays is 31 days. This maximum shipment time is six times the maximum normal expected shipment time. This justifies using a 31-day period for the basis of determining potential buildup of flammable concentrations in the package under the specified normal conditions with the absence of venting or operational controls during transport. However, to add an additional margin of safety, the shipping period is nearly double the total off-normal shipment time or 60 days, which is more than an order of magnitude longer than the maximum normal shipment time.

This page intentionally left blank.

APPENDIX 3.5

SHIPPING PERIOD ─ CLOSE-PROXIMITY SHIPMENTS

This page intentionally left blank.

3.5 Shipping Period—Close-Proximity Shipments

3.5.1 Introduction

This appendix presents the shipping period determination for close-proximity shipments (i.e., within a radius of approximately 1,000 miles). The three U.S. Department of Energy (DOE) facilities nearest to the Waste Isolation Pilot Plant (WIPP) (i.e., Los Alamos National Laboratory [LANL], Rocky Flats Environmental Technology Site [RFETS], and Nevada Test Site [NTS]) are within a radius of approximately 1,000 miles of WIPP. For close-proximity shipments, the TRUPACT-II or HalfPACT is loaded at the site, transported within a radius of approximately 1,000 miles, and vented within a maximum of 20 days from the closure (or sealing) of the inner containment vessel (ICV). The basis for the 20-day shipping period is defined in this appendix.

3.5.2 Approach

The shipping period is defined to begin with closure (or sealing) of the ICV during loading at the shipping facility and end with venting of the ICV during unloading at the receiving facility. Conservative time estimates for the following activities were used in determining the shipping period for close-proximity shipments:

- Loading time
- Transport time
- Unloading time.

3.5.2.1 Loading Time

The loading time begins with the sealing of the ICV and ends with the departure of the shipment of the package from the site. All steps in the normal, or expected, loading process for a single package (from attaching the lifting fixture to the crane until the lift fixture lift links are disconnected from the outer closure following loading) can be accomplished in two hours or less. Thus, the time associated with loading the three packages for a single truck shipment is expected to be less than eight hours. However, the maximum expected loading time is conservatively estimated as 24 hours (1 day).

The potential factors that could delay the expected loading time are as follows:

- Initiating loading on a day preceding a holiday weekend

- Difficulty associated with testing the ICV or outer containment vessel (OCV) seals

- Failure associated with payload handling equipment.

Loading could be delayed if initiated on a day preceding a holiday weekend or other scheduled facility closure period. This could result in a maximum loading time of 4 days. Potential delays associated with leak testing or payload handling equipment failures are typically reduced to a matter of hours by the backup or replacement equipment typically available at each shipping

facility. However, even with available standby equipment, any equipment failure is likely to result in a lost day due to the time required to identify the problem, attempt corrective measures, and then access the backup or replacement equipment. As a result, a 1-day delay is deemed adequate for either seal testing or payload handling equipment failures. Although unlikely, if loading is assumed to be initiated on a day preceding a holiday weekend and either a seal testing or payload handling equipment failure is assumed to occur simultaneously, 5 days could be required to load three payloads. It should be noted that if excessive loading delays beyond 5 days were to occur due to unanticipated events, the packages could be vented at the shipping facility.

3.5.2.2   Transport Time

The transport time begins with the departure of the shipment from the site and ends with the arrival of the shipment at the receiving site. The transport time is dependent upon the distance between the shipping and receiving sites. For close-proximity shipments, the distance will be within a radius of approximately 1,000 miles. The normal, or expected, travel time for a distance of 1,000 miles is 25 hours based on an average speed of 40 miles per hour (mph). This average speed takes into account stops for vehicle inspections every two hours, fueling, meals, driver relief, and state vehicle inspections.

The potential factors that could delay the expected transport time are as follows:

- Adverse weather
- Vehicle accidents
- Mechanical problems with the truck
- Driver illness.

Adverse weather could result in transport time delays due to road closures, slower driving speeds, or unforeseen stops.   Based on actual delays experienced to date by TRUPACT-II shipments, the average delay time attributed to weather is 23 hours (~1 day). Procedures at sites ensure that shipments are not initiated at times when adverse weather exists or is forecasted. Using operational experience, a 60-hour (2.5-day) delay is deemed adequate for any delay caused by adverse weather conditions.

Vehicle accidents have the potential for the longest transport time delays due to the time required to respond and perform required corrective actions. Based on the training programs provided to local emergency response personnel along the transport routes, accident response time would be minimal (less than one hour). However, additional time may be required for notification and response of other appropriate authorities such as Radiological Assistance Teams (if required). Deployment of other appropriate authorities from either the receiving or shipping facility, whichever is closer, would take no more than 0.5 day to reach an accident scene. The accident mitigation time for close-proximity shipments is considered to be prompt due to the relatively short distance that would be required to provide equipment to perform corrective measures. A backup truck and trailer, as well as special equipment (such as a crane and special lifting fixtures) could be required to return the shipment to the road. Either the shipping or receiving

facility, whichever is closer, could provide accident mitigation equipment and personnel. Therefore, up to 3 days is considered appropriate for completing accident corrective action. This time includes deployment of a backup truck and trailer, retrieving and transferring the packages to the backup vehicle, and performing any necessary surveys and/or inspections to confirm the shipment is prepared for transport.

Truck maintenance associated with common mechanical problems could result in transport time delays. The majority of routine mechanical problems (flat tires, belt or hose failures, etc.) can be rectified in a matter of hours. A worst-case mechanical problem would result in the need for a replacement truck, which is included in the time estimated for vehicle accident mitigation as described above.

The last remaining potential scenario for delaying the transport time is driver illness. The relatively short distances between close-proximity sites would enable prompt replacement of the ill driver(s). No more than 0.5 day would be required to provide a replacement driver if deployed from either the shipping or receiving facility, whichever is closer.

As a result, a 6.5-day transport time accounts for any unexpected impact to the expected transport time.

3.5.3 Unloading Time

The unloading time begins with the arrival of the shipment at the receiving site and ends with the venting of the ICV. The normal, or expected, unloading of a trailer with three packages will be accomplished in less than 0.5 day. However, the maximum expected unloading time is conservatively estimated at 24 hours (1 day).

The potential factors that could delay the expected unloading time are as follows:

- Shipment arrival preceding a holiday weekend
- Failure associated with venting or handling equipment.

Unloading could be delayed if the shipment arrives on a day preceding a holiday weekend or other scheduled facility closure period. This could result in a maximum unloading time of 4 days. Potential delays associated with venting or handling equipment failures are typically reduced to a matter of hours by the backup or replacement equipment typically available at each receiving facility. However, even with available standby equipment, any equipment failure is likely to result in a lost day due to the time required to identify the problem, attempt corrective measures, and deploy the backup or replacement equipment. As a result, a 1-day delay is deemed accurate for either venting or payload handling equipment failures. Although unlikely, if unloading is assumed to be initiated on a day preceding a holiday weekend and either a venting or payload handling equipment failure is assumed to occur simultaneously, 5 days could be required to unload three payloads. It should be noted that the packages could be vented, even if not completely unloaded, at the receiving facility within 5 days.

3.5.4 Summary and Conclusions

Based on an expected loading time of 24 hours, an estimated expected transport time of approximately 25 hours, and an expected unloading time of 24 hours, the maximum expected shipping period is approximately 3 days. The maximum shipment time that has been used in this analysis is based on conservative time estimates for loading (5 days), transport (6.5 days), and unloading (5 days). The additional contingency of a 3.5-day margin of safety results in a maximum shipping period of 20 days. Table 3.5-1 provides a summary of the activities comprising the shipping period.

Table 3.5-1 — Shipping Period Analysis Summary

Activity	Normal Expected Time (days)	Maximum Time Used in Analysis (days)
Loading Time	<1	5
Transport Time	~1	6.5
Unloading Time	<1	5
Margin of Safety	–	3.5
Shipment Time	3	20

This analysis justifies using a 20-day period as the basis for determining potential buildup of flammable concentrations in the package under the specified off-normal conditions with the absence of venting or operational controls during transport.

With twice the expected shipping period being just 6 days, the use of a 20-day shipping period is conservative. Data available for more than 1,800 shipments to the WIPP in more than 5 years show 20 days to be an extremely conservative estimate of shipping period. Sample shipping time data based on 1,467 shipments to WIPP from the three sites within a radius of approximately 1,000 miles are shown in Table 3.5-2. As shown, all shipments were made within a period of two days.

Table 3.5-2 — Sample Shipping Time Data

To WIPP From	Total Number of Shipments as of 04-20-04	Average Shipping Time (hours)*	% of Time Shipments are Completed within Average Time	Shipping Time Delays	
				Duration of Maximum Delay	Explanation
LANL	71	9	98%	1 day	Delay occurred at LANL as the result of generator site issues prior to shipment departure
NTS	7	30	100%	N/A	N/A
RFETS	1,389	18	99%	2 days	Weather delay; delay occurred at RFETS prior to shipment departure and en route following departure

*Average shipping times are estimated based on average speeds of 50 miles per hour and include time associated with safety inspections, fuel and food stops, and driver breaks.

N/A = Not applicable.

The 20-day shipping period justified herein may be used for any shipment to a destination within a radius of approximately 1,000 miles. For shipments to WIPP from within a radius of approximately 1,000 miles (i.e., from LANL, RFETS, and NTS), the 20-day shipping period is used exclusively.

This page intentionally left blank.

APPENDIX 3.6

SHIPPING PERIOD ─ CONTROLLED SHIPMENTS

This page intentionally left blank.

3.6 Shipping Period—Controlled Shipments

3.6.1 Introduction

This appendix presents the shipping period determination for shipments designated as controlled shipments. For these shipments, the TRUPACT-II or HalfPACT is loaded at the site, transported from the site to the Waste Isolation Pilot Plant (WIPP), and vented within a maximum of 10 days from the closure (or sealing) of the inner containment vessel (ICV). The basis for the 10-day shipping period is defined in this appendix. The use of a 10-day controlled shipment is an option available to sites that elect to impose administrative controls to ensure compliance with the conditions described herein.

3.6.2 Approach

The shipping period is defined to begin with closure (or sealing) of the ICV during loading at the shipping facility and end with venting of the ICV during unloading at the WIPP. Conservative time estimates for the following activities were used in determining the shipping period for controlled shipments:

- Loading time
- Transport time
- Unloading time.

3.6.2.1 Loading Time

The loading time begins with the sealing of the ICV and ends with the departure of the shipment of the package from the site. Activities to be completed during the loading time include leak testing and handling of the loaded package(s). As directed by site procedures for controlled shipments, these activities must be completed within 24 hours. If these activities are delayed beyond 24 hours, the package(s) must be vented and the closure process repeated in accordance with the administrative controls described in Section 6.2.3 of the Contact-Handled Transuranic Waste Authorized Methods for Payload Control (CH-TRAMPAC).

3.6.2.2 Transport Time

The transport time begins with the departure of the shipment from the site and ends with the arrival of the shipment at WIPP. The transport time is dependent upon the distance between the site and WIPP and capabilities for efficient response to potential transport time delays. As shown in Table 3.6-1, at an average speed of 40 miles per hour (mph) the longest travel time from a site to WIPP is 46.2 hours (corresponding to the 1,847-mile distance from Hanford to WIPP). Controlled shipments shall be made only when the shipping distance to WIPP is bound by that shown in Table 3.6-1. This average speed takes into account stops for vehicle inspections every two hours, fueling, meals, driver relief, and state vehicle inspections.

Table 3.6-1 — Normal Transit Times

To WIPP From	Distance (Miles)	Transit Time in Hours (Miles per Hour)				Transit Time in Days (Miles per Hour)			
		40	45	50	55	40	45	50	55
RFETS	666	16.7	14.8	13.3	12.1	0.7	0.6	0.6	0.5
INEEL	1484	37.1	33.0	29.7	27.0	1.5	1.4	1.2	1.1
Hanford	1847	46.2	41.0	36.9	33.6	1.9	1.7	1.5	1.4
LANL	352	8.8	7.8	7.0	6.4	0.4	0.3	0.3	0.3
SRS	1447	36.2	32.2	28.9	26.3	1.5	1.3	1.2	1.1
LLNL	1345	33.6	29.9	26.9	24.5	1.4	1.2	1.1	1.0
NTS	1017	25.4	22.6	20.3	18.5	1.1	0.9	0.8	0.8
ORNL	1493	37.3	33.2	29.9	27.1	1.6	1.4	1.2	1.1
Mound	1460	36.5	32.4	29.2	26.5	1.5	1.4	1.2	1.1
ANL	1404	35.1	31.2	28.1	25.5	1.5	1.3	1.2	1.1

The potential factors that could delay the normal transport time are as follows:

- Adverse weather
- Vehicle accidents
- Mechanical problems with the truck
- Driver illness.

Administrative controls in place at the shipping site prohibit the initiation of a controlled shipment at times when adverse weather exists or is forecasted. Any transport time delays associated with adverse weather are expected to be minimal and are, therefore, adequately covered by the margin of safety included in this analysis (see Section 3.6.4).

Prompt emergency response, truck maintenance, and driver or equipment replacement during the transport of controlled shipments is ensured by the application of additional resources. WIPP administrative controls require the designation of a shipment as a "controlled shipment" prior to initiation of the shipment from the site. This designation provides a trigger that requires additional resources to be available in order to provide accelerated response to avoid any significant delay during the transport time. This controlled shipment protocol is in addition to the routine use of the TRANSCOM system at WIPP, which provides continuous tracking of the shipment during transport from the site to WIPP.

Vehicle accidents have the potential for the longest transport time delays due to the time required to respond and perform required corrective actions. Based on the training programs provided to local emergency response personnel along the WIPP transport routes, accident response time would be minimal (less than one hour). However, additional time may be required for notification and response of other appropriate authorities such as Radiological Assistance Teams (if required). Deployment of other appropriate authorities from WIPP, the shipping facility, or other intermediate site, whichever is closer, would take no more than 1 day to reach an accident scene. Prompt mitigation of any accident is ensured by the application of WIPP protocol for controlled shipments. Due to the additional resources available during controlled shipments, up to 2 days is considered appropriate for completing accident corrective actions. This time

includes deployment of a backup truck and trailer, retrieving and transferring the package(s) to the backup vehicle, and performing any necessary surveys and/or inspections to confirm the shipment is prepared for continued transport.

Truck maintenance associated with common mechanical problems could result in transport time delays. The majority of routine mechanical problems (flat tires, belt or hose failures, etc.) can be rectified in a matter of hours. A worst case mechanical problem would result in the need for a replacement truck, which is included in the time estimated for vehicle accident mitigation as described above.

The last remaining potential scenario for delaying the transport time is driver illness. The additional resources available for controlled shipments ensure prompt replacement of an ill driver. The time required to replace a driver is conservatively estimated as 1 day.

As a result of WIPP protocols applied to shipments designated as controlled shipments, a 4-day transport time accounts for any unexpected impact to the expected transport time.

3.6.3 Unloading Time

The unloading time begins with the arrival of the shipment at WIPP and ends with the venting of the ICV. Operational procedures in place at WIPP ensure that processing and unloading procedures for controlled shipments are initiated within 24 hours of shipment arrival regardless of holidays or other schedules facility closure periods. Administrative controls imposed by WIPP procedures ensure that a shipment is not unattended beyond one day of arrival. Section 6.2.3 of the CH-TRAMPAC outlines administrative controls imposed to ensure venting of the ICV within 24 hours of shipment arrival.

3.6.4 Summary and Conclusions

Based on a loading time of 24 hours, an estimated transport time of less than 48 hours, and an unloading time of 24 hours, the normal expected shipping period for controlled shipments is 3 to 4 days. Using a conservatively estimated transport time of 4 days, the maximum expected shipping period for controlled shipments is 6 days. The additional contingency of a 4-day margin of safety results in a maximum shipping period of 10 days. Table 3.6-2 provides a summary of the activities comprising the shipping period.

Table 3.6-2 ─ Shipping Period Analysis Summary

Activity	Normal Expected Time (days)	Maximum Time Used in Analysis (days)
Loading Time	<1	1
Transport Time	1-2	4
Unloading Time	<1	1
Margin of Safety	–	4
Shipment Time	3-4	10

This analysis justifies using a 10-day period as the basis for determining compliance with gas generation requirements under rigorous operational controls during loading, transport, and unloading as specified in this appendix. With twice the normal expected shipping period being no more than 8 days, the use of a 10-day shipping period is conservative.

Sample shipping time data based on 2,503 shipments to WIPP to date are shown in Table 3.6-3. As shown, all shipments have been made in well under 10 days even without the use of administrative controls specified in this appendix. Therefore, the controlled shipments completed under the conditions specified in this appendix will readily comply with the 10-day shipping period.

Table 3.6-3 — Sample Shipping Time Data

To WIPP From	Total Number of Shipments as of 04-20-04	Average Shipping Time (hours)*	% of Time Shipments are Completed within Average Time	Shipping Time Delays	
				Duration of Maximum Delay	Explanation
ANL	11	43	100%	N/A	N/A
Hanford	76	43	98%	2 days	Weather delay; delay occurred at Hanford Site prior to shipment departure
INEEL	603	32	98%	5 days	Weather delay; delay occurred en route; shipment was returned to INEEL and delayed prior to second departure
LANL	71	9	98%	1 day	Delay occurred at LANL as the result of generator site issues prior to shipment departure
NTS	7	30	100%	N/A	N/A
RFETS	1,389	18	99%	2 days	Weather delay; delay occurred at RFETS prior to shipment departure and en route following departure
SRS	346	36	99%	3.7 days	Weather delay; delay occurred at SRS prior to shipment departure

*Average shipping times are estimated based on average speeds of 50 miles per hour and include time associated with safety inspections, fuel and food stops, and driver breaks.

N/A = Not applicable.

Only shipments designated as controlled shipments and, therefore, subject to the WIPP protocol described in this appendix and the administrative controls specified in Section 6.2.3 of the CH-TRAMPAC for loading and unloading are eligible for evaluation using the 10-day shipping period.

APPENDIX 3.7

**ASPIRATION OF UNVENTED PAYLOAD CONTAINERS
OF CH-TRU WASTE**

This page intentionally left blank.

3.7   Aspiration of Unvented Payload Containers of CH-TRU Waste

3.7.1   Introduction

Payload containers of contact-handled transuranic (CH-TRU) waste at U.S. Department of Energy (DOE) sites that have been stored in an unvented condition (without a filter or equivalent venting mechanism and/or without a punctured/vented liner) have the potential to accumulate hydrogen gas during storage. Prior to transport in a TRUPACT-II or a HalfPACT package, each container shall be vented for a sufficient period of time to aspirate. This is required to reduce the concentration of hydrogen present at the time of venting to steady state concentrations (generation rate equals release rate) within each of the layers of confinement in a payload container. Once steady state concentrations are achieved, there will be no change in the concentration of hydrogen in each of the volumes of confinement. "Venting" refers to the puncturing of the drum lid and rigid liner lid (if present) and the installation of one or more filter vent(s) or equivalent venting mechanism(s) in the drum lid of a payload container. The period of time for which a payload container needs to be vented before qualifying for transport in a package is defined as the "aspiration time." This appendix derives the aspiration times needed for unvented payload containers of waste for each payload shipping category.

Section 3.7.2 presents three options available to the sites to meet the aspiration requirements. Section 3.7.3 describes the methods used to derive the aspiration times including the computational procedure. A discussion of tables that must be used to determine the aspiration times for each payload shipping category is presented in Section 3.7.4. Specific procedures to be followed by the sites to implement any of the three options are presented in Section 3.7.5. All sites with unvented payload containers of waste shall follow one or more of these procedures as part of the waste qualification process.

3.7.2   Options to Determine Aspiration Times

Sites with unvented payload containers of waste have the following options to determine the aspiration time for a payload container. All of the options use bounding values for the hydrogen generation rates. For payload containers with waste types in packaging configurations that do not generate any flammable gas, aspiration is not required (i.e., Waste Material Type II.2). It is assumed that during the storage period and subsequent aspiration, hydrogen is being generated in the payload container at this bounding rate. These generation rates are the maximum allowable for each of the shipping categories. These rates are not a function of the G values, but depend on the packaging configurations within the payload containers. Since all the parameters used in the calculations are the same for containers with the same packaging configuration within a waste type (i.e., I, II, III, and IV), the aspiration times for the waste material types of a waste type (e.g., I.1, I.2, and I.3) are the same. In the aspiration tables for common shipping categories presented in Section 5.3 of the Contact-Handled Transuranic Waste Authorized Methods for Payload Control (CH-TRAMPAC), no distinction has therefore been made (or is necessary) between waste material types.

3.7.2.1 Option 1 - Aspiration Time Based on Date of Drum Closure

The aspiration time using Option 1 is calculated based on the amount of time that a payload container has been closed without venting. This option uses the bounding hydrogen generation rate for the payload shipping category (Appendices 2.3 and 6.7 of the CH-TRU Payload Appendices), and assumes that all of the hydrogen generated within the storage period will accumulate in the layers of confinement of the payload container. This approach will give a conservative estimate of the aspiration time, since the actual hydrogen generation rate will be less than the bounding value, and may decrease during storage due to matrix depletion. In addition, some of the hydrogen generated during storage may not be retained in the payload container. Many payload containers have gaskets that are manufactured to allow selected diffusion of hydrogen.

This analysis has been extended up to a possible accumulation of 40% hydrogen in the headspace of the payload container. As will be discussed in subsequent sections, this concentration is about an order of magnitude higher than the average concentration of hydrogen measured in sampling programs of CH-TRU waste drums at the DOE sites. If the DOE sites choose to implement this option, the age (period of time that the container has been closed) of the payload container will determine the aspiration time as shown in Section 5.3 of the CH-TRAMPAC.

3.7.2.2 Option 2 - Headspace Gas Sampling At The Time Of Venting

The second option is divided into two sub-options:

> Option 2A — Sampling of Container Headspace
> Option 2B — Sampling of Rigid Liner Headspace.

3.7.2.2.1 Option 2A — Container Headspace Gas Sampling at the Time of Venting

This option requires the sampling of payload containers for the container headspace concentration of hydrogen prior to puncturing the rigid drum liner. (Container headspace is the region between the payload container and the outermost layer of confinement, usually the rigid liner). This option allows credit for actual hydrogen generation rates inside the payload container during storage. In addition, this option allows credit for any diffusion of hydrogen through the gasket that can occur during storage. The aspiration time is determined based on the concentration of hydrogen in the container headspace. Bounding values for hydrogen generation are used to simulate the aspiration after venting. The required aspiration time for common shipping categories as a function of the headspace hydrogen concentration is presented in Section 5.3 of the CH-TRAMPAC. If the sites decide to implement this option, the payload container must be sampled for the container headspace concentration of hydrogen at the time of venting.

3.7.2.2.2 Option 2B — Rigid Drum Liner Headspace Gas Sampling at the Time of Venting

This option requires the sampling of payload containers for the rigid drum liner headspace concentration of hydrogen at the time of puncturing the rigid drum liner. (Rigid drum liner headspace is the region between the rigid drum liner and the next layer of confinement, usually a bag.) Bounding values for hydrogen are used to simulate the aspiration after venting. The required aspiration time for common shipping categories as a function of the rigid liner headspace hydrogen concentration is presented in Section 5.3 of the CH-TRAMPAC. If the sites decide to implement this option, the payload container must be sampled for the rigid drum liner headspace concentration of hydrogen at the time of venting.

3.7.2.3 Option 3 - Headspace Gas Sampling During Aspiration

The third option involves the sampling of payload containers for the container headspace concentration of hydrogen at least two weeks after venting. This accounts for actual hydrogen generation and release rates inside the container up to the time of sampling. Bounding values for hydrogen generation and release are then used to simulate the aspiration from the time of sampling. The required aspiration time for common shipping categories as a function of the headspace hydrogen concentration is presented in Section 5.3 of the CH-TRAMPAC. This option is similar to Option 2A except for the time of sampling the payload container. If the sites decide to implement this option, the payload container must be sampled for the headspace concentration of hydrogen at least two weeks after venting.

3.7.3 Derivation of Aspiration Times

3.7.3.1 Quantification of Aspiration Time Parameters

The purpose of this sub-section is to quantify the parameters which determine the aspiration times for each of the payload shipping categories. For common parameters, the values used are identical to those used in the calculation of decay heat limits (Appendices 2.3 and 6.7 of the CH-TRU Payload Appendices). These parameters include pressure, temperature, allowed hydrogen generation rates, and hydrogen release rates. The values of the release rates for the various confinement layers are summarized in Table 3.7-1. The release rates in the second column, expressed in units of liters/day/mole fraction, were computed using the ideal gas law.

Void Volumes for Waste Types: The total void volume for each waste type was determined by averaging the void volumes that were measured as part of the TRU Waste Sampling Program.[1] Containers that met the WAC restrictions and had a measured void volume were included in the calculations of average void volume. The aspiration model developed in this appendix is directly applicable to these waste containers.

---

[1] Clements, T.L., Jr., and D.E. Kudera, September 1985, "TRU Waste Sampling Program: Volume I, Waste Characterization," Report EGG-WM-6503," Idaho National Engineering Laboratory, Idaho Falls, Idaho.

Table 3.7-1 — Hydrogen Release Rates for Confinement Layers Used in Calculations

Confinement Layer	Release Rate (moles/sec/mole fraction)	Release Rate (liters/day/mole fraction)
Small Inner Bag[a]	5.58E-7 (Waste Type II, III) 4.17E-7 (Waste Type I)	1.163 0.869
Large Drum Liner Bag	4.67E-6	9.734
Rigid Drum Liner (intact without a puncture; this value was used in the accumulation step of the computational procedure)	1.83E-8	0.038[b]
Rigid Drum Liner (punctured; used in the aspiration step of the computational procedure)	5.09E-5	106.097
Carbon Composite Filter[a]	1.90E-6 (Waste Type II, III) 1.37E-6 (Waste Type I)	3.960 2.856

[a]   See Appendix 6.9 of the CH-TRU Payload Appendices for explanations of minimum release rates. The difference in release rates is due to the temperature at which the decay heat limit is calculated.

[b]   All values in the Table except for the release rates of an intact rigid liner without a puncture are from Appendix 6.7 of the CH-TRU Payload Appendices. The release rates for an intact rigid liner without a puncture are calculated from Kudera (Kudera, D.E., B.W. Brown, M.G. Bullock, K.S. Monti, and R.D. Sanders, Sr., September 1986, "Evaluation of the Aspiration Rate of Hydrogen from a Waste Drum," Informal Report EEG-WSM-7228, Idaho National Engineering Laboratory, Idaho Falls, Idaho).

A portion of the total void volume (28 liters) was assigned to the annular space (volume between drum and rigid liner) void volume[2]. This is based on actual measurement of the drum and liner dimensions. The remaining void volume was distributed proportionately to other layers of confinement based on the input values supplied to the PERM model, also developed as part of a study to determine aspiration rates at INEL.[2] The total void volume and the distribution of this volume among the different layers of confinement are summarized below.

Waste Type I. Solidified aqueous or homogeneous inorganic solids

> Annular void   = 28.0 liters
> Rigid liner void   = 26.7 liters
> Multiple bag void   = 34.0 liters
> _____
> Total void volume   = 88.7 liters

Waste Type II. Solid inorganic materials

> Annular void   = 28.0 liters
> Rigid liner void   = 13.9 liters
> Multiple bag void   = 125.1 liters
> _____
> Total void volume   = 167.0 liters

Waste Type III. Solid organic materials (including some absorbed liquids and cemented solid organics)

> Annular void   = 28.0 liters
> Rigid liner void   = 20.4 liters
> Multiple bag void   = 107.0 liters
> _____
> Total void volume   = 155.4 liters

In order to provide a conservative estimate for allocating the available void volume between the individual layers of confinement for multiple layers of bags, an effective release rate through all of the layers of bags in a drum was computed by summing the individual bag release rates in parallel, i.e.,

$$\frac{1}{Q_{eff}} = \Sigma \frac{1}{q_i}$$

where

---

[2] Kudera, D.E., B.W. Brown, M.G. Bullock, K.S. Monti, and R.D. Sanders, Sr., September 1986, "Evaluation of the Aspiration Rate of Hydrogen from a Waste Drum," Informal Report EEG-WSM-7228, Idaho National Engineering Laboratory, Idaho Falls, Idaho.

Q_{eff} = effective release rate through all layers of bags, (moles/sec/mole fraction)

q_i = release rate through layer (bag) "i," (moles/sec/mole fraction).

A sensitivity study was made to assess the change in aspiration time due to changes in the effective release rate from layers of bags. This assessment varied the distribution of the available void among the number of assumed bag confinement layers. The results indicate that the conservative approach is to assume the available void is in the innermost bag layer of confinement with outer layers (bags) having minimal void volumes. By adding all available void volume to the innermost layer, the summed release rate provides the longest aspiration time. A numerical example of this sensitivity study is provided in Table 3.7-2. Therefore, only the following three void volumes are used in the computations:

- a summed void volume inside the bags

- the void volume between the outermost bag and the rigid drum liner, and

- the annular void volume between the rigid drum liner and the drum.

Hydrogen Gas Generation Rates: The hydrogen gas generation rates used in estimating the aspiration times are as follows:

- For analytical categories, the maximum values for each payload shipping category are used

- For test categories, the measured values are used.

3.7.3.2 Mathematical Framework

The aspiration times for each option were calculated using the analytical solutions of the differential equations which describe the unsteady-state mass balances on hydrogen within each confinement volume of a payload container. As discussed in subsection 3.7.3.1, a maximum of three void volumes are used in the computations.

Two systems of differential equations have been solved for the following cases:

- a payload container with two void volumes and no bags

- a payload container with three void volumes.

Table 3.7-2 — Aspiration Times With Different Bag Void Volume Distributions

ASSUMPTIONS

1. All parameters except for the void volume distribution are the same in all cases. These were picked only for the purpose of a numerical example.

2. The total void volume for the bags is the same in all cases, and equal to 104.2 liters.

CASE 1:   Summing of bag void volumes (Approach used in model).
            Bag Void Volume = 104.2 liters
            Aspiration Time = 435 days

CASE 2:   Two bags with void volumes
            Bag 1 Void Volume = 100 liters
            Bag 2 Void Volume = 4.2 liters
            Aspiration Time   = 429 days

CASE 3:   Two bags with void volumes (Equal distribution between bags)
            Bag 1 Void Volume = 52.1 liters
            Bag 2 Void Volume = 52.1 liters
            Aspiration Time   = 370 days

CASE 4:   Three bags with void volumes
            Bag 1 Void Volume = 34.73 liters
            Bag 2 Void Volume = 34.73 liters
            Bag 3 Void Volume = 34.73 liters
            Aspiration Time   = 351 days

The assumptions that have been made in deriving the governing equations are:

- Hydrogen is an ideal gas and the ideal gas law applies

- The pressure and temperature are assumed to be one atmosphere and 21°C respectively. The assumption of isobaric conditions provides the longest aspiration times, since, with pressurization, the partial pressure of hydrogen would be greater implying faster aspiration than under isobaric conditions.

- Hydrogen is assumed to be nonreactive with any materials in the payload container.

- Hydrogen gas generation rates are not reduced by depletion of the waste matrix and thus remain constant.

- During aspiration simulations, the concentration of hydrogen outside the payload container is assumed to be zero.

The following list defines the variables that are used in equations for a payload container with two void volumes and no bags.

Nomenclature List: Payload Container With Two Voids and No Bags

Symbol	Definition
$X_1(t)$	mole fraction hydrogen within the drum liner void at time, t.
$X_2(t)$	mole fraction hydrogen within the headspace at time, t.
X_{10}	mole fraction hydrogen within the drum liner void at the time of venting.
X_{20}	mole fraction hydrogen within headspace of a drum at the time of venting.
R_1	The effective release rate of hydrogen from the rigid liner divided by the rigid liner void volume.
R_2	The effective release rate of hydrogen from the rigid liner divided by the headspace void volume.
R_3	The effective release rate of hydrogen from the container divided by the headspace void volume.
t	Time.
CG	The hydrogen gas generation rate per innermost confinement layer.

R   The gas law constant.

T   Absolute temperature.

P   Absolute pressure.

V_1 Void volume within innermost confinement layer.

For brevity in the equations a parameter G will be defined as:

$G = CG \times R \times T/(P \times V_1)$

Differential Equations for a Payload Container With Two Void Volumes and No Bags

$dX_1/dt = G - R_1(X_1 - X_2)$ (1A)

$dX_2/dt = R_2(X_1 - X_2) - R_3X_2$ (1B)

Solutions to Equations 1A and 1B For a Payload Container With Two Void Volumes and No Bags:

$X_1(t) = (R_2 + R_3)G/(P_1P_2)$
   $- \{X_{10}P_1^2-[(R_2+R_3)X_{10}+R_1X_{20}+G]P_1+(R_2+R_3)G\}/\{P_1(P_2-P_1)\}\exp(-P_1t)$

   $- \{X_{10}P_2^2-[(R_2+R_3)X_{10}+R_1X_{20}+G]P_2+(R_2+R_3)G\}/\{P_2(P_1-P_2)\}\exp(-P_2t)$

                                                                                     (2A)

$X_2(t) = GR_2/(P_1P_2)$

   $- \{X_{20}P_1^2-[R_2X_{10}+R_1X_{20}]P_1+R_2G\}/\{P_1(P_2-P_1)\}\exp(-P_1t)$

   $- \{X_{20}P_2^2-[R_2X_{10}+R_1X_{20}]P_2+R_2G\}/\{P_2(P_1-P_2)\}\exp(-P_2t)$

                                                                                     (2B)

where,

$A_1 = R_1 + R_2 + R_3$ (2C)

$P_1 = (A_1 + SQRT(A_1^2 - 4R_1R_3))/2$ (2D)

$P_2 = R_1R_3/P_1$ (2E)

Nomenclature List: Payload Container With Three Voids
Symbol   Definition

$X_1(t)$ mole fraction hydrogen within innermost void at time, t.

$X_2(t)$ mole fraction hydrogen within the rigid liner void at time, t.

$X_3(t)$ mole fraction hydrogen within the headspace at time, t.

X_{10} mole fraction hydrogen within innermost void at the time of venting.

X_{20} mole fraction hydrogen within the rigid liner void at the time of venting.

X_{30} mole fraction hydrogen within the headspace at the time of venting.

R_1 The effective release rate of hydrogen from all bags divided by the innermost void volume.

R_2 The effective release rate of hydrogen from all bags divided by the rigid liner void volume.

R_3 The effective release rate of hydrogen from the rigid liner divided by the liner void volume.

R_4 The effective release rate of hydrogen from the rigid liner divided by the headspace void volume.

R_5 The effective release rate of hydrogen from the container divided by the headspace void volume.

The other variables have been defined previously in the list for two void volumes.

Differential Equations for a Payload Container With Three Void Volumes

$$dX_1/dt = G - R_1(X_1 - X_2) \tag{3A}$$

$$dX_2/dt = R_2(X_1 - X_2) - R_3(X_2 - X_3) \tag{3B}$$

$$dX_3/dt = R_4(X_2 - X_3) - R_5X_3 \tag{3C}$$

Solutions to Equation 3A, 3B, and 3C for a Payload Container With Three Void Volumes

$$X_1(t) = \{X_{10}P_1{}^3-Z_{11}P_1{}^2+Z_{12}P_1-Z_{13}\}/\{P_1(P_2-P_1)(P_3-P_1)\}\exp(-P_1t)$$

$$+ \{X_{10}P_2{}^3-Z_{11}P_2{}^2+Z_{12}P_2-Z_{13}\}/\{P_2(P_1-P_2)(P_3-P_2)\}\exp(-P_2t)$$

$$+ \{X_{10}P_3{}^3 - Z_{11}P_3{}^2 + Z_{12}P_3 - Z_{13}\}/\{P_3(P_1 - P_3)(P_2 - P_3)\}\exp(-P_3 t)$$

$$+ Z_{13}/(P_1 P_2 P_3) \tag{4A}$$

$$X_2(t) = \{X_{20}P_1{}^3 - Z_{21}P_1{}^2 + Z_{22}P_1 - Z_{23}\}/\{P_1(P_2 - P_1)(P_3 - P_1)\}\exp(-P_1 t)$$

$$+ \{X_{20}P_2{}^3 - Z_{21}P_2{}^2 + Z_{22}P_2 - Z_{23}\}/\{P_2(P_1 - P_2)(P_3 - P_2)\}\exp(-P_2 t)$$

$$+ \{X_{20}P_3{}^3 - Z_{21}P_3{}^2 + Z_{22}P_3 - Z_{23}\}/\{P_3(P_1 - P_3)(P_2 - P_3)\}\exp(-P_3 t)$$

$$+ Z_{23}/(P_1 P_2 P_3) \tag{4B}$$

$$X_3(t) = \{X_{30}P_1{}^3 - Z_{31}P_1{}^2 + Z_{32}P_1 - Z_{33}\}/\{P_1(P_2 - P_1)(P_3 - P_1)\}\exp(-P_1 t)$$

$$+ \{X_{30}P_2{}^3 - Z_{31}P_2{}^2 + Z_{32}P_2 - Z_{33}\}/\{P_2(P_1 - P_2)(P_3 - P_2)\}\exp(-P_2 t)$$

$$+ \{X_{30}P_3{}^3 - Z_{31}P_3{}^2 + Z_{32}P_3 - Z_{33}\}/\{P_3(P_1 - P_3)(P_2 - P_3)\}\exp(-P_3 t)$$

$$+ Z_{33}/(P_1 P_2 P_3) \tag{4C}$$

where,

$$Z_{11} = (R_2 + R_3 + R_4 + R_5)X_{10} + R_1 X_{20} + G \tag{4D}$$

$$Z_{12} = (R_2 + R_3 + R_4 + R_5)G + (R_2 R_4 + R_2 R_5 + R_3 R_5)X_{10} + R_1(R_4 + R_5)X_{20} + R_1 R_3 X_{30} \tag{4E}$$

$$Z_{13} = (R_2 R_4 + R_2 R_5 + R_3 R_5)G \tag{4F}$$

$$Z_{21} = R_2 X_{10} + (R_1 + R_4 + R_5)X_{20} + R_3 X_{30} \tag{4G}$$

$$Z_{22} = R_2(R_4 + R_5)X_{10} + R_1(R_4 + R_5)X_{20} + R_1 R_3 X_{30} + R_2 G \tag{4H}$$

$$Z_{23} = R_2(R_4 + R_5)G \tag{4I}$$

$$Z_{31} = R_4 X_{20} + (R_1 + R_2 + R_3)X_{30} \tag{4J}$$

$$Z_{32} = R_2 R_4 X_{10} + R_1 R_4 X_{20} + R_1 R_3 X_{30} \tag{4K}$$

$$Z_{33} = R_2 R_4 G \tag{4L}$$

$$A_1 = R_1 + R_2 + R_3 + R_4 + R_5 \tag{4M}$$

$$A_2 = R_1(R_3 + R_4 + R_5) + R_2(R_4 + R_5) + R_3 R_5 \tag{4N}$$

$$A_3 = R_1R_3R_5 \tag{4O}$$

$$P_1 = [(A_1-A_3/C) + SQRT\{(A_1-A_3/C)^2-4C\}]/2 \tag{4P}$$

$$P_2 = C/P_1 \tag{4Q}$$

$$P_3 = A_3/(\tag{4R}$$

and C is a positive root of the cubic equation

$$C^3 - A_2C^2 + A_1A_3C - A_3^2 = 0 \tag{4S}$$

3.7.3.3 Computational Procedure

A consistent set of steps were followed in computing the aspiration time for each of the payload shipping categories for each of the three options. The steps for each option will be detailed in this subsection. An example of how aspiration times are specified for each of the three options is included in Attachment A of this appendix for shipping category 10 0040 0190 (or alpha-numeric shipping category I.3A2).

Option 1 - Aspiration Time Based On Date of Drum Closure

1.   Assuming a payload container has been closed for a time period (t_s) compute the concentration of hydrogen within each of the voids via Equations 2A, and 2B for a container with two void volumes and using Equations 4A, 4B, and 4C for a container with three void volumes.

2.   Recalculate R_i's to account for the puncturing of the rigid liner at the time of venting.

3.   Calculate the concentration, X_s, which is 1.05 times the steady-state value in the headspace. The steady state head space concentration is obtained from Equations 2B and 4C by letting time approach infinity. Hence, from Equation 2B for the case of a container with two voids the concentration (X_s) in the headspace is:

        $X_s = 1.05GR_2/(P_1P_2)$.

        From Equation 4C for a container with three voids the concentration (X_s) in the headspace is:

        $X_s = 1.05Z_{33}/(P_1P_2P_3)$

5.   Calculate the maximum concentration in the headspace (X_p) after venting. This is done by taking the derivative of Equations 2B and 4C with respect to time, setting the

derivative equal to zero and solving for time. At this time, (t_p) the concentration is thus a maximum.

6.   Calculate the maximum headspace concentration X_p corresponding to the time t_p using Equations 2B and 4C.

7.   If the maximum concentration X_p is less than X_s then there is no need to aspirate and thus the aspiration time (t_a) is zero. Otherwise, the aspiration time (t_a) is calculated using Equations 2B and 4C. The bisection method[3] is used to numerically solve for t_a in the nonlinear Equations 2B and 4C.

<u>Option 2A - Container Headspace Gas Sampling At The Time Of Venting</u>

1.   Assuming that the concentration of hydrogen in the container headspace at the time of venting is $X_2(t_s)$ for a container with two void volumes or $X_3(t_s)$ for a container with three void volumes, solve Equations 2B or 4C respectively for the storage time, $t=t_s$, which corresponds to these headspace concentrations.

2.   Compute the concentrations in the other void volumes, $X_1(t_s)$ and in $X_2(t_s)$ for three void volumes using Equations 2A or 4A and 4B at this storage time t_s. The concentrations $X_1(t_s)$, $X_2(t_s)$ and $X_3(t_s)$ are then assigned as the initial conditions X_{10}, X_{20} and X_{30} respectively in the aspiration Equations 2A and 2B and 4A, 4B and 4C.

3.   Recalculate the R_i's to account for the puncturing of the rigid liner at the time of venting.

4.   Calculate the concentration, (X_s), which is 1.05 times the steady-state value in the headspace. The steady state headspace concentration is obtained from Equations 2B and 4C by letting time approach infinity. Hence, from Equation 2B, for the case of a container with two voids the concentration (X_s) in the headspace is:

$X_s = 1.05GR_2/(P_1P_2)$.

From Equation 4C for a container with three voids the concentration (X_s) in the headspace is:

$X_s = 1.05Z_{33}/(P_1P_2P_3)$

5.   Calculate the maximum concentration in the headspace (X_p) after venting. This is done by taking the derivative of Equations 2B and 4C with respect to time, setting the derivative equal to zero and solving for time. At this time, (t_p) the concentration is thus a maximum.

---

[3] Reklaitis, G.V., A. Ravindran, and K.M. Ragsdell, 1983, "Engineering Optimization: Methods and Applications," John Wiley and Sons, New York, New York.

6.   Calculate the maximum headspace concentration X_p corresponding to the time t_p using Equations 2B and 4C.

7.   If the maximum concentration X_p is less than X_s then there is no need to aspirate and thus the aspiration time (t_a) is zero. Otherwise, the aspiration time (t_a) is calculated using Equations 2B and 4C. The bisection method[3] is used to numerically solve for t_a in the nonlinear Equations 2B and 4C.

Option 2B - Rigid Drum Liner Headspace Gas Sampling At The Time Of Venting

1.   Assuming that the concentration of hydrogen in the rigid liner headspace at the time of venting is $X_1(t_s)$ for a container with two void volumes or $X_2(t_s)$ for a container with three void volumes, solve Equations 2A or 4B respectively for the storage time, $t=t_s$, which corresponds to these headspace concentrations.

2.   Compute the concentrations in the other void volumes, $X_1(t_s)$ using Equations 2B for the case of two void volumes or $X_1(t_s)$ and $X_3(t_s)$ using Equations 4A and 4C for the case of three void volumes at this storage time t_s. The concentrations $X_1(t_s)$, $X_2(t_s)$ and $X_3(t_s)$ are then assigned as the initial conditions X_{10}, X_{20} and X_{30} respectively in the aspiration Equations 2A and 2B and 4A, 4B and 4C.

3.   Recalculate the R_i's to account for the puncturing of the rigid liner at the time of venting.

4.   Calculate the concentration, (X_s), which is 1.05 times the steady-state value in the headspace. The steady state headspace concentration is obtained from Equations 2B and 4C by letting time approach infinity. Hence, from Equation 2B, for the case of a container with two voids the concentration (X_s) in the headspace is:

$X_s = 1.05GR_2/(P_1P_2)$.

From Equation 4C for a container with three voids the concentration (X_s) in the headspace is:

$X_s = 1.05Z_{33}/(P_1P_2P_3)$

5.   Calculate the maximum concentration in the headspace (X_p) after venting. This is done by taking the derivative of Equations 2B and 4C with respect to time, setting the derivative equal to zero and solving for time. At this time, (t_p) the concentration is thus a maximum.

6.   Calculate the maximum headspace concentration X_p corresponding to the time t_p using Equations 2B and 4C.

7.   If the maximum concentration X_p is less than X_s then there is no need to aspirate and thus the aspiration time (t_a) is zero. Otherwise, the aspiration time (t_a) is calculated using

Equations 2B and 4C. The bisection method[3] is used to numerically solve for t_a in the nonlinear Equations 2B and 4C.

Option 3 - Headspace Gas Sampling During Aspiration

1.   Assume that the concentration of hydrogen in the headspace during aspiration is $X_2(t_p)$ for a container with two void volumes or $X_3(t_p)$ for a container with three void volumes. In order to determine the longest aspiration time, this concentration will be equivalent to the maximum concentration in the headspace after venting.

2.   The concentrations X_{10}, X_{20}, and X_{30} at the time of venting are not known and must be evaluated in order to calculate the aspiration time. The steps involved in this evaluation are:

   2A.   For an assumed storage time t_s prior to venting compute the concentrations in all void volumes, $X_1(t_s)$, $X_2(t_s)$ and $X_3(t_s)$, using Equations 2A, and 2B or 4A, 4B, and 4C.

   2B.   Assign concentrations $X_1(t_s)$, $X_2(t_s)$ and $X_3(t_s)$ as the initial conditions X_{10}, X_{20} and X_{30} respectively, in the container, at the time of venting.

   2C.   Recalculate the R_i's to account for the puncturing of the drum liner at the time of venting.

   2D.   Calculate the maximum concentration in the headspace (X_m) after venting. This is done by taking the derivative of Equation 2B or 4C with respect to time, setting the derivative equal to zero and solving for this time, (t_m) and evaluating X_m using Equation 2B or 4C. At this time (t_m) the concentration is thus a maximum.

   2E.   Compare the concentration X_m with $X_2(t_p)$ or with $X_3(t_p)$ and modify the storage time t_s accordingly using the bisection method[3.]

   2F.   Repeat steps 2A through 2E until the storage time, t_s is evaluated to an accuracy of at least 1/100 of a day.

3.   Calculate the concentration (X_s) which is 1.05 times the steady-state value in the headspace. The steady state headspace concentration is obtained from Equations 2B and 4C by letting time approach infinity. Hence, from Equation 2B, for the case of a container with two voids the concentration (X_s) in the headspace is:

$X_s = 1.05GR_2/(P_1P_2)$.

From Equation 4C for a container with three voids the concentration (X_s) in the headspace is:

$$X_s = 1.05Z_{33}/(P_1P_2P_3)$$

4.   The aspiration time, (t_a) is calculated using Equations 2B and 4C. The bisection method[3] is used to numerically solve for t_a in the nonlinear Equations 2B and 4C.

The aspiration times for Options 1 and 2 have been calculated up to a maximum concentration of 40 mole percent hydrogen in the container headspace, even though a majority of the stored waste containers are expected to have concentrations well below this value. The highest observed hydrogen concentration in a waste drum that could qualify for transport in a package is 32.4 mole percent.[1] Data collected as part of the TRU Waste Sampling Program[1] shows that the average hydrogen concentration in the headspace of the containers was 1.5 mole percent, with a standard deviation of 2.8 mole percent. These numbers include payload containers in Waste Types I, II, and III. Hence, a 40 mole percent hydrogen concentration in the container headspace should provide a bounding case for all of the stored waste, even if the waste had been stored for lengthy periods of time.

3.7.4 Aspiration Times for Shipping Categories

Example aspiration times under each of the options for common shipping categories are presented in Section 5.3 of the CH-TRAMPAC. The tables are categorized as per the waste type (I, II and III). The aspiration times using Option 1 are a function of the storage time for the payload containers. The aspiration times using Options 2A and 2B are a function of the headspace hydrogen concentration at the time of venting. The aspiration times using Option 3 are a function of the headspace hydrogen concentration, taken at least two weeks after the payload container had been vented.

3.7.5 Drum Aspiration Procedure

The procedures that will be followed in determining the aspiration time for a payload container are specified in this section. Three acceptable methods are available to the sites for establishing the required duration of aspiration. The first requires that the date of closure of the drum be known. The second involves sampling the headspace hydrogen concentration at the time of drum liner puncturing and installation of a filter vent. The third is based on sampling the headspace at least two weeks after the initiation of the payload container aspiration. A step-by-step procedure for the three options is presented in Section 5.3 of the CH-TRAMPAC.

Attachment A

This attachment provides a specific example for each of the three options in determining the aspiration times for the shipping category 10 0040 0190 (or I.3A2). As described in earlier sections of the Appendix, the mathematical basis for the three options is the same. The independent variable (with the aspiration time being the dependent variable) in the three options is different - the age of the waste in Option 1, the headspace hydrogen concentration at the time of venting in Option 2, and the headspace hydrogen concentration at the time of sampling (at least two weeks after venting) in Option 3.

Figure 3.7-1 is a plot of the hydrogen concentration in the different confinement layers in a payload container as a function of time. The container is a drum with two bag layers and a rigid drum liner. As mentioned in Section 3.7.3.1, the void volume in the layers of bags is combined into one single void volume; hence only three concentration profiles (labeled the inner bag, drum liner, and headspace) are shown in Figure 3.7-1. The figure is plotted from the program by calculating the hydrogen concentrations in the void volumes at different time steps.

From time t=0 to time t=t1 in Figure 3.7-1, the container is closed and hydrogen accumulates in the different layers as shown. The container is vented at time t1, with the drum liner punctured and the drum fitted with a filter vent or equivalent venting mechanism. The sharp increase in the headspace hydrogen concentration at this point is due to equilibration of the gases between the drum headspace and the void volume in the liner. The drum starts to aspirate at time t1, and approaches the steady state concentration in all layers at time t3. The drum can be part of a payload after time t3 and will comply with the 5% limit on the hydrogen concentration at the end of the 60-day shipping period.

The method of arriving at the aspiration times under each of the three options is described below for the case of this payload container.

<u>Aspiration Time from Option 1</u>: Under Option 1, the aspiration time is determined from the storage time of the waste, indicated as time t1 on Figure 3.7-1.

The aspiration time required is (t3 - t1). The aspiration times for different storage periods are derived similarly. These are the values reported for common shipping categories in Section 5.3 the CH-TRAMPAC. In the table, storage time of the waste (age) is read from the first column, rounded up to the next highest month.

<u>Aspiration Time from Option 2</u>: Under Option 2, the aspiration time is determined from the container (Option 2A) or rigid liner (Option 2B) headspace hydrogen concentration at the time of venting. In this example, the measured hydrogen concentration for a drum stored for t1 days is approximately 3% in the container headspace (Option 2A) or approximately 20% in the rigid liner headspace (Option 2B). The aspiration time for this headspace concentration is again (t3 - t1). The aspiration times for different headspace concentrations can be derived similarly. These are the values reported for common shipping categories in Section 5.3 of the CH-TRAMPAC.
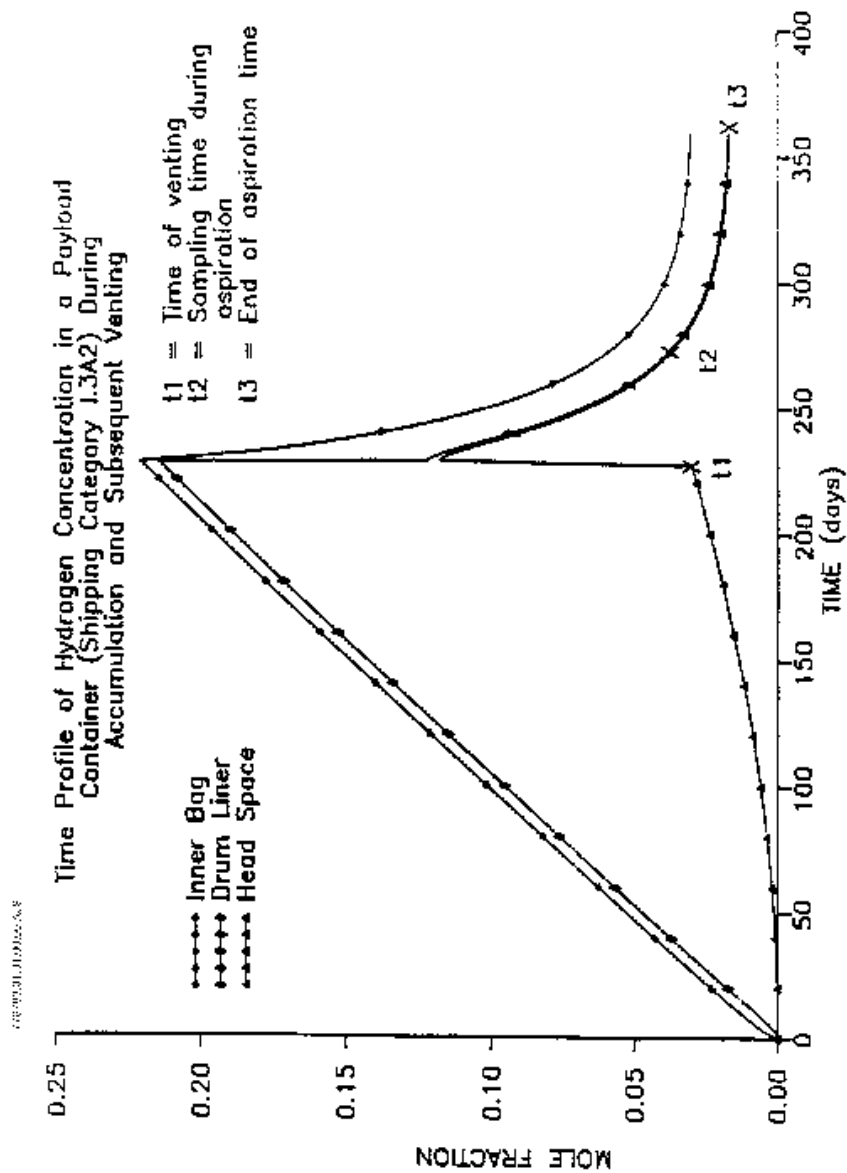
Figure 3.7-1—Time Profile of Hydrogen Concentration in a Payload Container (Shipping Category 1.3A2) During Accumulation and Subsequent Venting

3.7-18

Aspiration Time from Option 3: From Option 3, the aspiration time is determined from the headspace hydrogen concentration, measured at least two weeks from the time of venting. For this example (Figure 3.7-1), the measured headspace hydrogen concentration is 3.8% after aspiring for a time of (t2 - t1). The additional aspiration time required is (t3 - t2). The aspiration times for different samples of the headspace concentration can be derived similarly. These are the numbers reported for common shipping categories in Section 5.3 of the CH-TRAMPAC.

In summary, three options have been presented for the DOE sites to determine the required aspiration time for a given unvented payload container. The procedures to be followed by the sites in determining these aspiration times are completely mechanical as outlined in Section 5.3 of the CH-TRAMPAC. The aspiration times determined using Options 1, 2, and 3 are summarized in tables contained in Section 5.3 of the CH-TRAMPAC for common shipping categories.

This page intentionally left blank.

APPENDIX 3.8

SPECIFICATION FOR CLOSURE OF INNER CONFINEMENT LAYERS

This page intentionally left blank.

3.8   Specification for Closure of Inner Confinement Layers

For the payload of CH-TRU waste, a confinement layer is defined as follows:

>   A confinement layer is any boundary that restricts, but does not prohibit, the
>   release of hydrogen gas across the boundary.

Examples of confinement layers are plastic bags (smaller inner bags or larger container liner
bags) with the allowable closure methods described below and metal containers fitted with filter
vents. Note: Punctured plastic bags, liner bags open at the end, pieces of plastic sheeting
wrapped around the waste for handling, and metal containers with lid closures that allow free
hydrogen release are <u>not</u> considered as confinement layers.

Drum liner bags shall be made of materials belonging to the class of polyethylene (PE) or
polyvinyl chloride (PVC) with a nominal thickness between 5 - 15 mils and having a surface area
of at least 1.6 m^2. (This area is equal to that of a rigid drum liner – therefore, any bag larger in
size than the drum liner will meet this specification.) SWB liner bags shall be made of materials
belonging to the class of PE or PVC, unless another material is shown to be equivalent by testing
or analysis.

The only allowable methods of closure for plastic bags used for waste confinement are the
following:

- Twist and tape closure
- Fold and tape closure
- Heat-seal closure or twist and tape closure with a minimum of one filter vent
- Unvented heat-seal closure for a bag with a minimum surface area of approximately
  390 square inches. For example, a tube of plastic that is heat-sealed on both ends,
  with nominal dimensions of 14 inches by 14 inches when flattened, would have a
  surface area of 14 x 14 x 2 = 392 square inches. Larger bags are allowed, as the
  surface area for gas release is greater.

When the method of closure is twist and tape, the waste bag that is ready to be closed should be
twisted at the end and then taped tightly. The twisted portion of the bag that is taped should
generally have a length of six inches; however, procedures for twist and tape may be site
specific. Site-specific health and safety procedures shall govern the precautions to be taken by
the operators. Supplemental sealing devices such as clamps or heat sealing shall not be used
unless the hydrogen release has been quantified and is greater than or equal to that of the twist
and tape bag closure (see Appendices 6.7 and 6.13 of the CH-TRU Payload Appendices).
Quantification of hydrogen release can either be by testing or analysis.

The fold and tape procedure is applicable but not restricted to bags used in the SWB for which
twisting the top end is not practical.

Vented heat-sealed bags may be used to address site health and safety issues in specific configurations when the other closure methods may be difficult (see Section 2.5 of the CH-TRAMPAC). Appendix 3.11 of the CH-TRU Payload Appendices defines the authorized use of heat-sealed filtered bags. Unvented heat-sealed bags may be used provided they meet the requirements of this appendix.

Plastic bags that are closed by the twist and tape or fold and tape methods may also be vented for site-specific purposes.

Any other type of confinement layer (other than the types of plastic bags or metal or other rigid containers described) used at the sites shall be shown, by testing or analysis, to be equivalent to one of the allowable confinement layers for purposes of minimum hydrogen release. "Equivalency" shall be established by demonstration of a hydrogen release rate greater than or equal to the approved confinement layers.

APPENDIX 3.9

**DETERMINATION OF STEADY-STATE VOC CONCENTRATIONS
FROM DACs**

This page intentionally left blank.

3.9 Determination of Steady-State VOC Concentrations from DACs

3.9.1 Introduction

If a concentration of flammable volatile organic compounds (VOCs) in the payload container headspace of less than or equal to 500 parts per million (ppm) cannot be established based on waste generation procedures or records of process knowledge, headspace gas sampling for flammable VOCs is required. Prior to performing headspace sampling, drum age criteria (DACs) need to be met for headspace samples to be valid. DACs are estimates of time required for VOCs in a payload container to reach 90 percent of the equilibrium steady-state concentration within the different layers of confinement. Alternately, the headspace sample taken before the DAC has been met can be used to determine the 90 percent steady-state concentration in a waste container. The 90 percent steady-state concentration can then be correlated to the VOC concentration in the innermost layer of confinement by the use of prediction factors (PFs), which are multipliers to be applied to the headspace concentration. The methodology used for determining the steady-state (90%) VOC concentration from DACs (or measurement) and PFs is based on Liekhus et al., October 2000.[1] Three options are available:

Option 1   **No DACs Required.** If the concentration of flammable VOCs in a payload container can be shown to be less than or equal to 500 ppm from the waste generation procedures or records of process knowledge, then no DACs or PFs are required. Option 1 is discussed in Section 3.9.2.1.

Option 2   **Assignment of DACs for Common Packaging Configurations.** DACs for common representative packaging configurations used for contact-handled transuranic (CH-TRU) waste at the sites are presented in look-up tables. Under Option 2, there are three container venting and sampling scenarios. Option 2 and the associated scenarios and look-up tables are discussed in detail in Section 3.9.2.2.

Option 3   **Calculation of Steady-State VOC Concentrations for Specific Packaging Configurations.** For specific packaging configurations not covered by Option 2, the steady-state VOC concentration can be determined based on sampling (measurement) using the methodology described in Liekhus et al., October 2000.[1] Option 3 is described in Section 3.9.2.3.

A list of flammable VOCs identified by the sites in CH-TRU waste is provided as Table 3.9-1. If additional flammable VOCs (i.e., not listed in Table 3.9-1) are identified in concentrations greater than 500 ppm, Section 5.2.5.3.2 of the Contact-Handled Transuranic Waste Authorized Methods for Payload Control (CH-TRAMPAC) specifies a formalized process for including these VOCs in the analysis for compliance with the flammable (gas/VOC) limits.

---

[1] Liekhus, K.J., S.M. Djordjevic, M. Devarakonda, M.J. Connolly, October 2000, "Determination of Drum Age Criteria and Prediction Factors Based on Packaging Configurations," INEEL/EXT-2000-01207, Idaho National Engineering and Environmental Laboratory, Idaho Falls, Idaho.

Table 3.9-1 — List of Flammable Volatile Organic Compounds Identified by Sites in CH-TRU Wastes[a]

Acetone
Benzene
1-Butanol
Chlorobenzene
Cyclohexane
1,1-Dichloroethane
1,2-Dichloroethane
1,1-Dichloroethene
cis-1,2-Dichloroethene
Ethyl benzene
Ethyl ether
Methanol
Methyl ethyl ketone
Methyl isobutyl ketone
Toluene
1,2,4-Trimethylbenzene
1,3,5-Trimethylbenzene
Xylenes

[a]If additional flammable VOCs are identified in concentrations greater than 500 ppm total, the methodology documented in Section 5.2.5.3.2 of the CH-TRAMPAC shall be used.

3.9.2   Options For Determining DACs

The three options for determining DACs are discussed in the following sections. Figure 3.9-1 presents a flow chart for determining the appropriate option.

3.9.2.1   Option 1: No Drum Age Criteria Required

If the concentration of flammable VOCs in a payload container can be shown to be less than or equal to 500 ppm from the waste generation procedures or records of process knowledge, then no DACs or PFs are applicable.
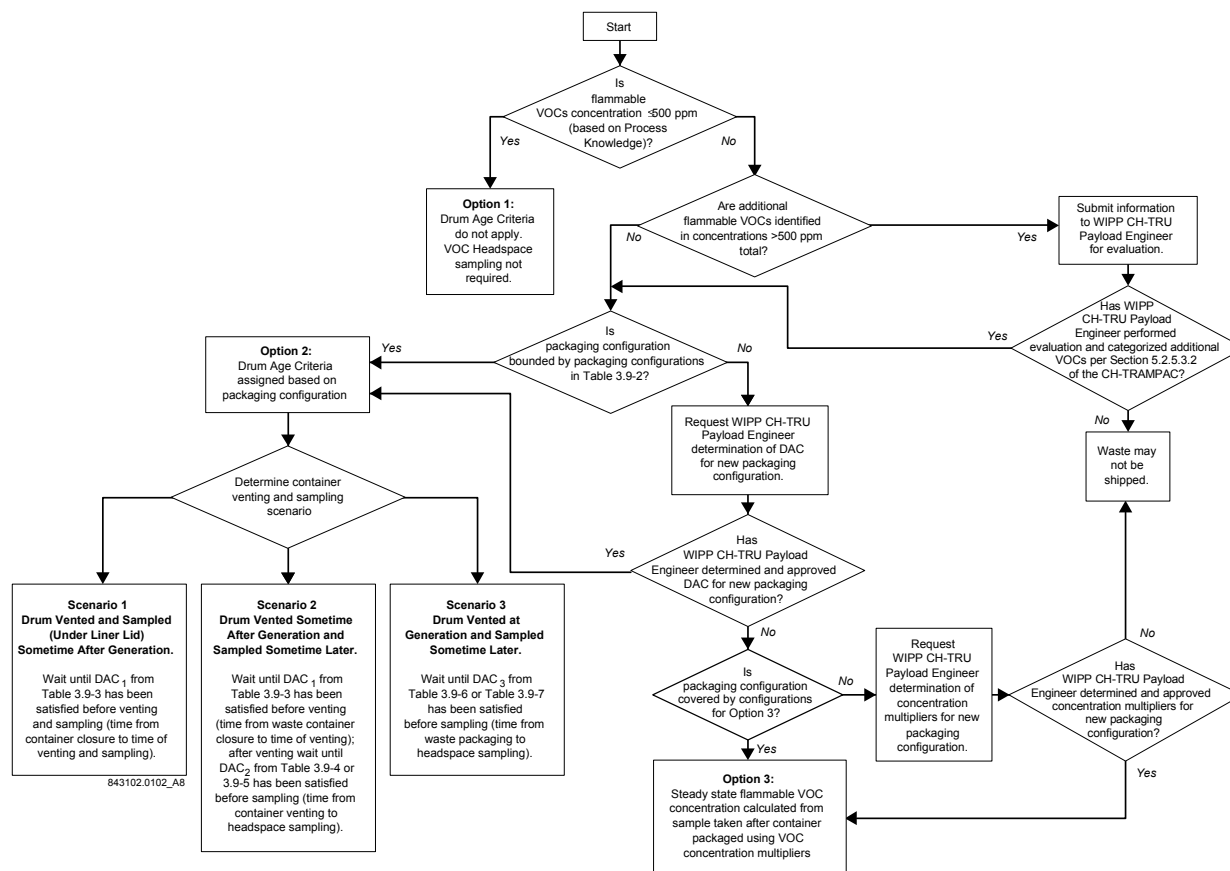
Figure 3.9-1 — Determination of DAC Option

If the concentration of flammable VOCs cannot be determined from the waste generation procedures or the records of process knowledge, headspace sampling must be performed and Option 2 or Option 3 below must be used.

3.9.2.2 Option 2: Drum Age Criteria for Common Packaging Configurations

The derivation of the DACs for Option 2 is based on specific packaging configurations and waste types commonly used at the TRU waste sites. The selection of representative packaging configurations for the DAC analysis under Option 2 was based on the following criteria:

- A review of the CH-TRU Waste Content Codes (CH-TRUCON) document[2] showing that currently, the majority of content code packaging configurations can be summarized into a set of common configurations. These configurations are divided into two groups: (1) packaging configurations included in either Waste Type I or Waste Type IV (solidified waste) content codes, and (2) packaging configurations included in either Waste Type II or Waste Type III (solid waste) content codes.

- A projection of future waste packaging configurations expected at U.S. Department of Energy (DOE) sites based on experience to date.

- A preliminary sensitivity analysis performed to determine which factors most influence the DACs.

The sensitivity analysis shows that four factors need to be considered when calculating the DACs. These factors include:

- Presence of a rigid drum liner
- Size of the hole in the drum liner lid
- Payload container filter diffusivity
- Number of plastic bags.

Other characteristics of packaging configurations were determined to have little or no impact on the DACs (e.g., filters on the plastic bags). For this reason, only the above-mentioned factors are considered in calculating DACs for the common waste packaging configurations.[1]

A computer program was used to calculate the DAC values for some of these common packaging configurations. The computer program is based on a VOC transport model that estimates the transient VOC gas-phase concentration throughout a waste container. The model consists of a series of material balance equations describing the transient VOC transport with

---

[2] U.S. Department of Energy (DOE), "CH-TRU Waste Content Codes (CH-TRUCON)," current revision, DOE/WIPP 01-3194, U.S. Department of Energy, Carlsbad Field Office, Carlsbad, New Mexico.

respect to a given layer of confinement. The governing equations for the model are presented in Liekhus et al., October 2000[1], and Connolly et al., June 1998[3].

Considering only the number of layers of confinement, the common packaging configurations currently described in the CH-TRUCON document[2] can be bound by the packaging configurations presented in Table 3.9-2.

Table 3.9-2 — Common CH-TRU Waste Packaging Configurations

Packaging Configuration	Waste Types II and III	Waste Types I and IV
Packaging Configuration 1 (55-gallon drums)	No inner bags, no liner bags	
Packaging Configuration 2 (55-gallon drums)	Up to 4 bag layers, up to 1 of which is a liner bag	Any configuration with 1 liner bag
Packaging Configuration 3 (55-gallon drums)	Up to 6 bag layers, up to 2 of which are liner bags	Any configuration with 2 liner bags
Packaging Configuration 4 (pipe components)	Up to 2 inner bags and 1 filtered metal can inside a pipe component (headspace sample taken inside the pipe component)	
Packaging Configuration 5 (SWBs or TDOPs)	SWB or TDOP with up to 1 bag layer (inner or liner)	
Packaging Configuration 6 (SWBs or TDOPs)	SWB or TDOP with up to 6 bag layers, up to 1 of which is a liner bag	
Packaging Configuration 7 (85- and 100-gallon drums)	85-gallon or 100-gallon drum with filtered inner lid (no inner or liner bags and no rigid liners)	

For example, a packaging configuration consisting of a single plastic bag in a 55-gallon drum for Waste Type II or III could be conservatively placed into Configuration 2 (i.e., the DAC for a packaging configuration consisting of 1 inner bag would be less than or equal to that for 3 inner bags and 1 liner bag). Similarly, a configuration of 2 inner bags and 2 liner bags in a 55-gallon drum for these waste types would be assigned to Configuration 3. In addition, filtered bag layers are also conservatively assigned to the configurations in Table 3.9-2. For example, a configuration of Waste Type II with 3 filtered inner bags and 1 filtered liner bag in a 55-gallon drum is bounded by Packaging Configuration 2. For Waste Types I and IV in 55-gallon drums, one or two liner bags are the configurations most commonly used. The DAC analysis conservatively assumes for solidified wastes that only the top of the liner bag is available for VOC transport. The presence of inner bags makes the entire liner bag area available and hence the DACs are bound by the configurations in Table 3.9-2.[1]

Any site requiring the transportation of TRU waste in the TRUPACT-II or HalfPACT that cannot be covered under a packaging configuration included in Table 5.2-3 must request the

[3] Connolly, M.J., S.M. Djordjevic, K.J. Liekhus, C.A. Loehr, L.R. Spangler, June 1998, "Position for Determining Gas Phase Volatile Organic Compound Concentrations in Transuranic Waste Containers," INEEL-95/0109, Rev. 2, Idaho National Engineering and Environmental Laboratory, Idaho Falls, Idaho.

determination of an appropriate DAC by submitting a request in writing to the WIPP CH-TRU Payload Engineer.

The WIPP CH-TRU Payload Engineer shall assign a conservative DAC for a packaging configuration not covered under Table 5.2-3 using the governing equations and methodology.[1,3] Compliance with all other transportation requirements of the CH-TRAMPAC document shall also be demonstrated. The WIPP CH-TRU Payload Engineer does not have the authority to change the transportation requirements for the TRUPACT-II or the HalfPACT as specified in the CH-TRAMPAC document without approval from the NRC. Section 1.5 of the CH-TRAMPAC describes the process for WIPP CH-TRU Payload Engineer approval of packaging configurations as part of the TRUCON code approval process.

DACs are defined for three unique venting and sampling scenarios (Figure 3.9-1). These drum venting and sampling scenarios are defined by the time elapsed after container closure and venting, as follows:

t_1 =   time (days) elapsed after container closure until venting

t_2 =   time (days) elapsed after venting.

Scenario 1: The drum liner headspace (under liner lid) can be sampled at the time of venting if t_1 is greater than DAC_1. The drum age criterion DAC_1 is defined as the time for a representative VOC to reach a concentration of at least 90% of its equilibrium concentration before drum venting. Table 3.9-3 presents the DAC_1 values.

Table 3.9-3 — DAC_1 Values (in Days)

Waste Type	DAC_1 (days)
Waste Types I and IV	127
Waste Types II and III	53

Scenario 2: For drums generated in an unvented condition and subsequently vented, the drum headspace can be sampled in a vented drum if t_1 is greater than DAC_1 and t_2 is greater than DAC_2.

The drum age criterion DAC_2 is defined as the time for a representative VOC to reach a headspace concentration of at least 90% of its steady-state concentration after venting a waste drum that was unvented for at least DAC_1. DAC_2 values are calculated for the two categories of waste types under Scenario 1 with four different opening sizes in the punctured drum liner lid and three different drum filter diffusivities.

In other words, under this scenario, if the drum has remained in an unvented condition for a period of at least 53 days for Waste Types II and III and 127 days for Waste Types I and IV, equilibration of VOCs is complete inside the drum. When the drum is subsequently vented, a time period for the appropriate DAC_2 listed in Table 3.9-4 or 3.9-5 is needed before sampling to ensure reequilibration between the liner and the drum headspace.

Table 3.9-4 — Packaging-Specific DAC$_2$ Values (in Days) for Solidified Waste (Waste Types I and IV)

Drum Filter Minimum Hydrogen Diffusivity (m/s/mf)	Liner Lid Opening			
	0.3-inch Diameter Hole	0.375-inch Diameter Hole	0.75-inch Diameter Hole	1-inch Diameter Hole
1.9×10^{-6}	36	30	23	22
3.7×10^{-6}	30	25	19	18
3.7×10^{-5}	13	11	11	11

m/s/mf = mole per second per mole fraction.

Table 3.9-5 — Packaging-Specific DAC$_2$ Values (in Days) for Solid Waste (Waste Types II and III)

Drum Filter Minimum Hydrogen Diffusivity (m/s/mf)	Liner Lid Opening			
	0.3-inch Diameter Hole	0.375-inch Diameter Hole	0.75-inch Diameter Hole	1-inch Diameter Hole
1.9×10^{-6}	29	22	13	12
3.7×10^{-6}	25	20	12	11
3.7×10^{-5}	7	6	6	4

m/s/mf = mole per second per mole fraction.

Scenario 3: If t_1 is less than DAC$_1$ when the container is vented, the container headspace can be sampled when t_2 is greater than DAC$_3$. Also, for newly generated payload containers that were vented at the time of generation, the container headspace can be sampled after DAC$_3$ has been exceeded.

The drum age criterion DAC$_3$ is defined as the time for a representative VOC to reach a headspace concentration of at least 90% of its steady-state concentration. DAC$_3$ values are calculated for the two categories of waste types each with different packaging configurations, different opening sizes in the drum liner lid as well as the case of no rigid liner inside the drum, and different filter diffusivities. The appropriate DAC$_3$ values are listed in Tables 3.9-6 and 3.9-7.

Table 3.9-6 — Packaging-Specific DAC$_3$ Values (in Days) for Solidified Waste (Waste Types I and IV)

Packaging Configuration 1						
Drum Filter Minimum Hydrogen Diffusivity (m/s/mf)	Liner Lid Opening				No Lid	No Liner
	0.3-inch Diameter Hole	0.375-inch Diameter Hole	0.75-inch Diameter Hole	1-inch Diameter Hole		
1.9×10^{-6}	131	95	37	24	4	4
3.7×10^{-6}	111	85	36	24	4	4
3.7×10^{-5}	28	28	23	19	4	4

Packaging Configuration 2						
Drum Filter Minimum Hydrogen Diffusivity (m/s/mf)	Liner Lid Opening				No Lid	No Liner
	0.3-inch Diameter Hole	0.375-inch Diameter Hole	0.75-inch Diameter Hole	1-inch Diameter Hole		
1.9×10^{-6}	213	175	108	92	56	18
3.7×10^{-6}	188	161	105	90	56	17
3.7×10^{-5}	80	80	75	71	49	10

Packaging Configuration 3						
Drum Filter Minimum Hydrogen Diffusivity (m/s/mf)	Liner Lid Opening				No Lid	No Liner
	0.3-inch Diameter Hole	0.375-inch Diameter Hole	0.75-inch Diameter Hole	1-inch Diameter Hole		
1.9×10^{-6}	283	243	171	154	107	34
3.7×10^{-6}	253	225	166	151	106	31
3.7×10^{-5}	121	121	115	110	84	13

Packaging Configuration 4	
Pipe Component Filter Minimum Hydrogen Diffusivity (m/s/mf)	Headspace Sample Taken Inside Pipe Component
1.9×10^{-6}	152

Table 3.9-6 — Packaging-Specific DAC$_3$ Values (in Days) for Solidified Waste (Waste Types I and IV) (Continued)

Packaging Configuration 5	
Minimum Total Filter Diffusivity (m/s/mf)	Headspace Sample Taken Inside Direct Load SWB/TDOP
7.4 x 10^{-6} (SWB)	15
3.33 x 10^{-5} (TDOP)	15

Packaging Configuration 6	
Minimum Total Filter Diffusivity (m/s/mf)	Headspace Sample Taken Inside Direct Load SWB/TDOP
7.4 x 10^{-6} (SWB)	56
3.33 x 10^{-5} (TDOP)	56

Packaging Configuration 7[a]			
Drum Filter Minimum Hydrogen Diffusivity (m/s/mf)	Inner Lid Filter Vent Minimum Hydrogen Diffusivity (m/s/mf)		
	7.4 x 10^{-6}	1.85 x 10^{-5}	9.25 x 10^{-5}
3.7 x 10^{-6}	13	7	2
7.4 x 10^{-6}	10	6	2
1.85 x 10^{-5}	6	4	2

[a]Headspace sample taken between inner and outer drum lids. If headspace sample is taken inside the filtered inner drum lid prior to placement of the outer drum lid, then a DAC$_3$ value of 2 days may be used.
m/s/mf = mole per second per mole fraction.

Table 3.9-7 — Packaging-Specific DAC$_3$ Values (in Days) for Solid Waste (Waste Types II and III)

Packaging Configuration 1						
Drum Filter Minimum Hydrogen Diffusivity (m/s/mf)	Liner Lid Opening				No Lid	No Liner
	0.3-inch Diameter Hole	0.375-inch Diameter Hole	0.75-inch Diameter Hole	1-inch Diameter Hole		
1.9×10^{-6}	131	95	37	24	4	4
3.7×10^{-6}	111	85	36	24	4	4
3.7×10^{-5}	28	28	23	19	4	4

Packaging Configuration 2						
Drum Filter Minimum Hydrogen Diffusivity (m/s/mf)	Liner Lid Opening				No Lid	No Liner
	0.3-inch Diameter Hole	0.375-inch Diameter Hole	0.75-inch Diameter Hole	1-inch Diameter Hole		
1.9×10^{-6}	175	138	75	60	30	11
3.7×10^{-6}	152	126	73	59	30	11
3.7×10^{-5}	58	57	52	47	28	8

Packaging Configuration 3						
Drum Filter Minimum Hydrogen Diffusivity (m/s/mf)	Liner Lid Opening				No Lid	No Liner
	0.3-inch Diameter Hole	0.375-inch Diameter Hole	0.75-inch Diameter Hole	1-inch Diameter Hole		
1.9×10^{-6}	199	161	96	80	46	16
3.7×10^{-6}	175	148[a]	93	79	46	16
3.7×10^{-5}	72	72	67	62	42	10

Packaging Configuration 4	
Pipe Component Filter Minimum Hydrogen Diffusivity (m/s/mf)	Headspace Sample Taken Inside Pipe Component
1.9×10^{-6}	152

Table 3.9-7 — Packaging-Specific DAC$_3$ Values (in Days) for Solid Waste (Waste Types II and III) (Continued)

Packaging Configuration 5	
Minimum Total Filter Diffusivity (m/s/mf)	**Headspace Sample Taken Inside Direct Load SWB/TDOP**
7.4×10^{-6} (SWB)	15
3.33×10^{-5} (TDOP)	15

Packaging Configuration 6	
Minimum Total Filter Diffusivity (m/s/mf)	**Headspace Sample Taken Inside Direct Load SWB/TDOP**
7.4×10^{-6} (SWB)	56
3.33×10^{-5} (TDOP)	56

Packaging Configuration 7[b]			
Drum Filter Minimum Hydrogen Diffusivity (m/s/mf)	**Inner Lid Filter Vent Minimum Hydrogen Diffusivity (m/s/mf)**		
	7.4×10^{-6}	**1.85×10^{-5}**	**9.25×10^{-5}**
3.7×10^{-6}	13	7	2
7.4×10^{-6}	10	6	2
1.85×10^{-5}	6	4	2

[a]DAC of 142 days is applicable provided that the packaging configuration does not exceed 3 inner bags and 2 liner bags. This DAC value for this bounding packaging configuration has been previously used to address headspace sampling issues at the sites for disposal purposes.[1]

[b]Headspace sample taken between inner and outer drum lids. If headspace sample is taken inside the filtered inner drum lid prior to placement of the outer drum lid, then a DAC$_3$ value of 2 days may be used.

m/s/mf = mole per second per mole fraction.

Because direct load TDOPs are equipped with a greater number of filters than SWBs, the SWB packaging configurations (Packaging Configurations 5 and 6) bound the direct load TDOP packaging configurations. Packaging Configuration 6 also includes bin overpack configurations with the headspace sample taken inside the bin.

Packaging Configuration 7 describes 85- and 100-gallon drums with a vented inner lid and no additional inner layers of confinement and no rigid liners. Sampling is performed between the inner and outer lids or inside the inner lid. The DAC values for an 85- or 100-gallon drum with no additional inner layers of confinement and no rigid liners are listed in Tables 3.9-6 and 3.9-7. If a 100-gallon drum contains a compacted 55-gallon drum containing a rigid drum liner, the 55-gallon drum must meet the appropriate 55-gallon drum DAC (DAC_3), listed in Tables 3.9-6 or 3.9-7, to ensure that VOC solubility associated with the presence of the 55-gallon rigid drum liner does not impact the DAC for the 100-gallon drum.

3.9.2.3 Option 3: Calculation of Steady-State VOC Concentrations for Specific Packaging Configurations

The steady-state VOC concentration for specific packaging configurations can be conservatively calculated by sampling the container headspace after container packaging and by the use of VOC concentration multipliers.[1] A VOC concentration multiplier is defined as the ratio of 90 percent of the steady-state VOC concentration in the sampling headspace divided by the VOC headspace concentration at a given time. The VOC concentration multipliers are determined by solving the governing transport equations.[1]

Therefore, Option 3 consists of sampling the container headspace at a point in time and multiplying by the appropriate VOC concentration multiplier. Option 3 is applicable to waste packaging configurations containing metal cans and pipe overpacks, which may require long time periods to achieve steady state. Three example packaging configurations of vented metal containers inside a vented drum are utilized in Option 3 as shown in Tables 3.9-8 through 3.9-11. These cases bound other packaging configurations with an equal or lesser number of bag layers (including filtered bags) in a similar fashion as described in Option 2. Cases where filtered cans are placed inside filtered cans are described by the bounding configuration containing a filtered can and filtered pipe component. VOC concentration multipliers for specific configurations with different filter characteristics are provided in Tables 3.9-8 through 3.9-11. Similar to the process described in Section 3.9.2.2, for configurations not covered by Tables 3.9-8 through 3.9-11, the site may request that the WIPP CH-TRU Payload Engineer direct the determination of appropriate concentration multipliers using the packaging configuration information and the governing equations and methodology[1].

Table 3.9-8 – VOC Concentration Multipliers

(Filtered Inner Containers and Drum Filter Minimum Hydrogen Diffusion Characteristic = 1.9 x 10^{-6} mole/sec/mole fraction)

Volatile Organic Compound	Days	2IB-PC-DL-DF*				3IB-FC-2LB-DL-DF*				2IB-FC-PC-DL-DF*			
		75	150	300	600	75	150	300	600	75	150	300	600
Carbon Tetrachloride		5.5	2.9	1.7	1.1	7.8	3.9	2.2	1.4	14.9	5.4	2.4	1.4
Cyclohexane		6.6	2.6	1.4	1.0	11.6	4.2	1.9	1.2	10.5	3.8	1.8	1.1
Methanol		2.8	1.8	1.2	1.0	4.0	2.4	1.5	1.1	5.3	2.6	1.5	1.1
Methylene chloride (Dichloromethane)		3.2	1.8	1.2	1.0	4.5	2.5	1.5	1.1	7.5	3.1	1.6	1.1
Toluene		22.7	11.5	6.0	3.2	32.6	15.5	7.7	4.0	64.9	22.9	9.5	4.5
1,1,1-Trichloroethane		4.3	2.3	1.4	1.0	6.2	3.2	1.8	1.2	11.2	4.2	2.0	1.2
Trichloroethene		11.2	5.7	3.1	1.8	15.4	7.6	4.0	2.2	31.2	11.1	4.8	2.4
1,1,2-Trichloro-1,2,2-trifluoroethane		4.5	2.1	1.3	1.0	6.7	3.1	1.7	1.1	9.9	3.6	1.7	1.1
p-Xylene		45.1	22.8	11.7	6.1	74.4	33.2	15.7	7.8	136.9	47.6	19.2	8.8
Acetone		3.1	1.8	1.2	1.0	4.5	2.4	1.5	1.1	7.4	2.9	1.5	1.0
1-Butanol		4.8	2.6	1.6	1.1	6.7	3.5	2.0	1.3	12.7	4.8	2.2	1.3
Chloroform		3.5	2.0	1.3	1.0	5.0	2.7	1.6	1.1	8.9	3.5	1.7	1.1
1,1-Dichloroethene		3.3	1.8	1.2	1.0	4.8	2.5	1.5	1.1	7.8	3.0	1.5	1.0
Methyl ethyl ketone		4.1	2.2	1.4	1.0	5.8	3.0	1.8	1.2	10.3	3.9	1.9	1.2
Methyl isobutyl ketone		7.1	3.6	2.0	1.3	10.1	5.0	2.7	1.6	19.6	6.9	3.0	1.6
1,1,2,2-Tetrachloroethane		17.0	8.8	4.6	2.6	23.8	11.6	5.9	3.1	49.4	17.5	7.3	3.6
Tetrachloroethene		9.1	4.7	2.6	1.6	12.5	6.3	3.3	1.9	26.4	9.4	4.0	2.1
Benzene		4.2	2.3	1.4	1.0	5.9	3.1	1.8	1.2	10.7	4.1	2.0	1.2
Bromoform		20.1	10.3	5.4	3.0	28.5	13.7	6.9	3.6	57.2	20.4	8.6	4.1
Chlorobenzene		10.2	5.3	2.9	1.7	14.1	7.0	3.7	2.1	29.7	10.6	4.5	2.3
1,1-Dichloroethane		3.3	1.9	1.2	1.0	4.8	2.6	1.5	1.1	8.3	3.3	1.6	1.1
1,2-Dichloroethane		4.5	2.5	1.5	1.1	6.2	3.3	1.9	1.2	11.7	4.5	2.1	1.3
Cis-1,2-Dichloroethene		3.4	1.9	1.2	1.0	4.8	2.6	1.5	1.1	8.4	3.3	1.7	1.1
Ethyl benzene		10.8	5.4	2.9	1.7	15.1	7.4	3.9	2.2	31.5	11.0	4.6	2.3
Ethyl ether		4.1	2.0	1.2	1.0	6.1	2.9	1.6	1.1	8.4	3.2	1.6	1.1
1,3,5-Trimethylbenzene		18.1	9.0	4.7	2.6	26.1	12.4	6.2	3.3	55.9	19.0	7.6	3.6
1,2,4-Trimethylbenzene		20.6	10.3	5.3	2.9	30.0	14.1	7.0	3.7	64.3	21.8	8.7	4.1
o-Xylene		12.4	6.3	3.4	1.9	17.4	8.5	4.4	2.4	36.9	12.9	5.3	2.6
m-Xylene		10.8	5.5	2.9	1.7	15.2	7.4	3.9	2.2	31.8	11.1	4.6	2.3

*IB = Inner bag; PC = Vented pipe component; FC = Filtered can; LB = Drum liner bag; DL = Drum liner; DF = Drum filter vent.

Table 3.9-9 — VOC Concentration Multipliers

(Filtered Inner Containers Minimum Hydrogen Diffusion Characteristic = 3.7×10^{-6} mole/sec/mole fraction; Drum Filter Minimum Hydrogen Diffusion Characteristic = 1.9×10^{-6} mole/sec/mole fraction)

Volatile Organic Compound		Waste Drum Packaging Configuration											
		2IB-PC-DL-DF*				3IB-FC-2LB-DL-DF*				2IB-FC-PC-DL-DF*			
	Days	75	150	300	600	75	150	300	600	75	150	300	600
Carbon tetrachloride		4.1	2.2	1.4	1.0	6.2	3.2	1.8	1.2	8.5	3.6	1.9	1.2
Cyclohexane		5.0	2.2	1.3	1.0	11.1	4.1	1.9	1.2	7.1	2.9	1.6	1.1
Methanol		2.3	1.5	1.1	1.0	3.5	2.2	1.4	1.0	3.6	2.1	1.3	1.0
Methylene chloride (Dichloromethane)		2.4	1.5	1.1	1.0	3.6	2.0	1.3	1.0	4.6	2.2	1.3	1.0
Toluene		15.8	8.1	4.3	2.4	23.5	11.2	5.7	3.0	35.3	14.4	6.7	3.4
1,1,1-Trichloroethane		3.2	1.8	1.2	1.0	5.1	2.7	1.6	1.1	6.6	2.9	1.6	1.1
Trichloroethene		7.9	4.1	2.3	1.4	11.2	5.6	3.0	1.7	17.2	7.1	3.5	1.9
1,1,2-Trichloro-1,2,2-trifluoroethane		3.5	1.8	1.1	1.0	6.1	2.9	1.6	1.1	6.3	2.7	1.5	1.0
p-Xylene		31.1	15.8	8.2	4.3	52.7	23.5	11.2	5.7	72.8	29.2	13.3	6.5
Acetone		2.4	1.4	1.0	1.0	3.8	2.1	1.3	1.0	4.6	2.1	1.3	1.0
1-Butanol		3.5	2.0	1.3	1.0	5.2	2.8	1.6	1.1	7.3	3.2	1.7	1.1
Chloroform		2.6	1.6	1.1	1.0	3.9	2.2	1.4	1.0	5.3	2.4	1.4	1.0
1,1-Dichloroethene		2.5	1.5	1.0	1.0	4.1	2.2	1.4	1.0	4.8	2.2	1.3	1.0
Methyl ethyl ketone		3.1	1.7	1.2	1.0	4.8	2.5	1.5	1.1	6.1	2.7	1.5	1.1
Methyl isobutyl ketone		5.3	2.7	1.6	1.1	8.3	4.1	2.3	1.4	11.2	4.6	2.3	1.4
1,1,2,2-Tetrachloroethane		11.8	6.1	3.3	1.9	16.5	8.1	4.2	2.3	26.6	11.0	5.2	2.7
Tetrachloroethene		6.4	3.4	2.0	1.3	9.1	4.6	2.5	1.5	14.4	6.0	2.9	1.7
Benzene		3.1	1.8	1.2	1.0	4.6	2.5	1.5	1.1	6.3	2.8	1.6	1.1
Bromoform		13.8	7.2	3.8	2.2	19.6	9.5	4.9	2.6	30.9	12.8	6.0	3.1
Chlorobenzene		7.2	3.8	2.2	1.4	10.3	5.2	2.8	1.7	16.2	6.7	3.3	1.8
1,1-Dichloroethane		2.5	1.5	1.1	1.0	3.9	2.1	1.3	1.0	5.0	2.3	1.3	1.0
1,2-Dichloroethane		3.3	1.9	1.2	1.0	4.7	2.5	1.5	1.1	6.7	3.0	1.7	1.1
Cis-1,2-Dichloroethene		2.5	1.5	1.1	1.0	3.8	2.1	1.3	1.0	5.0	2.3	1.4	1.0
Ethyl benzene		7.7	4.0	2.2	1.4	11.5	5.7	3.0	1.8	17.3	7.0	3.3	1.9
Ethyl ether		3.3	1.7	1.1	1.0	5.6	2.7	1.5	1.1	5.5	2.4	1.4	1.0
1,3,5-Trimethylbenzene		12.8	6.5	3.4	2.0	19.7	9.4	4.8	2.6	30.1	11.8	5.4	2.8
1,2,4-Trimethylbenzene		14.5	7.3	3.9	2.2	22.3	10.6	5.3	2.9	34.3	13.4	6.1	3.1
o-Xylene		8.8	4.6	2.5	1.5	13.0	6.4	3.4	1.9	20.0	8.1	3.8	2.1
m-Xylene		7.7	4.0	2.2	1.4	11.6	5.7	3.0	1.8	17.4	7.0	3.4	1.9

*IB - Inner bag; PC = Vented pipe component; FC = Filtered can; LB = Drum liner bag; DL = Drum liner; DF = Drum filter vent.

Table 3.9-10 — VOC Concentration Multipliers

(Filtered Inner Containers Minimum Hydrogen Diffusion Characteristic = 1.9 x 10^-6 mole/sec/mole fraction; Drum Filter Minimum Hydrogen Diffusion Characteristic = 3.7 x 10^-6 mole/sec/mole fraction)

| Volatile Organic Compound | Waste Drum Packaging Configuration | | | | | | | | | | | |
| | 2IB-PC-DL-DF* | | | | 3IB-FC-2LB-DL-DF* | | | | 2IB-FC-PC-DL-DF* | | | |
Days	75	150	300	600	75	150	300	600	75	150	300	600
Carbon Tetrachloride	3.9	2.1	1.3	1.0	5.3	2.8	1.6	1.1	9.3	3.5	1.7	1.1
Cyclohexane	4.3	1.9	1.1	1.0	6.9	2.6	1.4	1.0	6.4	2.5	1.3	1.0
Methanol	2.1	1.4	1.1	1.0	2.8	1.8	1.2	1.0	3.5	1.9	1.2	1.0
Methylene chloride (Dichloromethane)	2.3	1.4	1.0	1.0	3.2	1.8	1.2	1.0	4.8	2.1	1.2	1.0
Toluene	15.5	7.9	4.2	2.3	22.3	10.7	5.4	2.9	40.0	14.2	6.0	3.0
1,1,1-Trichloroethane	3.0	1.7	1.1	1.0	4.2	2.3	1.4	1.0	7.1	2.8	1.4	1.0
Trichloroethene	7.7	4.0	2.3	1.4	10.6	5.3	2.8	1.7	19.4	7.0	3.1	1.7
1,2-Trichloro-1,2,2-trifluoroethane	3.2	1.6	1.1	1.0	4.3	2.1	1.3	1.0	6.2	2.4	1.3	1.0
p-Xylene	30.7	15.6	8.0	4.3	50.7	22.7	10.9	5.5	84.1	29.4	11.9	5.6
Acetone	2.3	1.4	1.0	1.0	3.1	1.8	1.2	1.0	4.8	2.0	1.2	1.0
1-Butanol	3.4	1.9	1.2	1.0	4.7	2.5	1.5	1.1	8.0	3.1	1.6	1.1
Chloroform	2.5	1.5	1.1	1.0	3.5	2.0	1.3	1.0	5.7	2.4	1.3	1.0
1,1-Dichloroethene	2.3	1.4	1.0	1.0	3.3	1.8	1.2	1.0	5.0	2.1	1.2	1.0
Methyl ethyl ketone	2.9	1.6	1.1	1.0	4.0	2.2	1.4	1.0	6.5	2.6	1.4	1.0
Methyl isobutyl ketone	4.9	2.6	1.5	1.1	6.8	3.4	1.9	1.2	12.2	4.4	2.0	1.2
1,1,2,2-Tetrachloroethane	11.7	6.1	3.3	1.9	16.5	8.1	4.2	2.3	30.6	11.0	4.7	2.4
Tetrachloroethene	6.3	3.4	1.9	1.3	8.6	4.4	2.4	1.5	16.4	6.0	2.7	1.5
Benzene	3.0	1.7	1.2	1.0	4.1	2.2	1.4	1.0	6.8	2.7	1.4	1.0
Bromoform	13.8	7.2	3.8	2.2	19.7	9.6	4.9	2.7	35.4	12.7	5.4	2.7
Chlorobenzene	7.1	3.7	2.1	1.3	9.7	4.9	2.7	1.6	18.4	6.7	3.0	1.6
1,1-Dichloroethane	2.4	1.4	1.0	1.0	3.3	1.9	1.2	1.0	5.4	2.2	1.2	1.0
1,2-Dichloroethane	3.2	1.8	1.2	1.0	4.4	2.4	1.5	1.1	7.4	3.0	1.5	1.0
Cis-1,2-Dichloroethene	2.4	1.5	1.1	1.0	3.4	1.9	1.2	1.0	5.4	2.3	1.3	1.0
Ethyl benzene	7.4	3.8	2.1	1.4	10.3	5.1	2.7	1.6	19.5	6.9	3.0	1.6
Ethyl ether	2.9	1.5	1.0	1.0	3.9	2.0	1.2	1.0	5.3	2.2	1.2	1.0
1,3,5-Trimethylbenzene	12.4	6.2	3.3	1.9	17.7	8.4	4.3	2.4	34.4	11.8	4.8	2.4
1,2,4-Trimethylbenzene	14.1	7.1	3.7	2.1	20.3	9.7	4.9	2.7	39.6	13.6	5.5	2.7
o-Xylene	8.5	4.4	2.4	1.5	11.9	5.9	3.1	1.8	22.8	8.1	3.5	1.8
m-Xylene	7.4	3.8	2.2	1.4	10.3	5.1	2.8	1.6	19.7	7.0	3.0	1.6

*IB = Inner bag; PC = Vented pipe component; FC = Filtered can; LB = Drum liner bag; DL = Drum liner; DF = Drum filter vent.

Table 3.9-11 — VOC Concentration Multipliers

(Filtered Inner Containers and Drum Filter Minimum Hydrogen Diffusion Characteristic = 3.7 x 10^{-6} mole/sec/mole fraction)

Volatile Organic Compound	Waste Drum Packaging Configuration											
	2IB-PC-DL-DF*				3IB-FC-2LB-DL-DF*				2IB-FC-PC-DL-DF*			
Days	75	150	300	600	75	150	300	600	75	150	300	600
Carbon Tetrachloride	3.1	1.8	1.2	1.0	4.5	2.4	1.5	1.1	5.8	2.6	1.4	1.0
Cyclohexane	3.4	1.6	1.1	1.0	6.7	2.6	1.4	1.0	4.4	2.0	1.2	1.0
Methanol	1.8	1.3	1.0	1.0	2.6	1.7	1.2	1.0	2.6	1.6	1.1	1.0
Methylene chloride (Dichloromethane)	1.9	1.3	1.0	1.0	2.7	1.6	1.1	1.0	3.2	1.7	1.1	1.0
Toluene	12.0	6.2	3.3	1.9	17.6	8.5	4.4	2.4	23.9	9.8	4.7	2.5
1,1,1-Trichloroethane	2.5	1.5	1.0	1.0	3.7	2.0	1.3	1.0	4.6	2.1	1.2	1.0
Trichloroethene	6.0	3.2	1.9	1.2	8.5	4.3	2.4	1.4	11.7	5.0	2.5	1.5
1,1,2-Trichloro-1,2,2-trifluoroethane	2.6	1.4	1.0	1.0	4.1	2.0	1.2	1.0	4.2	1.9	1.2	1.0
p-Xylene	23.6	12.0	6.3	3.4	39.6	17.8	8.6	4.4	49.1	19.8	9.1	4.5
Acetone	1.9	1.2	1.0	1.0	2.8	1.6	1.1	1.0	3.2	1.6	1.1	1.0
1-Butanol	2.8	1.6	1.1	1.0	3.9	2.2	1.4	1.0	5.1	2.3	1.4	1.0
Chloroform	2.1	1.3	1.0	1.0	3.0	1.7	1.2	1.0	3.7	1.8	1.1	1.0
1,1-Dichloroethene	2.0	1.2	1.0	1.0	2.9	1.7	1.1	1.0	3.3	1.6	1.1	1.0
Methyl ethyl ketone	2.4	1.4	1.0	1.0	3.5	1.9	1.3	1.0	4.2	2.0	1.2	1.0
Methyl isobutyl ketone	4.0	2.1	1.3	1.0	5.9	3.0	1.7	1.2	7.6	3.2	1.7	1.1
1,1,2,2-Tetrachloroethane	9.0	4.8	2.6	1.6	12.7	6.3	3.3	1.9	18.1	7.6	3.7	2.0
Tetrachloroethene	4.9	2.7	1.6	1.1	6.9	3.6	2.0	1.3	9.9	4.2	2.1	1.3
Benzene	2.4	1.5	1.1	1.0	3.5	1.9	1.3	1.0	4.4	2.1	1.2	1.0
Bromoform	10.6	5.6	3.0	1.8	15.0	7.3	3.8	2.1	21.1	8.8	4.2	2.3
Chlorobenzene	5.5	3.0	1.8	1.2	7.8	4.0	2.2	1.4	11.0	4.7	2.4	1.4
1,1-Dichloroethane	2.0	1.3	1.0	1.0	2.9	1.7	1.1	1.0	3.5	1.7	1.1	1.0
1,2-Dichloroethane	2.6	1.5	1.1	1.0	3.6	2.0	1.3	1.0	4.7	2.2	1.3	1.0
Cis-1,2-Dichloroethene	2.0	1.3	1.0	1.0	2.9	1.7	1.1	1.0	3.5	1.7	1.1	1.0
Ethyl benzene	5.9	3.1	1.8	1.2	8.5	4.3	2.3	1.4	11.7	4.8	2.4	1.4
Ethyl ether	2.4	1.3	1.0	1.0	3.7	1.9	1.2	1.0	3.7	1.7	1.1	1.0
1,3,5-Trimethylbenzene	9.7	4.9	2.7	1.6	14.5	7.0	3.6	2.0	20.2	8.0	3.8	2.0
1,2,4-Trimethylbenzene	11.0	5.6	3.0	1.8	16.5	7.9	4.0	2.2	23.1	9.2	4.3	2.3
o-Xylene	6.7	3.5	2.0	1.3	9.7	4.8	2.6	1.6	13.6	5.6	2.7	1.6
m-Xylene	5.9	3.1	1.8	1.2	8.5	4.3	2.4	1.4	11.8	4.9	2.4	1.4

*IB = Inner bag; PC = Vented pipe component; FC = Filtered can; LB = Drum liner bag; DL = Drum liner; DF = Drum filter vent.

3.9.3 Methodology for Determining Packaging-Specific PFs

This section describes the methodology used for determining the PFs for a given packaging configuration. This methodology is based on the analysis presented in Liekhus et al., October 2000,[1] and Connolly et al., June 1998.[3] The PF is a variable with a unique value for each VOC and packaging configuration that, when multiplied by the measured VOC concentration in the container headspace, determines the concentration of the VOC in the innermost confinement layer. The PFs are applicable in cases where the headspace flammable VOC concentration exceeds 500 ppm.

At steady-state conditions, there is no accumulation of VOCs within any layer of confinement, the concentrations of VOCs are constant within each layer of confinement, and the VOC transport rate across each layer of confinement is equal to a constant rate. The equations describing VOC transport across layers of confinement are presented in Liekhus et al., October 2000.[1]

The relationship for the innermost confinement layer VOC concentration as a function of the measured container headspace VOC concentration is:

$$y_{icl} = y_{hs}\left[1 + n_{cf}\,D_{voc\text{-}cf}\left(\sum_{i=1}^{nl}\frac{n_i}{K_i}\right)\right]$$

where

y_{icl} =   innermost confinement layer VOC mole fraction (dimensionless)

y_{hs} =   VOC mole fraction within container headspace void volume (dimensionless)

n_i =   number of type "i" confinement layers in packaging configuration

n_{cf} =   number of container filters in packaging configuration

K_i =   transport characteristic of type "i" confinement layer (molecule [mol] sec^{-1})

nl =   number of different confinement layer types.

$D_{voc\text{-}cf}$ =   VOC-container filter diffusion characteristic (mol sec^{-1}), which is calculated using the following equation:

$$D_{VOC\text{-}cf} = \frac{D_{VOC\text{-}air}}{D_{H_2\text{-}air}}\,D_{H_2\text{-}cf}$$

where

$D_{VOC\text{-}air}$ = VOC diffusivity in air (cubic centimeters [cm^2] sec^{-1})

$D_{H_2\text{-}air}$ = hydrogen diffusivity in air (cm^2 sec^{-1})

$D_{H_2\text{-}cf}$ = hydrogen-container filter diffusion characteristic (mol sec^{-1}).

Multiplying both sides of equation 1 by a conversion factor (10^6 ppm/mole fraction) yields the following equation for the prediction factor:

$$Y_{icl} = Y_{hs}\left[1 + n_{cf}D_{voc\text{-}cf}\left(\sum_{i=1}^{nl}\frac{n_i}{K_i}\right)\right]$$

where

Y_{icl} = innermost confinement layer VOC concentration (ppm)

Y_{hs} = measured VOC concentration in container headspace (ppm).

Thus, the prediction factor, PF, is:

$$PF = \left[1 + n_{cf}D_{voc\text{-}cf}\left(\sum_{i=1}^{nl}\frac{n_i}{K_i}\right)\right]$$

Using this equation, the PFs for any packaging configuration can be established.

PFs are not applicable if the sample is taken after the appropriate DAC has been met inside the rigid liner of an unvented drum (Scenario 1), since all layers are at the equilibrium concentration.

APPENDIX 3.10

DETERMINATION OF FLAMMABLE GAS/VOLATILE ORGANIC COMPOUND CONCENTRATIONS BY MEASUREMENT

This page intentionally left blank.

3.10 Determination of Flammable Gas/Volatile Organic Compound Concentrations by Measurement

This appendix summarizes the logic and methodology of using headspace flammable gas/volatile organic compound (VOC) measurements for evaluating compliance with flammable gas/VOC concentrations during transport in the TRUPACT-II and HalfPACT packages. As described in Chapter 5.0 of the Contact-Handled Transuranic Waste Authorized Methods for Payload Control (CH-TRAMPAC) document, headspace gas/VOC measurement is one option for the following test category wastes:

- Containers that could potentially exceed 500 parts per million (ppm) flammable VOCs in the innermost confinement layer

- Containers that exceed decay heat limits or analytically determined hydrogen gas generation rate limits.

3.10.1 Calculation of Drum Flammable Gas Generation Methods: AltMeth

This section applies when the concentration of flammable VOCs is less than 500 ppm in the innermost layer of the payload container. The methodology is based on sampling the waste container headspace or inside the rigid drum liner for flammable gases to calculate the actual drum flammable gas generation rate. The use of headspace gas sampling results is an extension of the methodology for deriving aspiration times of contact-handled transuranic (CH-TRU) waste containers as documented in Appendix 3.7 of the CH-TRU Payload Appendices.

Containers are categorized as either (a) sealed and then vented or (b) newly packaged and vented. The conceptual model is described below:

- A payload container with either two or three void volumes is filled with waste within the innermost layer of confinement (multiple bag layers are conservatively classified as a single void with an equivalent resistance). The container is either sealed or vented with one or more filters at the time of waste packaging.

- Flammable gas is generated within the waste.

- Flammable gas accumulates and is transported across layers of confinement.

- After some time, sealed containers are vented and the headspace gas or the headspace inside the rigid drum liner may be sampled for flammable gas.

- At some point during aspiration or venting, the container headspace may be sampled for flammable gases.

3.10.1.1 Mathematical Model

The generation of flammable gas within the innermost confinement layer and subsequent transport across the various confinement layers of an actual container can be simulated by solving the differential equations that describe the unsteady-state mass balances on flammable gas within each confinement layer of the actual container. To account for the various packaging configurations and container conditions, two sets of differential equations must be solved along with the appropriate initial conditions that represent the initial state of a container. The two sets represent (a) a container with two void volumes, and (b) a container with three void volumes.

3.10.1.2 Differential Equations for a Container with Two Void Volumes

Differential Equations (1) and (2) represent the mass balances on flammable gas in a container with two void volumes.

$$\frac{dC_1}{dt} = G - R_1(C_1 - C_2) \tag{1}$$

$$\frac{dC_2}{dt} = R_2(C_1 - C_2) - R_3 C_2 \tag{2}$$

where,

C_1 = Mole or volume fraction of flammable gas within the drum liner void volume at time t (dimensionless).

C_2 = Mole or volume fraction flammable gas within the drum headspace at time t (dimensionless).

G = $C_g R T / (P V_1)$.

R_1 = Effective release rate of flammable gas from the container liner divided by the innermost void volume (day^{-1}).

R_2 = Effective release rate of flammable gas from the container liner divided by the headspace void volume. One value based on the release rate from an intact liner is used in the equations for the concentration in a sealed container. A different value is used with the aspiration equations based on the release of flammable gas from the punctured rigid liner hole (day^{-1}).

R_3 = Effective release rate of flammable gas from the container divided by the headspace void volume. One value based on the permeation characteristics of the drum gasket is used to calculate the concentration in a sealed container. A different value is used based on a combination of diffusion characteristic across the drum filter and permeation characteristic across the drum gasket to calculate concentrations in an aspirating container (day^{-1}).

t   = Time(s)/day.

R   = Universal gas constant (82.057 atm cm^3/mol K).

T   = Absolute temperature (K).

V_1 = Void volume within the innermost confinement layer (cm^3).

C_g = Flammable gas generation rate within the innermost confinement layer (mol/sec).

The following initial conditions represent the initial state of the container. At the time of container generation, there is no flammable gas within the container and the initial concentrations, C_{10} and C_{20}, are set equal to zero. If the container is sealed at the time of generation and then vented, the concentrations predicted in a sealed container at the time of venting serve as initial conditions for the differential equations that describe the mass balances of the aspirating container.

$$C_1(t = 0) = C_{10} \tag{3}$$

$$C_2(t = 0) = C_{20} \tag{4}$$

The solution to differential equations (1) and (2) is given by the following set of equations.

$$C_1(t) = (R_2 + R_3)\, G\, /\, (P_1\, P_2) \tag{5}$$
$$- \{C_{10}P_1^2 - [(R_2 + R_3)\, C_{10} + R_1 C_{20} + G]\, P_1 + (R_2 + R_3)\, G\} / \{P_1(P_2 - P_1)\} \exp(-P_1 t)$$
$$- \{C_{10}P_2^2 - [(R_2 + R_3)\, C_{10} + R_1 C_{20} + G]\, P_2 + (R_2 + R_3)\, G\} / \{P_2(P_1 - P_2)\} \exp(-P_2 t)$$

$$C_2(t) = G\, R_2\, /\, (P_1\, P_2) \tag{6}$$
$$- \{C_{20}P_1^2 - [R_2 C_{10} + R_1 C_{20}]P_1 + R_2 G\} / \{P_1(P_2 - P_1)\} \exp(-P_1 t)$$
$$- \{C_{20}P_2^2 - [R_2 C_{10} + R_1 C_{20}]\, P_2 + R_2 G\} / \{P_2(P_1 - P_2)\} \exp(-P_2 t)$$

where,

$$A_1 = R_1 + R_2 + R_3 \tag{7}$$

$$P_1 = (A_1 + \sqrt{A_1^2 - 4\, R_1\, R_3})) / 2 \tag{8}$$

$$P_2 = R_1\, R_3\, /\, P_1 \tag{9}$$

3.10.1.3 Differential Equations for a Container with Three Void Volumes

Differential Equations (10), (11), and (12) represent the mass balances on flammable gas in a container with three void volumes.

$$\frac{dC_1}{dt} = G - R_1(C_1 - C_2) \tag{10}$$

$$\frac{dC_2}{dt} = R_2(C_1 - C_2) - R_3(C_2 - C_3) \tag{11}$$

$$\frac{dC_3}{dt} = R_4(C_2 - C_3) - R_5C_3 \tag{12}$$

where,

G   = C_g R T / (P V_1)

C_1 = Mole or volume fraction flammable gas within the innermost void volume at time t (dimensionless).

C_2 = Mole or volume fraction flammable within the rigid drum liner at time t (dimensionless).

C_3 = Mole or volume fraction flammable within the drum headspace at time t (dimensionless).

R_1 = Effective release rate coefficient of hydrogen from all bags divided by the innermost void volume (day^{-1}).

R_2 = Effective release rate coefficient of hydrogen from all bags divided by the rigid liner void volume (day^{-1}).

R_3 = Effective release rate coefficient of flammable gas from the rigid liner divided by the liner void volume. (One value based on the release from an intact liner is used in the equations for the concentration profiles in a sealed container. A different value is used with the aspiration equations based on the release of flammable gas from the punctured drum liner.) (day^{-1}).

R_4 = Effective release rate coefficient of flammable gas from the rigid liner divided by the container headspace void volume. (One value based on the permeation characteristics of the drum gasket is used to calculate the concentration in a sealed container. A different value is used based on a combination of diffusion characteristic across the drum filter and permeation characteristic across the drum gasket to calculate concentrations in an aspirating container.) (day^{-1}).

R_5 = Effective release rate coefficient of flammable gas from the container divided by the container headspace void volume. (One value based on the permeation characteristics of the drum gasket is used to calculate the concentration in a sealed container. A different value is used based on a combination of diffusion characteristic across the drum filter and permeation characteristic across the drum gasket to calculate concentrations in an aspirating container.) (day^{-1}).

The following initial conditions represent the initial state of the container. At the time of container generation, there is no flammable gas within the container and the initial concentrations, C_{10}, C_{20}, and C_{30} are set equal to zero. If the container is sealed at the time of generation and then vented, the concentrations predicted in a sealed container at the time of venting serve as initial conditions for the differential equations that describe the mass balances of the aspirating container.

$$C_1(t = 0) = C_{10} \tag{13}$$

$$C_2(t = 0) = C_{20} \tag{14}$$

$$C_3(t = 0) = C_{30} \tag{15}$$

The solution to differential equations (10), (11) and (12) is given by the following set of equations.

$$
\begin{aligned}
C_1(t) = &\{ C_{10}P_1^3 - Z_{11}P_1^2 + Z_{12}P_1 - Z_{13} \} / \{ P_1(P_2 - P_1)(P_3 - P_1) \}\, exp(-P_1\, t) \\
&+ \{ C_{10}P_2^3 - Z_{11}P_2^2 + Z_{12}P_2 - Z_{13} \} / \{ P_2(P_1 - P_2)(P_3 - P_2) \} \exp(-P_2\, t) \\
&+ \{ C_{10}P_3^3 - Z_{11}P_3^2 + Z_{12}P_3 - Z_{13} \} / \{ P_3(P_1 - P_3)(P_2 - P_3) \} \exp(-P_3\, t) \\
&+ Z_{13} / (P_1\, P_2\, P_3)
\end{aligned}
\tag{16}
$$

$$
\begin{aligned}
C_2(t) = &\{ C_{20}P_1^3 - Z_{21}P_1^2 + Z_{22}P_1 - Z_{23} \} / \{ P_1(P_2 - P_1)(P_3 - P_1) \} \exp(-P_1\, t) \\
&+ \{ C_{20}P_2^3 - Z_{21}P_2^2 + Z_{22}P_2 - Z_{23} \} / \{ P_2(P_1 - P_2)(P_3 - P_2) \} \exp(-P_2\, t) \\
&+ \{ C_{20}P_3^3 - Z_{21}P_3^2 + Z_{22}P_3 - Z_{23} \} / \{ P_3(P_1 - P_3)(P_2 - P_3) \} \exp(-P_3\, t) \\
&+ Z_{23} / (P_1\, P_2\, P_3)
\end{aligned}
\tag{17}
$$

$$
\begin{aligned}
C_3(t) = &\{ C_{30}P_1^3 - Z_{31}P_1^2 + Z_{32}P_1 - Z_{33} \} / \{ P_1(P_2 - P_1)(P_3 - P_1) \} \exp(-P_1\, t) \\
&+ \{ C_{30}P_2^3 - Z_{31}P_2^2 + Z_{32}P_2 - Z_{33} \} / \{ P_2(P_1 - P_2)(P_3 - P_2) \} \exp(-P_2\, t) \\
&+ \{ C_{30}P_3^3 - Z_{31}P_3^2 + Z_{32}P_3 - Z_{33} \} / \{ P_3(P_1 - P_3)(P_2 - P_3) \} \exp(-P_3\, t) \\
&+ Z_{33} / (P_1\, P_2\, P_3)
\end{aligned}
\tag{18}
$$

where,

$$Z_{11} = (R_2 + R_3 + R_4 + R_5)\, C_{10} + R_1 C_{20} + G \tag{19}$$

$$Z_{12} = (R_2 + R_3 + R_4 + R_5)\, G + (R_2 R_4 + R_2 R_5 + R_3 R_5)\, C_{10} + R_1 (R_4 + R_5)\, C_{20} + R_1 R_3 C_{30} \tag{20}$$

$$Z_{13} = (R_2 R_4 + R_2 R_5 + R_3 R_5)\, G \tag{21}$$

$$Z_{21} = R_2 C_{10} + (R_1 + R_4 + R_5)\, C_{20} + R_3 C_{30} \tag{22}$$

$$Z_{22} = R_2 (R_4 + R_5)\, C_{10} + R_1 (R_4 + R_5)\, C_{20} + R_1 R_3 C_{30} + R_2 G \tag{23}$$

$$Z_{23} = R_2 (R_4 + R_5)\, G \tag{24}$$

$$Z_{31} = R_4 C_{20} + (R_1 + R_2 + R_3)\, C_{30} \tag{25}$$

$$Z_{32} = R_2 R_4 C_{10} + R_1 R_4 C_{20} + R_1 R_3 C_{30} \tag{26}$$

$$Z_{33} = R_2 R_4 G \tag{27}$$

$$A_1 = R_1 + R_2 + R_3 + R_4 + R_5 \tag{28}$$

$$A_2 = R_1 (R_3 + R_4 + R_5) + R_2 (R_4 + R_5) + R_3 R_5 \tag{29}$$

$$A_3 = R_1 R_3 R_5 \tag{30}$$

$$P_1 = [(A_1 - A_3 / C) + \sqrt{(A_1 - A_3 / C)^2 - 4C}] / 2 \tag{31}$$

$$P_2 = C / P_1 \tag{32}$$

$$P_3 = A_3 / (P_1 P_2) \tag{33}$$

where C is a positive root of the cubic equation

$$C^3 - A_2 C^2 + A_1 A_3 C - A_3^2 = 0 \tag{34}$$

The first step in applying the methodology is to establish the container history (i.e., dates of drum packaging, venting, and sampling). Next, the container headspace flammable gas concentration is obtained. The equations documented earlier are solved iteratively adjusting the flammable gas generation rate until the predicted flammable gas generation rate provides a headspace flammable gas concentration that matches the sampled headspace flammable gas

concentration. A validated software program can be used to apply this methodology to determine compliance with the 5-percent limit on hydrogen concentration by sampling the headspace of a container.

3.10.2 Calculation of Flammable Gas/Voc Concentrations: FAMP

The Flammability Assessment Methodology Program (FAMP) was established to investigate the flammability of gas mixtures found in CH-TRU waste containers. Central to the program was experimental testing and modeling to predict the gas mixture lower explosive limit (MLEL) of gases observed in CH-TRU waste containers. Flammability testing was conducted by the National Institute for Occupational Safety and Health (NIOSH) Pittsburgh Research Laboratory (PRL), as described in Loehr et al., 1997.[1] The MLELs of the gas mixtures in the flammability tests were used to develop and evaluate models for predicting the flammability of CH-TRU waste drum contents that could potentially have flammable gas/VOC mixtures. A summary of the test design, equipment and procedures, and results is provided below.

3.10.2.1 Experimental Design

The experimental design focused on investigating classes of compounds, including nonflammable VOCs, to predict MLELs and to provide data that represent a variety of CH-TRU waste gas mixtures for evaluating MLEL models. Table 3.10-1 lists the compounds (flammable VOCs, nonflammable VOCs, and flammable gases) observed in CH-TRU waste containers and considered in the FAMP. Flammable VOCs were classified according to their chemical structural characteristics and lower explosive limit (LEL) group (Table 3.10-2). The functional groups considered were aromatics, ketones, alcohols, and alkanes/alkenes. The LEL groups were designated by LELs of 0.9% to 1.3%, 1.4% to 2.6%, and 5.6% to 6.7%. In general, there is a correlation between functional and LEL group. LEL groups were chosen as classifications for flammable VOCs by functional and LEL groups.

In addition to LEL groups as classifications for flammable VOCs, flammable gases and nonflammable VOCs were two additional classes of compounds considered in the experimental design. Test mixtures for flammability testing were determined based on the following factors:

- Presence or absence of a flammable VOC from one or more of the three LEL groups
- Presence or absence of hydrogen
- Presence or absence of a nonflammable VOC.

VOCs were selected to represent compound classes based on prevalence in CH-TRU waste and on physical characteristics that facilitated testing.

---

[1] Loehr, C.A., S.M. Djordjevic, K.J. Liekhus, and M. J. Connolly (1997). Flammability Assessment Methodology Program Phase I: Final Report. INEEL/EXT-97-01073. Idaho National Engineering and Environmental Laboratory, Idaho Falls, Idaho.

Table 3.10-1 — Flammable and Nonflammable Volatile Organic Compounds and Flammable Gases Considered in the Flammability Assessment Methodology Program

Flammable VOCs	Nonflammable VOCs	Flammable Gases
Acetone	Bromoform	Hydrogen
Benzene	Carbon tetrachloride	Methane
1-Butanol	Chloroform	
Chlorobenzene	Formaldehyde	
Cyclohexane	Methylene chloride	
1,1-Dichloroethane	1,1,2,2-Tetrachloroethane	
1,2-Dichloroethane	Tetrachloroethene	
1,1-Dichloroethene	1,1,1-Trichloroethane	
Cis-1,2-Dichloroethene	Trichloroethene	
Ethyl benzene	1,1,2-Trichloro-1,2,2-trifluoroethane	
Ethyl ether		
Methanol		
Methyl ethyl ketone		
Methyl isobutyl ketone		
Toluene		
1,2,4-Trimethylbenzene		
1,3,5-Trimethylbenzene		
m-Xylene		
o-Xylene		
p-Xylene		

Table 3.10-2 — Classification of Flammable Volatile Organic Compounds

Flammable VOC	Structural Type	Functional Group Number	LEL (vol. %)	LEL Group Number
Acetone	Ketone	2	2.6	2
Benzene	Aromatic	1	1.3	1
1-Butanol	Alcohol	3	1.7	2
Chlorobenzene	Aromatic	1	1.3	1
Cyclohexane	Cycloalkane	-	1.3	1
1,1-Dichloroethane	Alkane	4	5.6	3
1,2-Dichloroethane	Alkane	4	~5	3
1,1-Dichloroethene	Alkene	4	6.5	3
cis-1,2-Dichloroethene	Alkene	4	5.6	3
Ethyl benzene	Aromatic	1	1.0	1
Ethyl ether	Ether	-	1.9	2
Methanol	Alcohol	3	6.7	3
Methyl ethyl ketone	Ketone	2	1.9	2
Methyl isobutyl ketone	Ketone	2	1.4	2
Toluene	Aromatic	1	1.2	1
1,2,4-Trimethylbenzene	Aromatic	1	0.9	1
1,3,5-Trimethylbenzene	Aromatic	1	1.0	1
o-Xylene	Aromatic	1	1.1	1
m-Xylene	Aromatic	1	1.1	1
p-Xylene	Aromatic	1	1.1	1

A full factorial design of the experimental factors plus a quarter replication and minus combinations that resulted in no gas in the mixture resulted in a test matrix of 38 gas mixtures. Replicate runs were included in the test matrix to assess the experimental error. All runs were performed in a random order to help ensure that experimental errors and factor effects were properly estimated and not confounded with experimental procedure trends and other possible experimental effects.

The experimental test mixtures consisted of hydrogen and four VOCs, including 1,2-dichloroethane, to represent chlorinated hydrocarbons and alkanes; methyl ethyl ketone (2-butanone) to represent oxygenated hydrocarbons and ketones; toluene to represent aromatic hydrocarbons; and carbon tetrachloride to represent nonflammable VOCs. These VOCs were chosen to represent the LEL and, thus, the functional groups, because they have sufficient vapor pressures to remain in the gas phase under conditions of standard temperature and pressure. Ethyl ether (an ether) and cyclohexane (a cycloalkane) were not included in the test mixtures because they are not prevalent in CH-TRU waste. The test mixtures contained equimolar amounts of the above constituents as shown in Table 3.10-3.

In planning the experiments, errors were anticipated for measuring the actual concentration of a mixture component injected into the test chamber, the component vapor pressure and associated

temperature, and the actual final mixture pressure. The required overall data quality objective (DQO) was to maintain the error in the experimental MLEL result to less than 5%.

Table 3.10-3 — Experimental Test Mixtures and MLEL Results

Mixture No.	1,2 - Dichloroethane (vol. %)	Methyl ethyl ketone (vol. %)	Toluene (vol. %)	Hydrogen (vol. %)	Carbon tetrachloride (vol. %)	MLEL(%)
1	20	20	20	20	20	3.40±0.10
2	100	0	0	0	0	4.85±0.05
3	50	50	0	0	0	2.65±0.05
4	33	33	33	0	0	1.95+0.03
5	25	25	25	25	0	2.40±0.05
6	33	33	0	33	0	3.40±0.07
7	25	25	0	25	25	5.15±0.05
8	33	33	0	0	33	4.85±0.10
9	25	25	25	0	25	2.80±0.05
10	50	0	50	0	0	2.05±0.03
11	33	0	33	0	33	3.50±0.05
12	33	0	33	33	0	2.65±0.05
13	25	0	25	25	25	3.95±0.05
14	50	0	0	50	0	5.35±0.20
15	33	0	0	33	33	9.7±0.50
16	50	0	0	0	50	Not Determined
17	0	100	0	0	0	1.95±0.03
18	0	50	0	0	50	4.65±0.03
19	0	50	50	0	0	1.45±0.05
20	0	50	0	50	0	3.15±0.07
21	0	25	25	25	25	2.90±0.05
22	0	0	100	0	0	1.20±0.03
23	0	0	50	0	50	2.90±0.05
24	0	0	50	50	0	2.05±0.03
25	0	0	33	33	33	3.65±0.10
26	0	0	0	100	0	5.00±0.40
27	0	0	0	50	50	10.8±0.80
28	0	33	33	0	33	2.45±0.05
29	0	33	33	33	0	2.00±0.05
30	0	33	0	33	33	5.20±0.10
31	0	0	0	0	100	Not Flammable
32	0	0	0	0	0	Not Applicable
33	33	0	33	0	33	3.45±0.10
34	0	33	33	0	33	2.35±0.05
35	33	0	0	33	33	10.1±0.50
36	0	33	0	33	33	5.20±0.07
37	0	0	0	0	0	Not Applicable
38	50	50	0	0	0	2.70±0.05
39	0	0	50	50	0	2.05±0.03
40	25	25	25	25	0	2.40±0.10

3.10.2.2 Flammability Testing Equipment and Procedures

A heavy-walled, stainless steel test chamber with an approximate volume of 19 liters was used for the gas mixture flammability tests. The chamber has been used extensively for dust and gas explosibility measurements. Such chambers are now the standard laboratory chambers for dust explosibility measurements[2], and are highly useful for gas explosibility measurements as well. They are considerably larger than the 5-liter spherical glass flasks specified in the ASTM vapor flammability test procedure[2,3], but are consistent with the ASTM standard. The larger size of the chamber allowed for the potential use of stronger igniters to ensure the absence of ignition limitations when measuring flammability limits, and minimized wall effects on flammability. The question of ignition limitations and wall effects are particularly important in testing halogenated VOCs. The equipment used objective pressure criteria for explosions rather that a purely visual and subjective criteria as in ASTM E681-94[3].

The chamber was equipped with viewing ports and various access ports for pressure and temperature sensors, electronic ignition, evacuation, gas admission, and VOC liquid injection. Ignition was attempted using a 41-joule energy spark, and the resulting pressure trace was monitored to determine flammability or nonflammability for each test. By using the test chamber, stronger ignition sources could be used to ensure the absence of ignition limitations when measuring flammability limits, and minimizing wall effects (i.e., heat losses) on flammability.

A computer-controlled data acquisition system was used to display the pressure, rate of pressure rise (dP/dt), and temperature data versus time. The partial pressures of the VOCs, hydrogen, and air were monitored using two Viatran pressure transducers for the explosion pressures and a Baratron pressure transducer for the component pressures. Chamber temperature was monitored by a Chromel-Alumel (type K) thermocouple.

The PRL measured the MLEL in dry air at a total pressure of 1 atm for the VOC mixtures. All testing used known amounts of the appropriate individual components. To ensure complete volatilization of the VOCs, each component was introduced under reduced pressure into the test chamber. Once the appropriate components were introduced into the chamber and pressures were checked to ensure proper component concentrations, the chamber was brought to atmospheric pressure using dry air. Once a uniform mixture was obtained, the test was started by energizing the appropriate ignition source and recording pressure and temperature. Ignition of the mixture was identified by the pressure rise of the test chamber vessel. A positive ignition was required for those test mixtures that contain a flammable gas.

---

[2] American Society for Testing and Materials (ASTM) (1997) E1515-96. Standard Test Method for Minimum Explosible Concentration of Combustible Dusts, American Society for Testing and Materials, West Conshohocken, Pennsylvania.

[3] American Society for Testing and Materials (ASTM) (1994) E681-94. Standard Test Method for Concentration Limits of Flammability of Chemicals, American Society for Testing and Materials, West Conshohocken, Pennsylvania.

This was accomplished by increasing the component concentrations, while maintaining the required component ratio, until the sample gave a positive ignition. The ignition source selected was of sufficient energy and duration as to avoid ignition limitations as discussed below.

An initial testing phase was completed prior to initiation of testing the 38 gas mixtures in order to verify and establish the following:

- *LEL of the individual components (hydrogen and VOCs).* The LELs determined through the initial testing were compared to values previously determined at the PRL for hydrogen and taken from the literature for the VOCs.

- *Criterion (i.e., pressure rise) for a positive ignition*. Based on the preliminary testing and comparisons to earlier measurements, a pressure rise of 0.5 psi was chosen as the LEL criterion.

- *Equipment performance*.

- *An appropriate ignition source for flammability tests*. Preliminary tests on the LELs of toluene and methyl ethyl ketone had used a stored spark energy of 17 joules. The LELs were found to be in agreement with the reported values from closed flammability tubes. Despite the apparent adequacy of the spark energy used, it was determined to use an even more energetic spark of 41 joules for the test series to help ensure that the more difficult to ignite halogenated VOCs (e.g., 1,2-dichloroethane) and mixtures (those with 1,2-dichloroethane or carbon tetrachloride) would not be ignition limited. Switching to the higher capacitance spark did not reduce the LEL for methyl ethyl ketone. There was, therefore, no indication that the more energetic spark was "overdriving" the chamber mixture, nor was there any expectation that the actual thermal energy deposited in the chamber by the spark (about 1 joule) could possibly do so.

The following measurements were made during an experimental run:

- *Pressure Measurements*. Individual component partial pressure (VOCs, hydrogen, and air) and total chamber pressure were established before each test. The time development of chamber pressure and rate of pressure rise in the chamber were recorded once the appropriate ignition source was energized. The pressure rise criterion, which was determined experimentally, was used to establish ignition of the test gas mixture. In addition to the pressure transducer used to measure component pressures (Baratron), two pressure transducers (Viatran) were used to measure the gas mixture explosion pressure.

- *Temperature measurements*. Test chamber temperature was monitored during each test using a Chromel-Alumel (type K) thermocouple and recoded as a function of time. The thermocouple was able to give qualitative data on flame propagation and temperature, but did not have the response time to allow the monitoring of the actual peak explosion temperature. Because the thermocouple was cemented in place inside

the reaction chamber, it was considered impractical to recalibrate the temperature output on a regular basis. Therefore, the temperature output was treated as a relative rather than an absolute measurement, with more significance given to the measured explosion temperature rise than on the absolute initial starting temperature.

- *Concentration Measurements*. The partial pressure of all gases (VOCs, hydrogen, and air) was used to determine concentrations prior to running a test.

Prior to their use, instruments used in the flammability tests were checked against known standards. Pressure transducers with built in calibrations were checked daily.

3.10.2.3 Experimental Results

The lowest flammable concentration in air of all mixtures specified in the experimental design was determined in the 19-liter laboratory chamber using a strong spark ignition source. Except for 1,2-dichloroethane, the LELs of pure VOCs were within the narrow range of literature values cited by the PRL. The experimental LEL for 1,2-dichloroethane is below the range of values cited in the literature, but may be more accurate because a larger chamber was used in combination with a more energetic spark and it is know that the halogenated species are prone to exhibiting wall effects and ignition limitations. Experimental MLELs generally agreed with calculated values for the mixtures to within 10%.[1]

Partial pressures of the VOC and hydrogen components were used to determine test mixture composition and concentration in air for MLEL determinations. Mixture explosion pressure and temperature data were also measured during the experimental tests. Temperature rise measurements and visual observations of the flame propagation were found to correlate well with pressure rise measurements.[1] MLELs for the various test mixtures listed in Table 3.10-3 are based on pressure versus component concentration data plots.

The precision of the MLELs reported in Table 3.10-3 is based on the number of data points in the near vicinity of the LEL value, how close the data points are to the LEL, the effect of using a range of pressure rise criteria (0.5 ± 02 psi), and sensitivity of explosion pressures near the LEL. The relative precision values form replicate runs, less than or equal to 5% of the LEL value, is consistent with the DQO identified in the FAMP Test Plan.[4]

The largest uncertainty in the MLEL determinations was due to a gradual increase in explosion pressure with hydrogen concentration and the dominance of hydrogen in some mixtures, particularly the hydrogen and carbon tetrachloride mixture, which combines the lightest, most diffusible molecule, hydrogen, with the heaviest VOC, carbon tetrachloride, selected for the experimental tests. The flammability of equimolar mixtures containing hydrogen is expected to be more influenced by hydrogen because of its diffusivity and reactivity as a fuel. This behavior is greatest when other mixture components are much heavier and slower than hydrogen, such as the halogenated components carbon tetrachloride and 1,2-dichloroethane. The other

---

[4] Connolly, M.J., S.M. Djordjevic, L. Evans, and C.A. Loehr (1997). Flammability Assessment Methodology Program Test Plan, Revision 0. INEL 96/0352. Idaho National Engineering and Environmental Laboratory, Idaho Falls, Idaho.

hydrogen-containing mixtures and the pure VOC mixtures (excluding hydrogen and carbon tetrachloride) show a sharp discontinuity at the flammability boundary and, therefore, have more well-defined MLEL and LEL values.[1]

3.10.2.4 Model Development, Evaluation, and Selection

The FAMP evaluated seven models for predicting MLELs for gas mixtures, including (a) the original method of Le Chatelier; (b) a modified Le Chatelier method based on accounting for the nonflammable VOC proportion in the mixture; (c) a group contribution factor method, which accounts for the compound stoichiometry; (d) a group contribution factor method that accounts only for flammable VOCs (Flammable Group method); (e) a group contribution method that uses experimental LELs as input; (f) predictions using the American Society for Testing and Materials code, CHETAH; and (g) linear regression of test MLELs on proportions of compounds in the classifications used for flammability testing. In addition, the effects of imposing bias on relatively unbiased models was investigated.

Model predictions for the test mixtures were compared to MLELs determined in flammability testing. Statistics on measures of the degree of consistency of agreement between predicted and test MLELs were generated. An evaluation of the models was also performed using innermost layer concentrations for 532 drums characterized under the CH-TRU waste characterization program at the Idaho National Engineering and Environmental Laboratory and the Rocky Flats Environmental Technology Site.

In applying the models to actual drum data, it was found that some methods resulted in unrealistic MLELs. For instance, all methods except the Flammable Group method resulted in extremely high MLELs predicted for some drums. Based on the results of model evaluations and because of favorable results in the experimental-based evaluations, the Flammable Group model was selected as a conservative approach to determine the MLEL of a mixture of flammable VOCs and flammable gas.

The Flammable Group method is based on an extension of the method presented in the American Institute of Chemical Engineers (AIChE) Procedure B: Method for Estimating Lower Flammability Limit of Pure Compounds in the Data Prediction Manual.[3] This method predicts the MLEL of a mixture based on knowledge of the chemical structure of each individual component in the mixture. The MLEL will be calculated by the following equation:

$$MLEL = \frac{100\%}{\sum f_i \, x \, GCF_i} \tag{35}$$

where,

$MLEL$ = mixture lower explosive limit (vol %)

f_i = fraction of flammable gas i in mixture on an air free and nonflammable VOC free basis (i.e., the concentration of flammable compound i divided by the sum of the concentrations of flammable VOCs and flammable gas).

GCF$_i$ = group contribution factor for compound i.

The GCF for a compound is calculated by the following method:

$$GCF_i = \sum n_j * GF_j \qquad\qquad (36)$$

where,

n_j =   number of group type j in compound i
GF_j =   group factor for group type j.

Table 3.10-4 contains the FAMP calculated group factor (GF) values for the various groups used to determine the GCF for a compound of interest. As an example, the GCF for methanol (CH_3OH) or structurally as

```
      H
      |
H — C — OH
      |
      H
```
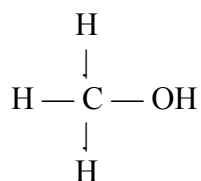
is calculated as 1 C group + 4 H groups + 1 O group or (9.10) + (4*2.17) + (-2.68) = 15.1. The GCF values for various flammable VOCs identified by the sites in CH-TRU waste are listed in Table 3.10-5. GCF values for additional flammable VOCs may be calculated by the WIPP CH-TRU Payload Engineer in the same manner. See Section 5.2.5.3.2 of the CH-TRAMPAC for the process of adding flammable VOCs.

Table 3.10-4 — FAMP Group Factor (GF) Values

Group	Group Factor
C	9.10
H	2.17
H_2	20.0
O	-2.68
N	1.38
Cl	-4.38
C=C	14.07
F (Number of H atoms > Number of F atoms)	-4.18
F (Number of H atoms < Number of F atoms)	-2.55
I	17.5
S	10.9
P	9.6

Table 3.10-5 — Compound Group Contribution Factors

Compound	Group Contribution Factor (GCF)
Flammable VOCs	
Acetone	37.64
Benzene	82.53
1-Butanol	55.42
Chlorobenzene	75.98
Cyclohexane	80.64
1,1-Dichloroethane	18.12
1,2-Dichloroethane	18.12
1,1-Dichloroethene	9.65
cis-1,2-Dichloroethene	9.65
Ethyl benzene	109.41
Ethyl ether	55.42
Methanol	15.1
Methyl ethyl ketone	51.08
Methyl isobutyl ketone	77.96
Toluene	95.97
1,2,4-Trimethylbenzene	122.85
1,3,5-Trimethylbenzene	122.85
o-Xylene	109.41
m/p-Xylene	109.41
Flammable Gases	
Hydrogen	20
Methane	20

APPENDIX 3.11

USE OF FILTERED BAGS AS CONFINEMENT LAYERS
FOR CH-TRU WASTES

This page intentionally left blank.

3.11 Use of Filtered Bags as Confinement Layers for CH-TRU Wastes

3.11.1 Introduction

Contact-handled-transuranic (CH-TRU) waste is typically packaged in closed, unfiltered plastic bags within authorized payload containers. However, filtered bags may also be used as layers of confinement within authorized payload containers for the shipment of specific CH-TRU waste forms in the TRUPACT-II and the HalfPACT. Filtered bags are used primarily for two purposes: (1) increasing allowable decay heat limits and (2) addressing site safety concerns for specific packaging configurations. This appendix describes the test procedures and analyses that validate the use of filtered bags, and provides the technical basis for increased allowable decay heat limits for specific shipping categories using filtered bags.

3.11.2 Description of Filtered Bag

The filtered bag is a plastic bag installed with a minimum of one filter vent. An example of a filtered bag configuration is presented in Figure 3.11-1. Other configurations meeting the requirements of Section 2.5 of the Contact-Handled Transuranic Waste Authorized Methods for Payload Control (CH-TRAMPAC), "Filter Vents," are acceptable. Appendix 3.8 of the CH-TRU Payload Appendices presents the specifications for allowable closure methods for any layers of confinement used in payload containers. Section 2.5 of the CH-TRAMPAC provides the specification for the plastic bag filter vent.

3.11.3 Testing

The flow rate and hydrogen diffusion characteristics of the bag filters were measured in experimental programs, designed similar to those for the filters used for the payload containers.[1,2] In the first series of tests, conducted in 1990, flow was measured as a function of differential air pressure across the filter vent, and diffusion was measured at zero differential pressure, with 4.78%, by volume, hydrogen in nitrogen.[3] Four bag filters were tested under both dry and wet conditions, and the test data were used to calculate filter flow and diffusion coefficients for each. The results indicate that flow increases linearly with pressure at a rate of 5.9 standard liters per minute (slpm)/pounds per square inch gauge (psig). This rate exceeds the minimum filter flow requirement specified by Section 2.5 of the CH-TRAMPAC (i.e., 1 slpm at 1 psig). Table 3.11-1 presents the flow coefficients of each tested filter.

---

[1] Peterson, S.H., E.E. Smeltzer, and R.D. Straw, March 1990, "Determination of Flow and Hydrogen Diffusion Characteristics of Carbon Composite Filters Used at the Waste Isolation Pilot Plant," Purchase Order No. 75WRS36917IZ, Westinghouse Science and Technology Center, Pittsburgh, Pennsylvania.

[2] Callis, E.L., J.H. Cappis, M.C. Smith, and R.S. Marshall, 1995, "Hydrogen Venting Characteristics of Commercial Carbon-Composite Filters and Applications to TRU Waste," LA-UR-95-1447, Los Alamos National Laboratory, Los Alamos, New Mexico.

[3] Callis, E.L., January 23, 1996, "Summary of January 1996 Filter Measurements," Letter Report to IT Corporation, Los Alamos National Laboratory, Los Alamos, New Mexico.

824499.01.01.00.00/A21   *NOT TO SCALE*
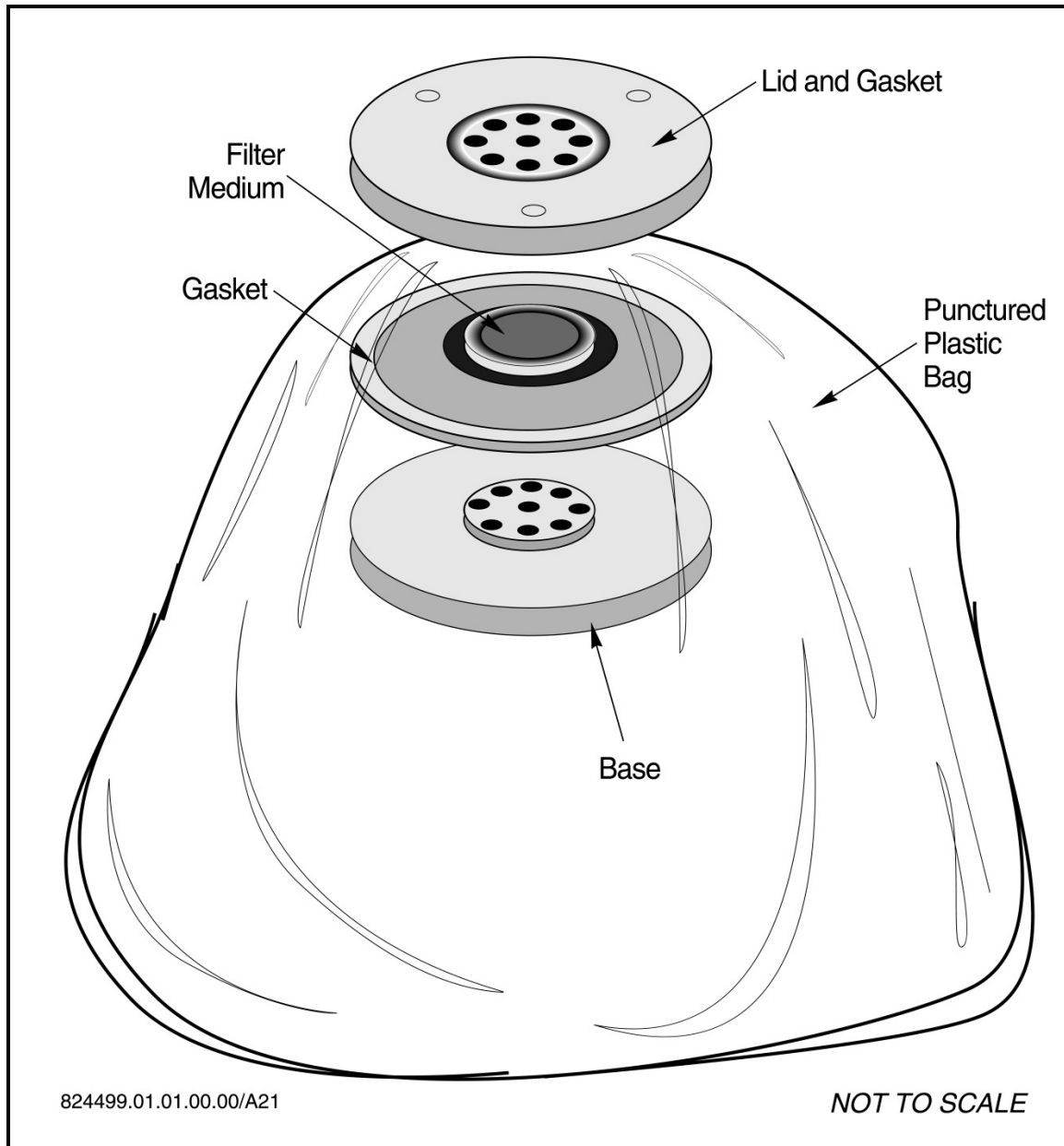
Figure 3.11-1 — Example of One Type of Filtered Bag

Table 3.11-1 — Flow Coefficients of Bag Filters Tested with Compressed Air, 0.2 to 10 psig

Filter Model	Filter Identification	Mean Flow Coefficient (slpm/psig)
NFT-030	WH-05	5.8
	WH-06	6.5
	WH-07	5.9
	WH-08	5.5
	AVERAGE	5.9

Source: Peterson, S.H., E.E. Smeltzer, and R.D. Straw, March 1990, "Determination of Flow and Hydrogen Diffusion Characteristics of Carbon Composite Filters Used at the Waste Isolation Pilot Plant," Purchase Order No. 75WRS36917IZ, Westinghouse Science and Technology Center, Pittsburgh, Pennsylvania.

Diffusion measurements in these tests showed that the hydrogen diffusivity values of the filters ranged from 4.17E-06 to 4.32E-06 mole/second/mole fraction (mol/sec/mol fraction) (Table 3.11-2).

Table 3.11-2 — Diffusion Coefficients of Bag Filters

Filter Model	Filter Identification	Diffusion Coefficient (mol/sec/mol Fraction)
NFT-030	WH-05	4.32E-06
	WH-06	4.26E-06
	WH-07	4.17E-06
	WH-08	4.31E-06
	AVERAGE	4.27E-06

Source: Peterson, S.H., E.E. Smeltzer, and R.D. Straw, March 1990, "Determination of Flow and Hydrogen Diffusion Characteristics of Carbon Composite Filters Used at the Waste Isolation Pilot Plant," Purchase Order No. 75WRS36917IZ, Westinghouse Science and Technology Center, Pittsburgh, Pennsylvania.

Table 3.11-3 presents a comparison of diffusion results for wet and dry filters. At applied pressures less than or equal to 1 psig the wet filters were ineffective.[1] At pressures greater than 1 psig, the water was forced out of the filter and the flow measurements paralleled that of the dry filter. A conservative approach precludes the use of filtered bags to directly package CH-TRU waste where the filters could come in contact with water (i.e., Waste Material Types I.1 [absorbed, adsorbed, or solidified inorganic liquids], I.2 [soils, solidified particulates, or sludges formed from precipitates], or Waste Type IV [solidified organics]). It should be noted that the CH-TRU waste forms do not exist as free liquids and are not likely to affect filter performance. Therefore, the use of a heat-sealed filtered bag as the innermost layer of confinement to package CH-TRU waste is limited to Waste Material Types I.3, II.1, III.1 and III.3 provided that there is no potential for contact of the filters with water. Waste Material Types II.2, II.3, and III.2, which by definition include a metal can as the innermost layer of confinement, may use heat-sealed

filtered bags outside of the innermost metal can. For other waste material types, heat-sealed filtered bags are not allowed as the innermost layer of confinement.

Table 3.11-3 — Comparison of Wet and Dry Diffusion Coefficients of Bag Filters

Filter Model	Filter Identification	Diffusion Coefficient (mol/sec/mol fraction)	
		Dry	Wet
NFT-030	WH-05	4.32E-06	0.040E-06
	WH-06	4.26E-06	0.044E-06
	WH-07	4.17E-06	0.022E-06
	WH-08	4.31E-06	0.041E-06
	AVERAGE	4.27E-06	0.037E-06

Source: Peterson, S.H., E.E. Smeltzer, and R.D. Straw, March 1990, "Determination of Flow and Hydrogen Diffusion Characteristics of Carbon Composite Filters Used at the Waste Isolation Pilot Plant," Purchase Order No. 75WRS36917IZ, Westinghouse Science and Technology Center, Pittsburgh, Pennsylvania.

In the second series of tests, conducted in 1995, 12 bag filters were tested for hydrogen diffusivity, with the results shown in Table 3.11-4.[2] The hydrogen diffusivity values ranged from 1.075E-05 mol/sec/mol fraction to 1.217E-05 mole/sec/mol fraction, with an average value of 1.127E-05 mol/sec/mol fraction. As may be seen by a comparison of Tables 3.11-2 and 3.11-4, these results are higher (approximately 3.7 times) than the results from the initial testing in 1990. Further investigations and retesting of the initial filters showed that the differences could be attributed to an improved design of the filters, which provided for nine gas release holes (in the 1995 filters) instead of only five (in the 1990 filters).[3] The use of bag filters is based only on the newer design. The minimum diffusivity value of 1.075E-05 mol/sec/mol fraction obtained in the 1995 testing will be used in the minimum specifications for the bag filters (Section 2.5 of the CH-TRAMPAC). As specified in Section 2.5 of the CH-TRAMPAC, high-diffusivity bag filters (HDBF) may be used to decrease the resistance to hydrogen diffusivity. The HDBFs allow credit to be taken for filters for which a hydrogen diffusivity value that is equal to or greater than 2 times, 5 times, 25 times, or 100 times the minimum specification for the bag filter has been demonstrated and documented through testing. As with other filter requirements, site-specific procedures ensure compliance with this limit through procurement and administrative controls. The value specified in Section 2.5 of the CH-TRAMPAC is used in determining the hydrogen release rate through the bag filters in the calculation of the decay heat limit for shipping categories using filtered bags (Section 3.11.5).

Table 3.11-4 — Diffusion Coefficients of Bag Filters

Filter Model	Filter Identification	Diffusion Coefficient (mol/sec/mol fraction)
NFT-030	LANL 1	1.105E-05
	LANL 2	1.116E-05
	LANL 4	1.170E-05
	LANL 6	1.130E-05
	LANL 13	1.128E-05
	LANL 14	1.145E-05
	LANL 15	1.217E-05
	LANL 16	1.075E-05
	LANL 25	1.092E-05
	LANL 26	1.125E-05
	LANL 27	1.121E-05
	LANL 28	1.105E-05
	AVERAGE	1.127E-05

Source: Callis, E.L., J.H. Cappis, M.C. Smith, and R.S. Marshall, 1995, "Hydrogen Venting Characteristics of Commercial Carbon-Composite Filters and Applications to TRU Waste," LA-UR-95-1447, Los Alamos National Laboratory, Los Alamos, New Mexico.

3.11.4 Shipping Category

Filtered bags shall be used only in packages as described in Section 3.11.3, Testing. The use of filtered bags in waste packaging configurations must be specified in approved content codes.

In the alpha-numeric shipping category notation scheme used until June 1999, the presence of filtered bags in a shipping category was indicated by using an alpha trailer designation of "f" in conjunction with the notation for the total number of bags. This designation indicated that all plastic bags were filtered bags. For example, the notation II.1A2f indicated CH-TRU Waste Material Type II.1 packaged in one 55-gallon drum with two filtered bags, each containing a minimum of one filter vent. In the numeric shipping category notation initiated in June 1999, the resistance of filtered bags is represented in the last four digits of the shipping category, as detailed in Appendix 2.2 of the CH-TRU Payload Appendices.

Filtered bags may be closed by any method, including heat-sealing. For estimation of gas release rates and decay heat limits, it is conservatively assumed that the bag closure allows no gas release (i.e., the bag is heat-sealed).

3.11.5 Decay Heat Limits

Decay heat limits, expressed as watts per payload container, are established for all shipping categories of authorized payload containers. Limits for the allowable decay heat value for each shipping category are specified in order to control the potential for combustible gas accumulation. The method for calculating decay heat limits for different shipping categories is provided in Appendix 2.3 of the CH-TRU Payload Appendices.

Because filtered bags allow higher rates of gas release, the maximum decay heat limits for specific shipping categories containing filtered bags may be increased. Allowable decay heat limits for shipping categories using filtered bags were calculated using data for hydrogen diffusivity through the bag filters and permeation through the liner bag(s). The calculation of decay heat limits is derived in Appendix 2.3 of the CH-TRU Payload Appendices, and is the same for the shipping categories using filtered bags, with the release rates being based on the testing described in this appendix.

APPENDIX 4.1

DESCRIPTION OF STANDARD PIPE OVERPACK

This page intentionally left blank.

4.1   Description of Standard Pipe Overpack

4.1.1   Introduction

The standard pipe overpack, also referred to as pipe overpack payload container, pipe overpack configuration, or pipe overpack assembly, consists of a pipe component, also referred to as pipe container, positioned by dunnage within a 55-gallon drum with a rigid liner. It is designed to be used for the shipment of specific contact-handled transuranic waste forms in the TRUPACT-II and the HalfPACT. Appendix 1.3.1 of the TRUPACT-II Safety Analysis Report (SAR), Appendix 1.3.1 of the HalfPACT SAR, and Section 2.9.2 of the Contact-Handled Transuranic Waste Authorized Methods for Payload Control (CH-TRAMPAC) describe the materials of construction, sizes, and other dimensional specifications for the standard pipe overpack. The purpose of the standard pipe overpack is to provide criticality control, shielding, and containment of fine particulate waste material and to increase the maximum fissile gram equivalent (FGE) loading within the package. This allows for the shipment of up to 7 pipe overpacks in a HalfPACT or up to 14 pipe overpacks in a TRUPACT-II with payload container and packaging FGE limits as presented in Section 4.1.6 of this appendix. This appendix describes the test procedures and analyses that validate the use of the standard pipe overpack, and provides the technical basis for the FGE limits for shipments of pipe overpacks. Appendices 4.2, 4.3, and 4.4 of the CH-TRU Payload Appendices describe the analyses that validate the use of shielded configurations of the pipe overpack and provide the technical basis for the shipment of specific gamma- and neutron-emitting wastes in shielded pipe overpacks in the TRUPACT-II and HalfPACT.

4.1.2 Description

The standard pipe overpack consists of a pipe component surrounded by cane fiberboard and plywood dunnage within a standard 55-gallon drum with a rigid polyethylene liner and lid. A schematic of the pipe overpack is shown in Figure 4.1-1.

The pipe component[1,2] provides three significant control functions with regard to waste materials: (1) criticality control, (2) shielding, and (3) containment of fine particulate waste material. The testing and analyses described in the following sections demonstrate the effectiveness of the pipe overpack design for normal conditions of transport and hypothetical accident conditions.

The pipe component is a stainless steel, cylindrical pipe with a welded or formed bottom cap and a bolted stainless steel lid sealed with a butyl rubber or ethylene propylene O-ring (Figure 4.1-2, Appendix 1.3.1 of the HalfPACT SAR, and Appendix 1.3.1 of the TRUPACT-II SAR). The pipe component is approximately 2 feet long and is available with either a 6-inch (in.) (0.280-in. nominal thickness) or a 12-in. (0.250-in. nominal thickness) diameter. The pipe component must be installed with a filter vent; Section 2.5 of the CH-TRAMPAC provides the specification for the pipe component filter vent. The pipe component is centered in the standard 55-gallon steel drum with dunnage consisting of cane fiberboard packing and plywood (see Figure 4.1-1).

---

[1] 6-inch Pipe Component Test Unit Fabrication Drawings:

> Rocky Flats Environmental Technology Site, March 1995. Residue Container Fabrication Drawing, P15630, Rocky Flats Environmental Technology Site.

> Rocky Flats Environmental Technology Site, September 1996. 6-inch Residue Container Assembly Drawing, SNMP 1001, Rocky Flats Environmental Technology Site.

[2] 12-inch Pipe Component Test Unit Fabrication Drawings:

> Rocky Flats Environmental Technology Site, October 1994. Residue Container Fabrication Drawing, P15706, Rocky Flats Environmental Technology Site.

> Rocky Flats Environmental Technology Site, September 1996. 12-inch Residue Container Assembly Drawing, SNMP 1019, Rocky Flats Environmental Technology Site.

55-GALLON DRUM
LID W/ FILTER VENT,
LID RING, AND
GASKET

55-GALLON DRUM
VENTED RIGID
LINER LID

PIPE COMPONENT
LID W/ FILTER VENT

PIPE COMPONENT
DUNNAGE

PIPE COMPONENT
BODY W/ GASKET

55-GALLON DRUM
BODY W/ RIGID
LINER BODY

CONTENTS

Figure 4.1-1 – Standard Pipe Overpack

Bolt

Filter Vent

Lift Attachment

Lift Attachment
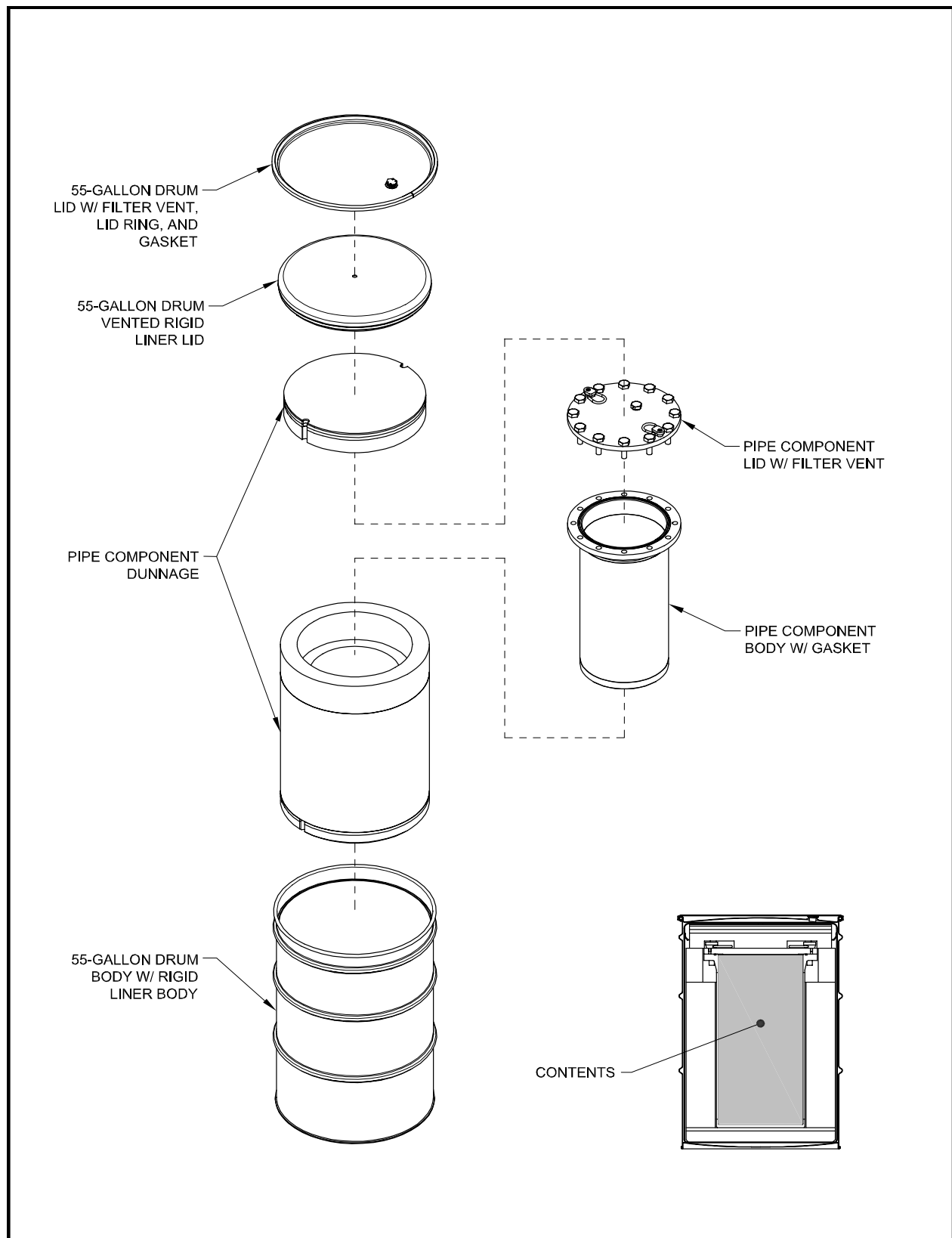
Filter Vent

Bolt

Body

824499.01.01.00.00/A15
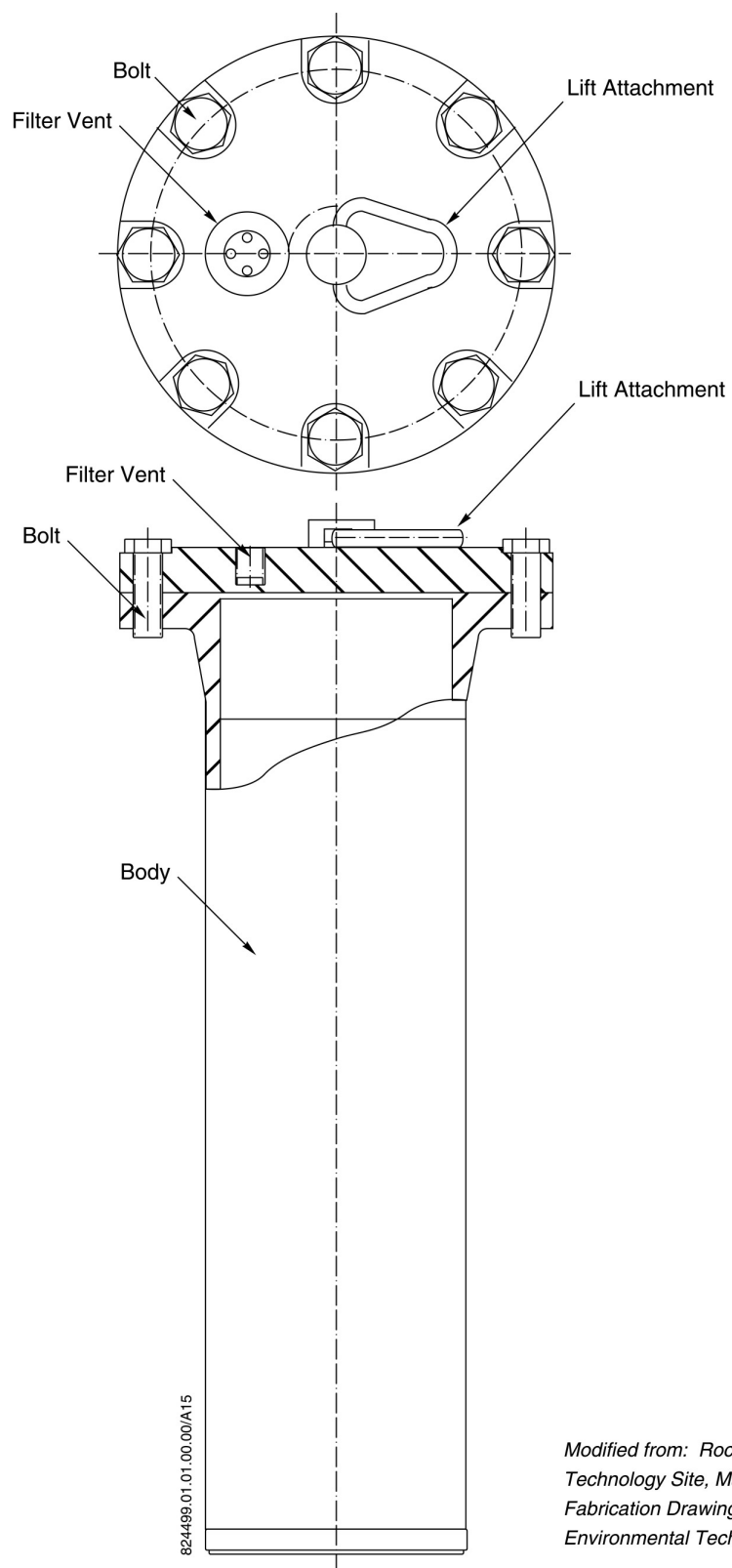
Modified from: Rocky Flats Environmental Technology Site, May 1994. Residue Container Fabrication Drawing, P15631, Rocky Flats Environmental Technology Site.

Figure 4.1-2 – Pipe Component

4.1.3   Description of Test Program for the Standard Pipe Overpack

A test program was developed and implemented to demonstrate the structural integrity of the pipe overpack under hypothetical accident conditions. Normal conditions of transport are also bounded by the test program. The test program procedures and results are documented in independent reports[3,4] and are summarized in this section.

Two series of testing, consisting of 30-foot top- and side-impact drops of loaded pipe overpacks, have been performed. The drop tests simulated the interaction effects of other fully loaded pipe overpacks within a TRUPACT-II without subjecting an actual TRUPACT-II packaging to the tests. This resulted in more conservative analyses of the performance of the pipe overpack, since potential damage to the pipe overpacks would be less severe within a TRUPACT-II or HalfPACT.

In the first series of testing, the empty weights of the 6-in. and 12-in. diameter pipe components were approximately 87 pounds and 195 pounds, respectively. Two 6-in. diameter aluminum rods weighing nominally 66 pounds total were placed one on top of the other in each 6-in. nominal diameter pipe component; and six 5.5-in. diameter aluminum rods weighing nominally 167 pounds total were placed in two layers of three in each 12-in. nominal diameter pipe component (Figure 4.1-3a). Nominal loaded weights of the 6-in. and 12-in. diameter pipe components were 153 pounds and 362 pounds, respectively. Six "dummy" pipe components were loaded with steel rods to approximately equal the loaded weights of the test pipe components. The purpose of the "dummy" pipe components was to complete the payload configuration; these components were not tested. The loaded pipe components were overpacked within standard 55-gallon drums. Nominal loaded weights of the pipe overpacks, containing the 6-in. and 12-in. diameter pipe components, were 328 pounds and 504 pounds, respectively.

The second series of testing was similar to the first and was conducted following a revision to the 12-in. diameter pipe component design. The design was revised to remove nonessential weight from the pipe component flange and lid. The revised 12-in. diameter lid design, similar to that of the 6-in. diameter pipe component, is thicker and eliminates the need for a shielding plate to be attached to the lid under the filter opening (see Section 4.1.7). This design increases the available payload weight by 60 pounds over the original design. The modifications to the 6-in. diameter pipe component design are negligible. The design drawings included in the SARs for the TRUPACT-II and HalfPACT encompass both the original and the revised pipe component designs.

---

[3] Ammerman, D.J., and J.G. Bobbe, October 1995. "Rocky Flats Pipe Component Testing," TTC-1434, Sandia National Laboratories, Albuquerque, New Mexico.

[4] Ammerman, D.J., J.G. Bobbe, M. Arviso, and D.R. Bronowski, April 1997. "Testing in Support of Transportation of Residues in the Pipe Overpack Container," TTC-1477, Sandia National Laboratories, Albuquerque, New Mexico.
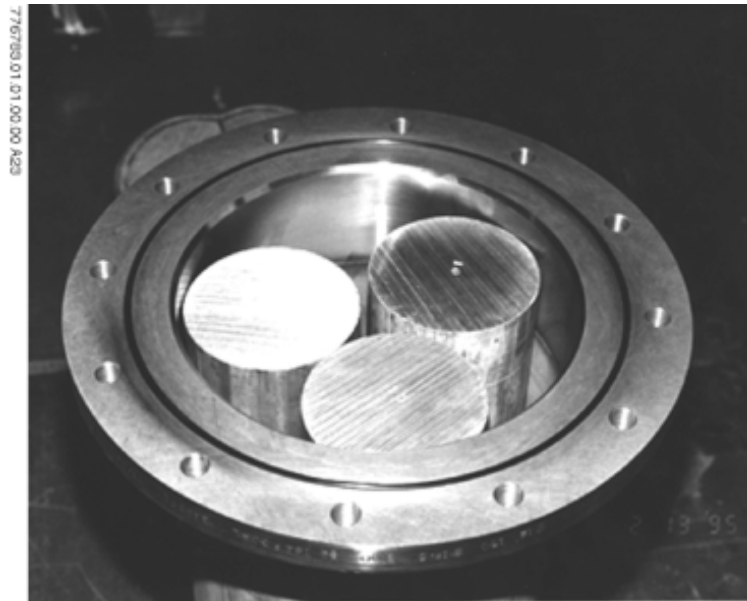
Figure 4.1-3a. Loaded Pipe Component (12-inch diameter)

Figure 4.1-3b. Top-Impact Drop Test Set-up
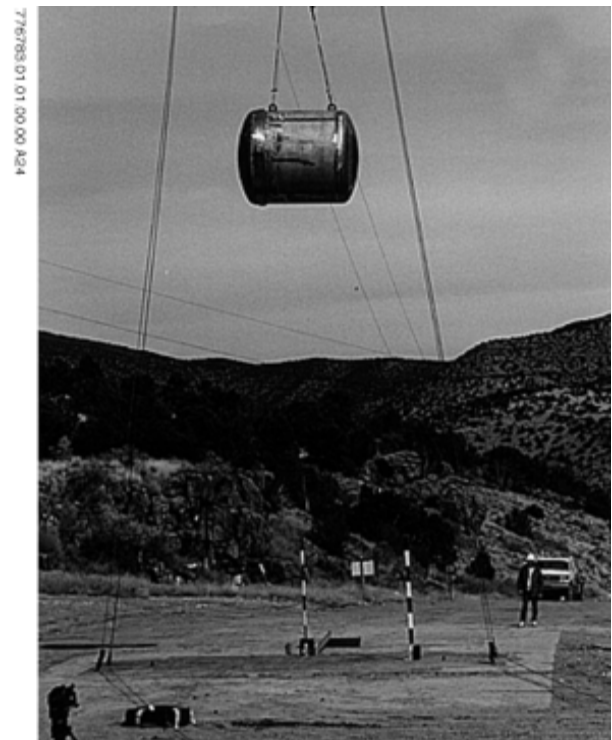
Figure 4.1-3c. Side-Impact Drop Test Set-up

Figure 4.1-3 – Test Program Photographs of the Standard Pipe Overpack (Pre-Test)

For the second series of tests, the nominal loaded weights of the 6-in. diameter pipe component and pipe overpack closely approximated the corresponding weights of the first test series. However, the nominal loaded weight of the revised 12-in. diameter pipe component was 407 pounds, which included contents weighing 225 pounds. The nominal loaded weight of the pipe overpack containing the 12-in. diameter pipe component was 547 pounds. The tests were designed to qualify not only TRUPACT-II payload assemblies of pipe overpacks, containing fourteen 6-in. or fourteen 12-in. diameter pipe components, but also a mixed assembly of pipe overpacks, containing a 7-pack of all 6-in. diameter and a 7-pack of all 12-in. diameter pipe components.

Three top-impact drop tests were performed during both series of tests. In each test, two drums were strapped end-to-end as if positioned for transport within a TRUPACT-II (Figure 4.1-3b). Top-impact drop tests were performed for the following three configurations of pipe overpacks:

- Two 55-gallon drums containing 6-in. diameter pipe components

- Two 55-gallon drums containing 12-in. diameter pipe components

- Two 55-gallon drums; one containing a 12-in. diameter pipe component and one containing a 6-in. diameter pipe component with the 6-in. impacting first.

One side-impact test was performed by dropping an uncertified but functional TRUPACT-II inner containment vessel (ICV) with a payload assembly, including a top layer of seven pipe overpacks containing 6-in. diameter pipe components and a bottom layer of seven pipe overpacks containing 12-in. diameter pipe components (Figure 4.1-3c and Figure 4.1-4). The drop demonstrated a worst case, since potential damage to the pipe overpacks would be less severe within the entire TRUPACT-II packaging, which includes 10 inches of impact-absorbing foam.

A leakage rate test using helium and a mass spectrometer leak detector was performed before and after each drop test to evaluate the containment provided by the pipe component. The pipe components used in the testing were fitted with leak-test ports to allow connection to the leak detector. The leak-test port is not a feature of the pipe component production model. To facilitate the test, the opening in the pipe component filter was sealed with vacuum putty. This allowed the gasket between the filter and the pipe component lid to be leak-tested. After the post-drop leak test, the filters were removed and an evaluation of filter performance was conducted by the filter manufacturer.

4.1.4 Results of Test Program for the Standard Pipe Overpack

The first test series was completed at Sandia National Laboratories/New Mexico in March 1995.[3] Testing of the revised pipe component was completed at the same location in December 1996.[4] There was no loss of containment in any drop test, and all pipe components had a leakage rate of less than 1×10^{-7} cc/sec. The filters showed no damage from the drop tests. Following the leak test, the filters were removed from the pipe components and verified by the filter manufacturer to have maintained undiminished flow and filtering characteristics in accordance with the requirements of Section 2.5 of the CH-TRAMPAC.

This page intentionally left blank.

TOP 7-PACK, 6-IN. PIPE

325 LB.
320 LB.
335 LB.
323 LB.
324 LB.
336 LB
322 LB.
ICV
IMPACT POINT

BOTTOM 7-PACK, 12-IN. PIPE

550 LB.
545 LB.
550 LB.
547 LB.
542 LB.
549 LB.
548 LB.
ICV
IMPACT POINT

SIDE DROP ORIENTATION

ICV
BOTTOM 7-PACK, 12-IN. PIPE
TOP 7-PACK, 6-IN. PIPE
IMPACT SIDE
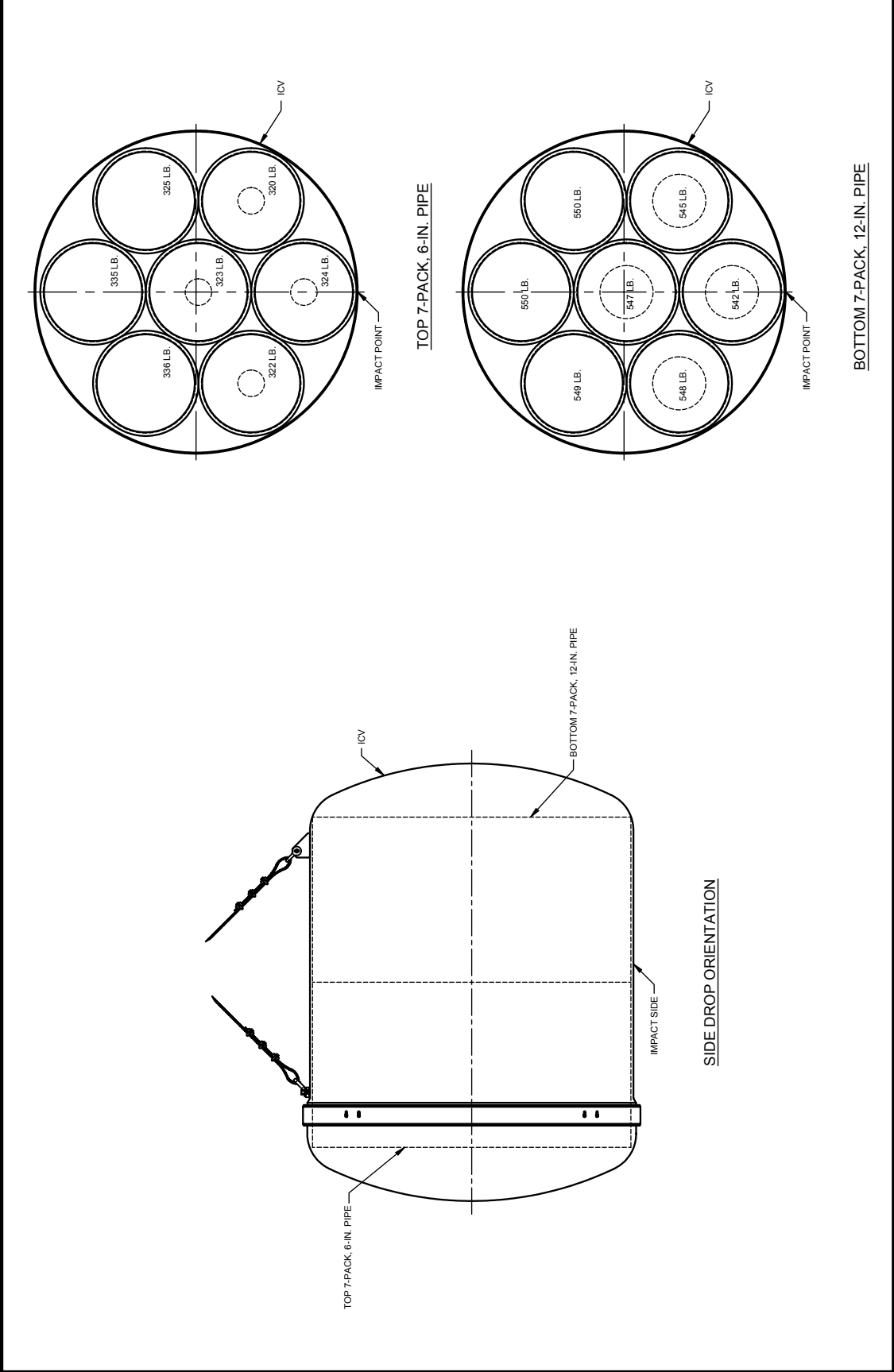
Figure 4.1-4 – Side Drop Configuration and Weights

4.1-9

This page intentionally left blank.

In the first test series, some of the bolts in the lids were observed to be loose upon post-test inspection of the two 6-in. diameter pipe components tested in the top-impact drop test. The cause of this anomaly was traced to the specification for bolt fabrication that allowed protruding die marks on the bearing surface of the bolts. During the top-impact drops, the protruding die marks cut into the surface of the pipe component lid causing a reduction of bolt tension. Although this irregularity did not affect the ability of the pipe components to maintain closure and pass the leak tests, the anomaly was corrected by modifying the specification for the screw-fasteners so that the result is a flat bearing-surface and uniform contact pressure.

The only other pipe overpack deformation observed during this test series was to the shielding plate of the 12-in. diameter pipe component lid. During the top-impact drop tests, the force of the pipe component contents pushed the shielding plate, which is located below the filter, closer to the lid surface. The shielding plate (see Section 4.1.7) prevents radiation emission through the filter vent and protects the filter media from potential damage if impacted by the component contents. While these functions were not compromised by the movement of the shielding plate, the abnormality was corrected in the production 12-in. diameter pipe components.

The 6-in. diameter pipe component and the revised 12-in. diameter pipe component do not have shielding plates. The lids of these designs are thicker than that of the original 12-in. diameter pipe component design and encase the bottom portion of the filter vent opening (see Section 4.1.7). Therefore, the lids of the 6-in. diameter pipe component and the revised 12-in. diameter pipe component provide adequate shielding without the addition of shielding plates.

Additionally, the maximum axial drum crush observed during the end drop test was 3.98 in. and 3.63 in. for the 6-in. and 12-in. pipe overpacks, respectively. The maximum diametrical drum crush observed during the side drop test was 4.31 in. and 2.25 in. for the 6-in. and 12-in. pipe overpacks, respectively.

In summary, the results of the test program for the standard pipe overpack demonstrate that under hypothetical accident conditions, the 6-in. and 12-in. diameter pipe components (both original and revised designs) maintain containment of material and do not incur any damage (see Figure 4.1-5).

4.1.5 Structural Analysis of the Standard Pipe Overpack

The pipe component is constructed of grade 304 stainless steel. Protective cane fiberboard and plywood packing material is used to center the pipe component within a standard 55-gallon drum to constitute a pipe overpack. In the original testing, the 20 pipe components involved in the drop tests sustained no visible damage or deformation with the exception of the minor items noted in Section 4.1.4, which have been corrected. The 14 pipe components that were leak tested showed no loss in containment capability. The capability of the pipe components to maintain structural integrity during hypothetical accident testing is due to the design and material construction of the closures.

Figure 4.1-5 – Test Program Photographs of the Standard Pipe Overpack (Post-Test)

The observed maximum drum crush values reported in Section 4.1.4 result in idealized minimum right-circular cylinder dimensions for the 6-in. and 12-in. pipe overpacks of 18.19 in. outside diameter by 29.27 in. height and 20.25 in. outside diameter by 29.62 in. height, respectively, utilized in the criticality analysis summarized in Section 4.1.6.

A butyl rubber or ethylene propylene O-ring seals the lid to the pipe component body. Both O-ring materials have a sustained temperature capability of 250 degrees Fahrenheit (°F), which exceeds temperatures realized within the TRUPACT-II ICV during previous testing. Likewise, the neoprene gasket that seals the filter housing to the lid has a 250°F temperature capability. The filter design used in the pipe component functions within specifications at temperatures ranging from well below –40°F to over 280°F. The filters have been shown to survive independent drop tests and impact tests.[5]

4.1.6 Criticality Analysis of the Standard Pipe Overpack

A criticality analysis was performed for two different payload cases, depending on the quantities of special reflector materials in the payload container (see Chapter 6.0 of TRUPACT-II SAR or Chapter 6.0 of HalfPACT SAR for description of special reflector materials), as described below:

- Case E: For Case E, the contents of the pipe overpack payload container contain less than or equal to 1% by weight quantities of special reflector materials. The pipe overpack payload container may contain greater than 1% by weight quantities of special reflector materials provided that one of the following conditions is met:
    o The special reflector materials are chemically or mechanically bound to the fissile material such that no reconfiguration or release of the bond is possible under normal or accident conditions, or
    o The special reflector materials are present in thicknesses and/or packing fractions that render them less effective than a 25% polyethylene/75% water equivalent reflector per the limits in Table 6.2-1 of the TRUPACT-II or HalfPACT SAR.
- Case F: For Case F, the contents of the pipe overpack payload container contain greater than 1% by weight quantities of special reflector materials that do not meet the exceptions listed for Case E.

The criticality analysis demonstrates that a TRUPACT-II shipment of 14 pipe overpacks with contents meeting the requirements of Case E at 200 FGE of ^{239}Pu each (for a total of 2,800 FGE per TRUPACT-II) or a HalfPACT shipment of 7 pipe overpacks with 200 FGE each (for a total of 1,400 FGE per HalfPACT) ensures compliance with the requirements of Title 10, Code of Federal Regulations (CFR), Sections 71.55 and 71.59 (10 CFR 71.55 and 71.59).[6] Additionally, shipments of pipe overpacks with contents meeting the requirements of Case F at 140 FGE for each payload container and 980 and 1960 FGE per HalfPACT and TRUPACT-II, respectively,

---

[5] Nuclear Filter Technology, Inc., February 1995. "The Effect of Extreme Temperatures, Impacts, and Vibrations on Nuclear Filter Technology, Inc.'s NucFil 013," Nuclear Filter Technology, Inc., Wheat Ridge, Colorado.

[6] Packaging Technology, Inc., May 2004, "Pipe Overpack Criticality Analysis for the TRUPACT-II Package," ED-076, Packaging Technology, Inc., Tacoma, Washington.

ensure compliance with 10 CFR 71.55 and 71.59. Based on an infinite array of undamaged or damaged packages, the criticality transport index is 0.0.

The key parameters in the pipe overpack analysis for Case E are (1) the maximum fissile loading per pipe component is 200 FGE, (2) no more than 1% by weight quantities of special reflector materials are present or greater than 1% by weight quantities of special reflectors are either bound to the fissile material or meet the limits in Table 6.2-1 of the TRUPACT-II or HalfPACT SAR, (3) the spacing between the components (i.e., effective drum diameter) is reduced by the maximum amount reported in Section 4.1.5, and (4) the package arrays are infinite arrays stacked two high.

The key parameters in the pipe overpack analysis for Case F are (1) the maximum fissile loading per pipe component is 140 FGE, (2) the spacing between the components (i.e., effective drum diameter) is reduced by the maximum amount reported in Section 4.1.5, and (3) the package arrays are infinite arrays stacked two high.

The detailed analysis presented in Packaging Technology, 2004[6], presents the results of a series of SCALE 4.4 CSAS25 module[7] (KENO-Va version 4) calculations that establish a maximum system reactivity ($k_s + 2\sigma$) of less than 0.933 and the corresponding Upper Subcriticality Limit (USL) of 0.9377. Therefore, the shipment of 200 FGE or 140 FGE per pipe overpack for Cases E and F, respectively, in the TRUPACT-II and HalfPACT is safely subcritical.

4.1.7 Shielding Analysis of the Standard Pipe Overpack

Adequate shielding is provided in the standard pipe overpack and TRUPACT-II or HalfPACT shipping configuration to ensure that no radioactive payload will exceed the dose rate limits established by 10 CFR 71.47(a) for normal conditions of transport (NCT) or 10 CFR 71.51(a)(2) for hypothetical accident conditions (HAC). Compliance with dose rate limits specified in Section 3.2 of the CH-TRAMPAC for individual pipe overpacks and loaded TRUPACT-IIs or HalfPACTs will be achieved by preshipment radiological surveys. Compliance with NCT and HAC radiation dose rate limits is ensured through the preshipment radiological surveys as demonstrated below. The 6-in. and 12-in. diameter pipe components provide a nominal 0.280 in. and 0.250 in. of steel (pipe wall thickness), respectively, for shielding of gamma radiation. Effective radiation shielding depends on a continuous barrier of dense material (i.e., steel) without "line-of-sight" openings that would allow radiation leakage or "streaming." The pipe components have design features to prevent radiation streaming through the relatively low density filter media of the filter vents.

Incorporated in the original design of the 12-in. diameter pipe component lid is a 3/16-in. thick steel shielding plate attached to the lid under the filter opening to prevent radiation streaming through the filter media material and to provide puncture protection to the filter media from any solid contents within the pipe component (see Figure 4.1-6a). These features are incorporated slightly differently in the 6-in. diameter pipe component and the revised design of the 12-in.

---

[7] SCALE4.4., "Modular Code System for Performing Standardized Computer Analyses for Licensing Evaluation for Workstations and Personal Computers," RSICC code package C00545/MNYCP00, Oak Ridge National Laboratory, September 1998.

diameter pipe component. Because their lids are thicker than that of the original 12-in. diameter pipe component, the filter vent does not penetrate the entire thickness of either lid, and shielding is provided by the remaining steel at the bottom of the tapped hole for the filter vent. Continuous venting is provided by four small holes that penetrate the remaining steel lid thickness. The holes are offset from the filter media and thereby avoid a line-of-sight radiation streaming path (see Figure 4.1-6b).

The NCT and HAC radiation dose rate limits are met by ensuring, through preshipment radiological surveys, that the surface dose rate of each pipe overpack is less than 200 millirem per hour (mrem/hr), the surface dose rate of the TRUPACT-II or HalfPACT is less than 200 mrem/hr, and the 2-meter dose rate of the TRUPACT-II or HalfPACT is less than 10 mrem/hr. Ammerman and Bobbe (1995)[3] bounds the radial crush of the pipe overpack during a HAC event at 2.16 in., while the TRUPACT-II and HalfPACT provide approximately 10 in. of additional distance attenuation beyond that of a single pipe overpack in the NCT configuration. The TRUPACT-II and HalfPACT also provide additional material attenuation in the form of the ICV, outer containment vessel, and outer containment assembly inner shells that have a combined thickness of 0.688 in. and 0.438 in. in the NCT and HAC configurations, respectively. The increase in distance and material attenuation provided by the TRUPACT-II and HalfPACT, in addition to the structural integrity of the pipe overpack, ensure that the NCT dose rates will not be significantly increased during a normal condition event and that the HAC dose rate limit will not be exceeded during a hypothetical accident condition.

4.1.8 Authorized Payload Contents for the Standard Pipe Overpack

The results of the criticality analyses show the pipe component to be an effective instrument for criticality control. TRUPACT-II or HalfPACT shipments of standard pipe overpacks with contents meeting the requirements of Case E at 200 FGE per standard pipe overpack are subcritical in all cases. Therefore, the pipe component FGE limit for payloads with Case E contents is 200 g, and 2,800 g per TRUPACT-II or 1,400 g per HalfPACT. The FGE limit for payloads with Case F contents is 140, 980, and 1,960 FGE for the pipe overpack, HalfPACT, and TRUPACT-II, respectively.

Section 3.2 of the CH-TRAMPAC requires that each individual standard pipe overpack and loaded TRUPACT-II or HalfPACT be measured prior to shipment to verify compliance with a dose rate limit of 200 mrem/hr at the surface. Additionally, Section 3.2 of the CH-TRAMPAC requires that each loaded TRUPACT-II or HalfPACT be measured prior to shipment to verify compliance with a dose rate limit of 10 mrem/hr at 2 meters. The results of the shielding evaluation show that, when the standard pipe overpack is in compliance with the preshipment survey surface dose rate limit, the dose rate requirements of 10 CFR 71.47(a) and 10 CFR 71.51(a)(2) are met for a TRUPACT-II loaded with 14 standard pipe overpacks or a HalfPACT loaded with 7 standard pipe overpacks.

The results of the pipe overpack test program and the structural analysis demonstrate the effectiveness of the pipe component to maintain containment of waste under normal conditions of transport and hypothetical accident conditions. As illustrated, the containment provided by the pipe component will allow for the effective immobilization of CH-TRU waste materials.
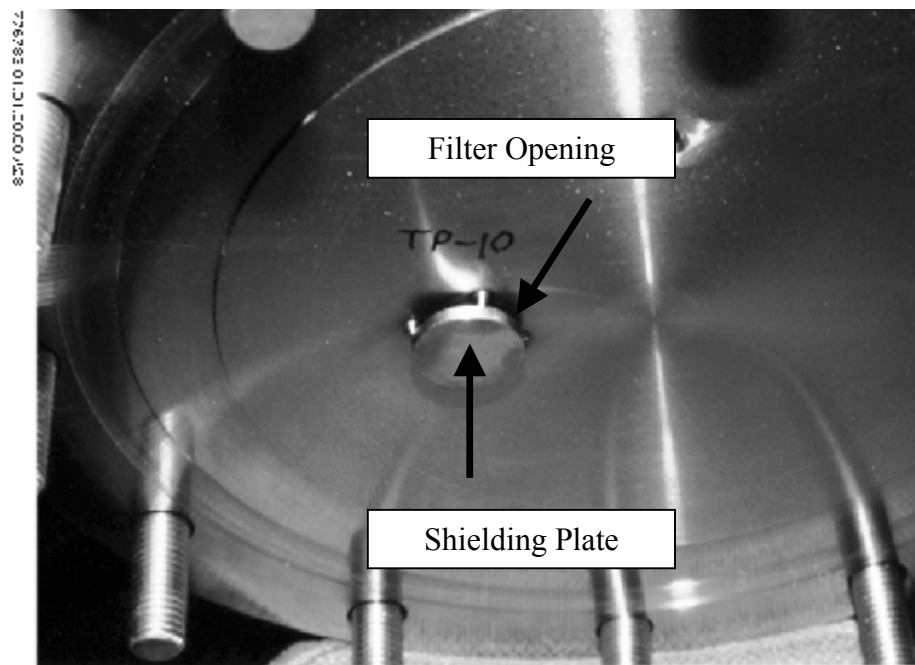
4.1-6a.   Lid of 12-inch diameter pipe component showing 3/16-inch thick steel shielding plate attached under filter opening (bottom view).
Lid of 12-inch diameter pipe component showing 3/16-inch thick steel
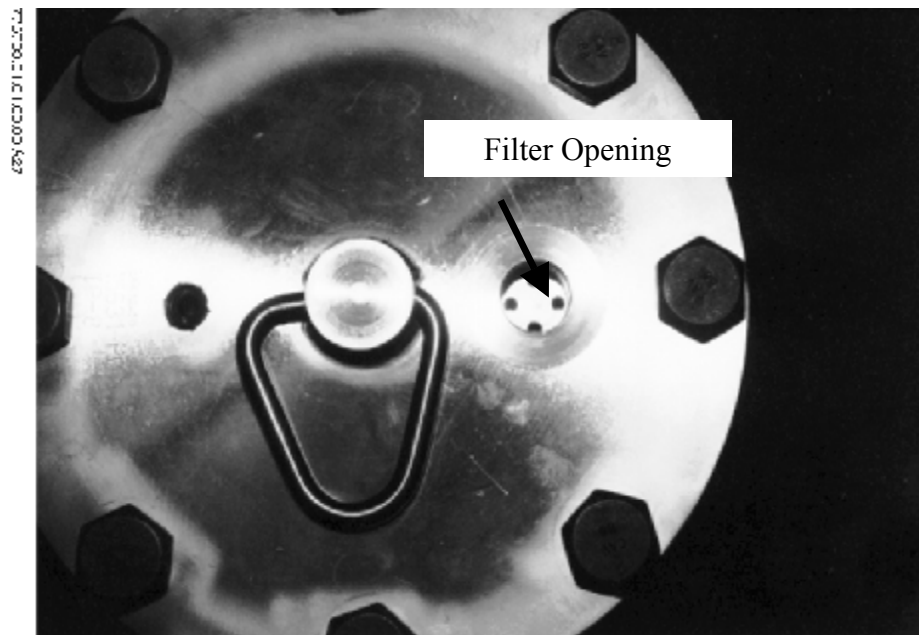
4.1-6b.   Lid of 6-inch diameter pipe component without filter showing four small holes, which penetrate the lid thickness (top view). The holes are offset from the filter media when the filter vent is installed.

Figure 4.1-6 – Photographs of Pipe Component Shielding Features

4.1.9 Conclusion

The standard pipe overpack consists of a pipe component positioned by dunnage within a 55-gallon drum with a rigid liner and lid. The tests and analyses summarized by this appendix demonstrate the ability of the pipe overpack to provide three significant control functions: (1) criticality control, (2) shielding, and (3) containment of fine particulate waste material during normal conditions of transport and hypothetical accident conditions.

The primary purpose of the pipe overpack is to allow the shipment of up to 7 pipe overpacks in a HalfPACT or up to 14 pipe overpacks in a TRUPACT-II, each with a maximum FGE loading of 200 g for payloads with contents meeting the requirements for Case E and 140 g for payloads with contents meeting the requirements for Case F. The results of the criticality analyses show that a payload of pipe overpacks is subcritical in all cases. As determined by the criticality analyses, the FGE limit is 2,800 g per TRUPACT-II and 1,400 g per HalfPACT for Case E shipments of waste packaged in standard pipe overpacks and 1,960 g per TRUPACT-II and 980 g per HalfPACT for Case F shipments of waste packaged in standard pipe overpacks.

The shielding evaluation shows that, when the standard pipe overpack is in compliance with the preshipment survey dose rate limit, the dose rate limits for NCT and HAC are met.

This page intentionally left blank.

APPENDIX 4.2

DESCRIPTION OF S100 PIPE OVERPACK

This page intentionally left blank.

4.2   Description of S100 Pipe Overpack

4.2.1   Introduction

The S100 pipe overpack is based closely on the standard pipe overpack described in Appendix 4.1 of the CH-TRU Payload Appendices. It differs from the standard pipe overpack in that most of the cane fiberboard dunnage is replaced with neutron shielding material. In addition, neutron shielding material is placed within the pipe component, above, below, and around the payload. It is intended for the shipment of sealed neutron sources in the TRUPACT-II and the HalfPACT. Appendix 1.3.1 of the TRUPACT-II Safety Analysis Report (SAR), Appendix 1.3.1 of the HalfPACT SAR, and Section 2.9.3 of the Contact-Handled Transuranic Waste Authorized Methods for Payload Control (CH-TRAMPAC) describe the materials of construction, size, and other dimensional specifications for the S100 pipe overpack. Up to 14 S100 pipe overpacks may be shipped in the TRUPACT-II, and up to 7 S100 pipe overpacks may be shipped in the HalfPACT. This appendix describes the structural, criticality, and shielding basis of the S100 pipe overpack.

4.2.2   Description

The S100 pipe overpack consists of a 6-inch (in.) pipe component surrounded by neutron shielding material on the sides and by cane fiberboard and plywood dunnage on the top and bottom, within a 55-gallon drum with a rigid polyethylene liner and lid. A schematic of the S100 pipe overpack is shown in Figure 4.2-1. The 6-in. pipe component used in the S100 pipe overpack is identical to the 6-in. pipe component used in the standard pipe overpack described in Appendix 4.1 of the CH-TRU Payload Appendices. Furthermore, the pipe component is placed within the drum, using the same type of cane fiberboard and plywood dunnage below the lower surface of the pipe component and above the upper surface of the pipe component. The space around the sides of the pipe component is filled with a neutron shielding material. The neutron shield may be in the form of a casting (such as a commercial neutron shielding casting compound), a solid monolith (such as a molded or machined unit of solid plastic), or fabricated component (such as a tightly wound roll of plastic film or other built-up fabrication). The minimum properties of the neutron shielding material are given in Section 4.2.6. The neutron shield extends from the lower edge of the pipe component up to the top surface of the lid of the pipe component, and rests on the lower plywood dunnage. The S100 Pipe Overpack is shown in Figure 4.2-1. To provide shielding for the top and bottom of the pipe component, rigid high-density polyethylene plugs approximately 6 in. in diameter and 6.5 in. long are placed below the payload (in the bottom of the pipe component), and above the payload (below the lid of the pipe component) as shown in Figure 4.2-1. A rigid high-density polyethylene shield sleeve is placed between the two end plugs, as shown in Figure 4.2-1.

55-GALLON DRUM
LID W/ FILTER VENT,
LID RING, AND
GASKET

55-GALLON DRUM
VENTED RIGID
LINER LID

PIPE COMPONENT
UPPER DUNNAGE

PIPE COMPONENT
LID W/FILTER

UPPER
SHIELD PLUG

SHIELD SLEEVE

LOWER
SHIELD PLUG

6 IN.
PIPE COMPONENT
BODY W/ GASKET

SIDE SHIELD

PIPE COMPONENT
LOWER DUNNAGE

55-GALLON DRUM
BODY W/ RIGID
LINER BODY

CONTENTS
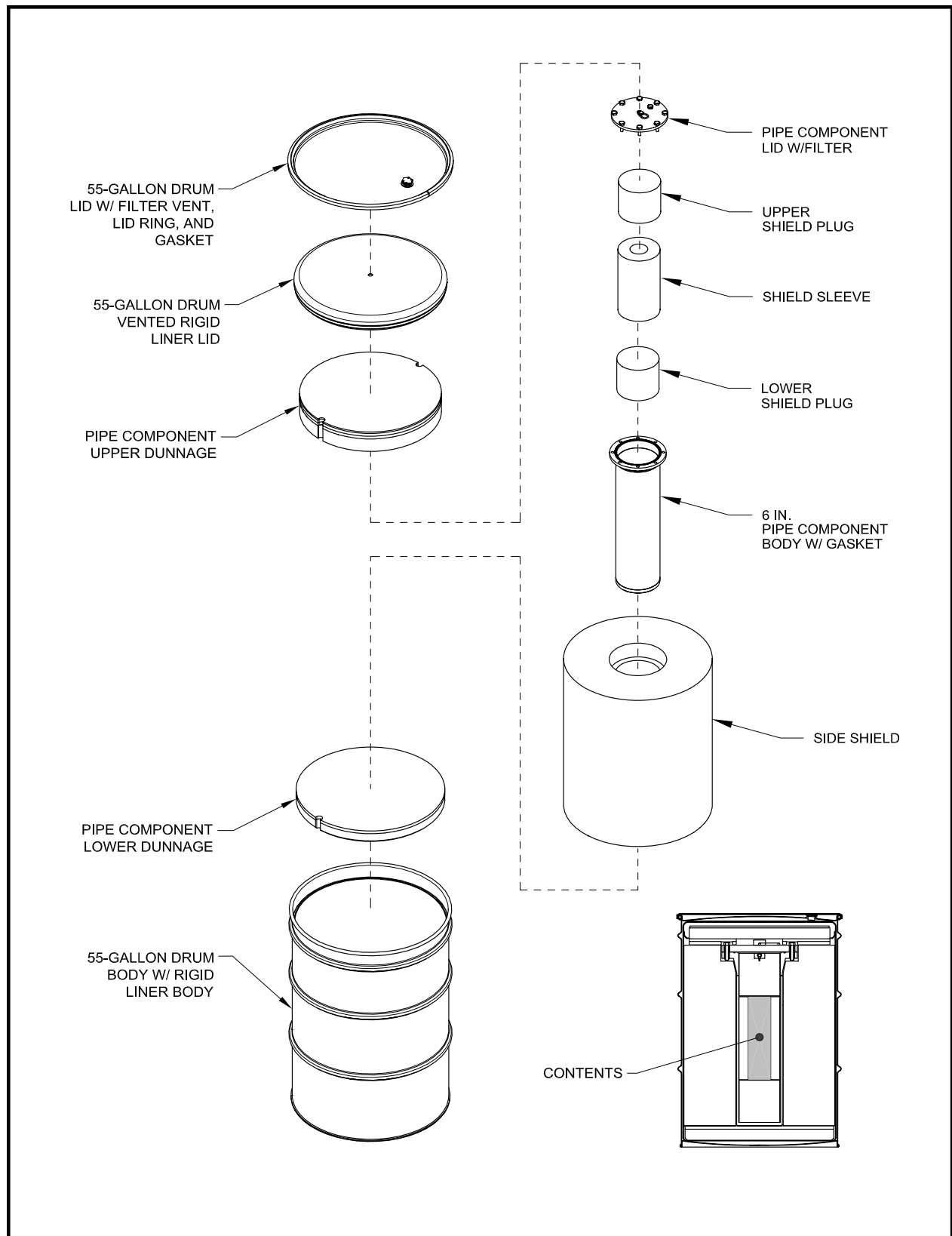
Figure 4.2-1 — S100 Pipe Overpack

The pipe component is a stainless steel, cylindrical pipe of 0.280 in. nominal thickness with a welded or formed bottom cap and a bolted stainless steel lid sealed with a butyl or ethylene-propylene rubber O-ring. The pipe component is approximately 2 feet (ft.) long and has an inner diameter of 6 in. The S100 pipe component is identical to the description of the standard 6-in. pipe component, including the filter vent, found in Appendix 4.1 of the CH-TRU Payload Appendices. The S100 pipe component provides three significant control functions: 1) criticality, 2) shielding, and 3) confinement of the payload. The S100 pipe overpack is designed for the transport of specific sealed neutron source waste forms. The following sections demonstrate the effectiveness of the S100 pipe overpack design for normal conditions of transport (NCT) and hypothetical accident conditions (HAC). All demonstrations are by analysis or by reference to the standard pipe overpack, unless stated otherwise.

4.2.3 Structural Analysis for Normal Conditions of Transport

Under NCT, the S100 pipe overpack remains leaktight and retains the sealed neutron sources within the pipe component. Since the pipe component remains leaktight under HAC as demonstrated in Section 4.2.4, this bounds all NCT, and demonstrations specific to NCT are not necessary.

The maximum damage that could occur to the shielding material in a normal condition free drop is evaluated as follows. As specified in Section 2.9.3 of the CH-TRAMPAC, the maximum weight of the loaded S100 pipe overpack is 550 pounds (lbs). The normal condition free drop height is 3 ft., or 36 in. The maximum damage to the shielding by crush deformation occurs in the side drop orientation. In this orientation, the weight of five of the drums in one layer may be conservatively assumed to be supported by a single drum in the lowest position as shown in Figure 4.2-2. (The two drums on either side of the lowest position each support their own weight.) A determination of crush distance is found by conservatively assuming that 25% of the drop energy of five drums is absorbed by the crush of the neutron absorbing material on one side of the lowest drum, where the percentage of energy absorbed by the neutron absorbing material is derived in Section 4.2.4. The drop energy (E), measured in inch-pounds (in.-lbs), to be absorbed by the neutron shield is:

$$E = 0.25 * (550 \text{ lbs} * 5 * 36 \text{ in.}) = 24,750 \text{ in.-lbs}$$

At the maximum payload temperature of 170ºF, the minimum crush strength of the neutron shielding material is $\sigma = 300$ pounds per square inch (psi). Therefore, to absorb this energy, the volume (V), measured in cubic inches (in^3), of crushed material is:

$$V = \frac{E \text{ in.-lbs}}{\sigma \text{ psi}} = 82.50 \text{ in}^3$$

5W
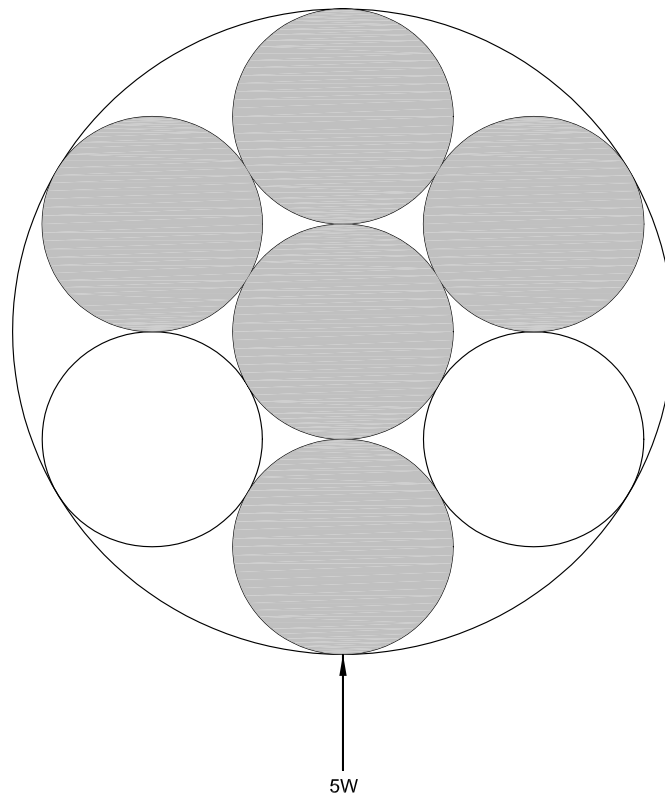
Figure 4.2-2 — NCT Side Drop Drum Loading Diagram

The volume is in the form of a segment of a cylinder having a length equal to the length of the neutron shielding material, or L = 26.7 in. The area (A) of the segment is therefore

$$A = \frac{V \text{ in}^3}{L \text{ in.}} = 3.08 \text{ in}^2$$

Based on the area of the circular segment and on the outer diameter of the shield material of 21.5 in., the depth of crush is computed to be 0.63 in. A conservative value of 2 inches is used in the normal condition shielding analysis discussed in Section 4.2.6 of this appendix.

As an alternative to specifying the shielding material crush strength, a test of the full-scale shielding component may be performed. The test shall demonstrate that the shield is capable of absorbing an amount of energy equal to 24,750 in-lbs with 2 in. or less of radial deformation. The energy absorbed may be calculated by integration of the force-deflection curve or other equivalent means. The test must be performed with a material temperature of at least 170ºF.

If cast neutron shielding material is used, some moisture may be hydrated by the material upon solidification. At the maximum payload container temperature of 170ºF, this moisture could produce a partial pressure of only 6 psi absolute, which would be the case for any moist payload. Therefore, the shielding material does not cause the pressure within the ICV to exceed the bounding maximum value of 61.2 psi absolute given in Section 2.6 of the TRUPACT-II and HalfPACT SARs.

4.2.4 Structural Analysis for Hypothetical Accident Conditions

Under HAC, the S100 pipe overpack remains leaktight and retains the sealed neutron sources within the pipe component. It is shown in Section 4.2.6 that an adequate level of biological shielding for HAC is achieved without any aid from the shielding in the S100 pipe overpack. Since the shielding in the S100 pipe overpack is not required for the HAC shielding analysis, the damage to the shielding material in the accident free drop does not need to be quantified. However, the reduced effective drum diameter, which prescribes the resultant pipe component spacing utilized in the criticality analysis, does need to be quantified.

To demonstrate that the pipe component remains leaktight and retains the sealed neutron sources within the pipe component in a 30 ft. free drop, reference is made to the testing of the Standard Pipe Overpack, as documented in Appendix 4.1 of the CH-TRU Payload Appendices. To account for design differences of the S100 Pipe Overpack, an additional test was performed, as documented below. Normal conditions of transport are bounded by these tests.[1]

The testing of the Standard Pipe Overpack, as documented in Appendix 4.1 of the CH-TRU Payload Appendices, consisted of two types of tests: 1) end drop testing, in which a stacked arrangement of drums was dropped from a height of 30 ft. in an end drop orientation, i.e., along

---

[1] Packaging Technology, Inc., July 2002, "30' Free Drop Test Report for the S100 Overpack," TR-013, Packaging Technology, Inc., Tacoma, Washington.

the axis of the drums, and 2) side drop testing, in which a bare TRUPACT-II ICV filled with test drums was dropped from 30 ft. in a horizontal orientation. Since, in the S100 design, the energy absorbing configuration at each axial end of the pipe component is identical to the Standard Pipe Overpack design, it was not necessary to repeat the end drop testing. In the side drop testing, however, the load path is through the material that is placed around the sides of the pipe component. In the prior Standard Pipe Overpack testing, this material was Celotex dunnage, and in the S100, it is made of neutron shielding material, which could have a different force-deflection behavior than the dunnage. Therefore, to clearly demonstrate that the S100 remains leaktight under hypothetical accident conditions, an additional drop test was performed.

The test consisted of a drop of a single, bare S100 package from a height of 30 ft. in a horizontal orientation onto an essentially unyielding surface. This test was conservative relative to a hypothetical accident drop inside a TRUPACT-II, since it neglected all of the impact absorption ability of the TRUPACT-II, and consequently, the impact was much higher. In addition, it was not necessary to place any weight on top of the S100 to represent the weight of the 'overburden' of drums ordinarily present within the ICV in a side drop orientation. This is because the effect of 'overburden' drums was conservatively included in the Standard Pipe Overpack drop testing using the 12-in. pipe component as follows:

- The 12-in. pipe version of the Standard Pipe Overpack weighed 547 lbs, which is essentially the same weight as the S100 at 550 lbs, and therefore the 'overburden' loading is equivalent;

- The 12-in. pipe component had a smaller nominal wall thickness and larger diameter than the 6-in. pipe component used in the S100, and thus was more liable to deformation under a given load;

- The 12-in. pipe component was surrounded by approximately 4.2 inches of Celotex dunnage, while the 6-in. pipe component in the S100 was surrounded by approximately 7 inches of neutron shielding, thus affording greater protection from the 'overburden' loads.

The test of the S100 focused, therefore, on the deceleration forces imposed on the 6-in. pipe component due to impact. Since the shielding material is generally stronger than the Celotex dunnage used to surround the 6-in. pipe component in the Standard Pipe Overpack, the impact forces on the pipe component in the S100 could be greater in a hypothetical accident free drop. Since the S100 is dropped bare, without any energy absorption materials present except the shield itself, it is very conservative compared to conditions within a complete TRUPACT-II or HalfPACT.

A helium mass spectrometer leakage rate test was performed before and after the drop test to evaluate the containment provided by the pipe component. There was no loss of leaktight containment as a result of the drop test. The leakage rate of the S100 pipe component after the 30 ft. drop was less than 1×10^{-7} cubic centimeters per second, air. In addition, the function of the filter vent in the lid of the pipe component was unimpaired, as verified by the filter manufacturer after the test.

The maximum radial crush of the S100 pipe overpack and the resulting minimum effective drum diameter from a 30 ft. free drop is determined by comparison of the crush strength and energy absorbing properties of the S100 Pipe Overpack's side neutron shield material and the 6-in. Standard Pipe Overpack's Celotex dunnage. The comparison demonstrates that the side neutron shield material will see less deformation than the Celotex material such that the maximum radial crush and resulting minimum effective drum diameter of 4.31 in. and 18.19 in., respectively observed in the 6-in. Standard Pipe Overpack drop testing and used in the S100 Pipe Overpack criticality analysis is conservative. The following analysis determines the percentage of total drop energy absorbed by the Celotex dunnage in the 6-in. Standard Pipe Overpack 30 ft. side drop.

Following the side drop crush logic provided in Section 4.2.3, the total drop energy from a 30 ft. side drop of an array of 6-in. standard pipe overpacks with a maximum weight of 328 lbs each (as specified in Section 2.9.2 of the CH-TRAMPAC) is given as follows:

$$E_{TOT} = (328 \text{ lbs} * 5 * 360 \text{ in.}) = 590,400 \text{ in.-lbs}$$

The actual energy absorbed by the Celotex dunnage in the lower drum can be determined from the measured radial drum crush value of 4.31 in. Based on the depth of crush and the outer diameter of the Celotex material of 21.5 in, the area (A) of the circular segment is computed to be 51.86 in^2. The crushed volume is in the form of a segment of a cylinder having a length equal to the length of the Celotex material, or L = 26.7 in. The crushed volume (V) is therefore

$$V = A \text{ in}^2 * L \text{ in.} = 1,384.66 \text{ in}^3$$

Based on the average plateau crush strength of Celotex at 150 °F of 90 psi[2], the actual energy (E) absorbed by the Celotex dunnage is

$$E_{ACT} = V \text{ in}^3 * \sigma \text{ psi} = 124,619 \text{ in.-lbs}$$

Therefore, the percentage of total to absorbed energy (f) is given as

$$f = \frac{E_{ACT}}{E_{TOT}} * 100 = 21\%$$

A conservative percentage of 25% is utilized in both the NCT and HAC crush determinations for the neutron shield material in the S100 pipe overpack. Accounting for the increased weight of the loaded S100 pipe overpack over that of the 6-in. standard pipe overpack and taking into account the fraction of total energy absorbed, the energy absorbed by the neutron shield material in a 30 ft. drop is given as follows:

---

[2] Walker, M.S., January 1991, "Packaging Materials Properties Data", Y/EN-4120, Martin Marietta Energy Systems, Inc., Oak Ridge, Tennessee.

$$E = 0.25 * \left(550 \text{ lbs} * 5 * 360 \text{ in.}\right) = 247,500 \text{ in.-lbs}$$

Following the calculational methodology employed for the NCT case with the minimum crush strength of the neutron shield material of $\sigma=300$ psi at 170ºF, the resulting maximum depth of crush of the neutron shield material is 3.01 in. where V=825.00 in^3, A=30.90 in^2, and L=26.7 in. Thus, the crush depth of neutron shielding material in the S100 pipe overpack is less than that observed for the 6-in. standard pipe overpack.

As an alternative to specifying the shielding material crush strength, a test of the full-scale shielding component may be performed. The test shall demonstrate that the shield is capable of absorbing an amount of energy equal to 247,500 in-lbs with 4 in. or less of radial deformation. The energy absorbed may be calculated by integration of the force-deflection curve or other equivalent means. The test must be performed with a material temperature of at least 170ºF. This energy absorption requirement is in addition to that specified for the NCT requirements (i.e., 24,750 in-lbs with 2 in. or less of radial deformation).

4.2.5 Criticality Analysis

A criticality analysis was performed for two different payload cases, depending on the quantities of special reflector materials in the payload container (see Chapter 6.0 of TRUPACT-II SAR or Chapter 6.0 of HalfPACT SAR for description of special reflector materials), as described below:

- Case E: For Case E, the contents of the pipe overpack payload container contain less than or equal to 1% by weight quantities of special reflector materials. The pipe overpack payload container may contain greater than 1% by weight quantities of special reflector materials provided that one of the following conditions is met:
  - o The special reflector materials are chemically or mechanically bound to the fissile material such that no reconfiguration or release of the bond is possible under normal or accident conditions, or
  - o The special reflector materials are present in thicknesses and/or packing fractions that render them less effective than a 25% polyethylene/75% water equivalent reflector per the limits in Table 6.2-1 of the TRUPACT-II or HalfPACT SAR.

- Case F: For Case F, the contents of the pipe overpack payload container contain greater than 1% by weight quantities of special reflector materials that do not meet the exceptions listed for Case E.

The criticality analysis demonstrates that a TRUPACT-II shipment of 14 pipe overpacks with contents meeting the requirements of Case E at 200 FGE of ^{239}Pu each (for a total of 2,800 FGE per TRUPACT-II) or a HalfPACT shipment of 7 pipe overpacks with 200 FGE each (for a total of 1,400 FGE per HalfPACT) ensures compliance with the requirements of Title 10, Code of

Federal Regulations (CFR), Sections 71.55 and 71.59 (10 CFR 71.55 and 71.59).[3] Additionally, shipments of pipe overpacks with contents meeting the requirements of Case F at 140 FGE for each payload container and 980 and 1960 FGE per HalfPACT and TRUPACT-II, respectively, ensure compliance with 10 CFR 71.55 and 71.59. Based on an infinite array of undamaged or damaged packages, the criticality transport index is 0.0.

The key parameters in the pipe overpack analysis for Case E are (1) the maximum fissile loading per pipe component is 200 FGE, (2) no more than 1% by weight quantities of special reflector materials are present or greater than 1% by weight quantities of special reflectors are either bound to the fissile material or meet the limits in Table 6.2-1 of the TRUPACT-II or HalfPACT SAR, (3) the spacing between the components (i.e., effective drum diameter) is reduced by the maximum amount reported in Section 4.2.4, and (4) the package arrays are infinite arrays stacked two high.

The key parameters in the pipe overpack analysis for Case F are (1) the maximum fissile loading per pipe component is 140 FGE, (2) the spacing between the components (i.e., effective drum diameter) is reduced by the maximum amount reported in Section 4.2.4, and (3) the package arrays are infinite arrays stacked two high.

The detailed analysis presented in Packaging Technology, 2004[3], presents the results of a series of SCALE 4.4 CSAS25 module[4] (KENO-Va version 4) calculations that establish a maximum system reactivity ($k_s + 2\sigma$) of less than 0.933 and the corresponding Upper Subcriticality Limit (USL) of 0.9377. Therefore, the shipment of 200 FGE or 140 FGE per pipe overpack for Cases E and F, respectively, in the TRUPACT-II and HalfPACT is safely subcritical.

4.2.6 Shielding Analysis

The payload of the S100 pipe overpack consists of neutron-emitting, actinide-bearing sealed sources, shown in Table 4.2-1. Source terms used in this analysis are for neutron emission and spectra for alpha-n reactions calculated by the SOURCES Version 4A computer code.[5] Of the sources shown in the table, the ^{238}Pu Be was determined to be the governing source for shielding calculations,[6] since it had the highest calculated unshielded dose rate of all the sources that will be transported in the S100.

---

[3] Packaging Technology, Inc., May 2004, "Pipe Overpack Criticality Analysis for the TRUPACT-II Package," ED-076, Packaging Technology, Inc., Tacoma, Washington.

[4] SCALE4.4., "Modular Code System for Performing Standardized Computer Analyses for Licensing Evaluation for Workstations and Personal Computers," RSICC code package C00545/MNYCP00, Oak Ridge National Laboratory, September 1998.

[5] Wilson, W.B., R.T. Perry, W. Charlton, et al., 1999, "SOURCES 4A: A Code for Calculating (alpha, n) Spontaneous Fission, and Delayed Neutron Sources and Spectra," LA-13639-MS, Los Alamos National Laboratory, Los Alamos, New Mexico.

[6] Gogol, S.L., and J. R. Bland, August 2002, "A Comparison of Dose Rates from (alpha, n) and Spontaneous Fission Neutron Sources," LA-UR-02-5120,.Los Alamos National Laboratory, Los Alamos, New Mexico.

Table 4.2-1 S100 Pipe Overpack Payloads

^{241}Am Be	^{238}Pu O	^{239}Pu Li	^{241}Am
^{238}Pu Be	^{239}Pu O	^{238}Pu B	^{238}Pu
^{239}Pu Be	^{244}Cm O	^{239}Pu F	^{239}Pu
^{241}Am O	^{241}Am Li	^{238}Pu ^{13}C	^{244}Cm

The radiation generated by the payload is in the form of neutrons and a relatively small amount of gamma radiation. Some additional gamma radiation is generated by capture of thermal neutrons in the neutron shielding. However, the gamma radiation remains a small fraction of the neutron radiation level.

Neutron shielding is afforded by placement of the pipe component within an annulus of shielding material, having an inner diameter of 7 in. and an outer diameter of 21.5 in. (conservatively neglecting the thickness of the drum poly liner). The side neutron shielding extends along the entire length of the pipe component as shown in Figure 4.2-1. The upper and lower shield plugs (6 in. in diameter and 6.5 in. long) and shield sleeve are made of solid high-density polyethylene and are placed within the pipe component. The side neutron shield may be in the form of a casting (such as a commercial neutron shielding casting compound), a solid monolith (such as a molded or machined unit of solid plastic), or fabricated component (such as a tightly wound roll of plastic film or other built-up fabrication). None of the materials of construction of the S100 pipe overpack, including the neutron shielding material, generate hydrogen gas in excess of 10^{-10} moles hydrogen per second per liter of headspace as a consequence of neutron or gamma irradiation by the payload sources.[7] A combination of the neutron shielding material and the materials of construction of the S100 pipe overpack provide sufficient shielding for both neutron and gamma radiation.

Any material used for the side neutron shield must meet minimum requirements for neutron attenuation and mechanical strength. Neutron attenuation must be at least as good as the reference material, which has an atomic fraction composition of 0.667 hydrogen and 0.333 carbon. A test shall be performed on any alternate materials used for the side shield assembly. The test sample, neutron source, test setup, and acceptance criteria shall be defined in a test specification. The acceptance criteria shall be that the measured neutron attenuation of the equivalent shielding material shall be equal to or greater than the attenuation predicted for the reference material, using the actual test setup and the shielding analysis code.

The side neutron shielding material will have a minimum mechanical strength at a temperature of 170ºF. The strength shall be defined as a minimum unit compressive crush strength of 300 psi. Alternatively, it may be defined as a maximum radial deformation of the full-scale shielding component under compressive load. The component must absorb a minimum of 24,750 in-lb. of

---

[7] Bustos, L.D., W.F. Sandoval, R. Villarreal, and L.R. Field, October 2000, "Hydrogen Generation Rate Potential from Neutron and Gamma Ray Interactions with Shielding/Packaging Materials Contained in the S100 Pipe Component Overpack," Los Alamos National Laboratory, Los Alamos, New Mexico.

energy with a maximum deformation of 2 in. and a minimum of 247,500 in-lb. of energy with a maximum deformation of 4 in., when loaded between the inner dimensions and outer dimensions of the component. Equivalent materials will not generate hydrogen gas in excess of 10^{-10} moles hydrogen per second per liter of headspace gas as a consequence of neutron or gamma irradiation.

Dose rate calculations were performed for a single S100 pipe overpack and for a TRUPACT-II in both the as-loaded and post-NCT free drop configurations.[8] The results were used to determine the maximum loading of the S100 pipe overpack such that the regulatory dose rate limits will be met in each case for NCT and HAC. In the analysis, the bounding payload of ^{238}Pu Be was used, as discussed above. Source gamma radiation was negligible and was not included, but capture gamma dose rate contribution was included in the calculated integrated dose rate. Dose rate calculations were made for a single S100 pipe overpack as presented for loading into a TRUPACT-II, for a TRUPACT-II as presented for transport with a payload of 14 identical S100 pipe overpacks each having the maximum payload, and for a TRUPACT-II including a conservative representation of NCT free drop damage with a payload of 14 identical S100 pipe overpacks each having the maximum payload. (The HAC case is discussed below.) Dose rates were calculated at the surface and at defined distances from the containers as shown in Table 4.2-2. As shown in the table, the limiting dose is for the TRUPACT-II package including NCT free drop damage, and is equal to 10 mrem/hr at a distance of 2 meters from the package surface. The corresponding S100 pipe overpack surface dose limit is 179 mrem/hr. This means that, as long as the surface dose rate of any S100 pipe overpack transported in a TRUPACT-II is at or below 179 mrem/hr, then the dose rate external to the TRUPACT-II will not exceed 10 mrem/hr at 2 meters including NCT free drop damage, nor will any of the other, less governing regulatory limits be exceeded. The TRUPACT-II calculations govern the case of the HalfPACT. Each S100 pipe overpack will be surveyed before loading into a TRUPACT-II or HalfPACT to ensure compliance with the limiting surface dose rate of 179 mrem/hr, as given in Section 3.2 of the CH-TRAMPAC.

The damage to the TRUPACT-II and payload under NCT is assumed to occur in the 3 ft. side drop, and is discussed in Section 4.2.3. The drums are modeled as resting on the inside of the TRUPACT-II ICV, which is resting on its side, and the bottom drum is crushed by a bounding distance of 2 in. The 2 in. of crushed shielding is conservatively assumed to be lost.

---

[8] Packaging Technology, Inc., August 2002, "Dose Rate Calculations for the S100 Pipe Overpack," ED-071, Packaging Technology, Inc., Tacoma, Washington.

Table 4.2-2 Maximum Dose Rates for S100 Pipe Overpack and TRUPACT-II

	Maximum Dose Rate (mrem/hr)	Limits (mrem/hr)④
S100 Surface	179 ±0.82	200
TRUPACT-II side Surface (undamaged) ①②	58.0 ±0.85	200
TRUPACT-II 2 meters (undamaged)	7.33 ±0.14	10
TRUPACT-II 5 meters (undamaged)③	1.76 ±0.04	2
TRUPACT-II side Surface (damaged)	128 ±1.4	200
TRUPACT-II 2 meters (damaged)	9.85 ±0.15	10

Notes:
1. TRUPACT-II contains 14 identical S100 pipe overpacks, each with a maximum surface dose rate of 179 mrem/hr or less.
2. Side dose rate governs over top or bottom dose rates.
3. The 5 meter distance corresponds to the normally occupied space of the truck cab.
4. Limits established by CH-TRAMPAC (S100 surface) or 10 CFR 71.47(b) (TRUPACT-II).

For HAC, the drums, neutron shielding material, pipe components, and internal dunnage are conservatively removed from consideration in the shielding calculation, and the sum total of all activity in the S100 payload is concentrated as a single point source resting on the inside surface of the TRUPACT-II ICV. In accordance with 10 CFR 71.51(a)(2), the dose point is located 1 meter from the external surface of the package. This is equivalent to a total distance from the source of 1 meter plus the minimum crushed wall thickness of the TRUPACT-II or HalfPACT. For simplicity and conservatism, the calculations assume that there is no material of any kind between the source and the dose point. The crushed wall thickness is found by subtracting the HAC 30-foot free drop side orientation crush damage from the original wall thickness of the package as follows. The outer diameter of the package is 94.38 inches, and the inner diameter of the ICV is 73.63 inches, which gives an undamaged wall thickness of 10.38 inches. The maximum crush damage is found in Table 2.10.3-1 of the TRUPACT-II SAR for Test No. 2, as equal to 3.63 inches. The remaining wall thickness is then equal to 10.38 – 3.63 = 6.75 inches. In the shielding calculations, a value of 6.5 inches is conservatively used. As already discussed, no material is assumed to fill this space. The resulting maximum allowable activity within the TRUPACT-II is a total of 406 Ci, and the resulting conservative dose rate is 999 mrem/hr at 1 meter from the crushed TRUPACT-II surface, which meets the requirements of 10 CFR 71.51(a)(2). As for NCT, the TRUPACT-II HAC calculations govern the case of the HalfPACT.

4.2.7 Authorized Payload Contents

As demonstrated in Section 4.2.6, when loaded with sealed neutron sources of the types specified in Table 4.2-1 (the authorized contents), the S100 pipe overpack meets all regulatory dose rate limits. The bounding payload is defined in three ways: (1) a maximum dose rate on the surface of the S100 pipe overpack of 179 mrem/hr for any S100 pipe overpack placed into the TRUPACT-II or HalfPACT, (2) a maximum activity of 406 Ci within a single TRUPACT-II or HalfPACT, and (3) a maximum payload of 200 FGE per S100 pipe overpack, or a total of 2,800 FGE per TRUPACT-II or 1,400 FGE per HalfPACT when the contents meet the requirements of Case E, or (4) a maximum payload of 140 FGE per S100 pipe overpack, or a total of 1,960 FGE per TRUPACT-II or 980 FGE per HalfPACT when the contents meet the requirements of Case F. Section 4.2.5 demonstrates that 200 FGE per S100 pipe overpack is safely subcritical for Case E shipments and that 140 FGE per S100 pipe overpack is safely subcritical for Case F shipments.

4.2.8 Conclusion

The S100 pipe overpack design is based on the standard pipe overpack. It consists of a 6-in. pipe component within a 55-gallon drum, including a rigid liner and lid. Dunnage is placed above and below the pipe component, and neutron shielding material is placed on the sides of the component. Within the pipe component are placed rigid high-density polyethylene shield plugs and insert. The analyses summarized in this appendix demonstrate the ability of the S100 pipe overpack to provide three significant control functions under NCT and HAC: (1) criticality, (2) shielding, and (3) confinement of the payload.

The primary purpose of the S100 pipe overpack is to allow the shipment of sealed neutron sources of the types listed in Table 4.2-1. The structural analysis shows that the pipe component remains leaktight and the neutron sources remain confined within the pipe component in conservatively bounded normal and accident free drops. For criticality, it is shown that 200 FGE per S100 pipe overpack for Case E payloads is safely subcritical and 140 FGE per S100 pipe overpack is safely subcritical for Case F payloads. The shielding analysis shows that, with the maximum authorized contents, the dose rate limits for NCT and HAC (including appropriate shielding damage assumptions in each case) are met.

This page intentionally left blank.

APPENDIX 4.3

DESCRIPTION OF S200 PIPE OVERPACK

This page intentionally left blank.

4.3   Description of S200 Pipe Overpack

4.3.1   Introduction

The S200 pipe overpack is based closely on the standard pipe overpack described in
Appendix 4.1 of the CH-TRU Payload Appendices. It differs from the standard pipe overpack
through the addition of a gamma shield insert located by dunnage inside the pipe component. It
is intended for the shipment of transuranic waste forms with high gamma energies in the
TRUPACT-II and HalfPACT. Appendix 1.3.1 of the TRUPACT-II Safety Analysis Report
(SAR), Appendix 1.3.1 of the HalfPACT SAR, and Section 2.9.4 of the Contact-Handled
Transuranic Waste Authorized Methods for Payload Control (CH-TRAMPAC) describe the
materials of construction, sizes, and other dimensional specifications for the S200 pipe overpack.
Up to 14 S200 pipe overpacks may be shipped in the TRUPACT-II, and up to 7 S200 pipe
overpacks may be shipped in the HalfPACT. This appendix describes the structural, criticality,
and shielding basis of the S200 pipe overpack.

4.3.2   Description

The S200 pipe overpack consists of a gamma shield insert located by rigid polyurethane foam
dunnage inside a standard 12-inch (in.) pipe component which is, in turn, located by cane
fiberboard and plywood dunnage within a standard 55-gallon drum with a rigid polyethylene
liner and lid. A schematic of the S200 pipe overpack is shown in Figure 4.3-1. The 12-in. pipe
component, cane fiberboard and plywood dunnage, and 55-gallon drum with rigid polyethylene
liner and lid are identical to the standard pipe overpack described in Appendix 4.1 of the
CH-TRU Payload Appendices.

The gamma shield insert is a lead two-component assembly consisting of a cylindrical body with
an integral bottom cap and a detachable lid. The shield insert is available in two sizes; the
S200-A shield insert has a nominal thickness of 1.000 in. and the S200-B shield insert has a
nominal thickness of 0.600 in. The overall dimensions of the S200-A and S200-B shield inserts
are nominally 10.125 in. diameter by 10.625 in. long and 9.325 in. diameter by 17.825 in. long,
respectively. The rigid polyurethane foam dunnage fills the bottom and annular space between
the shield insert and the 12-in. pipe component to position the insert near the lid of the pipe
component.

The pipe component provides three significant control functions: (1) criticality control,
(2) shielding, and (3) confinement of the waste material. Additionally, the gamma shield insert
also provides a shielding control function. The following sections demonstrate the effectiveness
of the S200 pipe overpack design for normal conditions of transport (NCT) and hypothetical
accident conditions (HAC). All demonstrations are by analysis or by reference to the standard
pipe overpack analysis and testing, unless stated otherwise.
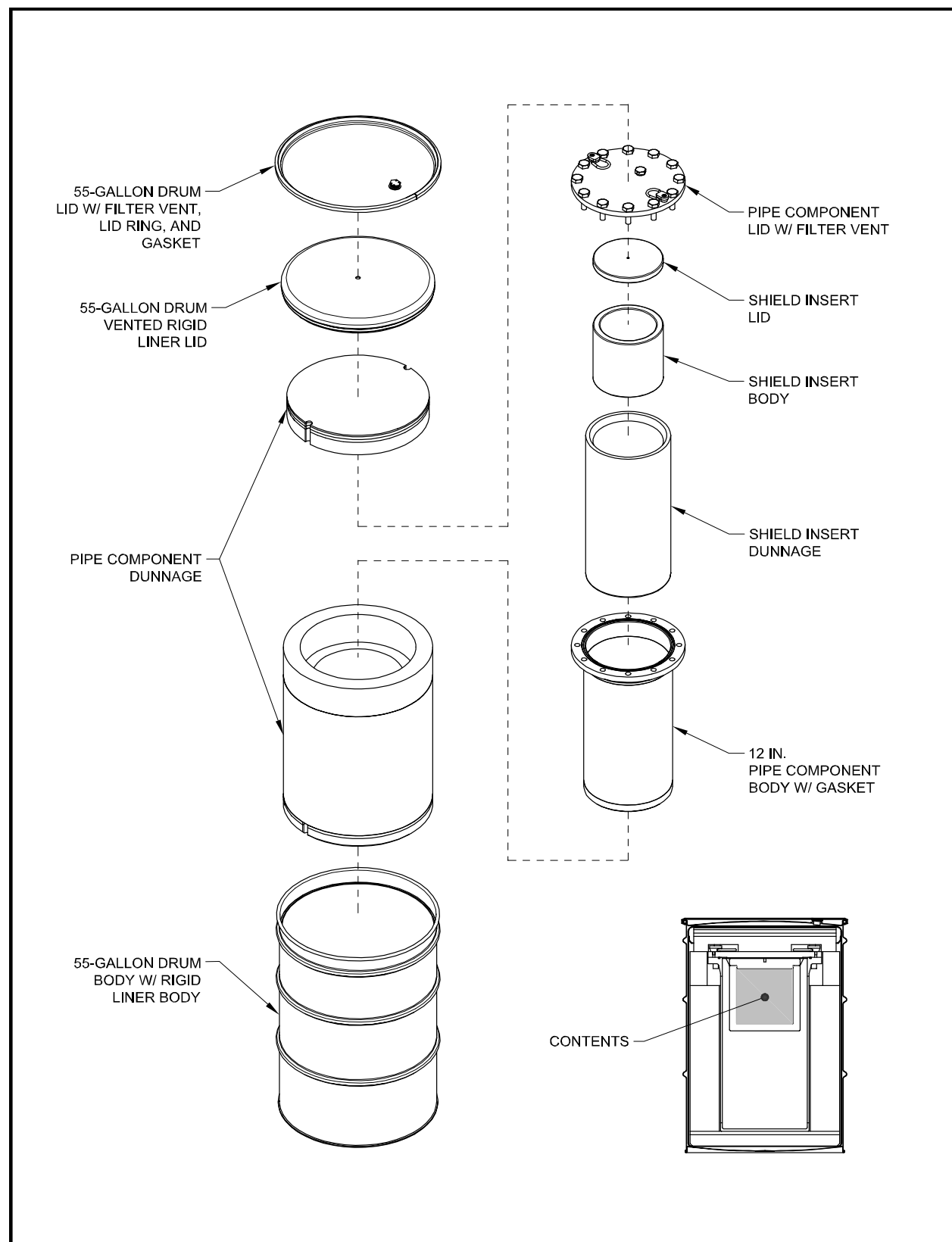
Figure 4.3-1 — S200 Pipe Overpack

4.3.3 Structural Analysis For NCT

The structural effectiveness of the S200 pipe overpack for NCT is demonstrated by showing that the waste contents are confined within the pipe component. The structural effectiveness of the pipe component for NCT is bounded by the structural effectiveness evaluation for HAC given in Section 4.3.4. It is shown in Section 4.3.6 that an adequate level of biological shielding for NCT is afforded by the materials of construction of the TRUPACT-II and HalfPACT, pipe components, and shield inserts themselves, with the 55-gallon drum, fiberboard dunnage, and foam dunnage providing only a distance attenuation contribution. The maximum deflection and resulting radial shift of the pipe overpack array for the NCT side drop, which is limiting for shielding calculations, is bounded by the HAC side drop analysis provided in Section 4.3.4. Additionally, the spacing between pipe components (i.e., effective drum diameter) utilized in the criticality analysis is also bounded by the HAC side drop analysis provided in Section 4.3.4. The following analysis evaluates the maximum damage to the shield insert rigid polyurethane foam dunnage in the end and side drop orientations and thereby shows that the shield lid remains engaged with the shield body and quantifies the maximum shift of the shield insert inside the pipe component.

The shield insert is positioned inside the pipe component by rigid polyurethane foam dunnage with a maximum clearance between the pipe component and shield insert lid of 0.125 in. The shield insert lid has a step feature that has a minimum length of 0.500 in. Therefore, limiting the axial crush of the foam dunnage to less than $(0.500 - 0.125) = 0.375$ in. in any drop orientation ensures that the shield lid remains engaged with the shield body. The maximum crush deformation of the foam in the end drop orientation may be bounded by assuming all of the drop energy of the shield insert and contents is absorbed by the foam beneath the shield insert body. The drop energy (E) to be absorbed for the S200-A and S200-B shield inserts is the product of the weight of the shield insert and contents in pounds (lbs) and the height of the drop (36 in.):

$$E_{S200-A} = (202 \text{ lbs}) (36 \text{ in.}) = 7{,}272 \text{ in.-lbs}$$
$$E_{S200-B} = (206 \text{ lbs}) (36 \text{ in.}) = 7{,}416 \text{ in.-lbs}$$

Under NCT, the average temperature of the contents of a drum is bounded by a temperature of 170°F for the case where decay heat is uniformly distributed among all drums, as shown in Table 3.4-1 of the HalfPACT SAR. The minimum parallel-to-rise compressive strength of the rigid polyurethane foam material is $\sigma = 400$ pounds per square inch (psi) at 170°F. Therefore, to absorb this energy, the volume (V) of the crush material in cubic inches (in^3) is:

$$V_{S200-A} = E_{S200-A} / \sigma = (7272 \text{ in.-lbs}) / (400 \text{ psi}) = 18.180 \text{ in}^3$$
$$V_{S200-B} = E_{S200-B} / \sigma = (7416 \text{ in.-lbs}) / (400 \text{ psi}) = 18.540 \text{ in}^3$$

This volume is in the form of a right circular cylinder with a diameter equal to the shield body that generates the following crush area (A) in square inches (in^2):

$$A_{S200-A} = (\pi/4) (D_{S200-A})^2 = (\pi/4) (10.125 \text{ in.})^2 = 80.516 \text{ in}^2$$
$$A_{S200-B} = (\pi/4) (D_{S200-B})^2 = (\pi/4) (9.325 \text{ in.})^2 = 68.295 \text{ in}^2$$

The bounding axial crush of the foam dunnage and resulting maximum separation of shield body and lid (H) is defined as:

$$H_{S200-A} = V_{S200-A} / A_{S200-A} = (18.180 \text{ in}^3) / (80.516 \text{ in}^2) = 0.226 \text{ in.}$$
$$H_{S200-B} = V_{S200-B} / A_{S200-B} = (18.540 \text{ in}^3) / (68.295 \text{ in}^2) = 0.271 \text{ in.}$$

Therefore, the minimum positive engagement between the shield body and lid in a maximum axial foam crush event is 0.104 in.

The maximum radial shift of the shield insert within the pipe component is also bounded through a volumetric crush analysis. The drop energy is the same as that defined above. The minimum perpendicular-to-rise compressive strength of the rigid polyurethane foam material is $\sigma = 300$ psi at 170°F. Therefore, to absorb this energy, the volume of the crush material is:

$$V_{S200-A} = E_{S200-A} / \sigma = (7272 \text{ in.-lbs}) / (300 \text{ psi}) = 24.240 \text{ in}^3$$
$$V_{S200-B} = E_{S200-B} / \sigma = (7416 \text{ in.-lbs}) / (300 \text{ psi}) = 24.720 \text{ in}^3$$

The product of the shield body length (L) and the crescent-shaped area generated by the radial shift defines the crush volume. Therefore, the area of crush material is given by:

$$A_{S200-A} = V_{S200-A} / L_{S200-A} = (24.240 \text{ in}^3) / (9.625 \text{ in.}) = 2.518 \text{ in}^2$$
$$A_{S200-B} = V_{S200-B} / L_{S200-B} = (24.720 \text{ in}^3) / (17.225 \text{ in.}) = 1.435 \text{ in}^2$$

The bounding radial crush of the foam dunnage and resulting maximum radial shift of the shield body and lid (R) is defined as:

$$R_{S200-A} = A_{S200-A} / D_{S200-A} = (2.518 \text{ in}^2) / (10.125 \text{ in.}) = 0.249 \text{ in.}$$
$$R_{S200-B} = A_{S200-B} / D_{S200-B} = (1.435 \text{ in}^2) / (9.325 \text{ in.}) = 0.154 \text{ in.}$$

The side drop crush distances are accounted for in the NCT shielding analysis discussed in Section 4.3.6.

4.3.4 Structural Analysis for HAC

The structural effectiveness of the S200 pipe overpack for HAC is demonstrated by showing that the waste contents remain confined within the pipe component. It is shown in Section 4.3.6 that an adequate level of biological shielding for HAC is afforded by the materials of construction of the TRUPACT-II or HalfPACT and pipe components, themselves, without any aid from the shield inserts inside the pipe components. The 55-gallon drum and fiberboard dunnage provides only a distance attenuation contribution. Since the shield insert in the S200 pipe overpack is not required for the HAC shielding analysis, the damage to the shielding material in the accident free drop does not need to be quantified. However, the maximum deflection and resulting radial shift of the pipe overpack array will be quantified for the side drop orientation, which is limiting for

shielding calculations. The following comparative analysis shows that the contents remain confined within the pipe component under the HAC free drop. Additionally, the analysis shows the maximum deflection of pipe overpacks and the resulting stacked array configuration resulting from the HAC free side drop.

As shown in Table 2.9-7 of Section 2.9.2 of the CH-TRAMPAC, the weight of the 12-in. standard pipe component contents is bounded by a value of 225 lbs. Additionally, as shown in Table 2.9-16 of Section 2.9.4 of the CH-TRAMPAC, the total weight of the S200 pipe overpack shield insert, dunnage, and contents is bounded by a value of 225 lbs. Because the design of the standard and S200 pipe overpacks are structurally identical except for items inside the pipe component and since the weight limit for items inside the pipe component are identical, all structural evaluations of the standard pipe overpack apply to the S200 pipe overpack. Ammerman and Bobbe, 1995,[1] demonstrates the leak tightness of the standard pipe overpack when subjected to HAC testing. Therefore, the waste contents will remain confined within the pipe component under the HAC free drop.

Additionally, Ammerman and Bobbe[1] report a 20.250 in. minimum deformed pipe overpack diameter resulting from a free side drop orientation. Therefore, conservatively using a 20.000 in. 55-gallon drum diameter bounds the radial shift of the pipe component with respect to the S200 pipe overpack at (22.500 – 20.000)/2 = 1.250 in. The resulting stacked array of 14 S200 pipe overpacks resting against the TRUPACT-II inner containment vessel is accounted for in the HAC shielding analysis discussed in Section 4.3.6. The maximum drum crush values reported in Ammerman and Bobbe of 20.25 in. outside diameter by 29.62 in. height are directly utilized in the criticality analysis summarized in Section 4.3.5.

4.3.5 Criticality Analysis

A criticality analysis was performed for two different payload cases, depending on the quantities of special reflector materials in the payload container (see Chapter 6.0 of TRUPACT-II SAR or Chapter 6.0 of HalfPACT SAR for description of special reflector materials), as described below:

- Case E: For Case E, the contents of the pipe overpack payload container contain less than or equal to 1% by weight quantities of special reflector materials. The pipe overpack payload container may contain greater than 1% by weight quantities of special reflector materials provided that one of the following conditions is met:
    - The special reflector materials are chemically or mechanically bound to the fissile material such that no reconfiguration or release of the bond is possible under normal or accident conditions, or
    - The special reflector materials are present in thicknesses and/or packing fractions that render them less effective than a 25% polyethylene/75% water equivalent reflector per the limits in Table 6.2-1 of the TRUPACT-II or HalfPACT SAR.

---

[1] Ammerman, D.J., and J.G. Bobbe, October 1995. "Rocky Flats Pipe Component Testing," TTC-1434, Sandia National Laboratories, Albuquerque, New Mexico.

- Case F: For Case F, the contents of the pipe overpack payload container contain greater than 1% by weight quantities of special reflector materials that do not meet the exceptions listed for Case E.

The criticality analysis demonstrates that a TRUPACT-II shipment of 14 pipe overpacks with contents meeting the requirements of Case E at 200 FGE of ^{239}Pu each (for a total of 2,800 FGE per TRUPACT-II) or a HalfPACT shipment of 7 pipe overpacks with 200 FGE each (for a total of 1,400 FGE per HalfPACT) ensures compliance with the requirements of Title 10, Code of Federal Regulations (CFR), Sections 71.55 and 71.59 (10 CFR 71.55 and 71.59).[2] Additionally, shipments of pipe overpacks with contents meeting the requirements of Case F at 140 FGE for each payload container and 980 and 1960 FGE per HalfPACT and TRUPACT-II, respectively, ensure compliance with 10 CFR 71.55 and 71.59. Based on an infinite array of undamaged or damaged packages, the criticality transport index is 0.0.

The key parameters in the pipe overpack analysis for Case E are (1) the maximum fissile loading per pipe component is 200 FGE, (2) no more than 1% by weight quantities of special reflector materials are present or greater than 1% by weight quantities of special reflectors are either bound to the fissile material or meet the limits in Table 6.2-1 of the TRUPACT-II or HalfPACT SAR, (3) the spacing between the components (i.e., effective drum diameter) is reduced by the maximum amount reported in Section 4.3.4, and (4) the package arrays are infinite arrays stacked two high.

The key parameters in the pipe overpack analysis for Case F are (1) the maximum fissile loading per pipe component is 140 FGE, (2) the spacing between the components (i.e., effective drum diameter) is reduced by the maximum amount reported in Section 4.3.4, and (3) the package arrays are infinite arrays stacked two high.

The detailed analysis presented in Packaging Technology, 2004[2], presents the results of a series of SCALE 4.4 CSAS25 module[3] (KENO-Va version 4) calculations that establish a maximum system reactivity ($k_s + 2\sigma$) of less than 0.933 and the corresponding Upper Subcriticality Limit (USL) of 0.9377. Therefore, the shipment of 200 FGE or 140 FGE per pipe overpack for less than or equal to 1% or greater than 1% by weight quantities of special reflector materials, respectively in the TRUPACT-II and HalfPACT is safely subcritical.

---

[2] Packaging Technology, Inc., May 2004, "Pipe Overpack Criticality Analysis for the TRUPACT-II Package," ED-076, Packaging Technology, Inc., Tacoma, Washington.

[3] SCALE4.4., "Modular Code System for Performing Standardized Computer Analyses for Licensing Evaluation for Workstations and Personal Computers," RSICC code package C00545/MNYCP00, Oak Ridge National Laboratory, September 1998.

4.3.6 Shielding Analysis

Adequate shielding is provided in the S200 pipe overpack and TRUPACT-II or HalfPACT shipping configuration to ensure that no radioactive payload will exceed the dose rate limits established by 10 CFR 71.47(a) for NCT or 10 CFR 71.51(a)(2) for HAC. Compliance with dose rate limits specified in Section 3.2 of the CH-TRAMPAC for individual S200 pipe overpacks and loaded TRUPACT-IIs or HalfPACTs will be achieved by pre-shipment radiological surveys. Compliance with NCT and HAC radiation dose rate limits will be ensured by limiting radionuclide quantities to satisfy the most-limiting NCT or HAC radiation dose rate limits for worst-case, reconfigured source and post-accident shielding geometries.

A shielding analysis of the S200 pipe overpack and TRUPACT-II shipping configuration was performed to establish the allowable quantities of the radionuclides shown in Table 4.3-1. The analysis utilized a point-source methodology developed by T. Rockwell III for gamma sources and the Nelson methodology for neutron sources.[4, 5, 6]

Table 4.3-1 — Radionuclide Inventory

^{3}H	^{85}Kr	^{103}Ru	^{123}Te	^{144m}Pr	^{209}Tl	^{214}Po	^{227}Ac	^{236}U	^{244}Pu	^{250}Bk
^{14}C	^{86}Rb	^{106}Ru	^{123m}Te	^{146}Pm	^{209}Pb	^{215}Po	^{228}Ac	^{237}U	^{241}Am	^{249}Cf
^{22}Na	^{89}Sr	^{103m}Rh	^{125m}Te	^{147}Pm	^{210}Pb	^{216}Po	^{227}Th	^{238}U	^{242}Am	^{250}Cf
^{32}P	^{90}Sr	^{106}Rh	^{127}Te	^{146}Sm	^{211}Pb	^{218}Po	^{228}Th	^{239}U	^{242m}Am	^{251}Cf
^{51}Cr	^{88}Y	^{107}Pd	^{127m}Te	^{147}Sm	^{212}Pb	^{211}At	^{229}Th	^{240}U	^{243}Am	^{252}Cf
^{54}Mn	^{90}Y	^{109m}Ag	^{125}I	^{151}Sm	^{214}Pb	^{217}At	^{230}Th	^{237}Np	^{245}Am	^{254}Cf
^{55}Fe	^{90m}Y	^{110}Ag	^{129}I	^{150}Eu	^{207}Bi	^{219}Rn	^{231}Th	^{238}Np	^{240}Cm	^{252}Es
^{59}Fe	^{91}Y	^{110m}Ag	^{131}I	^{152}Eu	^{210}Bi	^{220}Rn	^{232}Th	^{239}Np	^{242}Cm	^{253}Es
^{57}Co	^{88}Zr	^{109}Cd	^{134}Cs	^{154}Eu	^{211}Bi	^{222}Rn	^{234}Th	^{240}Np	^{243}Cm	^{254}Es
^{58}Co	^{90}Zr	^{113m}Cd	^{135}Cs	^{155}Eu	^{212}Bi	^{221}Fr	^{231}Pa	^{240m}Np	^{244}Cm	^{255}Es
^{60}Co	^{90m}Zr	^{119m}Sn	^{137}Cs	^{152}Gd	^{213}Bi	^{223}Fr	^{233}Pa	^{236}Pu	^{245}Cm	
^{59}Ni	^{93}Zr	^{121m}Sn	^{133}Ba	^{153}Gd	^{214}Bi	^{223}Ra	^{234}Pa	^{238}Pu	^{246}Cm	
^{63}Ni	^{95}Zr	^{123}Sn	^{137}Ba	^{168}Tm	^{209}Po	^{224}Ra	^{234m}Pa	^{239}Pu	^{247}Cm	
^{64}Cu	^{95}Nb	^{126}Sn	^{137m}Ba	^{182}Ta	^{210}Po	^{225}Ra	^{232}U	^{240}Pu	^{248}Cm	
^{65}Zn	^{95m}Nb	^{125}Sb	^{141}Ce	^{198}Au	^{211}Po	^{226}Ra	^{233}U	^{241}Pu	^{250}Cm	
^{73}As	^{99}Tc	^{126}Sb	^{144}Ce	^{207}Tl	^{212}Po	^{228}Ra	^{234}U	^{242}Pu	^{247}Bk	
^{79}Se	^{99m}Tc	^{126m}Sb	^{144}Pr	^{208}Tl	^{213}Po	^{225}Ac	^{235}U	^{243}Pu	^{249}Bk	

[4] T. Rockwell III, et al., Reactor Shielding Design Manual, TID-7004, First Edition, March 1956, U.S. Atomic Energy Commission, Oak Ridge, Tennessee.

[5] R.D. Wilson, Neutron Dose Rate Estimates for the 72-B Cask Using the Nelson Methodology, ENG-RCAL-021, Rev. 0, March 1999, Waste Management Federal Services, Inc., Northwest Operations, Richland, Washington.

[6] IT Corporation, June 2001, "Shielding Analysis of the S200 Pipe Overpack," IT Corporation, Albuquerque, New Mexico.

The primary shielding for the payload in the NCT configuration is the stainless steel and lead provided by the shield insert, pipe component, and TRUPACT-II. HAC configurations utilize the stainless steel in the pipe component and TRUPACT-II. A detailed description of the shield configurations utilized in the shielding analysis is presented in IT Corporation, 2001.[6]

The shielding analysis presented in IT Corporation, 2001,[6] calculates the maximum allowable radionuclide activity per S200 pipe overpack in the NCT at the surface, NCT at 2 meters, and HAC at 1 meter configurations inside a TRUPACT-II. The minimum of the calculated configuration activities is defined as the limiting activity and presented for both the S200-A and S200-B shield insert configurations in Table 4.3-2. The limiting activity per S200 pipe overpack provided in Table 4.3-2 is also conservative for the HalfPACT configuration because the number of S200 pipe overpacks (and the resulting total activity) is half that of the TRUPACT-II configuration.

Table 4.3-2 — Limiting Activity per S200 Pipe Overpack

Radio-nuclide Name	S200-A Limiting Activity (Ci)	S200-B Limiting Activity (Ci)	Radio-nuclide Name	S200-A Limiting Activity (Ci)	S200-B Limiting Activity (Ci)
^{3}H	unlimited	unlimited	^{103}Ru	6.524E-01	1.750E-01
^{14}C	unlimited	unlimited	^{106}Ru	unlimited	unlimited
^{22}Na	3.722E-02	2.343E-02	^{103m}Rh	1.618E+05	1.618E+05
^{32}P	unlimited	unlimited	^{106}Rh	6.710E-01	2.764E-01
^{51}Cr	1.226E+01	1.226E+01	^{107}Pd	unlimited	unlimited
^{54}Mn	8.440E-02	4.331E-02	^{109m}Ag	2.974E+03	2.974E+03
^{55}Fe	unlimited	unlimited	^{110}Ag	3.900E+00	1.594E+00
^{59}Fe	4.192E-02	2.577E-02	^{110m}Ag	2.521E-02	1.351E-02
^{57}Co	2.641E+01	2.641E+01	^{109}Cd	2.974E+03	2.974E+03
^{58}Co	8.829E-02	4.471E-02	^{113m}Cd	7.540E+03	7.540E+03
^{60}Co	1.906E-02	1.195E-02	^{119m}Sn	6.826E+02	6.826E+02
^{59}Ni	unlimited	unlimited	^{121m}Sn	5.948E+03	5.948E+03
^{63}Ni	unlimited	unlimited	^{123}Sn	7.589E+00	4.521E+00
^{64}Cu	7.156E+00	4.600E+00	^{126}Sn	1.726E+02	1.726E+02
^{65}Zn	9.129E-02	5.486E-02	^{125}Sb	5.782E-01	1.908E-01
^{73}As	1.055E+03	1.055E+03	^{126}Sb	4.239E-02	1.826E-02
^{79}Se	unlimited	unlimited	^{126m}Sb	9.044E-02	3.658E-02
^{85}Kr	1.363E+02	3.709E+01	^{123}Te	unlimited	unlimited
^{86}Rb	5.643E-01	3.353E-01	^{123m}Te	7.703E+00	7.703E+00
^{89}Sr	7.224E+02	3.920E+02	^{125m}Te	1.542E+03	1.542E+03
^{90}Sr	unlimited	unlimited	^{127}Te	7.613E+01	4.597E+01
^{88}Y	1.709E-02	1.110E-02	^{127m}Te	1.323E+03	5.207E+02
^{90}Y	1.328E+06	9.330E+05	^{125}I	1.647E+03	1.647E+03
^{90m}Y	6.476E-01	2.442E-01	^{129}I	1.465E+03	1.465E+03
^{91}Y	1.572E+01	9.695E+00	^{131}I	9.832E-01	5.754E-01
^{88}Zr	9.496E-01	7.384E-01	^{134}Cs	6.216E-02	2.832E-02
^{90}Zr	unlimited	unlimited	^{135}Cs	unlimited	unlimited
^{90m}Zr	unlimited	unlimited	^{137}Cs	2.181E-01	8.747E-02
^{93}Zr	1.975E+07	1.975E+07	^{133}Ba	1.142E+00	1.142E+00
^{95}Zr	1.248E-01	5.705E-02	^{137}Ba	unlimited	unlimited
^{95}Nb	1.100E-01	5.212E-02	^{137m}Ba	2.060E-01	8.261E-02
^{95m}Nb	8.103E+00	8.103E+00	^{141}Ce	2.011E+01	2.011E+01
^{99}Tc	1.693E+07	1.693E+07	^{144}Ce	1.539E+02	1.539E+02
^{99m}Tc	1.385E+01	1.385E+01	^{144}Pr	1.779E+00	1.126E+00

Table 4.3-2 — Limiting Activity per S200 Pipe Overpack (Continued)

Radio-nuclide Name	S200-A Limiting Activity (Ci)	S200-B Limiting Activity (Ci)	Radio-nuclide Name	S200-A Limiting Activity (Ci)	S200-B Limiting Activity (Ci)
^{144m}Pr	5.304E+01	3.512E+01	^{214}Po	unlimited	unlimited
^{146}Pm	1.958E-01	8.003E-02	^{215}Po	2.053E+03	9.111E+02
^{147}Pm	1.175E+06	1.175E+06	^{216}Po	4.824E+03	2.419E+03
^{146}Sm	unlimited	unlimited	^{218}Po	unlimited	unlimited
^{147}Sm	unlimited	unlimited	^{211}At	6.139E+01	2.565E+01
^{151}Sm	3.504E+05	3.504E+05	^{217}At	1.968E+03	8.069E+02
^{150}Eu	1.001E-01	4.605E-02	^{219}Rn	7.163E+00	7.163E+00
^{152}Eu	5.488E-02	3.263E-02	^{220}Rn	3.632E+02	1.115E+02
^{154}Eu	4.915E-02	2.843E-02	^{222}Rn	8.103E+02	2.176E+02
^{155}Eu	1.743E+02	1.743E+02	^{221}Fr	2.066E+01	2.066E+01
^{152}Gd	unlimited	unlimited	^{223}Fr	1.078E+01	5.211E+00
^{153}Gd	1.898E+02	1.898E+02	^{223}Ra	5.380E+00	5.380E+00
^{168}Tm	8.380E-02	4.045E-02	^{224}Ra	5.031E+01	5.031E+01
^{182}Ta	4.298E-02	2.631E-02	^{225}Ra	3.668E+02	3.668E+02
^{198}Au	9.004E-01	4.886E-01	^{226}Ra	1.065E+02	1.065E+02
^{207}Tl	2.733E+01	1.469E+01	^{228}Ra	5.749E+03	5.749E+03
^{208}Tl	1.497E-02	9.959E-03	^{225}Ac	8.245E+01	7.320E+01
^{209}Tl	2.596E-02	1.678E-02	^{227}Ac	3.927E+04	3.927E+04
^{209}Pb	unlimited	unlimited	^{228}Ac	7.672E-02	4.385E-02
^{210}Pb	2.589E+03	2.589E+03	^{227}Th	4.786E+00	4.786E+00
^{211}Pb	1.786E+00	8.441E-01	^{228}Th	7.082E+02	7.082E+02
^{212}Pb	4.342E+00	4.342E+00	^{229}Th	2.522E+01	2.522E+01
^{214}Pb	1.681E+00	1.589E+00	^{230}Th	1.352E+03	1.336E+03
^{207}Bi	4.786E-02	2.598E-02	^{231}Th	2.833E+02	2.833E+02
^{210}Bi	unlimited	unlimited	^{232}Th	2.841E+03	2.809E+03
^{211}Bi	8.296E+00	8.296E+00	^{234}Th	9.901E+02	9.901E+02
^{212}Bi	6.418E-01	3.564E-01	^{231}Pa	1.330E+01	1.330E+01
^{213}Bi	2.920E+00	1.052E+00	^{233}Pa	2.262E+00	2.262E+00
^{214}Bi	3.569E-02	2.213E-02	^{234}Pa	5.300E-02	2.859E-02
^{209}Po	1.519E+01	8.164E+00	^{234m}Pa	3.751E+00	2.161E+00
^{210}Po	7.613E+03	3.813E+03	^{232}U	8.615E+02	8.463E+02
^{211}Po	1.055E+01	5.124E+00	^{233}U	1.179E+03	1.130E+03
^{212}Po	unlimited	unlimited	^{234}U	1.202E+03	1.185E+03
^{213}Po	2.147E+03	1.038E+03	^{235}U	5.003E+00	5.003E+00

Table 4.3-2 — Limiting Activity per S200 Pipe Overpack (Continued)

Radio-nuclide Name	S200-A Limiting Activity (Ci)	S200-B Limiting Activity (Ci)	Radio-nuclide Name	S200-A Limiting Activity (Ci)	S200-B Limiting Activity (Ci)
^{236}U	1.301E+03	1.286E+03	^{245}Am	2.809E+01	2.809E+01
^{237}U	1.002E+01	1.002E+01	^{240}Cm	1.241E+02	1.227E+02
^{238}U	1.459E+01	1.443E+01	^{242}Cm	7.823E+01	7.722E+01
^{239}U	8.798E+00	4.327E+00	^{243}Cm	6.475E+00	6.475E+00
^{240}U	7.356E+02	7.356E+02	^{244}Cm	4.356E+00	4.306E+00
^{237}Np	1.416E+02	1.416E+02	^{245}Cm	2.649E+01	2.619E+01
^{238}Np	8.656E-02	4.996E-02	^{246}Cm	1.885E-02	1.864E-02
^{239}Np	5.101E+00	5.101E+00	^{247}Cm	1.175E+00	7.922E-01
^{240}Np	8.373E-02	4.282E-02	^{248}Cm	6.126E-05	6.057E-05
^{240m}Np	3.198E-01	1.524E-01	^{250}Cm	7.043E-06	6.963E-06
^{236}Pu	5.764E+02	5.597E+02	^{247}Bk	5.606E+00	5.606E+00
^{238}Pu	6.171E+02	6.087E+02	^{249}Bk	5.710E+03	5.644E+03
^{239}Pu	9.319E+02	8.655E+02	^{250}Bk	6.133E-02	3.558E-02
^{240}Pu	1.158E+02	1.145E+02	^{249}Cf	1.175E+00	1.175E+00
^{241}Pu	3.874E+06	3.874E+06	^{250}Cf	5.989E-03	5.921E-03
^{242}Pu	1.334E+00	1.318E+00	^{251}Cf	1.237E+01	1.237E+01
^{243}Pu	9.208E+01	9.208E+01	^{252}Cf	1.548E-04	1.530E-04
^{244}Pu	5.548E-03	5.485E-03	^{254}Cf	4.781E-06	4.727E-06
^{241}Am	2.788E+02	2.788E+02	^{252}Es	4.418E-01	2.180E-01
^{242}Am	7.973E+05	7.973E+05	^{253}Es	4.677E+01	4.453E+01
^{242m}Am	1.095E+02	1.095E+02	^{254}Es	3.681E+01	3.681E+01
^{243}Am	1.409E+02	1.409E+02	^{254m}Es	9.086E-03	8.561E-03

Note: The designation of "unlimited" is made for any radionuclide whose limiting activity is greater than 1×10^{8} curies (Ci).

4.3.7 Authorized Payload Contents

As demonstrated in Section 4.3.5, TRUPACT-II shipments of 14 S200 pipe overpacks and HalfPACT shipments of 7 S200 pipe overpacks containing 200 FGE per pipe overpack with contents meeting the requirements of Case E are subcritical in all cases. Therefore, the FGE limit for each S200 pipe overpack with Case E contents is 200 FGE. A maximum TRUPACT-II payload of 14 S200 pipe overpacks and HalfPACT payload of 7 S200 pipe overpacks have allowable FGE limits of 2,800 FGE and 1,400 FGE, respectively for Case E payloads. The FGE limit for Case F payloads is 140, 980, and 1,960 FGE for the S200 pipe overpack, HalfPACT, and TRUPACT-II, respectively.

Section 3.2 of the CH-TRAMPAC requires that each individual S200 pipe overpack and loaded TRUPACT-II or HalfPACT be measured prior to shipment to verify compliance with a dose rate limit of 200 millirem per hour (mrem/hr) at the surface. Additionally, Section 3.2 of the CH-TRAMPAC requires that each loaded TRUPACT-II or HalfPACT be measured prior to shipment to verify compliance with a dose rate limit of 10 mrem/hr at 2 meters. The results of the shielding analyses show that, when the S200 pipe overpack is loaded to the activity limits listed in Table 4.3-2 using a sum of partial fractions for multiple radionuclides, the dose rate limit requirements of 10 CFR 71.47(a) and 10 CFR 71.51(a)(2) are met for a TRUPACT-II loaded with 14 S200 pipe overpacks and a HalfPACT loaded with 7 S200 pipe overpacks.

4.3.8 Conclusion

The S200 pipe overpack design is very closely based on the standard pipe overpack. It consists of a standard 12-in. pipe component within a 55-gallon drum, including a rigid liner and lid. A gamma shield insert is placed inside the pipe component and located by polyurethane foam dunnage. The analyses summarized in this appendix demonstrate the ability of the S200 pipe overpack to provide three significant control functions under NCT and HAC: (1) criticality, (2) shielding, and (3) confinement of the waste contents. The payload of the S200 pipe overpack is transuranic waste with high gamma energies.

The structural analysis shows that the waste contents remain confined within the pipe component in conservatively bounded NCT and HAC free drops. For criticality, it is shown that 200 FGE per S200 pipe overpack is safely subcritical for Case E payloads and 140 FGE per S200 pipe overpack is safely subcritical for Case F payloads. The shielding analysis shows that, with maximum allowable activity specified in Table 4.3-2, the dose limits for NCT and HAC are met.

APPENDIX 4.4

DESCRIPTION OF S300 PIPE OVERPACK

This page intentionally left blank.

4.4   Description of S300 Pipe Overpack

4.4.1   Introduction

The S300 pipe overpack is based closely on the standard pipe overpack described in Appendix 4.1 of the CH-TRU Payload Appendices. It differs from the standard pipe overpack through the addition of neutron shielding within the pipe component. It is intended for the shipment of sealed neutron sources in the TRUPACT-II and HalfPACT. Appendix 1.3.1 of the TRUPACT-II Safety Analysis Report (SAR), Appendix 1.3.1 of the HalfPACT SAR, and Section 2.9.5 of the Contact-Handled Transuranic Waste Authorized Methods for Payload Control (CH-TRAMPAC) describe the materials of construction, sizes, and other dimensional specifications for the S300 pipe overpack. Up to 14 S300 pipe overpacks may be shipped in the TRUPACT-II, and up to 7 S300 pipe overpacks may be shipped in the HalfPACT. This appendix describes the structural, criticality, and shielding basis of the S300 pipe overpack.

4.4.2   Description

The S300 pipe overpack consists of a neutron shield insert placed inside a standard 12-inch (in.) pipe component which is, in turn, located by cane fiberboard and plywood dunnage within a standard 55-gallon drum with a rigid polyethylene liner and lid. A schematic of the S300 pipe overpack is shown in Figure 4.4-1. All of the components of the S300 pipe overpack, except the neutron shield insert, are identical to the 12-in. version of the standard pipe overpack described in Appendix 4.1 of the CH-TRU Payload Appendices.

The neutron shield insert is a two-part assembly consisting of a cylindrical body and stepped lid. With the exception of necessary clearances, the insert fits within and fills the 12-in. pipe component. The insert lid is held in place by the lid of the pipe component. The insert is made from solid, high-density polyethylene (HDPE), and has a nominal wall thickness of 4.13 inches.

The pipe component provides three significant control functions: (1) criticality control, (2) shielding, and (3) confinement of the sealed neutron sources. The following sections demonstrate the effectiveness of the S300 pipe overpack design for normal conditions of transport (NCT) and hypothetical accident conditions (HAC). All demonstrations are by analysis or by reference to the standard pipe overpack analysis and testing, unless stated otherwise.

4.4.3   Structural Analysis for NCT

The structural effectiveness of the S300 pipe overpack for NCT is demonstrated by showing that the source material contents are confined within the pipe component. The structural effectiveness of the pipe component for NCT is bounded by the structural effectiveness evaluation for HAC given in Section 4.4.4. It is shown in Section 4.4.6 that an adequate level of biological shielding for NCT is afforded by the shield insert itself, with all other materials providing mainly a distance attenuation function. The maximum deflection and resulting radial shift of the pipe overpack array for the NCT side drop, which is limiting for shielding calculations, is bounded by the HAC side drop analysis provided in Section 4.4.4. Additionally,

55-GALLON DRUM
LID W/ FILTER VENT,
LID RING, AND
GASKET

55-GALLON DRUM
VENTED RIGID
LINER LID

PIPE COMPONENT
DUNNAGE

55-GALLON DRUM
BODY W/ RIGID
LINER BODY

PIPE COMPONENT
LID W/ FILTER VENT

SHIELD INSERT
LID

SHIELD INSERT
BODY

12 IN.
PIPE COMPONENT
BODY W/ GASKET

CONTENTS
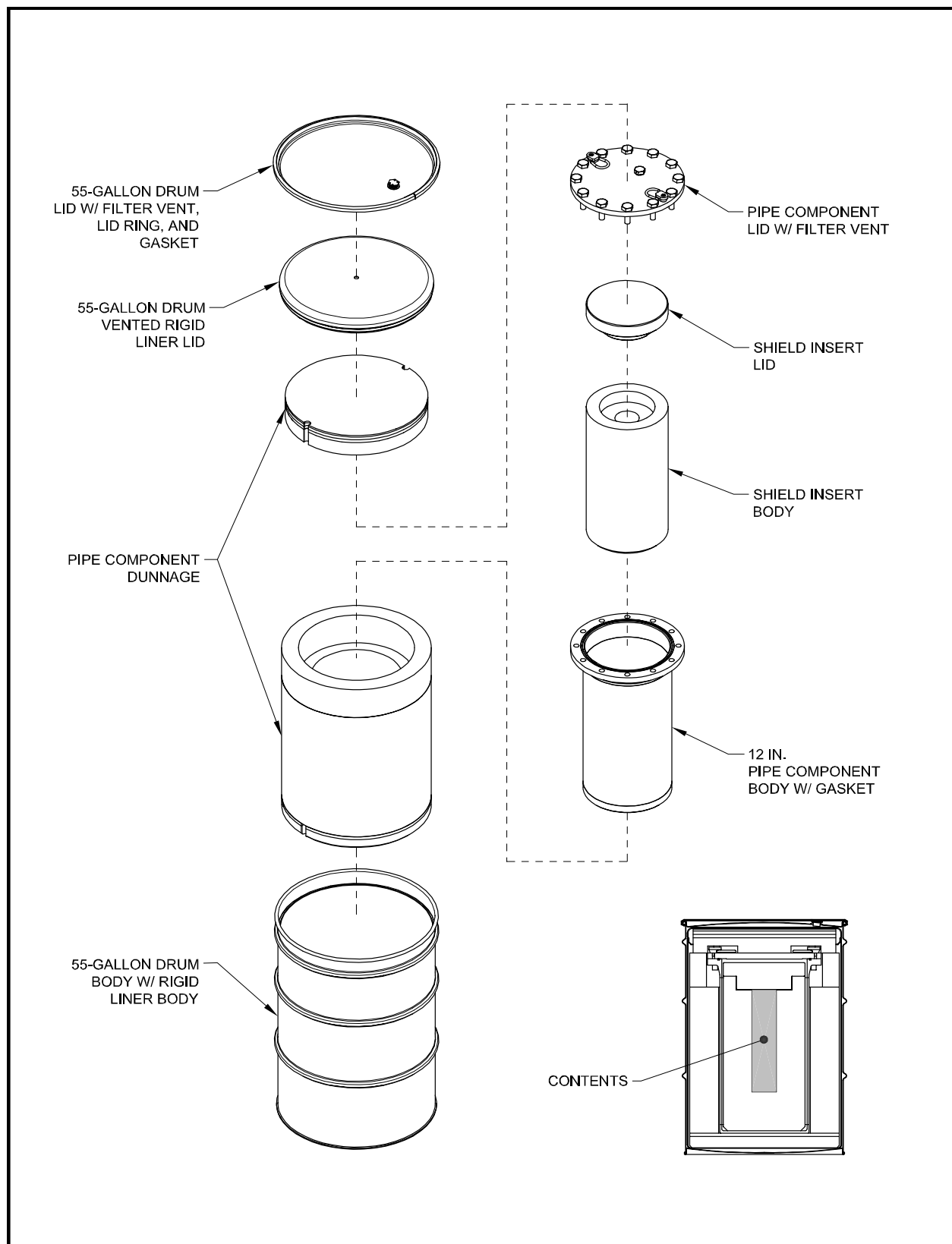
Figure 4.4-1 — S300 Pipe Overpack

the spacing between pipe components (i.e., effective drum diameter) utilized in the criticality analysis is also bounded by the HAC side drop analysis provided in Section 4.4.4.

4.4.4 Structural Analysis for HAC

The structural effectiveness of the S300 pipe overpack for HAC is demonstrated by showing that the source material contents remain confined within the pipe component. It is shown in Section 4.4.6 that an adequate level of biological shielding for HAC is afforded by distance attenuation considering the most conservative post-accident configuration of the TRUPACT-II or HalfPACT and pipe components. Since the shield insert in the S300 pipe overpack is not required for the HAC shielding analysis, the damage to the shielding material in the HAC free drop does not need to be quantified. However, the maximum deflection and resulting radial shift of the pipe overpack array will be quantified for the side drop orientation, which is limiting for shielding calculations. The following comparative analysis shows that the contents remain confined within the pipe component under the HAC free drop. Additionally, the analysis shows the maximum deflection of pipe overpacks and the resulting stacked array configuration resulting from the HAC free drop.

As shown in Table 2.9-7 of Section 2.9.2 of the CH-TRAMPAC, the weight of the 12-in. standard pipe component contents is bounded by a value of 225 lbs. Additionally, as shown in Table 2.9-20 of Section 2.9.5 of the CH-TRAMPAC, the total weight of the S300 pipe overpack shield insert and contents is also bounded by a weight of 225 lbs. Because the design of the standard and S300 pipe overpacks are structurally identical, and because the weight limit for items inside the pipe component are identical, all structural evaluations of the standard pipe overpack apply to the S300 pipe overpack. Ammerman and Bobbe, 1995,[1] demonstrates the leak tightness of the standard pipe overpack when subjected to HAC testing. Therefore, the source materials will remain confined within the pipe component under the HAC free drop.

Additionally, Ammerman and Bobbe[1] report a 20.250 in. minimum deformed pipe overpack diameter resulting from a free side drop orientation. Therefore, conservatively using a 20.000 in. 55-gallon drum diameter bounds the radial shift of the pipe component with respect to the S300 pipe overpack at (22.500 – 20.000)/2 = 1.250 in. The resulting stacked array of 14 S300 pipe overpacks resting against the TRUPACT-II inner containment vessel is accounted for in the HAC shielding analysis discussed in Section 4.4.6. The maximum drum crush values reported in Ammerman and Bobbe of 20.25 in. outside diameter by 29.62 in. height are directly utilized in the criticality analysis summarized in Section 4.4.5.

4.4.5 Criticality Analysis

A criticality analysis was performed for two different payload cases, depending on the quantities of special reflector materials in the payload container (see Chapter 6.0 of TRUPACT-II SAR or Chapter 6.0 of HalfPACT SAR for description of special reflector materials), as described below:

---

[1] Ammerman, D.J., and J.G. Bobbe, October 1995. "Rocky Flats Pipe Component Testing," TTC-1434, Sandia National Laboratories, Albuquerque, New Mexico.

- Case E: For Case E, the contents of the pipe overpack payload container contain less than or equal to 1% by weight quantities of special reflector materials. The pipe overpack payload container may contain greater than 1% by weight quantities of special reflector materials provided that one of the following conditions is met:
     - The special reflector materials are chemically or mechanically bound to the fissile material such that no reconfiguration or release of the bond is possible under normal or accident conditions, or
     - The special reflector materials are present in thicknesses and/or packing fractions that render them less effective than a 25% polyethylene/75% water equivalent reflector per the limits in Table 6.2-1 of the TRUPACT-II or HalfPACT SAR.
- Case F: For Case F, the contents of the pipe overpack payload container contain greater than 1% by weight quantities of special reflector materials that do not meet the exceptions listed for Case E.

The criticality analysis demonstrates that a TRUPACT-II shipment of 14 pipe overpacks with contents meeting the requirements of Case E at 200 FGE of ^{239}Pu each (for a total of 2,800 FGE per TRUPACT-II) or a HalfPACT shipment of 7 pipe overpacks with 200 FGE each (for a total of 1,400 FGE per HalfPACT) ensures compliance with the requirements of Title 10, Code of Federal Regulations (CFR), Sections 71.55 and 71.59 (10 CFR 71.55 and 71.59).[2] Additionally, shipments of pipe overpacks with contents meeting the requirements of Case F at 140 FGE for each payload container and 980 and 1960 FGE per HalfPACT and TRUPACT-II, respectively, ensure compliance with 10 CFR 71.55 and 71.59. Based on an infinite array of undamaged or damaged packages, the criticality transport index is 0.0.

The key parameters in the pipe overpack analysis for Case E are (1) the maximum fissile loading per pipe component is 200 FGE, (2) no more than 1% by weight quantities of special reflector materials are present or greater than 1% by weight quantities of special reflectors are either bound to the fissile material or meet the limits of Table 6.2-1 of the TRUPACT-II or HalfPACT SAR, (3) the spacing between the components (i.e., effective drum diameter) is reduced by the maximum amount reported in Section 4.4.4, and (4) the package arrays are infinite arrays stacked two high.

The key parameters in the pipe overpack analysis for Case F are (1) the maximum fissile loading per pipe component is 140 FGE, (2) the spacing between the components (i.e., effective drum diameter) is reduced by the maximum amount reported in Section 4.4.4, and (3) the package arrays are infinite arrays stacked two high.

The detailed analysis presented in Packaging Technology, 2004[2], presents the results of a series of SCALE 4.4 CSAS25 module[3] (KENO-Va version 4) calculations that establish a maximum

---

[2] Packaging Technology, Inc., May 2004, "Pipe Overpack Criticality Analysis for the TRUPACT-II Package," ED-076, Packaging Technology, Inc., Tacoma, Washington.

[3] SCALE4.4., "Modular Code System for Performing Standardized Computer Analyses for Licensing Evaluation for Workstations and Personal Computers," RSICC code package C00545/MNYCP00, Oak Ridge National Laboratory, September 1998.

system reactivity ($k_s + 2\sigma$) of less than 0.933 and the corresponding Upper Subcriticality Limit (USL) of 0.9377. Therefore, the shipment of 200 FGE or 140 FGE per pipe overpack for Cases E and F, respectively, in the TRUPACT-II and HalfPACT is safely subcritical.

4.4.6 Shielding Analysis

The payload of the S300 pipe overpack consists of neutron-emitting, actinide-bearing sealed sources, shown in Table 4.4-1. Source terms used in this analysis are for neutron emission and spectra for alpha-n reactions calculated by the SOURCES Version 4A computer code.[4] Of the sources shown in the table, the ^{238}Pu Be was determined to be the governing source for shielding calculations,[5] since it had the highest calculated unshielded dose rate of all the sources that will be transported in the S300.

Table 4.4-1 S300 Pipe Overpack Payloads

^{241}Am Be	^{238}Pu O	^{239}Pu Li	^{241}Am
^{238}Pu Be	^{239}Pu O	^{238}Pu B	^{238}Pu
^{239}Pu Be	^{244}Cm O	^{239}Pu F	^{239}Pu
^{241}Am O	^{241}Am Li	^{238}Pu ^{13}C	^{244}Cm

The radiation generated by the payload is in the form of neutrons and a relatively small amount of gamma radiation. Some additional gamma radiation is generated by capture of thermal neutrons in the neutron shielding. However, the gamma radiation remains a small fraction of the neutron radiation level.

Neutron shielding is provided by the shielding insert placed within the 12-in. pipe component. It has a minimum wall thickness of 4.06 in., and minimum end thicknesses of 3.58 in. at the bottom and 3.94 in. in the lid. None of the materials of construction of the S300 pipe overpack, including the neutron shielding material, generate hydrogen gas in excess of 10^{-10} moles hydrogen per second per liter of headspace as a consequence of neutron or gamma irradiation by the payload sources.[6] A combination of the neutron shielding material and the materials of construction of the S300 pipe overpack provide sufficient shielding for both neutron and gamma radiation.

---

[4] Wilson, W.B., R.T. Perry, W. Charlton, et al., 1999, "SOURCES 4A: A Code for Calculating (alpha, n) Spontaneous Fission, and Delayed Neutron Sources and Spectra," LA-13639-MS, Los Alamos National Laboratory, Los Alamos, New Mexico.

[5] Gogol, S.L., and J.R. Bland, August 2002, "A Comparison of Dose Rates from (alpha, n) and Spontaneous Fission Neutron Sources," LA-UR-02-5120,.Los Alamos National Laboratory, Los Alamos, New Mexico.

[6] Bustos, L.D., W.F. Sandoval, R. Villarreal, and L.R. Field, October 2000, "Hydrogen Generation Rate Potential from Neutron and Gamma Ray Interactions with Shielding/Packaging Materials Contained in the S100 Pipe Component Overpack," Los Alamos National Laboratory, Los Alamos, New Mexico.

Dose rate calculations were performed for a single S300 pipe overpack and for a TRUPACT-II in both the as-loaded and post-NCT free drop configurations.[7] The results were used to determine the maximum loading of the S300 pipe overpack such that the regulatory dose rate limits will be met in each case for NCT and HAC. In the analysis, the bounding payload of ^{238}Pu Be was used, as discussed above. Source gamma radiation was negligible and was not included, but capture gamma dose rate contribution was included in the calculated integrated dose rate. Dose rate calculations were made for a single S300 pipe overpack as presented for loading into a TRUPACT-II, for a TRUPACT-II as presented for transport with a payload of 14 identical S300 pipe overpacks each having the maximum payload, and for a TRUPACT-II including a conservative representation of NCT free drop damage with a payload of 14 identical S300 pipe overpacks each having the maximum payload. (The HAC case is discussed below.) Dose rates were calculated at the surface and at defined distances from the containers as shown in Table 4.4-2. As shown in the table, the limiting dose is for the TRUPACT-II package at a distance of 5 meters from the package surface (the truck cab, a normally occupied space), and is equal to 2 millirem per hour (mrem/hr). The corresponding S300 pipe overpack surface dose limit is 155 mrem/hr. This means that, as long as the surface dose rate of any S300 pipe overpack transported in a TRUPACT-II is at or below 155 mrem/hr, then the dose rate external to the TRUPACT-II will not exceed 2 mrem/hr at a distance of 5 meters, nor will any of the other, less governing regulatory limits be exceeded. The TRUPACT-II calculations govern the case of the HalfPACT. Each S300 pipe overpack will be surveyed before loading into a TRUPACT-II or HalfPACT to ensure compliance with the limiting surface dose rate of 155 mrem/hr, as given in Section 3.2 of the CH-TRAMPAC.

---

[7] Packaging Technology, Inc., August 2002, "Dose Rate Calculations for the S300 Pipe Overpack," ED-072, Packaging Technology, Inc., Tacoma, Washington.

Table 4.4-2 Maximum Dose Rates for S300 Pipe Overpack and TRUPACT-II

	Maximum Dose Rate (mrem/hr)	Limits (mrem/hr)④
S300 Surface	155 ±0.36	200
TRUPACT-II side Surface (undamaged) ①②	64.5 ±0.62	200
TRUPACT-II 2 meters (undamaged)	8.06 ±0.10	10
TRUPACT-II 5 meters (undamaged)③	1.97 ±0.03	2
TRUPACT-II side Surface (damaged)	120 ±0.20	200
TRUPACT-II 2 meters (damaged)	9.83 ±0.12	10

Notes:
1. TRUPACT-II contains 14 identical S300 pipe overpacks, each with a maximum surface dose rate of 155 mrem/hr or less.
2. Side dose rate governs over top or bottom dose rates.
3. The 5 meter distance corresponds to the normally occupied space of the truck cab.
4. Limits established by CH-TRAMPAC (S300 surface) or 10 CFR 71.47(b) (TRUPACT-II).

The damage to the TRUPACT-II and payload under NCT is assumed to occur in the 3 ft. side drop, and is discussed in Section 4.4.4. The drums are modeled as resting on the inside of the TRUPACT-II ICV, which is resting on its side. Each drum is conservatively reduced in size to a diameter of 20.0 in., and the array is accordingly compressed and shifted to be in contact with the inside surface of the TRUPACT-II ICV.

For HAC, the drums, neutron shielding material, pipe components, and internal dunnage are conservatively removed from consideration in the shielding calculation, and the sum total of all activity in the S300 payload is concentrated as a single point source resting on the inside surface of the TRUPACT-II ICV. In accordance with 10 CFR 71.51(a)(2), the dose point is located 1 meter from the external surface of the package. This is equivalent to a total distance from the source of 1 meter plus the minimum crushed wall thickness of the TRUPACT-II or HalfPACT. For simplicity and conservatism, the calculations assume that there is no material of any kind between the source and the dose point. The crushed wall thickness is found by subtracting the HAC 30-foot free drop side orientation crush damage from the original wall thickness of the package as follows. The outer diameter of the package is 94.38 inches, and the inner diameter of the ICV is 73.63 inches, which gives an undamaged wall thickness of 10.38 inches. The maximum crush damage is found in Table 2.10.3-1 of the TRUPACT-II SAR for Test No. 2, as equal to 3.63 inches. The remaining wall thickness is then equal to $10.38 - 3.63 = 6.75$ inches. In the shielding calculations, a value of 6.5 inches is conservatively used. As already discussed, no material is assumed to fill this space. The resulting maximum allowable activity within the

TRUPACT-II is a total of 406 Ci, and the resulting conservative dose rate is 999 mrem/hr at 1 meter from the crushed TRUPACT-II surface, which meets the requirements of 10 CFR 71.51(a)(2). As for NCT, the TRUPACT-II HAC calculations govern the case of the HalfPACT.

4.4.7 Authorized Payload Contents

As demonstrated in Section 4.4.6, when loaded with sealed neutron sources of the types specified in Table 4.4-1 (the authorized contents), the S300 pipe overpack meets all regulatory dose rate limits. The bounding payload is defined in three ways: (1) a maximum dose rate on the surface of the S300 pipe overpack of 155 mrem/hr for any S300 pipe overpack placed into the TRUPACT-II or HalfPACT, (2) a maximum activity of 406 Ci within a single TRUPACT-II or HalfPACT, and (3) a maximum payload of 200 FGE per S300 pipe overpack, or a total of 2,800 FGE per TRUPACT-II or 1,400 FGE per HalfPACT when the contents meet the requirements for Case E, or (4) a maximum payload of 140 FGE per S300 pipe overpack, or a total of 1,960 FGE per TRUPACT-II or 980 FGE per HalfPACT when the contents meet the reuqirements for Case F. Section 4.2.5 demonstrates that 200 FGE per S300 pipe overpack is safely subcritical for Case E contents and that 140 FGE per S300 pipe overpack is safely subcritical for Case E contents.

4.4.8 Conclusion

The S300 pipe overpack design is very closely based on the standard pipe overpack. It consists of a standard 12-in. pipe component within a 55-gallon drum, including a rigid liner and lid. A neutron shield insert is placed inside the pipe component. The analyses summarized in this appendix demonstrate the ability of the S300 pipe overpack to provide three significant control functions under NCT and HAC: (1) criticality, (2) shielding, and (3) confinement of the payload. The payload of the S300 is sealed neutron sources of the types listed in Table 4.4-1. The structural analysis shows that the source material remains confined within the pipe component in conservatively bounded NCT and HAC free drops. For criticality, it is shown that 200 FGE per S300 pipe overpack for Case E payloads is safely subcritical and 140 FGE per S300 pipe overpack is safely subcritical for Case F payloads. The shielding analysis shows that, with the maximum authorized contents, the dose rate limits for NCT and HAC (including appropriate shielding damage assumptions in each case) are met.

APPENDIX 5.1

REAL-TIME RADIOGRAPHY PROCEDURES

This page intentionally left blank.

5.1   Real-Time Radiography Procedures

5.1.1   Description of Real-Time Radiography

Real-time radiography (RTR) is a nondestructive testing method that allows the RTR operator to ascertain the physical waste form within a payload container without opening it. The examination method utilizes X rays to inspect the payload container and contents and allows the operator to view events in progress (real time) such as wave motion of free liquids. A typical RTR system consists of:

1.   An X-ray-producing device
2.   An imaging system
3.   An enclosure for radiation protection
4.   A payload container handling system
5.   An operator control station.

The X-ray-producing device has controls that allow the operator to vary the voltage, thereby controlling image quality. The voltage can be varied, typically between 150 and 400 kilovolts (kV), to provide an optimum degree of penetration through the waste. For example, high-density material (e.g., solidified liquid) is usually examined with the X-ray device set on the maximum voltage. This ensures maximum penetration through the payload container. Low-density material (e.g., plastics and cellulose) is usually examined at lower voltage settings to improve contrast and image definition. The imaging system typically utilizes a fluorescent screen and a low light television camera.

Payload containers are placed in the RTR vault. Waste drums are placed on a rotating platform. The platform or the X-ray tube and imaging system move up and down to allow total coverage of the drum. X rays are projected through the payload container and onto a fluorescent screen/image intensifier. The resultant image is transferred by a camera to a remotely located television screen. The operator conducts the examination by viewing the remote television screen. The operator scans the contents of the payload container during the examination. Waste boxes cannot be rotated during RTR inspection but are first inspected from one side and then rotated 180 degrees and inspected from the opposite side. The two-sided inspection is performed to compensate for magnification factors. Large magnification factors can occur depending upon the location of an object within a box. Scanning from two sides, 180 degrees apart, allows a higher degree of accuracy for determining sizes and quantities. The two scans, from opposite sides, also provide a higher degree of confidence for detection of objects that may be hidden when scanning from only one side. The waste payload is inspected for correct physical waste form description, sealed containers, pressurized containers, and free liquid waste forms.
The RTR operator documents the findings of the RTR examination of each waste payload by several means listed below:

- The results are recorded on an RTR examination form, and this form is included in the waste payload data package. The examination results may also be entered into a computerized data collection system.

- The examination is recorded on a videotape recorder.

- The RTR operator verbally describes the results of the RTR examination on the audio track of the videotape. The audio voice track on the videotape is an additional positive feature of RTR.

The advantage of viewing the examination in real time is that the X-ray device can be adjusted on the spot to obtain optimum imaging conditions, or the system can be stopped to focus on one object. RTR works extremely well for detecting free liquids due to its ability to view events in progress, such as wave motion. The presence of free liquids is verified by jogging the container or handling system (stopping and starting the container rotation) and then watching for the resulting wave motion. Free liquids in pressurized containers are easily detected, thereby assessing two parameters, liquids and pressurized containers. Items that may otherwise go undetected due to being shielded from the X rays by another object are often found because the operator is watching the inspection in real time while rotating or moving the payload container. Interpretation of results and disposition of the inspected payload containers are also accomplished at the time of inspection rather than waiting for X-ray film to be processed.

Operator training and experience are the most important control factor in ensuring the quality of RTR interpretation and inspection. Operator training, qualification, and certification are performed in accordance with Society for Nondestructive Testing (SNT)-TC1A.[1] SNT-TC1A is a nationally recognized guideline and is used by employers to train, qualify, and certify employees to perform specific nondestructive tests.

Recertification of operators is based upon evidence of continued satisfactory performance and is performed at least every two years. Unsatisfactory operator performance is cause for decertification. Retraining is required before an operator is again certified to interpret and disposition payload containers.

A training drum containing a variety of different container sizes and holding various amounts of liquid is periodically examined by each operator, as prescribed in the site waste certification and quality assurance (QA) procedures. The test videotape is then reviewed by supervision to ensure that the operator's interpretations remain consistent and accurate. The test tapes are also used for monitoring the imaging system characteristics and identifying other shapes or matrices.

QA oversight functions are performed by independent individuals who review videotape of examined payload containers. The frequency and number of payload containers included in these reviews is determined in accordance with Military Standard (MIL-STD)-105D, "Sampling Procedures and Tables for Inspection by Attributes".[2]

---

[1] SNT-TC-1A, August 1984, "Recommended Practice No. SNT-TC-1A, Personnel Qualification and Certification in Nondestructive Testing."

[2] MIL-STD-105D, April 29, 1963, "Military Standard, Sampling Procedures and Tables for Inspection by Attributes."

RTR has several inherent limitations. X rays with a high enough energy level to penetrate high-density waste forms or shielded containers present an image with such a large latitude that low-density materials (i.e., liquids) will be indiscernible. Therefore, high-density waste forms or shielded payload containers must have the physical waste form verified by other methods (e.g., visual examination during packaging) or be rejected.

RTR inspection is a semi-quantitative examination that can identify and verify the payload container's physical contents. RTR cannot determine the chemical composition of the waste.

This page intentionally left blank.

APPENDIX 5.2

**DOE ASSAY METHODS USED FOR DETERMINATION OF
FISSILE MATERIAL CONTENT AND DECAY HEAT VALUES
OF CH-TRU WASTES**

This page intentionally left blank.

Table of Contents

     Decay Heat Values of Contact-Handled Transuranic (CH-TRU) Wastes 5.2-1

     5.2.1 Introduction 5.2-1

     5.2.2 Assay Overview 5.2-3

     5.2.3 Assay Methods Descriptions, Characteristics, and Limitations 5.2-6

          5.2.3.1 Calorimetry 5.2-6
          5.2.3.2 Passive Gamma Assay 5.2-7
          5.2.3.3 Radiochemical Methods.. 5.2-14
          5.2.3.4 Passive Neutron Coincidence Counting (PNCC) Assays 5.2-15
          5.2.3.5 Passive-Active Neutron (PAN) Assay Systems............................. 5.2-19

     5.2.4 Fissile Material Content and Decay Heat Value Calculations 5.2-41

     5.2.5 New Assay Developments.. 5.2-43

     5.2.6 QA and QC Practices 5.2-44

List of Tables

List of Figures

This page intentionally left blank.

5.2   DOE Assay Methods Used for Determination of Fissile Material Content and Decay Heat Values of Contact-Handled Transuranic (CH-TRU) Wastes

5.2.1   Introduction

The isotopic composition of the waste may be determined from direct measurements taken on the product material during the processing or post-process certification at each site, analysis of the waste, or from existing records. The isotopic composition of the waste need not be determined by direct analysis or measurement of the waste unless process information is not available. Each U.S. Department of Energy (DOE) contractor CH-TRU waste generating and/or storage site may generate and/or store one or more types of waste forms (e.g., sludge, general laboratory waste, etc.) that must be assayed.

The major contractor sites that generate and/or store CH-TRU waste are listed in Table 5.2-1, and the assay techniques used by DOE contractor sites are listed in Table 5.2-2. The specific assay methods utilized at each site are given in Table 5.2-3.

Table 5.2-1 — DOE Contractor CH-TRU Waste Generator and/or Storage Sites

1.	Argonne National Laboratory - East (ANL-E)
2.	Idaho National Engineering and Environmental Laboratory (INEEL)
3.	Lawrence Livermore National Laboratory (LLNL)
4.	Los Alamos National Laboratory (LANL)
5.	Mound Facility (Mound)
6.	Nevada Test Site (NTS)
7.	Oak Ridge National Laboratory (ORNL)
8.	Richland Hanford (RH)
9.	Rocky Flats Environmental Technology Site (RFETS)
10.	Savannah River Site (SRS)

Table 5.2-2 — CH-TRU Waste Assay Methods

1.	Passive Gamma [HPGe, Ge(Li), NaI: transmission-corrected and noncorrected]
2.	Radiochemical assay: gross alpha and gamma spectrometry
3.	Passive neutron coincidence counting (PNCC)
4.	Passive/active neutron assay (PAN)
5.	Calorimetry

Table 5.2-3 — Summary of CH-TRU Waste Assay Methods Presently Used at DOE CH-TRU Waste Generating and Storage Sites[a]

Site	SGS or NaI	PNCC	PAN (drum)	PAN (box)	Radiochemistry	Mobile PAN
ANL-E	X				X	
Hanford	X		X			
INEEL			X	X		
LLNL	X				X	X
LANL	X	X	X		X	X
Mound	X				X	
NTS						X
ORNL	X		X			
RFETS	X	X	X	X	X	
SRS	X	X	X			

[a]Calorimetry method is also used to obtain quantitative radionuclide content.

The DOE and its site contractors have been historically, and continue to be, the dominant force in assay technology development and implementation, not only within the United States but internationally as well. Some of the assay technologies (passive gamma, radiochemistry, and passive neutron coincidence counting [PNCC]) are highly developed and have a long history of implementation first to nuclear products (in safeguards and material accounting) and eventually to nuclear scraps and wastes. Other assay technologies, such as passive/active neutron (PAN), are newer developments (circa 1980), and were developed especially for application to bulk TRU wastes assays under sponsorship of the DOE. Additional improvements to the assay technology continue to be made and implemented as indicated in this document.

Where practical, the DOE sites perform multiple independent assays of waste packages as well as real-time radiography (RTR) inspection. These independent assays generally take the form of a passive gamma assay (usually segmented gamma-ray scanning [SGS]) at the waste generator site followed by PAN assay at a central certification facility.

These practices, as well as quality assurance (QA) audits and administrative controls, provide assurances that correct values of fissile material and decay heat are assigned to each waste drum. In the case of special-case drums or of significant differences among independent assay measurements, personnel at each site review all available data, including the RTR information and assay records, to determine the appropriate action. If a reasonable assay value cannot be ascertained, remedial action is taken; either reassay if measurement errors are suspected, or repackaging if the drum is suspected of nonconformance with respect to fissile material content or decay heat.

This document describes the nondestructive and destructive assay methods for CH-TRU waste employed by the DOE sites. The assay methods employed by the DOE are shown to be reliable

and accurate means of determining fissile material, radionuclide, and decay heat content of CH-TRU wastes.

Assay topics addressed for an assay method include:

  (1)   An overview of the assay method
  (2)   Applicability to CH-TRU wastes
  (3)   Calibration standards and implementation
  (4)   Operator training requirements and practices
  (5)   Assay procedures
  (6)   Assay precision, bias, and limit of detection.

More details are presented for the SGS and PAN assay methods, which are the primary methods used within the DOE complex.

All systems or methods, except for PAN, have established American Society for Testing and Materials (ASTM), American National Standards Institute (ANSI), and/or U.S. Nuclear Regulatory Commission (NRC) guidelines or methods that describe proper calibration procedures, proper equipment set-up, etc. PAN is a new technique and does not yet have a guideline or method developed. However, comparisons of PAN data with the more established assay methods (e.g., SGS or radiochemistry) are discussed that demonstrate its reliability and accuracy.

QA and quality control (QC) practices used in assay methods are presented. New nondestructive assay developments such as neutron assay imaging are also discussed.

5.2.2 Assay Overview

This section describes the general features of nondestructive assay (NDA) and destructive assay methods used by the DOE site contractors to determine the TRU content of their bulk CH-TRU waste.

ANSI N15.20-1975[1] defines NDA to be "The observation of spontaneous or stimulated nuclear radiations, interpreted to estimate the content of one or more nuclides of interest in the item assayed, without affecting the physical or chemical form of the material.

active assay.   Assay based on the observation of radiation(s) induced by irradiation from and external source.

passive assay.   Assay based on the observation of naturally occurring or spontaneous nuclear radiation(s)."

---

[1] ANSI N15.20-1975, "American National Standard Guide to Calibrating Nondestructive Assay Systems."

Destructive assay refers to chemical analysis in which a sample aliquot is removed from the item (after assuring homogenization of the batch) to be assayed and prepared for alpha and/or gamma counting.

The NRC in NRC Regulatory Guide 5.11[2] describes the applicable NDA passive measurements: "Radiations attributable to alpha particle decay, to gamma-ray transitions following alpha and beta particle decay, and to spontaneous fission have served as the basis for practical passive NDA measurements."

Gamma rays, X-rays, and/or neutrons, as well as other subatomic particles, are emitted by the various TRU isotopes as they undergo de-excitation to their respective ground states or more stable energy levels. NDA techniques based on detection of each emitted radiation have been developed and utilized for CH-TRU bulk-waste assay.

The passive gamma, passive neutron coincidence counting, radiochemical, and calorimetric methods are techniques, which are described by the ASTM, ANSI, NRC, and American Society of Mechanical Engineers (ASME) standards, guidelines, and/or regulations. These documents[1,2,3,4,5,6,7,8,9,10] provide information to the user for proper implementation of these techniques.

Characteristics of any assay measurement include precision, bias, and detection limit. Proper calibration methods must also be employed to reduce or eliminate the bias of the assay results. Definitions of each of the above terms are given below and were obtained from

---

[2] USNRC Regulatory Guide 5.11, "Nondestructive Assay of Special Nuclear Material Contained in Scrap and Waste," Revision 1, April 1984.

[3] ASTM C 853-82, "Standard Test Methods for Nondestructive Assay of Special Nuclear Materials Contained in Scrap and Waste."

[4] ANSI N15.35, "Guide to Preparing Calibration Material for Nondestructive Assay Systems that Count Passive Gamma Rays."

[5] ASTM C 696-80, "Methods for Chemical, Mass Spectrometric, and Spectrochemical Analysis of Nuclear-Grade Uranium Dioxide Powders and Pellets."

[6] ASTM C 697-86, "Methods for Chemical, Mass Spectrometric, and Spectrochemical Analysis of Nuclear-Grade Plutonium Dioxide Powders and Pellets."

[7] ASTM C 759-79, Methods for Chemical, Mass Spectrometric, Spectrochemical, Nuclear, and Radiochemical Analysis of Nuclear-Grade Plutonium Nitrate Solutions."

[8] American National Standard Calibration Techniques for the Calorimetric Assay of Plutonium Bearing Solids Applied to Nuclear Materials Control, ANSI-N15.22, American National Standards Institute, New York, 1987.

[9] Standard Test Method for Determination of Plutonium Isotopic Composition by Gamma-Ray Spectrometry, ASTM C 1030-84, ibid.

[10] Standard Test Method for Nondestructive Assay of Special Nuclear Material in Low Density Scrap and Waste by Segmented Passive Gamma-Ray Scanning, ASTM C 853. This draft standard has been referenced with permission from ASTM Subcommittee C-26.10.

ASTM C 859-87[11]. Examples for each discussed assay method are found in the appropriate sections.

(1)   Precision: A generic term used to describe the dispersion of a set of measured values (also referred to as "random" or "statistical error").

(2)   Bias: A persistent positive or negative deviation of the method average from the correct value or accepted reference value (also referred to as "constant" or "systematic error").

(3)   Detection limit: A stated limiting value that designates the lowest concentration or mass that can be estimated or determined with confidence and that is specific to the analytical procedure used.

(4)   Calibration: The determination of the values of the significant parameters by comparison with values indicated by a reference instrument or by a set of reference standards.

Estimates of precision can be calculated by standard error propagation techniques.[10] Radioactive decay is random and described by Poisson statistics. For Poisson statistics, the variance in measuring N events in a detector is equal to N. (The standard deviation is the square root of the variance.)

The precision of a nondestructive assay measurement is not strongly related to the measurement item's adherence to ideal matrix and nuclide density assumptions. For destructive assay methods (e.g., radiochemical), which require sampling, the precision of repeat measurements of a single item will be strongly influenced by a lack of adherence to ideal nuclide density assumptions. However, for SGS systems, measurement bias depends primarily on the adherence of the measurement item to the assumptions of small particle size and homogeneity. Negative assay bias (reported value less than actual value) will be encountered, for example, when the nuclide is present in lumps that attenuate their own radiation to a greater extent than the surrounding material (self-absorption). Radiochemical methods that dissolve material samples will not be affected by lumps. Matrix and nuclide density have no effect on calorimeter measurements. Techniques used to correct for self-absorption effects are used in PNCC and PAN assay techniques.[3,12,13] Positive assay bias (reported value greater than actual value) can occur when, for example, system multiplication effects become severe at high-plutonium (Pu) sample

---

[11] ASTM C 859-87, "Standard Terminology Relating to Nuclear Materials."

[12] J. T. Caldwell, R.D. Hastings, G.C. Herrera, W.E. Kunz, E.R. Shunk, "The Los Alamos Second-Generation System for Passive and Active Neutron Assays of Drum-Size Containers," Los Alamos Formal Report LA-10774-MS, September 1986.

[13] J. T. Caldwell, et al., "System Evaluation Including Assay Algorithm, Matrix Corrections, and Operational Performance of the Los Alamos Passive/Active Neutron Assay Systems," Los Alamos Technical Report N2-87-222WP.

loadings during PNCC measurements. Typical techniques used to control this interference are: (1) equivalent reference standards used for calibration, or (2) use of source addition techniques.[14]

Of course, to obtain precise assay measurements, count-rate-dependent losses resulting from phenomena such as pulse pileup and analyzer dead-time characteristics must be monitored and corrected. These corrections are not required for calorimeter measurements. Analyzer dead-time is defined as that period of time, which is unique to the analyzer, in which it is unable to accept input signals for analysis. This correction is accomplished through the use of a combination of electronic modules, and/or radioactive sources, and/or computer algorithms (which have been obtained through the assay of calibration standards).

The uncertainty (w) in a measurement is the composite error, including both the precision and bias of the measurement. The uncertainty in a quantity f that is a function of n independent variables x_i is given by:

$$w = \left[\sum_{i=1}^{n} w_i^2 \right]^{\frac{1}{2}}$$

where w_j is the uncertainty in the variable x_i.

Assay item preparation is generally limited to good waste/scrap segregation practices that produce relatively homogeneous items that are required for any successful waste/inventory management and assay scheme, regardless of the measurement method used.

5.2.3 Assay Methods Descriptions, Characteristics, and Limitations

This section describes the various assay methods, presents their characteristics (precision, bias, and detection limits), and discusses their limitations and applicability to assay of CH-TRU wastes. Assay methods discussed include calorimetry, passive gamma assay (e.g., SGS), radiochemical methods, PNCC, and PAN assay.

5.2.3.1 Calorimetry

Calorimetry has been used for many years in the nuclear weapons program for product assay of weapons grade (WG) Pu. Many of the NDA Pu standards in use throughout the DOE complex have been characterized by calorimetry. A large number of standard radiochemical and gravimetric assay comparisons have been performed to verify the accuracy of calorimetric assay measurements.

Basically, calorimeters measure the heat flow out of contained small packages. Experimental difficulties grow exponentially with package size, so this method is generally used only with small packages, a few liters in volume at most. The primary heat release in WG Pu materials is from alpha and beta decay, and with a knowledge of isotopic composition, precise Pu mass

---

[14] R. B. Perry, R. W. Brandenburg, and N. S. Beyer, 1972, "The Effect of Induced Fission on Plutonium Assay with a Neutron Coincidence Well Counter," Transactions of the American Nuclear Society, 15 674.

values are readily obtained from virtually any physical or chemical form of Pu material, without knowledge of precise compound stoichiometry (e.g., Pu-to-oxygen ratio).

The kinetic energy of the emitted alpha or beta particle and the energy of the emitted alpha or beta particle and the recoil nucleus is transformed into heat, together with some fraction of the gamma ray energies and conversion electrons that may be emitted by the excited daughter nucleus in lowering its energy to a more stable nuclear configuration. The electrons and low-energy gamma rays are totally absorbed, while the higher-energy gamma rays that may escape from the calorimeter chamber comprise less than 0.01% of the total decay energy. Thus, most of the energy associated with these transitions of the daughter nucleus to ground state, as well as all of the energy associated with the alpha particle and recoil nucleus, is absorbed within the calorimeter.

The calorimeter method measures the total decay heat produced by an item. The relative isotopic abundances of the Pu and americium (Am) nuclides in the mixture and the values of decay heat per gram for each nuclide are used to calculate the average decay heat per gram of nuclide mixture. The total measured decay heat divided by the average decay heat per gram yields the grams of nuclide mixture.

ANSI N-15.22[8] describes the calorimetry procedure and equipment used for the assay technique. This standard method is used in DOE facilities for calorimetry calibrations, setup, and as the guide to operational measurements.

5.2.3.2 Passive Gamma Assay

5.2.3.2.1 Segmented Gamma Scanning (SGS)

High Resolution (Hyperpure Germanium [HPGe], Lithium-drifted Germanium GE[Li]), Transmission and Count-Rate Corrected Assays.

Overview

The first NDA measurements of TRU isotopes using passive gamma rays were performed by DOE contractor personnel more than 40 years ago. Passive gamma- ray NDA of TRU isotopes is a highly developed technology, and is also the most widely implemented. The introduction more than 20 years ago of germanium solid state detectors and the subsequent incorporation of these detectors into computer-based detection packages has improved the resolution and reliability of these systems. Commercial manufacturers of these systems include Canberra of Meriden, Connecticut, and Nuclear Data of Schaumberg, Illinois.

The number of individual TRU isotopes or their daughters that can be assayed with SGS is large; uranium (U)-233, Pu-238, Pu-239, neptunium (Np)-237, Am-241, Am-243 being among the more common ones. In each case, one or more characteristic moderate-to-high energy gamma rays are emitted in sufficient intensity to permit estimates of quantities in low-to-moderate density waste packages as large as 208-liter (L) drums. The recommended (ASTM C 853-82)[11] experimental arrangement for SGS assays is shown in Figure 5.2-1. This

figure displays the essential elements required for SGS assays of TRU isotopes in any package size.

To minimize assay errors due to axial inhomogeneities, assays are performed in segments along a waste package's vertical axis. The effects of radial inhomogeneities are minimized by rotating the drum during the assay measurement. The detector is shielded in such a manner so as to allow the waste drum to be scanned in segments (typically 10 to 20 segments).

Gamma-ray attenuation is measured for each segment with a transmission source in the indicated geometry of Figure 5.2-1. The energy of this source is selected to match that of the gamma-ray line(s) being measured (e.g., Oak Ridge National Laboratory [ORNL] uses a mixed europium (Eu)-152/Eu-154 oxide source for its large array of gamma-emitting radioisotopes [50 keV to 1600 keV], and selenium-75 is typically used for Pu-239 assays).

State-of-the-art counting electronics allow dynamic counting rate ranges of factors of 10^4 to 10^5 or more, with dead-time corrections measured with a second small, low-energy source positioned near the detector. Waste packaged are automatically rotated about their vertical axes and cycled through the required segment heights with standardized, computer-controlled electronic motors and precision mechanical turntable/elevator hardware. SGS hardware-software packages are commercially available from several manufacturers.

Applicability to CH-TRU Wastes

A prime factor that determines applicability of SGS to perform assay measurements of CH-TRU waste packages is gamma-ray transmission through the package. Other factors affecting assay measurements include particle self-absorption and nonhomogeneity of the assayed item ("lumping"). Two conditions must be met to optimize assay results. First, the particles containing the nuclide must be small to minimize self-absorption of emitted gamma radiation. Second, the mixture of material within a package segment must be reasonably uniform in order to apply an attenuation correction factor, computed from a single measurement of item transmission through the segment. Variations in item composition and density within a vertical segment lead to indeterminate errors. Such variations should be minimized through strict scrap and waste segregation procedures.

A combination of analytical error analysis[3] and experimental usage over many years has determined that transmission factors greater than or equal to 0.5% are required for accurate SGS assays. The physical density of a waste package that this requirement defines depends greatly on the package size [i.e., the radial distance from the gamma-emitting source(s) to detector] and the energy of the gamma rays used for the analysis. Four-liter packages having densities as high as 2 grams per cubic centimeter (g/cm^3) meet the criterion, whereas 208 L packages are limited to densities of 0.5 g/cm^3 or less. To assure compliance with these limits, all current SGS software packages include an automatic warning indicating when the transmission factor for any sector falls below the prescribed limiting value. The routine practice at some sites is to calculate a contribution from that sector based on the lower-limit transmission (e.g., 0.5%).
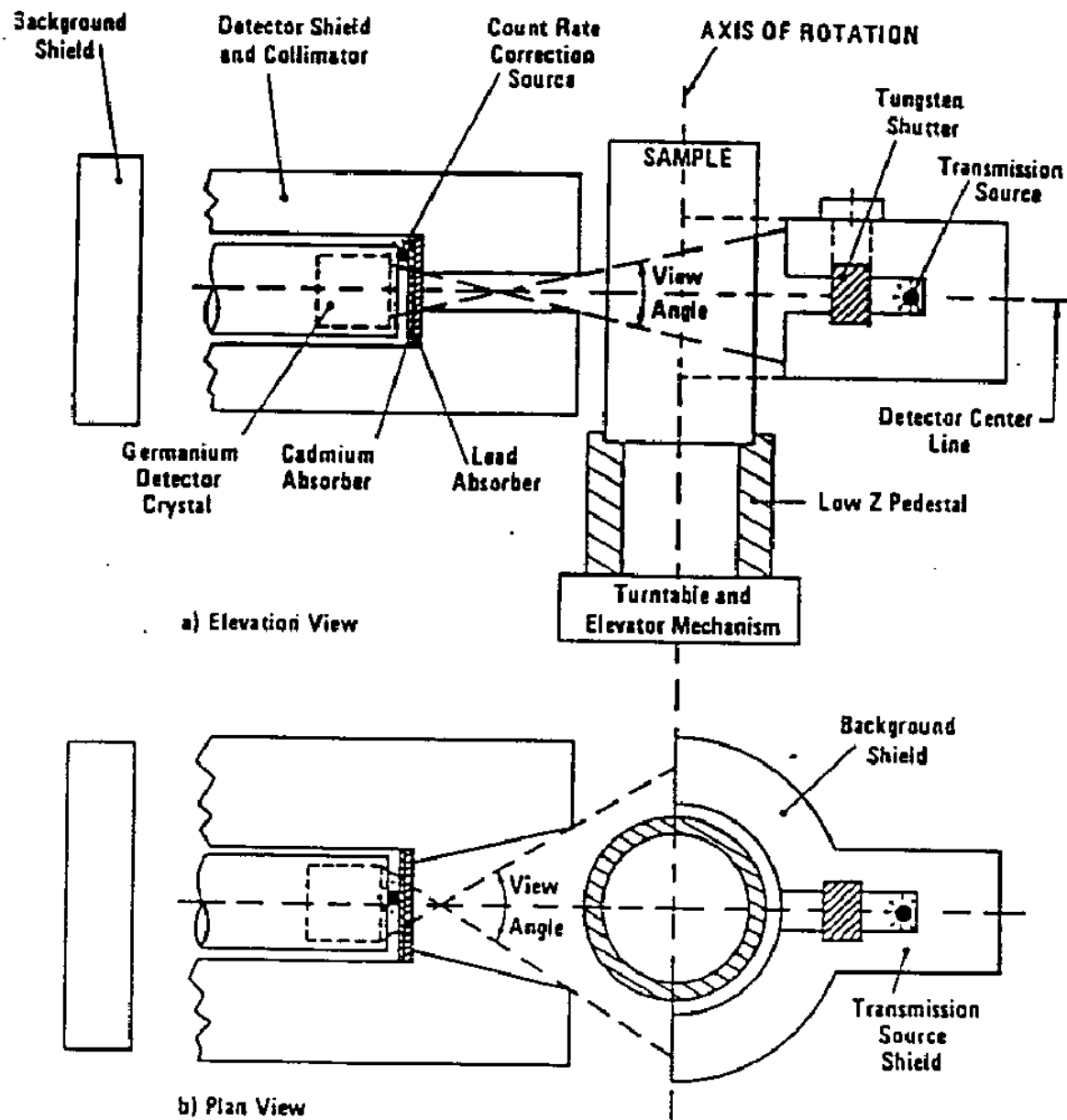
Figure 5.2-1—Schematic Arrangement for Segmented Gamma-Ray Scanning (SGS) System

The reason for maintaining the assay value, rather than disregarding it, is because most SGS transmission failures occur for only one sector out of the 10 to 20 drum sectors assayed. This sector, on the average, contains only a small fraction of the waste drum's total TRU inventory of gamma-emitting isotopes.

On the average, estimating the TRU content for one or two failed segments in this fashion results in only a small overall error for the waste drum. Other sites (e.g., Hanford) flag such drums for management decision on whether the item should be disassembled, examined, and repackaged, or reassayed on a neutron sensing assay instrument, which is less sensitive to density variations. Since the SGS assay value for a transmission failure is truly a lower limit, and as is discussed in detail in Section 5.2.3.4, passive neutron assays generally provide upper limit assay values (especially for WG Pu); the combination of SGS and passive neutron assay methods tends to bracket the actual assay value.

Some matrix forms are inherently unsuitable for SGS analysis. Such forms may contain 'lumps' of nuclide, that is, nuclides contained in small volumes of matrix material having a localized density substantially different from the bulk density of the rest of the container. The dimensions of nuclide particles that constitute a lump vary with the energy of the emitted radiation used for the analytical measurement. The possible magnitude of the problem may be estimated from the following example of attenuating effects. A plutonium metal sphere 0.02 cm in diameter will absorb approximately 4% of the 414 keV, Pu-239 gamma rays produced. Approximately 15% of the 186 keV gamma rays of U-235 will be absorbed in a uranium metal sphere of the same diameter.

As mentioned previously, another condition that will cause measurement problems is presented by containers with several irregular regions, highly variable in density, that prevent the calculation of a valid attenuation correction based on the transmission measurement. In case of such a condition, an analytical method less sensitive to nuclide and matrix densities, such as PNCC, should be employed.

Careful inspection of the transmission and nuclide peak areas for each segment may provide clues when a measurement should be suspect. Sudden, discontinuous changes in the transmission values for adjacent segments or high nuclide count values for isolated segments are examples of signals indicating possible problem items.

Instrument Calibration, Standards Preparation, and Implementation

The recommended DOE facility standard guide used for preparation of SGS standards is ANSI N-15.35.[4] The recommended DOE facility standard for implementation of these standards is ANSI N-15.20.[1] ANSI N-15.20 calls for the preparation of the calibration material using intimate and stable mixtures of the TRU isotope with matrix material and for preparation of a suitable number of calibration standards to cover the anticipated isotopic concentration region of interest (ROI). In the case of Pu-239, this range is 5 to 200 grams (g) for 208 L drums.

When establishing a calibration curve for the SGS instrument, as least two calibration standards are used for each content code. One standards drum contains a TRU isotopic mass near the low

end of the ROI (e.g., 5g Pu-239) while the other contains a TRU isotopic mass near the high end of the ROI (e.g., 200g Pu-239). Both drums contain waste stream matrix mixtures and densities designed to simulate the waste streams. Some sites use more than the two drums described above to ensure a proper calibration factor. Other sites measurement control programs require standards drums to be measured by the assay instrument multiple times, both before and after each measurement session.

Acceptable ranges for calibration data are specified in the operating procedures (e.g., ORNL accepts a variance of +/- 5%). If assay measurement falls outside the acceptable range, no production assay measurement is performed until the issue has been resolved by a designated NDA expert.

Operator Training Requirements and Practices

Present-day commercial SGS systems, such as the Canberra and Nuclear Data models, are highly-automated, computer-based systems. The instruments are computer-controlled using relatively interactive ("user-friendly") software. Only trained personnel are allowed to operate the assay equipment. Personnel are qualified according to DOE Order 5480.5.[15]

Each site provides a specialized training program for NDA instrument operators. The operators are directed and/or assisted by a designated site NDA expert. Expertise is attained by education and experience.

Assay Procedures

The assay procedures cited in ASTM C 853-82, "Standard Test Methods for Nondestructive Assay of Special Nuclear Materials Contained in Scrap and Waste,"[3] are recommended for use at all DOE facilities. These procedures stress usage of proper calibration standards, proper equipment and equipment setup, avoidance of practices (such as misalignment of the waste package) known to result in inaccurate assays, attention to proper record keeping and equipment maintenance, and safe operation of the equipment.

Assay Precision, Bias, and Detection Limit

Assay precision is generally taken to mean measurement repeatability. In the case of typical SGS systems, operated and calibrated according to the recommended procedures, repeatability of results is limited only by statistical counting errors. Counting statistics, in turn, are a strong function of TRU isotopic loading and counting time.

ASTM C 853[10] discusses SGS precision and bias in detail. Some of that discussion follows. The precision of an SGS assay is a function of the precision of the peak areas measured for each segment. The precision of an assay is normally better when the following conditions can be obtained:

---

[15] DOE Order 5480.5, "Safety of Nuclear Facilities," September 23, 1986.

- Increased count time
- High transmission source activity
- Low attenuation for gamma radiation in the energy range of interest.

Typical SGS assay precisions for low-density wastes are listed in Table 5.2-4. Certain matrices, such as graphite molds and cemented insulation, whose densities are above the prescribed SGS-applicability limit of 0.5 g/cm^3 for 208 L packages, and drum handling (homogeneity of calibration standards may be jeopardized) can have a deleterious effect on assay precision.[3]

Table 5.2-4 — Typical SGS Assay Precisions for WG Pu in Low-Density Wastes Contained in 208-L Drum

WG Pu (g)	Precision
1	+/- 100%
10	+/- 10%
30	+/- 3%

(Table 5.2-4 values reflect the assumption that the guidelines given in ASTM C 853-82[3] were adhered to in acquiring the data.)

The precision of an assay performed by SGS is not strongly related to the measurement item's adherence to ideal matrix and nuclide density assumptions. However, measurement bias depends primarily on the adherence of the measurement item to the assumptions of small particle size and homogeneity. Negative bias will be encountered when the nuclide is present in lumps that attenuate their own radiation to a greater extent than the surrounding material. Positive bias can result from low transmission items with over-corrected end effects. Items containing high-density areas may be biased either high or low or be unbiased, depending on the relative position of the high density area and the nuclide of interest. In the majority of measurement situations, however, it is expected that when biases exist, measurement results will be lower than true values.

Several SGS and destructive assay comparison studies of several waste forms indicate SGS assay biases of 10% or less, at the 95% confidence level.[16]   Assay biases for low-density waste matrices contained in 208-L drum packages are 5% or less. In small package applications (based on numerous Safeguards and Nuclear Materials Accounting applications), SGS assay biases of less than 0.5% have been reported.[16] The basic assay formalism associated with the SGS method, that is, transmission correction and the use of small segments, is conducive to very accurate results if recommended procedures are correctly followed. Heterogeneous matrices and isotopic concentration variations can have a severe and unpredictable effect on assay bias for a given waste drum.

Typical SGS assay biases for two types of wastes are summarized in Table 5.2-5.[16]

---

[16] Fleissner, John G. and Hume, Merril W., "Comparison of Destructive and Nondestructive Assay of Heterogeneous Salt Residues," RFP-3876, March 29, 1986.

Table 5.2-5 — Typical SGS Assay Biases

Waste Type	Biases
Heterogeneous salts	10%[a]
Low-density (e.g., combustibles)	5%

[a] Based upon assay of a number of 4-L waste packages prior to placing in a 208-L drum.

(Table 5.2-5 values reflect the assumption that the guidelines given in ASTM C 853-82 were adhered to in acquiring the data.)

SGS assay limit of detection for typical applicable wastes and standard counting times in current routine use in DOE facilities (30 min or less per assay measurement) is about 5g WG Pu. This is based on 30% assay precision. Usually SGS assays are only performed on 208-L drums when screening indicates 10 g or more WG Pu to be present.

SGS Assay Results Comparisons

Calorimetric assay measurements of heterogeneous molten salt residues have provided a total assay value for the Pu and Am, as an NDA comparison (referee) technique for an assessment of SGS assay of RFETS molten salts.[16] Reliable interpretation of the calorimetry measurements depended on an accurate determination of the Am/Pu ratio, since the relative amount of heat produced by the Am in these samples was typically 50% or more.

Gamma-ray spectral isotopic analysis coupled with calorimetry was performed at Mound on nine cans of molten salt, which were subsequently returned to RFETS for dissolution and solution quantification. Results of the Mound measurements show a relative standard deviation range from 0.032% to 0.50% for Pu values and 0.23% to 0.39% for Am values. No biases or statistical differences between pairs or measurements were noted.

5.2.3.2.2 NaI (low-resolution) Assays

Both transmission-corrected and transmission-uncorrected sodium iodide (NaI) assay units are used in DOE facilities. The transmission-uncorrected units are used, for example, at RFETS for low-density wastes containing up to 20 g Pu.

The NaI transmission-corrected assay instruments are special function units, servicing isolated waste streams producing a single type of waste under generally constant conditions. Typically, these NaI units consist of five individual collimated NaI detectors mounted at different heights that view a rotating drum, effecting a five-segment assay. Transmission source geometry is similar to that shown in Figure 5.2-1. The pertinent NDA guidelines outlined in ASTM C 853-82[3] are applied to these systems in a fashion similar to that described for SGS units. A two-window pulse height analysis is performed to correct for Am-241 and fission product interferences, and software indicators flag segments containing excessive Am or fission product amounts.

Calibration standards are carefully chosen for the particular waste stream being monitored, and assays are performed in a fashion similar to SGS assays. These units produce, on the average, reliable results as determined by numerous quantitative comparisons with SGS and PAN assays of the same waste drums.[17] Analytical studies of assay biases for these systems indicate +/-10% levels of bias. This has been verified with SGS and PAN comparisons of a large number of drums assayed with these NaI systems.[17] It should also be pointed out that assay standards practices and procedures are adhered to in accordance with ASTM C 853-82 and ANSI N-15.35. Duplicate assays with SGS or PAN (performed at the certification facility) provide additional assurance that proper TRU assay values are being generated with these systems.

5.2.3.3 Radiochemical Methods

The basic application of radiochemical methods in TRU waste assays is in quantifying radioisotopic content of process liquid or sludge waste forms. Before final drying or cementation, a batch of process sludge is contained in a single large tank. The sludge is then mixed for a sufficient period of time to assure a homogenous mixture. This mixture is then sampled at several points while circulating and the samples subjected to routine radiochemical processing and analysis (precipitation and separation followed by alpha and/or gamma spectrometry). The prepared aliquot samples are assayed in a standard alpha spectrometer. In the cases of higher-activity sludges, these samples are assayed using another method (e.g., passive gamma-ray spectroscopy). Assays of samples obtained from individual sludge drums may also be performed.

Using standard analyses, the individual TRU isotopic activities are determined; Pu-239, total Pu (WG Pu), and Am-241. These aliquot sample activities are then used to determine the original batch TRU activity, on an individual isotopic basis. By proper accounting for any volume reduction or increase produced in the drying or cementation process, these batch activities can then be used to determine an individual 208 L drum's specific Pu and Am content, simply by weighing the drum and accounting for the amount of original batch sludge that was deposited in that particular drum. Accurate final drum assays depend upon following the procedure outlined in a careful manner, with maintenance of a homogeneous mixture during both the crucial sampling and drum filling stages.

Standard test methods (e.g., ASTM C 696-80[5], ASTM C 697-86[6], and ASTM C 759-79[7]) describe the radiochemical standard aliquot sampling procedures used in the DOE facilities. Assay standards are prepared and used as indicated in the standard test methods. Sampling, weighing of the sample, and handling the sample are done under conditions that assure that the sample is representative of the lot or batch. A lot or batch is defined as any quantity of solution that is uniform in isotopic, chemical, and physical characteristics by virtue of having been mixed in such a manner as to be thoroughly homogeneous. All containers used for a lot or batch are positively identified as containing material from a particular homogeneous solution.

---

[17] F. J. Schultz and J. T. Caldwell 1988 DOE Model Conference paper.

Assay biases at the final filled-drum stage are difficult to estimate, since they depend primarily on the maintenance of homogeneous mixtures during the sampling, drying/cementing, and final drum-filling stages.

5.2.3.4 Passive Neutron Coincidence Counting (PNCC) Assays

5.2.3.4.1 Overview

PNCC assays include assays conducted on small packages that are summed to give the final reported assay value for a waste container, and the passive portion of the PAN assay system, which is discussed in detail in Section 5.2.3.5.

PNCC method for determination of Pu assay in product materials has been used for Safeguards verification purposes within the DOE complex for more than 20 years. PNCC has also been applied to the assay of TRU-bearing wastes and scraps for many years (ANSI N15-20-1975[1], subsections 20-28). In addition, the NRC Regulatory Guide 5.11[2] describes NDA techniques acceptable to the NRC for assay of wastes and scraps, which includes PNCC. These standards and regulatory guides are used to ensure proper application by the DOE of PNCC to scrap and waste assay. In fact, DOE laboratories, primarily Los Alamos National Laboratory (LANL), have been largely responsible for the development of PNCC as a reliable assay technique for TRU wastes, as well as for scraps and product.

The prototypical PNCC is comprised of a high-efficiency neutron detector large enough to accommodate the waste package of interest. It operates by detecting the number of time-correlated neutrons being emitted spontaneously by the assay item. In fission events, bursts of 2,3,4,5,... neutrons are emitted simultaneously, and the detection of two or more of these in time coincidence serves to identify the original fission event within the material being measured. Specialized counting electronics (e.g., shift register) have been devised to accomplish and record these measurements. These are discussed in detail in ASTM C 853-82[3].

Any TRU isotope that undergoes spontaneous fission at a measurable rate can be quantified by PNCC. Comprising this category are the even isotopes of Pu, curium (Cm), and californium (Cf). Most commonly within the DOE complex, the different grades of Pu [WG, reactor grades (RG) of different isotopic compositions, heat source grade (HSG)] are quantified by coincidence counting of the included mixture of even isotopes of Pu; predominantly Pu-240 for WG and RG, and Pu-238 for HSG. Thus, with knowledge of the Pu isotopics, the observed coincidence rates can be interpreted to yield total Pu mass.

5.2.3.4.2 Applicability to CH-TRU Wastes

The primary requirement for application of PNCC to CH-TRU waste assay is knowledge of the included isotopics, since normally the quantity of interest is the total elemental mass (i.e., total Pu mass) rather than the even isotope masses only. In addition, the wastes should not include mixed-element spontaneous fission emitters. For instance, it is undesirable to have Cm and Cf isotopes present in the same assay item containing Pu isotopes. Most DOE CH-TRU wastes contain Pu even-isotope spontaneous fission emitters. A typical average WG Pu isotope mix

contains 5.8% Pu-240. Pu-240 is responsible for more than 99% of coincidence neutrons detected in typical WG Pu wastes.

5.2.3.4.3 Instrument Calibration, Standards Preparation, and Implementation

Calibration of PNCC instruments, similar to SGS, is obtained by establishing a curve of instrument response versus isotopic mass.[1,3] A minimum of four calibration points are obtained over the mass range of interest using standards that are representative of the materials being measured. Within each content code, or waste category, the variation due to interference effects within the boundaries defining the limits of that category is measured. Calibration standards are constructed using containers identical to those for the scrap or waste, with contents that are representative of the range of matrix conditions to be encountered. It is not recommended to extrapolate beyond the calibration range established during instrument calibration. Encapsulated Cf-252 sources, such as those used at ORNL for passive PAN calibration, are available to be used for PNCC calibration purposes.

Acceptable ranges for calibration data are specified in the operating procedures. If assay measurement values fall outside the acceptable range, no production assay measurements are performed until the issue has been resolved. Operators contact a designated NDA expert for consultation.

5.2.3.4.4 Operator Training Requirements and Practices

Present-day commercial PNCC systems, such as the JOMAR or National Nuclear models, are highly-automated, computer-based systems. The instruments are computer-controlled using relatively interactive ("user-friendly") software. Only trained personnel are allowed to operate the assay equipment. Personnel are qualified according to DOE Order 5480.5.[15]

Each site provides a specialized training program for NDA instrument operators. The operators are directed and/or assisted by a designated site NDA expert. Expertise is attained by education and experience.

5.2.3.4.5 Assay Procedures

The assay procedures cited in ASTM C 853-82, "Standard Test Methods for Nondestructive Assay of Special Nuclear Materials Contained in Scrap and Waste,"[3] are recommended for use at all DOE facilities. These procedures stress usage of proper calibration standards, proper equipment and equipment setup, avoidance of practices (such as misalignment of the waste package) known to result in inaccurate assays, attention to proper record keeping and equipment maintenance, and safe operation of the equipment.

5.2.3.4.6 Assay Precision, Bias, and Limit of Detection

Most PNCC units are used to assay small packages (4-L size), which are then placed into larger waste containers, such as 208-L drums. Assuming proper administrative control of drum filling, this practice greatly reduces the assay errors associated with all PNCC performance effects except counting statistics and isotopics. Additional errors caused by self-multiplication or system dead-time are significant only when strong neutron sources are present.

Sources of assay biases and measurement uncertainties include:

(a)   Counting statistics: A significant source of error at both extremes of count rate. Measurement uncertainty can be significant at very low count rates for all assay conditions. For every high count rates, when the rate is due primarily to a strong (alpha, n) internal source or induced fissions, assay bias is increased.

(b)   Isotopics: For WG Pu waste assay biases produced by systematically incorrect actual Pu isotopics are 3% or less, based on use of historic average WG Pu isotopics. Uncertainties in the measurement of the isotopic composition, generally considered to be unbiased, increase the uncertainty of the assay value.

(c)   Self-multiplication (or induced fissions): Generally a problem when fairly large Pu amounts are present in conjunction with strong (alpha, n) sources within the same drum (measurement value greater than actual value). This phenomenon is a source of potential bias producing uncertainty in the assay value. Multiplication effects should not be significant when TRU gram loadings are low and waste volumes are large.

(d)   System dead-time: A problem when strong neutron sources are present (measurement value is less than actual value). This phenomenon is a source of potential bias with an associated uncertainty.

(e)   Calibration: Typically, assay uncertainties produced by uncertainties in calibration are 3% or less.

(f)   Matrix effects: Matrix effects include neutron poisons (e.g., boron, cadmium) and other neutron emitters [species that spontaneous fission or have strong (alpha, n) reactions] and neutron moderators. See Caldwell et al., 1986[12] for a discussion of moderator error estimation techniques.

Table 5.2-6 provides a summary of typical PNCC assay error contributions for low-density waste forms.

Table 5.2-6 — Summary of Typical PNCC Assay Error Contributions for Low-Density Waste Forms

Error Contribution	WG Pu	Typical Errors
Counting statistics	1 g	+/- 50%
	10 g	+/- 10%
	30 g	+/- 5%
	100 g	+/- 3%
Self-multiplication		+/- 5%
System dead-time		+/- 3%
Isotopics		+/- 3%
Calibration		+/- 3%
Matrix (low-density)		+/- 5-20%

Estimates of PNCC assay uncertainty can be calculated by standard error propagation techniques from the various bias contribution variances. The grams of plutonium calculated by PNCC is a function of net passive coincidence neutron count rate (gross neutron coincidence count rate minus accidental neutron coincidence rate) (SIGP), self-multiplication (MULT), system dead time (SYSDT), isotopics (ISOP), calibration (CALIBP), and moderator index (MI).

For 30 grams of plutonium, the uncertainty in the 30 grams of plutonium is given by (see Section 5.2.2):

$$w \quad = \quad [f(SIGP)^2 + f(MULT)^2 + f(SYSDT)^2 + f(ISOP)^2 + f(CALIBP)^2 + f(MI)^2]^{1/2}$$
$$= \quad [(0.05)^2 + (0.05)^2 + (0.03)^2 + (0.03)^2 + (0.03^2 + (0.20)^2]^{\frac{1}{2}}$$
$$= \quad 0.218 \text{ or } 21.8\%.$$

The passive mass assay value reported by the PNCC assay algorithm would then be:

Passive mass (grams) =   30.00 +/-   6.55.

Anderson and Lemming, 1982, MLM-3009, Table 5, p. 33, [18] shows overall neutron production rates for several of the more common TRU isotopes and several of the more common matrices that produce significant (alpha, n) reactions. For example, WG Pu, which has an average alpha energy of 5.15 megaelectron-volts (MeV), produces approximately 2 neutrons per second per millicuries-alpha (n/s/mCi-alpha) in an oxide matrix and 215 n/s/mCi-alpha in a fluoride matrix. Pu-238 and Am-241, which have an average alpha particle energy of 5.5 MeV, produce approximately 2.5 n/s/mCi-alpha in an oxide matrix and approximately 310 n/s/mCi-alpha in a fluoride matrix. These values are representative of pure chemicals and alloys. Neutron production rates for waste materials will be less, since the TRU isotopes are more widely dispersed and the alpha particles are less likely to encounter a productive target.

The more usual (alpha, n) reactions that can cause passive assay concerns consist of normal WG Pu in which a sizeable fraction of the Pu is chemically bound to either fluorides or bound in a salt mixture containing aluminum or magnesium. Typically, metal oxide or nitrate forms of TRU isotopes (which produce approximately 0.7 to 2 n/s/mCi-alpha) present no problems for passive neutron assays (both passive PAN and PNCC). In practice, rates ranging to 20 n/s/mCi-alpha do not decrease passive assay precisions drastically as long as the alpha sources present are only those associated with WG or RG Pu. However, waste streams that include additional Am-241 can be difficult to assay passively even if the TRU chemical form is the oxide.

---

[18] M. E. Anderson and J. F. Lemming, "Selected Measurement Data for Plutonium and Uranium," MLM-3009 (or ISPO-157), November 1982.

5.2.3.5 Passive-Active Neutron (PAN) Assay Systems

5.2.3.5.1 Overview

PAN assay systems consist of two independent assay units—passive and active neutron. The combination of passive and active neutron assays within a common system provides a unique set of information.

The passive assay portion of the PAN method described below is an adaptation of the PNCC method using "self-measurement" matrix corrections. Two complete passive assay detection systems are maintained with separate counting electronics. Two detection systems are used separately or in combination depending upon the neutron count rate. The passive coincidence measurement provides quantitative information on even isotopes present in the waste container, such as Pu-240. The passive singles neutron count rate (difference between total neutron rate and that due to spontaneous fission events) provides semi-quantitative information on alpha particle emitters present in the waste container, such as Am-241. The active assay provides quantitative information on the Pu-239 and other fissile isotope constituents. See Schultz et al., 1984[19] and WIPP-DOE-157, 1989[20] for a more complete description of the system.

For WG Pu, the passive coincidence and active assays provide independent total Pu assay values. This fact has been extremely important in verifying the accuracy or determining the bias of the PAN assay measurement technique, as presented in Caldwell, et al., 1986.[12] This formalism has also been verified by extensive comparisons of both passive and active neutron assays with SGS.[10] PAN assays systems have been developed for both drums and boxes (see Section 5.2.5 for discussion of box PAN assay systems). For these relatively large waste containers, effects of the waste material (matrix) on the neutron signals observed cannot be neglected.

5.2.3.5.2 Instrumentation

A basic cross-sectional view of a typical LANL PAN detection system, showing the schematic "interwoven" layout of the two distinct types of neutron detection packages (bare He-3 and cadmium (Cd)-shielded He-3 detector tubes), is shown in Figure 5.2-2.

Passive Assay Portion

The passive portion of the PAN assay system utilizes the two types of detection packages to:

(a)   determine a MI used to determine a correction to the assay calculation to account for the matrix characteristics, and

---

[19] F. J. Schultz, et al., Oak Ridge National Laboratory; J. T. Caldwell et al., Los Alamos National Laboratory, "First-Year Evaluation of a Nondestructive Assay System for the Examination of ORNL TRU Waste," ORNL-6007, April 1984.

[20] "Data Package Format for Certified Transuranic Waste for the Waste Isolation Pilot Plant," WIPP-DOE-157, Rev. 2, January 1989.

NEUTRON GENERATOR

BARE ^{3}He DETECTOR PACKAGE

CADMIUM SHIELDED ^{3}He DETECTOR PACKAGE

BORATED POLYETHYLENE

GRAPHITE

POLYETHYLENE
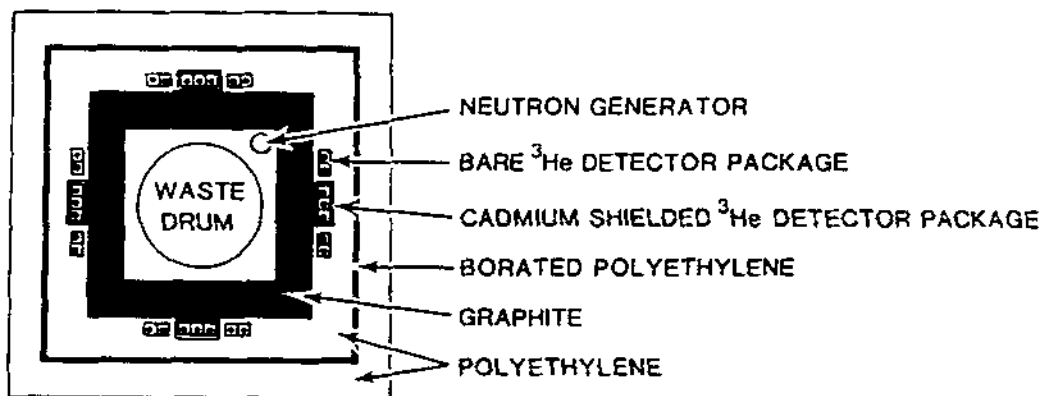
Cross-sectional views of the second-generation assay chamber show the layout and relative positions of both shielded and bare ^{3}He detector packages.

Figure 5.2-2—Schematic PAN System Layout

(b)   optimize counting statistics depending on the actual relative neutron sources encountered.

For low count-rate waste containers, all counts detected by the neutron detector packages are summed to yield the lowest assay limit of detection possible. All detector count rates (acquired by both bare and shielded detectors) are summed electronically to obtain a "System Totals" neutron detection efficiency of approximately 12%.

For waste containers with higher Pu loadings (e.g., 100 g or more) coupled with strong (alpha, n) backgrounds, the Cd-shielded detectors are summed independently, and the "Shielded Totals" count rate is formed with a resulting neutron detection efficiency of 2.9%. However, this detection package possesses a much faster "die-away" or "neutron-collection" time, approximately six times faster than that of the slower "Systems Totals", which is approximately 15 microseconds. At low count rates, the slower collection time is of no consequence [i.e., accidental coincidences due to (alpha, n) reactions are small] and, thus, the Systems Totals provides not only a more sensitive but also statistically more precise passive assay measurement.

At higher count rates the faster die-away time of the Shielded Totals gains a higher precision than the less specific count rate (Systems Totals). As a consequence, at high neutron count rates the Shielded Totals Coincidence rate is used to obtain the more precise passive assay measurement value.

The cross-over count rate (i.e., the count rate at which the assay measurement value obtained by the Shielded Totals supplants the Systems Totals) has been experimentally determined to be approximately 2000 counts per second (cps) (Systems Total count rate), and this value is used in the assay algorithm. There is a substantial range in which either Systems Coincidence or Shielded Coincidence rates both provide precise assay values. Many data comparisons have been performed in this cross-over region to verify the self-consistency between the two coincidence measurements.[17]

Active Assay Portion

The active portion of PAN systems performs a high-sensitivity, pulsed thermal neutron interrogation assay of waste drums. As shown schematically in Figure 5.2-2, a small 14-MeV neutron generator placed within the assay chamber between the waste drum and moderating walls provides short pulses (5-10 microseconds [ms] of high-energy interrogating neutrons. In approximately 0.5 ms, all original fast neutrons in this interrogating pulse have been thermalized by multiple collisions with the graphite and polyethylene walls and moderating materials within the waste drum. This "thermalized interrogating pulse" persists ($T^{1/2}$ about 400 ms) for some time, during which induced fissions within the waste drum are produced, primarily in Pu-239 or other fissile isotopes. These events, in turn, result in prompt-fission, spectrum neutrons being emitted by each fissioning nucleus.

The cadmium-shielded detection packages have been designed to reject an external thermal neutron flux to 1 part in 10^7, but to respond sensitively to fission spectrum neutrons. The

summed shielded detector packages shown in Figure 5.2-2 detect about 3% of all induced fission events that are produced within typical waste drums.

An additional measurement feature not shown in Figure 5.2-2, but discussed at length in Caldwell, et al., 1986,[12] is the set of thermal flux monitors, one Cd-shielded and collimated and the other bare, that are also positioned inside the assay chamber between the waste drum and the moderating walls. As discussed at length in Caldwell, et al., 1986,[12] the ratio of these flux monitors is highly sensitive to the neutron absorption characteristics of the waste drum contents. This ratio is used to form a drum "Absorption Index" (AI) (see Section 5.2.3.5.3).

5.2.3.5.3 PAN Assay Matrix Corrections

Two types of matrix effects can interfere with the active neutron measurements: absorption and moderation.[12] The absorption effects occur almost entirely as an attenuation of the interrogating thermal neutrons, caused by the presence of various neutron poisons within the waste matrix (e.g., boron, cadmium, chlorine, etc.).

Moderation effects occur at two stages of the measurement. The original burst of 14-MeV neutrons can be moderated to a considerable extent during passage through the waste matrix. Generally, this results in a larger thermal neutron interrogation flux than would have been produced in the absence of matrix. After the interrogation flux has produced fission reactions within the waste matrix, the same moderating materials can attenuate the prompt-fission signal neutrons resulting in a decrease in observed response relative to the no-matrix case. This attenuation of signal fission-neutrons also is the primary matrix effect for the passive measurement.

The approach to matrix corrections has been to base corrections on measured quantities determined as adjuncts to the primary active and passive TRU assay measurements. The systematic matrix correction algorithm is based on an analytic fit to assay measurements obtained for different positions of the source within a matrix drum. These analytic fits then provide estimates of uncertainty for the active and passive assay data.

The absorption matrix correction approach used by the PAN systems employs a ratio of an unshielded in-chamber flux monitor to a cadmium-collimated, in-chamber flux monitor (designated the barrel flux monitor). This ratio is termed the AI. The barrel flux monitor detects those neutrons that have undergone drum matrix interactions. The ratio of the monitors strongly reflects the neutronic properties of the matrix.

AI = [flux monitor response (0.7-4.7 ms)]/   (1)
                [barrel flux monitor response (0.7.4.7 ms)]

The MI depends upon the responses of the two detection systems (Cd-shielded and bare) to moderated neutrons. The shielded detectors are insensitive to thermal neutrons, while the bare detectors are very sensitive to the thermal neutron flux. In turn, the thermalized fraction depends very strongly on the moderator density of the matrix. To use this relationship in obtaining matrix correction factors, the ratio is normalized so that a value of zero is obtained when no moderator is present and, in addition, a small correction is made to account for self-absorption effects.

The general equation for a moderator index is given in Equation (2).

$$MI = \{1 - [(\text{shielded totals})/(\text{system totals})]/A_o\} \qquad (2)$$
$$x \: \{A_1 + A_2 \: x \: \ln(AI)\}$$

The term within the first set of brackets is the basic raw spectral data, and the term within the second set of brackets is the correction term for matrix absorption effects. The same MI values are used for both active and passive matrix corrections.

In order to obtain data to construct analytical models of matrix correction factors, 19 simulated waste matrices were fabricated,[12] and active and passive calibration standards were placed in known locations throughout the waste matrix drums. Both active and passive assay matrix response measurements were obtained as a function of location (radius, r, and height, z) of the standards. The resulting matrix response values varied smoothly as a function of r and z. These studies determined that the systematic effects are due only to gross neutron absorber and moderator amounts and are independent of the actual nature of the materials themselves. That is, a drum filled with Raschig rings (borated glass) produces the same responses as a drum filled with vermiculite mixed with an equally absorbing amount of borax.

Most of the observed distributions have been found to fit a power law as given in equation 3:

$$y = A + Br^N \qquad (3)$$

where A, B, and N are the fit parameters and r is the drum radius.

Volume-weighted average values were calculated using this equation, representing the most probable measurement result for either a totally uniform or a totally random distribution of source material within the matrix.

The matrix correction factor (MCFA) for an active assay measurement is a function of the AI and MI.

$$MCFA = MCFA(AI) \: x \: MCFA(MI) \qquad (4)$$

The MCFA values were fit to the power law (equation 3) as a function of their AI values for the 19 simulated waste matrices. The following set of equations describing the absorption portion of the active assay matrix correction factor were obtained for one PAN system:

$$MCFA(AI) = 1.00 \qquad (5)$$

for the AI less than or equal to 2.272, and

$$MCFA(AI) = 0.54x(AI)^{0.612} \tag{6}$$

for the AI greater than 2.72.

The moderator portion, MCFA(MI), of the active assay matrix correction factor is obtained by dividing the total measured MCFA values by the calculated MCFA(AI) values obtained in equations (5) or (6).

The analytic representation of these data is thus of the form

$$MCFA(MI) = 1.00, \tag{7}$$

for the MI less than or equal to 0.40,

$$MCFA(MI) = 0.483exp[1.817(MI)] \tag{8}$$

for the MI greater than 0.40.

The passive neutron matrix corrections are determined by systematic drum matrix measurements in a manner similar to the active measurements discussed previously. The passive matrix correction factors, MCFP, are a strong function of the MI.

The MCFP analytic fits to the four independent quantities measured during a passive assay scan are given below.

$$MCFP(system\ totals) = 1.00, \tag{9}$$

for the MI less than or equal to 0.355,

$$MCFP(system\ totals) = -0.16 + 3.28(MI), \tag{10}$$

for the MI greater than 0.355,

$$MCFP(shielded\ totals) = 1/[1 - MI], \tag{11}$$

$$MCFP(system\ coincidence) = [(0.5967)/(1 - MI) + 0.4187]^2, \tag{12}$$

$$MCFP(shielded\ coincidence) = [(0.8902)/(1 - MI) + 0.2337]^2. \tag{13}$$

The matrix correction equations given above or variations thereof are contained in the present PAN assay systems algorithms used throughout the DOE. Some sites perform additional matrix-dependent corrections to the assay results as discussed in Section 5.2.3.5.9.

Figure 5.2-3 shows the "Moderator Index" (see Caldwell, et al., 1986[12] for detailed discussion of the MI) obtained with mock matrix drums containing various hydrogen densities spanning the region of interest for general CH-TRU wastes. As can be seen, the MI varies smoothly with
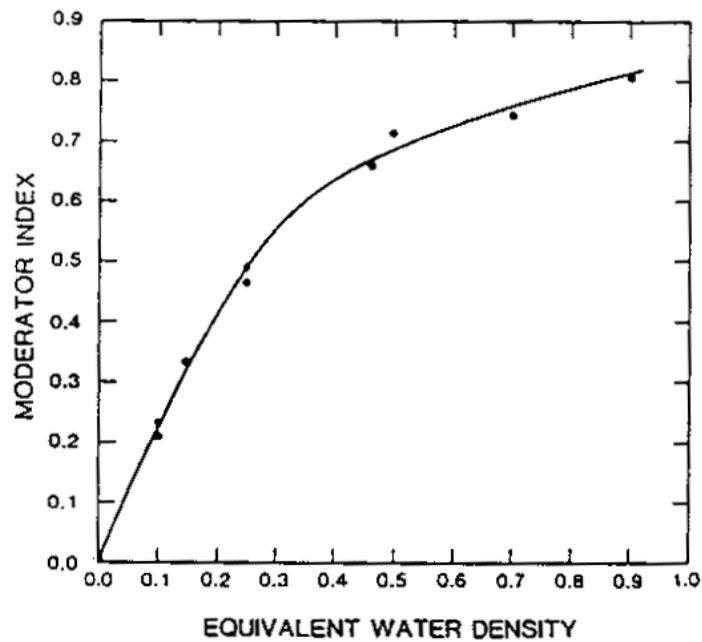
Figure 5.2-3—Moderator Index Measures for PAN Systems Using the Detector Ratio Method

average hydrogen density within a 208-L drum. Sludges display one of the higher average hydrogen densities of any CH-TRU waste form, with correspondingly high MIs (0.4 to 0.8). Lightly moderating matrices, such as combustibles, have MIs falling typically in the 0.1 to 0.3 region, and miscellaneous metals matrices, which generally contain no moderating materials, have measured MIs near 0.0.

Figure 5.2-4 shows the actual moderator correction factor (MCF) data[12] for the PNCC portion of the PAN systems as implemented at INEEL, Hanford, and SRS. The MCF value is the multiplicative factor required to normalize a given matrix measurement to the empty drum level of PNCC sensitivity. As can be seen, the MCF value varies smoothly as a function of the MI; Figure 5.2-4 can be used to estimate typical MCF values. For example,

  (a) Miscellaneous metals, MCF = 1.0 (i.e., same sensitivity as with empty drum),

  (b) Combustibles matrix, MCF = 1.35, and

  (c) Sludges, MCF = 3.6.

The MCF range observed for a 3,000 CH-TRU drum sludge assay campaign at INEEL was 1.8 to 10.0.

When performing PNCC assays of highly moderating matrices, such as sludges, measurement of a MCF value is essential for accurate assay results to be obtained. A "calibration" based on a "typical" sludge drum would result in assay errors of hundreds of per cent for some drums because of the large hydrogen density variations observed.

Figures 5.2-5a and 5.2-5b show plots of the systematic active assay correction factors. As can be seen in Figures 5.2-5a and 5.2-5b, some waste materials require no matrix correction (relative to a standard response measured in an empty drum). Examples of these waste matrices are cellulose-based combustibles, graphite molds and scarfings, aluminum scrap, dry-to-moderately-wet dirt, and silica.

5.2.3.5.4 Assay Algorithm and Data Acquisition System

All PAN units utilize a similar assay algorithm. At present, all drum- size units are equipped with IBM/PC-based data acquisition systems as described in Kuckertz, et al, 1987.[21] The system operating program (NEUT) controls all data acquisition and contains the assay algorithm.

Each data acquisition consists of sequential active and passive neutron assays, preceded by a user interactive initialization stage in which drum identification, content code information, drum weight, etc., can be entered from the PC keyboard, from a bar code reader, or from an RS-232 port by direct interaction with a site's data management computer. The weight of the drum's contents is used in calculating the nanocuries per gram (nCi/g) assay value that differentiates between TRU and non-TRU wastes. The content code input is used to flag difficult-to-assay

---

[21] T. H. Kuckertz et al., "Making Transuranics Assay Measurements Using Modern Controllers," Proceedings 9th ESARDA Symposium on Safeguards and Nuclear Material Management, London UK, pages 389-393, May 1987.
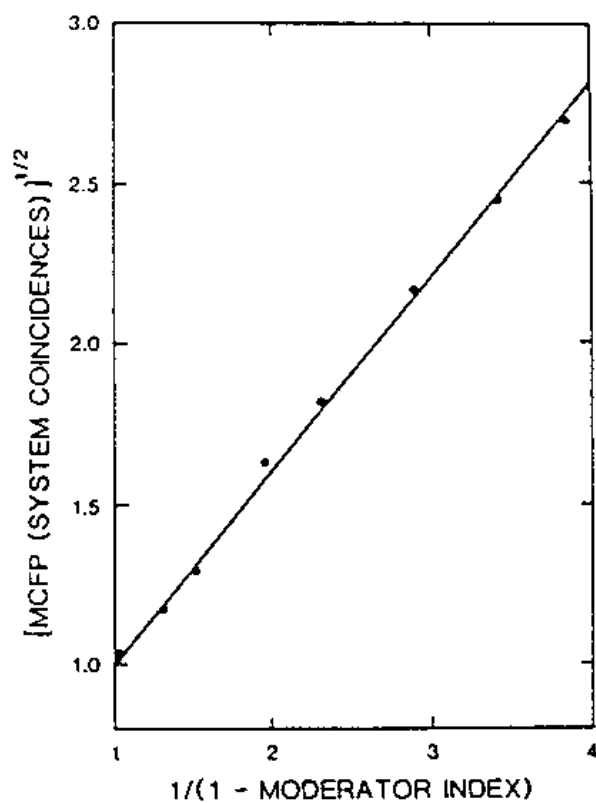
Figure 5.2-4—Use of the Moderator Index to Determine Passive Neutron Coincidence Matrix Correction Factors for a PAN System
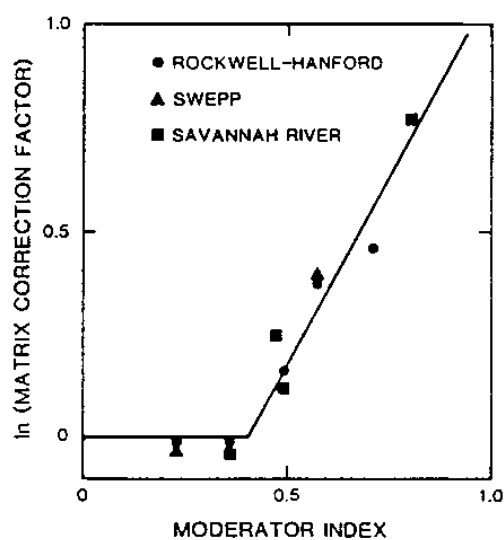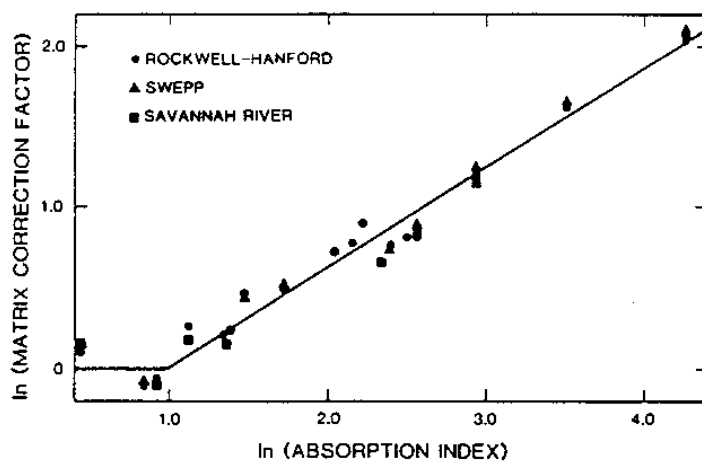
Figure 5.2-5—PAN System Active Assay Matrix Correction Factors Measured at Hanford, INEEL, and SRS with a Set of 20 Standard Matrix Drums

matrices or "special case" drums (see Section 5.2.3.5.11). All data input modes are in current use at the various sites. However obtained, that information becomes part of the permanent record stored with the TRU assay and matrix measurement data.

Modifications and upgrades have been performed at various times since the original algorithm was written in 1982. The development and upgrade of hardware and software has continued.[12,22,23,24] The software revisions can be readily accomplished within the Fortran software framework of NEUT.

Measured data as well as all initialization information, date and time stamp from the internal PC clock/calendar, and final analyzed results are archived. An on-line hard copy printout of the assay parameters and results is also generated. All background and calibration measurements are routinely recorded and archived in the same fashion as normal assays. Thus, a continuous and traceable record of all data is maintained. Most sites, in fact, are maintaining this complete set of data in interactive databases (e.g., Lotus 1,2,3 or dBASE III), wherein all single-run assay data occupies one row in a single spreadsheet or database record. In some cases, 10,000 such records exist at a site (e.g., INEEL). This data archiving technique is an extremely important development as such extensive waste drum assay databases have not been developed previously in the NDA field, much less put into such readily accessible form. This greatly facilitates internal consistency checks and comparisons of large numbers of individual drum assays results obtained with different assay techniques.

RG Pu (i.e., Pu containing high Pu-240 content) is accommodated within the same PAN algorithm as is used for WG Pu. The PAN operator is queried before each assay as to whether the drum contains WG Pu and, if not, what is the correct Pu-240 percentage for that waste drum. Once the Pu-240 percentage is entered, the algorithm automatically corrects both passive and active assays for the different Pu isotopics.

The basic Pu algorithm cannot, however, directly accommodate Pu-238 or HSG Pu. Those sites assaying HSG Pu waste exercise a special algorithm option in their Main Menus that allows for analysis of the basic passive and active data in terms of HSG Pu. If selected this option:

(a) Interprets the active assay results in terms of a Pu isotopic mix consisting of 18% Pu-239 and 82% Pu-238. Since only the Pu-239 fraction is fissile, total Pu mass is obtained by dividing the active assay result by the factor 0.18.

---

[22] J. T. Caldwell, J.M. Bieri, and A.P. Colarusso, "The Los Alamos Second-Generation Passive-Active Neutron Assay System--FY86 Operations Record and System Evaluation", Los Alamos Technical Report LA-Q2TN-86-106, September 1986.

[23] A. P. Colarusso, et al., "Mobile Nondestructive Assay System," Proceedings of 28th Annual INMM Meeting, Newport Beach, Ca, July 12-15, 1987.

[24] K. L. Coop, J. T. Caldwell, and C. A. Goulding, "Assay of Fissile Materials Using a Combined Thermal/Epithermal Neutron Interrogation Technique," Third International Conference on Facility Operations-Safeguards Interface, San Diego, CA, November 29 - December 4, 1987.

(b)   Interprets the passive assay data similarly. Pu-238 undergoes spontaneous fission at a rate of 2600 neutrons per second per gram (n/s/g) (for comparison, the Pu-240 rate is 990 n/s/g). Thus, passive coincidence counts can be used to obtain an estimate of Pu-238 mass.

(c)   As in all cases the Systems Totals Passive Singles rate can be used, assuming oxide as the dominant chemical form, to estimate a total alpha particle emission rate. This estimate can then be used to calculate the Pu-238 mass.

The SRS possesses most of the DOE's Pu-238 waste, and is currently evaluating their Pu-238 algorithm.

5.2.3.5.5 Applicability to CH-TRU Wastes

The PAN systematic matrix correction factors discussed in Caldwell, et al., 1986[12], and Section 5.2.3.5.3, and now implemented in all drum-size PAN units enables the quantitative assay of virtually all DOE wastes presently packaged in 208-L drums. At present, these six implemented PAN units have been used to assay, collectively, about 20,000 CH-TRU waste drums at the various sites, including 2,000 drum assays performed with the mobile drum unit at the Nevada Test Site (NTS) and Lawrence Livermore National Laboratory (LLNL).

5.2.3.5.6 Instrument Calibration, Standards Preparation, and Implementation

Calibration of PAN units includes a thorough initial calibration after fabrication and routine calibrations using secondary standards.

Caldwell, et al., 1986[12], lists the standards used in all the present PAN units, for which all passive and active calibration standards have National Bureau of Standards (NBS)-traceable or NBS-referenceable origins. Absolute and matrix standards calibrations were conducted of the PAN unit. The PAN units were then each provided a set of secondary standards (placed in "Pink Drums" for conspicuous identification) consisting of standard, NBS-referenceable Cf-252 passive assay and U-235 active assay materials. A baseline reference data set for both passive and active assays was obtained for each PAN unit with these unique "Pink Drum" standards, and each unit has subsequently performed standard Pink Drum assays prior to each set of PAN waste drum assays.

A typical set of these standards measurements performed with the INEEL PAN unit and extending for almost a three-year period is shown in Figure 5.2-6. The individual passive and active standards measurements fall well within a +/- 5% window, with no measurable systematic drift during the three-year operational history. Caldwell, et al., 1986[12], lists the corresponding Pink Drum measurements for Hanford, SRS, and the mobile drum unit. All display the same basic stability of response.
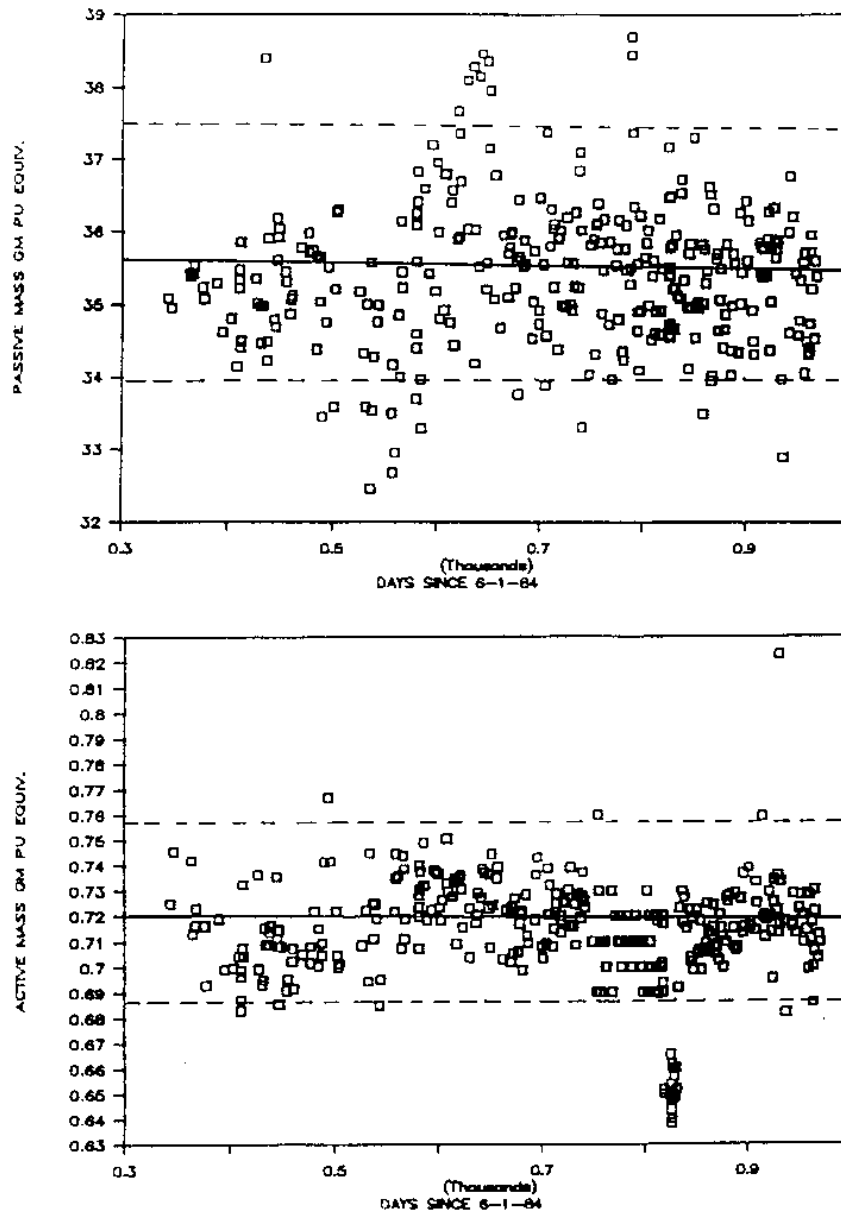
**Figure 5.2-6—INEEL PAN Standards Measurements (Pink Drum)
Performed Over a Three-Year Period.**
(Top Graph Shows Passive Standard and Bottom Graph Shows Active Standard.
Dashed Lines Indicate a +/-5% Measurement Error Band About Expected Standards
Assay Values.)

5.2.3.5.7 Operator Training Requirements and Practices

The present generation of PAN units are highly-automated, computer-based systems. The instruments are computer-controlled using relatively interactive ("user-friendly") software. Only trained personnel are allowed to operate the assay equipment. Personnel are qualified according to DOE Order 5480.5.[15]

Standardized training requirements and guidelines for all DOE assay operators are based upon such already-existing industry standard training requirements, such as SNT-TC-1A. Each site provides a specialized training program for NDA instrument operators. The operators are directed and/or assisted by a designated site NDA expert. Expertise is attained by education and experience.

5.2.3.5.8 Assay Procedures

As of 1989, the PAN assay systems were comparatively recent additions (approximately six years) to NDA instrumentation and, as a consequence, ASTM and ANSI standards have not been developed for PAN assay systems. Active assay techniques have been used for approximately 18 years, but the 14-MeV thermalized neutron assay (active portion of PAN) is comparatively recent. Of course, the passive coincidence portion of PAN is similar to the PNCC assay technique and, therefore, PNCC ASTM, ANSI, and NRC standard practices and guidelines are followed for that portion of the PAN system.

All PAN standard operating procedures instruct operators to acquire a background and a "Pink Drum" data set before any assays on waste containers are performed. These data sets are checked for consistency and, if the results fall outside a predetermined (e.g., +/-10%) acceptance window, remedial action is taken. The remedial action can include a repetition of the background and/or standards measurements. If the second measurement is successful, general assays can resume. If the problem persists qualified personnel are contacted to "debug" the system. No CH-TRU waste drum assays can resume until the problem is satisfactorily resolved. If the background or standards measurement is outside the acceptance window, the diagnostic generally assumed is that a hardware problem exists.

The assay procedure for PAN units equipped with the IBM/PC data acquisition system is relatively straightforward. An operator inserts a waste drum into the PAN unit and enters all drum identification information via an interactive dialogue (PAN assay system software, NEUT, prompts the operator for the specific information). Once NEUT has checked the information for correct format, the assay record and programmable electronics hardware are properly indexed, gates set, etc., NEUT then sends a message to the operator (via the CRT screen) that the system is ready to begin an assay.

At this point the operator presses one button, the start sequence button on the MA165C neutron generator controller unit. This initiates the PAN active assay. At the conclusion of the active assay, NEUT automatically records all data and initiates the PAN passive assay. At the conclusion of the PAN passive assay, all data is recorded, analyzed and printed out for

immediate inspection. The operator is then informed (via the CRT Screen) that the system is ready to perform another assay.

5.2.3.5.9 Assay Precision, Bias, and Limit of Detection

The PAN assay algorithm contains a calculation of the measurement uncertainty[12] that combines statistical uncertainties and estimated systematic biases based on the measured matrix correction factor. For a generally heterogeneous matrix and TRU materials distribution, the larger the indicated matrix correction, the larger the expected assay uncertainty. These values are reported with the actual assay values, for both passive and active neutron assays. For many well-characterized waste streams a typical value for the estimated uncertainty (not including the statistical contribution to the error) is 20%.

When a systematic matrix correction formalism is used, the corresponding systematic uncertainty in the passive assay measurement can be decreased to 5% or less. This low an uncertainty is valid for dry, combustible, low-hydrogen content waste, such as general laboratory waste. The passive assay value uncertainty is calculated as for PNCC. The algorithm used in the passive coincidence portion of the PAN units calculates a composite assay uncertainty based on combining all the effects discussed above, which becomes part of the permanent archived assay record.

The active assay value uncertainty estimate includes a systematic bias contribution, which is a function of the MCF (AI and MI). For reasonably uniform TRU isotope distributions (such as are found in sludges), AI measurements indicate assay uncertainties of +/- 10%. For nonuniform TRU isotope distributions, the uncertainty is a function of the magnitude of the MCF.[12] That is, the larger the MCF, the larger is the associated assay uncertainty. The effects on the assay measurement of concentrated TRU activity in different drum locations have been calculated and plotted as a function of the total MCF. For example, a matrix correction factor of approximately five yields a corresponding uncertainty of 50% in the assay measurement.

Extensive comparisons have been performed for passive and active neutron assays of the same drum, for a great variety of matrix types (e.g., four types of sludges, job-control wastes, combustibles, graphite scarfings, miscellaneous metals, tantalum crucibles, glassware, molten salts, filter media, dirt, and others.) Some of these comparisons are shown in the figures of this document and are discussed in Fleissner, et al., 1986, and Schultz and Caldwell, 1988.[16,17] It should be noted that the matrix corrections applied to passive and active assays for a given type of matrix (except where no matrix corrections are necessary) are quite distinct. Thus, there is a very low probability of obtaining agreement by accident between active and passive neutron assays for wastes with significant moderator and absorber amounts. If one obtains agreement, both independent PAN assay techniques are considered to yield unbiased assay measurement values.

The assay limit of detection for the active neutron portion of the PAN unit can be as low as a few milligrams of Pu-239 placed anywhere within a typical 208-L waste drum.

5.2.3.5.10   PAN Assay Results Comparisons

Comparisons of PAN assay results with SGS or radiochemical assay methods have been performed. The PAN assays, both passive and active, have been compared with SGS and radiochemistry assay results for (a) matrices requiring little or no matrix corrections, such as graphite molds and general laboratory wastes, and (b) homogeneous matrices (e.g., sludges).

Two papers[13,17] detail several comparisons of PAN and SGS assay measurements. Caldwell, et al.[13] includes a total database of some 5,000 assays performed at NTS, LLNL, Hanford, INEEL, LANL, and SRS. The drum assay and matrix correction formalism presented in Caldwell et al., 1986[12] was extensively evaluated for all types of waste matrices and waste content codes being generated within the DOE complex. Schultz and Caldwell 1988[17] encompasses an even larger database, but is confined to INEEL PAN assays and comparisons with RFETS SGS assays.

Figures 5.2-7a, 5.2-7b, and 5.2-7c show a recent PAN/SGS comparison performed by LANL personnel[11] using a mobile PAN drum-sized unit. The data was acquired at LLNL from assays of a set of some 200, 208-L, WG Pu waste drums consisting of general laboratory wastes (e.g., glassware, cellulosics, plastics, etc.) that had been assayed using the LLNL SGS unit. Figures 5.2-7a, 5.2-7b, and 5.2-7c show the PAN passive neutron, PAN active neutron, and SGS assay measurements comparisons. A statistical analysis of this data set indicates systematic agreement between both PAN neutron data sets and the SGS assay results at the 5% level (95% confidence level). Figure 5.2-8 shows a plot of similar waste stream assays performed with the Hanford PAN system, comparing passive and active neutron assay values for a set of 400 waste drums.

Figures 5.2-9a and 5.2-9b show a set of over 300 "graphite molds" matrix waste drums (RG Pu) assayed with the PAN unit at INEEL and also with an SGS unit located at the RFETS. A statistical analysis of this data set indicates systematic agreement of all three independent assay methods to within 10% on the average, at the 95% confidence level.

Quantitative comparisons between radiochemical Pu (WG) and Am-241 determinations and active PAN have been performed at the INEEL facility (SWEPP).[13] These comparison studies of approximately 1,300 drums of RFETS aqueous sludges comprise more than 100 individual sludge batches. These sludges contain low Pu and relatively high Am concentrations. The results of these comparisons are shown in Figure 5.2-10.

The batch-average drum Pu assay as determined at RFETS was compared to the same quantity as measured with the INEEL PAN unit. The indicated straight line shows the relationship RFETS Pu Mass = PAN Pu Mass. A statistical analysis of this same data indicates a best straight-line fit relationship of

$$\text{RFETS Pu Mass} = -0.06 + 0.85 * \text{PAN Pu Mass},$$

with a correlation factor of 0.51. The calculated correlation factor indicates that 51% of the variance does fit a straight line. The 0.85 constant indicates an approximately 15% average measurement bias between the two assay techniques.
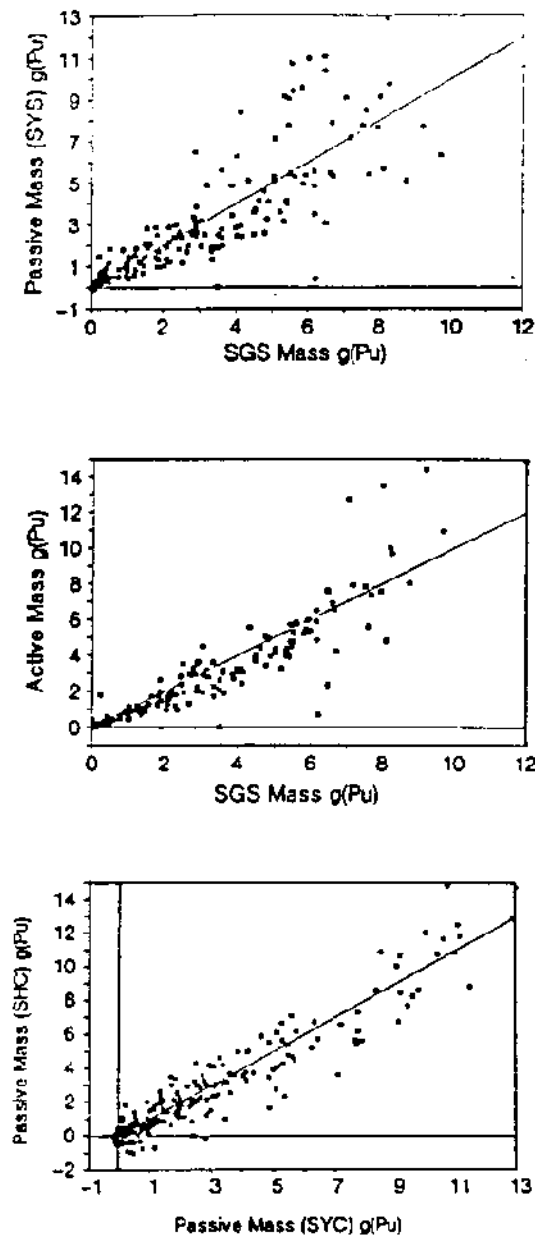
**Figure 5.2-7—Comparison of Assay Data Sets of 200 LLNL
CH-TRU Waste Drums.
Waste Matrix in Non-Segregated General Laboratory Waste.**
Top Graph Shows Passive Neutron (PAN) Compared to SGS. Middle Graph Shows
Active Neutron (PAN) Compared to SGS. Bottom Graph Shows Comparison of the Two
Independent PAN Passive Neutron Assay Systems. Straight Line (X=Y) Depicts Ideal
Case, Where Assay Techniques Shown Yield Identical Assay Measurement Results.
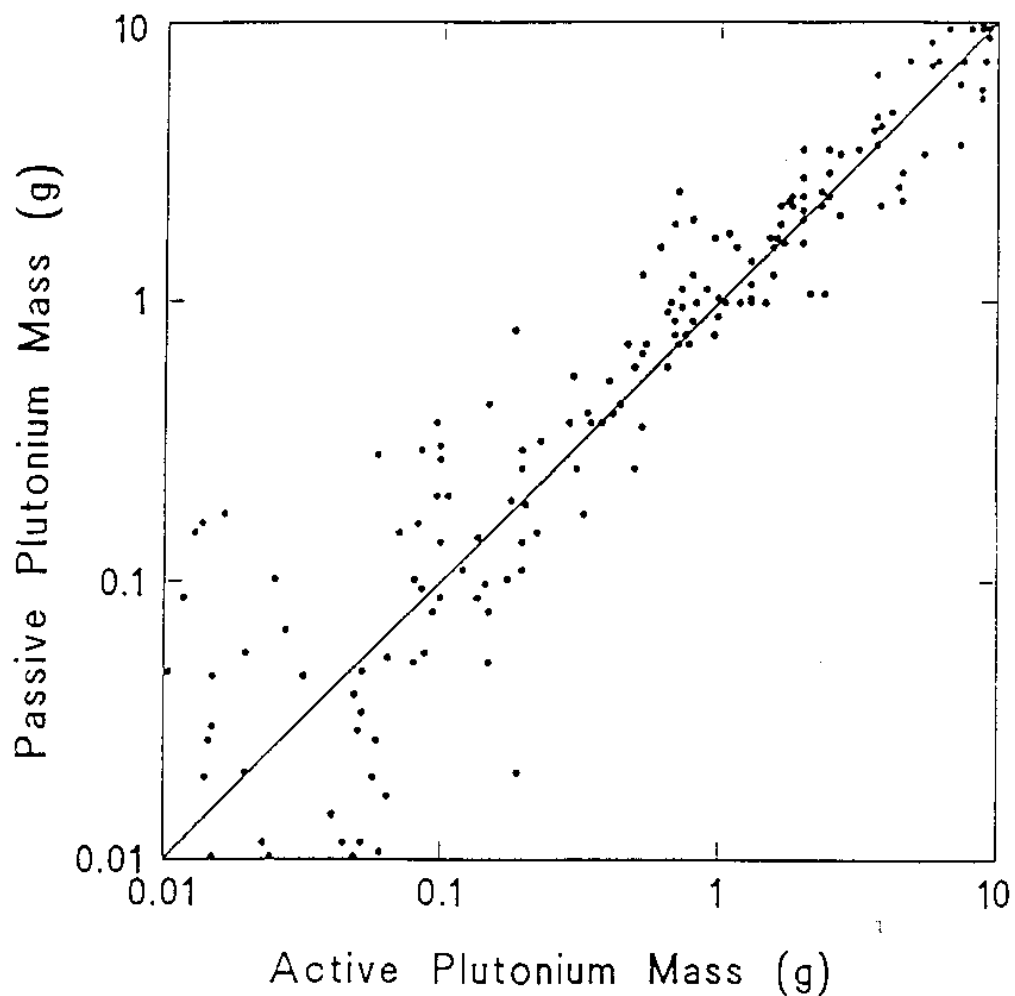
Figure 5.2-8—Comparison of 300 Hanford CH-TRU Waste Drum Assays Performed with the PAN System, Passive Neutron Compared to Active Neutron.
Straight Line (X=Y) Depicts Ideal Case, Where Assay Techniques Shown Yield Identical Assay Measurement Results.
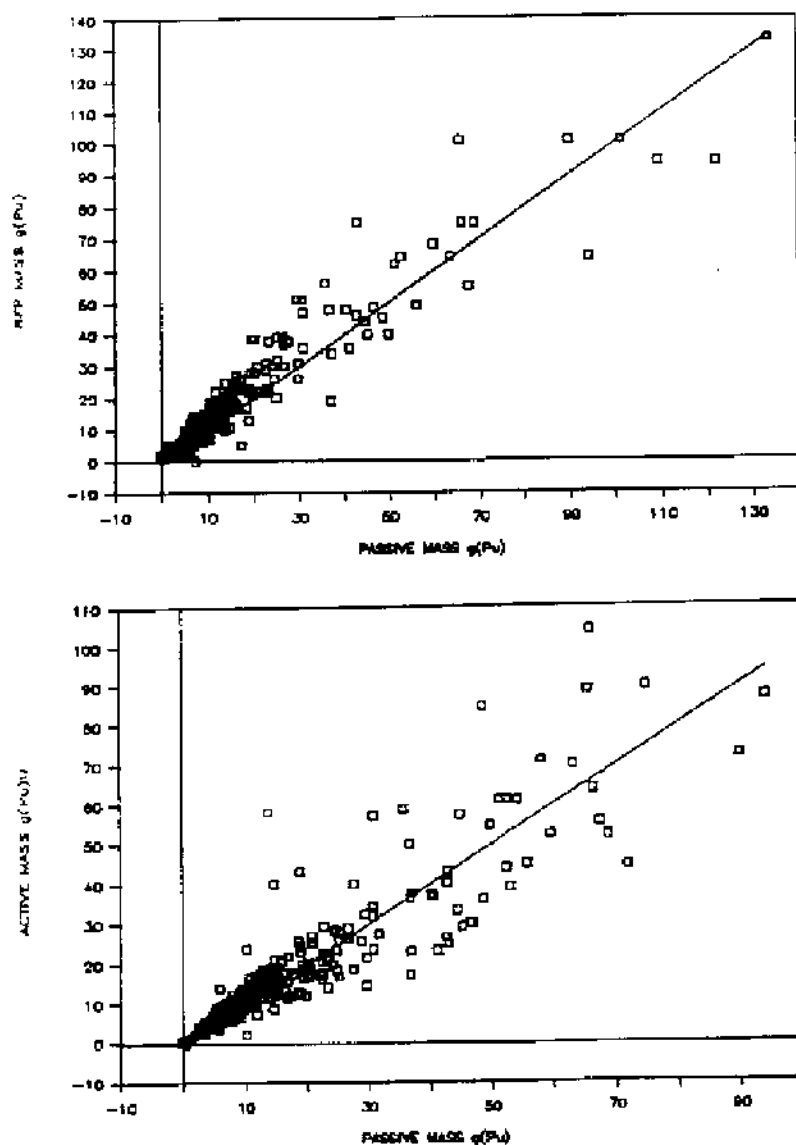
Figure 5.2-9—Assay Comparisons of a Set of 300 RFETS CH-TRU Waste Drums (Graphite Molds Matrix) Showing RFETS SGS System Assays Compared to INEEL PAN Unit Passive Neutron Assays (Top) and INEEL PAN Active Neutron and Passive Neutron Comparisons (Bottom).

Straight Lines (X=Y) Depict Ideal Case, Where Assay Techniques Shown Yield Identical Assay Measurement Results.
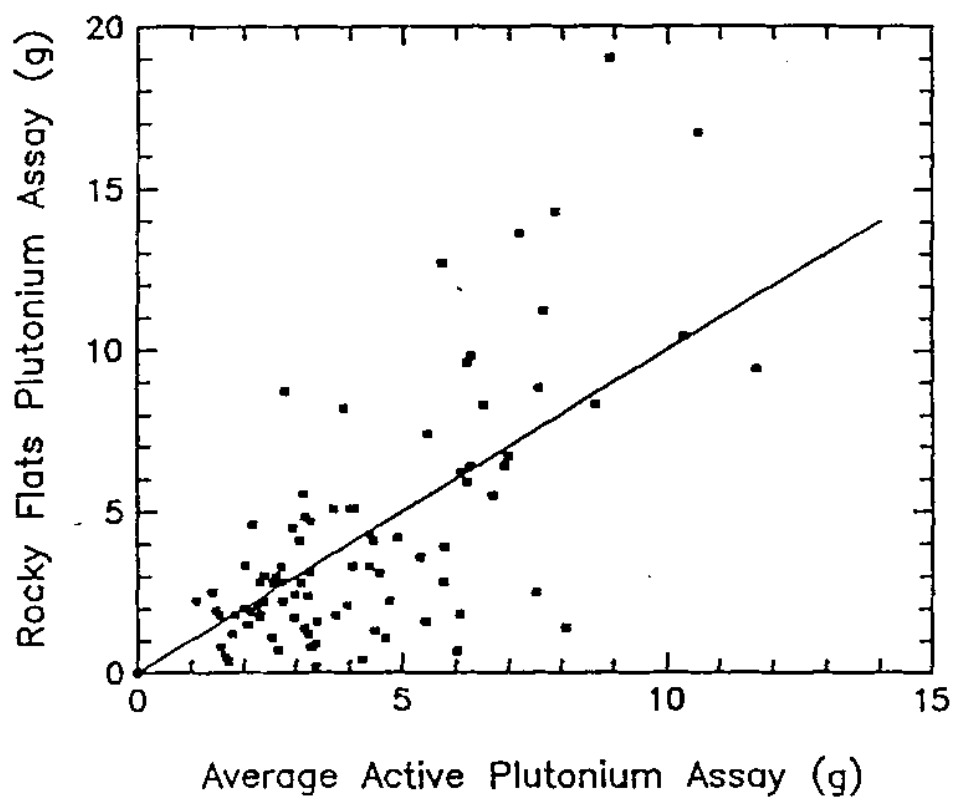
**Figure 5.2-10—Batch Average Pu Assays of 1300 Sludge Drums
Performed at RFETS Compared to PAN Assays of the Same Drums
Done at INEEL.**
Straight Line is a Linear Least Squares Fit to Data.

The individual PAN systematic measurement error (discussed in detail in Caldwell, et al., 1986[12]) for a typical sludge drum measurement is approximately 10% on average, due primarily to possible systematic errors in the matrix correction formalism. That error estimate is based on the observed standard deviation found for mockup sludge drum calibrations. PAN systems are able to measure the total uncorrelated neutrons, but cannot measure the individual contributions from mixed, uncorrelated sources of neutrons [e.g., (alpha, n) reactions due to Cm-244 and Am-241]. The contributions from Am-241, for example, can be calculated (obtained from passive single neutron rate) if no other (alpha, n) sources are present in the waste.

The two assay measurement techniques appear to agree within probable systematic errors associated with each technique (assuming a +/- 10% systematic error for both techniques). Other similar individual sludge drum NDA comparisons (passive and active PAN neutron assays of high-Pu, low-Am activity sludge drums[13] verify the basic PAN matrix corrections at the +/-10% level.

Schultz and Caldwell, 1988[17] details additional such comparisons for a great variety of matrix types, including heterogeneous matrices and highly neutron-absorbing matrices. In all cases the PAN assays are highly correlated with SGS assays and with each other. Comparison studies reported in Schultz and Caldwell, 1988[17] indicate a slightly better agreement between PAN and radiochemistry assay methods than the 10-15% discussed above.

5.2.3.5.11 Choice of Passive or Active Assay Value

Two assay values, a "passive" mass and an "active" mass, are obtained with each PAN assay. A choice of the values to be reported as the PAN assay value is performed within the assay algorithm by an analytical evaluation of assay conditions. Content-code-specific algorithm options are developed by a site based upon an evaluation by the assay data reviewer or expert of the individual site's waste content codes.

When specific content code or matrix information is available that indicates, for example, that passive assay results are more reliable than active assay results for that content code, then the algorithm selects the passive assay results when that content code is entered via the PAN operating software, NEUT. Similar overrides involve the statistical accuracy of a measurement. For example, if the passive measurement has a large error associated with it, then the active measurement is selected.

The default PAN assay algorithm is known to underestimate the absorption correction factor for various waste streams (e.g., tantalum crucibles). This phenomenon is due to neutron tunneling effects caused by the stacked arrangement of the crucibles. A correction factor based on the RFETS SGS assay value is used to adjust the PAN assay values.

A similar method is used at INEEL to modify the MI obtained during the assay of sludge drums. For sludge drums having low Pu content, an average MI is used in the assay value calculations. The average MI value used was obtained from previous assays of the same waste stream containing higher Pu loadings and, thus, higher count rates and improved counting statistics.

One algorithm option that is used by Hanford is based on experimental results indicating that fissile self-absorbing effects in several of their content codes were small for Pu mass loadings of 10 g or less, but increasingly probable for successively higher Pu mass loadings. It also took into account the experimental fact that Pu loadings in excess of 10 g led to statistically more precise passive assay measurements. Of course, the exact "cross-over" point between using the PAN active or passive assay measurement depends on several experimental factors such as waste form, (alpha, n) source strength, isotopics, etc.

INEEL has modified their PAN algorithm option to reflect the phenomenon that sufficiently strong (alpha, n) sources cause experimental measurement problems for the PAN passive assay measurement, rending it biased high. If the passive assay error bar exceeds 40 g Pu, then the option selects the self-absorption corrected active assay value. This algorithm option also reflects the development of a fissile self-absorption model that is applied to all PAN active assays. This model is purely empirical and assumes that the probability of fissile self-absorption is a monotonically increasing function of the total fissile loading in a waste drum. The function is determined from evaluations of large sets of actual CH-TRU waste drum assays employing PAN active and passive neutron and SGS measurements.[12] The derived functions, however, produce large error bars at the higher fissile mass values. In the "near 200 g Pu" regime, for example, the self-absorption corrected active assays may have relative errors of 40%.

PAN assay results may also be evaluated by the site NDA expert when special-case waste drums are encountered. The various factors that determine what is a "special case" drum include nominal assay values for CH-TRU waste drums near or in excess of the 200 g criticality limit and a lack of tag isotopics information (e.g., Pu-240 content). Both of these situations preclude proper interpretation of PAN assay measurement data.

Approximately one out of 500 RFP CH-TRU waste drums assayed with the INEEL PAN system are assigned an assay value near or in excess of the 200 g criticality limit. Typically, these drums contain very high (alpha, n) radioisotopic sources, which due to the high numbers of neutrons present, results in poor passive PAN coincidence measurements. The large numbers of neutrons (approximately 10^4 neutrons per second or greater) decrease the signal to noise ratio to below acceptable limits. Content codes 409 and 411 display this characteristic and also contain "lumps" of Pu that invalidates the active neutron assay. A panel of 3 or 4 INEEL experts examines and compares all assay and RTR information available, including a critical evaluation of the "tag" assay values. After a consensus of the expert panel is achieved a suitable resolution is proposed and the appropriate action taken. This action may include acceptance of the less than 200 g tag value or the waste drum is returned to the waste generator for repackaging. Both of these actions have occurred.

Hanford waste drum tag values obtained by using an SGS and the certification or check of the SGS assays with a PAN unit indicate assay values near or in excess of the 200 g criticality limit. The approach used at Hanford is basically the same one employed at INEEL, but a two-expert panel is used to evaluate the available data. The return-to-generator option is used frequently with drums having assay values near the 200 g limit.

Invalid or unavailable isotopics information occurred when a small set of Pacific Nuclear Laboratory (PNL) waste drums were assayed at Hanford using a PAN unit. These drums contained Cm-244, but this isotope was not originally listed on the accompanying data sheets. The PAN assay results indicated very high passive coincidence assay values. Many of the assay values were well in excess of the nominal 200 g limit. Experts resolved the problem through direct dialogues with the waste generator who, subsequently, agreed to provide the proper isotopic information that would then allow these drums to be properly assayed.

5.2.4   Fissile Material Content and Decay Heat Value Calculations

The fissile or fissionable isotope content for CH-TRU waste containers is expressed in terms of Pu-239 fissile gram equivalents (FGE), as defined in ANSI/ANS-8.15-1981.[25] The standard lists the maximum subcritical mass limits for fissile and non-fissile actinide nuclides. (U-233 and U-235 are considered equivalent to Pu-239.) The fissile material (e.g., Pu-239, U-235, etc.) or fissionable content of a CH-TRU waste container may be obtained by using any of the previously described assay techniques. However, to obtain the number of Pu-239 FGE present, the isotopic composition contained in the waste form must be known.

The PNCC assay method detects the coincident neutrons emitted by the even- number TRU isotopes (e.g., Pu-240 and Cm-244). (See Section 5.2.3.4 for a detailed discussion of the PNCC assay technique.) Once the coincident neutron (spontaneous fission) emitters have been quantified and the proper correction factors applied (e.g., self- multiplication, system dead-time, etc.), one can calculate the fissile material content by applying the known isotopic ratios.

After the mass of each TRU isotope present has been determined, the decay heat can be calculated by multiplying the mass of each isotope by the decay heat per gram of the isotope. For the general case of alpha and beta decay, the decay heat per gram can be calculated by using Eq. 10 in ANSI-N15.22.[8,20]

The original PAN system algorithm used a very conservative means to estimate a waste drum's decay heat. First, it was assumed that only the drum's alpha particle inventory was responsible for the waste drum's decay heating. Second, the conservative assumption was made that all neutrons detected were produced by (alpha, n) reactions within the drum's waste matrix. In the original algorithm this assumption led to the value of 98,000,000 MeV of alpha decay heat energy being associated with each neutron emitted. This estimate is conservative for two reasons:

(1)   In all cases of WG Pu, a fraction of the neutrons detected are produced by Pu-240 or other spontaneous fission reactions, with a much lower decay-heat-per-neutron factor. Typically each spontaneous fission neutron is associated with approximately 100 MeV of decay heat energy.

(2)   In many waste packages the actual (alpha, n) production factor is higher than the conservative value (2 n/s/mCi-alpha) used in the PAN algorithm. Production factors

---

[25] ANSI/ANS-8.15-1981, "Nuclear Criticality Control of Special Actinide Elements."

as high as 14 n/s/mCi-alpha were observed for RFETS CH-TRU waste drums when assayed with the INEEL PAN system.[26] For the various fluoride, magnesium (Mg), aluminum (Al) salt, and typical sludge matrices values as high as 100 n/s/mCi-alpha are observed.

To obtain more realistic estimates of the decay heat value for sludge wastes and those containing fluorides, INEEL has used an experimentally determined (alpha, n) production factor. For example, an experimentally determined production factor is being used for RFETS aqueous sludges.[26] This derived production factor has been incorporated into the PAN assay algorithm.

Hanford and SRS use an (alpha, n) production factor based on given Pu isotopics contained in the waste drum. The modified PAN assay algorithm assumes that the entire 241 mass (i.e., sum of Pu-241 and Am-241) is in the form of Am-241. This assumption is very conservative since Am-241 produces approximately 35 times the decay heating associated with Pu-241.

ORNL uses a PAN decay heat calculation algorithm based upon the subtraction of the spontaneous fission neutron portion (passive neutron coincidence) from the observed total neutron count rate.

Error bars associated with the decay heat calculation propagate in the same fashion as that described for PAN Pu mass calculation (see Section 5.2.3.5.9).

The administrative classification of 200 millirem per hour (mrem/h) for container surface dose rate imposed for CH-TRU waste automatically limits the decay heat contributions from beta- and gamma-emitting radioisotopes.

To calculate the fission product inventories required to generate a surface dose rate of 200 mr/h one can assume the total external surface dose rate is produced by fission products (the beta-and gamma-emitters). Any TRU radioisotopes present are conservatively assumed not to contribute to the observed external dose rate. One also assumes that the short-lived fission products have decayed sufficiently to be of no concern. This is a conservative assumption since most waste drums are more than one year old. Consequently, only a small number of "pure" beta-emitters would then be present (e.g., strontium [Sr]-90). The remaining predominant radioisotopes producing the heat-generating radiation other than Sr-90 would then be cesium (Cs)-137 and cobalt (Co)-60.

Consider a CH-TRU waste drum containing 100 kilograms (kg) of medium atomic number wastes. Assume the maximum allowable container external dose rate of 200 mrem/h and that this rate is attributable solely to beta- and gamma-emitters (conservative assumption). Also, assume that the radioisotope inventory of this waste drum is a mixture of the dominant long-lived fission product species Sr-90 and Cs-137. For long-term decay 6.5% Cs-137 and 2.2% Sr-

---

[26] C. E. Moss and J. T. Caldwell, "Assay of TRU Wastes Containing (alpha, n) Sources," LA UR 86-2220, June 22, 1986.

90 are produced by reactor fissions.[27] This fission product mixture produces a decay heating of 0.91 MeV, 50% derived from beta emission and 50% derived from gamma-ray emission.[28]

If one also makes the following conservative assumptions: (1) that only the Cs-137 0.67 MeV gamma ray exits the waste drum, (2) the Cs-137 is located in the center of the waste drum, and (3) the mass attenuation factor is very conservative (i.e., 0.74 cm^2/g), one can calculate the curies required to produce an container external dose rate of 200 mrem/h. These assumptions and calculations yield an estimate of 0.25 Ci of Cs-137 present in the example waste drum. Using the isotopic ratio discussed earlier, one calculates a beta and gamma decay heating of 0.001 watt. This decay heating value is equivalent to that produced by the alpha emissions of 0.4 g WG Pu.

Detailed gamma-ray spectral studies of ORNL and RFETS CH-TRU waste drums[19,26,29] indicate that the detected gamma rays were attributable to TRU isotopes and not to fission products. Consequently, from the calculations above and the small quantities of observed fission products the contributions to the waste drum decay heat from beta- and gamma-emitters is negligible.

5.2.5 New Assay Developments

In keeping with the DOE's general policy of upgrading NDA hardware, software and procedures, the DOE continues to support a vigorous NDA development program, with specific support of TRU waste assay-related instrumentation. One recent example of this development is a significantly improved digital processing unit (upgraded shift register) for use with PNCC units that greatly reduces basic dead-time limitations associated with older PNCC units. The improvement considerably lowers processing errors. These newer processors are now either installed or in the process of being installed in all DOE facilities using PNCC assay techniques.

Another development nearing the implementation phase in support of the PAN assay method is "neutron imaging" of 208 L waste drums.[30] With very little change in the basic PAN hardware, 208 L waste drum assay data may be acquired in a fashion that allows it to be processed with existing imaging software similar to that used in medical CAT scans. Neutron imaging has already been demonstrated using an upgraded DOE PAN unit,[30] the Mobile Drum System. Improved matrix and self-absorption corrections to the basic assay data will then be possible using the neutron imaging technique. Accurate determination of the TRU material distribution should result in considerably improved assay accuracies since it is known that incomplete matrix and self-absorption corrections are a major source of assay errors.

PAN box assay systems have been used in the DOE complex for several years. The earlier versions are discussed in several of the references[13,21,22] that include assay campaigns at NTS and RFETS. Recently, some improvements in the box PAN systems have been made and

---

[27] "Chart of the Nuclides," Knolls Atomic Power Laboratory.

[28] David C. Kocher, "Radioactive Decay Data Tables," DOE/TIC-11026, 1981.

[29] F. J. Schultz, et al., "Neutron and Gamma-Ray Nondestructive Examination of Contact-Handled Transuranic Waste at the ORNL TRU Waste Drum Assay Facility," ORNL-6103, March 1985.

[30] San Horton, "Neutron Imaging," U. S. Army, Ph.D. thesis, 1988.

implemented at some sites. The new box assay unit at INEEL and the Mobile System box assay unit are examples of this implemented PAN technology. The improvements have been in four areas:

(a)   Improved matrix corrections made possible by development and deployment of a "moving" shielded flux monitor that samples the emergent interrogating flux along the entire length of a box.

(b)   Improved detection uniformity throughout the box volume made possible by a better detector layout.

(c)   Smaller matrix inhomogeneity assay errors, achieved by implementation of a source location algorithm, which effects matrix corrections correlated with the location of the TRU material is based on crude neutron imaging, and

(d)   Implementation of IBM/PC data acquisition/controller hardware and software.

Improvement (a) is similar to the shielded flux monitor described in Section 5.2.3.5 that is used in the drum-size PAN. These new developments are being implemented simultaneously with the institution of the standard waste box.

5.2.6 QA and QC Practices

QA and QC are important functions at all DOE facilities, especially in special nuclear materials (SNM) accounting areas. The 18 elements of NQA-1 are being implemented throughout the DOE.[15] TRU waste assay QA and QC practices adhere to the guidelines established in NQA-1. Some of these practices have been discussed previously in relationship to other subjects. A brief listing of some of these QA/QC practices in common use to assay newly generated and stored CH-TRU waste throughout the DOE complex are:

(1)   Expert NDA personnel check of NDA records before assay values assigned to the waste package (NQA-1 Elements 1. Organization and 10. Inspection). (The functions of these site NDA reviewers or experts have been discussed previously in Sections 5.2.3.2, 5.2.3.4, and 5.2.3.5),

(2)   Assay standards used before and after waste assays (NQA-1 Element 12. Control of Measuring and Test Equipment). Detailed discussions of the instrument calibration and calibrations standards preparation and implementation have been discussed in detail for each assay method in Sections 5.2.3.2.1.3, 5.2.3.4.3, and 5.2.3.5.6),

(3)   Automatic electronic system gain stabilization. (Element 3. Design Control). For each assay method manufacturer's system instructions and site operating procedures suggest to the assay system operators the correct settings for proper system gain and stabilization,

(4)   Automatic software flagging and tagging for special-case waste containers (NQA-1 Element 5. Instructions, Procedures, and Drawings). For example, less than 0.5%

transmission segments are flagged for SGS assay measurements and special-case waste matrices are flagged by the computer algorithm in PAN assay measurements,

(5)   Administrative tagging of failed segment assays as "LOWER LIMITS" (NQA-1 Element 15. Control of Nonconforming Items). This procedure is performed for those SGS waste drums that qualify.

(6)   Original segment assay and calibration data archived for future reference (NQA-1 Elements 6. Document Control and 17. Quality Assurance Records). PAN assay algorithm automatically archives all calibration data acquired (see Section 5.2.3.5.6),

(7)   Detailed data sheets are prepared for each drum and accompany the drum through all NDA, RTR, etc. stations. Some sites (e.g., INEEL) use automated, computerized data sheets and bar codes (NQA-1 Element 9. Control of Processes),

(8)   Most sites' SGS assays verified by one or two other independent NDA measurements (at the certification facility). For example, RFETS SGS assays are verified by the INEEL PAN passive and active assay measurements (NQA-1 Elements 9. Control of Processes and 18. Audits),

(9)   Nonconforming drums returned for repackaging (NQA-1 Element 15. Control of Nonconforming Items). When a drum is found to contain non-conforming items after RTR inspection or to contain, for example, greater than the acceptable nuclear criticality limit, it is returned to the waste generator for repackaging,

(10)   RTR inspection is used in appraisal of NDA "Special-Case" waste containers to aid in the evaluation of matrix problems (NQA-1 Element 16. Corrective Action). For example, special-case waste drums (e.g., INEEL. tantalum crucible content code) are flagged by the PAN assay algorithm through previous evaluation and identification of the content code by the site NDA reviewer (expert). See Section 5.2.3.5.11 for a more detailed discussion of the special-case waste drums,

(11)   RTR inspection is used routinely to verify or evaluate waste form or content code of all waste drums (NQA-1 Element 8. Identification and Control of Items). RTR inspections are used to confirm the proper identification of waste content codes.

(12)   General practice of upgrading NDA hardware, software, and procedures whenever available and fiscally possible is pursued (NQA-1 Elements 2. Quality Assurance Program and 3. Design Control). See Section 5.2.5 for a discussion of new NDA developments.

It is DOE policy to conduct periodic audits of all Waste Isolation Pilot Plant certification activities at each site.[31] The audit teams consist of technical NDA (and nondestructive

---

[31] WIPP-DOE 120, Quality Assurance.

examination [NDE]) and administrative personnel knowledgeable in several of the NDA technologies discussed in Section 5.2.3. The purpose of these audits is to provide independent monitoring and evaluation of each site's NDA and NDE activities on a regular basis and to foster compliance with certification plans. These in-depth evaluations take place on site, and a detailed audit team report, including recommendations for improvements in areas judged deficient, follow each such audit. In addition, each site conducts independent internal audits on at least an annual basis, covering the same overall procedures as performed in the DOE external audits. The effect of these audits is to provide considerable independent oversight of each DOE site's NDA and NDE operations, as overlays to each site's routine operations activities.

APPENDIX 5.3

CH-TRU WASTE SAMPLING PROGRAMS AT DOE SITES

This page intentionally left blank.

5.3   CH-TRU Waste Sampling Programs at DOE Sites

5.3.1   Summary

Previous and existing sampling programs at U.S. Department of Energy (DOE) sites provide valuable information about the properties and transport parameters of retrievably stored and newly generated waste. Results from these programs have provided a basis for certifying retrievably stored waste with existing records and process knowledge as the primary source of information, and with real-time radiography (RTR) as a verification technique. Actual sampling of a statistically significant number of waste containers can then be used as secondary verification. Although these sampling programs were primarily aimed at meeting the Waste Isolation Pilot Plant Waste Acceptance Criteria (WIPP WAC), they can be extended to meet transportation requirements as well.

Sampling programs also provide a historical perspective of waste generation processes and operations at the sites. Knowledge of these can be used to address some of the issues that are transportation concerns (i.e. production of HCl from payload containers, presence of volatile organics). This Appendix provides a description of the sampling programs and their relevance to the transportation parameters.

5.3.2   Introduction

The objective of this Appendix is to summarize the past and present sampling programs for contact handled transuranic (CH-TRU) waste at sites and to demonstrate how the information obtained through these programs is applicable for qualifying waste for transport. The available data on sampling of TRU waste originates from three sources:

1)   The TRU Waste Sampling Program that consists of extensive random sampling programs conducted between 1983-1985 at the Idaho National Engineering Laboratory (INEL).[1]

2)   Stored Waste Examination Pilot Plant (SWEPP) Certified Waste Sampling Program conducted from 1986 to present at INEL.[2,3]

3)   A controlled study of INEL retrievably stored waste to estimate gas generation rates from CH-TRU waste containers.[4]

---

[1] Clements, T. L., Kudera, D. E., September 1985, "TRU Waste Sampling Program: Volume I -- Waste Characterization," EG&G-WM-6503, EG&G Idaho, Inc., Idaho Falls, Idaho.

[2] Arnold, P. M., October 1986, "EG&G Drum Sampling Program Results FY 1986," RFP 4250, Rocky Flats Plant, Golden, Colorado.

[3] Watson, L. E., December 1987, "EG&G Sampling Program Results," RFP 4251 Rocky Flats Plant, Golden, Colorado.

[4] Clements, T. L. and Kudera, D. E., September 1985, "TRU Waste Sampling Program: Volume II -- Gas Generation Studies," EG&G-WM-6503, EG&G Idaho, Inc., Idaho Falls, Idaho.

A background and summary of each of these programs will be provided with an evaluation of the aspects related to the transportation requirements.

5.3.3 TRU Waste Sampling Program at INEL

The INEL TRU Waste Sampling Program[1] randomly selected and sampled 181 TRU unvented waste (payload) containers from retrievable storage. The waste ranged in age from six months to twelve years. The main objectives of the study were to examine the waste contents both visually and by RTR to determine waste form compliance with the WIPP WAC, and to assess the validity of using RTR as a nondestructive certification technique. The sampling program included:

- Analysis of the waste container's headspace gas for composition
- Determination of the packaging configuration
- Description of the waste form
- Reporting the physical state of the waste for each item description code (IDC)

Each of these parameters was assessed by visual, analytical analysis or RTR examination.

It should be noted that the TRU Waste Sampling Program was initiated before the shipping requirements were conceived. However, most of the proposed controls for shipment of TRU waste were examined during the sampling process. These results assist in generating a database that demonstrates a safe history of handling, shipping and storage for the waste.

5.3.4 The SWEPP Sampling Program

The SWEPP Certified Waste Sampling Program has incorporated the results from the TRU Waste Sampling Program described above, to determine acceptable sample sizes. This program has been in progress since 1986, and the percentage of containers to be sampled is updated yearly to incorporate the total number of nonconformances for the previous year's input. The purpose of the SWEPP Certified Waste Sampling Program is to provide quality control in support of the waste certification process. The program consists of selecting a statistically valid portion of the TRU waste containers that have been WIPP WAC certified, and visually examining the contents for compliance. This program supplements 100% RTR of the waste containers.

The combined data from the TRU Waste Sampling Program and the FY-1986 and FY-1987 SWEPP Certified Waste Sampling Program demonstrated that, when all waste forms are taken into consideration only 3 out of 228 (1.32%) sampled containers showed nonconformances to the WIPP WAC. These were uncemented sludge drums that showed no visible liquid during RTR examination, yet actually contained liquid in excess of 0.7 gallons when examined visually. The failure to detect the liquid was because the surface movement was restricted due to formation of a solid layer. It is important to note that the visual examinations did not reveal any problems with any other WIPP WAC requirements, which include restrictions on the presence of non-radioactive pyrophoric materials, explosives, and compressed gases.

An overall WIPP WAC miscertification of 1.3% is considered acceptable for continuation of the SWEPP certification process without requiring any major changes. INEL has defined[5] the sample size and sampling frequencies for FY-1988 based on these results. Sampling 30 out of the 2,900 drums expected to be SWEPP-certified in FY-1988 is expected to give a 95% confidence level that the estimate is correct. This is based on the assumption that 2% of the SWEPP-certified drums are WIPP WAC miscertified, and the actual range of percent of miscertification is 0-7%.

5.3.5 Gas Generation Studies

The gas generation studies of the TRU Waste Sampling Program[4] were conducted to evaluate the effectiveness of different venting devices in maintaining pressure equilibrium between the payload containers and ambient conditions. In addition, concentrations of hydrogen and other gases were measured in an effort to quantify the gas generation rates in the drums.

A total of sixteen newly generated Pu-239 waste drums from the Rocky Flats Plant and six Pu-238 drums from Los Alamos National Laboratory were evaluated under controlled conditions in this study. The Pu-239 drums were vented for a period of 13 weeks and later sealed to measure gas generation rates and temporal variations in composition. Results from these studies are discussed in Section 5.3.6.4 of this Appendix.

5.3.6   Evaluation of Transportation Parameters From Sampling Programs

The transportation parameters and their methods for determination and control are described in the Contact-Handled Transuranic Waste Authorized Methods for Payload Control (CH-TRAMPAC). Sampling programs provide confirmatory data on these parameters and the adequacy of the verification techniques used (records and data base, consistency of waste generation processes, RTR, etc.). The transportation parameters that can be addressed in a sampling program are listed below, and each is discussed with respect to the sampling programs below:

- Physical form
- Chemical properties
- Chemical compatibilities
- Gas distribution and pressure buildup

5.3.6.1 Physical Form

The transportation requirements for physical form are the same as WIPP WAC requirements. The previous results from the sampling programs (see Section 5.3.4) have shown the nonconformance rates for these criteria to be very low.[5]

---

[5] Kudera, D., 1989, Personal Communication.

5.3.6.2 Chemical Properties and Waste Type

The waste type restrictions on payload materials are described in the CH-TRAMPAC. The restrictions on non-radioactive pyrophorics and explosives are regulated by the WAC and the sampling programs show that these requirements are consistently met at the sites.

Sampling programs have demonstrated no visible deterioration of the plastic confinement layers, even for containers that have been in storage for up to fifteen years. This indicates the absence of reactive materials or corrosives in the wastes. Inspections performed on the drums verified that they had not deteriorated appreciably during storage.

All of the content codes from DOE sites are grouped into waste material types (e.g., solidified aqueous or homogeneous inorganic solids, solid inorganics, solid organics, and solidified organics), based on their gas generation potential, which is quantified by the effective G values (see Appendix 3.2 of the CH-TRU Payload Appendices). In order to conform to these limits, the chemicals/materials within a given waste material type are restricted. The waste material types are further classified into shipping categories depending on the type of the payload container and the bagging configuration. The correlations between content codes and shipping categories are listed in the CH-TRU Waste Content Codes (CH-TRUCON) document. Only compatible waste content codes are included in the CH-TRUCON document and considered for transport. The TRU Waste Sampling Program discovered only one payload container in 181 of the sampled containers to have been assigned an incorrect IDC that would have resulted in a change of shipping categories. These results indicated that procedural controls and process technology information have ensured compliance with the waste type restrictions.

5.3.6.3 Chemical Compatibility

5.3.6.3.1 Chemical Compatibility within Payload Containers

Payload materials must be chemically compatible with each other and with the materials of construction of the packaging ICV. The TRU waste sampling program at INEL included examination of several drums that had been in storage for up to fifteen years. No effects of any adverse chemical reactions were detected in any of these drums. Waste containers generated in 1973 and sampled in 1988 showed little or no chemical deterioration of the inner confinement layers, except for coloring of the plastic bags in some cases.[6] The sampling of WAC certified drums in the SWEPP Sampling Program also showed no evidence of adverse chemical reactions. The results of these sampling programs indicate that the waste materials are chemically compatible with themselves and with the payload containers. The detailed chemical compatibility analysis performed on waste from each DOE site demonstrates that no appreciable chemical reactions will occur in the wastes or between the wastes and the payload containers. Details of this analysis are presented in Appendix 6.1 of the CH-TRU Payload Appendices.

---

[6] Roggenthen, D. K., McFeeters, T. L., Nieweg, R. G., March 1989 (in Press), "Waste Drum Gas Generation Sampling Program at Rocky Flats During FY 1988," RFP-4311, Rocky Flats Plant, Golden, Colorado.

5.3.6.3.2 Occurrence of Free Chlorides

None of the sampling programs reported the presence of HCl gas in the headspace of the sampled containers or (where applicable) in the inner confinement layers. The production of HCl gas is of concern due to its potential for causing stress corrosion cracking of the package. Actual waste data shows that even though HCl production is possible, it is highly improbable that gaseous HCl would ever be produced and released from the payload containers. An analysis of the source terms and release conditions for HCl in the payload materials is presented in Appendix 6.2 of the CH-TRU Payload Appendices.

5.3.6.3.3 Occurrence of Volatile Organic Compounds

Sampling programs also provide information on the relative amounts of volatile organic compounds (VOCs) in the payload materials. VOCs are a concern due to potential incompatibilities with the butyl rubber O-rings of the packaging and due to the potential for pressure buildup from their vapor pressures. A detailed discussion of the existing information on VOCs in the waste from sampling programs is presented in Appendix 6.4 of the CH-TRU Payload Appendices. Results from the sampling programs listed above are:

- The source term for VOCs in the waste is limited.

- Headspace concentrations of VOCs in the payload containers are below the range for saturation values.

- Even in the case of organic sludges (which contain the VOCs in bound form and belong to the test category) the release of the VOCs from the waste is limited.

- VOC release rates from the payload containers are extremely small and the effects of any interaction between the VOCs and the butyl rubber O-rings would be minimal and not affect the sealing properties.

- Ongoing sampling programs show that compared to retrievably stored waste, newly generated waste has much lower concentrations of the VOCs.

5.3.6.4 Gas Concentrations and Pressure Build-Up

Generation of gases from the payload materials is of concern due to the potential for pressure buildup and the occurrence of potentially flammable mixtures of gases. The controls in place to restrict these parameters are described in the CH-TRAMPAC, and are summarized below:

- Restrictions on materials that can be present within each payload (limits on hydrogen generation potential of waste materials).

- Limits on the number of internal layers of confinement within each payload container.

- Limits on the decay heat within each payload container.

The relevance of the sampling programs to each of these parameters is addressed below.

5.3.6.4.1 Restrictions on Materials

The restriction on the materials that can be present in a payload is addressed in Section 5.3.6.2 of this document. Sampling programs show that for waste that is certified to the WAC, the waste type restrictions are consistently met, and none of the sampling programs showed any effects of chemical activity within the drums.

5.3.6.4.2 Restrictions on Packaging Configuration

The second listed control is a packaging requirement, which restricts the maximum number of plastic bag layers that can be present for a given content code. This number is defined for each content code in the CH-TRUCON document. The TRU Waste Sampling Program[1] conducted at INEL documented packaging configurations for each payload container sampled. This includes information on the number and type of liner bags and bagout bags used for waste packaging. This data has provided a basis for the retrievably stored waste to be qualified for shipment. The packaging requirements listed in the CH-TRUCON document for each content code (and correlating IDCs) are consistent with the reported data from the TRU Waste Sampling Program.

5.3.6.4.3 Restrictions on Decay Heat

This parameter controls gas generation in the payload containers by limiting the decay heat of the radionuclides in each shipping category. These decay heats are determined based on an effective G value for generation of flammable gas for each shipping category. An analysis of effective G values measured for real wastes is provided in Appendix 3.1 of the CH-TRU Payload Appendices. An average G value in any waste type (I, II, III) was consistently less than the effective G values being used to establish possible hydrogen generation rates. Experimental results on estimates for hydrogen release rates are provided in Appendix 6.8 of the CH-TRU Payload Appendices. The radionuclide content of a payload container is restricted such that given the release rates and the effective G values, the hydrogen concentration will not exceed 5% in any of the confinement layers. The concentrations of hydrogen predicted in these calculations are derived using steady-state assumptions, and are much higher than those that could be produced in an average drum in a given shipping category. For example, the wattage limit on a drum of Waste Type III with four layers of plastic is 0.0207 watts, or 6.89 grams of weapons grade plutonium.

Sampling programs mentioned above have shown that containers at steady-state with much higher decay heat loadings had hydrogen concentrations well below 5% for payload containers belonging to an analytical category. Especially for retrievably stored waste that had not been vented, the analytical calculations show hydrogen concentrations much greater than the actual measured concentrations. The observed low concentrations could be due to lower hydrogen production rates, matrix depletion (reduction in the G value with time) and/or the escape of hydrogen from the payload containers. Very few of the sealed drums in the sampling programs were overpressurized, indicating possibly low gas generation rates, simultaneous consumption of oxygen or periodic leakage of gas from the drums due to overpressurization (the drums were not vented).

5.3.7   Complexity of Real Waste Sampling

For visual inspection of the waste contents, necessary precautions must be taken to ensure the safety of personnel performing the task. In the handling of materials contaminated with TRU radionuclides, a barrier is always in place between the individual and the radioactive materials (e.g., glove boxes, gloves, bubblesuits, etc). Whenever a waste container is opened for sampling or inspection, necessary precautions must be taken to prevent contamination from the radioactive material. Sites have, in the past, utilized containment structures under ventilation control with the individuals in supplied-air bubblesuits to open and inspect the waste contents. Although the internal exposures have been low, the sites have changed their waste handling techniques by developing in some cases multi-million dollar remote handling concepts to prevent this potential exposure. Due to the unique difficulties associated with actual sampling of the waste (i.e., additional potential exposure to workers and generation of excessive waste as byproduct of waste sampling), alternate and effective nondestructive techniques are necessary to supply the primary source of information on the waste. Visual inspection on a limited basis can then serve as a supplemental verification system.

5.3.8   Conclusions

The following conclusions can be drawn from the waste characterization data obtained through the various sampling programs:

1)   A transportation qualification process using a statistical sampling approach is valid for retrievably stored waste when 100% RTR is supplemented with visual examination sampling programs.

2)   The use of an RTR system is an adequate non-destructive certification technique for meeting certain WAC requirements, as described in this appendix.

3)   Process knowledge, existing records and database information adequately provide primary sources for characterizing the shipping parameter requirements of stored waste. RTR and sampling programs can serve as secondary verification techniques.

4)   Existing data on the sampling of real waste and ongoing sampling programs can be used to assess the potential for gas generation and to quantify effective G values.

This page intentionally left blank.

APPENDIX 6.1

CHEMICAL COMPATIBILITY OF WASTE FORMS

This page intentionally left blank.

6.1   Chemical Compatibility of Waste Forms

6.1.1   Introduction

This appendix describes the method used for demonstrating chemical compatibility in a given payload container, within a given waste type, and among waste types to simulate mixing of waste during hypothetical accident conditions.

6.1.2   Chemical Compatibility Analyses

The chemical compatibility analysis was performed using the methods described in the U.S. Environmental Protection Agency (EPA) document "A Method for Determining the Compatibility of Hazardous Wastes."[1] Content codes are classified as 'incompatible' if the potential exists for any of the following reactions:

- explosion
- heat generation
- gas generation (flammable gases)
- pressure build up (nonflammable gases)
- toxic by-product generation
- fire
- violent polymerization
- solubilization of toxic substances.

Note: Solubilization of toxic substances and toxic byproduct generation is not directly a concern for transportation of waste in the TRUPACT-II or HalfPACT but has been included for completeness.

Each generator and storage site has produced a comprehensive list of chemicals present in an approved content code. The chemical components found in each waste generation process are determined by examining the process technology, by chemical analysis, or by process flow analysis. Under this system, all chemical inputs into the system are accounted for, even though all of these components may not be a part of the waste. For example, generator sites might include both acids and bases in their lists, even though the two groups have been neutralized prior to placement in a payload container.

The chemical concentration levels are reported as either Trace (T)(<1% by weight), Minor (M)(1-10%), or Dominant (D)(>10%). The list is divided into groups based on chemical properties and structure (e.g., acids, caustics, metals, etc.). Table 6.1-1 lists all the groups and their number designations. As noted in the table, the groups and examples listed are only for illustrative purposes, and do not necessarily represent components of waste materials in a payload. A listing of chemicals allowed in the waste in quantities >1% (weight) by waste

---

[1] Hatayama, H.K., J.J. Chen, E.R. deVera, R.D. Stephens, and D.L. Storm, 1980, "A Method for Determining the Compatibility of Hazardous Wastes," EPA-600/2-80-076, U.S. Environmental Protection Agency, Cincinnati, Ohio.

material type is provided in Section 4.3 of the Contact-Handled Transuranic Waste Authorized Methods for Payload Control (CH-TRAMPAC). Other chemicals or materials not identified in the lists of allowable materials (Tables 4.3-1 through 4.3-8 in the CH-TRAMPAC) as specified by Section 4.3 of the CH-TRAMPAC are restricted to less than 5 weight percent total.

Table 6.1-1 — EPA List of Chemical Groups and Materials*

Group Number	Group Name	Example
1	Acids, Mineral, Non-Oxidizing	Hydrochloric Acid
2	Acids, Mineral, Oxidizing	Nitric Acid (>1%)
3	Acids, Organic	Acetic Acid
4	Alcohols and Glycols	Methanol
5	Aldehydes	Formaldehyde
6	Amides	Acetamide
7	Amines, Aliphatic and Aromatic	Aniline
8	Azo Compounds, Diazo Compounds and Hydrazines	Hydrazine
9	Carbamates	Carbaryl
10	Caustics	Sodium Hydroxide
11	Cyanides	Potassium Cyanide
12	Dithiocarbamates	Maneb
13	Esters	Vinyl Acetate
14	Ethers	Tetrahydrofuran
15	Fluorides, Inorganic	Potassium Fluoride
16	Hydrocarbons, Aromatic	Toluene
17	Halogenated Organics	Carbon Tetrachloride
18	Isocyanates	Methyl Isocyanate
19	Ketones	Acetone
20	Mercaptans and other Organic Sulfides	Carbon Disulfide
21	Metals, Alkali and Alkaline Earth, Elemental	Metallic Sodium
22	Metals, other Elemental and Alloys in the form of Powders, Vapors or Sponges	Titanium
23	Metals, other Elemental and Alloys as Sheets, Rods, Moldings, Drops, etc.	Aluminum
24	Metals and Metal Compounds, Toxic	Beryllium
25	Nitrides	Sodium Nitride
26	Nitriles	Acetonitrile
27	Nitro Compounds	Dinitrobenzene
28	Hydrocarbons, Aliphatic, Unsaturated	Butadiene
29	Hydrocarbons, Aliphatic, Saturated	Cyclohexane
30	Peroxides and Hydroperoxides Organic	Acetyl Peroxide
31	Phenols, Cresols	Phenol

Table 6.1-1 — EPA List of Chemical Groups and Materials[a] (Continued)

Group Number	Group Name	Example
32	Organophosphates, Phosphothioates, and Phosphodithioates	Malathion
33	Sulfides, Inorganic	Zinc Sulfide
34	Epoxides	Epoxybutane
101	Combustible and Flammable Materials, Miscellaneous	Cellulose
102	Explosives	Ammonium Nitrate
103	Polymerizable Compounds	Acrylonitrile
104	Oxidizing Agents, Strong	Hydrogen Peroxide
105	Reducing Agents, Strong	Metallic Sodium
106	Water and Mixtures Containing Water	Water
107	Water Reactive Substances	Sulfuric Acid (>70%)

a   Modified from "A Method for Determining the Compatibility of Hazardous Wastes." [1]

NOTE: The chemical groups and materials listed in this table are a comprehensive listing of chemical compounds that may be incompatible. This is not meant to infer that all the listed chemical compounds and materials are present in TRU waste.

Interactions between compounds present in trace quantities (<1 percent by weight) and compounds present in concentrations ≥ 1 percent by weight (i.e., D x T, M x T, or T x T) do not pose an incompatibility problem for the following reasons:

- The trace chemicals reported by the sites are in concentrations well below the trace limit of less than 1 weight percent. An example is the volatile organic compounds (VOCs) discussed in detail in Appendix 6.4 of the CH-TRU Payload Appendices. Sampling programs show that the concentration levels of these compounds are significantly lower than the upper limit of 1%.

- The trace chemicals are usually dispersed in the waste, which further dilutes concentrations of these materials.

- Trace chemicals that might be incompatible with materials/chemicals >1 weight percent would have reacted during the waste generating process prior to placement in payload containers.

- Because of restrictions imposed by the EPA on reporting of hazardous wastes, some chemicals are listed in trace quantities even if they have already reacted. Hazardous waste regulations as promulgated by the EPA[2] (known as the mixture rule) require that a mixture of any solid waste and a hazardous waste listed in 40 CFR Part 261, Subpart D

---

[2] U.S. Environmental Protection Agency, Title 40, Code of Federal Regulations, Part 261, Subpart D, U.S Environmental Protection Agency, Washington, D.C.

be considered a hazardous waste subject to RCRA regulations. However, Subpart D does not list minimum concentrations for these listed wastes, with the result that any such mixtures must be considered hazardous waste even if the Subpart D constituent is at or below detection limits.

- The waste is either solidified and immobilized (solidified materials) or present in bulk form as a solid (solid materials). In almost all cases, any possible reactions take place before the waste is generated in its final form.

As specified in the CH-TRAMPAC, the total quantity of chemicals/materials not listed as allowed materials for a given waste material type in any payload container is restricted to less than 5 weight percent total. Potential incompatibilities between minor and dominant compounds have been analyzed for the payload using the lists of allowable materials for each waste material type in Section 4.3 of the CH-TRAMPAC. The analysis combined the lists of allowable materials for all waste material types (to simulate a bounding case where different waste material types may be shipped together in a package) and assigned EPA chemical reactivity group numbers and names to each allowable constituent. The reactivity group numbers were assigned based on information provided in Hatayama, et al.[1] If the allowable material (or chemical) is a non-reactive inorganic material (not covered under the EPA reactivity group numbers), it was assigned a reactivity group number of "0" to reflect a complete analysis for all allowable materials (materials assigned a reactivity group number of "0" do not present a compatibility concern). The compiled list of allowable materials and assigned reactivity group numbers is provided in Attachment A of this appendix.

The list of allowable materials and assigned reactivity group numbers was sorted by reactivity group number and then condensed to form a list of the represented reactivity groups (Attachment B of this appendix).

Using the list of represented reactivity groups, a hazardous waste compatibility chart was generated. The chart, which is provided in Attachment C, is a reduced version of the hazardous waste compatibility chart presented in Hatayama, et al.[1] The chart summarizes the potential types of reactions possible between each of the reactivity groups represented in the lists of allowable materials for each waste material type. The reaction codes and consequences of the reactions are specified for each combination of two reactivity groups.

Using the hazardous waste compatibility chart, a list of potential chemical incompatibilities in the TRU waste was generated. The list, which is presented in Attachment D, also presents explanations why the reaction associated with each of the potential chemical incompatibilities will not occur.

The results of the analysis demonstrate chemical compatibility across all waste material types (I.1, I.2, I.3, II.1, II.2, II.3, III.1, III.2, III.3, and IV.1). As previously discussed, each content code is required to have an associated chemical list. Chemical incompatibilities do not exist in approved content codes. This has been ensured by a knowledge of the processes generating the wastes and the chemical compatibility analysis described in this appendix. The chemical constituents present in quantities >1% (weight) (documented as minor and dominant quantities)

in the chemical list associated with each content code are evaluated for compliance with the list of allowable materials for the appropriate waste material type specified in Section 4.3 of the CH-TRAMPAC. Only content codes with chemical lists that have been evaluated by this process and determined to be compatible shall be approved for shipment in the package. As described in Section 4.3 of the CH-TRAMPAC, any change to the chemical list of an approved content code, as well as requests for additional waste forms, must be submitted to the Cognizant Engineer for evaluation for compliance with the lists of allowable materials of the CH-TRAMPAC.

This page intentionally left blank.

Attachment A
Lists of Allowable Materials and
Associated Reactivity Groups

Lists of Allowable Materials and Associated Reactivity Groups

Waste Material Type	Allowable Chemical/Material[a]	Reactivity Group[b]	
		Name	Number[c]
I.1	Absorbents/adsorbents (e.g., Celite®, diatomaceous earth, diatomite, Florco®, Oil-Dri®, perlite, vermiculite)	Other solidification materials and absorbents/adsorbents	0
I.1	*Acids, inorganic*	Acids, Mineral, Non-oxidizing	1
I.1	*Acids, inorganic*	Acids, Mineral, Oxidizing	2
I.1	Alumina cement	Water reactive substance	107
I.1	Aquaset® products (for aqueous solutions)	Other solidification materials and absorbents/adsorbents	0
I.1	Aqueous sludges	Other solidification materials and absorbents/adsorbents	0
I.1	Aqueous solutions/water	Water and Mixtures containing water	106
I.1	Asbestos	Other Inorganics (non-reactive)	0
I.1	Ash (e.g., ash bottoms, fly ash, soot)	Other Inorganics (non-reactive)	0
I.1	Batteries, dry (e.g., flashlight)	Metals, alkali and alkaline earth, elemental and alloys	21
I.1	Ceramics (e.g., molds and crucibles)	Other Inorganics (non-reactive)	0
I.1	Clays (e.g., bentonite)	Other Inorganics (non-reactive)	0
I.1	Concrete	Other solidification materials and absorbents/adsorbents	0
I.1	Envirostone® (no organic emulsifiers allowed)	Other solidification materials and absorbents/adsorbents	0
I.1	Fiberglass, inorganic	Other Inorganics (non-reactive)	0
I.1	Filter media, inorganic	Other Inorganics (non-reactive)	0
I.1	Firebrick	Other Inorganics (non-reactive)	0
I.1	Glass (e.g., borosilicate glass, labware, leaded glass, Raschig rings)	Other Inorganics (non-reactive)	0
I.1	Graphite (e.g., molds and crucibles)	Metals, Other elemental, and alloy, as sheets, rods, moldings, vapors, or sponges	23
I.1	Grit	Other Inorganics (non-reactive)	0
I.1	Heel (e.g., ash heel; soot heel; firebrick heel; sand, slag, and crucible heel)	Other Inorganics (non-reactive)	0
I.1	Insulation, inorganic	Other Inorganics (non-reactive)	0
I.1	Magnesia cement (e.g., Ramcote® cement)	Water reactive substance	107
I.1	Metal hydroxides	Other Inorganics (non-reactive)	0
I.1	Metal oxides (e.g., slag)	Other Inorganics (non-reactive)	0
I.1	*Metals (e.g., aluminum, cadmium, copper, steel, tantalum, tungsten, zinc)*	Metals, Other elemental, and alloy, as sheets, rods, moldings, vapors, or sponges	23
I.1	*Metals (e.g., aluminum, cadmium, copper, steel, tantalum, tungsten, zinc)*	Metals, Other elemental and alloy in the form of powders, vapors, or sponges	22

6.1-8

Waste Material Type	Allowable Chemical/Material[a]	Reactivity Group[b]	
		Name	Number[c]
I.1	*Metals (e.g., aluminum, cadmium, copper, steel, tantalum, tungsten, zinc)*	Metals and metal compounds, toxic	24
I.1	*Metals (e.g., aluminum, cadmium, copper, steel, tantalum, tungsten, zinc)*	Reducing agents, strong	105
I.1	Nitrates (e.g., ammonium nitrate, sodium nitrate)	Oxidizing Agents, Strong	104
I.1	Petroset® products (for aqueous solutions)	Other solidification materials and absorbents/adsorbents	0
I.1	*Portland cement*	Water reactive substance	107
I.1	*Portland cement*	Caustics	10
I.1	Sand/soil, inorganic	Other Inorganics (non-reactive)	0
I.1	*Salts (e.g., calcium chloride, calcium fluoride, sodium chloride)*	Other Inorganics (non-reactive)	0
I.1	*Salts (e.g., calcium chloride, calcium fluoride, sodium chloride)*	Fluorides, inorganic	15
I.1	Other inorganic materials	Other Inorganics (non-reactive)	0
I.2	Absorbents/adsorbents (e.g., Celite®, diatomaceous earth, diatomite, Florco®, Oil-Dri®, perlite, vermiculite)	Other solidification materials and absorbents/adsorbents	0
I.2	Alumina cement	Water reactive substance	107
I.2	Aquaset® products (for aqueous solutions)	Other solidification materials and absorbents/adsorbents	0
I.2	Aqueous sludges	Other solidification materials and absorbents/adsorbents	0
I.2	Aqueous solutions/water	Water and Mixtures containing water	106
I.2	Asbestos	Other Inorganics (non-reactive)	0
I.2	Ash (e.g., ash bottoms, fly ash, soot)	Other Inorganics (non-reactive)	0
I.2	Batteries, dry (e.g., flashlight)	Metals, alkali and alkaline earth, elemental and alloys	21
I.2	Ceramics (e.g., molds and crucibles)	Other Inorganics (non-reactive)	0
I.2	Clays (e.g., bentonite)	Other Inorganics (non-reactive)	0
I.2	Concrete	Other solidification materials and absorbents/adsorbents	0
I.2	Fiberglass, inorganic	Other Inorganics (non-reactive)	0
I.2	Filter media, inorganic	Other Inorganics (non-reactive)	0
I.2	Firebrick	Other Inorganics (non-reactive)	0
I.2	Glass (e.g., borosilicate glass, labware, leaded glass, Raschig rings)	Other Inorganics (non-reactive)	0
I.2	Graphite (e.g., molds and crucibles)	Metals, Other elemental, and alloy, as sheets, rods, moldings, vapors, or sponges	23
I.2	Grit	Other Inorganics (non-reactive)	0
I.2	Heel (e.g., ash heel; soot heel; firebrick heel; sand, slag, and crucible heel)	Other Inorganics (non-reactive)	0
I.2	Insulation, inorganic	Other Inorganics (non-reactive)	0

Waste Material Type	Allowable Chemical/Material[a]	Reactivity Group[b]	
		Name	Number[c]
I.2	Magnesia cement (e.g., Ramcote® cement)	Water reactive substance	107
I.2	Metal hydroxides	Other Inorganics (non-reactive)	0
I.2	Metal oxides (e.g., slag)	Other Inorganics (non-reactive)	0
I.2	*Metals (e.g., aluminum, cadmium, copper, steel, tantalum, tungsten, zinc)*	Metals, Other elemental, and alloy, as sheets, rods, moldings, vapors, or sponges	23
I.2	*Metals (e.g., aluminum, cadmium, copper, steel, tantalum, tungsten, zinc)*	Metals, Other elemental and alloy in the form of powders, vapors, or sponges	22
I.2	*Metals (e.g., aluminum, cadmium, copper, steel, tantalum, tungsten, zinc)*	Metals and metal compounds, toxic	24
I.2	*Metals (e.g., aluminum, cadmium, copper, steel, tantalum, tungsten, zinc)*	Reducing agents, strong	105
I.2	Nitrates (e.g., ammonium nitrate, sodium nitrate)	Oxidizing Agents, Strong	104
I.2	Petroset® products (for aqueous solutions)	Other solidification materials and absorbents/adsorbents	0
I.2	*Portland cement*	Water reactive substance	107
I.2	*Portland cement*	Caustics	10
I.2	Sand/soil, inorganic	Other Inorganics (non-reactive)	0
I.2	*Salts (e.g., calcium chloride, calcium fluoride, sodium chloride)*	Other Inorganics (non-reactive)	0
I.2	*Salts (e.g., calcium chloride, calcium fluoride, sodium chloride)*	Fluorides, inorganic	15
I.2	Other inorganic materials	Other Inorganics (non-reactive)	0
I.3	Absorbents/adsorbents (e.g., Celite®, diatomaceous earth, diatomite, Florco®, Oil-Dri®, perlite, vermiculite)	Other solidification materials and absorbents/adsorbents	0
I.3	Asbestos	Other Inorganics (non-reactive)	0
I.3	Ash (e.g., ash bottoms, fly ash, soot)	Other Inorganics (non-reactive)	0
I.3	Batteries, dry (e.g., flashlight)	Metals, alkali and alkaline earth, elemental and alloys	21
I.3	Ceramics (e.g., molds and crucibles)	Other Inorganics (non-reactive)	0
I.3	Clays (e.g., bentonite)	Other Inorganics (non-reactive)	0
I.3	Concrete	Other solidification materials and absorbents/adsorbents	0
I.3	Fiberglass, inorganic	Other Inorganics (non-reactive)	0
I.3	Filter media, inorganic	Other Inorganics (non-reactive)	0
I.3	Firebrick	Other Inorganics (non-reactive)	0
I.3	Glass (e.g., borosilicate glass, labware, leaded glass, Raschig rings)	Other Inorganics (non-reactive)	0
I.3	Graphite (e.g., molds and crucibles)	Metals, Other elemental, and alloy, as sheets, rods, moldings, vapors, or sponges	23
I.3	Grit	Other Inorganics (non-reactive)	0

Waste Material Type	Allowable Chemical/Material[a]	Reactivity Group[b]	
		Name	Number[c]
I.3	Heel (e.g., ash heel; soot heel; firebrick heel; sand, slag, and crucible heel)	Other Inorganics (non-reactive)	0
I.3	Insulation, inorganic	Other Inorganics (non-reactive)	0
I.3	Metal hydroxides	Other Inorganics (non-reactive)	0
I.3	Metal oxides (e.g., slag)	Other Inorganics (non-reactive)	0
I.3	*Metals (e.g., aluminum, cadmium, copper, steel, tantalum, tungsten, zinc)*	Metals, Other elemental, and alloy, as sheets, rods, moldings, vapors, or sponges	23
I.3	*Metals (e.g., aluminum, cadmium, copper, steel, tantalum, tungsten, zinc)*	Metals, Other elemental and alloy in the form of powders, vapors, or sponges	22
I.3	*Metals (e.g., aluminum, cadmium, copper, steel, tantalum, tungsten, zinc)*	Metals and metal compounds, toxic	24
I.3	*Metals (e.g., aluminum, cadmium, copper, steel, tantalum, tungsten, zinc)*	Reducing agents, strong	105
I.3	Nitrates (e.g., ammonium nitrate, sodium nitrate)	Oxidizing Agents, Strong	104
I.3	*Portland cement*	Water reactive substance	107
I.3	*Portland cement*	Caustics	10
I.3	Sand/soil, inorganic	Other Inorganics (non-reactive)	0
I.3	*Salts (e.g., calcium chloride, calcium fluoride, sodium chloride)*	Other Inorganics (non-reactive)	0
I.3	*Salts (e.g., calcium chloride, calcium fluoride, sodium chloride)*	Fluorides, inorganic	15
I.3	Water (maximum of 30 weight percent unbound water)	Water and Mixtures containing water	106
I.3	Other inorganic materials	Other Inorganics (non-reactive)	0
II.1 II.2 II.3	Absorbents/adsorbents (e.g., Celite®, Florco®, Oil-Dri®, diatomite, perlite, vermiculite)	Other solidification materials and absorbents/adsorbents	0
II.1 II.2 II.3	Asbestos	Other Inorganics (non-reactive)	0
II.1 II.2 II.3	Ash (e.g., ash bottoms, fly ash, soot)	Other Inorganics (non-reactive)	0
II.1 II.2 II.3	Batteries, dry (e.g., flashlight)	Metals, alkali and alkaline earth, elemental and alloys	21
II.1 II.2 II.3	Ceramics (e.g., molds and crucibles)	Other Inorganics (non-reactive)	0
II.1 II.2 II.3	Clays (e.g., bentonite)	Other Inorganics (non-reactive)	0
II.1 II.2 II.3	Concrete/Portland cement (surface contaminated only)	Other solidification materials and absorbents/adsorbents	0
II.1 II.2 II.3	Fiberglass, inorganic	Other Inorganics (non-reactive)	0
II.1 II.2 II.3	Filter media, inorganic	Other Inorganics (non-reactive)	0

Waste Material Type	Allowable Chemical/Material[a]	Reactivity Group[b]	
		Name	Number[c]
II.1 II.2 II.3	Firebrick	Other Inorganics (non-reactive)	0
II.1 II.2 II.3	Glass (e.g., borosilicate glass, labware, leaded glass, Raschig rings)	Other Inorganics (non-reactive)	0
II.1 II.2 II.3	Graphite (e.g., molds and crucibles)	Metals, Other elemental, and alloy, as sheets, rods, moldings, vapors, or sponges	23
II.1 II.2 II.3	Grit	Other Inorganics (non-reactive)	0
II.1 II.2 II.3	Heel (e.g., ash heel; soot heel; firebrick heel; sand, slag, and crucible heel)	Other Inorganics (non-reactive)	0
II.1 II.2 II.3	Insulation, inorganic	Other Inorganics (non-reactive)	0
II.1 II.2 II.3	Magnesium alloy	Metals, Other elemental, and alloy, as sheets, rods, moldings, vapors, or sponges	23
II.1 II.2 II.3	Metal oxides (e.g., slag)	Other Inorganics (non-reactive)	0
II.1 II.2 II.3	*Metals (e.g., aluminum, cadmium, copper, steel, tantalum, tungsten, zinc)*	Metals, Other elemental, and alloy, as sheets, rods, moldings, vapors, or sponges	23
II.1 II.2 II.3	*Metals (e.g., aluminum, cadmium, copper, steel, tantalum, tungsten, zinc)*	Metals, Other elemental and alloy in the form of powders, vapors, or sponges	22
II.1 II.2 II.3	*Metals (e.g., aluminum, cadmium, copper, steel, tantalum, tungsten, zinc)*	Metals and metal compounds, toxic	24
II.1 II.2 II.3	*Metals (e.g., aluminum, cadmium, copper, steel, tantalum, tungsten, zinc)*	Reducing agents, strong	105
II.1 II.2 II.3	Nitrates (e.g., ammonium nitrate, sodium nitrate)	Oxidizing Agents, Strong	104
II.1 II.2 II.3	*Salts (e.g., calcium chloride, calcium fluoride, sodium chloride)*	Other Inorganics (non-reactive)	0
II.1 II.2 II.3	*Salts (e.g., calcium chloride, calcium fluoride, sodium chloride)*	Fluorides, inorganic	15
II.1 II.2 II.3	Sand/soil, inorganic	Other Inorganics (non-reactive)	0
II.1 II.2 II.3	Other inorganic materials	Other Inorganics (non-reactive)	0
II.3	Aqueous solutions/water	Water and Mixtures containing water	106
III.1	Absorbent polymers, organic	Combustible and flammable materials, miscellaneous	101
III.1	Acids, solid, organic	Acids, organic	3
III.1	Asphalt	Combustible and flammable materials, miscellaneous	101

Waste Material Type	Allowable Chemical/Material[a]	Reactivity Group[b] Name	Number[c]
III.1	Bakelite®	Combustible and flammable materials, miscellaneous	101
III.1	Cellulose (e.g., Benelex®, cotton Conwed®, paper, rags, rayon, wood)	Combustible and flammable materials, miscellaneous	101
III.1	Cellulose acetate butyrate	Polymerizable compounds	103
III.1	Cellulose propionate	Polymerizable compounds	103
III.1	Chlorinated polyether	Ethers	14
III.1	*Detergent, solid (e.g., emulsifiers, surfactants)*	Esters	13
III.1	*Detergent, solid (e.g., emulsifiers, surfactants)*	Hydrocarbons, Aromatic	16
III.1	*Detergent, solid (e.g., emulsifiers, surfactants)*	Hydrocarbon, aliphatic, unsaturated	28
III.1	*Detergent, solid (e.g., emulsifiers, surfactants)*	Organophosphates, phosphothioates, and phosphodithioates	32
III.1	Fiberglass, organic	Combustible and flammable materials, miscellaneous	101
III.1	Filter media, organic	Combustible and flammable materials, miscellaneous	101
III.1	Greases, commercial brands	Combustible and flammable materials, miscellaneous	101
III.1	Insulation, organic	Combustible and flammable materials, miscellaneous	101
III.1	*Leaded rubber (e.g., gloves, aprons, sheet material)*	Metals, Other elemental, and alloy, as sheets, rods, moldings, vapors, or sponges	23
III.1	*Leaded rubber (e.g., gloves, aprons, sheet material)*	Metals and metal compounds, toxic	24
III.1	*Leaded rubber (e.g., gloves, aprons, sheet material)*	Combustible and flammable materials, miscellaneous	101
III.1	Leather	Combustible and flammable materials, miscellaneous	101
III.1	Oil (e.g., petroleum, mineral)	Combustible and flammable materials, miscellaneous	101
III.1	Organophosphates (e.g., tributyl phosphate, dibutyl phosphate, monobutyl phosphite)	Organophosphates, phosphothioates, and phosphodithioates	32
III.1	Paint, dry (e.g., floor/wall paint, ALARA)	Combustible and flammable materials, miscellaneous	101
III.1	Plastics [e.g., polycarbonate, polyethylene, polymethyl methacrylate (Plexiglas®, Lucite®), polysulfone, polytetrafluoroethylene (Teflon®), polyvinyl acetate, polyvinyl chloride (PVC), polyvinylidene chloride (saran)]	Combustible and flammable materials, miscellaneous	101
III.1	*Polyamides (nylon)*	Combustible and flammable materials, miscellaneous	101
III.1	*Polyamides (nylon)*	Amides	6

Waste Material Type	Allowable Chemical/Material[a]	Reactivity Group[b]	
		Name	Number[c]
III.1	Polychlorotrifluoroethylene (e.g., Kel-F®)	Combustible and flammable materials, miscellaneous	101
III.1	*Polyesters (e.g., Dacron®, Mylar®)*	Combustible and flammable materials, miscellaneous	101
III.1	*Polyesters (e.g., Dacron®, Mylar®)*	Esters	13
III.1	*Polyethylene glycol (e.g., Carbowax®)*	Alcohols and Glycols	4
III.1	*Polyethylene glycol (e.g., Carbowax®)*	Combustible and flammable materials, miscellaneous	101
III.1	Polyimides	Hydrocarbons, aromatic	16
III.1	Polyphenyl methacrylate	Combustible and flammable materials, miscellaneous	101
III.1	Polypropylene (e.g., Ful-Flo® filters)	Combustible and flammable materials, miscellaneous	101
III.1	Polyurethane	Combustible and flammable materials, miscellaneous	101
III.1	Polyvinyl alcohol	Alcohols and Glycols	4
III.1	*Resins (e.g., aniline-formaldehyde, melamine-formaldehyde, organic resins, phenol-formaldehyde, phenolic resins, urea-formaldehyde)*	Aldehydes	5
III.1	*Resins (e.g., aniline-formaldehyde, melamine-formaldehyde, organic resins, phenol-formaldehyde, phenolic resins, urea-formaldehyde)*	Phenols and Creosols	31
III.1	Rubber, natural or synthetic [e.g., chlorosulfonated polyethylene (Hypalon®), ethylene-propylene rubber, EPDM, polybutadiene, polychloroprene (neoprene), polyisobutylene, polyisoprene, polystyrene, rubber hydrochloride (pliofilm®)]	Combustible and flammable materials, miscellaneous	101
III.1	*Sand/Soil*	Other Inorganics (non-reactive)	0
III.1	*Sand/Soil*	Combustible and flammable materials, miscellaneous	101
III.1	Waxes, commercial brands	Combustible and flammable materials, miscellaneous	101
IV.1	Acids, organic	Acids, organic	3
IV.1	Alcohols (e.g., butanol, ethanol, isopropanol, methanol)	Alcohols and Glycols	4
IV.1	Esters (e.g., ethyl acetate, polyethylene glycol ester)	Esters	13
IV.1	Ethers (e.g., ethyl ether)	Ethers	14

Waste Material Type	Allowable Chemical/Material[a]	Reactivity Group[b]	
		Name	Number[c]
IV.1	Halogenated organics (e.g., bromoform; carbon tetrachloride; chlorobenzene; chloroform; 1,1-dichloroethane; 1,2-dichloroethane; 1,1-dichloroethylene; cis-1,2-dichloroethylene; methylene chloride; 1,1,2,2-tetrachloroethane; tetrachloroethylene; 1,1,1-trichloroethane; 1,1,2-trichloroethane; trichloroethylene; 1,1,2-trichloro-1,2,2-trifluoroethane)	Halogenated Organics	17
IV.1	***Hydrocarbons, aliphatic (e.g., cyclohexane, n-paraffin hydrocarbons)***	Hydrocarbon, aliphatic, unsaturated	28
IV.1	***Hydrocarbons, aliphatic (e.g., cyclohexane, n-paraffin hydrocarbons)***	Hydrocarbon, aliphatic, saturated	29
IV.1	Hydrocarbons, aromatic (e.g., benzene; ethyl benzene; toluene; 1,2,4-trimethylbenzene; 1,3,5-trimethylbenzene; xylene)	Hydrocarbons, aromatic	16
IV.1	Ketones (e.g., acetone, methyl ethyl ketone, methyl isobutyl ketone)	Ketones	19
IV.1	Trioctyl phosphine oxide	Organophosphates, phosphothioates, and phosphodithioates	32

[a] Chemicals in ***bold italic*** have been assigned to more than one reactivity group.

[b] Reactivity group from Hatayama, H.K., J. J. Chen, E.R. deVera, R.D. Stephens, and D.L. Storm, 1980, "A Method for Determining the Compatibility of Hazardous Wastes," EPA-600/2-80-076, U.S. Environmental Protection Agency, Cincinnati, Ohio.

[c] Non-reactive inorganic materials or chemicals are assigned a reactivity group number of "0."

This page intentionally left blank.

Attachment B
List of Unique Reactivity Group Numbers in Lists of
Allowable Materials

List of Unique Reactivity Group Numbers in
Lists of Allowable Materials

Allowable Chemical/Material[a]	Reactivity Group[b]	
	Name	Number
Absorbents/adsorbents (e.g., Celite®, diatomaceous earth, diatomite, Florco®, Oil-Dri®, perlite, vermiculite)	Other solidification materials and absorbents/adsorbents	0
Acids, inorganic	Acids, Mineral, Non-oxidizing	1
Acids, inorganic	Acids, Mineral, Oxidizing	2
Acids, solid, organic	Acids, Organic	3
Polyethylene glycol (e.g., Carbowax®)	Alcohols and Glycols	4
Resins (e.g., aniline-formaldehyde, melamine-formaldehyde, organic resins, phenol-formaldehyde, phenolic resins, urea-formaldehyde)	Aldehydes	5
Polyamides (nylon)	Amides	6
Portland cement	Caustics	10
Esters (e.g., ethyl acetate, polyethylene glycol ester)	Esters	13
Ethers (e.g., ethyl ether)	Ethers	14
Salts (e.g., calcium chloride, calcium fluoride, sodium chloride)	Fluorides, inorganic	15
Hydrocarbons, aromatic (e.g., benzene; ethyl benzene; toluene; 1,2,4-trimethylbenzene; 1,3,5-trimethylbenzene; xylene)	Hydrocarbons, aromatic	16
Halogenated organics (e.g., bromoform; carbon tetrachloride; chlorobenzene; chloroform; 1,1-dichloroethane; 1,2-dichloroethane; 1,1-dichloroethylene; cis-1,2-dichloroethylene; methylene chloride; 1,1,2,2-tetrachloroethane; tetrachloroethylene; 1,1,1-trichloroethane; 1,1,2-trichloroethane; trichloroethylene; 1,1,2-trichloro-1,2,2-trifluoroethane)	Halogenated Organics	17
Ketones (e.g., acetone, methyl ethyl ketone, methyl isobutyl ketone)	Ketones	19
Batteries, dry (e.g., flashlight)	Metals, alkali and alkaline earth, elemental and alloys	21
Metals (e.g., aluminum, cadmium, copper, steel, tantalum, tungsten, zinc)	Metals, Other elemental and alloy in the form of powders, vapors, or sponges	22
Metals (e.g., aluminum, cadmium, copper, steel, tantalum, tungsten, zinc)	Metals, Other elemental, and alloy, as sheets, rods, moldings, vapors, or sponges	23
Leaded rubber (e.g., gloves, aprons, sheet material)	Metals and metal compounds, toxic	24
Hydrocarbons, aliphatic (e.g., cyclohexane, n-paraffin hydrocarbons)	Hydrocarbon, aliphatic, unsaturated	28
Hydrocarbons, aliphatic (e.g., cyclohexane, n-paraffin hydrocarbons)	Hydrocarbon, aliphatic, saturated	29

Allowable Chemical/Material[a]	Reactivity Group[b]	
	Name	Number
Resins (e.g., aniline-formaldehyde, melamine-formaldehyde, organic resins, phenol-formaldehyde, phenolic resins, urea-formaldehyde)	Phenols and Creosols	31
Organophosphates (e.g., tributyl phosphate, dibutyl phosphate, monobutyl phosphite)	Organophosphates, phosphothioates, and phosphodithioates	32
Asphalt	Combustible and flammable materials, miscellaneous	101
Cellulose acetate butyrate	Polymerizable compounds	103
Nitrates (e.g., ammonium nitrate, sodium nitrate)	Oxidizing Agents, Strong	104
Metals (e.g., aluminum, cadmium, copper, steel, tantalum, tungsten, zinc)	Reducing agents, strong	105
Aqueous solutions/water	Water and Mixtures containing water	106
Portland cement	Water reactive substances	107

[a] Chemicals in **bold italic** have been assigned to more than one reactivity group.
[b] Reactivity group from Hatayama, H.K., J.J. Chen, E.R. deVera, R.D. Stephens, and D.L. Storm, 1980, "A Method for Determining the Compatibility of Hazardous Wastes," EPA-600/2-80-076, U.S. Environmental Protection Agency, Cincinnati, Ohio.

This page intentionally left blank.

**Attachment C
Hazardous Waste Chemical Compatibility Chart**

Waste Chemical Compatibility Chart

Legend

Symbol	Meaning
E	= Explosion
F	= Fire
G	= Innocuous and Non-Flammable Gas Generation
GF	= Flammable Gas Generation
GT	= Toxic Gas Generation
H	= Heat Generation
P	= Violent Polymerization
S	= Solubilization of Toxic Substances

Group No.	Reactivity Group Name	1	2	3	4	5	6	10	13	14	15	16	17	19	21	22	23	24	28	29	31	32	101	103	104	105	106	107
1	Acids, Mineral, Non-Oxidizing	**1**																										
2	Acids, Mineral, Oxidizing	H	**2**																									
3	Acids, Organic		G, H	**3**																								
4	Alcohols and Glycols	H	H, P	H, P	**4**																							
5	Aldehydes	H, P	H, F	H, P		**5**																						
6	Amides	H	H, GT				**6**																					
10	Caustics	H	H	H		H		**10**																				
13	Esters	H	H, F						**13**																			
14	Ethers	H	H, F							**14**																		
15	Fluorides, Inorganic	GT	GT	GT							**15**																	
16	Hydrocarbons, Aromatic	H, F	H, F									**16**																
17	Halogenated Organics	H, GT	H, F, GT				H, GT	H					**17**															
19	Ketones	H	H, F				H	H						**19**														
21	Metals, Alkali and Alkaline Earth, Elemental	GF, H, F	GF, H, F	GF, H, F	GF, H, F	GF, H, F	GF, H	GF, H	GF, H			GF, H	H, E	H, E	**21**													
22	Metals, Other Elemental and Alloys as Powders, Vapors, or Sponges	GF, H, F	GF, H, F	GF		F		GF, H	GF, H				H, E			**22**												
23	Metals, Other Elemental and Alloys as Sheets, Rods, Drops, Moldings, etc	GF, H, F	GF, H, F			F		GF, H	GF, H				H, F				**23**											
24	Metals and Metal Compounds, Toxic	S		S		S	S	S										**24**										
28	Hydrocarbons, Aliphatic, Unsaturated	H				H									H, E				**28**									
29	Hydrocarbons, Aliphatic, Saturated		H, F												H					**29**								
31	Phenols and Creosols	H													GF, H						**31**							
32	Organophosphates, Phosphothioates, Phosphodithioates	H, GT	H, GT												H				H, E			**32**						
101	Combustible and Flammable Materials, Miscellaneous	H, G	H, F, GT												H, G, F								**101**					
103	Polymerizable Compounds	P, H	P, H	P, H											P, H	P, H	P, H	P, H			P, H			**103**				
104	Oxidizing Agents, Strong	H, GT		H, GT		H, F, GT			H, F	H, F			H, F		H, F, E	H, F, E	H, F		H, F	H, F		H, F			**104**			
105	Reducing Agents, Strong	H, GF	H, F, GT	H, GF	H, GF, F	H, GF, F	H, GF		H, E	GF, H			H, E	GF, H											H, F, E	**105**		
106	Water and Mixtures Containing Water	H	H												GF, H			S							GT, GF, H	H, P, GF	**106**	
107	Water Reactive Substances	←----- Extremely Reactive ----- Do Not Mix with Any Chemical or Waste Material ----- Extremely Reactive -----→																								H, F, E	GF, GT	**107**
Reactivity Group Number		1	2	3	4	5	6	10	13	14	15	16	17	19	21	22	23	24	28	29	31	32	101	103	104	105	106	107

Source: Hatayama, H.K., J.J. Chen, E.R. deVera, R.D. Stephens, and D.L. Storm, "A Method for Determining the Compatibility of Hazardous Wastes," EPA-600/2-80-076, U.S. Environmental Protection Agency, Cincinnati, Ohio, 1980.

**Attachment D
Potential Chemical Incompatibilities**

Potential Chemical Incompatibilities

Combination of Reactivity Groups		Reaction Result (A x B)	Explanation of Potential Incompatibility
Group A	Group B		
1	4	Heat Generation	Reaction will not occur – Acids are neutralized and solidified/immobilized prior to shipping
1	5	Heat Generation	Reaction will not occur – Acids are neutralized and solidified/immobilized prior to shipping
1	5	Violent Polymerization	Reaction will not occur – Acids are neutralized and solidified/immobilized prior to shipping
1	6	Heat Generation	Reaction will not occur – Acids are neutralized and solidified/immobilized prior to shipping
1	10	Heat Generation	Reaction will not occur – Acids are neutralized and solidified/immobilized prior to shipping; Bases/caustic materials are neutralized and solidified/immobilized prior to shipping
1	13	Heat Generation	Reaction will not occur – Acids are neutralized and solidified/immobilized prior to shipping
1	14	Heat Generation	Reaction will not occur – Acids are neutralized and solidified/immobilized prior to shipping
1	15	Toxic Gas Generation	Reaction will not occur – Acids are neutralized and solidified/immobilized prior to shipping
1	17	Heat Generation	Reaction will not occur – Acids are neutralized and solidified/immobilized prior to shipping
1	17	Toxic Gas Generation	Reaction will not occur – Acids are neutralized and solidified/immobilized prior to shipping
1	19	Heat Generation	Reaction will not occur – Acids are neutralized and solidified/immobilized prior to shipping
1	21	Flammable Gas Generation	Reaction will not occur – Acids are neutralized and solidified/immobilized prior to shipping
1	21	Heat Generation	Reaction will not occur – Acids are neutralized and solidified/immobilized prior to shipping
1	21	Fire	Reaction will not occur – Acids are neutralized and solidified/immobilized prior to shipping
1	22	Flammable Gas Generation	Reaction will not occur – Acids are neutralized and solidified/immobilized prior to shipping
1	22	Heat Generation	Reaction will not occur – Acids are neutralized and solidified/immobilized prior to shipping
1	22	Fire	Reaction will not occur – Acids are neutralized and solidified/immobilized prior to shipping
1	23	Flammable Gas Generation	Reaction will not occur – Acids are neutralized and solidified/immobilized prior to shipping
1	23	Heat Generation	Reaction will not occur – Acids are neutralized and solidified/immobilized prior to shipping
1	23	Fire	Reaction will not occur – Acids are neutralized and solidified/immobilized prior to shipping
1	24	Solubilization of	Reaction will not occur – Acids are neutralized and

Combination of Reactivity Groups		Reaction Result (A x B)	Explanation of Potential Incompatibility
Group A	**Group B**		
		Toxic Substances	solidified/immobilized prior to shipping Additionally, any solubilization of toxic substances will not affect transportation of wastes.
1	28	Heat Generation	Reaction will not occur – Acids are neutralized and solidified/immobilized prior to shipping
1	31	Heat Generation	Reaction will not occur – Acids are neutralized and solidified/immobilized prior to shipping
1	32	Heat Generation	Reaction will not occur – Acids are neutralized and solidified/immobilized prior to shipping
1	32	Toxic Gas Generation	Reaction will not occur – Acids are neutralized and solidified/immobilized prior to shipping
1	101	Heat Generation	Reaction will not occur – Acids are neutralized and solidified/immobilized prior to shipping
1	101	Innocuous and Non-Flammable Gas Generation	Reaction will not occur – Acids are neutralized and solidified/immobilized prior to shipping
1	103	Violent Polymerization	Reaction will not occur – Acids are neutralized and solidified/immobilized prior to shipping
1	103	Heat Generation	Reaction will not occur – Acids are neutralized and solidified/immobilized prior to shipping
1	104	Heat Generation	Reaction will not occur – Acids are neutralized and solidified/immobilized prior to shipping; oxidizing agents are reacted prior to being placed in the waste/shipped.
1	104	Toxic Gas Generation	Reaction will not occur – Acids are neutralized and solidified/immobilized prior to shipping; oxidizing agents are reacted prior to being placed in the waste/shipped.
1	105	Heat Generation	Reaction will not occur – Acids are neutralized and solidified/immobilized prior to shipping; reducing agents are reacted prior to being placed in the waste/shipped.
1	105	Flammable Gas Generation	Reaction will not occur – Acids are neutralized and solidified/immobilized prior to shipping; reducing agents are reacted prior to being placed in the waste/shipped.
1	106	Heat Generation	Reaction will not occur – Acids are neutralized and solidified/immobilized prior to shipping; free liquid content is limited to less than 1% of waste volume

Combination of Reactivity Groups		Reaction Result (A x B)	Explanation of Potential Incompatibility
Group A	Group B		
1	107	Highly Reactive	Reaction will not occur – Acids are neutralized and solidified/immobilized prior to shipping; free liquid content is limited to less than 1% of waste volume; water reactive substances are reacted prior to being placed in the waste/shipped. Lime in Portland cement is most common water reactive substance expected in the waste. Portland cement is used as an absorbent and solidification agent for the wastes.
2	3	Innocuous and Non-Flammable Gas Generation	Reaction will not occur – Acids are neutralized and solidified/immobilized prior to shipping
2	3	Heat Generation	Reaction will not occur – Acids are neutralized and solidified/immobilized prior to shipping
2	4	Heat Generation	Reaction will not occur – Acids are neutralized and solidified/immobilized prior to shipping
2	4	Fire	Reaction will not occur – Acids are neutralized and solidified/immobilized prior to shipping
2	5	Heat Generation	Reaction will not occur – Acids are neutralized and solidified/immobilized prior to shipping
2	5	Fire	Reaction will not occur – Acids are neutralized and solidified/immobilized prior to shipping
2	6	Heat Generation	Reaction will not occur – Acids are neutralized and solidified/immobilized prior to shipping
2	6	Toxic Gas Generation	Reaction will not occur – Acids are neutralized and solidified/immobilized prior to shipping
2	10	Heat Generation	Reaction will not occur – Acids are neutralized and solidified/immobilized prior to shipping; Bases/caustic materials are neutralized and solidified/immobilized prior to shipping
2	13	Heat Generation	Reaction will not occur – Acids are neutralized and solidified/immobilized prior to shipping
2	13	Fire	Reaction will not occur – Acids are neutralized and solidified/immobilized prior to shipping
2	14	Heat Generation	Reaction will not occur – Acids are neutralized and solidified/immobilized prior to shipping
2	14	Fire	Reaction will not occur – Acids are neutralized and solidified/immobilized prior to shipping
2	15	Toxic Gas Generation	Reaction will not occur – Acids are neutralized and solidified/immobilized prior to shipping
2	16	Heat Generation	Reaction will not occur – Acids are neutralized and solidified/immobilized prior to shipping
2	16	Fire	Reaction will not occur – Acids are neutralized and solidified/immobilized prior to shipping

Combination of Reactivity Groups		Reaction Result (A x B)	Explanation of Potential Incompatibility
Group A	Group B		
2	17	Heat Generation	Reaction will not occur – Acids are neutralized and solidified/immobilized prior to shipping
2	17	Fire	Reaction will not occur – Acids are neutralized and solidified/immobilized prior to shipping
2	17	Toxic Gas Generation	Reaction will not occur – Acids are neutralized and solidified/immobilized prior to shipping
2	19	Heat Generation	Reaction will not occur – Acids are neutralized and solidified/immobilized prior to shipping
2	19	Fire	Reaction will not occur – Acids are neutralized and solidified/immobilized prior to shipping
2	21	Flammable Gas Generation	Reaction will not occur – Acids are neutralized and solidified/immobilized prior to shipping
2	21	Heat Generation	Reaction will not occur – Acids are neutralized and solidified/immobilized prior to shipping
2	21	Fire	Reaction will not occur – Acids are neutralized and solidified/immobilized prior to shipping
2	22	Flammable Gas Generation	Reaction will not occur – Acids are neutralized and solidified/immobilized prior to shipping
2	22	Heat Generation	Reaction will not occur – Acids are neutralized and solidified/immobilized prior to shipping
2	22	Fire	Reaction will not occur – Acids are neutralized and solidified/immobilized prior to shipping
2	23	Flammable Gas Generation	Reaction will not occur – Acids are neutralized and solidified/immobilized prior to shipping
2	23	Heat Generation	Reaction will not occur – Acids are neutralized and solidified/immobilized prior to shipping
2	23	Fire	Reaction will not occur – Acids are neutralized and solidified/immobilized prior to shipping
2	24	Solubilization of Toxic Substances	Reaction will not occur – Acids are neutralized and solidified/immobilized prior to shipping Additionally, any solubilization of toxic substances will not affect transportation of wastes.
2	28	Heat Generation	Reaction will not occur – Acids are neutralized and solidified/immobilized prior to shipping
2	28	Fire	Reaction will not occur – Acids are neutralized and solidified/immobilized prior to shipping
2	29	Heat Generation	Reaction will not occur – Acids are neutralized and solidified/immobilized prior to shipping
2	29	Fire	Reaction will not occur – Acids are neutralized and solidified/immobilized prior to shipping
2	31	Heat Generation	Reaction will not occur – Acids are neutralized and solidified/immobilized prior to shipping
2	31	Fire	Reaction will not occur – Acids are neutralized and solidified/immobilized prior to shipping

Combination of Reactivity Groups		Reaction Result (A x B)	Explanation of Potential Incompatibility
Group A	Group B		
2	32	Heat Generation	Reaction will not occur – Acids are neutralized and solidified/immobilized prior to shipping
2	32	Toxic Gas Generation	Reaction will not occur – Acids are neutralized and solidified/immobilized prior to shipping
2	101	Heat Generation	Reaction will not occur – Acids are neutralized and solidified/immobilized prior to shipping
2	101	Fire	Reaction will not occur – Acids are neutralized and solidified/immobilized prior to shipping
2	101	Toxic Gas Generation	Reaction will not occur – Acids are neutralized and solidified/immobilized prior to shipping
2	103	Violent Polymerization	Reaction will not occur – Acids are neutralized and solidified/immobilized prior to shipping
2	103	Heat Generation	Reaction will not occur – Acids are neutralized and solidified/immobilized prior to shipping
2	105	Heat Generation	Reaction will not occur – Acids are neutralized and solidified/immobilized prior to shipping; reducing agents are reacted prior to being placed in the waste/shipped.
2	105	Fire	Reaction will not occur – Acids are neutralized and solidified/immobilized prior to shipping; reducing agents are reacted prior to being placed in the waste/shipped.
2	105	Toxic Gas Generation	Reaction will not occur – Acids are neutralized and solidified/immobilized prior to shipping; reducing agents are reacted prior to being placed in the waste/shipped.
2	106	Heat Generation	Reaction will not occur – Acids are neutralized and solidified/immobilized prior to shipping; free liquid content is limited to less than 1% of waste volume
2	107	Highly Reactive	Reaction will not occur – Acids are neutralized and solidified/immobilized prior to shipping; free liquid content is limited to less than 1% of waste volume; water reactive substances are reacted prior to being placed in the waste/shipped. Lime in Portland cement is most common water reactive substance expected in the waste. Portland cement is used as an absorbent and solidification agent for the wastes.
3	4	Heat Generation	Reaction will not occur – Acids are neutralized and solidified/immobilized prior to shipping
3	4	Violent Polymerization	Reaction will not occur – Acids are neutralized and solidified/immobilized prior to shipping
3	5	Heat Generation	Reaction will not occur – Acids are neutralized and solidified/immobilized prior to shipping
3	5	Violent Polymerization	Reaction will not occur – Acids are neutralized and solidified/immobilized prior to shipping

Combination of Reactivity Groups		Reaction Result (A x B)	Explanation of Potential Incompatibility
Group A	Group B		
3	10	Heat Generation	Reaction will not occur – Acids are neutralized and solidified/immobilized prior to shipping; Bases/caustic materials are neutralized and solidified/immobilized prior to shipping
3	15	Toxic Gas Generation	Reaction will not occur – Acids are neutralized and solidified/immobilized prior to shipping
3	21	Flammable Gas Generation	Reaction will not occur – Acids are neutralized and solidified/immobilized prior to shipping
3	21	Heat Generation	Reaction will not occur – Acids are neutralized and solidified/immobilized prior to shipping
3	21	Fire	Reaction will not occur – Acids are neutralized and solidified/immobilized prior to shipping
3	22	Flammable Gas Generation	Reaction will not occur – Acids are neutralized and solidified/immobilized prior to shipping
3	24	Solubilization of Toxic Substances	Reaction will not occur – Acids are neutralized and solidified/immobilized prior to shipping Additionally, any solubilization of toxic substances will not affect transportation of wastes.
3	103	Violent Polymerization	Reaction will not occur – Acids are neutralized and solidified/immobilized prior to shipping
3	103	Heat Generation	Reaction will not occur – Acids are neutralized and solidified/immobilized prior to shipping
3	104	Heat Generation	Reaction will not occur – Acids are neutralized and solidified/immobilized prior to shipping; oxidizing agents are reacted prior to being placed in the waste/shipped.
3	104	Toxic Gas Generation	Reaction will not occur – Acids are neutralized and solidified/immobilized prior to shipping; oxidizing agents are reacted prior to being placed in the waste/shipped.
3	105	Heat Generation	Reaction will not occur – Acids are neutralized and solidified/immobilized prior to shipping; reducing agents are reacted prior to being placed in the waste/shipped.
3	105	Flammable Gas Generation	Reaction will not occur – Acids are neutralized and solidified/immobilized prior to shipping; reducing agents are reacted prior to being placed in the waste/shipped.
3	107	Highly Reactive	Reaction will not occur – Acids are neutralized and solidified/immobilized prior to shipping; free liquid content is limited to less than 1% of waste volume; water reactive substances are reacted prior to being placed in the waste/shipped. Lime in Portland cement is most common water reactive substance expected in the waste. Portland cement is used as an absorbent and solidification agent for the wastes.

Combination of Reactivity Groups		Reaction Result (A x B)	Explanation of Potential Incompatibility
Group A	Group B		
4	21	Flammable Gas Generation	Reaction will not occur – Alcohols and Glycols are solidified/immobilized prior to shipping
4	21	Heat Generation	Reaction will not occur – Alcohols and Glycols are solidified/immobilized prior to shipping
4	21	Fire	Reaction will not occur – Alcohols and Glycols are solidified/immobilized prior to shipping
4	104	Heat Generation	Reaction will not occur – Alcohols and Glycols are solidified/immobilized prior to shipping; oxidizing agents are reacted prior to being placed in the waste/shipped.
4	104	Fire	Reaction will not occur – Alcohols and Glycols are solidified/immobilized prior to shipping; oxidizing agents are reacted prior to being placed in the waste/shipped.
4	105	Heat Generation	Reaction will not occur – Alcohols and Glycols are solidified/immobilized prior to shipping; reducing agents are reacted prior to being placed in the waste/shipped.
4	105	Flammable Gas Generation	Reaction will not occur – Alcohols and Glycols are solidified/immobilized prior to shipping; reducing agents are reacted prior to being placed in the waste/shipped.
4	105	Fire	Reaction will not occur – Alcohols and Glycols are solidified/immobilized prior to shipping; reducing agents are reacted prior to being placed in the waste/shipped.
4	107	Highly Reactive	Reaction will not occur – Alcohols and Glycols are solidified/immobilized prior to shipping; free liquid content is limited to less than 1% of waste volume; water reactive substances are reacted prior to being placed in the waste/shipped. Lime in Portland cement is most common water reactive substance expected in the waste. Portland cement is used as an absorbent and solidification agent for the wastes.
5	10	Heat Generation	Reaction will not occur – Aldehydes are solidified/immobilized prior to shipping; bases/caustic materials are neutralized and solidified/immobilized prior to shipping
5	21	Flammable Gas Generation	Reaction will not occur – Aldehydes are solidified/immobilized prior to shipping
5	21	Heat Generation	Reaction will not occur – Aldehydes are solidified/immobilized prior to shipping
5	21	Fire	Reaction will not occur – Aldehydes are solidified/immobilized prior to shipping

6.1-30

Combination of Reactivity Groups		Reaction Result (A x B)	Explanation of Potential Incompatibility
Group A	Group B		
5	28	Heat Generation	Reaction will not occur – Aldehydes are solidified/immobilized prior to shipping
5	104	Heat Generation	Reaction will not occur – Aldehydes are solidified/immobilized prior to shipping; oxidizing agents are reacted prior to being placed in the waste/shipped.
5	104	Fire	Reaction will not occur – Aldehydes are solidified/immobilized prior to shipping; oxidizing agents are reacted prior to being placed in the waste/shipped.
5	105	Heat Generation	Reaction will not occur – Aldehydes are solidified/immobilized prior to shipping; reducing agents are reacted prior to being placed in the waste/shipped.
5	105	Flammable Gas Generation	Reaction will not occur – Aldehydes are solidified/immobilized prior to shipping; reducing agents are reacted prior to being placed in the waste/shipped.
5	105	Fire	Reaction will not occur – Aldehydes are solidified/immobilized prior to shipping; reducing agents are reacted prior to being placed in the waste/shipped.
5	107	Highly Reactive	Reaction will not occur – Aldehydes are solidified/immobilized prior to shipping; free liquid content is limited to less than 1% of waste volume; water reactive substances are reacted prior to being placed in the waste/shipped. Lime in Portland cement is most common water reactive substance expected in the waste. Portland cement is used as an absorbent and solidification agent for the wastes.
6	17	Heat Generation	Reaction will not occur – Amides are solidified/immobilized prior to shipping
6	17	Toxic Gas Generation	Reaction will not occur – Amides are solidified/immobilized prior to shipping
6	21	Flammable Gas Generation	Reaction will not occur – Amides are solidified/immobilized prior to shipping
6	21	Heat Generation	Reaction will not occur – Amides are solidified/immobilized prior to shipping
6	24	Solubilization of Toxic Substances	Reaction will not occur – Amides are solidified/immobilized prior to shipping Additionally, any solubilization of toxic substances will not affect transportation of wastes.

Combination of Reactivity Groups		Reaction Result (A x B)	Explanation of Potential Incompatibility
Group A	Group B		
6	104	Heat Generation	Reaction will not occur – Amides are solidified/immobilized prior to shipping; oxidizing agents are reacted prior to being placed in the waste/shipped.
6	104	Fire	Reaction will not occur – Amides are solidified/immobilized prior to shipping; oxidizing agents are reacted prior to being placed in the waste/shipped.
6	104	Toxic Gas Generation	Reaction will not occur – Amides are solidified/immobilized prior to shipping; oxidizing agents are reacted prior to being placed in the waste/shipped.
6	105	Heat Generation	Reaction will not occur – Amides are solidified/immobilized prior to shipping; reducing agents are reacted prior to being placed in the waste/shipped.
6	105	Flammable Gas Generation	Reaction will not occur – Amides are solidified/immobilized prior to shipping; reducing agents are reacted prior to being placed in the waste/shipped.
6	107	Highly Reactive	Reaction will not occur – Amides are solidified/immobilized prior to shipping; free liquid content is limited to less than 1% of waste volume; water reactive substances are reacted prior to being placed in the waste/shipped. Lime in Portland cement is most common water reactive substance expected in the waste. Portland cement is used as an absorbent and solidification agent for the wastes.
10	13	Heat Generation	Reaction will not occur – Caustics/bases are neutralized and solidified/immobilized prior to shipping
10	17	Heat Generation	Reaction will not occur – Caustics/bases are neutralized and solidified/immobilized prior to shipping
10	19	Heat Generation	Reaction will not occur – Caustics/bases are neutralized and solidified/immobilized prior to shipping
10	21	Flammable Gas Generation	Reaction will not occur – Caustics/bases are neutralized and solidified/immobilized prior to shipping
10	21	Heat Generation	Reaction will not occur – Caustics/bases are neutralized and solidified/immobilized prior to shipping

Combination of Reactivity Groups		Reaction Result (A x B)	Explanation of Potential Incompatibility
Group A	**Group B**		
10	22	Flammable Gas Generation	Reaction will not occur – Caustics/bases are neutralized and solidified/immobilized prior to shipping
10	22	Heat Generation	Reaction will not occur – Caustics/bases are neutralized and solidified/immobilized prior to shipping
10	23	Flammable Gas Generation	Reaction will not occur – Caustics/bases are neutralized and solidified/immobilized prior to shipping
10	23	Heat Generation	Reaction will not occur – Caustics/bases are neutralized and solidified/immobilized prior to shipping
10	24	Solubilization of Toxic Substances	Reaction will not occur – Caustics/bases are neutralized and solidified/immobilized prior to shipping; Additionally, any solubilization of toxic substances will not affect transportation of wastes.
10	32	Heat Generation	Reaction will not occur – Caustics/bases are neutralized and solidified/immobilized prior to shipping
10	32	Explosion	Reaction will not occur – Caustics/bases are neutralized and solidified/immobilized prior to shipping
10	103	Violent Polymerization	Reaction will not occur – Caustics/bases are neutralized and solidified/immobilized prior to shipping
10	103	Heat Generation	Reaction will not occur – Caustics/bases are neutralized and solidified/immobilized prior to shipping
10	107	Highly Reactive	Reaction will not occur – Caustics/bases are neutralized and solidified/immobilized prior to shipping; free liquid content is limited to less than 1% of waste volume; water reactive substances are reacted prior to being placed in the waste/shipped. Lime in Portland cement is most common water reactive substance expected in the waste. Portland cement is used as an absorbent and solidification agent for the wastes.
13	21	Flammable Gas Generation	Reaction will not occur – Esters are solidified/immobilized prior to shipping
13	21	Heat Generation	Reaction will not occur – Esters are solidified/immobilized prior to shipping
13	104	Heat Generation	Reaction will not occur – Esters are solidified/immobilized prior to shipping; oxidizing agents are reacted prior to being placed in the waste/shipped.

Combination of Reactivity Groups		Reaction Result (A x B)	Explanation of Potential Incompatibility
Group A	Group B		
13	104	Fire	Reaction will not occur – Esters are solidified/immobilized prior to shipping; oxidizing agents are reacted prior to being placed in the waste/shipped.
13	105	Heat Generation	Reaction will not occur – Esters are solidified/immobilized prior to shipping; reducing agents are reacted prior to being placed in the waste/shipped.
13	105	Fire	Reaction will not occur – Esters are solidified/immobilized prior to shipping; reducing agents are reacted prior to being placed in the waste/shipped.
13	107	Highly Reactive	Reaction will not occur – Esters are solidified/immobilized prior to shipping; free liquid content is limited to less than 1% of waste volume; water reactive substances are reacted prior to being placed in the waste/shipped. Lime in Portland cement is most common water reactive substance expected in the waste. Portland cement is used as an absorbent and solidification agent for the wastes.
14	104	Heat Generation	Reaction will not occur – Ethers are solidified / immobilized prior to shipping. Oxidizing agents are reacted prior to being placed in the waste/shipped.
14	104	Fire	Reaction will not occur – Ethers are solidified / immobilized prior to shipping. Oxidizing agents are reacted prior to being placed in the waste/shipped.
14	107	Highly Reactive	Reaction will not occur – Ethers are solidified / immobilized prior to shipping. Free liquid content is limited to less than 1% of waste volume; water reactive substances are reacted prior to being placed in the waste/shipped. Lime in Portland cement is most common water reactive substance expected in the waste. Portland cement is used as an absorbent and solidification agent for the wastes.
15	107	Highly Reactive	Reaction will not occur – Salts are reacted during use and processing; Free liquid content is limited to less than 1% of waste volume; water reactive substances are reacted prior to being placed in the waste/shipped. Lime in Portland cement is most common water reactive substance expected in the waste. Portland cement is used as an absorbent and solidification agent for the wastes.

Combination of Reactivity Groups		Reaction Result (A x B)	Explanation of Potential Incompatibility
Group A	Group B		
16	104	Heat Generation	Reaction will not occur – Aromatic hydrocarbons are solidified/immobilized prior to shipping. Oxidizing agents are reacted prior to being placed in the waste/shipped.
16	104	Fire	Reaction will not occur – Aromatic hydrocarbons are solidified/immobilized prior to shipping. Oxidizing agents are reacted prior to being placed in the waste/shipped.
16	107	Highly Reactive	Reaction will not occur – Aromatic hydrocarbons are solidified/immobilized prior to shipping. Free liquid content is limited to less than 1% of waste volume; water reactive substances are reacted prior to being placed in the waste/shipped. Lime in Portland cement is most common water reactive substance expected in the waste. Portland cement is used as an absorbent and solidification agent for the wastes.
17	21	Heat Generation	Reaction will not occur – Halogenated organics are solidified/immobilized prior to shipping
17	21	Explosion	Reaction will not occur – Halogenated organics are solidified/immobilized prior to shipping
17	22	Heat Generation	Reaction will not occur – Halogenated organics are solidified/immobilized prior to shipping
17	22	Explosion	Reaction will not occur – Halogenated organics are solidified/immobilized prior to shipping
17	23	Heat Generation	Reaction will not occur – Halogenated organics are solidified/immobilized prior to shipping
17	23	Fire	Reaction will not occur – Halogenated organics are solidified/immobilized prior to shipping
17	104	Heat Generation	Reaction will not occur – Halogenated organics are solidified/immobilized prior to shipping; oxidizing agents are reacted prior to being placed in the waste/shipped.
17	104	Toxic Gas Generation	Reaction will not occur – Halogenated organics are solidified/immobilized prior to shipping; oxidizing agents are reacted prior to being placed in the waste/shipped.
17	105	Heat Generation	Reaction will not occur – Halogenated organics are solidified/immobilized prior to shipping; reducing agents are reacted prior to being placed in the waste/shipped.
17	105	Explosion	Reaction will not occur – Halogenated organics are solidified/immobilized prior to shipping; reducing agents are reacted prior to being placed in the waste/shipped.

6.1-35

Combination of Reactivity Groups		Reaction Result (A x B)	Explanation of Potential Incompatibility
Group A	Group B		
17	107	Highly Reactive	Reaction will not occur – Halogenated organics are solidified/immobilized prior to shipping; free liquid content is limited to less than 1% of waste volume; water reactive substances are reacted prior to being placed in the waste/shipped. Lime in Portland cement is most common water reactive substance expected in the waste. Portland cement is used as an absorbent and solidification agent for the wastes.
19	21	Flammable Gas Generation	Reaction will not occur – Ketones are solidified/immobilized prior to shipping
19	21	Heat Generation	Reaction will not occur – Ketones are solidified/immobilized prior to shipping
19	104	Heat Generation	Reaction will not occur –Ketones are solidified/immobilized prior to shipping; oxidizing agents are reacted prior to being placed in the waste/shipped.
19	104	Fire	Reaction will not occur –Ketones are solidified/immobilized prior to shipping; oxidizing agents are reacted prior to being placed in the waste/shipped.
19	105	Flammable Gas Generation	Reaction will not occur –Ketones are solidified/immobilized prior to shipping; reducing agents are reacted prior to being placed in the waste/shipped.
19	105	Heat Generation	Reaction will not occur –Ketones are solidified/immobilized prior to shipping; reducing agents are reacted prior to being placed in the waste/shipped.
19	107	Highly Reactive	Reaction will not occur – Ketones are solidified/immobilized prior to shipping; free liquid content is limited to less than 1% of waste volume; water reactive substances are reacted prior to being placed in the waste/shipped. Lime in Portland cement is most common water reactive substance expected in the waste. Portland cement is used as an absorbent and solidification agent for the wastes.
21	31	Flammable Gas Generation	Reaction will not occur – Phenols and Creosols are solidified/immobilized prior to shipping; metals are typically in oxide form
21	31	Heat Generation	Reaction will not occur – Phenols and Creosols are solidified/immobilized prior to shipping; metals are typically in oxide form

Combination of Reactivity Groups		Reaction Result (A x B)	Explanation of Potential Incompatibility
Group A	Group B		
21	32	Heat Generation	Reaction will not occur – Organophosphates are solidified/immobilized prior to shipping; metals are typically in oxide form
21	101	Heat Generation	Reaction will not occur – Combustible materials are dry; free liquid content is limited to less than 1% of waste volume; metals are typically in oxide form
21	101	Innocuous and Non-Flammable Gas Generation	Reaction will not occur – Combustible materials are dry; free liquid content is limited to less than 1% of waste volume; metals are typically in oxide form
21	101	Fire	Reaction will not occur – Combustible materials are dry; free liquid content is limited to less than 1% of waste volume; metals are typically in oxide form
21	103	Violent Polymerization	Reaction will not occur – Polymerizable compounds are reacted or immobilized/solidified prior to shipping; metals are typically in oxide form
21	103	Heat Generation	Reaction will not occur – Polymerizable compounds are reacted or immobilized/solidified prior to shipping; metals are typically in oxide form
21	104	Heat Generation	Reaction will not occur –Oxidizing agents are reacted prior to being placed in the waste/shipped; metals are typically in oxide form
21	104	Fire	Reaction will not occur –Oxidizing agents are reacted prior to being placed in the waste/shipped; metals are typically in oxide form
21	104	Explosion	Reaction will not occur –Oxidizing agents are reacted prior to being placed in the waste/shipped; metals are typically in oxide form
21	106	Flammable Gas Generation	Reaction will not occur – Free liquids are limited to less than 1% of waste volume; metals are typically in oxide form.
21	106	Heat Generation	Reaction will not occur – Free liquids are limited to less than 1% of waste volume; metals are typically in oxide form.
21	107	Highly Reactive	Reaction will not occur – Metals are typically in oxide form; water reactive substances are reacted prior to being placed in the waste/shipped. Lime in Portland cement is most common water reactive substance expected in the waste. Portland cement is used as an absorbent and solidification agent for the wastes.
22	28	Heat Generation	Reaction will not occur – Unsaturated aliphatic hydrocarbons are solidified/immobilized prior to shipping
22	28	Explosion	Reaction will not occur – Unsaturated aliphatic hydrocarbons are solidified/immobilized prior to shipping

Combination of Reactivity Groups		Reaction Result (A x B)	Explanation of Potential Incompatibility
Group A	Group B		
22	103	Violent Polymerization	Reaction will not occur – Polymerizable compounds are reacted or immobilized/solidified prior to shipping
22	103	Heat Generation	Reaction will not occur – Polymerizable compounds are reacted or immobilized/solidified prior to shipping
22	104	Heat Generation	Reaction will not occur – Oxidizing agents are reacted prior to being placed in the waste/shipped
22	104	Fire	Reaction will not occur – Oxidizing agents are reacted prior to being placed in the waste/shipped
22	104	Explosion	Reaction will not occur – Oxidizing agents are reacted prior to being placed in the waste/shipped
22	106	Flammable Gas Generation	Reaction will not occur – Free liquids are limited to less than 1% of waste volume; water reactive metals are reacted prior to shipping
22	106	Heat Generation	Reaction will not occur – Free liquids are limited to less than 1% of waste volume; water reactive metals are reacted prior to shipping
22	107	Highly Reactive	Reaction will not occur –Water reactive substances are reacted prior to being placed in the waste/shipped. Lime in Portland cement is most common water reactive substance expected in the waste. Portland cement is used as an absorbent and solidification agent for the wastes.
23	103	Violent Polymerization	Reaction will not occur – Polymerizable compounds are reacted or immobilized/solidified prior to shipping
23	103	Heat Generation	Reaction will not occur – Polymerizable compounds are reacted or immobilized/solidified prior to shipping
23	104	Heat Generation	Reaction will not occur – Oxidizing agents are reacted prior to being placed in the waste/shipped
23	104	Fire	Reaction will not occur – Oxidizing agents are reacted prior to being placed in the waste/shipped
23	107	Highly Reactive	Reaction will not occur –Water reactive substances are reacted prior to being placed in the waste/shipped. Lime in Portland cement is most common water reactive substance expected in the waste. Portland cement is used as an absorbent and solidification agent for the wastes.
24	103	Violent Polymerization	Reaction will not occur – Polymerizable compounds are reacted or immobilized/solidified prior to shipping
24	103	Heat Generation	Reaction will not occur – Polymerizable compounds are reacted or immobilized/solidified prior to shipping
24	106	Solubilization of Toxic Substances	Reaction will not occur – Free liquid content is limited to less than 1% of waste volume; Additionally, any solubilization of toxic substances will not affect transportation of wastes.

Combination of Reactivity Groups		Reaction Result (A x B)	Explanation of Potential Incompatibility
Group A	Group B		
24	107	Highly Reactive	Reaction will not occur – Water reactive substances are reacted prior to being placed in the waste/shipped. Lime in Portland cement is most common water reactive substance expected in the waste. Portland cement is used as an absorbent and solidification agent for the wastes.
28	104	Heat Generation	Reaction will not occur – Unsaturated aliphatic hydrocarbons are immobilized/solidified prior to shipping; oxidizing agents are reacted prior to being placed in the waste/shipped
28	104	Fire	Reaction will not occur – Unsaturated aliphatic hydrocarbons are immobilized/solidified prior to shipping; oxidizing agents are reacted prior to being placed in the waste/shipped
28	107	Highly Reactive	Reaction will not occur – Unsaturated aliphatic hydrocarbons are immobilized/solidified prior to shipping; free liquid content is limited to less than 1% of waste volume; water reactive substances are reacted prior to being placed in the waste/shipped. Lime in Portland cement is most common water reactive substance expected in the waste. Portland cement is used as an absorbent and solidification agent for the wastes.
29	104	Heat Generation	Reaction will not occur – Saturated aliphatic hydrocarbons are immobilized/solidified prior to shipping; oxidizing agents are reacted prior to being placed in the waste/shipped
29	104	Fire	Reaction will not occur – Saturated aliphatic hydrocarbons are immobilized/solidified prior to shipping; oxidizing agents are reacted prior to being placed in the waste/shipped
29	107	Highly Reactive	Reaction will not occur – Saturated aliphatic hydrocarbons are immobilized/solidified prior to shipping; free liquid content is limited to less than 1% of waste volume; water reactive substances are reacted prior to being placed in the waste/shipped. Lime in Portland cement is most common water reactive substance expected in the waste. Portland cement is used as an absorbent and solidification agent for the wastes.

Combination of Reactivity Groups		Reaction Result (A x B)	Explanation of Potential Incompatibility
Group A	Group B		
31	103	Violent Polymerization	Reaction will not occur – Polymerizable compounds are reacted or immobilized/solidified prior to shipping; phenols and creosols are immobilized/solidified prior to shipping
31	103	Heat Generation	Reaction will not occur – Polymerizable compounds are reacted or immobilized/solidified prior to shipping; phenols and creosols are immobilized/solidified prior to shipping
31	104	Heat Generation	Reaction will not occur – Phenols and creosols are immobilized/solidified prior to shipping; oxidizing agents are reacted prior to being placed in the waste/shipped
31	104	Fire	Reaction will not occur – Phenols and creosols are immobilized/solidified prior to shipping; oxidizing agents are reacted prior to being placed in the waste/shipped
31	105	Flammable Gas Generation	Reaction will not occur – Phenols and creosols are immobilized/solidified prior to shipping; reducing agents are reacted prior to being placed in the waste/shipped
31	105	Heat Generation	Reaction will not occur – Phenols and creosols are immobilized/solidified prior to shipping; reducing agents are reacted prior to being placed in the waste/shipped
31	107	Highly Reactive	Reaction will not occur – Phenols and creosols are immobilized/solidified prior to shipping; free liquid content is limited to less than 1% of waste volume; water reactive substances are reacted prior to being placed in the waste/shipped. Lime in Portland cement is most common water reactive substance expected in the waste. Portland cement is used as an absorbent and solidification agent for the wastes.
32	104	Heat Generation	Reaction will not occur – Organophosphates are immobilized/solidified prior to shipping; oxidizing agents are reacted prior to being placed in the waste/shipped
32	104	Fire	Reaction will not occur – Organophosphates are immobilized/solidified prior to shipping; oxidizing agents are reacted prior to being placed in the waste/shipped
32	104	Toxic Gas Generation	Reaction will not occur – Organophosphates are immobilized/solidified prior to shipping; oxidizing agents are reacted prior to being placed in the waste/shipped

Combination of Reactivity Groups		Reaction Result (A x B)	Explanation of Potential Incompatibility
Group A	Group B		
32	105	Toxic Gas Generation	Reaction will not occur – Organophosphates are immobilized/solidified prior to shipping; reducing agents are reacted prior to being placed in the waste/shipped
32	105	Flammable Gas Generation	Reaction will not occur – Organophosphates are immobilized/solidified prior to shipping; reducing agents are reacted prior to being placed in the waste/shipped
32	105	Heat Generation	Reaction will not occur – Organophosphates are immobilized/solidified prior to shipping; reducing agents are reacted prior to being placed in the waste/shipped
32	107	Highly Reactive	Reaction will not occur – Organophosphates are immobilized/solidified prior to shipping; free liquid content is limited to less than 1% of waste volume; water reactive substances are reacted prior to being placed in the waste/shipped. Lime in Portland cement is most common water reactive substance expected in the waste. Portland cement is used as an absorbent and solidification agent for the wastes.
101	104	Heat Generation	Reaction will not occur – Combustible materials are dry; oxidizing agents are reacted prior to being placed in the waste/shipped
101	104	Fire	Reaction will not occur – Combustible materials are dry; oxidizing agents are reacted prior to being placed in the waste/shipped
101	104	Innocuous and Non-Flammable Gas Generation	Reaction will not occur – Combustible materials are dry; oxidizing agents are reacted prior to being placed in the waste/shipped
101	105	Flammable Gas Generation	Reaction will not occur – Combustible materials are dry; reducing agents are reacted prior to being placed in the waste/shipped
101	105	Heat Generation	Reaction will not occur – Combustible materials are dry; reducing agents are reacted prior to being placed in the waste/shipped
101	107	Highly Reactive	Reaction will not occur – Combustible materials are dry; free liquid content is limited to less than 1% of waste volume; water reactive substances are reacted prior to being placed in the waste/shipped. Lime in Portland cement is most common water reactive substance expected in the waste. Portland cement is used as an absorbent and solidification agent for the wastes.

Combination of Reactivity Groups		Reaction Result (A x B)	Explanation of Potential Incompatibility
Group A	Group B		
103	104	Heat Generation	Reaction will not occur – Polymerizable compounds are reacted or immobilized/solidified prior to shipping; oxidizing agents are reacted prior to being placed in the waste/shipped
103	104	Fire	Reaction will not occur – Polymerizable compounds are reacted or immobilized/solidified prior to shipping; oxidizing agents are reacted prior to being placed in the waste/shipped
103	104	Toxic Gas Generation	Reaction will not occur – Polymerizable compounds are reacted or immobilized/solidified prior to shipping; oxidizing agents are reacted prior to being placed in the waste/shipped
103	105	Heat Generation	Reaction will not occur – Polymerizable compounds are reacted or immobilized/solidified prior to shipping; reducing agents are reacted prior to being placed in the waste/shipped
103	105	Violent Polymerization	Reaction will not occur – Polymerizable compounds are reacted or immobilized/solidified prior to shipping; reducing agents are reacted prior to being placed in the waste/shipped
103	105	Flammable Gas Generation	Reaction will not occur – Polymerizable compounds are reacted or immobilized/solidified prior to shipping; reducing agents are reacted prior to being placed in the waste/shipped
103	107	Highly Reactive	Reaction will not occur – Polymerizable compounds are reacted or immobilized/solidified prior to shipping; free liquid content is limited to less than 1% of waste volume; water reactive substances are reacted prior to being placed in the waste/shipped. Lime in Portland cement is most common water reactive substance expected in the waste. Portland cement is used as an absorbent and solidification agent for the wastes.
104	105	Heat Generation	Reaction will not occur – Oxidizing agents are reacted prior to being placed in the waste/shipped; reducing agents are reacted prior to being placed in the waste/shipped
104	105	Fire	Reaction will not occur – Oxidizing agents are reacted prior to being placed in the waste/shipped; reducing agents are reacted prior to being placed in the waste/shipped
104	105	Explosion	Reaction will not occur – Oxidizing agents are reacted prior to being placed in the waste/shipped; reducing agents are reacted prior to being placed in the waste/shipped

Combination of Reactivity Groups		Reaction Result (A x B)	Explanation of Potential Incompatibility
Group A	Group B		
104	107	Highly Reactive	Reaction will not occur – Oxidizing agents are reacted prior to being placed in the waste/shipped; free liquid content is limited to less than 1% of waste volume; water reactive substances are reacted prior to being placed in the waste/shipped. Lime in Portland cement is most common water reactive substance expected in the waste. Portland cement is used as an absorbent and solidification agent for the wastes.
105	106	Flammable Gas Generation	Reaction will not occur – Reducing agents are reacted prior to being placed in the waste/shipped; free liquid content is limited to less than 1% of waste volume
105	106	Toxic Gas Generation	Reaction will not occur – Reducing agents are reacted prior to being placed in the waste/shipped; free liquid content is limited to less than 1% of waste volume
105	107	Highly Reactive	Reaction will not occur – Reducing agents are reacted prior to being placed in the waste/shipped; free liquid content is limited to less than 1% of waste volume; water reactive substances are reacted prior to being placed in the waste/shipped. Lime in Portland cement is most common water reactive substance expected in the waste. Portland cement is used as an absorbent and solidification agent for the wastes.
106	107	Highly Reactive	Reaction will not occur – Free liquid content is limited to less than 1% of waste volume; water reactive substances are reacted prior to being placed in the waste/shipped. Lime in Portland cement is most common water reactive substance expected in the waste. Portland cement is used as an absorbent and solidification agent for the wastes.

This page intentionally left blank.

APPENDIX 6.2

**FREE HALIDES IN THE CH-TRU WASTE PAYLOAD—SOURCE TERM
AND RELEASE RATE ESTIMATES**

This page intentionally left blank.

6.2   Free Halides in the CH-TRU Waste Payload-Source Term and Release Rate Estimates

6.2.1   Summary

An evaluation of source terms for halides has demonstrated that very small amounts of halides are available for chemical reaction to cause stress corrosion cracking (SCC) of the Inner Containment Vessel (ICV) of TRUPACT-II or HalfPACT. This is substantiated with sampling data from actual waste drums and radiolysis experiments conducted on TRU waste materials. Extensive sampling programs of both retrievably stored and newly generated waste did not detect hydrogen chloride (HCl) gas in the headspace of any of the payload containers. Experiments designed to simulate alpha and gamma radiolysis of actual bagging and TRU waste materials from generator sites demonstrated HCl gas generation to be very low.

These observations support the conclusions that alpha radiolysis of actual waste produces little or no HCl gas. Any small quantities of HCl gas produced are likely either to dissolve readily in any absorbed water or moisture present in the waste, or to react with the waste contents or payload containers. This will retard the release of HCl gas from the payload containers, precluding the possibility of stress corrosion cracking of the ICV.

6.2.2   Introduction

The production of free halides from radiolysis of the payload materials can potentially cause SCC of the package. The primary material of construction used for the ICV and the Outer Containment Vessel (OCV) of the package is Type 304 stainless steel (austenitic). This material may be susceptible in the sensitized condition to SCC in the presence of chloride contamination. However, Tokiwai et al.[1], have shown 304 stainless steel to be resistant to SCC at temperatures below 55°C, even for heavily sensitized material at stresses near yield, for maximum allowable levels of NaCl concentration and relative humidities. Normal operating temperatures of the cavity headspace or ICV walls are not expected to exceed 55EC. The following discussion will provide an analysis of the source terms for the halides and their potential to reach the ICV.

6.2.3   Source Terms for Chlorides and Fluorides in Waste Material

The contaminants of concern are hydrogen chloride (HCl) and hydrogen fluoride (HF), which could originate from the radiolysis of polyvinyl chloride or halogenated organics.

6.2.3.1   Potential for Fluoride Production in Waste

Compounds containing fluorides considered as potential sources for HF gas have not been identified in the CH-TRU materials in significant amounts. Only Teflon, inorganic fluoride salts and a trace amount of Freon-113 occur in the waste, and these do not produce HF from radiolysis (Appendix 3.1 of the CH-TRU Payload Appendices).

---

[1] Tokiwai, M., H. Kimiura, and H. Kusangi, 1985, Corrosion Science, Vol. 25, No. 89, pp. 837-844.

6.2.3.2 Potential for Chloride Production in Waste

The potential for chloride production in the payload materials comes primarily from radiolysis of the chlorinated compounds. Volatile organic compounds (VOCs) capable of generating HCl are not present in sufficient amounts in the waste to be of concern for SCC. Appendix 6.4 of the CH-TRU Payload Appendices discusses the source terms and release rates of VOCs. The only other compound present in the waste with a potential for HCl production is polyvinyl chloride (PVC).

Experimental evidence has shown average G(HCl) (moles of HCl in the gas or liquid state released per 100 eV of energy absorbed) values for radiolysis of commercial grades of plasticized stabilized PVC to be quite small (see Appendix 3.2 of the CH-TRU Payload Appendices). Table 6.2-1 summarizes the available data on generation of HCl from radiolysis of PVC. Three independent experiments of alpha radiolysis on actual waste and packaging material from three U.S. DOE sites revealed very little or no HCl. Contact handled TRU waste to be shipped in the TRUPACT-II or HalfPACT is contaminated predominantly with alpha-emitting radionuclides. For the two gamma radiolysis experiments cited in Table 6.2-1 that measured G(HCl), the quantitative measurement was made by titration of acidity in samples with a weak base. No direct evidence of HCl gas was reported in these experiments other than a qualitative indication of Cl^-.[2]

In conclusion, radiolytic activity within the drums of CH-TRU waste will not result in the generation of any substantial amounts of HCl gas. The source term for HCl gas itself (without any consideration of transport to the ICV) is expected to be insignificant in payload containers transported in the TRUPACT-II or HalfPACT.

6.2.3.3 Gas Sampling of CH-TRU Waste Drums

Sampling programs at Idaho National Engineering Laboratory (INEL)[3] and Rocky Flats Plant[4] did not detect HF or HCl gas in the head space of any of the 249 drums of retrievably stored and newly generated TRU waste that were sampled. In addition to drum headspace sampling, twenty-two drums of retrievably stored and newly generated waste were sampled for gases within successive layers of confinement up to the innermost layer with the waste. In all cases, HF or HCl were never detected in any layers of confinement.

---

[2] Kazanjian, A.R, and A.K. Brown, December 1969, "Radiation Chemistry of Materials Used in Plutonium Processing," The Dow Chemical Company, Rocky Flats Division, RFP-1376.

[3] Clements, T.L., Jr., and D.E. Kudera, September 1985, "TRU Waste Sampling Program: Volume I, Waste Characterization," EGG-WM-6503, EG&G Idaho, Inc., Idaho Falls, Idaho.

[4] Roggenthen, D.K., T.L. McFeeters, and R.A. Nieweg, March 1989, "Waste Drum Gas Generation Sampling Program at Rocky Flats During FY 1988," RFP-4311.

Table 6.2-1 — G(HCl) Values for Plasticized Polyvinyl Chloride Materials in CH-TRU Waste

	Irradiation	G(HCl)
Average G(HCl) for Plasticized PVC	α,γ	0.64[a]
Values for Materials used at U.S. DOE site		
PVC bagout bag (Los Alamos National Laboratory)[b]	α	~0[c]
Nine samples of PVC bag material (Rocky Flats Plant)[d]	γ	0.21[e]
Samples of PVC bagout material (Rocky Flats Plant)[f]	α	0
Samples of PVC gloves (Los Alamos National Laboratory)[g]	γ	0
Samples of PVC bags (Savannah River Plant)[h]	γ	<0.01[i]

[a]   Average of 27 literature values for plasticized PVC (Appendix 3.2 of the CH-TRU Payload Appendices).

[b]   Zerwekh, A., 1979, "Gas Generation from Radiolytic Attack of TRU- Contaminated Hydrogeneous Waste," Los Alamos National Laboratory, LA- 7674-MS, June 1979.

[c]   Mass spectrometric analysis of gases did not detect any Cl⁻ or HCl. Wet chemistry analysis of material inside glass reaction vessel yielded 0.06% Cl⁻.

[d]   Kazanjian, A.R, and A.K. Brown, "Radiation Chemistry of Materials Used in Plutonium Processing," The Dow Chemical Company, Rocky Flats Division, RFP-1376, December 1969.

[e]   Tubes of irradiated PVC were opened under water, shaken, and titrated with NaOH. The presence of chlorides in solution was identified qualitatively. Only acid content (not Cl⁻) was measured quantitatively. Acid concentration in water could be due to CO_2 dissolved from atmosphere.

[f]   Kazanjian, A. R, "Radiolytic Gas Generation in Plutonium Contaminated Waste Materials," Rockwell International, Rocky Flats Plant, RFP-2469, October 1976.

[g]   Kosiewicz, S.T., "Gas Generation from Organic Transuranic Wastes. I. Alpha Radiolysis at Atmospheric Pressure," Nuclear Technology 54, pp. 92-99, 1981.

[h]   Hobbs, David, Personal Communication, Savannah River Plant, Feb. 1989.

[i]   Personal communication for ongoing experiments.

6.2.4   Mechanisms for Retardation of Chlorides Inside Payload Containers

Production of chlorides by radiolysis of waste materials in payload containers does not necessarily imply the presence of a gaseous phase. Some of the radiolysis experiments did not observe HCl gas in the void space of the experimental apparatus but did measure chlorides after washing of the interior of the reaction vessel.[5] This suggests the existence of mechanisms that can retard the release of gaseous HCl.

6.2.4.1   Solubility of HCl in Water

The presence of any free HCl that is produced in a payload container will be controlled in the headspace by the high solubility of HCl gas in water. Transfer of HCl gas to the aqueous phase occurs with very little resistance in the liquid phase and with very little back pressure of the gas.[6] For small quantities of HCl gas produced in the payload containers, the moisture content of the waste materials would probably be sufficient to absorb the gas generated.

---

[5] Zerwekh, A., 1979, "Gas Generation from Radiolytic Attack of TRU- Contaminated Hydrogeneous Waste," Los Alamos National Laboratory, LA- 7674-MS, June 1979.

[6] Treybal, R.E., 1980, Mass Transfer Operations, McGraw-Hill Book Company, New York, New York.

The partial pressures of gaseous HCl over aqueous solutions of HCl are extremely small even at appreciable concentrations of HCl, due to its high solubility.[6] Table 6.2-2 provides the partial pressure of HCl above HCl aqueous solutions over a wide range of temperatures.[7] The partial pressures reported in the normal operating ranges of the TRUPACT-II or HalfPACT (Table 6.2-2) would minimize the possibility of HCl being present as a gaseous phase.

Waste types to be transported in payload containers contain varying amounts of adsorbed/absorbed water as a by-product of processes (without the presence of free liquids) in addition to water vapor from atmospheric humidity inside the layers of confinement. Although water vapor was not quantitatively measured in the headspaces of the drums examined at RFP as part of the TRU waste sampling program,[3] water was noted in all gas samples.[8] Hence it is probable that any HCl produced would dissolve within the drums. It should be noted that anhydrous HCl is noncorrosive to 304 stainless steel.[9] Therefore, sufficient moisture exists in the form of adsorbed/absorbed water in layers of containment in payload containers to depress the vapor pressure of any HCl that may be present.

6.2.4.2 Reactivity of Waste Materials and Internal Surfaces of the Payload Containers

For any small quantities of HCl gas that could be present in the payload containers, it is highly unlikely that any chlorides would reach the ICV. The payload containers in which the waste is packaged are either carbon or galvanized steel. HCl is much more reactive with these materials than the 304 SS. HCl will also have an affinity for some contents of the waste. An example of this is hydrolization of cellulose, which is present in substantial amounts in the waste.[10] The small amounts of HCl produced are expected to be consumed in reactions with these materials and therefore be unavailable for transport into the ICV.

6.2.5 Conclusion

In assessing the potential for stress corrosion cracking, it is apparent that the nature of the waste and the conditions under which the waste will be transported, should preclude the possibility of

---

[7] Perry, C.H., and D. Green, Eds., 1984, Chemical Engineers Handbook, McGraw-Hill Book Company, New York.

[8] Simmons, Bill, Rocky Flats Plant Personal Communications, 1988.

[9] Kirk, R.E., and D.F. Othmer, Eds., 1966, Encyclopedia of Chemical Technology, Vol. 11, John Wiley and Sons, New York.

[10] Young, R. A., and R. M. Rowell, Eds., 1986, Cellulose: Structure Modification, and Hydrolysis, John Wiley and Sons, New York.

producing significant quantities of free HCl gas in the payload containers. Alpha radiolysis of PVC does not produce appreciable amounts of HCl gas, and any small quantities of the gas generated are likely to be retained in the payload containers, thereby limiting transport to the ICV cavity.

Table 6.2-2 — Partial Pressures of HCl Over Aqueous Solutions of HCl mmHg°C[a,b]

%HCL	A	B	0°	5°	10°	15°	20°	25°	30°	35°	40°	45°	50°	60°	70°	80°
2	11.8037	4736	----	----	0.0000117	0.000023	0.000044	0.000084	0.000151	0.000275	0.00047	0.00083	0.00140	0.00380	0.0100	0
4	11.6400	4471	0.000018	0.000036	0.000069	0.000131	0.00024	0.00044	0.00077	0.00134	0.0023	0.00385	0.0064	0.0165	0.0405	0
6	11.2144	4202	0.000066	0.000125	0.000234	0.000425	0.00076	0.00131	0.00225	0.0038	0.0062	0.0102	0.163	0.040	0.094	0
8	11.0406	4042	0.000118	0.000323	0.000583	0.00104	0.00178	0.0031	0.00515	0.0085	0.0136	0.022	0.0344	0.081	0.183	0
10	10.9311	3908	0.00042	0.00075	0.00134	0.00232	0.00395	0.0067	0.0111	0.0178	0.0282	0.045	0.069	0.157	0.35	0
12	10.7900	3765	0.00099	0.00175	0.00305	0.0052	0.0088	0.0145	0.0234	0.037	0.058	0.091	0.136	0.305	0.66	1
14	10.6954	3636	0.0024	0.00415	0.0071	0.0118	0.0196	0.0316	0.050	0.078	0.121	0.185	0.275	0.60	1.25	2
16	10.6261	3516	0.0056	0.0095	0.016	0.0265	0.0428	0.0685	0.106	0.163	0.247	0.375	0.55	1.17	2.40	4
18	10.4957	3376	0.0135	0.0225	0.037	0.060	0.095	0.148	0.228	0.345	0.515	0.77	1.11	2.3	4.55	8
20	10.3833	3245	0.0316	0.052	0.084	0.132	0.205	0.32	0.48	0.72	1.06	1.55	2.21	4.4	8.5	15
22	10.3172	3125	0.0734	0.119	0.187	0.294	0.45	0.68	1.02	1.50	2.18	3.14	4.42	8.6	16.3	29
24	10.2185	2995	0.175	0.277	0.43	0.66	1.00	1.49	2.17	3.14	4.5	6.4	8.9	16.9	31.0	54
26	10.1303	2870	0.41	0.64	0.98	1.47	2.17	3.20	4.56	6.50	9.2	12.7	17.5	32.5	58.5	100
28	10.0115	2732	1.0	1.52	2.27	3.36	4.90	7.05	9.90	13.8	19.1	26.4	35.7	64	112	188
30	9.8763	2593	2.4	3.57	5.23	7.60	10.6	15.1	21.0	28.6	39.4	53	71	124	208	340
32	9.7523	2457	5.7	8.3	11.8	16.8	23.5	32.5	44.5	60.0	81	107	141	238	390	623
34	9.6061	2316	13.1	18.8	26.4	36.8	50.5	68.5	92	122	161	211	273	450	720	
36	9.5262	2229	29.0	41.0	56.4	78	105.5	142	188	246	322	416	535	860		
38	9.4670	2094	63.0	87.0	117	158	210	277	360	465	598	758	955			
40	9.2156	1939	130	176	233	307	399	515	627	830						
42	8.9925	1800	253	332	430	560	709	900								
44	8.8621	1681	510	655	840											
46	----	----	940													

[a]Perry, C.H., and D. Green, Eds., 1984 Chemical Engineers Handbook, McGraw Hill Book Company, New York, New York.
[b]Log$_{10}$pmm = A - B/T, which, however, agrees only approximately with the table. The table is more nearly correct.

APPENDIX 6.3

PAYLOAD COMPATIBILITY WITH BUTYL RUBBER O-RING SEALS

This page intentionally left blank.

6.3 Payload Compatibility with Butyl Rubber O-Ring Seals

6.3.1 Summary

Payload materials and chemicals in the TRUPACT-II or HalfPACT do not present an incompatibility concern with respect to the butyl rubber O-rings. Chemicals that are of concern are not present in the waste in any significant amounts. Strong oxidizing acids are neutralized or basified prior to being generated as contact-handled transuranic (CH-TRU) waste. Organic solvents of concern that are present in residual amounts in the payload containers are usually bound with the waste materials.

6.3.2 Introduction

This appendix evaluates the compatibility of the payload materials with the butyl rubber O-rings of the package. Chemicals that are reported as potentially incompatible with the butyl rubber O-rings (for liquid immersion or in saturated vapors) include the following:

- Concentrated oxidizing acids, (e.g., nitric acid)

- Aromatic hydrocarbons, (e.g., xylene and toluene)

- Halogenated organic solvents, (e.g., 1,1,2-trichloro-1,2,2-trifluoroethane [Freon-113], methylene chloride, carbon tetrachloride, and 1,1,1-trichloroethane).

6.3.3 Restrictions on Acids

The payload materials do not contain any free liquid acids, because the waste is in a solid form or is solidified. Acidic components from process operations are neutralized or basified before being generated as CH-TRU waste. All aqueous liquids are neutralized or basified to a pH range of 5.5 to 12 prior to solidification. Strong (concentrated) acids are prohibited through restrictions on corrosives.

6.3.4 Restrictions on Aromatic Hydrocarbons

The aromatic hydrocarbons (e.g., xylene) are also flammable and are generally present in concentrations less than or equal to 500 parts per million (ppm) in the headspace of the payload containers. As an upper limit, they are restricted to the mixture lower explosive limit (MLEL) for the total flammable (gas/VOC) mixture as described in Section 5.2 of the Contact-Handled Transuranic Waste Authorized Methods for Payload Control (CH-TRAMPAC). While this is an upper limit, process operations limit the presence and release of these hydrocarbons:

- Very few waste streams use flammable organic solvents at the sites, limiting the number of content codes that could contain these compounds.

- Permeabilities of the aromatic hydrocarbons through the plastic bags used as confinement layers are extremely high.[1] Residual amounts of these compounds should escape from the bags before the waste is emplaced in the payload containers.

- Analysis of solidified aqueous inorganic materials with ppm levels of aromatic hydrocarbons in the waste (Appendix 6.4 of the CH-TRU Payload Appendices) did not have any detectable levels in the headspace above the waste.

This class of compounds is therefore not an incompatibility concern for the payload materials and the package.

6.3.5 Restrictions on Halogenated Organic Solvents

Some of the organic solvents that are incompatible with butyl rubber are used in operations at the sites. Appendix 6.4 of the CH-TRU Payload Appendices evaluates the sources and release of these from the payload materials. Real waste data shows these solvents to be present in extremely small amounts in the waste (Waste Types I, II and III). Any residual amounts of these solvents present will diffuse at very slow rates through the filters in the payload containers. As discussed in Appendix 6.4 of the CH-TRU Payload Appendices, Waste Type IV, which may contain higher levels of VOCs, can be shipped only under the test category.

The total accumulation of organic solvents in the package cavity during transportation is expected to be low (Appendix 6.4 of the CH-TRU Payload Appendices). At these low concentrations, even if the solvents interact with the butyl rubber O-rings, the only possible effect on the O-rings would be a negligible amount of swelling. This should not effect their sealing properties.

6.3.6 Conclusions

In summary, the payload materials in the TRUPACT-II or HalfPACT do not present an incompatibility concern with respect to the butyl rubber O-rings. Chemicals that are of concern are not present in the waste in any significant amounts. Residual amounts of any solvents present are not expected to accumulate above low ppm amounts in the package cavity. These low concentrations are not sufficient to degrade the material properties of the butyl rubber O-rings and affect the sealing properties.

---

[1] Brandrup, J., and Immergut, E. H., eds., "Permeability Coefficients and Transmission Rates," Polymer Handbook, (Interscience Publishers, New York, 1966).

APPENDIX 6.4

VOLATILE ORGANIC COMPOUNDS (VOC) IN THE CH-TRU PAYLOAD—SOURCE TERM AND RELEASE RATE ESTIMATES

This page intentionally left blank.

6.4   Volatile Organic Compounds (VOC) in the CH-TRU Waste Payload—Source Term and Release Rate Estimates

6.4.1   Summary

Volatile organic compounds (VOC) are used by some of the Department of Energy (DOE) sites as part of their process operations. The presence of VOCs in the Transuranic Package Transporter (TRUPACT)-II or HalfPACT payload, and their possible release into the package cavity during transport, are of concern for two reasons: (1) potential damage to the butyl rubber O-ring seals due to interaction with the VOC vapors that could diffuse from the payload containers, and (2) contribution to the overall pressure in the inner containment vessel (ICV) cavity by the vapor pressure that might be exerted by these chemicals. This appendix evaluates these concerns by an analysis of waste generation processes at the sites, current and past sampling programs, and the payload configuration.

Waste types that are known to contain VOCs in appreciable amounts (solidified organics) are restricted from being a part of the payload, unless it can be shown by actual testing that these content codes are safe for transport. The VOCs can be present in the other waste types only in trace amounts of less than one percent by weight. Solidified aqueous or homogeneous inorganic solids (Waste Type I) are processed through a vacuum filtration technique prior to solidification in a payload container. The vacuum filtration process greatly reduces the amount of trace VOCs in the waste. A similar reduction in VOCs also occurs for many inorganic and organic solid wastes (Waste Types II and III) generated in processes that are operated under slightly negative pressures. Examples are wastes generated from glovebox lines. Results from sampling programs support these conclusions.

Any residual amounts of VOCs within the waste in a payload container are impeded from being released during transport because of additional chemical and physical barriers. For waste types with bound water (i.e., solidified aqueous or homogeneous inorganic solids), the vapor pressure of the organics is reduced appreciably. Quantitative analysis, along with data from sampling programs, is presented in following sections.

Due to the multiple processes mentioned above, the source term for the VOCs is limited. VOCs present in residual amounts in the waste are not expected to diffuse from the headspace of the payload containers into the ICV in any significant quantities. Therefore, for the waste types expected to be transported in the TRUPACT-II and HalfPACT, the presence of VOCs in the package cavity should not be an issue of concern.

6.4.2   Introduction

VOCs include those organic compounds that exert appreciable vapor pressures at normal temperatures. Examples are halogenated compounds like Freon-113 and methylene chloride, and lower molecular weight alcohols (e.g., methanol). Some of these compounds are used at the DOE sites as industrial solvents and in decontamination operations. The potential of these volatiles being present in the payload is of concern for the following reasons:

- The vapor pressure exerted by the volatiles may contribute to the total pressure in the package cavity.

- Some of the organic solvents could potentially cause damage to the butyl rubber O-rings in the package during transport.

Hence, evaluation of the VOCs with respect to the payload and the package is necessary in order to ensure safe transport. The following sections discuss the source term of the VOCs in the payload and estimates of the release of these VOCs into the package cavity. Data from past and ongoing sampling programs at the DOE sites and laboratory experiments are analyzed to draw conclusions about these parameters. Wherever relevant, the different waste types expected to be part of the payload are discussed separately. (For a description of the classification of waste materials into waste types, see Appendix 2.1 of the CH-TRU Payload Appendices.

6.4.3 Source Term of VOCS in Different Waste Types

Solidified organics (Waste Type IV) are the only waste type with organic solvents as the main constituents of the waste. At the present time, payload containers belonging to this waste type cannot qualify for shipment unless it can be demonstrated by testing each payload container that it is safe for transport purposes. The test procedure to be followed is detailed in Section 5.2.5 of the Contact-Handled Transuranic Waste Authorized Methods for Payload Control (CH-TRAMPAC). For example, a container in this class would have to be tested under normal transport conditions to demonstrate that the maximum pressure limits imposed on the package are not exceeded. The same is true for the other transport parameters. Testing of a population of payload containers from a content code belonging to Waste Type IV could qualify the content code for shipment.

The remainder of the waste types have VOCs only in trace amounts of less than 1 percent by weight. While this is an upper bound on the amount of VOCs, waste generation procedures limit the VOC concentrations in these waste streams to much lower concentrations:

- Generation of solidified aqueous or homogeneous inorganic solids (Waste Type I) usually involves a vacuum filtration step (to dewater the waste stream), which reduces the amount of trace VOCs in the waste.

- Solid inorganic and organic wastes (Waste Types II and III) are generated from gloveboxes that are operated under negative pressures which acts to reduce the amounts of residual VOCs in the waste.

- Generator and storage sites will cite reportable quantities of some VOCs even if the material is suspected of being present in negligible quantities. This reporting is necessary to comply with Resource Conservation and Recovery Act (RCRA) regulations that a listed material is in a waste until proven to be absent (below testability limit).

6.4.4   Occurrence of VOCs in CH-TRU Waste from Sampling Programs

6.4.4.1   Evidence from Sampling Program at Rocky Flats Plant (RFP)

As part of a recent sampling program at Rocky Flats Plant (RFP),[1] 22 drums were sampled for headspace-gas composition and for organic compounds in the inner confinement layers, and where possible, in the innermost layer of confinement with the waste. Table 6.4-1 lists the results of this sampling along with relevant information on the individual drums. The results of this sampling program are discussed by waste type below.

6.4.4.1.1   Analyses of Solidified Aqueous Inorganic Solids - Waste Type I

Ten drums in this category were tested as part of the sampling program. The drums were analyzed for thirty-six (36) compounds that are listed in Table 6.4-2. The ten waste drums represent a cross section of drums generated at the Rocky Flats Plant and retrievably stored at INEL. Five of the ten drums were filled between 1983 and 1984, two were filled in 1973, and three were newly generated in 1988. Only two of the ten drums had carbon composite filter vents in the drum lids prior to opening. For five of the ten drums, the sludge also was analyzed for volatile organic compounds.

Table 6.4-1 — Summary of Rocky Flats Plant Sampling Program

Drum Number	Waste Type	Date Drum Filled	Gas Sample Analysis[a,b] (Headspace) (Vol %)			
			CCl_4	TRIC	FREON	CH_2Cl_2
62542	I	6-21-88				
59728	I	6-20-88				
62815	I	7-10-88				
7411-2808	I	4-9-73				
7411-2578	I	2-9-73				
7412-03850	I	8-2-84				
7412-02917	I	9-7-83				
7412-03492	I	3-9-84				
41450	III	6-7-88				
58642	III	6-7-88				
74402387	III	1-22-73				
240658	II	6-22-83				
74316881	IV	4-3-84	3.9		0.3	
74317069	IV	12-5-84	1.5		0.8	
741204577	I	3-26-85				

---

[1] Roggenthen, D.K., T.C. McFeeters, and R.G. Nieweg, "Waste Drum Gas Generation Sampling Program at Rocky Flats During FY 1988," RFP 4311, March 1989.

Table 6.4-1 — Summary of Rocky Flats Plant Sampling Program (Concluded)

Drum Number	Waste Type	Date Drum Filled	Gas Sample Analysis[a,b] (Headspace) (Vol %)			
			CCl_4	TRIC	FREON	CH_2Cl_2
74703446	I	1-7-85				
74316930	IV	5-25-84				
2500484	IV	4-17-85	3.5	0.8		0.8
002800658	II	9-28-82		0.4		
242533	II	2-21-84		0.1		
234906	II	2-21-84				
3201073	II	12-5-83				

[a] $CC1_4$ = Carbon tetrachloride
   TRIC   = 1,1,1-Trichloroethane
   FREON = 1,1,2-Trichloro-1,2,2-trifluoroethane
   CH_2C1_2 = Methylene chloride (dichlormethane)
[b] Detection limit: 500 ppm for all gases.

Table 6.4-2 — Organic Compounds Sampled for in Rocky Flats Plant Program

Chloromethane
Bromomethane
Vinyl chloride
Chloroethane
Methylene chloride
Acetone
Carbon disulfide
1,1-Dichloroethene
1,1-Dichloroethane
1,2-Dichloroethene (total)
Chloroform
1,2-Dichloroethane
2-Butanone
1,1,1-Trichloroethane
Carbon tetrachloride
FREON TF
Bromodichloromethane
1,2-Dichloropropane
cis-1,3-Dichloropropene
Trichloroethene
Dibromochloromethane
1,1,2-Trichloroethane
Benzene
trans-1,3-Dichloropropene
Bromoform
4-Methyl-2-pentanone
2-Hexanone
Tetrachloroethene
1,1,2,2-Tetrachloroethane
Toluene
Chlorobenzene
Ethylbenzene
Styrene
Xylenes (total)
Isopropanol
Butanol

None of the drums had detectable quantities of VOCs in the headspace (between the liner and the outer bag), the outer and inner bags or inside the inner bag next to the waste. Analysis of solidified inorganic waste from five retrievably stored drums did not detect any traces of VOCs in four out the five drums (Table 6.4-3). The waste from one drum (No. 7411-2808) contained nine of the organics at low ppm levels (0.9 ppm to 19 ppm). These organics did not appear in any of the containment layers or in the headspace of the drum between the liner and outermost drum liner bag.

Table 6.4-3 — Volatile Organic Analysis of Sludge Samples

Volatile Compounds	Amount (PPM) by Drum Number					
	7411–2808	7412–02917	7412–03492	7412–03850	7411–2578	BLD[b]
1,2-Dichloroethene (Total)	7.8	U[a]	U	U	U	0.1 PPM
Chloroform	1.8	U	U	U	U	0.1
1,1,1-Trichloroethane	8.8	U	U	U	U	0.1
Tetrachloroethene	1.7	U	U	U	U	0.1
1,1,2,2-Tetrachloroethane	4.7	U	U	U	U	0.1
Toluene	0.9	U	U	U	U	0.1
Ethylbenzene	5.3	U	U	U	U	0.1
Styrene	9.6	U	U	U	U	0.1
Total Xylenes	19.0	U	U	U	U	0.1

[a]   U = undetected.
[b]   BLD = Beyond lower detection limit.

None of the newly generated waste drums showed any traces of the organics in the headspace or layers of confinement. The drum with the ppm levels of some of the organics was the one filled in 1973 and vented at the INEL facility. This means that the drum had been vented for at least a period of eight weeks prior to being part of the sampling program. The absence of detectable quantities of VOCs in nine of ten solidified inorganic solids demonstrates that the vacuum filtration technique for these sludges is effective in lowering the concentration of VOCs in the waste. The presence of ppm amounts of the VOCs in the one sludge and the absence of the VOCs from the headspace (in spite of the vented drum) are evidence to the fact that any residual VOCs tend to stay with the waste. These data support the conclusion that the VOCs present in the waste are in low ppm or less amounts, with the source term itself being very limited.

6.4.4.1.2 Analysis of Solid Inorganics - Waste Type II

Five drums of Waste Type II were analyzed for gaseous components in the different confinement layers and the headspace of the drums. Three of the five drums did not show any of the organics, one (No. 242553) had up to 0.1 volume percent of 1,1,1-trichlorethane, while the fifth drum (No. 002800658) had up to a maximum of 0.4 volume percent of 1,1,1-trichloroethane in some of the individual packages. These drums were made up of mostly glassware, some of which contained residual amounts of the 1,1,1-trichloroethane. The concentrations measured in these drums are well below the saturation concentration of the organic liquid (13% from vapor pressure considerations), indicating that the organic liquid is present in only very small amounts.

6.4.4.1.3 Analysis of Solid Organics - Waste Type III

Three drums belonging to this waste type were analyzed in the sampling program, and none of them had any detectable amounts of the halogenated organics. Low concentrations (0.08 volume %) of hydrocarbons were present in one of the three drums.

6.4.4.1.4 Analysis of Solidified Organics - Waste Type IV

As mentioned earlier in this appendix, Waste Type IV belongs in the test category due to the possible presence of appreciable amounts of VOCs in the headspace of the payload containers. Results from the sampling of four of the drums in this waste type are presented here as supporting evidence that the VOCs are generally present in a non-volatile form in the waste. While VOCs could have been present at near-saturation levels in these drums (solidified organics waste type and the drum not vented), the results show that the VOCs are present in fairly low concentrations. One of the four drums (No. 74316930) did not have any detectable quantities of VOCs in any of the confinement layers. No analyses of the organic sludge samples are available. The maximum concentration of any VOC found in the three other drums was 3.9 volume percent for carbon tetrachloride.

These results seem to indicate that even if a finite supply of the organics was available, the nature of the waste limits release of the vapors into the headspace. Until quantified information can be obtained, this waste type is assigned to the test category.

Carbon tetrachloride has the lowest saturated vapor pressure (Table 6.4-4) of the four common solvents found in defense waste (i.e., carbon tetrachloride, Freon-113, methylene chloride and 1,1,1-trichloroethane). The fact that only carbon tetrachloride was detected in the headspace of the solidified organic drums provides evidence that the other organic solvents commonly associated with this waste form have volatilized prior to drum closure.

6.4.4.2 TRU Waste Sampling Program at INEL

The TRU Waste Sampling Program was conducted between 1983-1985 at INEL[2] in an effort to characterize the retrievably stored waste at INEL. In this program, 210 drums were sampled and analyzed for headspace gas composition. Table 6.4-5 summarizes the results on the VOC analyses by waste type and provides maximum, minimum and average concentrations along with the sample size.

Among the thirty-two drums sampled in Waste Type I, four of the VOCs were not present in any of the drums, and average concentrations of the other four ranged between 0.0025 and 0.198 volume percent. This sampling program was conducted even before transport requirements for the package were formulated. The results of the program indicate that by process history, the source term of the VOCs is limited. Similar results can be seen for Waste Types II and III where the average VOC concentrations were orders of magnitude below their saturation levels. Even among the twenty-three drums of Waste Type IV that were sampled, three of the VOCs were not present in the head space at all, and average concentrations of those present were below 1.4 volume percent. These results once again illustrate that the VOCs are in the waste in limited quantities and/or the bound nature of the VOCs even in the case of the organic sludges.

---

[2] Clements, T.L., and D.E. Kudera, "TRU Waste Sampling Program: Volume I--Waste Characterization," EG&G Idaho, Inc., Idaho Falls, Idaho, EGG-WM-6503, September 1985.

Table 6.4-4 — Vapor Pressures of Organic Solvents Above a Pure Liquid Phase[a]

Compound	Vapor Pressure	Temperature	Vapor Pressure	Temperature
Xylene	20 mm Hg	104°F	60 mm Hg	146°F
1,1,1-Trichloroethane	400 mm Hg	130°F	760 mm Hg	165°F
1,1,2-Trichloro-1,2,2-trifluoroethane (Freon-113)	760 mm Hg	118°F	1520 mm Hg	158°F
Carbon tetrachloride	200 mm Hg	100°F	760 mm Hg	170°F
Methlyene chloride (Dichloromethane)	760 mm Hg	105°F	---	---

[a]Green, D.W., 1984, Perry's Chemical Engineers' Handbook, 6th edition, McGraw-Hill Book Company, New York, New York.

Table 6.4-5 — Summary VOC Analysis in TRU Waste Sampling Program

Waste Type	TRICH[a]	IPROP[b]	TRCETHY[c]	CCl$_4$[d]	DCM[e]	1,2-DCETHA[f]	FREON[g]	CYCHEX[h]	DCETHY[i]	TOTAL VOC[n]
I[j] MAX	0.94	0	0.04	0.04	0.22	0	0	0	0	1.17
I MIN	0	0	0	0	0	0	0	0	0	--
I AVG	0.1978	0	0.005	0.0025	0.0203	0	0	0	0	--
II[k] MAX	2.84	0	0.17	0.09	0.42	0.4	0.81	0.17	0.03	2.84
II MIN	0	0	0	0	0	0	0	0	0	--
II AVG	0.2669	0	0.0043	0.0029	0.0230	0.0106	0.0103	0.0021	0.0003	--
III[l] MAX	1.06	0.62	0.14	0.29	0.25	0	2.87	0	0	3.37
III MIN	0	0	0	0	0	0	0	0	0	--
III AVG	0.1238	0.0201	0.0087	0.0068	0.0089	0	0.0389	0	0	--
IV[m] MAX	7.48	0	0.14	4.09	0.71	0	10.4	0	0	17.88
IV MIN	0	0	0	0	0	0	0	0	0	--
IV AVG	1.3582	0	0.0213	0.6734	0.0726	0	1.0717	0	0	--

[a]TRICH = Trichloroethane

[b]IPROP = Isopropyl alcohol

[c]TRCETHY = Trichlorethylene

[d]CCl$_4$ = Carbon tetrachloride

[e]DCM = Dichloromethane

[f]1,2-DCETHA = 1,2-Dichloroethane

[g]FREON = FREON-113 (1,1,2-Trichloro-1,2,2-trifluoroethane)

[h]CYCHEX = Cyclohexane

[i]DCETHY = Dichloroethylene

[j]32 drums Waste Type I were sampled

[k]78 drums Waste Type II were sampled

[l]77 drums Waste Type III were sampled

[m]23 drums Waste Type IV were sampled

[n]Maximum total volatile organic compounds in any drum

6.4.5   Release of VOCs from the Waste into the Payload Container

The vapor pressure of a pure compound is generally not completely exerted when the compound is in a combined form with other substances. Any residual VOCs present in the waste will therefore exert only a portion of their vapor pressures and tend to stay in a bound form. An

example is presented below for the case of methyl alcohol, which is the most volatile alcohol documented in the waste from an analysis of process technology.

The maximum amount of methyl alcohol expected in any of the waste forms based on process technology is 250 ppm. If a waste form contains bound water, the volatility of the alcohol will be reduced. A waste type containing 50% bound water (typical for Waste Type I) and 250 ppm of methyl alcohol would have the alcohol exerting a vapor pressure of only 0.12 mm Hg over the aqueous mixture at 40°C.[3] The vapor pressure at 60°C would be 0.26 mm Hg. The data presented in the previous section for halogenated organic compounds displayed evidence of reduced volatilities in actual waste materials.

6.4.6 Release of VOCs from Payload Containers

All payload containers in the payload are vented as specified in Section 2.5 of the CH-TRAMPAC. Release of the VOCs from the payload containers is seen from the experimental studies conducted at the INEL facility.[4] The concentrations of trichloroethane and methylene chloride in the headspace of a drum of combustible waste (which was vented with a carbon composite filter) remained constant at 6 and 1.5% respectively during thirteen weeks of venting (see Figure A-8d of Clements and Kudera[4]). These concentrations were lower than the saturated concentrations of 13% for trichloroethane and 33% for methylene chloride, which indicates that the source of the VOCs in the waste is limiting. It is also possible that the vapor presence of the organics are depressed by the presence of other compounds. After purging and sealing the drum, the concentration of each VOC remained below 3%, once again indicating that the source term of the VOCs was limited.

6.4.7 Conclusions

The following conclusions can be drawn from an evaluation of existing information on VOCs in CH-TRU waste:

1.   For materials expected to be shipped in the TRUPACT-II or HalfPACT, the source term of the VOCs is very small by the very nature of waste generation processes. Waste types known to contain appreciable amounts of VOCs are not allowed to be a part of the payload unless each container is tested under shipping conditions and shown to be safe for transport until sufficient data have been collected to allow a content code to be certified for shipment.

2.   Experimental studies show that VOCs present in the waste are well below saturation levels and in ppm levels in most cases.

---

[3] Perry, R.H., 1984, Perry's Chemical Engineers' Handbook, 6th edition, McGraw-Hill, Inc., New York, New York, Table 3-8, p. 3-61.

[4] Clements, T.L., and D.E. Kudera, "TRU Waste Sampling Program: Volume II--Gas Generation Studies," EG&G Idaho, Inc., Idaho Falls, Idaho, EGG-WM-6503, September 1985.

3.   The residual VOCs in the waste tend to be bound in the waste and do not migrate out of the payload containers. Thus, the residual VOCs do not pose a problem with respect to incompatibilities with the package.

This page intentionally left blank.

APPENDIX 6.5

BIOLOGICAL ACTIVITY ASSESSMENT

This page intentionally left blank.

6.5   Biological Activity Assessment

6.5.1   Summary

This appendix addresses the impact of biological activity within the waste on TRUPACT-II and HalfPACT shipments. The primary concerns in this regard are the possible generation of gases by biotic processes that might contribute to the build up of pressure in the cavity, or produce potentially flammable gases. An analysis of the waste forms and their environment shows that biological activity will be minimal and will have little impact on the package during a potential shipping period of up to 60-days. Gas production by microbial processes is not a concern for transport of contact-handled transuranic (CH-TRU) waste.

6.5.2   Introduction

Some of the CH-TRU waste forms and most of the packaging inside the payload containers (polyethylene [PE] and polyvinyl chloride [PVC] bags in drums or standard waste boxes) are organic in nature. The potential for microbial activity would exist if a suitable environment exists for the degradation of these organics. As will be shown in the following sections, the waste environment during transport is not conducive for microbial proliferation. Wherever a distinction between retrievably stored and newly generated waste is necessary, it will be made.

6.5.3   Types of Biological Activity

There are different types of microorganisms to be considered in the degradation of CH-TRU waste. Aerobic microorganisms, which produce carbon dioxide (CO_2) and water (H_2O), require oxygen for growth.[1] Anaerobic microorganisms, which can produce CO_2 and hydrogen (H_2, predominantly as an intermediate) or methane (CH_4), as well as other products, degrade materials in anoxic (oxygen-free) environments.[1] Facultative anaerobes can live with or without oxygen. Obligate anaerobes, on the other hand, cannot tolerate any oxygen and will only grow in strict anoxic environments. Microorganisms most likely to be found in waste products include bacteria and fungi. Bacteria utilize only the surface of a material and can be either aerobic or anaerobic. Fungi can access the matrix of the material but are generally only found in aerobic environments. Microorganisms can also be classified based on the optimum temperature they require for growth. Mesophiles have an optimum temperature for growth between 20 and 55°C, while thermophiles grow best at temperatures above 50°C.

---

[1]Atlas, R. M., 1984, "Microbiology: Fundamentals and Applications," Macmillan Publishing Company, New York , New York.

6.5.4 Waste Forms--Implications of Substrate and Nutrient Availability

Various waste forms will be transported in the package, but, in terms of the potential for gas generation, only one form is important; namely, cellulosic materials (solid organics). Materials made of rubber and plastic are more resistant to microbial actions. The contribution of these compounds to the total gas generated will be negligible, (especially over the shipping period of 60 days) primarily because of their inert nature. Evidence from stored drums (in retrievable storage for periods up to 15 years) that were opened up as part of a sampling program shows little or no degradation of the packaging materials (see Appendix 5.3 of the CH-TRU Payload Appendices). Even under conditions designed to promote microbial proliferation, these compounds degrade very slowly, if at all. Similarly, the solidified inorganic sludges should not exhibit any significant microbial gas generation due to their relatively high alkalinity (pH = 10-12), which would be hostile for most common microorganisms. This aspect is discussed further in the next section on environmental factors affecting microbial growth.

Examples of cellulosic materials that could be present in the payload are cotton, Kimwipes, and paper. Cellulose is a polymer composed of chains of glucose monomers. Biodegradation of cellulose requires the hydrolysis of the polymer into the monomer units. Biological depolymerization is a slow process that can significantly inhibit fermentation rates. Even though there are organisms that can degrade cellulose under different conditions, it is a complex process requiring very specific enzymes. Wood will also be present in TRU waste but is degraded at a much slower rate than cellulose in the form of cotton. Wood contains lignin which is much more resistant to microbial attack than cellulose. In addition, bacterial action is a strong function of surface area and substrate availability. The bulk form and segregated nature of the TRU waste creates conditions that are not very conducive to high microbial metabolic activities, especially during a limited period of sixty days. As shown in subsequent sections, the waste environment is such that, even for stored waste, the relatively long time period in itself is not sufficient to promote active microbial growth.

The availability of the nutrients, nitrogen and phosphorus, is another factor that can severely limit the extent of microbial activity in the package. The dry weight of a bacterial cell typically contains 14% nitrogen and 3% phosphorus.[2] While some of the waste forms do contain sources of nitrogen, phosphorus is limiting in most cases. Even where sources of nitrogen are present, the waste form environments are far from optimum for bacterial growth. An example is inorganic sludges which contain nitrates but are lacking in carbon substrates, and which are basified to a pH of 10-12. In other words, even without any consideration of the non-ideal environmental conditions of the payload, substrate and nutrient limitations by themselves will maintain microbial activity at minimal levels in the cavity.

---

[2]Bailey, J. E., and D.F. Ollis, 1977, "Biochemical Engineering Fundamentals," McGraw Hill Book Company, New York , New York.

6.5.5 Environmental Factors Affecting Microbial Activity in the Payload

Environmental factors such as temperature, pH, Eh, oxygen, moisture content, and water availability are very important in determining the rates (kinetics) and feasibility (thermodynamic aspects) of microbial activity. For the payload, almost all of these environmental variables are either sub-optimal or hostile. Each of these is considered in detail below.

6.5.5.1 pH and Temperature

The pH is an important factor to consider in the microbial degradation of CH-TRU waste. Usually, most bacteria will be most active at neutral pHs. The sludges to be transported in the package are fairly basic (pH of 10-12), which will inhibit the activity of most bacteria and fungi. Specific organism groups like the methanogens (methane producers) also have sensitive pH ranges for growth.[2] Even under carefully controlled laboratory conditions, methanogenesis has a very long start-up phase and a fairly unstable operating phase. Establishment of an active population of methanogens is therefore unlikely during the shipping period.

As mentioned in Section 6.5.3, microorganisms can be classified based on the optimum temperature they require for growth. Methanogens, for example, have an optimum temperature range between 90 to 100°F. Anaerobic digestion units (aimed at digesting sewage sludge and the production of methane) are usually provided with external heat exchangers to maintain optimum temperatures for methanogenesis.[2] These constant and optimal conditions are not likely to exist even for waste that has been stored for long periods of time. Fluctuations in the temperature also prevent the establishment of a stable microbial population in the waste containers.

6.5.5.2 Eh and Oxygen Availability

Eh (the redox potential) is an indication of whether an environment is oxidizing or reducing. Many microorganisms have strict Eh requirements for growth. Methanogens, for example, require a very reducing environment in which the Eh must be less than -200 mV.[3] They are obligate anaerobes and cannot tolerate even small amounts of oxygen. It is very unlikely that any significant quantities of methane will be produced during transport of CH-TRU waste. Methanogenesis from cellulose requires a complex set of organisms and conditions to be successful and is easily upset if favorable conditions are not maintained. The production of methane requires not only the depletion of oxygen but also the reduction of nitrates and sulfates.[3] Even in a process plant under optimum conditions, it is difficult to produce methane from cellulose. Even experiments done under controlled laboratory conditions showed no methane generation with CO_2 being the major gaseous product.[4] (These experiments are not applicable to

---

[3]Weiss, A. J., R. L. Tate III, and P. Colombo, 1982, "Assessment of Microbial Processes on Gas Production at Radioactive Low-Level Waste Disposal Sites," BNL-51557, Brookhaven National Laboratories, Brookhaven, New York.

[4]Molecke, M. A., 1979, "Gas Generation from Transuranic Waste Degradation: Data Summary and Interpretation," SAND79-1245, Sandia National Laboratories, Albuquerque, New Mexico.

the transport conditions - a bacterial inoculum was added to synthetic waste along with required nutrients in these experiments.) Radiolytic production of oxygen even in trace quantities would act as an inhibitor of anaerobic activity. In addition, the requirement of having a filter vent on all the waste containers before transport provides a means of communication with the environment, further destabilizing a constant environment even for the stored waste.

6.5.5.3 Moisture Content and Water Availability

One of the prime requirements for microbial proliferation is the availability of sufficient amounts of water. Approximately 80% of a bacterial cell mass is water. Microbial activity can be sustained even at relative humidities below the saturation value, but metabolic activities under these conditions will be very slow. Hence, microbial gas generation rates in short time periods (like the sixty-day shipping period) will be insignificant. As pointed out earlier, even if some of the content codes have pockets of damp waste, other requirements for biological activity (substrate, nutrients, suitable pH and Eh conditions) will not necessarily be present in these areas.

6.5.5.4 Radiation Effects on the Microorganisms

An additional factor that contributes to making the microbial environment non-ideal in the package is the radiation from the payload, which can result in the death of a portion of the microbial population. Radiation effects can potentially compound the existing hostile environment of the microorganisms in the payload.

6.5.6 Source Term of the Microorganisms

The waste packaging configuration in the payload containers restricts the source term for the microorganisms. While an initial microbial inoculum may be present in the waste, the plastic bagging acts as a barrier for the availability of the waste substrates to the microorganisms. In addition, the filter vents on the waste containers have a filtering efficiency of ≥99.9%, with 0.3 to 0.5 micron particles, DOP (dioctyl phthalate) smoke (Section 2.5 of the Contact-Handled Transuranic Waste Authorized Methods for Payload Control [CH-TRAMPAC]). Typical dimensions of bacteria are between 0.5 to 3 microns.[2] This means that the filter vents would act as effective bacterial filters (though not 100%) to prevent continuous contamination of the waste with microorganisms.

6.5.7 Conclusions

The nature and configuration of the payload for the TRUPACT-II and HalfPACT are such that biological activity will be minimal and of very little concern during the 60-day shipping period. The environment in the cavity will be suboptimal or hostile for the growth of most microorganisms due to the segregation of the waste and essential nutrients and the limitations of usable substrate, nitrogen and phosphorus sources. The following factors support this statement:

1.   Cellulose, which is the most likely waste product to be degraded by bacteria, is degraded by a complex process that requires a specific set of organisms. Some of these organisms may be present in the waste but may not be in a sufficient quantity to contribute to the overall gas generation.

2.   The proper nutrients (primarily nitrogen and phosphorus) must be present in order for the microorganisms to degrade any material. Nitrogen from the air cannot be efficiently utilized by microorganisms; it must come from a source such as nitrate. Sufficient phosphorus, however, is very likely to be missing or limiting in many drums.

3.   It is very unlikely that methane would be produced during transportation of the waste for several reasons:

      -    The environment for methanogenesis must be very reducing (no oxygen)

      -    Very specific microorganisms are required, which exist in narrow ranges of suitable environments, and

      -    The process can be self-poisoning if intermediates produced are not controlled or neutralized.

4.   Although hydrogen may be produced during intermediate steps in anaerobic processes, it is very unlikely that it will be present as a final product. It is used as a reducing agent almost as quickly as it is produced.

5.   Another factor limiting bacterial degradation is substrate surface area. The cellulosic materials that are put into bags are in a very bulky form that is not easily accessible to surface-decomposing bacteria.

6.   Any aerobic decomposition will result in insignificant pressure changes due to the simultaneous consumption of oxygen with the production of carbon dioxide.

7.   Even retrievably stored waste does not provide the necessary conditions for continuous and prolonged microbial activity. Fluctuations in environmental variables like the temperature and oxygen availability (due to the filter vent) act to prevent anaerobic biological activity at any significant level. Evidence from sampling programs shows very little deterioration of the packaging materials even after years of storage. In addition, limitations in substrate and nutrient availability and segregation of these nutrients apply to retrievably stored waste as well.

This page intentionally left blank.

APPENDIX 6.6

THERMAL STABILITY OF PAYLOAD MATERIALS AT TRANSPORT TEMPERATURES

This page intentionally left blank.

6.6 Thermal Stability of Payload Materials at Transport Temperatures

6.6.1 Summary

This appendix describes the thermal stability of payload materials, demonstrating that thermal degradation will be minimal for payload materials during transport in the TRUPACT-II or HalfPACT.

6.6.2 Introduction

The thermal stability of the payload materials is addressed for the wastes inside drums or Standard Waste Boxes, and payload materials outside the waste containers, including the drum binding material (stretch wrap), plastic reinforcement plates, and slip sheets.

Inorganic payload materials will be thermally inert, with the possible exception of small amounts of gases adsorbed on the surfaces, most of which will be water vapor. The pressure calculations performed in the TRUPACT-II and HalfPACT Safety Analysis Reports (SARs) assume saturated water vapor is present in all cases.

Organic materials are placed into shipping categories that are shown to meet transport requirements by analysis or into shipping categories which are shown to meet transport requirements by test, depending on the chemical makeup and decay heat of the wastes. Thermal analyses discussed in the TRUPACT-II and HalfPACT SARs show that a waste temperature of 238 degrees Fahrenheit (^{o}F) (114 degrees Celcius [^{o}C]) bounds the payload temperature for all wastes transported in analytically determined shipping categories. Thermal stability of payload materials at and below 238°F (114°C) is addressed in terms of the threshold decomposition temperatures. The effect of irradiation on the materials at this temperature is shown to be negligible. For the test shipping categories of Waste Type IV, any gases produced thermally are included in the measurement of total gas generation.

Plasticizers added to polymers to increase flexibility are typically less thermally or chemically stable than the polymers.[1] However, the vapor pressures of most common plasticizers (e.g., phthalates, sebacates, and other esters) are only 1 millimeter of mercury at 160°F (71°C) or above[2] and can be ignored in pressure calculations.

Oxidation is the major degradation process for polymers heated in the presence of oxygen. In a sealed system, oxygen typically is depleted at a rate faster than the rate of formation of oxygen-containing gases such as carbon dioxide or carbon monoxide, leading to a net pressure decrease.

---

[1] Deanin, R. D., Polymer Structure, Properties and Applications, Chaners Books, Boston, 1972.

[2] AIP Handbook, American Institute of Physics Handbook, Second Edition, McGraw-Hill Book Company, New York, 1963.

The SAR analyses also show that the maximum drum wall temperature during normal conditions of transport is 162ºF (72ºC). This temperature is used to evaluate the thermal stability of the polyethylene stretch wrap, reinforcement plates, and slip sheets. These materials are outside the waste containers and will have experienced little or no radiation.

6.6.3 Threshold Decomposition Temperatures for Plastics and Other Polymers

Waste material and packaging components may be a combination of cellulosics, plastics, and rubber. Representative materials from each of these categories were studied to determine threshold decomposition temperatures.[3] The temperature at which a material loses weight, not including drying, is the threshold decomposition temperature. Gas generation from thermal decomposition was measured by pressure increases in sealed containers over long periods of time. Experiments were performed in aerobic and anaerobic atmospheres.

The threshold decomposition temperature for materials in air is shown in Table 6.6-1. Pylox gloves (polyvinyl chloride) have the lowest threshold decomposition temperature of 302ºF (150ºC). Results of anaerobic experiments and experiments with potential catalysts that may be present in the waste yielded no significant lowering of the threshold decomposition temperatures.

The generation of gas through thermal decomposition of the waste materials did not occur at temperatures lower than 302ºF (150ºC) and will, therefore, be negligible at 238ºF (114ºC).

6.6.4 Effect of Radiation on Thermal Properties of Materials

Radiation chemically changes materials and can affect their thermal properties. For example, for an absorbed dose of 500 millirad in vacuum, the melting point of polyethylene was decreased about 9ºF (5ºC).[4]

Polyethylene film irradiated in vacuum or under a nitrogen atmosphere were subsequently heated in the presence of oxygen at 230ºF (110ºC). The weight change between unirradiated and irradiated polyethylene films (exposure times up to 1150 hours [hr]) was compared.[5] The major difference between irradiated and unirradiated materials was that the irradiated materials began to absorb oxygen and increase in weight after 50 hr without antioxidant, or after 500 hr with antioxidant.

The rate of weight loss versus temperature of polyethylene was measured for samples irradiated in air and then heated in air.[6] Thermal degradation was detectable above about 302ºF (150ºC), with only minor differences found between irradiated and unirradiated materials.

---

[3] Kosiewicz, S. "Cellulose Thermally Decomposes at 70ºC," Thermochimica Acta, Vol. 40, pp 319-326, 1980.

[4] Black, R. M., and A. Charlesby, "The Oxidation of Irradiated Polyethylene-II Thermal Oxidation," Inter. J. Appl. Radiat. Isotopes 7, PP. 134-140, 1959.

[5] Kato, K., et al., "Structural Changes and Melting Behavior of Gamma-Irradiated Polyethylene," Jap. J. Appl. Phys. 20, pp. 691-697, 1981.

[6] Igarashi, S., "Thermogravimetric Analysis of the Effect of Ionizing Radiation on Thermal Stability of Polyethylene," J. Appl. Polym. Sci., Vol. 8, pp 1455 - 1464, 1964.

The conclusions reached are that while there are measurable differences in the thermal properties of polymers when they are irradiated, the effects are relatively small even near 392°F (200°C), and can be neglected for temperatures less than or equal to 238°F (114°C).

Table 6.6-1 — Threshold Decomposition Temperatures in Air

Material	Temperature (°C)
Cellulosics[a]	
Scott utility wipes	185
Kleenex tissues	185
Diaper paper (PE-backed)	190-185
Cloth (cotton twill)	185
T-shirt (cotton)	185-190
Cheesecloth	205
Wood	175
Fiberboard	185-190
Plastics	
Pylox gloves (PVC)	150
Tygon tubing (PVC)	175
Polyethylene	210
Polypropylene	195-200
Lucite [poly(methyl methacrylate)]	170-175
Teflon [poly(fluoroethylene)]	430-435
Rubbers	
Hypalon	165
Neoprene	175-180
Durasol/neosol	180
Latex	195
Bitumen[b]	275

Source: Kosiewicz, S. "Cellulose Thermally Decomposes at 70°C," Thermochimica Acta, Vol. 40, pp 319-326, 1980.

[a] Water loss observed at 40-110°C.
[b] Not a rubber material.

6.6.5 Thermal Degradation of Polyethylene at 162°F (72°C)

The temperature of the polyethylene stretch wrap, reinforcement plates, and slip sheets may exceed the maximum normal-use temperature for polyethylene (nominally 140°F [60°C]). These materials will have experienced little or no radiation, since they are outside the waste containers.

Thermal degradation of organic materials occurs according to an Arrhenius relationship:

$$k = A\exp(E_a/RT)$$

where k = rate constant

   A = pre-exponential factor (1/time)

   E_a = activation energy for thermal degradation (calories/mole)

   T = temperature (K)

   R = gas constant.

Thermal oxidation of low-density polyethylene shows gradual energy absorption until melting occurs at about 230^oF (110^oC), and then combustion occurs at about 482^oF (250^oC).[7] Demas concludes that polyethylene can be used as an electrical insulation material for temperatures up to $140\text{-}167^oF$ ($60\text{-}75^oC$) without creating a toxicological problem for humans, indicating that production of toxic or flammable gases is minimal at these temperatures.

Kosiewicz[8] describes experiments measuring thermal degradation of common waste materials at $68°$, $104°$, $158°$, and $212°F$ ($20°$, $40°$, $70°$, and $100°C$), including various cellulosics, plastics, and rubbers. He measured the amount of gas evolved at a given temperature that was maintained for a long period of time. The gas amount was determined by the pressure reached in an experimental cylinder. A gas production rate of 1E-7 mole/day-gram was reported for experiments conducted at $158°F$ ($70°C$) for more than 340 days for both uncontaminated samples and samples contaminated with plutonium at 4E5 nanocuries per gram of material. None of the samples were sterilized, so some of the gas evolved could have come from microbial degradation. The gas composition was not reported. Similar experiments conducted using paper resulted in a very low gas generation rate at $104°F$ ($40°C$) and a maximum rate of 7E-8 moles/day-gram at $158°F$ ($70°C$).

Over the 60-day transport time, the moles of gas generated per pound of material would be:

   moles/lb = 1E-7 moles/day-gram x 60 days x 1E3 gram/2.2 pounds
         = 2.7E-3 moles/pound.

Carbon dioxide and carbon monoxide are common thermal degradation products of polymers, so much of this gas would be nonflammable.

---

[7] Demas, P., "Emissions of Volatiles from Non-Metallic Shipboard Materials -- Electrical Insulations," 75-ENAs-35, American Society of Mechanical Engineers, New York, 1975.

[8] Kosiewicz, S. T., et al., "Studies of Transuranic Waste Storage under Conditions Expected in the Waste Isolation Pilot Plant (WIPP)," Interim Summary Report, LA-7931-PR, October 1, 1977 -- June 15, 1979.

The maximum weight of the slip sheets and stretch wrap is 100 pounds. The maximum amount of gas generated during transport for a maximum drum wall temperature of at 162°F (72°C) would then be 0.3 moles for 60 days. This gas would be generated outside the payload containers.

6.6.6 Conclusions

The conclusions reached are that generation of gases through thermal degradation of the waste materials up to 238°F (114°C) and of polyethylene at 162°F (72°C) (stretch wrap, reinforcement plates, and slip sheets) will be negligible.

This page intentionally left blank.

APPENDIX 6.7

GAS RELEASE ASSESSMENT

This page intentionally left blank.

6.7   Gas Release Assessment

6.7.1   Summary

The hydrogen concentration will be maintained below 5% in all void volumes within the payload and packaging inner containment vessel (ICV) during transport of contact-handled transuranic (CH-TRU) materials. This document describes the logic and methodology used in evaluating payload characteristics which meet this requirement. Appendix 6.8 of the CH-TRU Payload Appendices describes the experiments relating to the quantification of hydrogen release rates from the payload containers.

Parameters that govern the maximum decay heat limits per shipping category are listed below:

- Waste configuration (i.e., the number and type of confinement layers).

- Release rates of hydrogen from each of these confinement layers.

- Hydrogen generation rates quantified by the effective G value of a waste material (the number of molecules of hydrogen produced per 100 eV of energy absorbed).

- Operating temperature for the payload in the ICV during a 60-day shipping period.

- Void volume in the ICV outside the payload containers available for gas accumulation.

- Duration of the shipping period.

A computational spreadsheet was used to perform the calculations required to determine the maximum decay heat values based on a pseudo steady-state model of gas release. The computed maximum decay heats are based on an approach that will ensure that hydrogen concentrations are safely maintained below the 5% limit during normal and accident conditions of transport. Among the factors that include a margin of safety to ensure an acceptably low hydrogen concentration are:

- Effective G values used in analytical calculations are higher than values reported for actual waste containers as part of sampling programs (see Appendix 5.3 of the CH-TRU Payload Appendices).

- Minimum measured hydrogen diffusion coefficients through the drum and standard waste box (SWB) filters rather than the average values.

- Minimum drum liner release rate.

- Only the leakage rate from the small bag closure used as the release rate from small bags (i.e., no credit taken for permeation through the plastic bag material).

- Lowest measured total release rate for a large bag was used.

- Void volumes inside each inner confinement layer and in the payload containers assumed to be zero.

- A 60-day shipping period compared to typical shipping periods of 5 days or less.

6.7.2 Introduction

In order to ensure safe transport of the payload in a package, the concentration of hydrogen within any void volume in a layer of confinement of the payload or in the ICV shall be less than or equal to 5% during an assumed 60-day shipping period.[1] The predominant mechanism by which hydrogen is generated within the payload is by radiolysis of the hydrogen-containing waste materials and plastic bags or sheets present in the payload (see Section 5.2 of the Contact-Handled Transuranic Waste Authorized Methods for Payload Control [CH-TRAMPAC]). This document describes the logic and methodology used to quantify the maximum decay heats, which will ensure acceptably low hydrogen concentrations.

A description of the payload configuration in the package comprises the next section. The factors affecting and controlling the maximum permissible release rate of hydrogen are discussed in Section 6.7.4. The margins of safety for the parameters that are used to quantify the decay heat limits are discussed in Section 6.7.5. The computational method that was developed to perform the mathematical analysis is described in Appendix 2.3 of the CH-TRU Payload Appendices.

6.7.3 The Payload and the Package

The term "payload" refers to the waste contents that will be transported in the package as defined by the CH-TRAMPAC. The classification of shipping categories is described in Appendix 2.1 of the CH-TRU Payload Appendices. The content codes in the different shipping categories are described in the CH-TRU Waste Content Codes (CH-TRUCON) document.[2] Payloads will be assembled in accordance with the CH-TRAMPAC.

6.7.3.1 Payload Configuration

Typically, for purposes of radiological safety, the CH-TRU waste is packaged in one or more layers of confinement (plastic bags). Bags are closed according to the specifications of Appendix 3.8 of the CH-TRU Payload Appendices. When a drum is the payload container, a punctured or filtered rigid drum liner may separate the waste bags and the steel drum shell (Section 2.9 of the CH-TRAMPAC). Each container is vented in accordance with Section 2.5 of the CH-TRAMPAC. The filter releases generated gases, while acting as a barrier for particulates. Authorized payload containers and payload configurations are specified in Section 2.1 of the CH-TRAMPAC.

---

[1] U.S. Nuclear Regulatory Commission, SSINS No. 6835, IE Information Notice No. 84-72: "Clarification of Conditions for Waste Shipments Subject to Hydrogen Generation," September, 1984.

[2] U.S. Department of Energy (DOE), "CH-TRU Waste Content Codes (CH-TRUCON)," DOE/WIPP 01-3194, current revision, U.S. Department of Energy, Carlsbad Field Office, Carlsbad, New Mexico.

6.7.4   Parameters Affecting Release Rates and Decay Heat Limits

Specific parameters that affect these release rates are described below.

6.7.4.1   Permeability of Bags

The permeability coefficient or simply the permeability is a measure of the rate at which a gas passes through a material. Permeability may be defined as the number of moles of gas passing per unit time through a material of unit area that is of unit thickness under a unit partial pressure gradient at a specified temperature. Typical units for permeability are: (mole*cm)/(sec*sq. cm*mmHg). Therefore, the mass flow rate of a gas (e.g., hydrogen) through a material will increase with an increase in the available surface area, an increase in the partial pressure gradient of the gas across the membrane and with a decrease in the thickness of the material, and an increase in temperature.

6.7.4.2   Leakage Through Bag Closures

In addition to permeation through the plastic bags, hydrogen is also released through the closure at the end of the bags (Appendix 3.8 of the CH-TRU Payload Appendices). For bags closed by the twist and tape method, the twisted portion of the bag that is taped generally has a length of six inches. Hydrogen is then released by diffusion through the twisted closure. Bags that are folded and taped would be expected to offer very little resistance to the passage of hydrogen. Vented bags that are heat-sealed are installed with a minimum of one filter vent, with gas release occurring through the filter vent in addition to permeation (Section 2.5 of the CH-TRAMPAC). Bags that are closed with a twist and tape or fold and tape closure may be installed with a filter vent as a measure of safety. The closure methods described in Appendix 3.8 of the CH-TRU Payload Appendices are mandatory for all payload containers to be transported, as specified by Section 5.1 of the CH-TRAMPAC, and hence these release mechanisms for hydrogen will be in operation.

6.7.4.3   Bag Materials

Two kinds of bag materials are typically used by the waste generator sites, polyvinyl chloride (PVC) and polyethylene (PE). The permeability depends on the type of material, and any additives that are added to the polymer during manufacturing. For example, the permeability of a PVC bag generally increases with the amount of plasticizer used in making the film.[3]

6.7.4.4   Radiation Effects on Bags

The radiation from the decay of radionuclides within a bag may affect the properties of the bag including the permeability to hydrogen and other gases. Gamma radiation doses up to 800 Krad seem to have no significant effect on the permeability of PE or PVC to nitrogen, oxygen, carbon dioxide and water vapor.[4] The permeability of these materials to hydrogen can also be expected to yield similar results. Polymers like PE and PVC preferentially crosslink as a result of radiolysis, yet data from Deanin (1972)[3] seem to indicate that significant permeability changes

---

[3]Deanin R. D., 1972, "Polymer Structure, Properties, and Applications," Chaners Books; Boston, Massachusetts.

[4]Varsanyi, 1975, "Investigations into the Permeability of Polymer Membranes of Food Packaging Quality to Gases and Water Vapour after Radiation Treatment with Radurizing Doses," Acta Alimentaria 4, pp. 169-251.

do not result from this effect. Preliminary permeability data from an actual waste drum, that has been stored for a period of 15 years, indicate that the hydrogen permeability rates through both PE and PVC are higher when compared with new plastic samples.[5]

6.7.4.5 Temperature

Permeabilities are highly dependent on temperature. For this reason, values of permeability are and should be quoted at a specific temperature. The temperature dependence of the permeability may be represented by an Arrhenius type equation:[6]

$$P \text{ "is proportional to the" } \exp(-E/RT) \qquad\qquad (\text{Equation 1})$$

where,

P   = permeability
E   = activation energy for permeation
R   = gas constant
T   = absolute temperature.

Typically, for polymeric membranes the activation energies for hydrogen per-meation are between 1 and 10 Kcal/gmole. The estimated activation energies for hydrogen permeating through PE and PVC membranes are 8.2 Kcal/gmole and 1.9 Kcal/gmole respectively.[6] Therefore, the permeability of hydrogen through PE is much more sensitive to changes in temperature than through PVC.

6.7.4.6 Diffusion Coefficients Through Filters

Each container must be vented in accordance with Section 2.5 of the CH-TRAMPAC. These filter vents prevent a potential pressure buildup due to generation of gases by allowing the venting of gaseous products while retaining particulates. Hydrogen molecules diffuse through a filter at a rate that follows Fick's first law of diffusion, which states that the diffusion rate is equal to the product of:

- Effective diffusion coefficient
- Cross-sectional area of the filter, and
- Concentration gradient across the filter.

The temperature dependence of hydrogen release through bag closures is a function of the diffusion process, as well as the closure configuration. While pure diffusion shows a slight decrease with decreasing temperature, actual tests (described in Appendix 6.8 of the CH-TRU Payload Appendices) show that the total release of hydrogen from bags can increase with

---

[5]Roggenthen, D. K., McFeeters, T. L., Nieweg, R. G., March 1989, "Waste Drum Gas Generation Sampling Program at Rocky Flats During FY 1988," RFP-4311.

[6]Perry, R. H., 1984, "Perry's Chemical Engineers' Handbook," 6th Edition, McGraw Hill Book Company, New York.

decreasing temperature. This aspect is discussed further in Appendix 6.9 of the CH-TRU Payload Appendices.

The effective diffusion coefficient of hydrogen through the filter is a fraction of that in air due to the presence of the solid filter medium.

6.7.4.7 Diffusion Through Drum Liner

If a rigid plastic drum liner is placed inside a drum to be transported, the liner must be punctured with a hole that has a minimum diameter of 0.3 inches, or a filter with hydrogen release rates equivalent to or greater than a 0.3-inch minimum diameter hole. Otherwise, the liner must be treated as any other confinement layer with the associated resistance calculated in accordance with Appendix 2.2 of the CH-TRU Payload Appendices. The release of hydrogen from this liner will therefore be comprised of two components: permeation of the gas through the material and diffusion of hydrogen through the punctured hole. The diffusion rate through the hole will be equal to the product of:

- Cross-sectional area of the hole
- Diffusion coefficient of hydrogen in air
- Concentration gradient of hydrogen.

6.7.5 Quantification of Decay Heat Parameters

6.7.5.1 Margins of Safety in Calculations

The purpose of this section is to identify the margins of safety associated with the parameters that determine the maximum permissible decay heat for each payload shipping category. The watts of decay heat have been derived incorporating several margins of safety as explained in the following sub-sections. The maximum decay heat values will ensure that the concentrations of hydrogen will be below the 5% limit during normal and accident conditions of transport.

6.7.5.2 Temperature and Pressure

The temperature dependence of hydrogen release rates is discussed in Appendix 6.9 of the CH-TRU Payload Appendices.

The pressure being used in the hydrogen release calculations is assumed to be constant at 1 atm. Since production of any gases would tend to increase the pressure (and reduce mole fractions of hydrogen), neglecting gas generation and any decrease in ambient pressure should not alter the margins of safety being used in the release calculations. Any increase in pressure in the inner confinement layers due to gas production would result in flow of the gases and higher release rates.

6.7.5.3 High G Values

The effective G values provided in Appendix 3.2 of the CH-TRU Payload Appendices bound the worst-case hydrogen producing material while allowing credit for weight percent water in the waste and self-absorption of alpha decay energy by radioactive particulates. For Waste Types II

and III, the assumption is made that all of the decay heat is absorbed by the material with the highest G value for hydrogen.

6.7.5.4 Minimum Hydrogen Diffusion Coefficients

Each payload container to be shipped will be vented as specified in Section 2.5 of the CH-TRAMPAC. The filters provide for venting of gaseous products while retaining particulates. A total of 18 filters of the carbon composite filter design (12 drum and 6 SWB) have been tested for hydrogen diffusivity[7] to calculate the hydrogen diffusion coefficient for each. Four of the Kevlar filters to be used in the bins have also been tested for their hydrogen diffusivity characteristics. As a margin of safety, the hydrogen diffusion coefficient assumed for the drum filter vent decay heat limit calculations is the lowest diffusion coefficient which has been measured. The value of this parameter is 1.90E-6 mole/sec/mole fraction[7] as opposed to the average value of 3.10E-6 mole/sec/mole fraction (Table 6.7-1). The value of the lowest measured diffusion coefficient for the SWB filter vent is 3.70E-6 mole/sec/mole fraction whereas the average was 4.87E-6 mole/sec/mole fraction (Table 6.7-2). This minimum hydrogen diffusivity value for the SWB filter vent is also used for

the bin filter vents, even though the hydrogen diffusivities of these filter vents are about four times higher than this value (Table 6.7-3). Testing and hydrogen diffusivity values for filter vents used in bags are discussed in Appendix 3.11 of the CH-TRU Payload Appendices.

6.7.5.5 Minimum Drum Liner Release Rate

If a rigid plastic liner is used in a drum, the liner must have a hole with a minimum diameter of 0.3 inches or a filter with hydrogen release rates equivalent to or greater than a 0.3-inch minimum diameter hole. Otherwise, the liner must be treated as any other confinement layer with the associated resistance calculated in accordance with Appendix 2.2 of the CH-TRU Payload Appendices before the drum can be transported. Release of hydrogen through the liner will occur by two mechanisms:

- Diffusion through the punctured hole or filter vent and
- Permeation through the material.

As a margin of safety, no credit will be taken for the release of hydrogen by permeation through the liner material. The release rate through the punctured hole is equal to the product of:

---

[7]Peterson S. H., July 1988, "Determination of Hydrogen Flow and Diffusion Properties of Selected Graphite Filters," Westinghouse Research and Development Center, Chemical and Process Development Department, Pittsburgh, Pennsylvania.

Table 6.7-1 — Hydrogen Diffusion Coefficients Through Drum Filters

Filter ID #	Diffusion Coefficient (mole/sec/mole fraction)
NFT-D1	3.60E-6
NFT-D2	3.30E-6
NFT-D3	5.70E-6
NFT-D4	4.23E-6
NFT-D5	3.22E-6
NFT-E5	3.38E-6
NFT-16	2.46E-6
NFT-17	2.43E-6
NFT-18	1.90E-6
NFT-21	2.10E-6
NFT-22	2.37E-6
NFT-23	2.50E-6

Source: Peterson S. H., July 1988, "Determination of Hydrogen Flow and Diffusion Properties of Selected Graphite Filters," Westinghouse Research and Development Center, Chemical and Process Development Department, Pittsburgh, Pennsylvania.

Table 6.7-2 — Hydrogen Diffusion Coefficients Through SWB Filters

Filter ID #	Diffusion Coefficient (mole/sec/mole fraction)
NFT-9026	5.43E-6
NFT-9027	3.70E-6
NFT-9032	5.19E-6
NFT-9033	4.80E-6
NFT-9034	5.19E-6
NFT-9035	4.90E-6

Source: Peterson S. H., July 1988, "Determination of Hydrogen Flow and Diffusion Properties of Selected Graphite Filters," Westinghouse Research and Development Center, Chemical and Process Development Department, Pittsburgh, Pennsylvania.

Table 6.7-3 — Hydrogen Diffusion Coefficients Through Kevlar Bin Filters

Filter ID #	Diffusion Coefficient (mole/sec/mole fraction)
K-23	7.7E-6
K-25	7.2E-6
K-27	7.4E-6
K-28	7.3E-6
K-25 (repeat)	7.7E-6

Source: Peterson S. H., and E. E. Smeltzer, August 1990, "Determination of Flow and Hydrogen Diffusion Characteristics of Kevlar Filters for WIPP," Westinghouse Science and Technology Center, Pittsburgh, Pennsylvania.

- Minimum cross sectional area of the hole (0.456 sq. cm)
- Diffusion coefficient of hydrogen in air, and
- Concentration gradient of hydrogen across the hole.

Another margin of safety that has been incorporated is that the diffusion coefficient of hydrogen in air at -29°C will be used in calculations of decay heat limits. With this value of the diffusion coefficient (0.511 sq. cm/sec) the release rate through the drum liner has been computed as 5.09E-5 mole/sec/mole fraction. Since the diffusion coefficient varies with temperature to the 1.75 power[5] the release rate would be higher by a factor of 1.22 at 25 ^{o}C but is not considered in the calculations for the decay heat limits. The sites that use a carbon composite filter to vent the liner will ensure that the release rate is equal to or higher than this value.

6.7.5.6 Release Rates From Bags

Several margins of safety have been incorporated in deriving the release rates from bags. These may be summarized as follows:

- For small bags (not large drum liner bags), such as those used to bag-out solid inorganics and organics, only the leakage through the worst-case bag material closure has been used as the release rate. All decay heat is assumed to be in the innermost layer of confinement. These bags do have a finite surface area which is typically around 0.6 sq. meters which would correspond to an additional release rate of around 2E-6 mole/sec/mole fraction at 25°C.

- Credit has been taken for only one closure, although the majority of the small bags have two closures. The release rate by this mechanism has been quantified as 5.58E-7 mole/sec/mole fraction based on experimental measurements (Appendix 6.8 of the CH-TRU Payload Appendices).

- For large bags the total release (closure leakage and bag permeation) as measured at three different temperatures (Appendix 6.8 of the CH-TRU Payload Appendices). For purposes of calculating the decay heat limits, the lowest measured total release rate of 4.67E-6 mole/sec/mole fraction was used.

- For the SWB and ten-drum overpack (TDOP) liners the total release rate is the sum of the release rates by permeation through the liner and the release rate through the small bag closure. The actual release rates through the SWB and TDOP liners are expected to be much higher due to the fold and tape closures that offer minimal resistance.

- For filtered small bags, only the diffusion through the filter vent has been used as the release rate. The lowest measured value for the hydrogen diffusivity was used in calculating decay heats.

- For filtered large bags, the total release consists of permeation through the bag and diffusion through the filter vent. The lowest measured values for the hydrogen diffusivity and permeation from the liner bags are used in calculating decay heats.

6.7.5.7 Void Volumes

A pseudo-steady-state analysis was used to compute the decay heat limit for each shipping category and will be described in detail in the following section. For the purpose of these calculations, an assumption of zero void volume inside each of the layers of confinement in a payload container has been made. This results in higher calculated concentrations of hydrogen in the different confinement layers and the ICV cavity. (The smaller the available volume for a given amount of hydrogen, the higher its concentration.) For fixed release rates of hydrogen through the various layers of confinement, this approach gives the lowest decay heat limits.

6.7.6 Decay Heat Limits for Shipping Categories

The method of arriving at a decay heat limit for the different shipping categories is presented in Appendix 2.3 of the CH-TRU Payload Appendices. The decay heat limit in watts per generator for each payload shipping category is presented in the CH-TRAMPAC.

This page intentionally left blank.

APPENDIX 6.8

GAS RELEASE TESTING

This page intentionally left blank.

6.8 Gas Release Testing

6.8.1 Summary

This document provides a summary of a testing program designed to obtain data on hydrogen release rates from confinement layer configurations that mimic real waste drums of contact-handled transuranic (CH-TRU) waste. Several different confinement layer configurations have been tested.

A test consists of simulating hydrogen gas generation in the innermost bag by a controlled release of hydrogen and monitoring the resulting hydrogen concentration within each of the void volumes between layers of confinement. All layers of confinement are initially purged with nitrogen. The tests are terminated when steady state conditions are achieved, (i.e., when the hydrogen volume percentage remains constant in all void volumes for twelve consecutive hours with a concentration of around 4.0 percent in the inner bag.) A mass balance for hydrogen at steady state permits the computation of effective release rates from each of the confinement layers since the flowrates across each layer are equal to each other and to the hydrogen gas injection rate.

The release of hydrogen from a waste confinement layer consists of two components:

- Permeation through the bag material

- Release through the bag closure ("twist and tape" or "fold and tape"), or through the filter vents in heat-sealed bags.

Only the release rate through the bag closure (5.6E-7 mole/sec/mole fraction) was used as the total release rate from small inner bags (Appendix 6.7 of the CH-TRU Payload Appendices). This value was computed as the difference in values obtained from Tests 9A and 9C. The contribution of bag permeation was not considered in the calculations in order to provide a margin of safety. Results of test 9B demonstrate that the bag permeability for small bags is nearly 80% of the value being used for the bag closure of the small bag.

The lowest measured total release rate (4.67E-6 mole/sec/mole fraction), based on Test 10C, was used as the total release rate from large drum liner bags in the computations of decay heat limits. These release rates serve as inputs to the hydrogen release estimates described in Appendix 6.7 of the CH-TRU Payload Appendices.

6.8.2 Introduction

The purpose of this document is to provide a summary of whole-bag hydrogen release tests that were conducted at Pacific Nuclear Systems, Inc., Richland, Washington. The objective of this test program was to obtain data on the release rates of hydrogen from each of several layers of confinement in drums that simulate the typical packaging configuration of CH-TRU waste.

The scope of the testing program is presented in the next section (6.8.3). A description of the experimental equipment can be found in Section 6.8.4. The details of the experimental procedure that was used are contained within Section 6.8.5. The quality assurance and quality control measures pertinent to the testing program are discussed in Section 6.8.6. The final section contains an analysis and summary of the experimental results.

6.8.3 Test Program

6.8.3.1 Task

The scope of the testing program is to obtain hydrogen release rate data for different configurations that mimic typically packaged CH-TRU waste drums (payload container). For purposes of radiological safety, the CH-TRU waste is packaged in multiple layers of plastic bags that are closed by one of the allowable methods specified in Appendix 3.8 of the CH-TRU Payload Appendices and subsequently placed in a payload container. The payload containers are vented as specified in Section 2.5 of the CH-TRAMPAC.

6.8.3.2 Configuration of Test Drums

The drums used to measure hydrogen release rates were generally configured as follows (from the drum to the innermost layer of confinement):

- 55-gallon drum (with gasket) and with a carbon composite filter installed in drum lid.
- 90-mil rigid high density polyethylene (HDPE) liner, punctured with 0.75"-diameter hole (bung removed).
- One or more layers of plastic bagging.

A detailed description of the test apparatus is presented in the following section.

6.8.4 Equipment Description

The purpose of this section is to describe the equipment that was used in conducting the hydrogen release tests. A schematic diagram of the external test equipment assembly is presented in Figure 6.8-1.
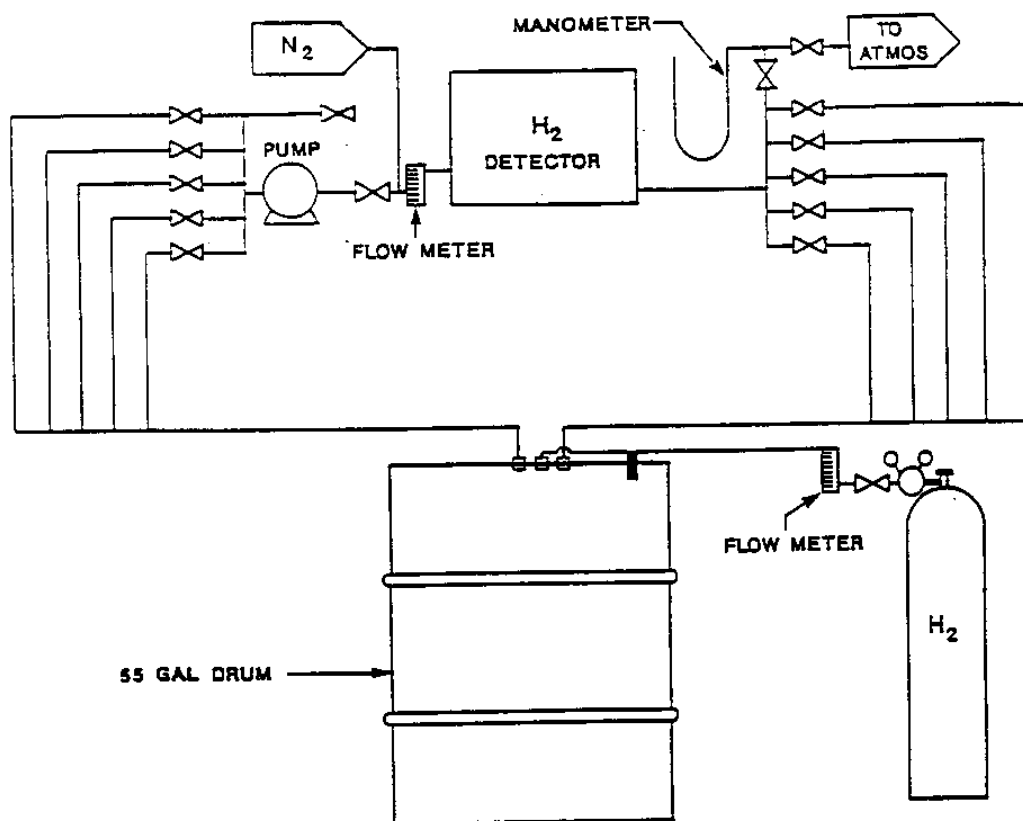
Figure 6.8-1—External Test Equipment Assembly

6.8.4.1 Plastic Bags

The four different types of bags used in the experiments were:

- 9 - 14 mil, 55-gallon PVC O-ring drum liner bag manufactured by Vinyl Tech Inc, used by Rocky Flats Environmental Technology Site (RFETS) and typical of bags used at all sites.

- 10 - 12 mil, 55-gallon PE round-bottom drum liner bag manufactured by the Hedwin Corp, used by RFETS and typical of large drum liner bags used at all sites.

- 9 - 14 mil, PVC bag-out (small inner bag) manufactured by Vinyl Tech Inc., used by RFETS and typical of bags used at all sites to bag-out waste from gloveboxes.

- 5-mil PE (small inner bag) manufactured by Parade Packaging Materials, used at RFETS and typical of bags used at all sites.

6.8.4.2 Drum Liner

This is a rigid, 90-mil, high density polyethylene (HDPE) liner for a 55-gallon drum, which is black opaque with a removable lid and seal. The lid has a 0.75-inch diameter hole near the center of the lid (after removal of the bung).

6.8.4.3 55-Gallon Drum

A drum made of carbon steel and painted white. The drum has a white neoprene rubber gasket between the body and lid. A filter vent is installed in the drum lid.

6.8.4.4 Filter Vents

The specifications for the filter vents are provided in Section 2.5 of the CH-TRAMPAC. The filters are installed in the lids of a drum. The filters release any gases that might be generated in the payload containers, while acting as a barrier for particulates (efficiency in excess of 99.9%). Model numbers and characteristics of the filters used in the hydrogen release tests are:

- Model 012, which is in service at RFETS. Two filters of this model, lot numbers NFT-17 and NFT-21, were used in the tests. The 3/4-inch threaded bung plug is made of mild steel.

- Model 013, which is in service at Savannah River Site (drums) will be used in SWBs. Two filters of this model, lot numbers NFT-9034 and NFT-9035, were used in the tests. The lid to this filter is distinct in that it is suspended 1/16-inch in the air by dimples stamped onto the lid. The 3/4-inch threaded bung plug is made of 304 stainless steel.
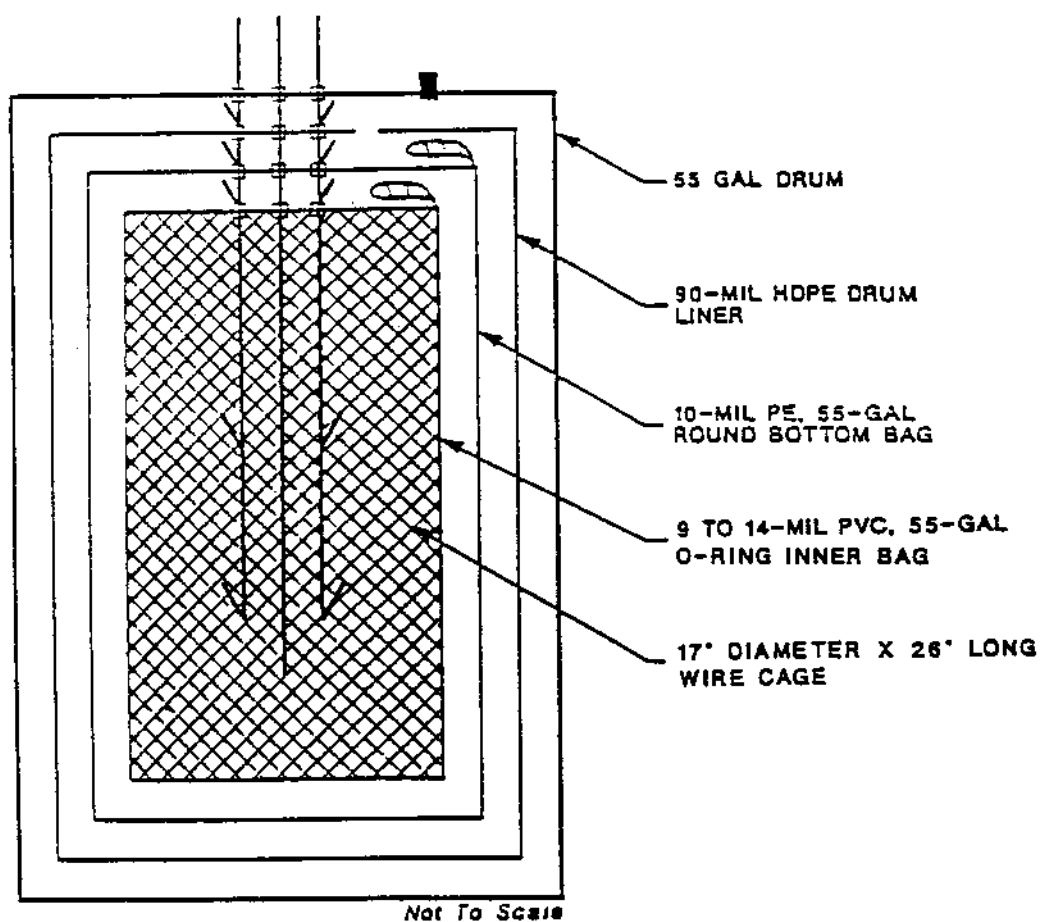
- Model 020, Lot number NFT-E filter, is used at the Idaho National Engineering and Environmental Laboratory and the Nevada Test Site. The 7/16-inch self-tapping threaded plug is made of 303 stainless steel.

6.8.4.5 Whole Drum Configuration

The experiments were set up with one, two, three, or four bags. Examples of the test configurations are shown in Figures 6.8-2 to 6.8-5 for Tests 4 to 7. The shaded areas in the figures represent a three-dimensional cage that was used inside the test apparatus to prevent the bags from collapsing and to sustain their shape. The experimental procedures for the tests are summarized in Table 6.8-1. Table 6.8-1 lists the exact configuration of each test set-up. The parameters that are listed in the table are defined below, in the order in which they appear.

PARAMETER	DEFINITION
Test Number	Uniquely identifies each test. For Tests 4 - 7, the B test was a repeat of the A test.
Temperature At Steady State (^{o}F)	The temperature of the room measured at steady state.
Dimensions (in)	The dimensions of the bag as specified by the manufacturer.
Total Surface Area (sq. ft.)	Effective surface area of bag in test. (Does not include the closure area).
Confinement Layers	The confinement layer configuration for each test. (See next section for a complete description of each layer.)
Filter Type and Number	The filter (identified by model lot and serial numbers) that is installed in the lid of the drum.
Bulkhead -Duct Seal Used/Unused	A yes or no denotes whether duct seal was used to seal the bulkhead connections.
Type of Bag Seal	Denotes whether the method of sealing the bag was twist and tape or heat-sealing (for experimental purposes only).
Notes	Refers to the figure number in this appendix that depicts the confinement layer configuration.

Most of the experiments were set up to simulate typical waste configurations at the sites, except for Tests 9B and 9C that were specifically designed to measure individual components of the release rates (i.e., bag plus bulkhead plus closure, bag plus closure and bag only). The bag used in these tests was heat sealed for the purpose of the experiments. The following descriptions of the components of the test assembly refer to the experimental set up shown in Figure 6.8-1.

55 GAL DRUM

90-MIL HDPE DRUM LINER

10-MIL PE. 55-GAL ROUND BOTTOM BAG

9 TO 14-MIL PVC, 55-GAL O-RING INNER BAG

17" DIAMETER X 26" LONG WIRE CAGE

Not To Scale

LEGEND

■ CARBON COMPOSITE FILTER

☐ BULKHEAD FITTING

SAMPLING TUBING

HORSETAIL-Last 6" of plastic bag tied off with tape (Not heat-sealed)

Figure 6.8-2—Test 4. Confinement Layer Configuration

Figure 6.8-3—Test 5. Confinement Layer Configuration

Not To Scale

55 GAL 17-C DRUM

90-MIL HDPE DRUM LINER

10-MIL PE, 55-GAL ROUND BOTTOM BAG

9 TO 14-MIL PVC, 55-GAL O-RING BAG

17" DIAMETER X 26" LONG WIRE CAGE

5 MIL PE INNER BAG

9 1/2" DIAMETER X 14" LONG WIRE CAGE

9 TO 14- MIL PVC, 55-GAL INNER BAG

LEGEND

CARBON COMPOSITE FILTER

BULKHEAD FITTING

SAMPLING TUBING

HORSETAIL—Last 6" of plastic bag tied off with tape (Not heat-sealed)
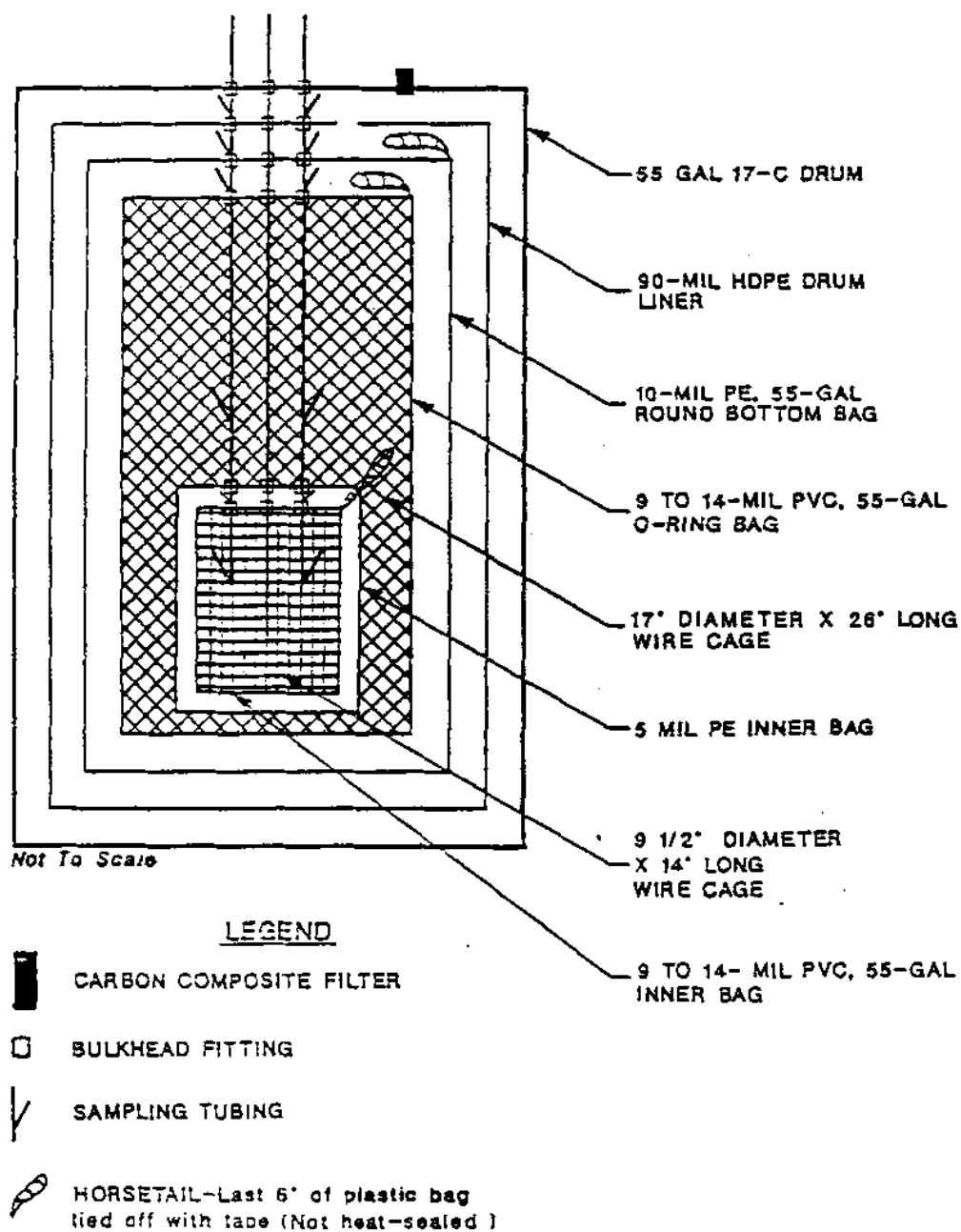
Figure 6.8-4—Test 6. Confinement Layer Configuration

55 GAL 17-C DRUM

90-MIL HDPE DRUM LINER

10-MIL PE, 55-GAL ROUND BOTTOM BAG

9 TO 14-MIL PVC, 55-GAL O-RING BAG

17" DIAMETER X 26" LONG WIRE CAGE

5 MIL PE INNER BAG

10 1/4" DIAMETER X 14" LONG WIRE CAGE

Not To Scale

LEGEND

■ CARBON COMPOSITE FILTER

□ BULKHEAD FITTING

⌿ SAMPLING TUBING

⌀ HORSETAIL—Last 6" of plastic bag tied off with tape (Not heat-sealed)

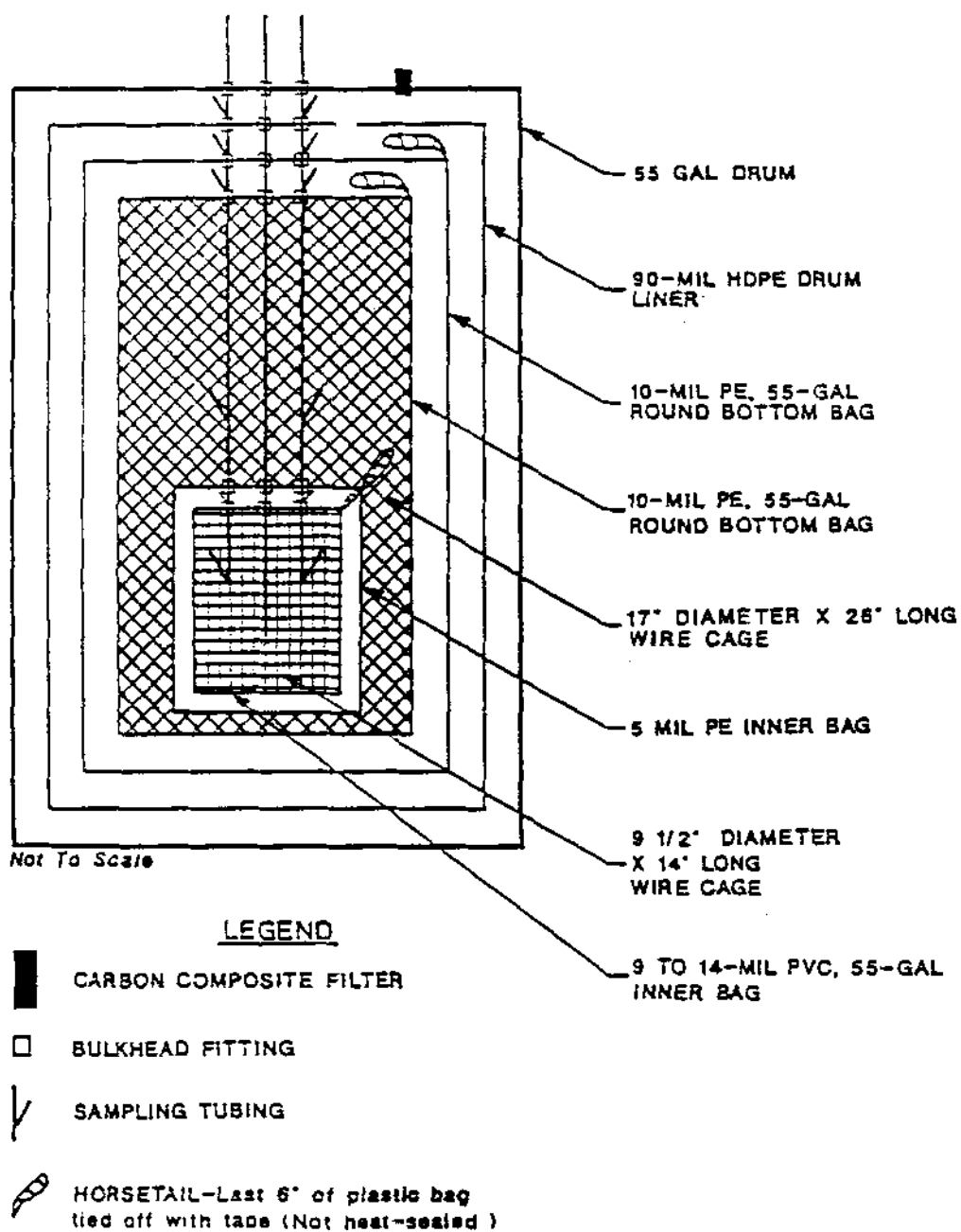**Figure 6.8-5—Test 7. Confinement Layer Configuration**
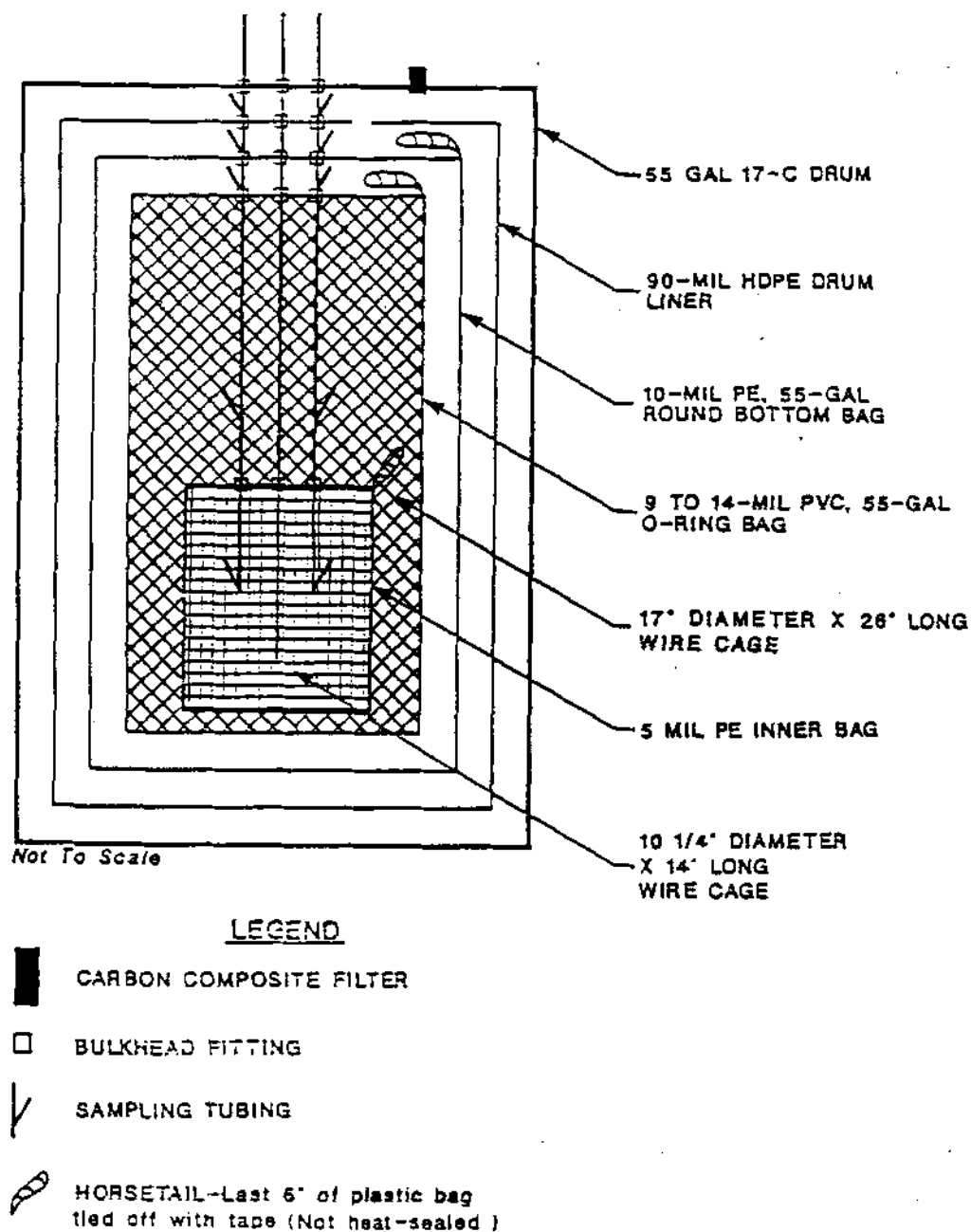
Table 6.8-1 — Test Descriptions

Test Number	Temperature at Steady State (°F)	Dimensions (in.)	Total Surface Area (ft²)	Confinement Layers	Filter Type and Number	Bulkhead Duct Seal Used	Type of Bag Seal	Notes
4A	74.0	36.875 x 86.5 37.625 x 58	36.6 29.4	14 mil PVC liner bag 10 mil PE liner bag 90 mil HDPE drum liner	NFT-E INEL Design	No	Twist and tape closure	Figure 6.8-2
4B	76.0	36.875 x 86.5 37.625 x 58	36.6 29.4	14 mil PVC liner bag 10 mil PE liner bag 90 mil HDPE drum liner	NFT-21 RFP Design	No	Twist and tape closure	Figure 6.8-2
5A	78.0	10 x 72 24.625 x 30.5 37.625 x 58 37.625 x 58	6.3 8.4 29.4 29.4	14 mil PVC inner bag-out 5 mil PE inner bag 10 mil PE liner bag 10 mil PE liner bag 90 mil HDPE drum liner	NFT-21 RFP Design	No	Twist and tape closure	Figure 6.8-3
5B	82.0	10 x 72 24.625 x 30.5 37.625 x 58 37.625 x 58	6.3 8.4 29.4 29.4	14 mil PVC inner bag-out 5 mil PE inner bag 10 mil PE liner bag 10 mil PE liner bag 90 mil HDPE drum liner	NFT-21 RFP Design	No	Twist and tape closure	Figure 6.8-3
6A	68.0	10 x 72 24.625 x 30.5 36.875 x 86.5 37.625 x 58	6.3 8.4 36.6 29.4	14 mil PVC inner bag-out 5 mil PE inner bag 14 mil PVC liner bag 10 mil PE liner bag 90 mil HDPE drum liner	NFT-17 RFP Design	No	Twist and tape closure	Figure 6.8-4
6B	66.0	10 x 72 24.625 x 30.5 36.875 x 86.5 37.625 x 58	6.3 8.4 36.6 29.4	14 mil PVC inner bag-out 5 mil PE inner bag 14 mil PVC liner bag 10 mil PE liner bag 90 mil HDPE drum liner	NFT-21 RFP Design	No	Twist and tape closure	Figure 6.8-4
7A	77.0	24.625 x 30.5 36.875 x 86.5 37.625 x 58	8.4 36.6 29.4	5 mil PE inner bag 14 mil PVC liner bag 10 mil PE liner bag 90 mil HDPE drum liner	NFT-17 RFP Design	No	Twist and tape closure	Figure 6.8-5
7B	71.0	24.625 x 30.5 36.875 x 86.5 37.625 x 58	8.4 36.6 29.4	5 mil PE inner bag 14 mil PVC liner bag 10 mil PE liner bag 90 mil HDPE drum liner	NFT-17 RFP Design	No	Twist and tape closure	Figure 6.8-5
9A	70.0	10 x 72	6.3	14 mil PVC inner bag-out	NFT-17 RFP Design	No	Twist and tape closure	

Table 6.8-1 — Test Descriptions (Concluded)

Test Number	Temperature at Steady State (°F)	Dimensions (in.)	Total Surface Area (ft²)	Confinement Layers	Filter Type and Number	Bulk Head Duct Seal Used	Type of Bag Seal	Notes
9B	50.0	10 x 72	6.3	14 mil PVC inner bag-out	NFT-9035 SRP Design	Yes	Heat sealed	
9C	59.0	10 x 72	6.3	14 mil PVC inner bag-out	NFT-9035 SRP Design	No	Heat sealed	
10A	10.0	37.625 x 58	29.4	10 mil PE liner bag	NFT-17 RFP Design	Yes	Twist and tape closure	
10B	–18.0	37.625 x 58	29.4	10 mil PE liner bag	NFT-17 RFP Design	Yes	Twist and tape closure	
10C	57.0	37.625 x 58	29.4	10 mil PE liner bag	NFT-9034 SRP Design	Yes	Twist and tape closure	
11A	63.0	36.875 x 86.5	36.6	14 mil PVC liner bag	NFT-21 RFP Design	Yes	Twist and tape closure	

6.8.4.6 Sampling Tubing

Small diameter (0.125-inch O.D., 0.08-inch I.D.) Nylaflow tubing is used to penetrate the confinement layers to allow recycling of gas to measure H_2 concentration in confinement layers and to input H_2 into the innermost confinement layer.

6.8.4.7 Manometer

A water-filled manometer measures the pressure inside each confinement layer or void volume to a sensitivity of 0.1 inch of water. These measurements were discontinued once it was established that there is no pressure differential across any of the layers of confinement.

6.8.4.8 Hydrogen Cylinder and Two-Stage Regulator

A hydrogen cylinder (high purity), fitted with a two-stage regulator model #TSA-15-350, provides a steady flow of H_2 irrespective of changes in pressure inside the cylinder. Both of these items are manufactured by Oxarc Inc., Pasco, Washington.

6.8.4.9 Hydrogen Rotameter Assembly

A precision flowmeter, model FL-310, manufactured by Omega Engineering, Stanford, Connecticut, provides a flow rate of 0.03 to 30 ml/minute of H_2 at ambient temperature and pressure to the innermost bag confinement layer.

6.8.4.10 Bulkhead Fittings

All plastic (Nylaflow) tubing used to sample head spaces in layers of confinement were guided through bulkhead fittings to provide leak-tight seals. A combination of plastic, threaded bulkhead fittings with neoprene seal rings and multi-tube compression fittings (i.e., conax type) are used to prevent leakage of gases between confinement barriers around tubing penetrations. These fittings were supplied by Harrington Plastics, Seattle, Washington.

For the initial tests (Tests 4, 5, 6, and 7), a bubble test was used to detect any leaks that may occur around the bulkhead fittings. For the quantification of minimum release rates, the bubble test proved to be inadequate, and a special duct seal was used around the bulkheads to completely seal all possible areas of gas leakage. An independent study, utilizing Freon gas and commercial leak detection equipment, confirmed that with the duct seal, the system did not have any detectable gas leaks. The details for each individual test are summarized in Section 6.8.7.

6.8.4.11 Hydrogen Analyzer

A Beckman Model No. 6139-1-1-0-0-1-000 thermal conductivity analyzer is used for detecting hydrogen in nitrogen mixtures in the range of 0-5 percent by volume. The sensitivity of these detectors is ±0.05 percent H_2 by volume.

6.8.4.12 Gas Manifolds

Two valve manifolds are used for directing the flow from each of the different sample lines through the hydrogen analyzer (Figure 6.8-1).

6.8.4.13 Pump

A rotary, peristaltic, tygon tubing pump shown in Figure 6.8-1 is used for recirculating the atmosphere of each void volume between confinement layers. After aligning the appropriate inlet and return valves, the pump draws the gas out of a selected void volume and discharges it through the hydrogen analyzer (to measure H_2 concentration). The exhaust from the analyzer is returned (recycled) back to the same void volume through a gas diffuser.

6.8.4.14 Gas Diffuser

A porous plastic gas diffuser is used on each sample return line to reduce the gas velocity at the tubing exit.

6.8.4.15 Nitrogen Supply

Nitrogen gas is used for purging the atmosphere within the test drum and within each bag at the initiation of the experiment.

6.8.4.16 Nitrogen Purged Filter Vent Assembly

The open end of an inverted plastic beaker is sealed to the surface of the drum lid, covering the drum filter vent. A stream of nitrogen gas will continually purge the beaker to prevent the diffusion of air into the drum during testing. A small hole in the closed end of the beaker will allow introduction of a nitrogen purge tube and escape path for nitrogen purge.

6.8.4.17 Timer Solenoid H_2-Flow Control

A programmable timer, electric solenoid, and air-operated bellows valve system automatically control the H_2 flow rate. The timer can be programmed to supply H_2 for a desired amount of time per time period. This allows very low flow rates of H_2 to be supplied to the innermost bag. If the hydrogen flow is below the rotameter range or if the rotameter accuracy/repeatability is in question over a given hydrogen flow range, the hydrogen metering valve and regulator pressure

can be set at a fixed setting and the timer on/off cycle can be varied to provide the desired hydrogen injection rate. These are all manufactured by Seattle Valve and Fitting, Bellevue, Washington.

6.8.5 Experimental Procedure

6.8.5.1 General Requirements

The general requirements for all of the hydrogen release tests can be summarized as follows:

- All fittings for tubing penetrations into confinement layers are ensured to be gas tight in order to prevent leakage of hydrogen. For initial experiments, a soap bubble test was used for all fittings. Additional testing demonstrated that the seal in the bulkheads was not adequate. Starting with Test 9B, duct seal is used in all experiments to prevent any gas leakage around fittings.

- The atmosphere within the test drum and within each void volume is purged and replaced by inert nitrogen prior to the introduction of hydrogen for safety purposes.

- Hydrogen is injected into the inner bag until a concentration of 5 volume percent is attained. The hydrogen supply is turned off and the inner bag void volume is allowed to decay to four percent. The purpose of this is to obtain an approximate estimate of the hydrogen release rate from each layer.

- Hydrogen gas concentration is analyzed at regular time intervals from each void volume and recorded. Utilizing the timer and the hydrogen solenoid valve, the flow rate of hydrogen is adjusted to achieve steady state at 4 percent in the inner bag.

- The test is terminated when steady state is achieved in all void volumes between confinement layers with a concentration of approximately 4 percent in the innermost bag. The test is continued for approximately 12 hours after steady state conditions are achieved.

For each test, the pertinent information is recorded on a "Datasheet." A copy of a sample Datasheet is included as Table 6.8-2. In addition to the parameters listed on the Datasheet, the confinement layer configuration (i.e., type and number of bags), vendor, and sizes are also included to completely define each test.

The following sections describe the detailed experimental procedure that was followed for each test.

Table 6.8-2 — Example Datasheet For Hydrogen Release Experiments

Time	Sample	H$_2$ Conc. (% Vol)	Pressure Static	Baro. (in of H$_2$O)	Temp. (F^o)	Observations/Initials
2/1/89						
0000	Drum	1.14			70	
	Inner Bag	3.99				
0800	Drum	1.15			69	
	Inner Bag	3.99				
1000	Drum	1.15			72	
	Inner Bag	3.99				
2330	Drum	1.15			71	
	Inner Bag	3.99				

Date   HYDROGEN RELEASE TEST FOR TYPICAL
          RFETS CH-TRU DRUM

6.8.5.2 Installation of the Gas Flow Tubing

- Make the penetrations through confinement layers and install the bulkhead fittings and sample tubes through the drum lid, drum liner lid (if used), and each bag.

- Install a gas diffuser on the end of each sample return line in the bags.

- Label the outside ends of the tubing.

- Assemble the appropriate bag configuration system for each test per instructions (list of tests is in Table 6.8-1).

- Place the appropriate bag system adjacent to the drum liner lid and place the drum liner lid adjacent to the 55-gallon drum.

- Adjust the tubing lengths so that they are placed in the desired area of the appropriate bag or container lid. Tighten the compression fitting nut on the tubing seals approximately 1/3 turn from hand tight. Then apply duct seal putty to all bulkhead fittings if applicable to the particular test.

- Verify that the outside end of each tube is attached to the appropriate connection on the gas manifolds. Cycle the gas flow pump to ascertain that unrestricted flow can occur through each tube.

6.8.5.3 Closure of the 55-gallon Drum

- Cut the small 14-mil PVC bag-out bag in concurrence with dimensions of the bag listed in Table 6.8-1 and insert a rigid frame (wire cage) inside the bag to maintain the size of the bag for Tests 5, 6, 9, and 11. For Tests 4 and 7, cut the 14-mil PVC 55 gallon O-ring drum liner bag as identified in Table 6.8-1 and insert rigid frame inside the bag to maintain the size of the bag (Figures 6.8-2 to 6.8-5 show typical configurations of these bags). Utilize maximum size frame in all cases. For Test 7, place maximum size frame inside the 5-mil PE bag. Record dimensions and details of frame construction on Datasheet.

- Place wire frame inside third bag to support bag volume around inner and second bag for Tests 5 and 6. For Test 7, place the second wire frame inside second bag to support bag volume around the inner bag. Record dimensions and details of frame construction on Datasheet.

- Insert nitrogen purge tube into bottom of each bag. Purge for five to ten minutes. Remove purge tube and then, if not a heat-sealed bag (only experiments 9B and 9C), make a twist-and-tape closure as follows:

    — Twist top 6 inches of bag into "horsetail" closure. Twist the 55-gallon PVC O-ring bag and the 55-gallon PE round-bottom bag each four turns at 180 degrees

each. Twist both the small PVC bag-out bag and the small PE bag six turns at 180 degrees each.

— Hold the twisted end, tape around the horsetail, starting at the bag end of the twist and wrapping in upward spirals until the end of the horsetail is reached. Continue wrapping up and down horsetail until three or four layers of tape have been reached.

— Repeat nitrogen purge and seal open end of each bag used as per Table 6.8-1.

- Insert carefully the bags with internal frames inside the 90 mil rigid liner if used (refer to Table 6.8-1). Install the lid of the 90-mil liner on top of the liner and snap it into place. Adjust tubing lengths through bulkhead fittings and tighten the compression fitting nut on the tubing seals approximately 1/3 turn from hand tight. Then apply duct seal to bulkhead fittings as per the individual test procedure.

- Guide all the sampling lines through the holes in the lid for the 55-gallon drum as the lid is placed and secured to the top of the 55-gallon drum. After placement of the 55-gallon drum lid, adjust tubing lengths through the bulkhead fittings and tighten the compression fitting nut on the tubing seals approximately 1/3 turn from hand tight. Do not kink or crimp the nylon tubing.

- Test the manifolds for any leaks.

6.8.5.4 Purging of Drum

- Start nitrogen purge of drum and 90-mil rigid drum liner by removing drum bung and connecting nitrogen supply to drum return tubing and 90-mil drum liner inlet tubing. Establish flow of nitrogen into drum cavity while performing the next step. Adjust the nitrogen flow to produce noticeable flow of nitrogen out of the open bung hole.

- Place inverted plastic beaker on top center of drum lid and seal with RTV or duct seal. Insert N_2 purge tube through small hole in top of beaker.

- Isolate nitrogen purge on drum and 90-mil drum liner and reinstall bung in drum lid.

- Test static pressure inside each bag void volume with water manometer. Record on Datasheet. Open return valves as required to vent all bags to atmosphere until pressure inside each bag is less than 1/8-inch water prior to starting test. Following commencement of test no static pressure readings are required.

6.8.5.5 Testing of Drum

- Record actual flowrate of hydrogen or timer interval on Datasheet. The source of hydrogen for the experiment will be a cylinder with a two-stage regulator that will

provide a large decrease in pressure to the rotameter and help stabilize the flowrate as the pressure in the cylinder decreases with usage. The two-stage regulator will be connected to the hydrogen rotameter.

- Verify zero and span calibration of hydrogen monitor as described in Section 6.8 by connecting calibration gas to the nitrogen inlet of the hydrogen monitor. Record data on Datasheet.

- Sample for gas analysis from each void volume at periodic intervals as follows. Three samples per day at approximately 8-hour intervals until steady state is reached. Record data on Datasheet.

- Turn off or reduce the hydrogen supply after the inner bag attains 4.5 to 5% hydrogen and allow the system to decay to approximately 4%. Initiate hydrogen gas input into the inner bag to sustain a 4% hydrogen level. Utilizing the timer and hydrogen solenoid valve, adjust flowrate to achieve steady state at 4% in inner bag. Terminate test when steady state is achieved in all void volumes with a concentration of around 4% in the innermost bag for 12 consecutive hours.

6.8.5.6 Sampling of Gases

- The sampling procedure is based upon the following operational parameters of the Beckman Thermal Conductivity Analyzer. Important operating parameters are:

  — A sample of nitrogen gas should always be flowing through the hydrogen monitor, except during valve manipulations.

  — A flow of 100 to 200 cc/min of sample gas is required during recirculation of gas within a layer of confinement void volume.

  — If sample gas flow must be interrupted for more than 1 hour, it will be necessary to turn off the hydrogen monitor. Operations should be planned to avoid deenergizing the hydrogen monitor to prevent delays caused by heat up stabilization and recalibration.

  — The sampling order is:
     1. Drum
     2. Drum Liner
     3. Large Bag
     4. Second Large Bag (If used)
     5. Inner Bag
     6. Bag-out Bag

- Sample all void volumes as follows:
  — Verify hydrogen meter reads zero percent. If meter is more than 0.05 percent off zero, recalibrate as described in next section.

— Isolate nitrogen purge gas to monitor by closing upper nitrogen valve and then close gas out valve on return manifold.

— Record temperature at each recording on Datasheet.

— Turn on sample pump to 35% to 45% speed to provide 100 to 200 cc/min sample gas flow through monitor. Open and then close appropriate inlet and return valves for desired void volume to allow sample gas to flow through manifold. Continue sample gas flow for 1 to 5 minutes until hydrogen monitor stabilizes. Record hydrogen concentration on Datasheet.

— After all void volumes are sampled, verify that all sample valves are closed and the pump is on.

— Open gas-out and manometer valves and throttle open lower nitrogen valve to provide nitrogen purge flow (10-50 cc/min) to pump and monitor through the inlet manifold.

— Close lower nitrogen valve (inlet manifold) and then stop sample pump.

— Throttle open upper nitrogen valve to provide a continuous nitrogen purge (10-50 cc/min) to monitor. Verify purge flow is directed to inverted beaker on top of drum.

• Repeat the sampling of gases per schedule.

• Repeat calibration check on hydrogen monitor as described in the next section.

6.8.5.7 Calibration Check

• Check calibration of hydrogen monitor with known calibration gas (5 percent hydrogen by volume in nitrogen) as follows:

— Verify hydrogen monitor reads zero percent with nitrogen purge gas at 50-200 cc/min to monitor. Rezero by changing zero dial as required.

— Disconnect nitrogen inlet to monitor and connect calibration gas.

— Meter in calibration gas carefully and stabilize flow at 50-200 cc/min. Allow monitor to stabilize, one to five minutes. Recalibrate monitor to full scale (5 percent) by changing span dial, as required. Record hydrogen concentration on Datasheet.

— Isolate calibration gas and disconnect.

6.8-19

— Reinstall nitrogen purge tubing and valve in nitrogen purge flow (10-50 cc/min) to monitor.

6.8.6 Quality Assurance and Quality Control

6.8.6.1 Documentation

The following information is recorded throughout the test program for each test on the Datasheet:

- Chronological log with time at each sampling

- Hydrogen concentrations within each containment layer void volume at each sampling

- Temperature in the testing room at each sampling

- Any visual observations.

6.8.6.2 Verification of Rotameter Calibration

The hydrogen rotameter factory calibration is verified by flowing hydrogen through the rotameter into a water-filled, inverted graduated cylinder provided with a water seal.

6.8.6.3 Verification of Hydrogen Monitor Calibration

The hydrogen monitor (i.e., Beckman thermal conductivity analyzer) calibration should be verified as described in Section 6.8.5.7 at the beginning and end of the test, or more frequently if sufficient drift in the calibration is observed. Record the hydrogen calibration check on the Datasheet.

6.8.7 Analysis of Experimental Data

6.8.7.1 Testing Program Versus Waste Generation Procedures at Sites

The testing program described here has been formulated to obtaining release rates of hydrogen through systems that were representative of real waste, but with a margin of safety. The bag closure methods used in these tests (described in Section 6.8.5.3), for example, are more stringent (tighter wrapping and more layers of plastic tape) than what is usually practiced at the sites. The tie off procedure in the tests is usually carried out by two individuals in order to obtain as tight a closure as possible. Independent (and qualitative) tests were also performed using easily detectable gases (i.e., Freon) to verify that variations in closure methods including double bent tie offs are not less restrictive than the procedure used for closure during the testing. Soap bubble tests were also performed to determine the relative amount of release through the closure.

All of these tests showed that in most cases, the leakage of hydrogen through the closure was the dominant release mechanism. At some of the U.S. Department of Energy sites, two or more of the bags are sometimes tied off in single tieoffs, which should further increase the release of hydrogen (compared to two layers with independent closures). Results from these tests are therefore expected to provide a reasonable margin of safety in estimating release rates of hydrogen.

6.8.7.2 Determination of Release Rates

6.8.7.2.1 Introduction

The tests were terminated when steady state conditions were achieved, i.e., when the hydrogen volume percentages remained constant in all void volumes. Figures 6.8-6 through 6.8-20 are plots of the hydrogen concentration in each of the bag layers in a given test versus time. The test numbers can be correlated with the test configuration through Table 6.8-1. When steady state conditions are achieved, the hydrogen concentrations in the different layers do not change with time. The figures also serve to highlight the relative resistances of the different layers to the release of hydrogen. Higher the gradient of hydrogen across a barrier, higher is its resistance. For example, from Figure 6.8-8, it can be seen that the concentration gradient of hydrogen across the liner is very small. This is because the punctured liner offers very little resistance to the release of hydrogen compared to the other bag layers.

Once steady state is achieved, the molar flowrates of hydrogen across each of the confinement layers are equal to each other and to the hydrogen generation rate (simulated in the tests by injection of a controlled stream of hydrogen). The flowrate across a layer is equal to the product of the hydrogen release rate and the mole fraction difference across a layer of confinement. The gas injection rate was converted from a volumetric flowrate in (ml/hr) to a molar flowrate in (mole/sec) via the ideal gas law equation. The pressure was assumed to be atmospheric (i.e., 1 atm.). The temperature at steady state for each test was used in the ideal gas law equation.

The release rate for a confinement layer was therefore computed using the following relation:

$$R_r = \frac{CG \, x \, P/(RT) \, x \, hr/3600 \, \text{sec}}{Delta \, x}$$

where,

R_r	=	Release rate from a confinement layer (mole/sec)
CG	=	Hydrogen gas injection rate (ml/hr)
P	=	Atmospheric pressure (1 atm)
R	=	Gas law constant (82.054 atm*ml/mole*K)
T	=	Absolute temperature at steady state (K)
Delta x	=	Volume (mole) fraction hydrogen gradient across the confinement layer.

Figure 6.8-6—Hydrogen Concentration Profiles in Confinement Layers, Test Number 4A

TIME (HRS)

H2 CONCENTRATION (% in N2)

[ ] Inner Liner   + Outer Liner   ◇ Drum Liner   △ Drum

Figure 6.8-7—Hydrogen Concentration Profiles in Confinement Layers, Test Number 4B

Figure 6.8-8—Hydrogen Concentration Profiles in Confinement Layers, Test Number 5A

Figure 6.8-9—Hydrogen Concentration Profiles in Confinement Layers, Test Number 5B

Figure 6.8-10—Hydrogen Concentration Profiles in Confinement Layers, Test Number 6A

Figure 6.8-11—Hydrogen Concentration Profiles in Confinement Layers, Test Number 6B
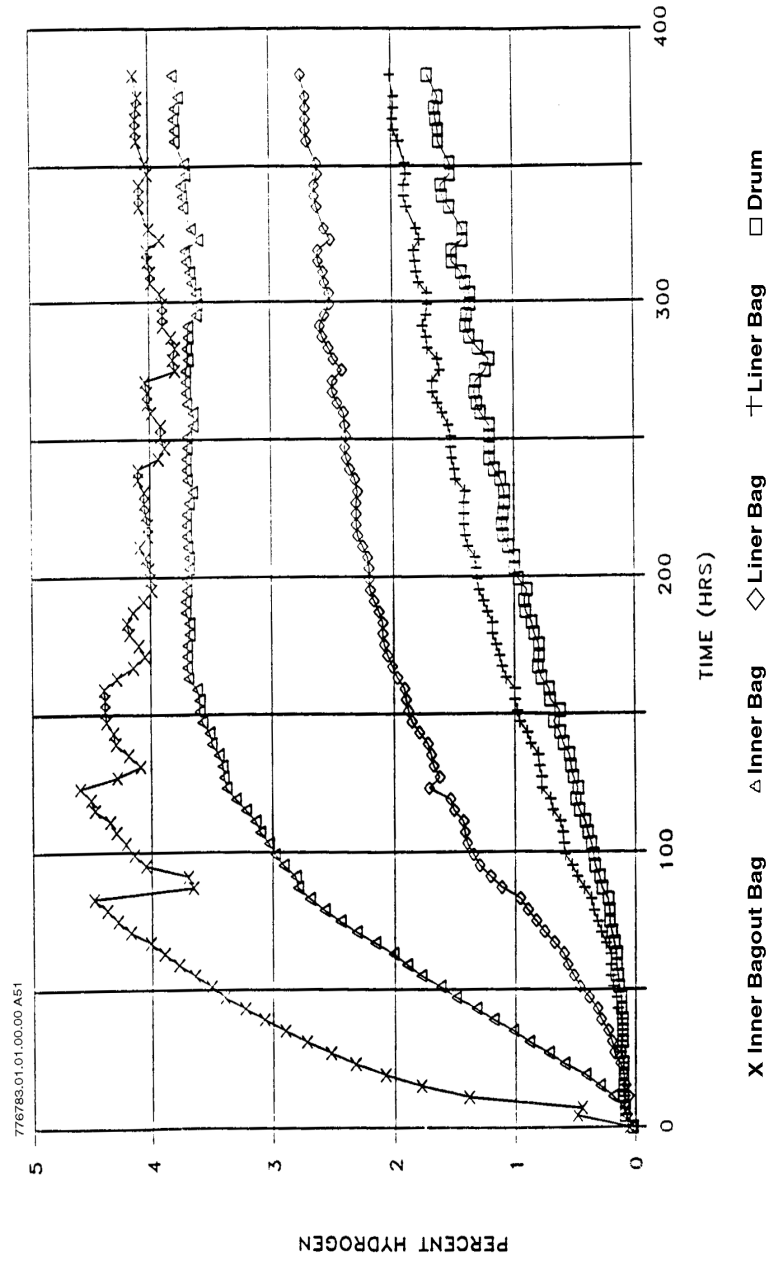
Figure 6.8-12—Hydrogen Concentration Profiles in Confinement Layers, Test Number 7A
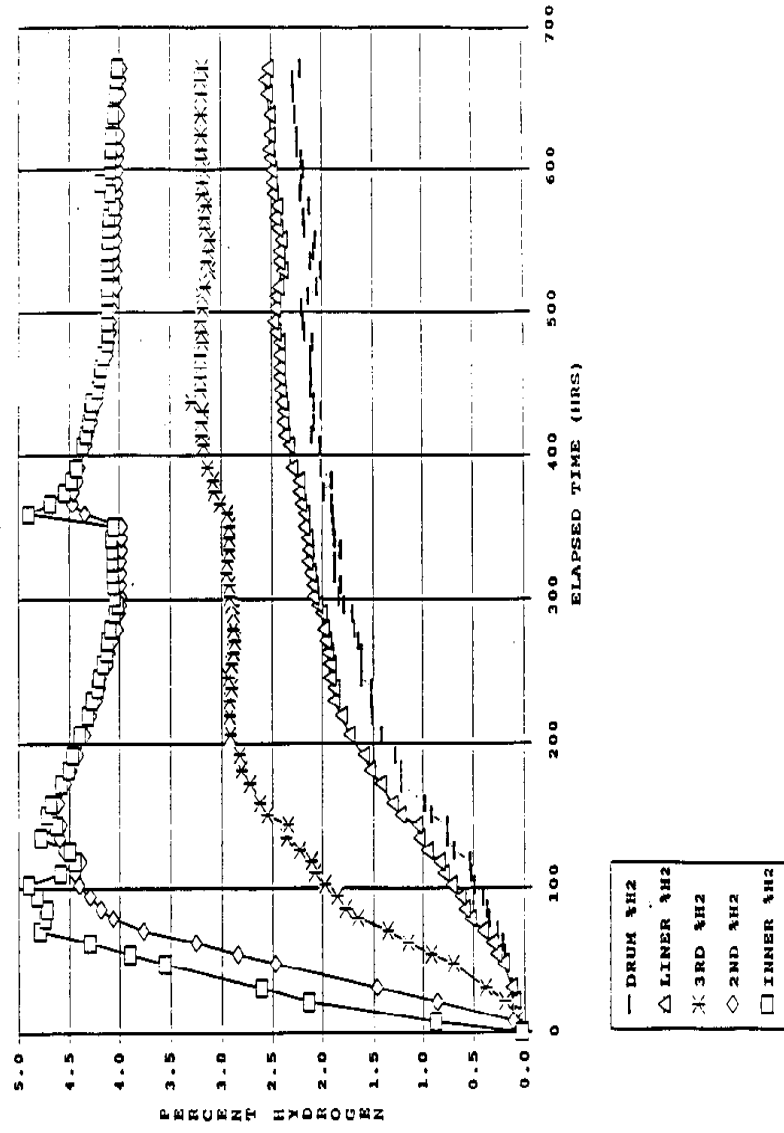
Figure 6.8-13—Hydrogen Concentration Profiles in Confinement Layers, Test Number 7B
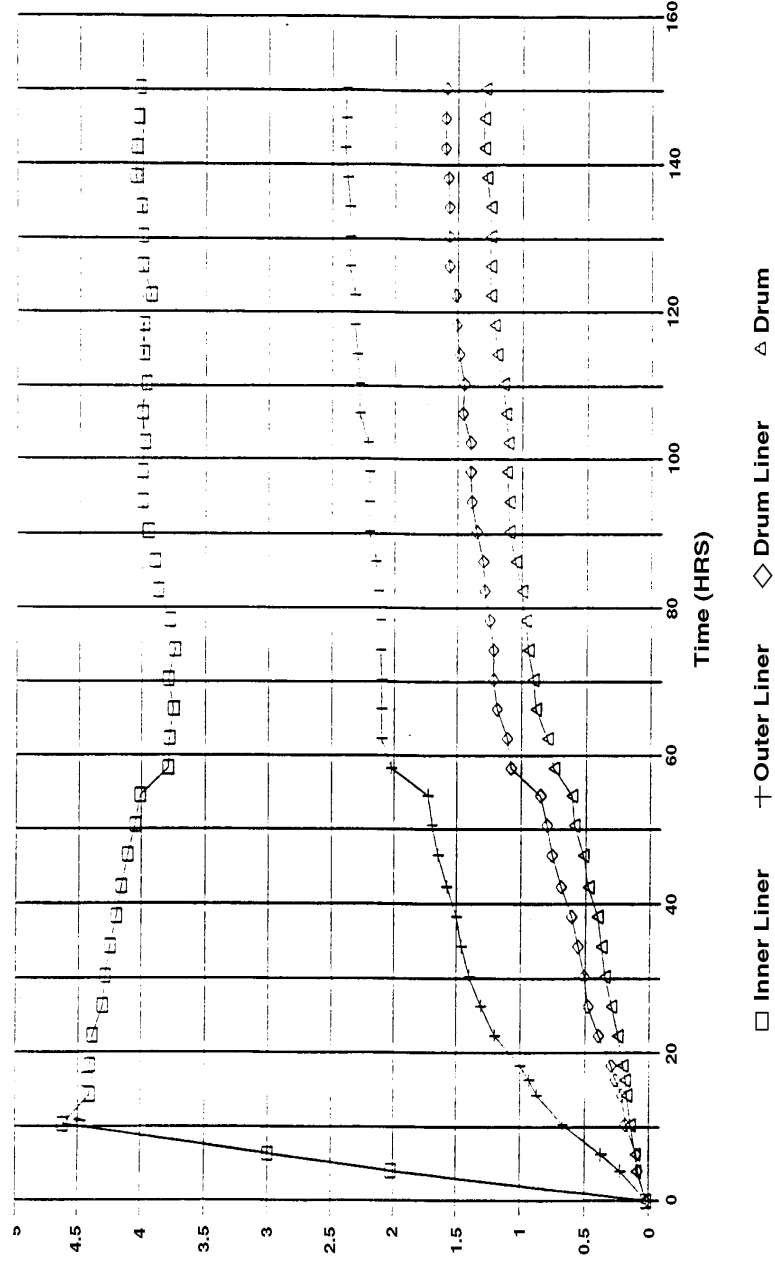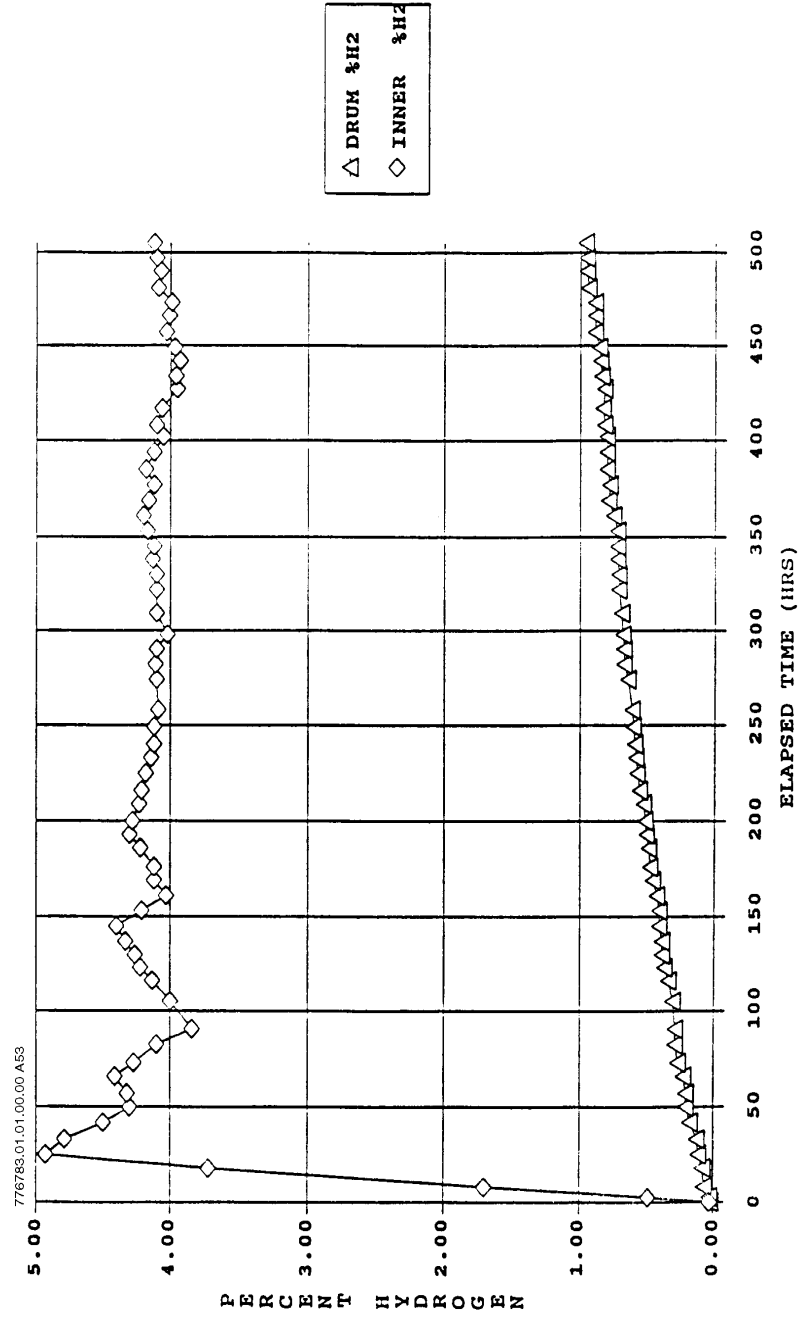
Figure 6.8-14—Hydrogen Concentration Profiles in Confinement Layers, Test Number 9A

Figure 6.8-15—Hydrogen Concentration Profiles in Confinement Layers, Test Number 9B
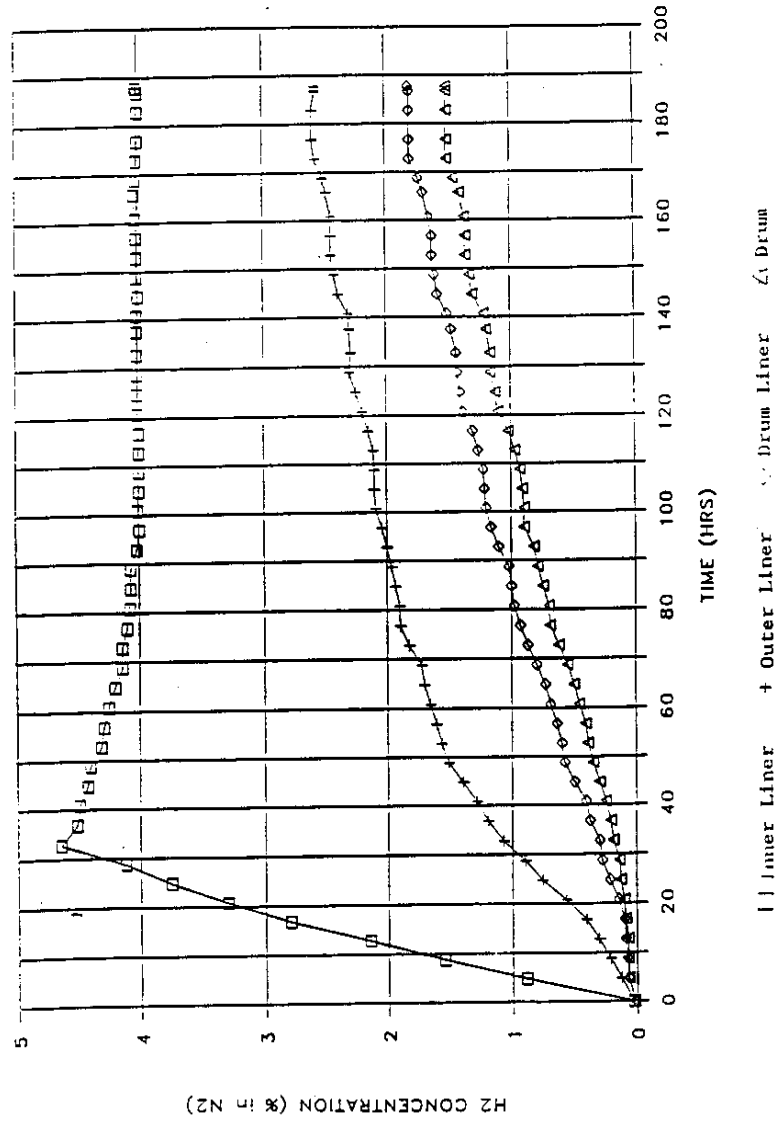
Figure 6.8-16—Hydrogen Concentration Profiles in Confinement Layers, Test Number 9C

Figure 6.8-17—Hydrogen Concentration Profiles in Confinement Layers, Test Number 10A
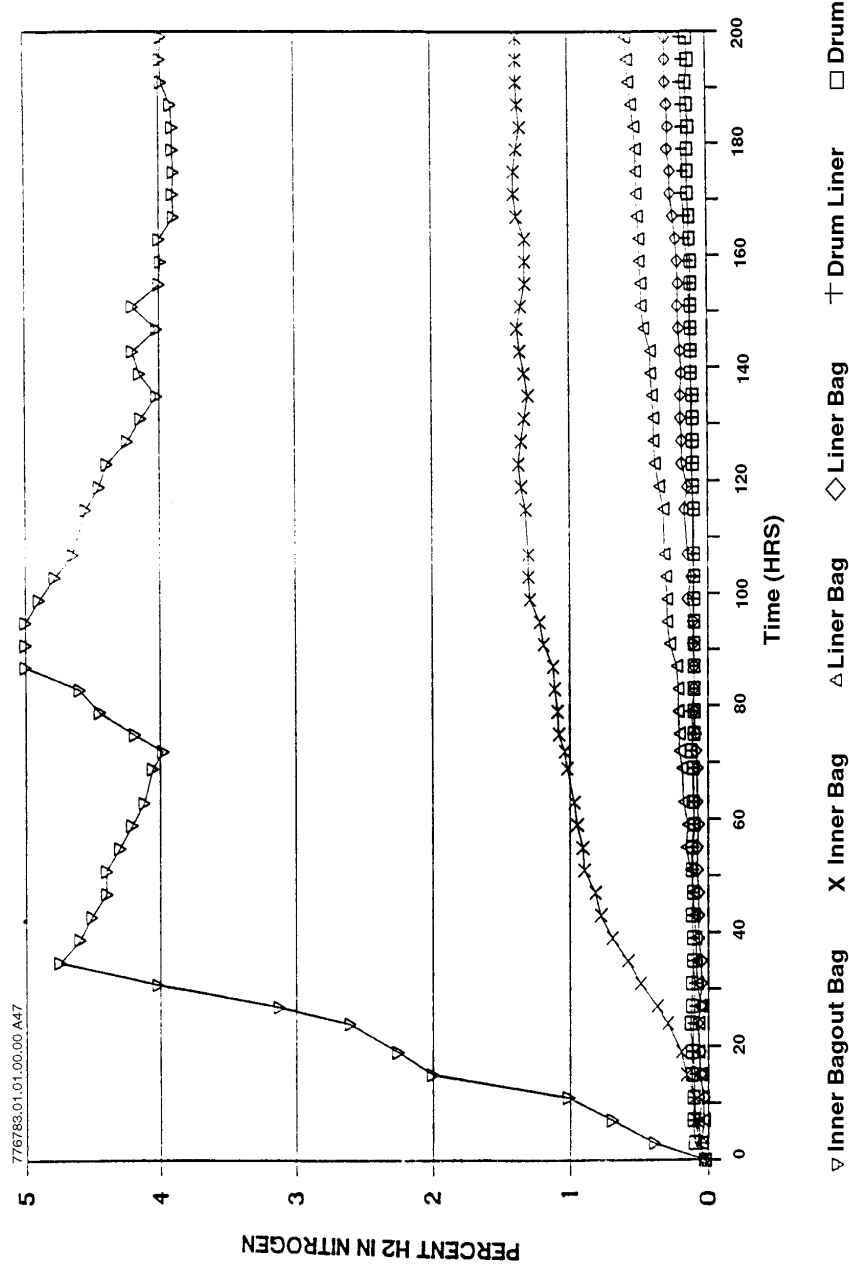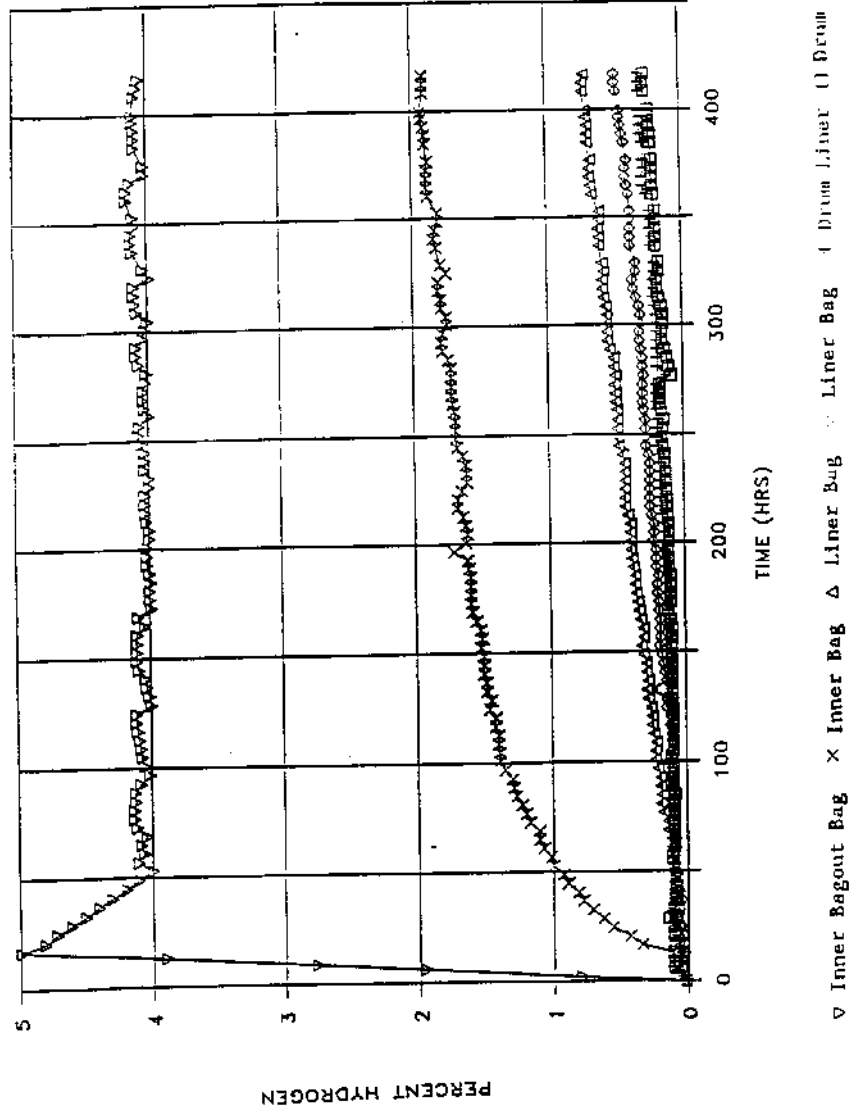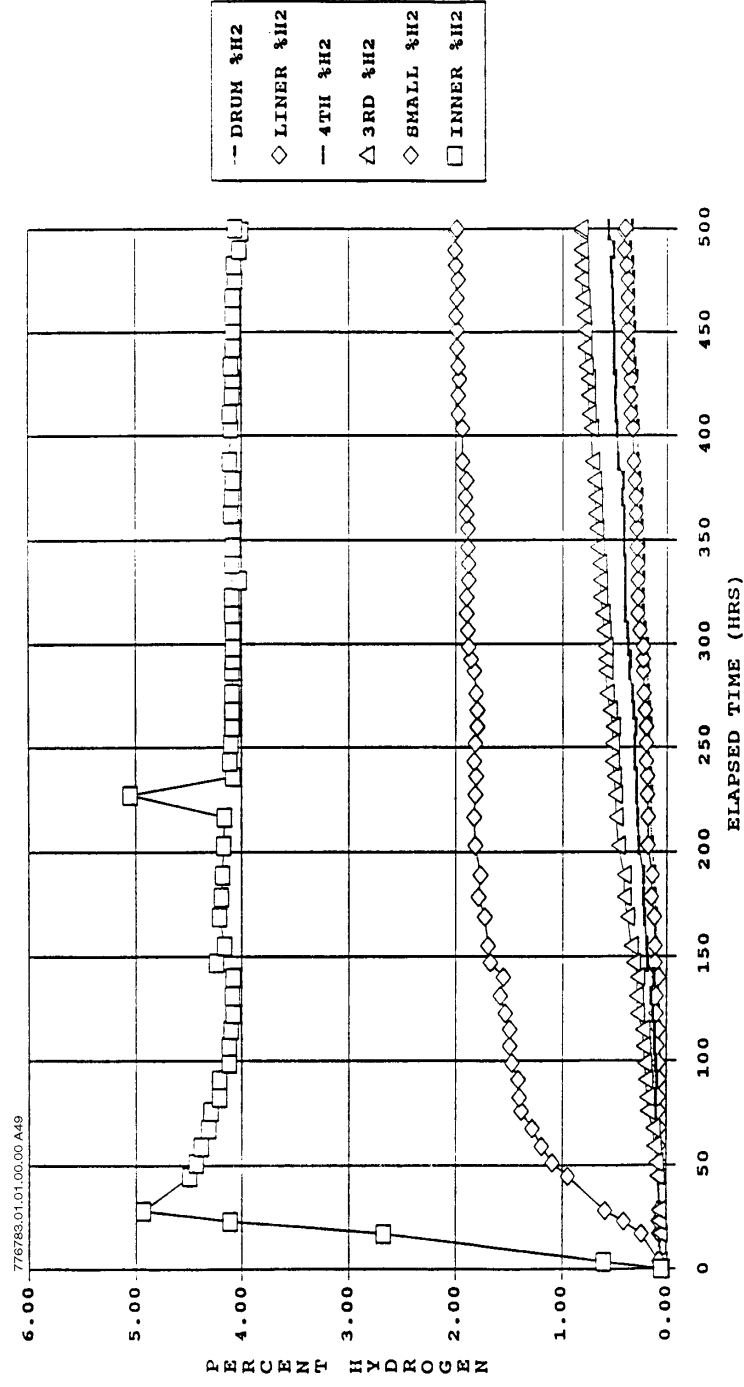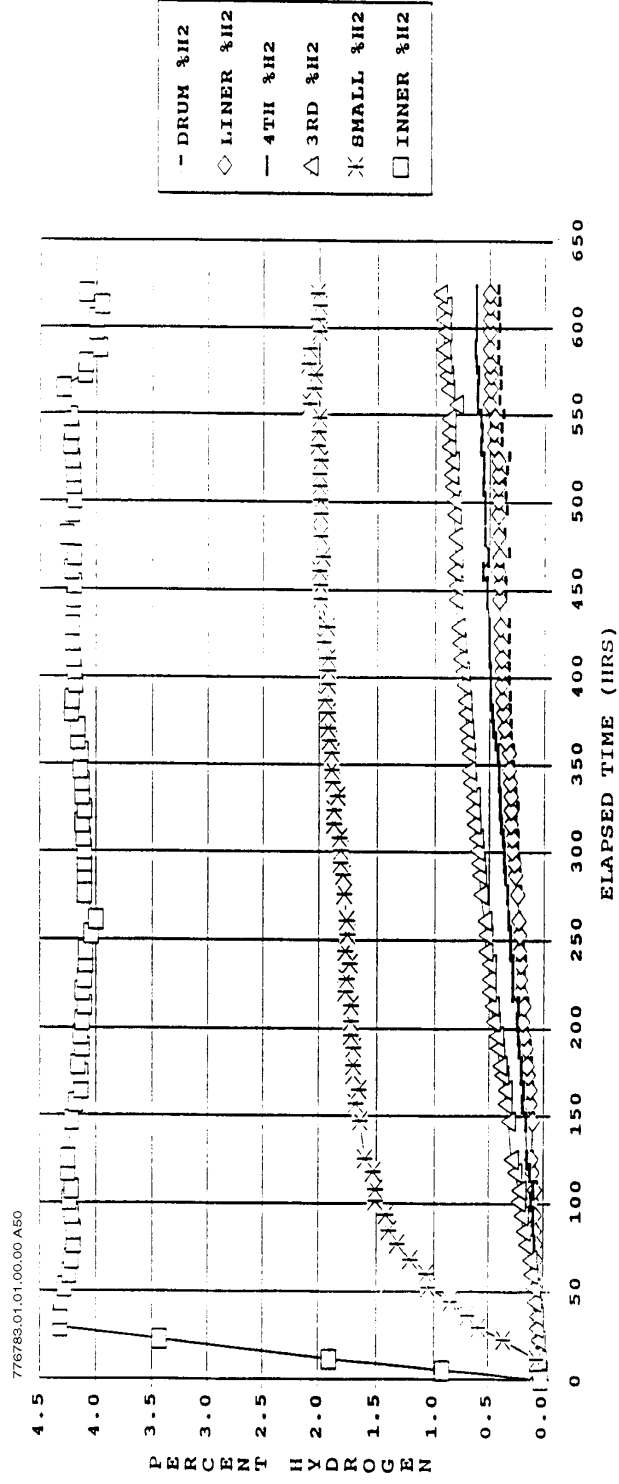
6.8-33

Figure 6.8-18—Hydrogen Concentration Profiles in Confinement Layers, Test Number 10B

6.8-34

Figure 6.8-19—Hydrogen Concentration Profiles in Confinement Layers, Test Number 10C

6.8-35

Figure 6.8-20—Hydrogen Concentration Profiles in Confinement Layers, Test Number 11A
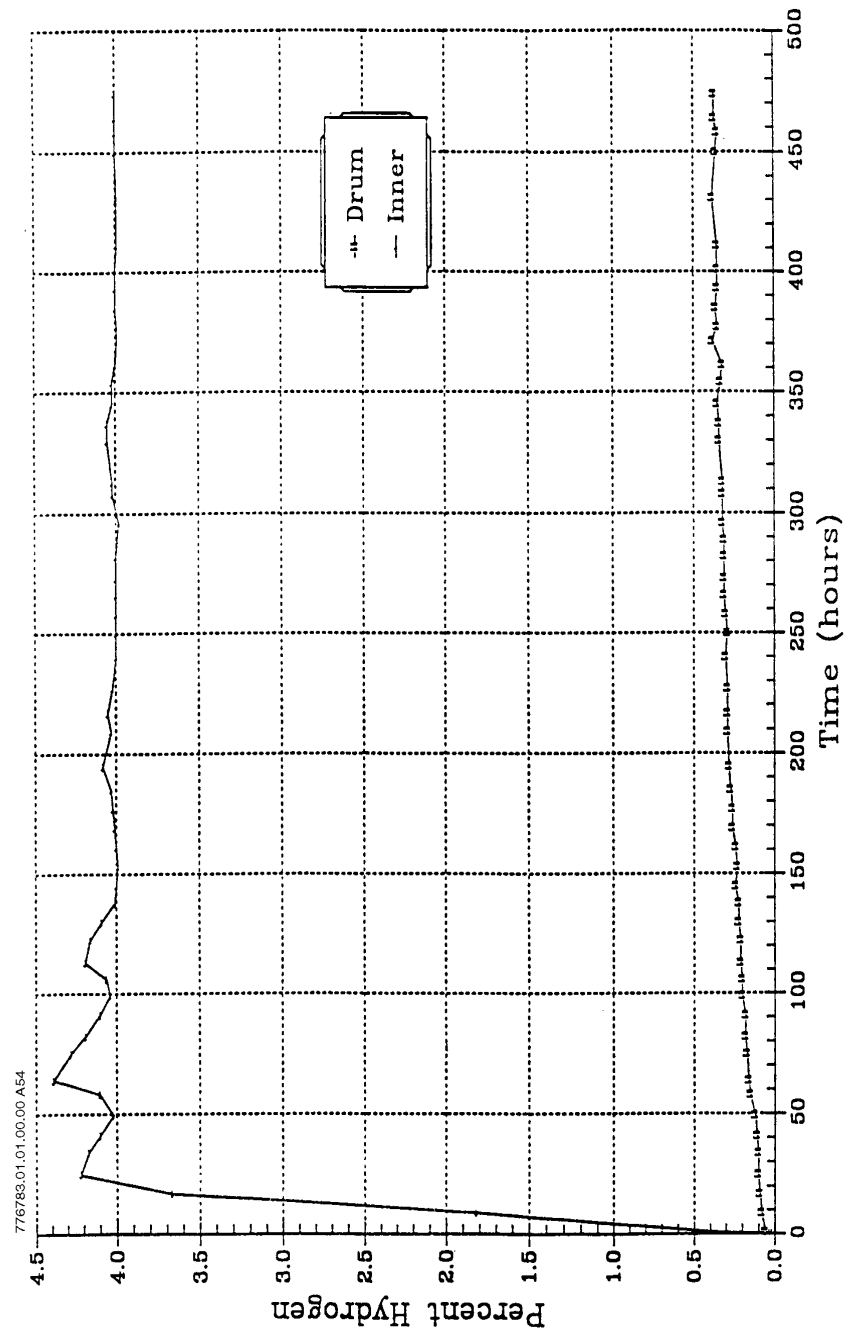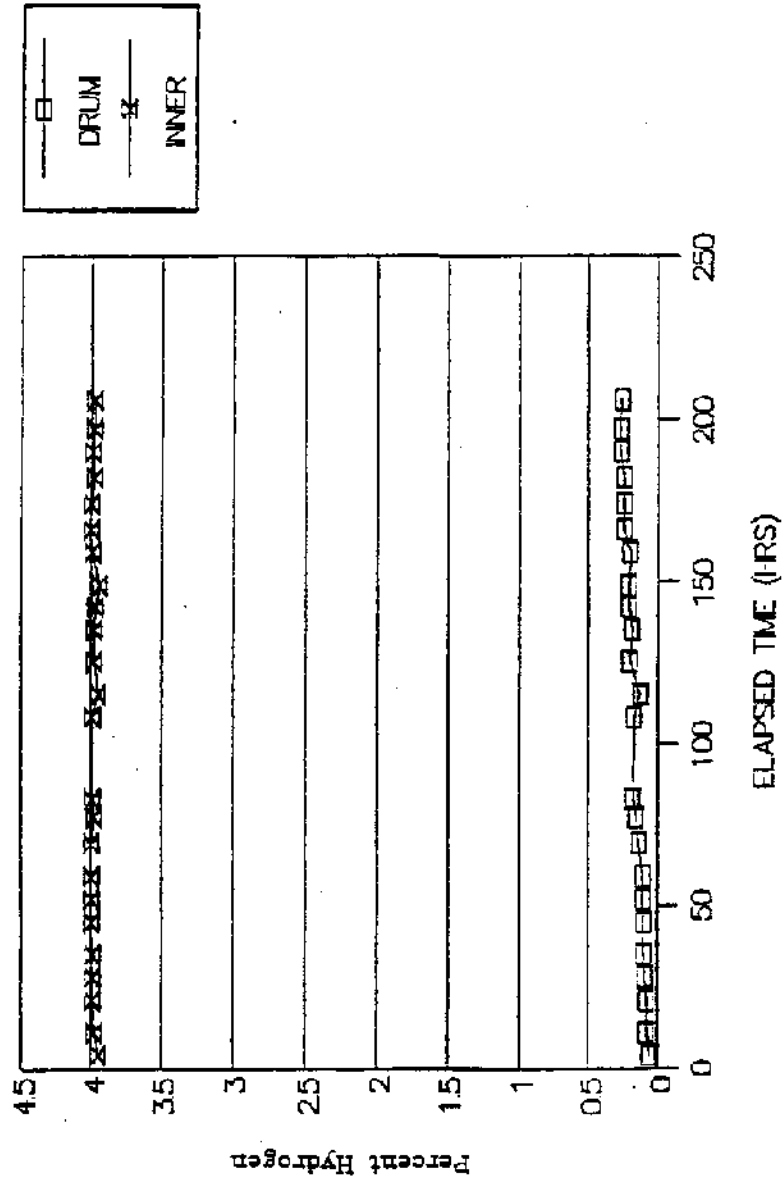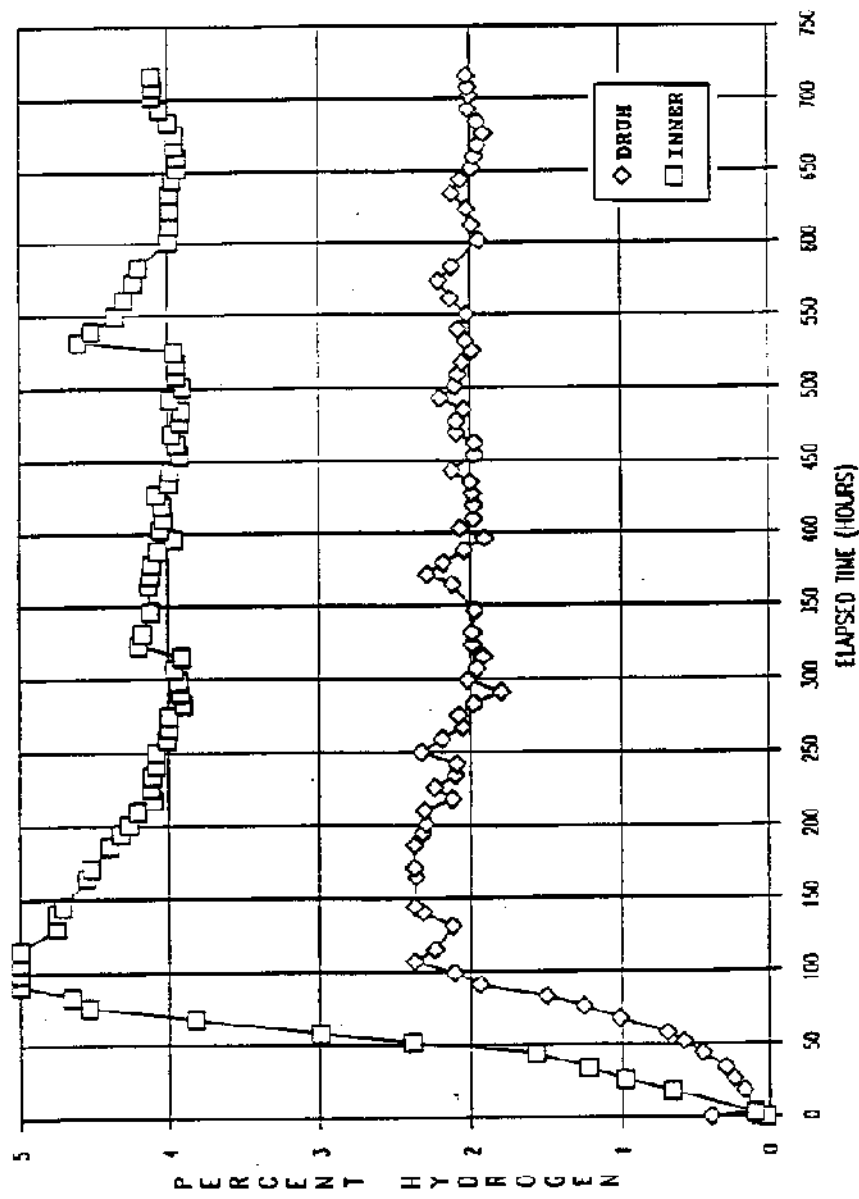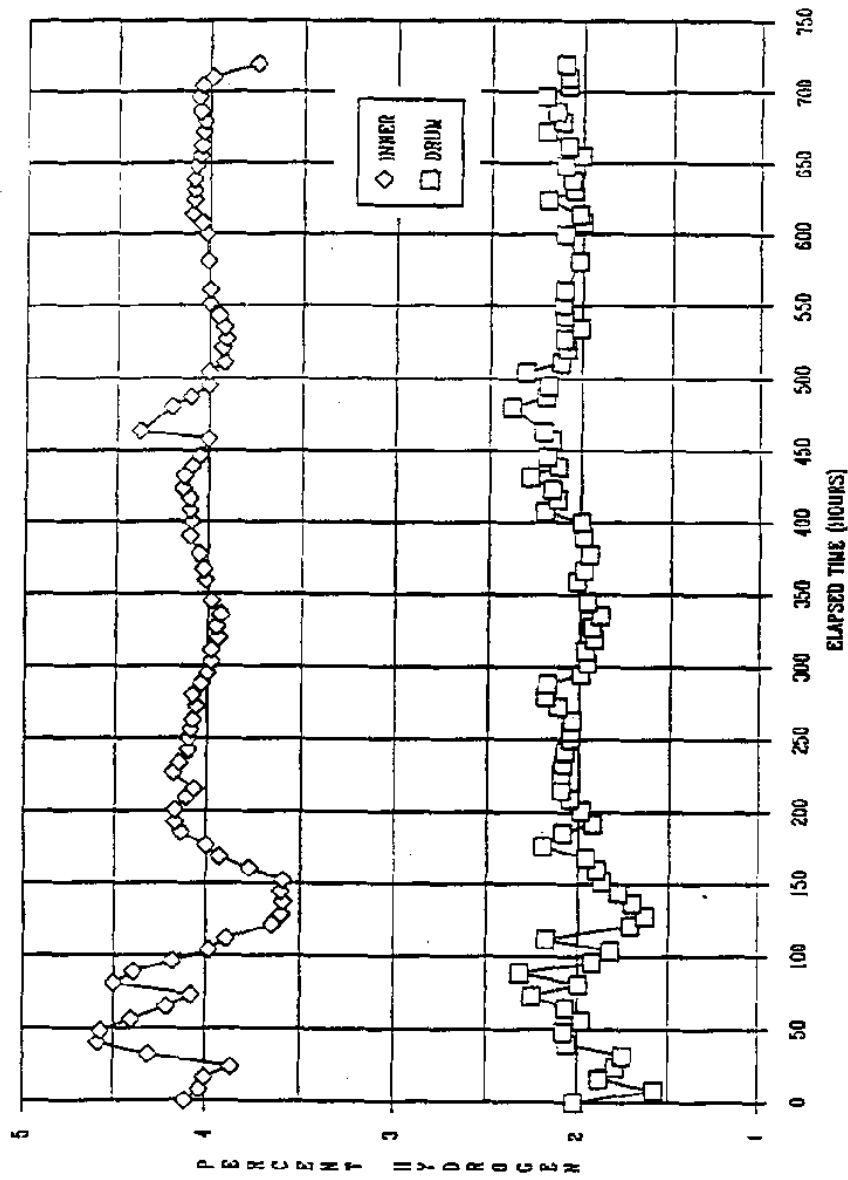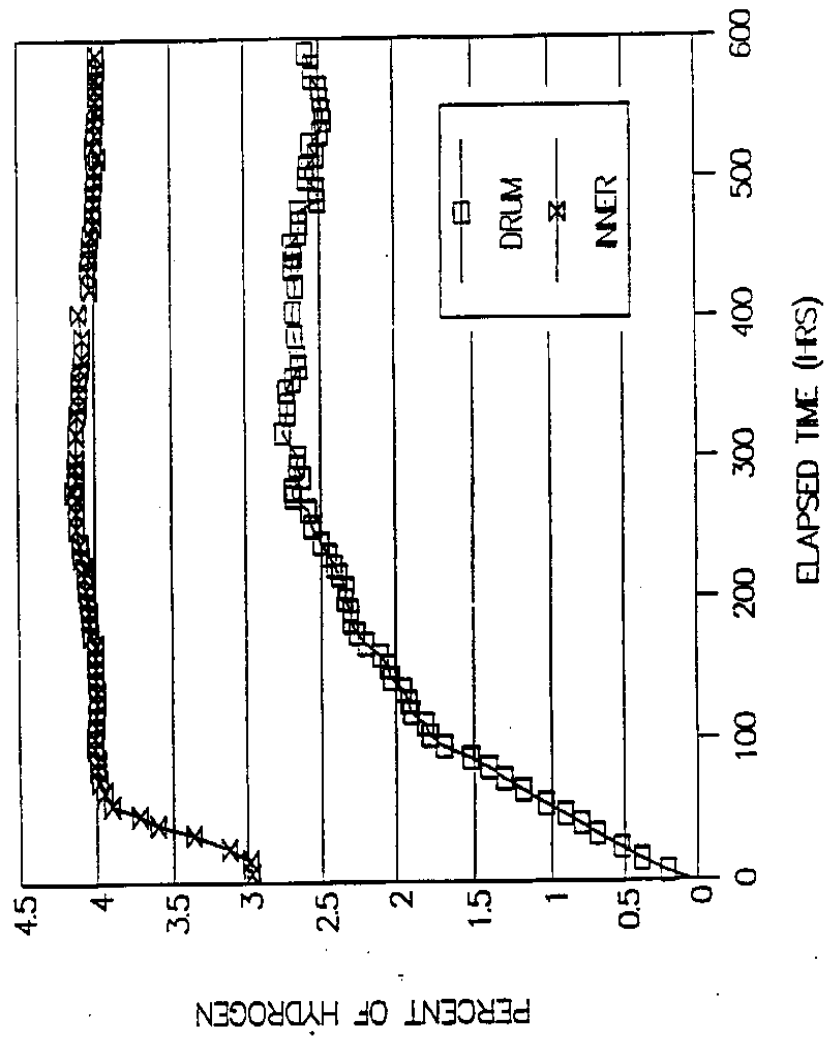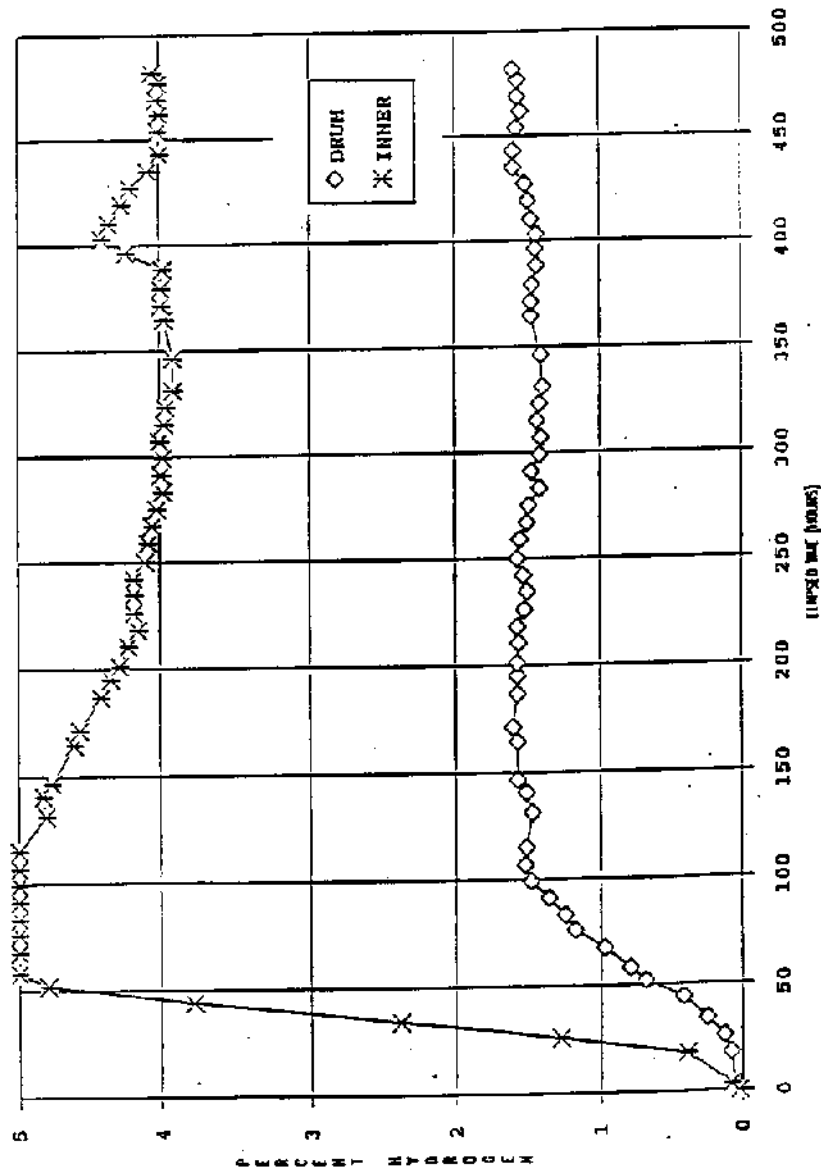
6.8-36

For each test, the number of the test, hydrogen injection rate, temperature at steady state, bag type, the mole percent hydrogen in the void volume of each confinement layer at steady state, and the computed release rates for each of the plastic bag confinement layers are summarized in Table 6.8-3. Similar information for the filters is provided in Table 6.8-4.

The contribution to the total release rate by any leakage of hydrogen around the bulkhead fittings was eliminated in experiments 9B, 10A, 10B, 10C, and 11A with the use of the duct seal. The release rate data of Tests 4, 5, 6, and 7 have not been used in quantifying the total release rates from bags since only the lowest measured release rates were being used as inputs into the calculations (Appendix 6.7 of the CH-TRU Payload Appendices).

6.8.7.2.2 Release Rates from Small Inner Bags

Tests 9A through 9C were conducted specifically in order to quantify the various contributions to the total release rate in the case of the small inner bags. The various contributions are summarized in Table 6.8-5.

The release rate by permeation through the small inner bag is equal to the total release rate from Test 9B, since there was no leakage around the bulkhead fitting nor through the twisted closure because this test had the twist-and-tape closure cut off and the end heat-sealed. The leakage through the closure is equal to the difference of the values measured in Test 9A and 9C, that is, 5.6E-7 mole/sec/mole fraction. The leakage rate around the bulkhead fitting is the difference between Tests 9B and 9C or 2.96E-7 mole/sec/mole fraction.

6.8.7.2.3 Temperature Dependence of Gas Release

Tests 10A through 10C were conducted in order to quantify the temperature dependence of the total release rate at the low end of the operating temperatures. The results show that the total release rate at the low temperatures (Tests 10A and 10B at 10^oF and -18^oF, respectively) do not decrease as would be predicted by considerations of pure permeation and diffusion. The total release rate at 10^oF was approximately 70% higher than the release rate at 57^oF. The release rates at 10^oF and at -18^oF appear to be the same. The increased release rates at the low temperatures probably result from a stiffening of the plastic material and changes in the closure configuration. The similar release rates at 10^oF and -18^oF suggest that the dependence of release rates on these low temperatures is not functional. That is, there would not be a continuous decrease in the release rate with increasing temperatures. At higher than room temperature, the normal dependence of diffusion on temperature (increasing as the 1.75 power of temperature) would be valid.

6.8.7.2.4 Bounding Release Rate for Decay Heat Calculations

The release rate from the small PVC bag closure leakage (5.6E-7 mole/sec/mole fraction) was used as the total release rate from small bags in computations of decay heat limits (Appendix 6.7 of Payload Appendices). As mentioned earlier, the bag permeability was not considered in this case even though its contribution to the release of hydrogen is approximately equal to the closure release rate (Table 6.8-5). This should provide a margin of safety in keeping concentrations of hydrogen at lower concentration than what is predicted by analytical calculations. The lowest measured total release rate (4.67E-6 mole/sec/mole fraction) based on Test 10C results

(Table 6.8-3) was used as the total release rate from large bags (Appendix 6.7 of Payload Appendices).

The filter diffusivities presented in Table 6.8-4 are not actual measurements on the filters but are effective diffusivities in the configuration of the waste. For the purposes of specifying a minimum diffusivity for the filters, actual diffusivity measurements on the filters have been used since these are representative of what would be measured by the manufacturer. In a drum (or SWB) configuration, release of hydrogen can depend on the way the filter is installed, hydrogen leakage through the gasket material and any other available paths for the hydrogen.

In summary, this test program determined the release rates through different bagging configurations that serve as conservative inputs into the decay heat calculations outlined in Appendix 6.7 of the CH-TRU Payload Appendices. Release rates in actual waste drums are expected to be much higher than what is predicted by this experimental data. This, coupled with the lower hydrogen production rates (as opposed to the effective values being used in the calculations), should provide a high margin of safety for safe transport of the CH-TRU waste. Sampling programs at the sites prove this to be true and are discussed in Appendix 5.3 of the CH-TRU Payload Appendices.

Table 6.8-3 — Summary of Total Release Rates from Plastic Confinement Layers

Test Number	H₂ Flow Rate (Ml/hr)	Temperature at Steady State (°F)	Confinement Layer	Steady State Hydrogen mol%	Total Release (mol/sec/mol fraction)
4A	15.6	74.0	14 mil PVC liner bag 10 mil PE liner bag 90 mil HDPE drum liner	4.02 2.39 1.59	1.09E−05 2.23E−05 5.94E−05
4B	13.6	76.0	14 mil PVC liner bag 10 mil PE liner bag 90 mil HDPE drum liner	4.01 2.58 1.81	1.08E−05 2.00E−05 4.99E−05
5A	3.1	78.0	14 mil PVC inner bag-out 5 mil PE inner bag 10 mil PE liner bag 10 mil PE liner bag 90 mil HDPE drum liner	4.00 1.93 0.90 0.50 0.29	1.35E−06 4.45E−06 1.21E−05 3.19E−05 7.03E−05
5B	3.5	82.0	14 mil PVC inner bag-out 5 mil PE inner bag 10 mil PE liner bag 10 mil PE liner bag 90 mil HDPE drum liner	4.05 1.91 0.72 0.49 0.31	1.84E−06 3.31E−06 1.71E−05 2.19E−05 9.84E−05
6A	2.8	68.0	14 mil PVC inner bag-out 5 mil PE inner bag 14 mil PVC inner bag 10 mil PE liner bag 90 mil HDPE drum liner	4.06 1.99 0.83 0.56 0.40	1.56E−06 2.79E−06 1.20E−05 2.02E−05 4.62E−05
6B	2.2	66.0	14 mil PVC inner bag-out 5 mil PE inner bag 14 mil PVC liner bag 10 mil PE liner bag 90 mil HDPE drum liner	4.09 2.02 0.96 0.62 0.50	1.23E−06 2.40E−06 7.47E−06 2.12E−05 3.18E−05
7A	17	77.0	5 mil PE inner bag 14 mil PVC liner bag 10 mil PE liner bag 90 mil HDPE drum liner	4.09 3.75 2.70 1.98	5.68E−05 1.84E−05 2.68E−05 5.22E−05
7B	2.8	71.0	5 mil PE inner bag 14 mil PVC liner bag 10 mil PE liner bag 90 mil HDPE drum liner	4.02 3.98 3.18 2.53	8.07E−05 4.04E−06 4.97E−06 1.01E−05
9A	3.7	70.0	14 mil PVC inner bag-out bulkhead; not sealed	4.12	1.35E−06
9B	1.5	50.0	14 mil PVC inner bag-out less horsetail; bulkhead; end sealed	4.00	4.94E−07
9C	2.5	59.0	14 mil PVC inner bag-out less horsetail; no duct seal used on bulkhead fittings	3.98	7.90E−07
10A	25	10.0	10 mil PE liner bag	4.11	1.55E−05
10B	20.9	−18.0	10 mil PE liner bag	4.02	1.52E−05
10C	5.9	57.0	10 mil PE liner bag	3.98	4.67E−06
11A	12.5	63.0	14 mil PVC liner bag	4.01	5.97E−06

Table 6.8-4 — Summary of Total Release Rates from Filters

Test Number	H$_2$ Flow Rate (ml/hr)	Temperature at Steady State (°F)	Filter Type and Number	Steady State Hydrogen mol%	Total Release Rate (mol/sec/mol fraction)
4A	15.6	74.0	NFT-E INEL Design	1.29	1.38E−05
4B	13.6	76.0	NFT-21 RFP Design	1.50	1.03E−05
5A	3.1	78.0	NFT-21 RFP Design	0.22	2.51E−05
5B	3.5	82.0	NFT-21 RFP Design	0.27	1.46E−05
6A	2.8	68.0	NFT-17 RFP Design	0.33	9.80E−06
6B	2.2	66.0	NFT-21 RFP Design	0.42	6.05E−06
7A	17	77.0	NFT-17 RFP Design	1.61	1.20E−05
7B	2.8	71.0	NFT-17 RFP Design	2.21	1.46E−06
9A	3.7	70.0	NFT-17 RFP Design	0.96	4.44E−06
9B	1.5	50.0	NFT-9035 SRP SRP Design	0.37	4.85E−06
9C	2.5	59.0	NFT-9035 SRP SRP Design	0.26	1.13E−05
10A	25	10.0	NFT-17 RFP Design	2.02	1.60E−05
10B	20.9	−18.0	NFT-17 RFP Design	2.12	1.36E−05
10C	5.9	57.0	NFT-9034 SRP Design	2.49	2.80E−06
11A	12.5	63.0	NFT-21 RFP Design	1.57	9.28E−06

Table 6.8-5 — Summary of Release Rates for Small Bag Confinement Layers

Contributor to Total Release Rate	Permeation Through Small PVC	Bag Closure Leakage	Bulkhead Fittings Leakage
Relation to Tests	9B	9A-9C	9C-9B
Value*	4.94E-7	5.6E-7	2.96E-7

*Values reported in mole/sec/mole fraction.

APPENDIX 6.9

**TEMPERATURE DEPENDENCE OF HYDROGEN GAS GENERATION
AND RELEASE RATES**

This page intentionally left blank.

6.9   Temperature Dependence Of Hydrogen Gas Generation And Release Rates

6.9.1   Summary

The temperature dependence of hydrogen gas generation and release rates is presented in this document. These parameters determine the maximum allowable decay heat limit for each shipping category. The assumptions and equations used in calculating the analytical decay heat limits are presented in this document. The analysis presented here demonstrates that for Waste Types II and III, under worst-case assumptions, the minimum decay heats occur at room temperatures. The minimum decay heat limits for shipping categories in Waste Type I occur at the lowest operating temperature, -20°F (-29°C). As examples of the results from determining the decay heat limits from each shipping category, plots of the decay heat limit as a function of temperature are provided for the shipping categories II.1A4 and I.1A3.

For Waste Types II and III, the total hydrogen release rate (from the different layers of confinement in a payload container) and the hydrogen generation rate (calculated using the temperature corrected effective G value) increase with increasing temperatures. The resultant decay heat limit varies only minimally with temperature [a difference of 2.2% between the extremes of the operating temperature range from -20°F (-29°C) to 154°F (68°C) applicable to analytical category waste], and room temperatures result in the minimum values for the decay heat limits.

For Waste Type I, the effective G value does not change with temperature (see Appendix 3.2 of the CH-TRU Payload Appendices). Using the same set of assumptions for the hydrogen release rate (as for Waste Types II and III), the total hydrogen release rate increases with increasing temperatures and are a minimum at the lowest operating temperature, -20°F (-29°C). Since the effective G value does not decrease with decreasing temperature for Waste Type I (while the equations show a decrease in the hydrogen release rates with decreasing temperatures), the minimum decay heat limit is obtained at the lowest operating temperature in each shipping category.

Experiments conducted at lower than room temperature show the release rates from plastic bags to be much higher than those assumed in these calculations (Appendices 6.7 and 6.8 of the CH-TRU Payload Appendices). No credit is taken for the experimentally measured increased hydrogen release rates through the twist-and-tape closure of the bags at the low temperatures. These assumptions add a margin of safety to the decay heat limit used for each payload shipping category in Waste Type I and Waste Material Type II.3.

An example calculation for obtaining the decay heat limit for the shipping category II.1A4 at the maximum operating temperature is presented in Attachment A. This attachment presents the steps for obtaining the decay heat limit for any shipping category at any temperature. The analysis presented in Attachment A of this appendix shows that porosity effects on the twist-and-tape closure are negligible in calculating the decay heat limits. Any decrease in porosity of the closure at high temperatures is offset by increased diffusion.

Attachment B of this appendix provides example calculations for decay heat limits using less restrictive assumptions (taking credit for increased permeation from the liner bags at higher temperatures, etc.). These values are provided for illustrative purposes only.

6.9.2 Introduction

The release of hydrogen gas from the layers of plastic bags and the payload containers occurs by two mechanisms. The first is release of hydrogen by diffusion through the twist-and-tape closure of the bags, through the drum liner lid hole, and drum filter. The second is permeation of the hydrogen through the bag materials. The temperature dependence of pure diffusion and permeation processes is well characterized. Diffusion is directly proportional to the 1.75 power of the absolute temperature.[1] Permeation through plastics increases exponentially with temperature, with an activation energy characteristic of a given material.[1] In the flammable gas calculations presented in Appendix 2.3 of the CH-TRU Payload Appendices, the release rates used to calculate the decay heat limit for each payload category assume the following (see Appendix 6.7 of the CH-TRU Payload Appendices for details):

- Room temperature conditions are assumed for Waste Material Type II.1 and Waste Type III. Minimum operating temperature conditions [-20°F (-29°C)] are assumed for Waste Type I and Waste Material Type II.3. As shown in this appendix, the most conservative decay heat limits are obtained under these conditions.

- For small inner bags (excluding the drum liner bags), only the diffusion through the twist-and-tape closure is used in determining the total release rate. No credit is taken for permeation through the bag material.

- For the drum liner bags, the sum of diffusion through the bag closure and permeation of the bag material is used in determining the total release rate. The lowest measured total hydrogen release rate at three different test temperatures [-18°F (-28°C), 10°F (-12°C), and 57°F (14°C)] (Appendix 6.8 of the CH-TRU Payload Appendices) is used as the hydrogen release rate.

- For the rigid drum liner, the diffusion through a 0.3" diameter hole at -20°F (-29°C) is used to determine total hydrogen release rate (see Appendix 6.7 of the CH-TRU Payload Appendices). No credit is taken for permeation through the liner material.

- For the filter vents in the payload containers, the lowest measured diffusion coefficient is used to determine the total hydrogen release rate (Appendix 6.7 of the CH-TRU Payload Appendices) and is corrected for temperature as described by equation (2) of Table 6.9-1.

---

[1] Perry, R.H., "1984, Perry's Chemical Engineers Handbook," 6th Edition , McGraw Hill Book Company, New York, New York.

Table 6.9-1 —Equations Summarizing Temperature Dependence Of Decay Heat Parameters[*]

1. <u>Effective G Value for Hydrogen</u>

   The effective G value for hydrogen is calculated using an Arrhenius type dependence on temperature (see Appendix 3.2 of the CH-TRU Payload Appendices). The effective G value, $G_{eff(T2)}$, at temperature T_2 is computed as:

   $$G_{eff(T2)} = G_{eff(T1)} \quad exp[(E_G/R)\{(T_2\text{-}T_1)/(T_2 \text{ x } T_1)\}] \tag{1}$$

2. <u>Release through Drum Filter</u>

   The mechanism of release through the filter is by diffusion, which varies with temperature raised to the 1.75 power. Using the minimum measured diffusion coefficient of $1.9(10)^{-6}$ mole/sec at 70^oF (21^oC) (Appendix 6.7 of the CH-TRU Payload Appendices), the total release rate of hydrogen from the filter, RS(drum filter) at temperature, T_2 is:

   $$RS(drum\ filter, T_2) = 1.9(10)^{-6}\ mole/sec\ (T_2/T_1)^{1.75} \tag{2}$$

3. <u>Release through Punctured Rigid Drum Liner</u>

   The release rate from the rigid drum liner is the minimum value based on diffusion of hydrogen in air at -20^oF (-29^oC). The value of this release rate is:

   $$RS(drum\ liner, T) = 5.09(10)^{-5}\ mole/sec \tag{3}$$

4. <u>Release through Liner Bags</u>

   The lowest measured total release rate is used as the release rate at all temperatures. The value of this release rate is:

   $$RS(liner\ bag, T) = 4.67(10)^{-6}\ mole/sec \tag{4}$$

5. <u>Release through Inner Bags</u>

   The release rate is corrected for temperature and closure porosity dependence. The dependence of the porosity ($\in$) on temperature is discussed in Attachment A of this appendix. The release rate at temperature, T_2 is:

   $$RS(inner\ bag, T_2) = 1.58(10)^{-7}(T_2/T_1)^{1.75} \quad (\in_2/\in_1)^2\ mole/sec \tag{5}$$

[*] All variables are defined in Table 6.9-2.

Table 6.9-2 — Nomenclature List For Variables

E_G Hydrogen generation activation energy.
[0.8 kcal/g-mole] for polyethylene (Waste Material Type II.1 and Waste Type III)
[0.0 kcal/g-mole] for water (Waste Type I and Waste Material Type II.3))
(Appendix 3.2 of the CH-TRU Payload Appendices)

E_p Activation energy for hydrogen permeation through polyethylene.
[8.2 kcal/g-mole]
(Appendix 6.7 of the CH-TRU Payload Appendices)

R Gas law constant.
[$1.987(10)^{-3}$ kcal/g-mole K]

T_1 Absolute temperature at which the reference value of a decay heat parameter is specified.
[294 ^{o}K] (70 ^{o}F).

T_2 Absolute temperature at which the value of a decay heat parameter is to be evaluated (K).

$G_{eff(T1)}$ Reference effective G value for hydrogen
[1.70 molecules/100eV] at 70 ^{o}F for Waste Material Type II.1
[1.60 molecules/100eV] at 70 ^{o}F for Waste Material Type I.1
(Appendix 3.2 of the CH-TRU Payload Appendices)

$G_{eff(T2)}$ Temperature corrected effective G value for hydrogen at temperature, T_2.

ϵ_1 Porosity of the twist-and-tape closure at temperature, T_1.

ϵ_2 Porosity of the twist-and-tape closure at temperature, T_2.

$RS(I)$ Total release rate from confinement layer "I" (mole/sec).

$r(i)$ Resistance of confinement layer "I" to the flow of hydrogen; equal to the reciprocal of the total release rate = $1/RS(I)$ in (sec/mole).

r_{eff} Effective resistance of all layers of confinement.
$r_{eff} = \Sigma\, r(I)$ for I = 1 to number of confinement layers (sec/mole).

CG Allowable hydrogen gas generation rate per innermost confinement layer (mole/sec).

Table 6.9-2 — Nomenclature List For Variables (Concluded)

X_{inner} Maximum permissible concentration (mole fraction) of hydrogen in innermost
                 confinement layer.
                 [0.05]

t   Shipping period duration.
                 [60 days]

n_{gen} Number of hydrogen generators per packaging.
                 - 14 for drums
                 - 8 for overpack of drums in an SWB
                 - 2 for SWBs and bins overpacked in SWBs

N_{tg} Total moles of gas inside the packaging inner containment vessel (ICV) cavity.
                 [101.56 moles for drums and 72.54 moles for SWBs]
                 (Appendix 2.3 of the CH-TRU Payload Appendices)

Q_i Decay heat per innermost confinement layer (watt).

N_A Avogadro's number.
                 [$6.023(10)^{23}$ molecules/g-mole].

6.9.3 Temperature Dependence Of Parameters In Decay Heat Calculations

The temperature dependent parameters in the decay heat limit calculations include the effective G value for hydrogen, porosity of the twist-and-tape closure, and the hydrogen release rates through the different layers of confinement. The equations describing these temperature dependencies, and the values for parameters used in these equations, are described in this section. The nomenclature for the variables in the equations is presented in Table 6.9-2. A summary of the variables as a function of temperature is presented in Table 6.9-2, and each is discussed in detail below:

1. <u>G value for Hydrogen</u>: The effective G values for hydrogen generation used for Waste Material Type II.1 and Waste Type III are based on polyethylene (Appendix 3.2 of the CH-TRU Payload Appendices). The effective G values have an Arrhenius type dependence with temperature with an activation energy of 0.8 kcal/g-mole for polyethylene (Appendix 3.2 of the CH-TRU Payload Appendices). For Waste Type I and Waste Material Type II.3, the effective G values for hydrogen are due to water. These effective G values do not vary as a result of temperature changes; that is, water has an activation energy of zero (Appendix 3.2 of the CH-TRU Payload Appendices). The temperature-corrected effective G value as a function of temperature is given in equation (1) of Table 6.9-1.

2. <u>Hydrogen Release Rate through a Drum Filter</u>: The diffusion of hydrogen through the drum filter varies directly as the 1.75 power of the absolute temperature.[1] Equation (2) of Table 6.9-1 defines the temperature dependence of this hydrogen release rate.

3. <u>Hydrogen Release Rate through the Punctured Rigid Drum Liner</u>: The diffusion of hydrogen through the punctured rigid drum liner varies directly as the 1.75 power of the absolute temperature. No credit is taken for permeation through the rigid drum liner material, and the minimum rigid drum liner hydrogen release rate through the puncture hole [at -20°F (-29°C)] is used in the decay heat limit calculations. Equation (3) of Table 6.9-1 defines the hydrogen release rate through the punctured rigid drum liner used in the decay heat calculations.

4. <u>Hydrogen Release Rate through the Liner Bags</u>: Total hydrogen release rate through the liner bags considers both diffusion through the twist-and-tape closure and permeation through the plastic. Total release rates through liner bags were measured at three temperatures [-18°F (-28°C), 10°F (-12°C), and 57°F (14°C)] to quantify the effect of lower (than room) temperatures on these release rates (Appendix 6.8 of the CH-TRU Payload Appendices). These experiments showed that release rates at the lower end of the operating temperatures [-18°F (-28°C) and 10°F (-12°C)] are higher than would be expected from analytical consideration of permeation and diffusion alone. At temperatures at or above 10°F (-12°C), stiffening of the plastic material in the twist-and-tape closure results in a lesser restriction to the release of hydrogen. The increased release rates at the lower temperatures are not of a functional form. That is, as seen from Table 6.8-3 of Appendix 6.8 of the CH-TRU Payload Appendices, the release rates at 10°F (-12°C), and -18°F (-28°C) are nearly

the same. Hence, the hydrogen release rate is not a continuously decreasing function from low temperatures to higher temperatures.

In the decay heat limit calculations, the lowest measured total hydrogen release rate is used as the release rate at all temperatures in the operating range. No credit is taken for the increased hydrogen release rate at the lower (than room) temperatures found in the experiments. No corrections for increased permeation or diffusion are made for the higher (than room) temperatures. Equation (4) of Table 6.9-1 defines the temperature dependence of this hydrogen release rate.

5. <u>Hydrogen Release Rate through the Inner Bags</u>: As mentioned in the summary above, no credit is taken for permeation through the inner bags in estimating the total hydrogen release rates. In the decay heat limit calculations, the release rate through the inner bags has been modeled as strict diffusion through the twist-and-tape closure (directly proportional to the 1.75 power of the absolute temperature). No credit is taken for the experimentally measured increased hydrogen release rates through the twist-and-tape closure at the lower (than room) operating temperatures. In addition, a decrease in porosity of the closure with increasing temperatures is considered in the calculations. As shown in Attachment A, the decrease in porosity at the higher (than room) temperatures is minimal. Equation (5) of Table 6.9-1 defines the temperature dependence of this release rate.

These release rates serve as inputs into the decay heat limit calculations as described below.

6.9.4 Decay Heat Limits as Functions of Temperature—Waste Types II and III

The methodology for calculating the decay heat limits is described in Appendix 2.3 of the CH-TRU Payload Appendices (with an example for shipping category I.1A2), and in Attachment A of this appendix for the shipping category II.1A4. The equations in the decay heat calculations are summarized in Table 6.9-3. As shown in Equation (3) of Table 6.9-3, the decay heat limit for a shipping category is directly proportional to the maximum allowable hydrogen generation rate and inversely proportional to the temperature-corrected effective G value. The temperature-corrected effective G value as a function of temperature is plotted in Figure 6.9-1 for the shipping category II.1A4. The maximum allowable hydrogen generation rate is equal to the hydrogen release rate (across each layer of confinement) at equilibrium. Equation (2) of Table 6.9-3 defines the maximum allowable hydrogen generation rate in terms of the release rate parameters and the number of moles of gas in the packaging ICV. This parameter (the maximum allowable hydrogen generation rate) is plotted as a function of temperature for the shipping category II.1A4 in Figure 6.9-2. The decay heat limit as a function of temperature can be calculated from the values on Figures 6.9-1 and 6.9-2 at each temperature, as defined by equation (3) of Table 6.9-3. The decay heat limits at 5 degree (^{o}F) intervals are summarized in Table 6.9-4, along with the values of the other variables that enter into the calculations. The decay heat limit as a function of temperature is plotted in Figure 6.9-3.

Table 6.9-3 — Equations For Decay Heat Calculations

1.   Calculation of Effective Resistance

The resistance of a confinement layer "i" to the flow of hydrogen is the reciprocal of the total release rate from that confinement layer. Therefore,

$$r(i) \text{ (sec/mole)} = 1/RS(i) \tag{1}$$

The effective resistance is computed by summing the individual confinement layer resistances.

$$r_{eff} = \Sigma \, r(i) \text{ for i = 1 to number of confinement layers}$$

2.   Calculation of Maximum Allowable Hydrogen Generation Rate

The maximum allowable hydrogen generation rate per innermost confinement layer may be computed as:

$$CG \text{ (mole/sec)} = (X_{inner})/\{r_{eff} + [(t)(n_{gen})/N_{tg}]\} \tag{2}$$

For 14 drum payload containers

$$(t)(n_{gen})/N_{tg} = (60 \text{ days})(14 \text{ drums})(86400 \text{ sec/day})/101.56 \text{ mole}$$
$$= 714{,}612 \text{ sec/mole}$$

3.   Calculation of Decay Heat Limit

The decay heat limit per innermost confinement layer, may be computed as:

$$Q_i \text{ (watts)} = [(CG)(N_A)/(G_{eff} \text{ molecules/100eV})][1.602(10)^{-19} \text{ watt-sec/eV}] \tag{3}$$
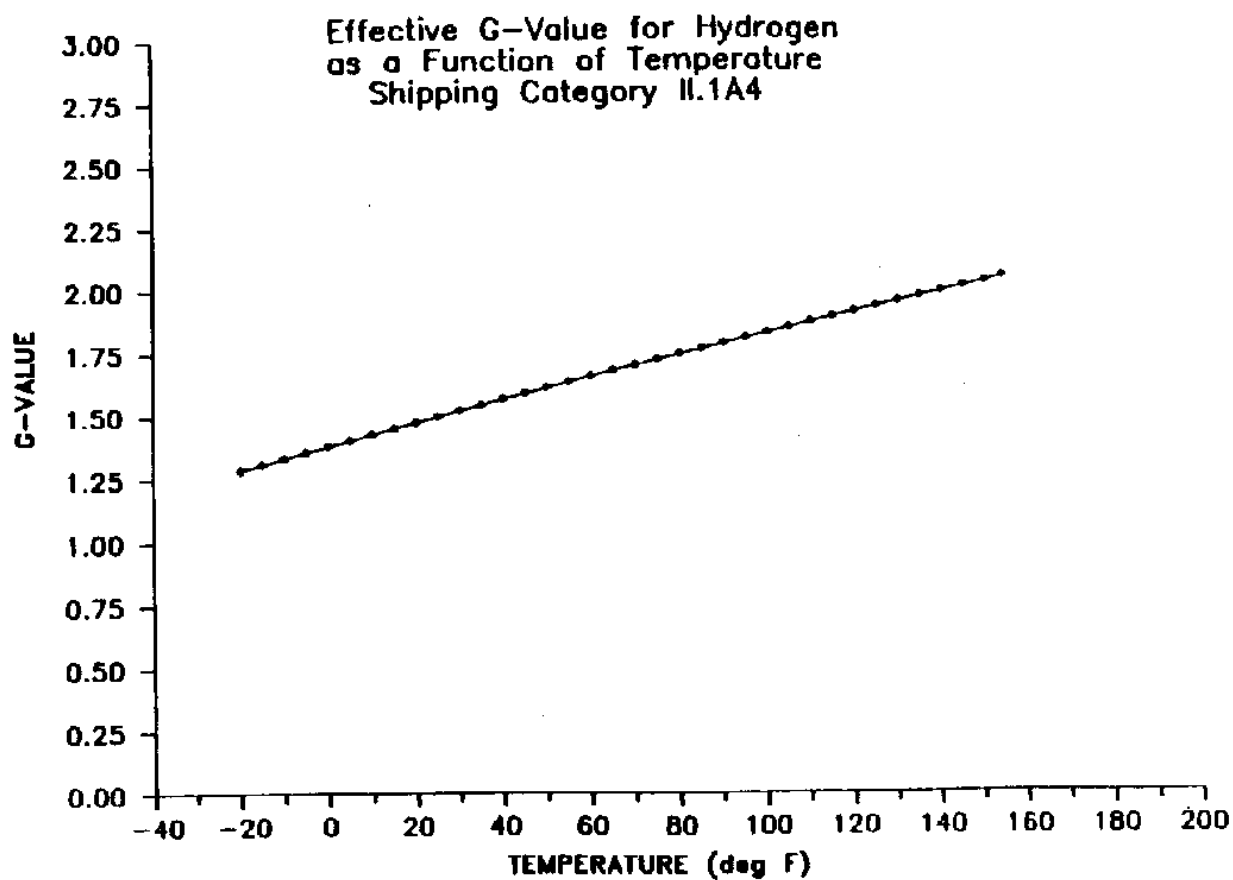
Figure 6.9-1—Effective G-Value for Hydrogen as a Function of Temperature (Shipping Category II.1A4)
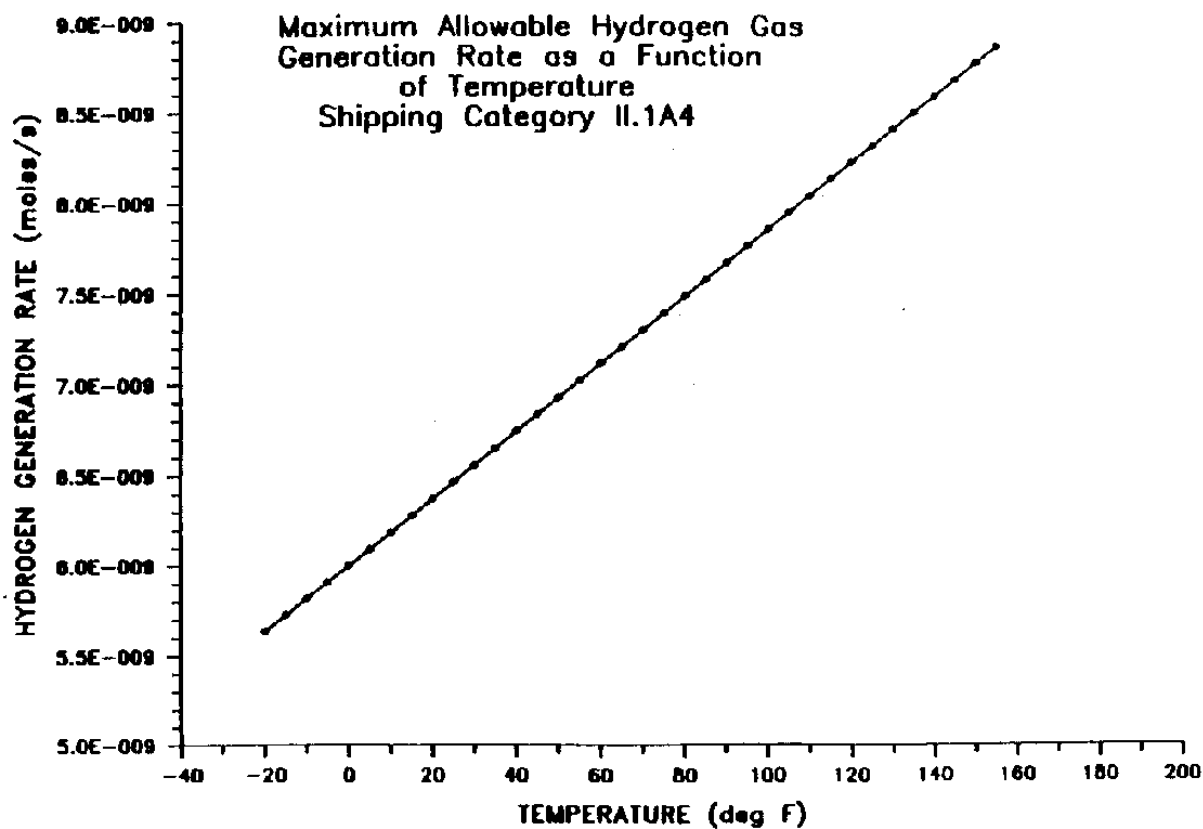
Figure 6.9-2—Maximum Allowable Hydrogen Gas Generation Rate as a Function of Temperature (Shipping Category II.1A4)
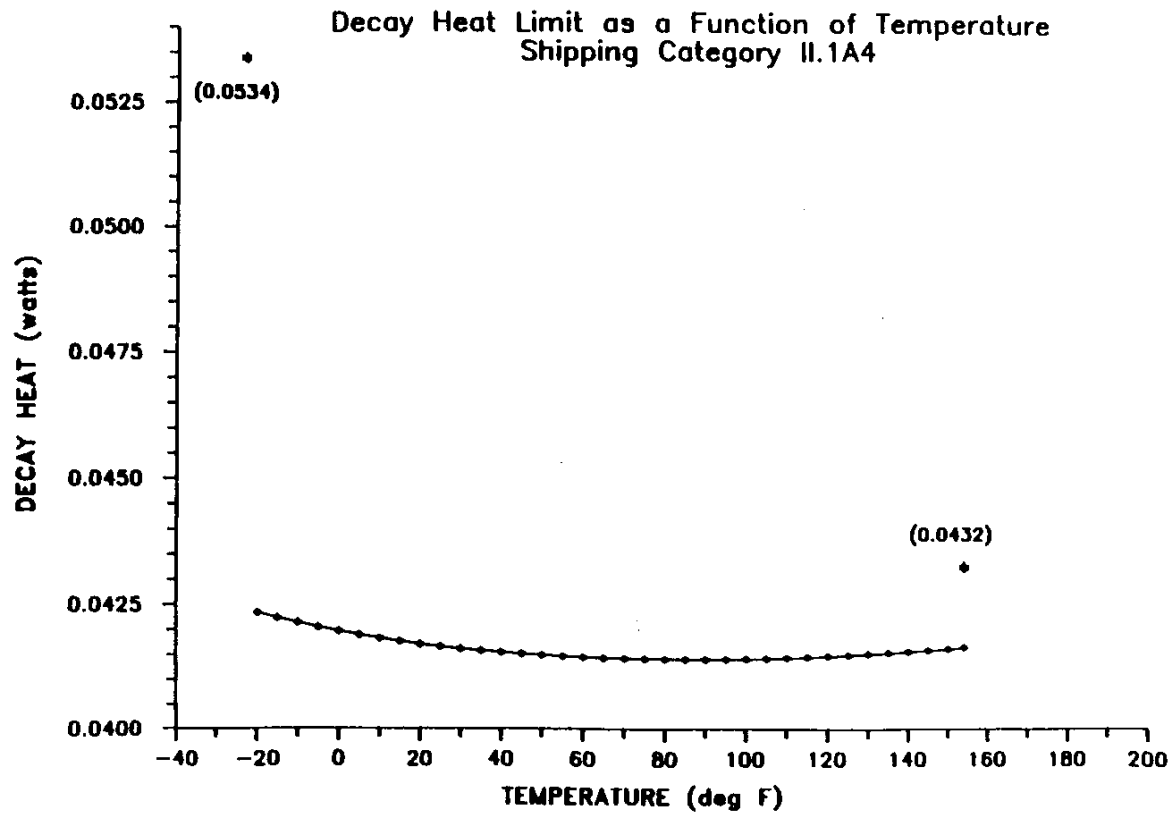
Figure 6.9-3—Decay Heat Limit as a Function of Temperature (Shipping Category II.1A4)

Table 6.9-4 — Decay Heat Parameters For Shipping Category II.1A4

Temp (F)	Temp (K)	Porosity	r(inner bag) (s/mol)	r(liner bag) (s/mol)	r(drum liner) (s/mol)	r(drum filter) (s/mol)	r(eff) (s/mol)	G(eff)	CG (mol/s)	Q$_i$ (Watt)
−20	244	0.6934	2398864	214133	19646	729327	8159697	1.28	5.634E−09	0.0423
−15	247	0.6927	2352856	214133	19646	713896	8006243	1.31	5.733E−09	0.0422
−10	250	0.6920	2308332	214133	19646	698971	7857746	1.34	5.833E−09	0.0421
−5	253	0.6913	2265225	214133	19646	684532	7713986	1.36	5.932E−09	0.0420
0	255	0.6908	2237461	214133	19646	675164	7621325	1.38	5.998E−09	0.0420
5	258	0.6901	2196579	214133	19646	661485	7485002	1.40	6.098E−09	0.0419
10	261	0.6894	2156959	214133	19646	648237	7352894	1.43	6.198E−09	0.0418
15	264	0.6887	2118548	214133	19646	635400	7224825	1.46	6.298E−09	0.0418
20	266	0.6882	2093790	214133	19646	627064	7142214	1.47	6.364E−09	0.0417
25	269	0.6875	2057281	214133	19646	614877	7020497	1.50	6.464E−09	0.0417
30	272	0.6867	2022440	214133	19646	603058	6904158	1.52	6.563E−09	0.0416
35	275	0.6860	1988039	214133	19646	591592	6789489	1.55	6.663E−09	0.0416
40	278	0.6853	1954635	214133	19646	580465	6678148	1.57	6.763E−09	0.0415
45	280	0.6848	1933087	214133	19646	573229	6606268	1.59	6.830E−09	0.0415
50	283	0.6841	1901253	214133	19646	562637	6500176	1.61	6.930E−09	0.0415
55	286	0.6834	1870316	214133	19646	552349	6397075	1.64	7.031E−09	0.0415
60	289	0.6827	1840240	214133	19646	542354	6296852	1.66	7.131E−09	0.0414
65	291	0.6822	1820829	214133	19646	535848	6232115	1.68	7.198E−09	0.0414
70	294	0.6815	1792115	214133	19646	526316	6136440	1.70	7.298E−09	0.0414
75	297	0.6808	1764179	214133	19646	517048	6043362	1.72	7.399E−09	0.0414
80	300	0.6801	1736991	214133	19646	508033	5952787	1.75	7.499E−09	0.0414
85	303	0.6793	1711030	214133	19646	499263	5866132	1.77	7.598E−09	0.0414
90	305	0.6789	1693437	214133	19646	493548	5807639	1.79	7.666E−09	0.0414
95	308	0.6781	1668607	214133	19646	485166	5724768	1.81	7.765E−09	0.0414
100	311	0.6774	1643934	214133	19646	477006	5642587	1.83	7.865E−09	0.0414
105	314	0.6767	1619892	214133	19646	469059	5562515	1.85	7.965E−09	0.0414
110	316	0.6762	1604363	214133	19646	463876	5510745	1.87	8.032E−09	0.0414
115	319	0.6755	1581325	214133	19646	456269	5434021	1.89	8.132E−09	0.0415
120	322	0.6748	1558861	214133	19646	448856	5359219	1.91	8.232E−09	0.0415
125	325	0.6741	1536954	214133	19646	441630	5286271	1.94	8.332E−09	0.0415
130	328	0.6734	1515584	214133	19646	434585	5215116	1.96	8.432E−09	0.0415
135	330	0.6729	1501775	214133	19646	429987	5169092	1.97	8.498E−09	0.0415
140	333	0.6722	1481259	214133	19646	423231	5100786	2.00	8.598E−09	0.0416
145	336	0.6715	1461234	214133	19646	416640	5034120	2.02	8.698E−09	0.0416
150	339	0.6707	1442113	214133	19646	410209	4970327	2.04	8.795E−09	0.0416
154	341	0.6703	1429048	214133	19646	406008	4926931	2.05	8.863E−09	0.0417

Figures 6.9-1 and 6.9-2 show that both the temperature-corrected effective G value and the maximum allowable hydrogen generation rate increase with increasing temperatures. Figure 6.9-3 shows that the decay heat limits have a minimum at room temperatures and are slightly higher at both lower and higher operating temperatures. The largest difference between the lowest and the highest decay heat limit values in the operating temperature range is only 2.2%. These results show that for Waste Material Type II.1 and Waste Type III (the analysis for Waste Type III is identical to that for Waste Material Type II.1), the minimum decay heat limits are obtained assuming room temperature conditions.

In Figure 6.9-3, points are shown above the decay heat limit curve at each end of the operating temperature range. These decay heat limits would result at the two temperatures shown if the following more realistic assumptions for the hydrogen release rates through the inner bags and the liner bags are made:

- Credit is taken for increased hydrogen release through the liner bags at higher (than room) temperatures due to increased permeation and diffusion.

- Credit is taken for the experimental results (Appendices 6.7 and 6.8 of the CH-TRU Payload Appendices) at lower (than room) temperatures in order to use a constant value (measured at room temperatures) for the release rate through the inner bags.

Attachment B of this appendix provides the derivation of the decay heat limits with these assumptions. The two additional points have been provided in Figure 6.9-3 for illustrative purposes to demonstrate an added margin of safety in the analysis for the decay heat limits.

6.9.5 Decay Heat Limits as Functions of Temperature—Waste Type I and Waste Material Type II.3

For Waste Type I and Waste Material Type II.3, the effective G value does not change with temperature, while the maximum allowable hydrogen generation rate is an increasing function of temperature. Figures 6.9-4 and 6.9-5 are plots of the G value and the maximum allowable hydrogen generation rate as functions of temperature for the shipping category I.1A3. Table 6.9-5 presents the decay heat limit and related variables at 5 ^{o}F intervals through the operating temperature range. The decay heat limit as a function of temperature is plotted in Figure 6.9-6. Due to the constant values for the effective G values for waste material types in Waste Type I and Waste Material Type II.3, the decay heat limits are an increasing function of temperature, and are a minimum at the minimum operating temperature of -20°F.

In Figure 6.9-6, points are shown above the decay heat limit curve at each end of the operating temperature range. These decay heat limits would result at the two temperatures shown if the more realistic assumptions are made as listed above for the hydrogen release rates through the inner bags and the liner bags. Attachment B of this appendix provides the derivation of the decay heat limits with these assumptions. These assumptions have not been used in the decay heat limit calculations, and the conservative decay heat limits obtained at the minimum operating temperature have been used for shipping categories in Waste Type I and Waste Material Type II.3.

Effective G-Value for Hydrogen
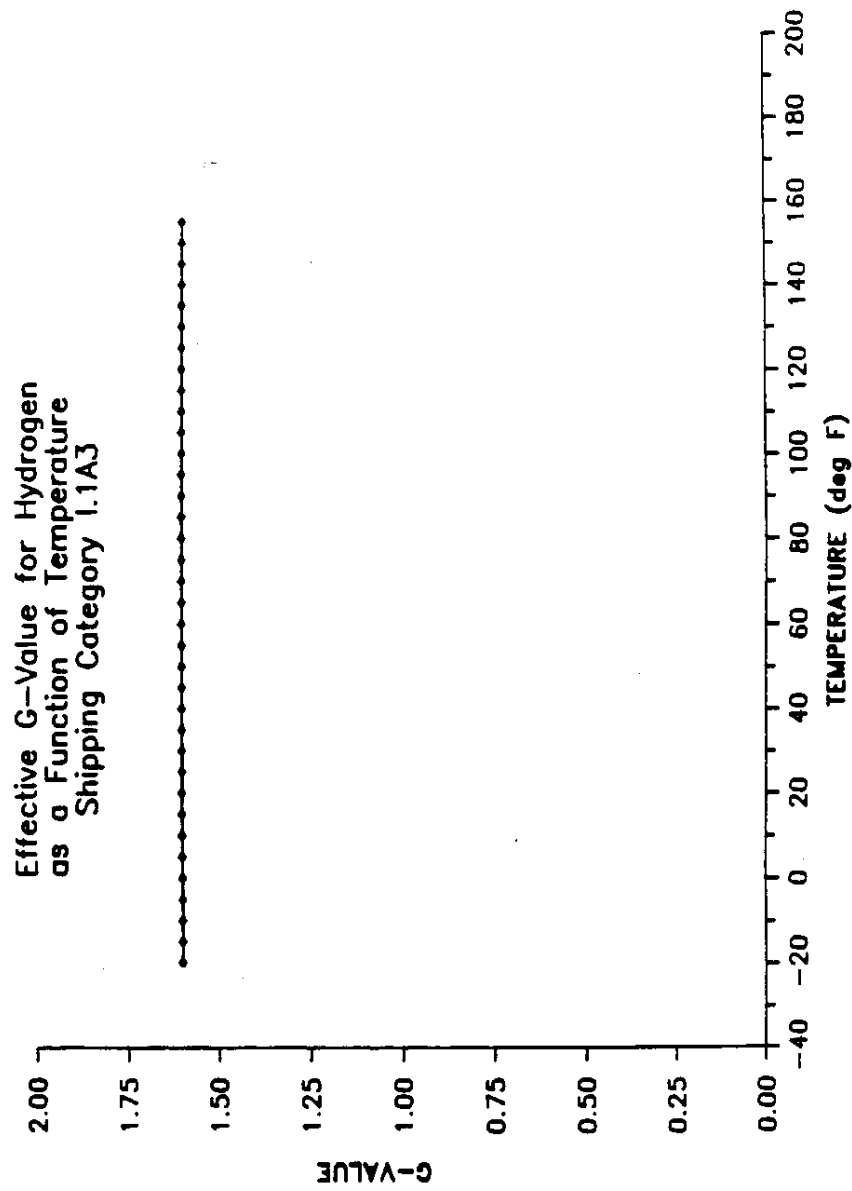as a Function of Temperature
Shipping Category I.1A3

Figure 6.9-4— Effective G-Value for Hydrogen as a Function of Temperature (Shipping Category I.1A3)
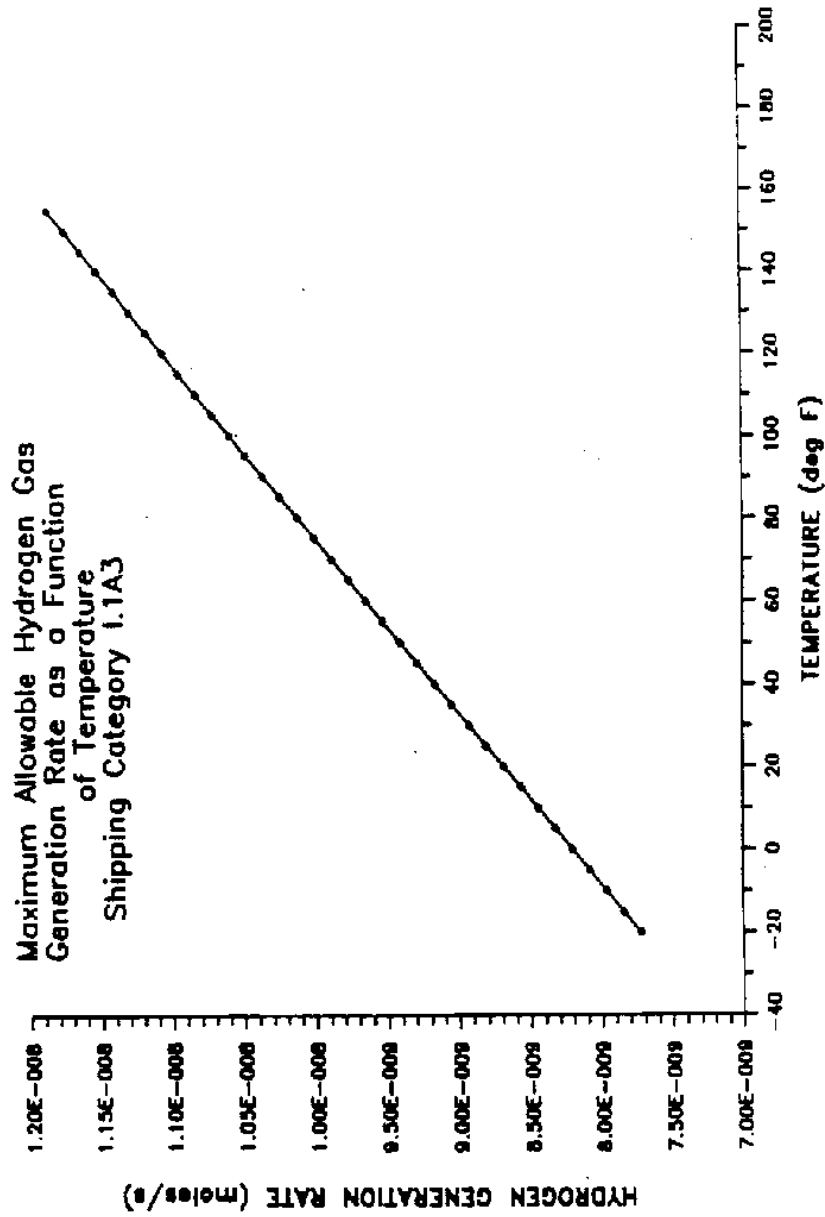
Figure 6.9-5— Maximum Allowable Hydrogen Gas Generation Rate as a Function of Temperature (Shipping Category I.1A3)

Table 6.9-5 — Decay Heat Parameters For Shipping Category I.1A3

Temp (F)	Temp (K)	Porosity	r(inner bag) (s/mol)	r(liner bag) (s/mol)	r(drum liner) (s/mol)	r(drum filter) (s/mol)	r(eff) (s/mol)	G(eff)	CG (mol/s)	Q$_i$ (Watt)
−20	244	0.6934	2398864	214133	19646	729327	5760833	1.60	7.721E−09	0.0466
−15	247	0.6927	2352856	214133	19646	713896	5653387	1.60	7.852E−09	0.0474
−10	250	0.6920	2308332	214133	19646	698971	5549414	1.60	7.982E−09	0.0481
−5	253	0.6913	2265225	214133	19646	684532	5448761	1.60	8.112E−09	0.0489
0	255	0.6908	2237461	214133	19646	675164	5383864	1.60	8.199E−09	0.0494
5	258	0.6901	2196579	214133	19646	661485	5288422	1.60	8.329E−09	0.0502
10	261	0.6894	2156959	214133	19646	648237	5195934	1.60	8.459E−09	0.0510
15	264	0.6887	2118548	214133	19646	635400	5106276	1.60	8.590E−09	0.0518
20	266	0.6882	2093790	214133	19646	627064	5048424	1.60	8.676E−09	0.0523
25	269	0.6875	2057281	214133	19646	614877	4963217	1.60	8.806E−09	0.0531
30	272	0.6867	2022440	214133	19646	603058	4881718	1.60	8.934E−09	0.0539
35	275	0.6860	1988039	214133	19646	591592	4801450	1.60	9.064E−09	0.0547
40	278	0.6853	1954635	214133	19646	580465	4723513	1.60	9.194E−09	0.0554
45	280	0.6848	1933087	214133	19646	573229	4673181	1.60	9.280E−09	0.0560
50	283	0.6841	1901253	214133	19646	562637	4598922	1.60	9.410E−09	0.0567
55	286	0.6834	1870316	214133	19646	552349	4526760	1.60	9.539E−09	0.0575
60	289	0.6827	1840240	214133	19646	542354	4456613	1.60	9.669E−09	0.0583
65	291	0.6822	1820829	214133	19646	535848	4411286	1.60	9.754E−09	0.0588
70	294	0.6815	1792115	214133	19646	526316	4344325	1.60	9.883E−09	0.0596
75	297	0.6808	1764179	214133	19646	517048	4279184	1.60	1.001E−08	0.0604
80	300	0.6801	1736991	214133	19646	508033	4215795	1.60	1.014E−08	0.0612
85	303	0.6793	1711030	214133	19646	499263	4155102	1.60	1.027E−08	0.0619
90	305	0.6789	1693437	214133	19646	493548	4114202	1.60	1.035E−08	0.0624
95	308	0.6781	1668607	214133	19646	485166	4056160	1.60	1.048E−08	0.0632
100	311	0.6774	1643934	214133	19646	477006	3998653	1.60	1.061E−08	0.0640
105	314	0.6767	1619892	214133	19646	469059	3942623	1.60	1.074E−08	0.0647
110	316	0.6762	1604363	214133	19646	463876	3906382	1.60	1.082E−08	0.0653
115	319	0.6755	1581325	214133	19646	456269	3852697	1.60	1.095E−08	0.0660
120	322	0.6748	1558861	214133	19646	448856	3800357	1.60	1.107E−08	0.0668
125	325	0.6741	1536954	214133	19646	441630	3749317	1.60	1.120E−08	0.0675
130	328	0.6734	1515584	214133	19646	434585	3699532	1.60	1.133E−08	0.0683
135	330	0.6729	1501775	214133	19646	429987	3667316	1.60	1.141E−08	0.0688
140	333	0.6722	1481259	214133	19646	423231	3619528	1.60	1.154E−08	0.0696
145	336	0.6715	1461234	214133	19646	416640	3572886	1.60	1.166E−08	0.0703
150	339	0.6707	1442113	214133	19646	410209	3528214	1.60	1.178E−08	0.0711
154	341	0.6703	1429048	214133	19646	406008	3497883	1.60	1.187E−08	0.0716
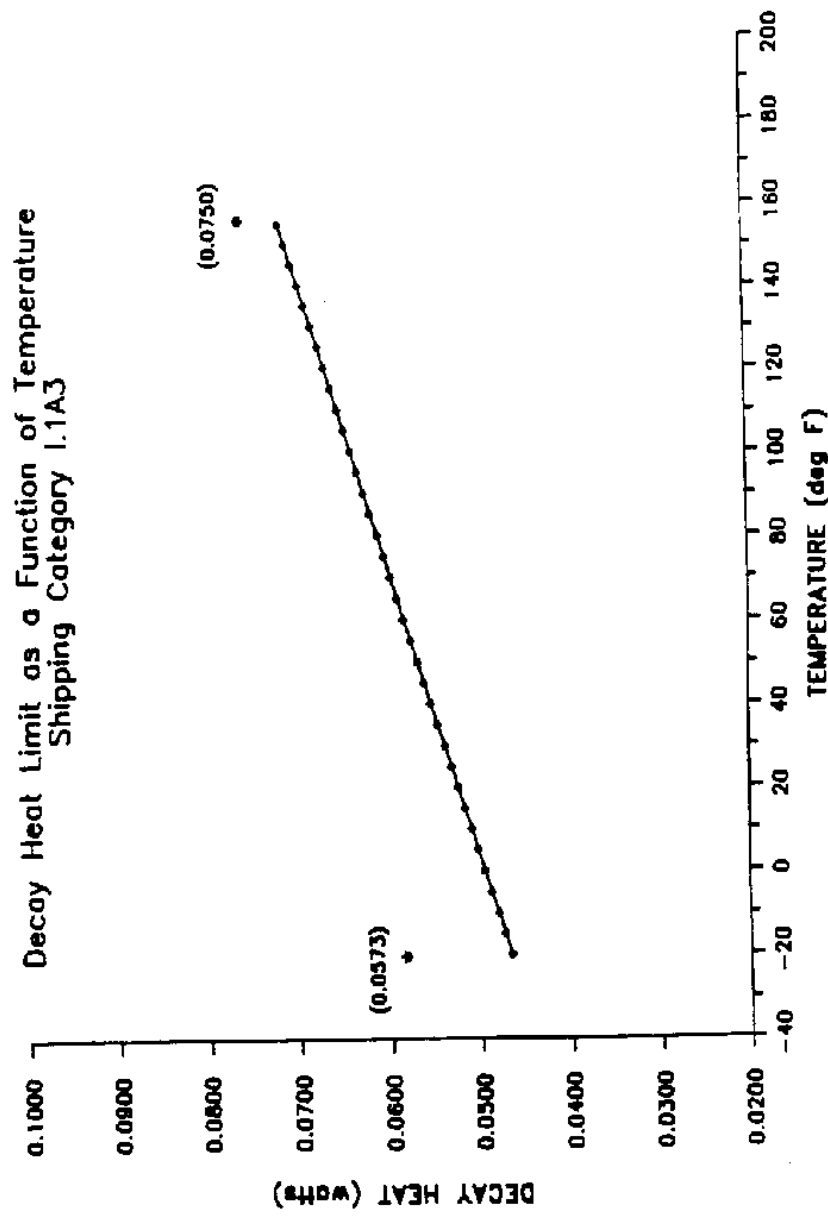
Figure 6.9-6—Decay Heat Limit as a Function of Temperature (Shipping Category I.1A3)

6.9.6 Conclusions

Hydrogen generation and release rates determined at room temperatures provide the most conservative decay heat limits for shipping categories in Waste Material Type II.1 and Waste Type III. Hydrogen generation and release rates determined at the minimum operating temperature provide the most conservative decay heat limits for shipping categories in Waste Type I and Waste Material Type II.3. This is because the effective G value for hydrogen for Waste Type I and Waste Material Type II.3 remains constant with temperature, while the hydrogen release rates are conservatively assumed to be lower than that for room temperatures.

ATTACHMENT A

DECAY HEAT LIMIT AT THE MAXIMUM OPERATING TEMPERATURE
SHIPPING CATEGORY II.1A4

A1.0   Introduction

This attachment presents the steps for obtaining the decay heat limit for any shipping category at any temperature. The shipping category II.1A4 at the maximum operating temperature is used as an example for the calculations. The analysis presented here also shows that porosity effects on the twist-and-tape closure are negligible in calculating a decay heat limit.

The following is a list of assumptions that will be used in the calculation for the decay heat limit:

- A temperature of 154^oF (68^oC) will be assumed.

- All bags are assumed to be made of polyethylene. This will result in the highest effective G value for hydrogen at 68^oC.

- The total moles of gas in the ICV cavity will remain constant during a 60-day shipping period and will be equal to 101.56 moles based on a void volume of 2,450 liters for a 14-drum payload assembly and conditions inside the ICV when the ICV is sealed for transport [70^oF, and 1 atm pressure].

Other assumptions are listed in the appropriate subsections of this attachment.

A2.0   Release Rates at Maximum Temperature

The release rate of hydrogen through the bag closures is governed by the effective diffusion coefficient of hydrogen through each bag closure, which is a function of the binary diffusion coefficient of hydrogen in air and the porosity of the closure.[1] The release rate by molecular diffusion is directly proportional to temperature raised to the 1.75 power.[2] The porosity of the closure may be evaluated from the geometry of the closure. The resistance of a bag layer (to the release of hydrogen) is the reciprocal of the release rate. That is, while the release rate increases with temperature, the resistance decreases with temperature. The resistances of each of the different confinement layers at 154^oF (68^oC) are computed below.

---

[1] Smith, J.M., 1981, "Chemical Engineering Kinetics," 3rd Edition, McGraw-Hill Book Company, New York, New York, pp. 462-467.

[2] Perry, R.H., D.W. Green, and J.O. Maloney, 1984, "Perry's Chemical Engineers' Handbook," 6th Edition, McGraw-Hill Book Company, New York, New York.

A2.1 Resistance of Inner Bags

The Random-Pore Model of gaseous diffusion in porous media[1] predicts that the effective diffusion coefficient is equal to the product of effective binary diffusion coefficient of the hydrogen in air system and the square of the porosity.

Therefore,

$$D_e = D_{Hydrogen-Air} \, \in^2 \tag{1}$$

where,

D_e $\qquad\qquad$ = $\quad$ effective diffusion coefficient of hydrogen through closure (mole/sec)

$D_{Hydrogen-Air}$ $\quad$ = $\quad$ binary diffusion coefficient of hydrogen in air (mole/sec)

$\in$ $\qquad\qquad$ = $\quad$ porosity of the closure.

Since the binary diffusion coefficient varies with temperature raised to the 1.75 power[2], the effective diffusion coefficient of hydrogen through the closure (the release rate) at temperature T_2 may be computed from the release rate at temperature T_1 using the relationship:

$$D_{e2} = D_{e1} \, (T_2/T_1)^{1.75} \, (\in_2/\in_1)^2 \tag{2}$$

where,

D_{e2} $\qquad\qquad$ = $\quad$ release rate of hydrogen through closure at temperature T_2 (mole/sec)

D_{e1} $\qquad\qquad$ = $\quad$ release rate of hydrogen through closure at temperature T_1 (mole/sec)

$\in_2$ $\qquad\qquad$ = $\quad$ porosity of closure at temperature T_2

$\in_1$ $\qquad\qquad$ = $\quad$ porosity of closure at temperature T_1

T $\qquad\qquad$ = $\quad$ absolute temperature (K).

By definition the porosity is the volume of voids per total volume. The volume of the bag material in the closure may be computed as:

$$V_m = 2lhw \tag{3}$$

where,

V_m $\qquad\qquad$ = $\quad$ volume of the bag material in the closure

l   =   length of bag comprising closure, 5.5 inches (see Spurgeon[3])

h   =   width of bag comprising closure, 10.0 inches (Appendix 6.8 of the CH-TRU
                    Payload Appendices)

w   =   thickness of bag material, 14 mil or 0.014 inch (Appendix 6.8 of the CH-TRU
                    Payload Appendices)

V_m =   2(5.5 inches)(10.0 inches)(0.014 inch) = 1.540 in^3.

The total volume of the closure is evaluated as:

$$V_T = \pi r^2 l \tag{4}$$

where,

V_T =   total volume of the closure

r   =   radius of the closure, average of 0.529 inches (see Spurgeon[3])

V_T = $\pi(0.529 \text{ inches})^2(5.5 \text{ inches}) = 4.835 \text{ in}^3$.

The porosity of the closure at 21°C, ϵ_1, is then computed as:

$\epsilon_1 = (V_T - V_m(21^oC))/V_T = (4.835 - 1.540)/4.835 = 0.6815$

The volumetric expansion of the bag material due to thermal stress induced by a temperature increase may be derived from Sears and Zemansky (1963)[4] as:

$$\triangle V_m = 3\alpha V_m \Delta T \tag{5}$$

where,

ΔV_m =   volumetric expansion of bag material due to thermal stress (in^3)

α =   linear coefficient of thermal expansion of the bag material (K^{-1})

ΔT = $T_2 - T_1$ =   temperature increase (K)

---

[3] Spurgeon, B., Personal Communication, PN Services, Inc., Richland, Washington, July 1989.

[4] Sears, F.W., and M.W. Zemansky, 1963, "University Physics," 3rd Edition, Addison-Wesley Publishing Company, Inc., Reading Massachusetts, p. 347.

The highest reported linear coefficient of thermal expansion for polymers of $25(10)^{-5}$ K^{-1} will be used in the calculation.[5] This a conservative assumption since it will provide the maximum reduction in closure porosity with temperature.

$\Delta V_m = 3(25(10)^{-5}$ K$^{-1})(1.540$ in$^3)(341$K - 294K)

$\Delta V_m = 0.054$ in^3

The volume of the bag material in the closure at temperature T_2 (68°C) will then be:

$V_m(68^oC) = V_m(21^oC) + \Delta V_m = 1.540$ in^3 + 0.054 in^3

$V_m(68^oC) = 1.594$ in^3

The porosity of the closure at 68°C, ϵ_2, is then computed as:

$\epsilon_2 = (V_T - V_m(68^oC))/V_T = (4.835 - 1.594)/4.835 = 0.6703$

The release rate of hydrogen from the closure at 21°C, D_{e1}, is $5.58(10)^{-7}$ mole/sec.

The release rate from the closure at 68°C, D_{e2} is then computed from equation (2) as:

$D_{e2} = 5.58(10)^{-7}$ mole/sec $(341$K $/ 294$K$)^{1.75}$ $(0.6703 / 0.6815)^2$

$D_{e2} = 7.00(10)^{-7}$ mole/sec

The resistance of the inner bag to the release of hydrogen at 68°C, r(inner bag, 68°C), is then:

r(inner bag, 68°C) =   1/D_{e2}
$\quad\quad\quad\quad$ =   1 / (7.00(10)$^{-7}$ mole/sec)
$\quad\quad\quad\quad$ =   1,429,048 sec/mole

For comparison purposes,

r(inner bag, 21°C) = 1,792,115 sec/mole

A2.2 Resistance of Liner Bags

The release rate from a large liner bag at 68°C is assumed to be the lowest measured total release. No credit is taken for increased release through the liner bags at the higher temperature due to increased permeation and diffusion.

---

[5] Rodriguez, F., 1982, "Principles of Polymer Systems," 2nd Edition, McGraw-Hill Book Company, New York, New York, pp. 532-537.

The resistance of the liner bag, r(liner bag) is from Appendix 6.7 of the CH-TRU Payload Appendices,

r(liner bag) = $1/(29.15(10)^{-6}$ mole/sec) = 34,303 sec/mole.

A2.3 Resistance of Filter

The mechanism of release through the filter is also by diffusion; therefore, using the minimum measured diffusion coefficient of $1.9(10)^{-6}$ mole/sec at $70^{o}F$ ($21^{o}C$) (Appendix 6.7 of the CH-TRU Payload Appendices), the resistance at $154^{o}F$ ($68^{o}C$) is:

r(drum filter)   = $1/(1.9(10)^{-6})$mole/sec x $(294/341)^{1.75}$
                 = 406,008 sec/mole

A2.4 Resistance of Drum Liner

The diffusion through a 0.3 inch diameter hole at $-20^{o}F$ ($-29^{o}C$) is used to determine the total release rate (see Appendix 6.7 of the CH-TRU Payload Appendices). No credit is taken for permeation through the liner material or for increased diffusion through the hole at the higher temperature. Therefore, the resistance of the liner is: (Appendix 6.7 of the CH-TRU Payload Appendices)

r(drum liner)   = 19,646 sec/mole

A2.5 Effective Resistance

The effective resistance for the layers of confinement in a payload container in the payload shipping category II.1A4 is the sum of the individual resistances of each layer. There are 3 inner bags, 1 liner bag, the punctured rigid drum liner and the drum filter. Therefore, the effective resistance at $154^{o}F$ ($68^{o}C$), r_{eff}, is:

$r_{eff}(68^{o}C)$ = 3 x r(inner bag) + r(liner bag) + r(rigid drum liner) + r(drum filter)

$r_{eff}(68^{o}C)$ = {3(1,429,048) + 214,133 + 19,646 + 406,008} sec/mole

$r_{eff}(68^{o}C)$ = 4,926,931 sec/mole

A2.6 Increase in G Value With Temperature

The temperature corrected effective G value for hydrogen at $154^{o}F$ ($68^{o}C$) is calculated using an Arrhenius type dependence on temperature (see Appendix 3.2 of the CH-TRU Payload Appendices):

$G_{eff(T2)}$ = $G_{eff(T1)}$ $\exp[(E_G/R)\{(T_2-T_1)/(T_2 \text{ x } T_1)\}]$,

where,

E_G =   is the hydrogen generation activation energy = 0.8 kcal/g-mole for polyethylene (see Appendix 3.2 of the CH-TRU Payload Appendices).

R =   gas law constant = $1.987(10)^{-3}$ kcal/g-mole.

T_1 =   Temperature which provides the basis for the effective G values 70°F (21°C).

T_2 =   Maximum temperature in the ICV during transport of payload 154°F (68°C).

$G_{eff(T1)}$ =   Effective G value for hydrogen for Waste Material Type II.1 = 1.70 at 70°F (21°C) (see Appendix 3.2 of the CH-TRU Payload Appendices).

$G_{eff(T2)}$ =   Temperature corrected effective G value for hydrogen for Waste Material Type II.1 at 154°F (68°C).

Substituting the above values in the Arrhenius equation for the temperature corrected effective G value for hydrogen:

$G_{eff(T2)}$ =   1.70 exp[{(0.8 kcal/g-mole)/$1.987(10)^{-3}$ kcal/g-mole} x (341 - 294)/(341 x 294)}]

$G_{eff(T2)}$ =   2.05.

A2.7 Decay Heat Limit at Maximum Temperature

The allowable hydrogen gas generation rate per innermost confinement layer is computed using equation (4) of Appendix 2.3 of the CH-TRU Payload Appendices:

$$CG = (X_{inner})/(r_{eff} + (t)(N_{gen})/N_{tg})$$

$$CG = (0.05)/\{4,926,931 \text{ sec/mole} + [(60 \text{ days})(86,400 \text{ sec/day})(14)/(101.56 \text{ moles})]\}$$

$$= 8.863(10)^{-9} \text{ mole/sec}.$$

For shipping category II.1A4, the temperature corrected effective G value for hydrogen at 154^oF (68^oC) is 2.05. Therefore, the decay heat limit per innermost confinement layer, Q_i, is:

$$Q_i = [8.863(10)^{-9} \text{ mole/sec}][6.023(10)^{23} \text{ molecules/mole}]$$

$$\text{x } [1.602(10)^{-19} \text{ watt-sec/eV}]/[2.05 \text{ molecules/100 eV}]$$

$$= 0.0417 \text{ watt.}$$

The computed decay heat of 0.0417 watt at 154^oF (68^oC) is higher than the decay heat of 0.0414 watt that was calculated assuming a temperature of 70^oF (21^oC).

The sample calculation above demonstrates that the decay heat limit would be higher for the maximum operating temperature than at room temperatures even when the increase in the effective G value and possible closure restriction effects are considered.

This page intentionally left blank.

ATTACHMENT B

DECAY HEAT LIMITS USING MORE REALISTIC RELEASE RATES

B1.0 Introduction

This attachment presents the derivation of decay heat limits using more realistic hydrogen release rate assumptions than those used to obtain the decay heat limits in the CH-TRAMPAC (assumptions listed in Attachment A of this appendix). The limits indicated as single points in Figures 6.9-3 and 6.9-6 of this appendix would be applicable at each end of the operating temperature range. This attachment is provided for illustrative purposes to demonstrate the added margin of safety included in the analysis for the decay heat limits that are applicable to each payload shipping category.

The following is a list of assumptions that will be used in the calculations:

- For small inner bags (excluding the drum liner bags), only the diffusion through the twist-and-tape closure is used in determining the total release rate. No credit is taken for permeation through the bag material. As indicated by actual experimental measurements (Appendix 6.8 of the CH-TRU Payload Appendices), the release rate through the inner bags is not decreased at the lower operating temperatures. At temperatures above room temperature, the release rate (by diffusion) from the inner bags is a function of temperature raised to the 1.75 power and the square of porosity.

- For the drum liner bags, the sum of diffusion through the bag closure and permeation of the bag material is used in determining the total release rate. The lowest measured total release rate at three different test temperatures (Appendix 6.8 of the CH-TRU Payload Appendices) will be used for the release rate from a liner bag at temperatures below 70°F (21°C). Credit is taken for increased release through the liner bags at the higher temperature end due to increased permeation and diffusion.

- For the rigid drum liner, the diffusion through a 0.3" diameter hole will vary with the 1.75 power of temperature. No credit was taken for permeation through the liner material.

- For the filter vent in the payload containers, the lowest measured diffusion coefficient was used to determine the total release rate (Appendix 6.7 of the CH-TRU Payload Appendices) at room temperature. The release rate from the filter by diffusion will vary with the 1.75 power of temperature.

B2.0 Quantification of Confinement Layer Resistances at Minimum and Maximum Temperatures

The resistances of each of the different confinement layers at -20°F (-29°C) and at 154°F (68°C) are computed below based on the aforementioned assumptions. The resistance of a confinement layer to the release of hydrogen is the reciprocal of the hydrogen release rate from that layer.

B2.1 Resistance of Drum Liner

The drum liner resistance at -20°F, r(drum liner, -20°F) is 19,646 sec/mole. The resistance at 154°F (68°F) will be computed using equation (5) of Table 6.9-1 of this document.

r(drum liner 154°F)   = 19,646 sec/mole x (244/341)$^{1.75}$
                                 = 10,937 sec/mole.

B2.2 Resistance of Filter

The mechanism of release through the filter is by diffusion, with a temperature dependence described by equation (2) in Table 6.9-1 of this document. The resistance of the filter at the minimum and maximum temperatures are:

r(drum filter, -20°F) = 1/1.9(10)$^{-6}$ sec/mole x (294/244)$^{1.75}$
r(drum filter, -20°F) = 729,327 sec/mole

r(drum filter, 154°F) = 1/1.9(10)$^{-6}$ sec/mole x (294/341)$^{1.75}$
r(drum filter, 154°F) = 406,008 sec/mole.

B2.3 Resistance of Inner Bags

The release rate through the inner bags is not decreased at lower operating temperatures, therefore:

r(inner bag, -20°F) = r(inner bag, 70°F) = 1,792,115 sec/mole

At 154°F (68°C), equation (5) of this document is used for the dependence of the hydrogen release rate from the inner bag with temperature. The porosities values were computed in Attachment A of this appendix.

r(inner bag, 154°F) = 1/1.58(10)$^{-7}$(T$_1$/T$_2$)$^{1.75}$ ($\in_1/\in_2$)^2
r(inner bag, 154°F) = 1,792,115 sec/mole x (294/341)$^{1.75}$(0.6815/0.6703)^2
r(inner bag, 154°F) = 1,429,048 sec/mole

B2.4 Resistance of Liner Bags

The lowest measured total release rate at three different test temperatures (Appendix 6.8 of the CH-TRU Payload Appendices) will be used for the release rate from a liner bag at temperatures below $70^{o}F$ ($21^{o}C$). Therefore:

r(liner bag, $-20^{o}F$) = r(liner bag, $70^{o}F$) = 214,133 sec/mole

The hydrogen release rate from a large liner bag at $154^{o}F$ ($68^{o}C$) will be calculated as the sum of the following three terms:

a.   the total release rate (sum of the diffusion through the bag closure and bag permeation) from a large liner bag at $70^{o}F$ ($21^{o}C$)

   = $4.67(10)^{-6}$ mole/sec (Appendix 6.7 of the CH-TRU Payload Appendices)

b.   the increase in the diffusion rate from the bag closure due to increased temperature. This value is taken to be the same as for the increase seen in the small bag closure

   =   (1/1,429,048 - 1/1,792,115)
   = $1.4(10)^{-7}$ mole/sec

c.   the increase in the release rate due to higher permeation rates (P) as a result of the increase in temperature

   = $P(154^{o}F)$ - $P(70^{o}F)$.

   The rate of release by permeation at $154^{o}F$ ($68^{o}C$) will be computed from the release rate dependence on temperature in an Arrhenius function (Appendix 6.7 of the CH-TRU Payload Appendices) as

   $$P(154^{o}F) = P(70^{o}F)\exp\{(E_p/R) \times (T_2 - T_1)/(T_2 \times T_1)\}$$

where,

   E_p = activation energy for hydrogen permeation through polyethylene.
      = [8.2 kcal/g-mole] (Appendix 6.7 of the CH-TRU Payload Appendices)

   $P(21^{o}C)$ is the difference between the total release and the bag closure release.

   $P(21^{o}C)$ = $4.67(10)^{-6}$ mole/sec - $5.58(10)^{-7}$ mole/sec
              = $4.11(10)^{-6}$ mole/sec

   Substituting for these values:
   $P(68^{o}C)$ - $P(21^{o}C)$ = $24.34(10)^{-6}$ mole/sec

Therefore the hydrogen release rate from a large liner bag at 154°F (68°C) is:

$$= 4.67(10)^{-6} + 1.4(10)^{-7} + 24.34(10)^{-6} \text{ mole/sec}$$
$$= 29.15(10)^{-6} \text{ mole/sec}$$

The resistance of the liner bag, r(liner bag) is the reciprocal of the release rate,

$$r(\text{liner bag}) = 1/29.15(10)^{-6} \text{ sec/ mole} = 34,305 \text{ sec/mole}$$

B3.0 G Values at Minimum and Maximum Temperatures

The temperature corrected effective G value for hydrogen at both -20°F (-29°C) and at 154°F (68°C) for shipping category II.1A4 were computed as

G_{eff} (II.1A4 at -20°F) = 1.28

G_{eff} (II.1A4 at 154°F) = 2.05

For Waste Type I, the G value does not change with temperature (Appendix 3.2 of the CH-TRU Payload Appendices), therefore,

G_{eff} (I.1A3 at 70°F) = G_{eff} (I.1A3 at -20°F) = G_{eff} (I.1A3 at 154°F) = 1.60

B4.0 Decay Heat Limit At Minimum Normal Operating Temperature For Shipping Category I.1A3

The effective resistance for shipping category I.1A3 is the sum of the individual resistances. There are 2 inner bags, 1 liner bag, the punctured rigid drum liner, and the drum filter. Therefore, the effective resistance, r_{eff} is

$r_{eff(I.1A3, -20°F)}$ $= 2 \times r(\text{inner bag}) + r(\text{liner bag}) + r(\text{drum liner}) + r(\text{drum filter})$

$r_{eff(I.1A3, -20°F)}$ $= \{2(1,792,115) + 214,133 + 19,646 + 729,327\} \text{ sec/mole}$

$r_{eff(I.1A3, -20°F)}$ $= 4,547,336 \text{ sec/mole}.$

The maximum allowable hydrogen generation rate is computed from equation (2) of Table 6.9-3 as:

CG (I.1A3, -20°F) = 0.05/(4,547,336 + 714,612) mole/sec
CG (I.1A3, -20°F) = $9.502(10)^{-9}$ mole/sec

The decay heat limit is computed from equation (3) of Table 6.9-3 as:

Q_i(I.1A3 at -20°F) = [9.502(10)$^{-9}$ mole/sec][6.023(10)^{23} molecules/mole] x [1.602(10)$^{-19}$ watt-sec/eV]/(1.60 molecules/100 eV]

Q_i(I.1A3 at -20°F) = 0.0573 watt.

B5.0 Decay Heat Limit At Minimum Normal Operating Temperature for Shipping Category II.1A4

The effective resistance for shipping category II.1A4 is the sum of the individual resistances. There are 3 inner bags, 1 liner bag, the punctured drum liner, and the drum filter. Therefore, the effective resistance, r_{eff} is

$r_{eff(II.1A4,-20°F)}$ =   3 x r(inner bag) + r(liner bag)
                                           + r(drum liner) + r(drum filter)

$r_{eff(II.1A4,-20°F)}$ =   {3(1,792,115) + 214,133 + 19,646 + 729,327} sec/mole

$r_{eff(II.1A4,-20°F)}$ =   6,339,451 sec/mole

The maximum allowable hydrogen generation rate is computed from equation (2) of Table 6.9-3 as:

CG (II.1A4, -20°F) = 0.05/(6,339,451 + 714,612) mole/sec

CG (II.1A4, -20°F) = 7.088(10)$^{-9}$ mole/sec

The decay heat limit is computed from equation (3) of Table 6.9-3 as:

Q_i (II.1A4 at -20°F)   =   [7.088(10)$^{-9}$ mole/sec] [6.023(10)^{23} molecules/mole]
                                         x [1.602(10)$^{-19}$ watt-sec/eV]/(1.28 molecules/100 eV]

Q_i(II.1A4 at -20°F) = 0.0534 watt.

B6.0 Decay Heat Limit at Maximum Normal Operating Temperature for Shipping Category I.1A3

The effective resistance for shipping category I.1A3 at 154°F (68°C) is evaluated using the resistances computed above as:

$r_{eff(I.1A3,154°F)}$ = {2(1,429,048) + 34,305 + 10,937 + 406,008} sec/mole

$r_{eff(I.1A3,154°F)}$ = 3,309,346 sec/mole

The maximum allowable hydrogen generation rate is computed from equation (2) of Table 6.9-3 as:

CG (I.1A3, 154°F) = 0.05/(3,309,364 + 714,612) mole/sec
CG (I.1A3, 154°F) = 1.243(10)$^{-8}$ mole/sec

The decay heat limit is computed from equation (3) of Table 6.9-3 as:

Q_i (I.1A3 at 154°F)   =   [1.243(10)$^{-8}$ mole/sec] [6.023(10)^{23} molecules/mole] x [1.602(10)$^{-19}$
watt-sec/eV]/(1.60 molecules/100 eV]

Q_i(I.1A3 at -20°F) = 0.0750 watt.

B7.0 Decay Heat Limit at Maximum Normal Operating Temperature for Shipping Category II.1A4

The effective resistance for shipping category II.1A4 at 154°F (68°C) is evaluated using the resistances computed above as:

$r_{eff(II.1A4,154°F)}$ = {3(1,429,048) + 34,305 + 10,937 + 406,008} sec/mole

$r_{eff(II.1A4,154°F)}$ = 4,738,394 sec/mole

The maximum allowable hydrogen generation rate is computed from equation (2) of Table 6.9-3 as:

CG (II.1A4, 154°F) = 0.05/(4,738,394 + 714,612) mole/sec
CG (II.1A4, 154°F) = 9.169(10)$^{-9}$ mole/sec

The decay heat limit is computed from equation (3) of Table 6.9-3 as:

Q_i (II.1A4 at 154°F)   =   [9.169(10)$^{-9}$ mole/sec] [6.023(10)^{23} molecules/mole] x [1.602(10)$^{-19}$
watt-sec/eV]/(2.05 molecules/100 eV]

Q_i(II.1A4 at 154°F) = 0.0432 watt.

The four decay heat limits derived above in Sections B4.0, B5.0, B6.0 and B7.0 of this attachment are the points marked in Figures 6.9-3 and 6.9-6 of this appendix. The use of the assumptions outlined in this Attachment provides decay heat limits at each end of the operating temperature range that are higher than the limits applied to each shipping category, as shown in the two figures.

APPENDIX 6.10

EFFECT ON DECAY HEAT LIMITS OF OVERPACKING PAYLOAD CONTAINERS

This page intentionally left blank.

6.10 Effect on Decay Heat Limits of Overpacking Payload Containers

6.10.1 Summary

The ten-drum overpack (TDOP) and standard waste box (SWB) are containers that will be primarily used to overpack other payload containers. One of the transportation parameters that could be affected as a result of this overpacking is the allowable decay heat limit per each payload container. The analyses presented in this appendix show that overpacking payload containers in a TDOP fitted with nine filters (total hydrogen diffusivity of 3.33E-5 moles per second per mole fraction [m/s/mf]) or an SWB fitted with four filters (total hydrogen diffusivity of 1.48E-5 m/s/mf) will not decrease the allowable decay heat limits, even when payload containers are allowed to remain overpacked in a TDOP or an SWB fitted with four filters for indefinite periods of time before transport. For example, a 55-gallon drum that meets the decay heat limit for a 14-drum payload in a TRUPACT-II can also be shipped in a 10-drum configuration in a TDOP inside a TRUPACT-II or in a 4-drum configuration in an SWB (fitted with four filters) with two SWBs inside a TRUPACT-II. This is due to the following reasons:

- The TDOP is fitted with a minimum of nine filters (total hydrogen diffusivity of 3.33E-5 m/s/mf) that allow hydrogen release from the TDOP. The SWB fitted with four filters (total hydrogen diffusivity of 1.48E-5 m/s/mf) will allow hydrogen release from the SWB.

- The number of payload containers per shipment is less when overpacked in a TDOP or SWB compared to the case when containers are not overpacked in a TDOP or SWB. For example, when drums are overpacked in a TDOP, there is a 10 drum payload compared to a 14-drum payload without the overpacking. Similarly, there is only an 8-drum payload when overpacked in an SWB compared to a 14-drum payload without the overpacking. The lesser number of payload containers result in less accumulation of hydrogen in the ICV and the payload containers during shipment.

- There is a known amount of additional void volume available in payload configurations overpacked in the TDOP or SWB, which reduces overall concentrations of the hydrogen generated.

This appendix describes the mathematical analyses supporting the conclusion that no reduction in decay heat limits occurs for payload configurations overpacked in a TDOP or in an SWB fitted with four filters (total hydrogen diffusivity of 1.48E-5 m/s/mf). Decay heat limits for all other overpacked configurations can be conservatively classified into one of the existing configurations for which decay heat limits have been specified in the Contact-Handled Transuranic Waste Authorized Methods for Payload Control (CH-TRAMPAC) document.

6.10.2 Introduction

The TDOP is an authorized payload container in the TRUPACT-II that will be used primarily for the overpacking of other payload containers (it can also be used for the direct loading of waste). Specifications for the TDOP are given in Section 2.9 of the CH-TRAMPAC.

In addition, the SWB can be used to overpack up to four 55-gallon drums with either two or four filters installed in the SWB. It is possible that these overpacked payload configurations may be kept in interim storage for indefinite periods of time before shipment in a TRUPACT-II (i.e., it is not necessary that shipment occur immediately after overpacking in a TDOP or SWB). Decay heat limits for drums overpacked in SWBs with two filters are derived as described in the CH-TRAMPAC document. Overpacking in a TDOP or an SWB fitted with four filters could potentially affect the allowable decay heat limits for payload containers due to the following differences from equivalent configurations that are not overpacked:

- There is an additional layer of resistance to the release of hydrogen when containers are overpacked.

- The number of payload containers is less when overpacked in a TDOP or in two SWBs (e.g., 10 drums per TDOP and TRUPACT-II compared to 14 drums per TRUPACT-II when not overpacked in a TDOP; one SWB per TDOP and TRUPACT-II compared to two SWBs per TRUPACT-II when not overpacked in a TDOP). The lesser number of payload containers results in less accumulation of hydrogen in the TRUPACT-II during shipment, compared to shipments where payload containers are not overpacked.

- Due to the lesser number of containers overpacked, there is additional void volume available for gas accumulation in payload configurations using overpacking.

The purpose of this appendix is to analyze these potential impacts on decay heat limits. As shown by the mathematical analysis in the following sections, decay heat limits for payload containers are not decreased by overpacking in a TDOP or in an SWB fitted with four filters (total hydrogen diffusivity of 1.48E-5 m/s/mf), and the decay heat limits that have been calculated for the payload containers without the overpacking are applicable even in the overpacked condition in a TDOP or in an SWB fitted with four filters.

6.10.3 Assumptions and Quantification of Input Parameters

Values of the input parameters used in the analysis, with applicable assumptions, are presented in this section.

6.10.3.1 Resistances of the Confinement Layers

The resistances of the various confinement layers to the release of hydrogen are quantified in Appendix 6.7 of the CH-TRU Payload Appendices, and are summarized in Table 6.10-1. The logic for the two different values of a confinement layer resistance (one value for Waste Type I and a second value for Waste Types II and III) is provided in Appendix 6.9 of the CH-TRU Payload Appendices. The analysis assumes the use of nine filters on the TDOP or four filters on the SWB. Each filter has a hydrogen diffusivity of 3.7E-6 m/s/mf. A lesser number of filters may be used provided the total hydrogen diffusivity is equal to or greater than 3.33E-5 m/s/mf for the TDOP and 1.48E-5 m/s/mf for the SWB.

Table 6.10-1 — Resistances of the Confinement Layers

Confinement Layer	Resistances (sec/mole)	
	Waste Type I	Waste Types II and III
Drum Filter	729,327	526,316
SWB/Bin Filter	374,519	270,270
85-Gallon Drum Filter	374,519	270,270
TDOP Filter	374,519	270,270
Inner Bag	2,398,864	1,792,115
Drum Liner Bag	214,133	214,133
SWB/Bin/TDOP Liner	125,660	125,660
Punctured Drum Liner	19,646	19,646

6.10.3.2 Void Volumes

Based on the specifications for the TDOP in Section 2.9.9 of the CH-TRAMPAC, the external volume occupied by a TDOP is 4,473 liters and the internal volume is 4,426 liters. The void volume within an empty TRUPACT-II ICV is approximately 5,750 liters. The void volume between the TDOP and the TRUPACT-II ICV is approximately 1,277 liters. The void volume inside a TDOP with a payload of 10 55-gallon drums is 2,069 liters. The volume occupied by two SWBs is approximately 4,000 liters. The net void volume for gas accumulation in the ICV is 1,750 liters for an assembly of SWBs. These void volumes serve to reduce hydrogen concentrations in the different layers of the package and payload.

6.10.3.3 Other Input Parameters

All other input parameters for the decay heat calculations are the same as those presented in Appendices 6.7 and 6.9 of the CH-TRU Payload Appendices.

6.10.4 Methodology and Mathematical Analyses

The analysis conservatively assumes that the overpacked payload containers inside the TDOP or SWB can remain inside indefinitely, i.e., steady-state conditions with the maximum gas concentrations are attained. The TDOP or SWB is then loaded into the TRUPACT-II for a 60-day shipping period. Each of the payload configurations to be overpacked is analyzed below to determine impacts on decay heat limits.

Configuration 1: 10 55-gallon Drums Overpacked in a TDOP

The analysis for the configuration of 10 55-gallon drums overpacked in a TDOP is based on modeling the buildup of flammable gas within the TRUPACT-II payload assembly during the 60-day shipping period. The first step in the analysis was the calculation of a pseudo steady-

state gas generated concentrations within the TDOP as a first approximation. The following equations calculate these concentrations:

$$X_{TDOP} \quad = \quad C_g{}' \, (10 \, r_{TDOP \, filter}/n_{TDOP})$$

$$X_{Annular} \quad = \quad C_g{}' \, r_{df} + X_{TDOP}$$

$$X_{Drum \, Liner} \quad = \quad C_g{}' \, r_{dl} + X_{Annular}$$

$$X_{Multiple \, Bag \, Void} \quad = \quad C_g{}' \, (r_{Inner \, Bags} + r_{liner \, bags}) + X_{Drum \, Liner}$$

where:

X_{TDOP} $\quad = \quad$ mole fraction of flammable gas within the TDOP void volume

$X_{Annular}$ $\quad = \quad$ mole fraction of flammable gas within the annular space between the drum liner and the drum

$X_{Drum \, Liner}$ $\quad = \quad$ mole fraction of flammable gas within the drum liner void volume

$X_{Multiple \, Bag \, Void}$ $=$ mole fraction of flammable gas within the innermost confinement layer

$r_{inner \, bags}$ $\quad = \quad$ total resistance of the inner bags to the release of flammable gas (sec/mole)

$r_{liner \, bags}$ $\quad = \quad$ total resistance of the liner bags to the release of flammable gas (sec/mole)

r_{dl} $\quad = \quad$ resistance of the drum liner to the release of flammable gas (sec/mole)

r_{df} $\quad = \quad$ resistance of the 55-gallon drum filter to the release of flammable gas (sec/mole)

$r_{TDOP \, filter}$ $\quad = \quad$ resistance of a single filter on the TDOP to the release of flammable gas (sec/mole)

n_{TDOP} $\quad = \quad$ number of filters on the TDOP

$C_g{}'$ $\quad = \quad$ first approximation for maximum allowable flammable gas generation rate (mole/sec)

For example, if pseudo-steady-state flammable gas generation rate is used as the first approximation:

$$C_g{}' \quad = \quad \frac{0.05}{r_{eff} + \left(10\dfrac{t}{N_{tg}}\right)}$$

where

r_{eff} = effective resistance of all confinement layers of the generating container to the release of flammable gas (sec/mole)

t = maximum shipping period duration (60 days)

N_{tg} = total moles of gas inside the TRUPACT-II ICV cavity outside of the TDOP,

= $P\ V_{void}/RT$

where:

P = pressure inside the TRUPACT-II, assumed to be constant at 1 atm., because the amount of gas generated is much less than the total amount of air originally present in the cavity

V_{void} = void volume inside the TRUPACT-II ICV and outside of the TDOP, i.e. 1,277 liters with a TDOP inside the TRUPACT-II

R = gas constant = 0.08206 atm-liter/mole-K

T = absolute temperature = 294 K.

Equations were then developed to calculate the flammable gas concentration within the various payload assembly layers as a function of time during the shipping period. Collectively, these equations model the diffusion of flammable gas generated within the waste across the various resistance layers present in the payload assembly.

$$\frac{dX_{Multiple\ Bag\ Void}}{dt} = \frac{C_g\ RT}{PV_{Multiple\ Bag\ Void}} - \frac{R_{bags}}{V_{Multiple\ Bag\ Void}}(X_{Multiple\ Bag\ Void} - X_{Drum\ Liner})$$

$$\frac{dX_{Drum\ Liner}}{dt} = \frac{R_{bags}}{V_{Drum\ Liner}}(X_{Multiple\ Bag\ Void} - X_{Drum\ Liner}) - \frac{R_{dl}}{V_{Drum\ Liner}}(X_{Drum\ Liner} - X_{Annular})$$

$$\frac{dX_{Annular}}{dt} = \frac{R_{dl}}{V_{Annular}} (X_{Drum\ Liner} - X_{Annular}) - \frac{R_{df}}{V_{Annular}} (X_{Annular} - X_{TDOP})$$

$$\frac{dX_{TDOP}}{dt} = \frac{10\ R_{df}}{V_{TDOP}} (X_{Annular} - X_{TDOP}) - \frac{n_{TDOP}\ R_{TDOP\ filter}}{V_{TDOP}} (X_{TDOP} - X_{ICV})$$

$$\frac{dX_{ICV}}{dt} = \frac{n_{TDOP}\ R_{TDOP\ filter}}{V_{void}} (X_{TDOP} - X_{ICV})$$

where:

R_{bags} = release rate across the inner bags and liner bags of flammable gas (liters/day)

R_{dl} = release rate of flammable gas across the drum liner (liters/day)

R_{df} = release rate of flammable gas across the drum filter (liters/day)

$R_{TDOP\ filter}$ = release rate of flammable gas across one TDOP filter (liters/day)

$V_{Multiple\ Bag\ Void}$ = void volume inside bag layers (conservatively assumed to be 1 liter)

$V_{Drum\ Liner}$ = void volume inside drum liner (conservatively assumed to be 1 liter)

$V_{Annular}$ = void volume between drum liner and drum (conservatively assumed to be 1 liter)

V_{TDOP} = void volume inside the TDOP with a payload of 10 55-gallon drums (2,069 liters)

X_{ICV} = mole fraction of flammable gas within the TRUPACT-II ICV cavity

C_g = maximum allowable flammable gas generation rate (mole/sec)

This system of equations must be solved simultaneously to find the maximum flammable gas generation rate that results in a concentration of five percent in the innermost confinement layer during the 60-day shipping period. The steady-state flammable gas generation rate is used as a first approximation of the allowable transient flammable gas generation rate. An iterative calculation process using the Runge-Kutta method was adapted to solve the system of equations.

Configuration 2: 8 55-Gallon Drums Overpacked in Two SWBs With Four Filters in Each SWB

The analysis for the configuration of eight 55-gallon drums overpacked in two SWBs fitted with four filters (total hydrogen diffusivity of 1.48E-5 m/s/mf) each is based on the modeling build-up of flammable gases within the payload assembly during the 60-day shipping period. The first step in the analysis was the calculation of a pseudo-steady-state gas generation concentration within the SWBs as a first approximation. The following equations calculate those concentrations:

X_{SWB} $\quad=\quad$ $C_g{'} (4\ r_{SWB\ Filter} / n_{SWB})$

$X_{Annular}$ $\quad=\quad$ $C_g{'}\ r_{df} + X_{SWB}$

$X_{Drum\ Liner}$ $\quad=\quad$ $C_g{'}\ r_{dl} + X_{Annular}$

$X_{Multiple\ Bag\ Void} =$ $\quad$ $C_g{'}\ (r_{Inner\ Bags} + r_{Liner\ Bags}) + X_{Drum\ Liner}$

where $C_g{'}$, $X_{Annular}$, r_{df}, $X_{Drum\ Liner}$, r_{dl}, $X_{Multiple\ Bag\ Void}$, $r_{Inner\ Bags}$, and $r_{Liner\ Bags}$ are defined above and where:

X_{SWB} $\quad=\quad$ mole fraction of flammable gas within the SWB void volume

$r_{SWB\ Filter}$ $\quad=\quad$ resistance of a single filter on the SWB to the release of flammable gas (sec/mole)

n_{SWB} $\quad=\quad$ number of filters on the SWB.

As in Configuration 1, equations were developed to calculate the flammable gas concentration within the various payload assembly layers as a function of time during the shipping period.

$$\frac{dX_{Multiple\ Bag\ Void}}{dt} = \frac{C_g\ RT}{PV_{Multiple\ Bag\ Void}} - \frac{R_{Bags}}{V_{Multiple\ Bag\ Void}} \left(X_{Multiple\ Bag\ Void} - X_{Drum\ Liner} \right)$$

$$\frac{dX_{Drum\ Liner}}{dt} = \frac{R_{Bags}}{V_{Drum\ Liner}} \left(X_{Multiple\ Bag\ Void} - X_{Drum\ Liner} \right) - \frac{R_{dl}}{V_{Drum\ Liner}} \left(X_{Drum\ Liner} - X_{Annular} \right)$$

$$\frac{dX_{Annular}}{dt} = \frac{R_{dl}}{V_{Annular}} \left(X_{Drum\ Liner} - X_{Annular} \right) - \frac{R_{df}}{V_{Annular}} \left(X_{Annular} - X_{SWB} \right)$$

$$\frac{dX_{SWB}}{dt} = \frac{4\ R_{df}}{V_{SWB}} \left(X_{Annular} - X_{SWB} \right) - \frac{n_{SWB}\ R_{SWB\ Filter}}{V_{SWB}} \left(X_{SWB} - X_{ICV} \right)$$

$$\frac{dX_{ICV}}{dt} = \frac{2\, n_{SWB}\, R_{SWB\, Filter}}{V_{Void}}\, (X_{SWB} - X_{ICV})$$

where:

$R_{SWB\, Filter}$ =   release rate of flammable gas across one SWB filter (liters/day)

V_{SWB} =   void volume inside the SWB with a payload of four 55-gallon drums
                    (conservatively assumed to be 10 liters).

This system of equations was again solved simultaneously to find the maximum flammable gas generation rate that results in a concentration of 5 percent in the innermost confinement layer during the 60-day shipping period.

Four different packaging configurations were considered for overpacking 55-gallon drums in the SWB. The system of equations summarized above is the same for all of the packaging configurations. These packaging configurations represent the lower and upper ends of the flammable gas generation range. The four configurations were as follows:

- Four drums of Shipping Category 10 0160 0147 per SWB fitted with four SWB filters and two SWBs per TRUPACT-II. Each drum has one low hydrogen diffusivity filter (diffusion coefficient of 1.9×10^{-6} mole/sec/mole fraction).

- Four drums of Shipping Category 30 0340 1044 per SWB fitted with four SWB filters and two SWBs per TRUPACT-II. Each drum has one low hydrogen diffusivity filter.

- Four drums of Shipping Category 10 0160 0111 per SWB fitted with four SWB filters and two SWBs per TRUPACT-II. Each drum has one high hydrogen diffusivity filter (diffusion coefficient of 3.7×10^{-6} mole/sec/mole fraction).

- Four drums of Shipping Category 30 0340 1018 per SWB fitted with four SWB filters and two SWBs per TRUPACT-II. Each drum has one high hydrogen diffusivity filter.

Configuration 3: 6 85-gallon Drums Overpacked in a TDOP

The analysis for the configuration of 6 85-gallon drums overpacked in a TDOP is based on modeling the buildup of flammable gas within the TRUPACT-II payload assembly during the 60-day shipping period. The first step in the analysis was the calculation of a pseudo steady-state gas generated concentrations within the TDOP as a first approximation. The following equations calculate these concentrations:

X_{TDOP} = $C_g' (6\, r_{TDOP\, filter}/n_{TDOP})$

$X_{Annular}$ = $C_g'\, r_{85df} + X_{TDOP}$

$$X_{\text{Drum Liner}} \quad = \quad C_g{}' \, r_{dl} + X_{\text{Annular}}$$

$$X_{\text{Multiple Bag Void}} \quad = \quad C_g{}' \, (r_{\text{Inner Bags}} + r_{\text{liner bags}}) + X_{\text{Drum Liner}}$$

where:

r_{85df} =   resistance of the 85-gallon drum filter to the release of flammable gas (sec/mole)

As in Configuration 1, equations were then developed to calculate the flammable gas concentration within the various payload assembly layers as a function of time during the shipping period. Collectively, these equations model the diffusion of flammable gas generated within the waste across the various resistance layers present in the payload assembly.

$$\frac{dX_{\text{Multiple Bag Void}}}{dt} = \frac{C_g \, RT}{PV_{\text{Multiple Bag Void}}} - \frac{R_{\text{bags}}}{V_{\text{Multiple Bag Void}}} \left(X_{\text{Multiple Bag Void}} - X_{\text{Drum Liner}} \right)$$

$$\frac{dX_{\text{Drum Liner}}}{dt} = \frac{R_{\text{bags}}}{V_{\text{Drum Liner}}} \left(X_{\text{Multiple Bag Void}} - X_{\text{Drum Liner}} \right) - \frac{R_{dl}}{V_{\text{Drum Liner}}} \left(X_{\text{Drum Liner}} - X_{\text{Annular}} \right)$$

$$\frac{dX_{\text{Annular}}}{dt} = \frac{R_{dl}}{V_{\text{Annular}}} \left(X_{\text{Drum Liner}} - X_{\text{Annular}} \right) - \frac{R_{85df}}{V_{\text{Annular}}} \left(X_{\text{Annular}} - X_{\text{TDOP}} \right)$$

$$\frac{dX_{\text{TDOP}}}{dt} = \frac{6 R_{85df}}{V_{\text{TDOP}}} \left(X_{\text{Annular}} - X_{\text{TDOP}} \right) - \frac{n_{\text{TDOP}} \, R_{\text{TDOP filter}}}{V_{\text{TDOP}}} \left(X_{\text{TDOP}} - X_{\text{ICV}} \right)$$

$$\frac{dX_{\text{ICV}}}{dt} = \frac{n_{\text{TDOP}} \, R_{\text{TDOP filter}}}{V_{\text{void}}} \left(X_{\text{TDOP}} - X_{\text{ICV}} \right)$$

where:

R_{85df} =   release rate of flammable gas across the 85-gallon drum filter (liters/day)

$V_{\text{Multiple Bag Void}}$ =   void volume inside bag layers (from Appendix 3.7 of the CH-TRU Payload Appendices)

$V_{\text{Drum Liner}}$ =   void volume inside drum liner (from Appendix 3.7 of the CH-TRU Payload Appendices)

V_{Annular} =   void volume between drum liner and drum (from Appendix 3.7 of the CH-TRU Payload Appendices)

V_{TDOP} =   void volume inside the TDOP with a payload of 6 85-gallon drums (2,210 liters)

This system of equations must be solved simultaneously to find the maximum flammable gas generation rate that results in a concentration of five percent in the innermost confinement layer during the 60-day shipping period.

Other Payload Configurations

For other payload configurations, the pseudo steady-state analysis (used as a first approximation for the 10-drum configuration) is sufficient to demonstrate that decay heat limits are not decreased by overpacking in a TDOP. No further refinement of the pseudo steady-state condition is necessary since the conservative pseudo steady-state analysis itself demonstrates that decay heat limits are not decreased.

For these configurations, an equation was developed (for each of the four additional configurations) that relates the innermost confinement layer flammable gas concentration to the sum of the resistances of the confinement layers and the allowable flammable gas generation rate. These equations are summarized below for the four configurations considered. The governing equations are the same as those used in Appendix 2.3 of the CH-TRU Payload Appendices. The equations solve for the allowable gas generation rates and decay heats when overpacked in a TDOP.

Configuration 4: 4 55-gallon Drums Overpacked in an SWB Overpacked in a TDOP

$$X_1 \ = \ C_g[r_{\text{inner bags}} + r_{\text{liner bags}} + r_{dl} + r_{df} + 4r_{\text{SWB filters}} + r_{\text{TDOP filter}}/n_{\text{TDOP}} + 4(t/N_{tg})]$$

$$X_1 \ = \ C_g[r_{\text{eff}} + 4r_{\text{SWB filters}} + r_{\text{TDOP filter}}/n_{\text{TDOP}} + 4(t/N_{tg})]$$

Configuration 5: 1 SWB Overpacked in a TDOP

$$X_1 \ = \ C_g(r_{\text{inner bags}} + r_{\text{SWB liners}} + r_{\text{SWB filters}} + r_{\text{TDOP filter}}/n_{\text{TDOP}} + t/N_{tg})$$

$$X_1 \ = \ C_g(r_{\text{eff}} + r_{\text{TDOP filter}}/n_{\text{TDOP}} + t/N_{tg})$$

Configuration 6: 1 Experimental Bin Inside an SWB Overpacked in a TDOP

$$X_1 \ = \ C_g(r_{\text{inner bags}} + r_{\text{bin liners}} + r_{\text{bin filters}} + r_{\text{SWB filters}} + r_{\text{TDOP filter}}/n_{\text{TDOP}} + t/N_{tg})$$

$$X_1 \ = \ C_g(r_{\text{eff}} + r_{\text{SWB filters}} + r_{\text{TDOP filter}}/n_{\text{TDOP}} + t/N_{tg})$$

Configuration 7: 6 85-Gallon Drums Overpacked in a TDOP

X_1 = $C_g[r_{inner\ bags} + r_{liner\ bags} + r_{dl} + r_{df} + r_{85df} + 6r_{TDOP\ filter}/n_{TDOP} + 6(t/N_{tg})]$

X_1 = $C_g[r_{eff} + r_{85df} + 6r_{TDOP\ filter}/n_{TDOP} + 6(t/N_{tg})]$

where:

X_1 = mole fraction flammable gas within innermost confinement layer

$r_{bin\ liners}$ = total resistance of the bin liners to the release of flammable gas (sec/mole)

$r_{SWB\ liners}$ = total resistance of the SWB liners to the release of flammable gas (sec/mole)

$r_{SWB\ filters}$ = total resistance of the SWB filters to the release of flammable gas (sec/mole)

$r_{bin\ filters}$ = total resistance of the bin filters to the release of flammable gas (sec/mole)

The resistance terms, r_{eff}, $r_{SWB\ filters}$, and r_{85df}, represent the effective resistance of all confinement layers within the TDOP to the release of flammable gas. The next resistance term in these equations represents the resistance of the filters on the TDOP to the release of flammable gas. Since these filters act in parallel, increasing the number of filters decreases the total resistance. The last resistance term in the equations, t/N_{tg}, represents the effective resistance offered by the accumulation of flammable gas within the ICV during a 60-day shipping period.

6.10.5 Discussion of Results

Tables 6.10-2 through 6.10-8 present examples of the results of the analyses for all six overpacked configurations. The decay heat limit under the Configuration column (last column of each table) is the limit that could be applied under the overpacked condition. The decay heat limit under the Base Case column is the limit for each payload container without being overpacked in a TDOP or SWB. As can be seen in all cases, the overpacked configuration decay heat numbers are higher than the numbers for the base case. Therefore, decay heat numbers are not decreased due to overpacking in a TDOP or SWB. It is conservative to use the base case decay heat limits for the overpacked configurations. The tables cover shipping categories with no bags (least resistance) to multiple bags (high resistance). Other shipping categories not included in the tables would fall within this range of shipping categories.

6.10.6 Conclusions

The analysis presented in this appendix demonstrates that overpacking payload containers in a TDOP or an SWB fitted with four filters (total hydrogen diffusivity of 1.48E-5 m/s/mf) does not decrease the allowable decay heat limits for the payload containers. The overpacked configurations can be conservatively assigned the same decay heat limits as the equivalent configurations not using the TDOP or SWB for overpacking. A payload container in a shipping category that meets the decay heat limit for shipment without being overpacked in a TDOP fitted

with nine filters (total hydrogen diffusivity of 3.33E-5 m/s/mf) or an SWB fitted with four filters automatically meets the required decay heat limit when overpacked. In summary, for purposes of <u>flammable gas generation and decay heat limits</u>, overpacked payload configurations can be considered as follows:

Ten 55-gallon drums overpacked in a TDOP	Same as 14 55-gallon drums in a TRUPACT-II
Eight 55-gallon drums overpacked in two SWBs with four filters in each SWB	Same as 14 55-gallon drums in a TRUPACT-II
Four 55-gallon drums overpacked in an SWB overpacked in a TDOP	Same as eight 55-gallon drums overpacked in two SWBs with two filters (total hydrogen diffusivity of 7.40E-6 m/s/mf) each in a TRUPACT-II
One SWB overpacked in a TDOP	Same as two SWBs in a TRUPACT-II
One experimental bin in an SWB overpacked in a TDOP	Same as two experimental bins in two SWBs in a TRUPACT-II
Six 55-gallon drums in six 85-gallon drums overpacked in a TDOP	Same as eight 55-gallon drums overpacked in two SWBs with two filters (total hydrogen diffusivity of 7.40E-6 m/s/mf) each in a TRUPACT-II
Six 85-gallon drums overpacked in a TDOP	Same as eight 85-gallon drums in a TRUPACT-II

Table 6.10-2 — Configuration 1: 10 55-gallon Drums Overpacked in a TDOP Example Comparison of Maximum Allowable Gas Generation Rates and Decay Heats with Base Case*

Alpha-numeric Payload Shipping Category	Numeric Payload Shipping Category	Base Case		Configuration 1	
		Cg-Gas Generation (moles/sec)	Decay Heat Limit	Cg - Gas Generation (moles/sec)	Decay Heat Limit
I.1A0	10 0160 0147	3.416E-08	**0.2060**	3.474E-08	**0.2095**
I.1A1	10 0160 0168	2.980E-08	**0.1797**	3.035E-08	**0.1830**
I.1A2	10 0160 0190	2.643E-08	**0.1594**	2.687E-08	**0.1620**
I.1A3	10 0160 0648	7.721E-09	**0.0466**	7.775E-09	**0.0469**
I.2A0	10 0130 0147	3.416E-08	**0.2536**	3.474E-08	**0.2578**
I.2A1	10 0130 0168	2.980E-08	**0.2212**	3.035E-08	**0.2253**
I.2A2	10 0130 0190	2.643E-08	**0.1962**	2.687E-08	**0.1994**
I.2A3	10 0130 0648	7.721E-09	**0.0573**	7.775E-09	**0.0577**
I.2A4	10 0130 0888	5.634E-09	**0.0418**	5.667E-09	**0.0421**
I.3A0	10 0040 0147	3.416E-08	**0.8241**	3.474E-08	**0.8380**
I.3A1	10 0040 0168	2.980E-08	**0.7189**	3.035E-08	**0.7321**
I.3A2	10 0040 0190	2.643E-08	**0.6375**	2.687E-08	**0.6482**
I.3A3	10 0040 0648	7.721E-09	**0.1863**	7.775E-09	**0.1875**
I.3A4	10 0040 0888	5.634E-09	**0.1359**	5.667E-09	**0.1367**
II.1A0	20 0170 0127	3.966E-08	**0.2251**	4.368E-08	**0.2479**
II.1A1	20 0170 0148	3.390E-08	**0.1924**	3.689E-08	**0.2094**
II.1A2a	20 0170 0327	2.961E-08	**0.1680**	3.187E-08	**0.1809**
II.1A2	20 0170 0169	1.531E-08	**0.0869**	1.591E-08	**0.0903**
II.1A3	20 0170 0506	9.883E-09	**0.0561**	1.014E-08	**0.0576**
II.1A4	20 0170 0686	7.298E-09	**0.0414**	7.445E-09	**0.0423**
II.1A5	20 0170 0865	5.785E-09	**0.0328**	5.880E-09	**0.0334**
II.1A6	20 0170 1044	4.791E-09	**0.0272**	4.859E-09	**0.0276**
II.2AM	20 0000 0000	NA	**40.000**	NA	**40.000**
III.1A0	30 0340 0127	3.966E-08	**0.1126**	4.368E-08	**0.1240**
III.1A1	30 0340 0148	3.390E-08	**0.0962**	3.689E-08	**0.1047**
III.1A2a	30 0340 0327	2.961E-08	**0.0840**	3.187E-08	**0.0904**
III.1A2	30 0340 0169	1.531E-08	**0.0434**	1.591E-08	**0.0452**
III.1A3	30 0340 0506	9.883E-09	**0.0280**	1.014E-08	**0.0288**
III.1A4	30 0340 0686	7.298E-09	**0.0207**	7.445E-09	**0.0211**
III.1A5	30 0340 0865	5.785E-09	**0.0164**	5.880E-09	**0.0167**
III.1A6	30 0340 1044	4.791E-09	**0.0136**	4.859E-09	**0.0138**

* Base Case: 14 55-gallon drums (as two 7-packs) loaded directly into a TRUPACT-II

Table 6.10-3 — Configuration 2: 4 55-gallon Drums Overpacked in an SWB Fitted with Four Filters, Two SWBs per TRUPACT-II Example Comparison of Maximum Allowable Gas Generation Rates and Decay Heats with Base Case*

Alpha-numeric Payload Shipping Category	Numeric Payload Shipping Category	Base Case		Configuration 2	
		Cg-Gas Generation (moles/sec)	Decay Heat Limit	Cg - Gas Generation (moles/sec)	Decay Heat Limit
I.1A0	10 0160 0147	3.416E-08	**0.2060**	3.742E-08	**0.2257**
III.1A6	30 0340 1044	4.791E-09	**0.0136**	4.996E-09	**0.0142**
—	10 0160 0111	4.505E-08	**0.2716**	4.872E-08	**0.2938**
—	30 0340 1018	4.912E-09	**0.0139**	**5.126E**-09	**0.0145**

* Base Case: 14 55-gallon drums (as two 7-packs) loaded directly into a TRUPACT-II

Table 6.10-4 – Configuration 3: 6 85-gallon Drums Overpacked in a TDOP   Example Comparison of Maximum Allowable Gas Generation Rates and Decay Heats with Base Case*

Alpha-numeric Payload Shipping Category	Numeric Payload Shipping Category	Base Case		Configuration 3	
		Cg-Gas Generation (moles/sec)	Decay Heat Limit	Cg-Gas Generation (moles/sec)	Decay Heat Limit
—	10 0160 0050	1.000E-07	**0.6031**	1.478E-07	**0.8913**
—	30 0340 0995	5.025E-09	**0.0143**	5.178E-09	**0.0147**

*Base Case: 8 85-gallon drums loaded directly into a TRUPACT-II

Table 6.10-5 — Configuration 4: 4 55-gallon Drums Overpacked in an SWB Overpacked in a TDOP Example Comparison of Maximum Allowable Gas Generation Rates and Decay Heats with Base Case*

Alpha-numeric Payload Shipping Category	Numeric Payload Shipping Category	Base Case		Configuration 4	
		Cg-Gas Generation (moles/sec)	Decay Heat Limit	Cg - Gas Generation (moles/sec)	Decay Heat Limit
I.1B0	10 0160 0207	2.416E-08	**0.1457**	2.432E-08	**0.1466**
I.1B1	10 0160 0229	2.189E-08	**0.1320**	2.202E-08	**0.1328**
I.1B2	10 0160 0250	2.002E-08	**0.1207**	2.013E-08	**0.1214**
I.1B3	10 0160 0709	7.061E-09	**0.0426**	7.074E-09	**0.0427**
I.2B0	10 0130 0207	2.416E-08	**0.1793**	2.432E-08	**0.1805**
I.2B1	10 0130 0229	2.189E-08	**0.1625**	2.202E-08	**0.1635**
I.2B2	10 0130 0250	2.002E-08	**0.1486**	2.013E-08	**0.1494**
I.2B3	10 0130 0709	7.061E-09	**0.0524**	7.074E-09	**0.0525**
I.2B4	10 0130 0949	5.274E-09	**0.0391**	5.282E-09	**0.0392**
I.3B0	10 0040 0207	2.416E-08	**0.5827**	2.432E-08	**0.5866**
I.3B1	10 0040 0229	2.189E-08	**0.5281**	2.202E-08	**0.5312**
I.3B2	10 0040 0250	2.002E-08	**0.4828**	2.013E-08	**0.4855**
I.3B3	10 0040 0709	7.061E-09	**0.1703**	7.074E-09	**0.1706**
I.3B4	10 0040 0949	5.274E-09	**0.1272**	5.282E-09	**0.1274**

Table 6.10-5 — Configuration 4: 4 55-gallon Drums Overpacked in an SWB Overpacked in a TDOP Example Comparison of Maximum Allowable Gas Generation Rates and Decay Heats with Base Case* (Concluded)

Alpha-numeric Payload Shipping Category	Numeric Payload Shipping Category	Base Case		Configuration 4	
		Cg-Gas Generation (moles/sec)	Decay Heat Limit	Cg - Gas Generation (moles/sec)	Decay Heat Limit
II.1B0	20 0170 0166	3.015E-08	**0.1711**	3.128E-08	**0.1776**
II.1B1	20 0170 0188	2.670E-08	**0.1516**	2.759E-08	**0.1566**
II.1B2	20 0170 0367	1.364E-08	**0.0774**	1.387E-08	**0.0787**
II.1B2a	20 0170 0209	2.396E-08	**0.1360**	2.467E-08	**0.1400**
II.1B3	20 0170 0546	9.163E-09	**0.0520**	9.265E-09	**0.0526**
II.1B4	20 0170 0725	6.898E-09	**0.0392**	6.955E-09	**0.0395**
II.1B5	20 0170 0905	5.530E-09	**0.0314**	5.567E-09	**0.0316**
II.1B6	20 0170 1084	4.616E-09	**0.0262**	4.641E-09	**0.0263**
II.2BM	20 0000 0000	NA	**40.0000**	NA	**40.0000**
III.1B0	30 0340 0166	3.015E-08	**0.0856**	3.128E-08	**0.0888**
III.1B1	30 0340 0188	2.670E-08	**0.0758**	2.759E-08	**0.0783**
III.1B2	30 0340 0367	1.364E-08	**0.0387**	1.387E-08	**0.0394**
III.1B2a	30 0340 0209	2.396E-08	**0.0680**	2.467E-08	**0.0700**
III.1B3	30 0340 0546	9.163E-09	**0.0260**	9.265E-09	**0.0263**
III.1B4	30 0340 0725	6.898E-09	**0.0196**	6.955E-09	**0.0197**
III.1B5	30 0340 0905	5.530E-09	**0.0157**	5.567E-09	**0.0158**
III.1B6	30 0340 1084	4.616E-09	**0.0131**	4.641E-09	**0.0132**

*Base Case: Up to 4 55-gallon drums overpacked in a Standard Waste Box.

Table 6.10-6 — Configuration 5: 1 SWB Overpacked in a TDOP Example Comparison of Maximum Allowable Gas Generation Rates and Decay Heats with Base Case*

Alpha-numeric Payload Shipping Category	Numeric Payload Shipping Category	Base Case		Configuration 5	
		Cg-Gas Generation (moles/sec)	Decay Heat Limit	Cg - Gas Generation (moles/sec)	Decay Heat Limit
I.1C0	10 0160 0034	1.514E-07	**0.9132**	1.530E-07	**0.9226**
I.1C2	10 0160 0059	8.598E-08	**0.5185**	8.649E-08	**0.5216**
I.1C2b	10 0160 0286	1.751E-08	**0.1056**	1.754E-08	**0.1057**
I.2C0	10 0130 0034	1.514E-07	**1.1239**	1.530E-07	**1.1356**
I.3C0	10 0040 0034	1.514E-07	**3.6528**	1.530E-07	**3.6906**
II.1C0	20 0170 0028	1.798E-07	**1.0206**	1.900E-07	**1.0786**
II.1C1	20 0170 0041	1.238E-07	**0.7029**	1.286E-07	**0.7300**
II.1C1f	20 0170 0034	1.501E-07	**0.8518**	1.571E-07	**0.8919**
II.1C2	20 0170 0053	9.445E-08	**0.5361**	9.720E-08	**0.5517**
II.1C2b	20 0170 0220	2.277E-08	**0.1292**	2.293E-08	**0.1301**
II.1C2f	20 0170 0039	1.288E-07	**0.7309**	1.339E-07	**0.7602**
II.1C2bf	20 0170 0043	1.173E-07	**0.6659**	1.216E-07	**0.6901**
II.1C3	20 0170 0233	2.154E-08	**0.1222**	2.168E-08	**0.1230**
II.1C3f	20 0170 0049	1.039E-07	**0.5897**	1.072E-07	**0.6086**
II.1C4	20 0170 0412	1.215E-08	**0.0690**	1.220E-08	**0.0692**
II.2CM	20 0000 0000	NA	**40.0000**	NA	**40.0000**
III.1C0	30 0340 0028	1.798E-07	**0.5103**	1.900E-07	**0.5393**
III.1C1	30 0340 0041	1.238E-07	**0.3515**	1.286E-07	**0.3650**
III.1C1f	30 0340 0034	1.501E-07	**0.4259**	1.571E-07	**0.4459**
III.1C2	30 0340 0053	9.445E-08	**0.2680**	9.720E-08	**0.2758**
III.1C2b	30 0340 0220	2.277E-08	**0.0646**	2.293E-08	**0.0651**
III.1C2f	30 0340 0039	1.288E-07	**0.3655**	1.339E-07	**0.3801**
III.1C2bf	30 0340 0043	1.173E-07	**0.3329**	1.216E-07	**0.3451**
III.1C3	30 0340 0233	2.154E-08	**0.0611**	2.168E-08	**0.0615**
III.1C3f	30 0340 0049	1.039E-07	**0.2948**	1.072E-07	**0.3043**
III.1C4	30 0340 0412	1.215E-08	**0.0345**	1.220E-08	**0.0346**

*Base Case: Direct loaded Standard Waste Box.

Table 6.10-7 — Configuration 6: 1 Experimental Bin Inside an SWB Overpacked in a TDOP Example Comparison of Maximum Allowable Gas Generation Rates and Decay Heats with Base Case*

Alpha-numeric Payload Shipping Category	Numeric Payload Shipping Category	Base Case		Configuration 6	
		Cg-Gas Generation (moles/sec)	Decay Heat Limit	Cg - Gas Generation (moles/sec)	Decay Heat Limit
II.1D2	20 0170 0067	7.524E-08	**0.4271**	7.698E-08	**0.4369**
III.1D2	30 0340 0067	7.524E-08	0.2135	7.698E-08	**0.2184**

*Base Case: Experimental Bin overpacked in a Standard Waste Box.

Table 6.10-8 — Configuration 7: 6 85-gallon Drum Overpacks Overpacked in a TDOP Example Comparison of Maximum Allowable Gas Generation Rates and Decay Heats with Base Case*

Alpha-numeric Payload Shipping Category	Numeric Payload Shipping Category	Base Case		Configuration 7	
		Cg-Gas Generation (moles/sec)	Decay Heat Limit	Cg - Gas Generation (moles/sec)	Decay Heat Limit
I.1B0	10 0160 0207	2.416E-08	**0.1457**	2.550E-08	**0.1538**
I.1B1	10 0160 0229	2.189E-08	**0.1320**	2.299E-08	**0.1386**
I.1B2	10 0160 0250	2.002E-08	**0.1207**	2.093E-08	**0.1262**
I.1B3	10 0160 0709	7.061E-09	**0.0426**	7.171E-09	**0.0432**
I.2B0	10 0130 0207	2.416E-08	**0.1793**	2.550E-08	**0.1893**
I.2B1	10 0130 0229	2.189E-08	**0.1625**	2.299E-08	**0.1706**
I.2B2	10 0130 0250	2.002E-08	**0.1486**	2.093E-08	**0.1553**
I.2B3	10 0130 0709	7.061E-09	**0.0524**	7.171E-09	**0.0532**
I.2B4	10 0130 0949	5.274E-09	**0.0391**	5.335E-09	**0.0396**
I.3B0	10 0040 0207	2.416E-08	**0.5827**	2.550E-08	**0.6151**
I.3B1	10 0040 0229	2.189E-08	**0.5281**	2.299E-08	**0.5546**
I.3B2	10 0040 0250	2.002E-08	**0.4828**	2.093E-08	**0.5048**
I.3B3	10 0040 0709	7.061E-09	**0.1703**	7.171E-09	**0.1730**
I.3B4	10 0040 0949	5.274E-09	**0.1272**	5.335E-09	**0.1287**
II.1B0	20 0170 0166	3.015E-08	**0.1711**	3.157E-08	**0.1792**
II.1B1	20 0170 0188	2.670E-08	**0.1516**	2.781E-08	**0.1578**
II.1B2	20 0170 0367	1.364E-08	**0.0774**	1.393E-08	**0.0790**
II.1B2a	20 0170 0209	2.396E-08	**0.1360**	2.485E-08	**0.1410**
II.1B3	20 0170 0546	9.163E-09	**0.0520**	9.290E-09	**0.0527**
II.1B4	20 0170 0725	6.898E-09	**0.0392**	6.969E-09	**0.0396**

Table 6.10-8 — Configuration 7: 6 85-gallon Drums Overpacked in a TDOP Example Comparison of Maximum Allowable Gas Generation Rates and Decay Heats with Base Case* (Concluded)

Alpha-numeric Payload Shipping Category	Numeric Payload Shipping Category		Base Case		Configuration 7	
			Cg-Gas Generation (moles/sec)	Decay Heat Limit	Cg - Gas Generation (moles/sec)	Decay Heat Limit
II.1B5	20 0170	0905	5.530E-09	**0.0314**	5.576E-09	**0.0316**
II.1B6	20 0170	1084	4.616E-09	**0.0262**	4.647E-09	**0.0264**
II.2BM	20 0000	0000	NA	**40.0000**	NA	**40.0000**
III.1B0	30 0340	0166	3.015E-08	**0.0856**	3.157E-08	**0.0896**
III.1B1	30 0340	0188	2.670E-08	**0.0758**	2.781E-08	**0.0789**
III.1B2	30 0340	0367	1.364E-08	**0.0387**	1.393E-08	**0.0395**
III.1B2a	30 0340	0209	2.396E-08	**0.0680**	2.485E-08	**0.0705**
III.1B3	30 0340	0546	9.163E-09	**0.0260**	9.290E-09	**0.0264**
III.1B4	30 0340	0725	6.898E-09	**0.0196**	6.969E-09	**0.0198**
III.1B5	30 0340	0905	5.530E-09	**0.0157**	5.576E-09	**0.0158**
III.1B6	30 0340	1084	4.616E-09	**0.0131**	4.647E-09	**0.0132**

*Base Case: 55-gallon drum overpacked in a Standard Waste Box or 85-gallon drum.

This page intentionally left blank.

APPENDIX 6.11

SHIPMENT OF TRITIUM-CONTAMINATED WASTE

This page intentionally left blank.

6.11 Shipment of Tritium-Contaminated Waste

6.11.1 General Information

The TRUPACT-II and HalfPACT shipping packages have been designed and licensed to transport contact-handled transuranic (CH-TRU) materials for the U.S. Department of Energy (DOE). The DOE - Carlsbad Field Office has been requested to make shipments of tritium-contaminated materials (e.g., solidified or bonded materials) from various national laboratories to storage and/or disposal facilities using the packagings. The purpose of this appendix is to describe and justify the addition of tritium-contaminated materials as a content condition for the TRUPACT-II and the HalfPACT.

6.11.2 Description of Contents

6.11.2.1 Adsorbed/Solidified Tritium-Contaminated Liquid Waste

A high-quality stainless steel pressure vessel (primary container) is filled with adsorbent material, water containing small quantities of tritium is added, the water is adsorbed, and the primary container is sealed. The primary container is placed inside a 55-gallon drum and surrounded by dunnage and additional adsorbent material. An example of specific details and compliance with the Contact-Handled Transuranic Waste Authorized Methods for Payload Control (CH-TRAMPAC) is described in Content Code SL 111, see CH-TRU Waste Content Codes (CH-TRUCON) document.[1] The content description (for this code) is as follows:

- Type and form of material—Dewatered or solidified tritium contaminated waste adsorbed onto inorganic material. The waste is sealed in a high-quality stainless steel pressure vessel. Explosives, corrosives, nonradioactive pyrophorics, free liquids and flammable organics are prohibited. The internal volume of each primary container is limited to not more than 20 liters, and the internal pressure of each primary container is limited to not more than 1 atmosphere at the time of shipment. The primary containers are overpacked in 55-gallon drums.

6.11.2.2 Titanium-Contaminated Inorganic Waste

Titanium sponge, in which some of the titanium has been previously reacted at high temperature with tritium to form TiT_2, TiHT, and TiDT, is placed in a high-quality aluminum (primary) container. The primary container is then sealed. The primary container is placed inside a 55-gallon drum and surrounded by dunnage and adsorbent material. An example of specific details and compliance with the transportation requirements is detailed in Content Code LL 111B, see CH-TRUCON document.[1] The content description (for this code) is as follows:

- Type and form of material—Solidified tritium contaminated waste in the form of titanium sponge in which some of the titanium has been previously reacted at high

---

[1] U.S. DOE, "CH-TRU Waste Content Codes (CH-TRUCON)," current revision, DOE/WIPP 01-3194, U.S. Department of Energy, Carlsbad Field Office, Carlsbad, New Mexico.

temperature with tritium to form TiT_2, TiHT, and TiDT. The waste is sealed in aluminum containers that are overpacked into 55-gallon drums. Explosives, corrosives, nonradioactive pyrophorics, free liquids and flammable organics are prohibited. The internal pressure of each primary container is limited to not more than 1 atmosphere at the time of shipment.

*   Maximum quantity of material per package—Contents not to exceed 7,265 pounds in a TRUPACT-II or 7,600 pounds in a HalfPACT including shoring and secondary containers, with no more than 1,000 pounds per 55-gallon drum. The maximum number of 55-gallon drums per package is 14 in a TRUPACT-II or 7 in a HalfPACT as shown in Section 2.9 of the CH-TRAMPAC. Decay heat not to exceed the values given in the CH-TRAMPAC.

6.11.3 Structural Evaluation

The 55-gallon drums of tritium waste will be assembled in compliance with Section 2.9 of the CH-TRAMPAC. The maximum weights will be verified to be less than or equal to the limits specified in Section 2.3 of the CH-TRAMPAC.

The inorganic nature of the waste and limited wattage due to the small amount of tritium present inside the primary payload containers limit the potential buildup of pressure that could occur inside the TRUPACT-II or HalfPACT inner containment vessel (ICV) to less than or equal to the 50 psig design pressure during one year. Since payload containers are 55-gallon drums, there are no special structural considerations for either normal or hypothetical conditions of transport that are not already discussed in the TRUPACT-II Safety Analysis Report (SAR) and the HalfPACT SAR. In summary, there are no structural impacts to the TRUPACT-II or HalfPACT packagings resulting from the shipment of 55-gallon drums containing tritium waste.

6.11.4 Thermal Evaluation

The thermal limit for tritium shipments remains the same as discussed in Section 3.0 of both the TRUPACT-II and HalfPACT SARs—not to exceed a total of 40 thermal watts in a TRUPACT-II and 30 thermal watts in a HalfPACT. There will be no thermal impact to the TRUPACT-II or HalfPACT packagings as a result of shipping tritium waste for either normal or hypothetical accident conditions of transport.

6.11.5 Containment Evaluation

The containment criteria for tritium shipments remains the same as for other shipments using the TRUPACT-II or HalfPACT as discussed in the respective SARs. Prior to shipment, both the inner and outer containment vessels of the packaging will be tested in accordance with the appropriate SAR. There will be no impact on the containment capability of the TRUPACT-II or HalfPACT as a result of shipping 55-gallon drums of tritium waste for either normal or hypothetical accident conditions of transport.

6.11.6 Shielding Evaluation

Tritium is a low-energy beta particle emitter and will be shielded by the stainless steel primary container. For normal conditions of transport, the 55-gallon drums containing the solidified tritium waste may be contact handled as with other TRUPACT-II or HalfPACT authorized contents—each 55-gallon drum shall have a surface dose rate of less than or equal to 200 mrem/hr at the surface. If one assumes as a worst case that both the primary container and the payload container were damaged during a hypothetical accident, the stainless steel 1/4-inch thick ICV would provide adequate shielding. The shipment of tritium waste in the TRUPACT-II or HalfPACT poses no radiation safety impact for normal or hypothetical accident conditions of transport.

6.11.7 Criticality Evaluation

Tritium is not a fissile material and, therefore, there will be no impact on the current criticality capabilities of the transportation packaging for both normal and hypothetical accident conditions of transport.

6.11.8 Operating Procedures

The TRUPACT-II and HalfPACT will be loaded and unloaded in accordance with the standard operating procedures described in the respective SARs. Prior to transport, each transportation package will be leakage rate tested in accordance with the appropriate SAR. There are no changes to the operating procedures resulting from the handling of 55-gallon drums of tritium waste.

6.11.9 Acceptance Tests and Maintenance

There are no changes to the TRUPACT-II or HalfPACT acceptance tests and maintenance (as described in the appropriate SAR) due to the shipment of drums of tritium waste. The packaging will be in full compliance with the acceptance tests and maintenance requirements prior to transport when loaded with 55-gallon drums of tritium waste.

This page intentionally left blank.

APPENDIX 6.12

**USE OF TRUPACT-II FOR THE SHIPMENT OF HIGH-WATTAGE
CH-TRU WASTE**

This page intentionally left blank.

6.12 Use of TRUPACT-II for the Shipment of High-Wattage CH-TRU Waste

6.12.1 Introduction

The purpose of this appendix is to describe the shipment of payload containers of high-wattage contact-handled transuranic (CH-TRU) waste from U.S. Department of Energy (DOE) sites as authorized contents in the TRUPACT-II. This appendix defines the conditions and controls under which this waste can be shipped in the TRUPACT-II. This appendix includes analyses demonstrating compliance with gas generation requirements and establishes conditions for compliance with all Contact-Handled Transuranic Waste Authorized Methods for Payload Control (CH-TRAMPAC) requirements. The key elements of this appendix are as follows:

- After assembly in a TRUPACT-II inner containment vessel (ICV), the payload containers that meet all applicable limits described in this appendix undergo the application of a vacuum to remove hydrogen that may have accumulated during storage. This process is described in Section 6.12.8 of this appendix. The implementation of the vacuum application is controlled as described in Section 6.12.8.1 of this appendix. After application of the vacuum process, the ICV is backfilled with an inert gas (e.g., nitrogen or argon) as an additional margin of safety (no credit is taken for this inerting in the analysis).

- The loaded TRUPACT-II is evacuated and backfilled at the site, transported from the site to the Waste Isolation Pilot Plant (WIPP), and vented at WIPP within the applicable maximum period of time (i.e., five (5) or ten (10) days) from the completion of the vacuum process at the site. The basis for the shipping period is defined in Section 6.12.6.1 of this appendix. Administrative controls required to ensure that the shipping period is not exceeded are defined in Section 6.12.8.2 of this appendix.

- The controls defined in this appendix ensure that the maximum normal operating pressure (MNOP) for this payload is well below the TRUPACT-II design pressure of 50 pounds per square inch gauge (psig), as shown in Section 6.12.6.3 of this appendix.

The operating controls and conditions to be exercised by the site and WIPP to ensure the safe shipment of high-wattage CH-TRU waste are identified in Section 6.12.8 of this appendix.

6.12.2 Scope

This appendix applies to payload containers of high-wattage CH-TRU waste currently stored at the DOE sites. These high-wattage payload containers contain inorganic and organic debris belonging to Waste Material Type III.1, as defined in Appendix 2.1 of the CH-TRU Payload Appendices. The payload containers and packaging configurations governed by this appendix are described by Content Codes LA 154, SQ 154, and SQ 156, which are provided in Section 6.12.10 of this appendix. Only CH-TRU waste containers that belong to these content codes may be qualified for TRUPACT-II shipment under the conditions specified in this appendix.

6.12.3 Container and Physical Properties

For Content Codes LA 154, SQ 154, and SQ 156, the container and physical properties requirements and the associated methods of compliance are the same as those described in Section 2.0 of the CH-TRAMPAC.

6.12.4 Nuclear Properties

For Content Codes LA 154, SQ 154, and SQ 156, the nuclear properties requirements and the associated methods of compliance are the same as those described in Section 3.0 of the CH-TRAMPAC.

6.12.5 Chemical Properties

For Content Codes LA 154, SQ 154, and SQ 156, the chemical properties requirements and the associated methods of compliance are the same as those described in Section 4.0 of the CH-TRAMPAC.

6.12.6 Gas Generation

For Content Codes LA 154, SQ 154, and SQ 156, the gas generation requirements are the same as those described in Section 5.0 of the CH-TRAMPAC. As discussed in Section 6.12.6.2 of this appendix, the effective flammable gas G value assigned to Content Codes LA 154 and SQ 154 is that established for Waste Material Type III.1 in Section 5.0 of the CH-TRAMPAC. The effective flammable gas G value assigned to Content Code SQ 156 is based on the high-dose criterion of >1.2 watt*year. The G value determined for Content Code SQ 156 is specified in Section 6.12.6.2.3 of this appendix. For Content Codes LA 154, SQ 154, and SQ 156, the compliance methodology associated with the gas generation requirements is summarized below and detailed in Section 6.12.9 of this appendix.

The gas generation requirements compliance methodology for Content Codes LA 154, SQ 154, and SQ 156 involves the use of a process with the following two objectives:

- Reduction of hydrogen gas that may have accumulated in the internal layers of confinement during storage of the payload containers

- Minimization of hydrogen gas accumulation during transport of the payload containers from the site to WIPP.

The first objective is achieved through the application of a vacuum to the loaded ICV prior to transportation. The application of a vacuum removes the accumulated hydrogen gas from the payload containers and internal confinement layers. This evacuation process is shown to reduce the hydrogen gas concentration to a conservative value as demonstrated in Section 6.12.9 of this appendix. An iterative procedure was used to identify the limiting operating conditions for the evacuation process and the maximum allowable decay heat for each packaging configuration of Content Codes LA 154, SQ 154, and SQ 156. A minimum flow rate (at ambient pressure) of 11.9 standard cubic feet per minute (scfm) and a maximum allowable ultimate vacuum pump pressure of 50 millitorr (mtorr) was used to calculate a minimum vacuum duration of 12 hours (corresponding to an ICV internal vacuum pressure of 2 torr) to achieve the required hydrogen concentration in the innermost void volume.

Following the vacuum application, an inert backfill gas (e.g., nitrogen or argon) is introduced into the evacuated ICV. The use of an inert gas as backfill provides an additional margin of safety; no credit is taken for this in the demonstration of compliance. Section 6.12.9 of this appendix presents the mathematical analysis supporting the evacuation and backfill process.

The second objective is achieved by requiring shipments of Content Codes LA 154, SQ 154, and SQ 156 to be completed in controlled short shipping periods as described in Section 6.12.6.1 of this appendix.

6.12.6.1 Shipping Period Analysis

6.12.6.1.1 Content Code LA 154

For payloads comprised of containers belonging to Content Code LA 154, the shipping period begins at the completion of the hydrogen evacuation process at LANL and ends when the ICV is vented at WIPP. Conservative time estimates for the various activities determining the shipping period for Content Code LA 154 payloads are as follows:

- **Loading Time**. Loading time begins with the completion of the vacuum application to the ICV and ends with the departure of the shipment of the TRUPACT-II from LANL. Activities to be completed during the loading time include backfilling, leak testing, and handling of the loaded TRUPACT-II(s). As directed by LANL procedures, these activities are sequenced for completion within 24 hours. If these activities are delayed beyond 24 hours, the package(s) will be vented and the vacuum re-applied at LANL in accordance with the controls described in Section 6.12.8.2 of this appendix.

- **Transport Time**. Transport time begins with the departure of the shipment from LANL and ends with the arrival of the shipment at WIPP. The transport time is dependent upon the distance between LANL and WIPP. As shown in Table 6.12-1, at an average speed of 40 miles per hour (mph) the longest travel time from LANL to WIPP is 8.8 hours. This average speed takes into account stops for vehicle inspections every two hours, fueling, meals, driver relief, and state vehicle inspections.

Table 6.12-1 – Distance Between WIPP and LANL

Distance to WIPP (miles)	Transit Time (hours)			
	40 mph	45 mph	50 mph	55 mph
352	8.8	7.8	7.0	6.4

While the expected shipment time from LANL to WIPP is approximately 8.8 hours, the transport time is conservatively estimated as 48 hours. This estimate is conservative because administrative controls imposed by LANL procedures (as outlined in Section 6.12.8.2 of this appendix) eliminate the potential for departure delays associated with holiday weekends or other scheduled facility closure periods. In addition, the use of the TRANSCOM system at WIPP provides continuous tracking of the shipment during transit from LANL to WIPP. The 352-mile distance between LANL and WIPP allows for prompt emergency response, truck maintenance, and driver or equipment replacement, if needed. With approximately 20 shipments being made to WIPP each

week, the resources exist at WIPP to expeditiously attend to any contingencies for Content Code LA 154 shipments. A 48-hour transport time accounts for any unexpected impact to the normal transit time.

- **Unloading Time**. Unloading time begins with the arrival of the shipment at WIPP and ends with the venting of the ICV. Operational procedures in place at WIPP ensure that processing and unloading procedures for shipments of Content Code LA 154 are initiated within 24 hours of shipment arrival regardless of holidays or other scheduled facility closure periods. Administrative controls imposed by WIPP procedures ensure that a shipment is not unattended beyond one day of arrival. Section 6.12.8.2 of this appendix outlines controls imposed to ensure venting of the ICV within 24 hours of shipment arrival.

Based on a loading time of 24 hours, a conservatively estimated transport time of 48 hours, and an unloading time of 24 hours, the maximum shipping period for shipments of Content Code LA 154 is 4 days (96 hours). The additional contingency of a one-day (24-hour) margin of safety results in a maximum shipping period of 5 days (120 hours). Table 6.12-2 provides a summary of the activities comprising the shipping period.

Table 6.12-2– Content Code LA 154 Shipping Period Analysis Summary

Activity	Normal Expected Time (days)	Maximum Time Used in Analysis (days)
Loading Time	<1	1
Transport Time	0.37	2
Unloading Time	<1	1
Margin of Safety	—	1
Shipment Time	2.37	**5**

This analysis justifies using a 5-day period as the basis for determining compliance with gas generation requirements under rigorous operational controls during loading, transport, and unloading as specified in this appendix. Only shipments of Content Code LA 154 are eligible for evaluation using the 5-day shipping period.

6.12.6.1.2 Content Codes SQ 154 and SQ 156

Payloads comprised of containers belonging to Content Codes SQ 154 and SQ 156 shall be transported as controlled shipments (i.e., 10-day shipping period) as outlined in Appendix 3.6 of the CH-TRU Payload Appendices. In addition to the controls specified in Appendix 3.6 of the CH-TRU Payload Appendices, controls for the completion of the additional activities required for shipments of Content Codes SQ 154 and SQ 156 (i.e., evacuation and backfill of the ICV) prior to the initiation of the 24-hour loading time required for controlled shipments must be established.

For controlled shipments of Content Codes SQ 154 and SQ 156, the 24-hour loading time begins with the completion of the evacuation and backfill process and ends with the departure of the

shipment of the TRUPACT-II from the site. Site procedures must be implemented for controlled shipments of Content Codes SQ 154 and SQ 156 to ensure that loading, as defined herein, is completed within 24 hours. If the loading activities are delayed beyond 24 hours, the package(s) must be vented and the vacuum reapplied in accordance with the administrative controls described in Section 6.12.8.2 of this appendix.

6.12.6.2 Determination of Limits

Section 6.12.9 of this appendix documents the mathematical analysis used to arrive at the flammable gas generation limits for Content Codes LA 154, SQ 154, and SQ 156. The derivation of flammable gas generation rate and decay heat limits for these content codes, all of which are classified as Waste Material Type III.1, Solid Organic Waste, are discussed in the following sections. The G value assigned to Content Codes LA 154 and SQ 154 (1.09) is the same as that specified in Section 5.0 of the CH-TRAMPAC for containers meeting the matrix-depletion criterion of >0.012 watt*year. As discussed in Section 6.12.6.2.3, the G value assigned to Content Code SQ 156 (0.53) is based on the high-dose properties of the containers described by Content Code SQ 156 (i.e., Content Code SQ 156 containers must meet a "high-dose criterion" of >1.2 watt*year). In addition, the use of Content Code SQ 156 is subject to the specific requirements delineated in Section 6.12.6.2.3. For all content codes, the release rates for the confinement layers are the same as those specified in Appendices 2.2 and 2.3 of the CH-TRU Payload Appendices.

The initial conditions for hydrogen are established for each of the packaging configurations authorized under Content Codes LA 154, SQ 154, and SQ 156 by the application of the vacuum as specified in this appendix. Using these initial hydrogen conditions along with the G value and maximum shipping period associated with each content code, a flammable gas generation rate limit and decay heat limit are calculated for each packaging configuration such that the flammable gas concentration within the innermost confinement layer of a payload container at the end of the shipping period is no more than 5 percent by volume. The flammable gas generation limits for individual containers belonging to Content Codes LA 154, SQ 154, and SQ 156 are specified in the following sections.

In addition, all payloads comprised of containers belonging to Content Codes LA 154, SQ 154, and SQ 156 must meet the design limit of 40 watts per TRUPACT-II.

Shipments of Content Codes LA 154, SQ 154, and SQ 156 under the test category [exceeding 500 parts per million flammable volatile organic compounds (VOCs) or the decay heat limits specified in the following sections] are as described in Section 5.2 of the CH-TRAMPAC and Section 6.12.9 of this appendix. Limits applicable under mixing of shipping categories are also described in Section 6.12.9 of this appendix. Mixing of shipping categories is allowed only within containers of a single content code (e.g., all containers comprising a payload must belong to Content Code LA 154).

6.12.6.2.1 Content Code LA 154

Assuming a Content Code LA 154 payload assembly comprised of fourteen 55-gallon drums belonging to a single packaging configuration (i.e., either Content Code LA 154A or LA 154B), up to six 85-gallon drum overpacks in a ten-drum overpack (TDOP) (Content Code LA 154C), or two standard waste boxes (SWBs) each overpacking up to four 55-gallon drums (Content

Code LA 154D), the maximum allowable flammable gas generation rate and decay heat limits are as specified in Table 6.12-3.

Table 6.12-3 – Content Code LA 154 Flammable Gas Generation Rate and Decay Heat Limits

Content Code	Flammable Gas Generation Rate Limit per Drum (moles per second)	Decay Heat Limit per Drum (watts)
LA 154A	2.0581E-7	1.8219
LA 154B	2.7172E-7	2.4053
LA 154C	1.8936E-7	1.6762
LA 154D	2.3173E-7	2.0513

6.12.6.2.2 Content Code SQ 154

Assuming a Content Code SQ 154 payload assembly comprised of fourteen 55-gallon drums belonging to a single packaging configuration (i.e., either Content Code SQ 154A or SQ 154B), two SWBs each overpacking up to four 55-gallon drums belonging to a single packaging configuration (i.e., either Content Code SQ 154C or SQ 154D), two direct loaded SWBs belonging to a single packaging configuration (i.e., Content Code SQ 154E, or SQ 154F), or a TDOP overpacking up to ten 55-gallon drums (i.e., SQ 154G), the maximum allowable flammable gas generation rate and decay heat limits are as specified in Table 6.12-4.

Table 6.12-4 – Content Code SQ 154 Flammable Gas Generation Rate and Decay Heat Limits

Content Code	Flammable Gas Generation Rate Limit per Drum or Directly Loaded SWB (moles per second)	Decay Heat Limit per Drum or Directly Loaded SWB (watts)
SQ 154A	1.0924E-7	0.9670
SQ 154B	1.6075E-7	1.4230
SQ 154C	1.2298E-7	1.0886
SQ 154D	1.4949E-7	1.3233
SQ 154E	9.8873E-8	0.8752
SQ 154F	2.6261E-7	2.3247
SQ 154G	1.0633E-7	0.9412

6.12.6.2.3 Content Code SQ 156

Content Code SQ 156 describes high-wattage CH-TRU wastes that must meet a high-dose criterion of >1.2 watt*year (Section 6.12.10 of this appendix). Based on an evaluation of gas

generation data from containers meeting this criterion, an effective flammable gas G value of 0.53 has been established for Content Code SQ 156.[1] The use of Content Code SQ 156 is authorized only for waste populations that meet the following requirements:

1. The site must document the basis for grouping containers into a population, based on similar gas generation characteristics (e.g., grouping of containers generated from the same process).

2. The site must collect sufficient data on a subpopulation of waste containers in the population in accordance with WIPP Certification Program protocols such that the flammable gas G value for the population is shown to be statistically bound by that for Content Code SQ 156, as measured by the 95th UTL. The methodology for determining the subpopulation size to result in sufficient data is as described in Section 5.2.5.5.2 of the CH-TRAMPAC, "Statistics for Required Subpopulation Size." The determination of flammable gas G values from gas generation data is as described in the Shaw Environmental, Inc., report[1].

3. The site must request DOE-Carlsbad Field Office (CBFO) approval of site-specific use of Content Code SQ 156, based on the above data and documentation. Use of Content Code SQ 156 and the high-dose range G value shall be formally approved by DOE-CBFO for each site and population of waste.

Assuming a Content Code SQ 156 payload assembly comprised of fourteen 55-gallon drums belonging to a single packaging configuration (i.e., either Content Code SQ 156A or SQ 156B), two SWBs each overpacking up to four 55-gallon drums belonging to a single packaging configuration (i.e., either Content Code SQ 156C or SQ 156D), two direct loaded SWBs belonging to a single packaging configuration (i.e., Content Code SQ 156E or SQ 156F), two SWBs each overpacking three filtered containers (i.e., SQ 156H), or a TDOP overpacking up to ten 55-gallon drums (i.e., SQ 156G), the maximum allowable flammable gas generation rate and decay heat limits are as specified in Table 6.12-5.

Table 6.12-5 – Content Code SQ 156 Flammable Gas Generation Rate and Decay Heat Limits

Content Code	Flammable Gas Generation Rate Limit per Drum/Filtered Container or Directly Loaded SWB (moles per second)	Decay Heat Limit per Drum/Filtered Container or Directly Loaded SWB (watts)
SQ 156A	1.0364E-07	1.8868
SQ 156B	1.5906E-07	2.8571①
SQ 156C	1.1645E-07	2.1200

---

[1] Shaw Environmental, Inc., February 2005, *High-Dose Criterion for Flammable Gas G Values and Dose-Dependent Net Gas G Values for Contact-Handled Transuranic Wastes*, Shaw Environmental, Inc., Albuquerque, New Mexico.

Content Code	Flammable Gas Generation Rate Limit per Drum/Filtered Container or Directly Loaded SWB (moles per second)	Decay Heat Limit per Drum/Filtered Container or Directly Loaded SWB (watts)
SQ 156D	1.4665E-07	2.6698
SQ 156E	9.8232E-08	1.7883
SQ 156F	2.6222E-07	4.7738
SQ 156G	1.0089E-07	1.8367
SQ 156H	1.0005E-07	1.8214

Note:

① Decay heat limit per drum is limited by the 40-watt TRUPACT-II payload limit.

6.12.6.3 Pressure Analysis

The MNOP for the Content Code LA 154 payload and the Content Code SQ 154 and SQ 156 payloads is calculated for the maximum shipping period of 5 days and 10 days, respectively. The administrative controls imposed on shipments of Content Codes LA 154, SQ 154, and SQ 156 are identified in Sections 6.12.6.1 and 6.12.8 of this appendix.

The mathematical analysis for the determination of the MNOP for shipments of Content Codes LA 154, SQ 154, or SQ 156 is the same as that presented in Section 3.0 of the TRUPACT-II Safety Analysis Report (SAR). Table 6.12-6 through Table 6.12-8 present the results of the pressure analyses for Content Codes LA 154, SQ 154, and SQ 156. The highest pressure increase at the end of the applicable shipping period for each content code is as follows:

- For Content Code LA 154, at the end of a 5-day shipping period, the highest pressure increase is 8.17 psig (Content Code LA 154B) at a decay heat of 33.674 watts per TRUPACT-II.

- For Content Code SQ 154, at the end of a 10-day shipping period, the highest pressure increase is 7.81 psig (Content Code SQ 154B) at a decay heat of 19.922 watts per TRUPACT-II.

- For Content Code SQ 156, at the end of a 10-day shipping period, the highest pressure increase is 13.35 psig (Content Code SQ 156B) at a decay heat of 40 watts per TRUPACT-II. Note: The 40-watt limit per TRUPACT-II will govern in this case.

Therefore, the MNOP for Content Code LA 154, SQ 154, and SQ 156 payloads will be well below the TRUPACT-II design pressure of 50 psig. In all cases, the MNOP will be well below 50 psig even at the design limit of 40 watts per TRUPACT-II. As shown in Table 6.12-6 through Table 6.12-8, the TRUPACT-II design pressure is approached only after approximately 68 days for Content Code LA 154, after approximately 126 days for Content Code SQ 154, and after approximately 55 days for Content Code SQ 156. Because shipments of Content Code LA 154 and Content Codes SQ 154 and SQ 156 are restricted to 5 days and 10 days, respectively, a large margin of safety exists with respect to compliance with the time at which the design pressure is approached

Table 6.12-6 – TRUPACT-II Pressure Increase for Content Code LA 154

TRUPACT-II Pressure Increase for Content Code LA 154 at 5 days

Content Code	Decay Heat per Drum (watts)	Decay Heat per TRUPACT-II (watts)	Average Contents Temperature (deg. F)	Effective G Value for Total Gas (molecules/100eV)	Activation Energy (kcal/g-mole)	Temp Corrected Effective G Value (molecules/100eV)	Radiolytic Gas Generation Rate (moles/sec)	Radiolytic Gas Generation STP at 5 days (liters)	Average ICV Gas Temperature (deg. F)	Radiolytic Gas Pressure Increase (psia)	Increased Initial Gas Pressure (psia)	Minimum ICV Wall Temperature (deg. F)	Water Vapor Pressure (psia)	Pressure Increase at 5 days (psig)
LA 154A	1.8219	25.507	149.1	8.4	2.1	12.8	3.39E-05	327.91	140.2	2.40	16.65	134.3	2.50	6.85
LA 154B	2.4053	33.674	156.4	8.4	2.1	13.3	4.64E-05	449.14	144.7	3.31	16.77	138.6	2.79	8.17
LA 154C	1.6762	10.057	135.4	8.4	2.1	11.9	1.24E-05	120.30	131.7	0.96	16.41	126.1	2.01	4.68
LA 154D	2.0513	16.410	173.1	8.4	2.1	14.4	2.45E-05	237.42	135.3	2.41	16.51	131.3	2.30	6.52

Time to Attain the TRUPACT-II Design Pressure Limit of 50 psig for Content Code LA 154

Content Code	Decay Heat per Drum (watts)	Decay Heat per TRUPACT-II (watts)	Average Contents Temperature (deg. F)	Effective G Value for Total Gas (molecules/100eV)	Activation Energy (kcal/g-mole)	Temp Corrected Effective G Value (molecules/100eV)	Radiolytic Gas Generation Rate (moles/sec)	Radiolytic Gas Generation STP (liters)	Average ICV Gas Temperature (deg. F)	Radiolytic Gas Pressure Increase (psia)	Increased Initial Gas Pressure (psia)	Minimum ICV Wall Temperature (deg. F)	Water Vapor Pressure (psia)	Pressure Increase (psig)	Time (days)
LA 154A	1.8219	25.507	149.1	8.4	2.1	12.8	3.39E-05	6223.04	140.2	45.55	16.65	134.3	2.50	50.00	94.89
LA 154B	2.4053	33.674	156.4	8.4	2.1	13.3	4.64E-05	6120.95	144.7	45.14	16.77	138.6	2.79	50.00	68.14
LA 154C	1.6762	10.057	135.4	8.4	2.1	11.9	1.24E-05	5785.66	131.7	46.28	16.41	126.1	2.01	50.00	240.47
LA 154D	2.0513	16.410	173.1	8.4	2.1	14.4	2.45E-05	4515.80	135.3	45.89	16.51	131.3	2.30	50.00	95.10

Table 6.12-7 – TRUPACT-II Pressure Increase for Content Code SQ 154

TRUPACT-II Pressure Increase for Content Code SQ 154 at 10 days

Content Code	Decay Heat per Drum or SWB (watts)	Decay Heat per TRUPACT-II (watts)	Average Contents Temperature (deg. F)	Effective G Value for Total Gas (molecules/100eV)	Activation Energy (kcal/g-mole)	Temp Corrected Effective G Value (molecules/100eV)	Radiolytic Gas Generation Rate (moles/sec)	Radiolytic Gas Generation STP at 10 days (liters)	Average ICV Gas Temperature (deg. F)	Radiolytic Gas Pressure Increase (psia)	Increased Initial Gas Pressure (psia)	Minimum ICV Wall Temperature (deg. F)	Water Vapor Pressure (psia)	Pressure Increase at 10 days (psig)
SQ 154A	0.9670	13.538	138.4	8.4	2.1	12.1	1.70E-05	329.27	133.6	2.38	16.47	128.0	2.11	6.26
SQ 154B	1.4230	19.922	144.1	8.4	2.1	12.5	2.58E-05	499.24	137.2	3.64	16.56	131.4	2.31	7.81
SQ 154C	1.0886	8.709	151.7	8.4	2.1	12.9	1.17E-05	226.93	131.1	2.29	16.39	127.1	2.06	6.04
SQ 154D	1.3233	10.586	156.9	8.4	2.1	13.3	1.46E-05	283.19	132.1	2.86	16.42	128.1	2.12	6.70
SQ 154E	0.8752	1.750	132.4	8.4	2.1	11.7	2.13E-06	41.22	127.3	0.41	16.29	123.3	1.86	3.86
SQ 154F	2.3247	4.649	140.5	8.4	2.1	12.2	5.91E-06	114.30	128.9	1.15	16.33	124.9	1.94	4.72
SQ 154G	0.9412	9.412	153.7	8.4	2.1	13.1	1.28E-05	247.69	131.5	1.31	16.41	127.5	2.08	5.10

Time to Attain the TRUPACT-II Design Pressure Limit of 50 psig for Content Code SQ 154

Content Code	Decay Heat per Drum or SWB (watts)	Decay Heat per TRUPACT-II (watts)	Average Contents Temperature (deg. F)	Effective G Value for Total Gas (molecules/100eV)	Activation Energy (kcal/g-mole)	Temp Corrected Effective G Value (molecules/100eV)	Radiolytic Gas Generation Rate (moles/sec)	Radiolytic Gas Generation STP (liters)	Average ICV Gas Temperature (deg. F)	Radiolytic Gas Pressure Increase (psia)	Increased Initial Gas Pressure (psia)	Minimum ICV Wall Temperature (deg. F)	Water Vapor Pressure (psia)	Pressure Increase (psig)	Time (days)
SQ 154A	0.9670	13.538	138.4	8.4	2.1	12.1	1.70E-05	6368.06	133.6	46.10	16.47	128.0	2.11	49.98	193.4
SQ 154B	1.4230	19.922	144.1	8.4	2.1	12.5	2.58E-05	6290.40	137.2	45.81	16.56	131.4	2.31	49.98	126.0
SQ 154C	1.0886	8.709	151.7	8.4	2.1	12.9	1.17E-05	4581.80	131.1	46.24	16.39	127.1	2.06	49.99	201.9
SQ 154D	1.3233	10.586	156.9	8.4	2.1	13.3	1.46E-05	4564.95	132.1	46.15	16.42	128.1	2.12	49.99	161.2
SQ 154E	0.8752	1.750	132.4	8.4	2.1	11.7	2.13E-06	4642.31	127.3	46.55	16.29	123.3	1.86	50.00	1126.1
SQ 154F	2.3247	4.649	140.5	8.4	2.1	12.2	5.91E-06	4617.85	128.9	46.43	16.33	124.9	1.94	50.00	404.0
SQ 154G	0.9412	9.412	153.7	8.4	2.1	13.1	1.28E-05	8748.42	131.5	46.21	16.41	127.5	2.08	50.00	353.2

Table 6.12-8 – TRUPACT-II Pressure Increase for Content Code SQ 156

TRUPACT-II Pressure Increase for Content Code SQ 156 at 10 days

Content Code	Decay Heat per Drum or SWB (watts)	Decay Heat per TRUPACT-II (watts)	Average Contents Temperature (deg. F)	Effective G Value for Total Gas (molecules/100eV)	Activation Energy (kcal/g-mole)	Temp Corrected Effective G Value (molecules/100eV)	Radiolytic Gas Generation Rate (moles/sec)	Radiolytic Gas Generation STP at 10 days (liters)	Average ICV Gas Temperature (deg. F)	Radiolytic Gas Pressure Increase (psia)	Increased Initial Gas Pressure (psia)	Minimum ICV Wall Temperature (deg. F)	Water Vapor Pressure (psia)	Pressure Increase at 10 days (psig)
SQ 156A	1.8868	26.415	149.9	8.4	2.1	12.8	3.52E-05	681.99	140.7	5.00	16.66	134.8	2.53	9.49
SQ 156B	2.8571	40.000	162.0	8.4	2.1	13.6	5.67E-05	1097.23	148.2	8.14	16.87	142.0	3.04	13.35
SQ 156C	2.1200	16.960	174.6	8.4	2.1	14.5	2.55E-05	494.30	135.6	5.03	16.52	131.6	2.32	9.17
SQ 156D	2.6698	21.358	186.8	8.4	2.1	15.3	3.40E-05	658.64	137.9	6.72	16.58	133.9	2.47	11.07
SQ 156E	1.7883	3.577	137.5	8.4	2.1	12.0	4.47E-06	86.55	128.3	0.87	16.32	124.3	1.91	4.40
SQ 156F	4.7738	9.548	154.0	8.4	2.1	13.1	1.30E-05	251.74	131.6	2.54	16.41	127.6	2.08	6.33
SQ 156G	1.8367	18.367	178.5	8.4	2.1	14.7	2.82E-05	545.19	136.3	2.90	16.54	132.3	2.37	7.11
SQ 156H	1.8214	10.928	157.9	8.4	2.1	13.4	1.52E-05	293.72	132.3	2.97	16.43	128.3	2.13	6.83

Time to Attain the TRUPACT-II Design Pressure Limit of 50 psig for Content Code SQ 156

Content Code	Decay Heat per Drum or SWB (watts)	Decay Heat per TRUPACT-II (watts)	Average Contents Temperature (deg. F)	Effective G Value for Total Gas (molecules/100eV)	Activation Energy (kcal/g-mole)	Temp Corrected Effective G Value (molecules/100eV)	Radiolytic Gas Generation Rate (moles/sec)	Radiolytic Gas Generation STP (liters)	Average ICV Gas Temperature (deg. F)	Radiolytic Gas Pressure Increase (psia)	Increased Initial Gas Pressure (psia)	Minimum ICV Wall Temperature (deg. F)	Water Vapor Pressure (psia)	Pressure Increase (psig)	Time (days)
SQ 156A	1.8868	26.415	149.9	8.4	2.1	12.8	3.52E-05	6206.15	140.7	45.47	16.66	134.8	2.53	49.96	91.0
SQ 156B	2.8571	40.000	162.0	8.4	2.1	13.6	5.67E-05	6034.78	148.2	44.76	16.87	142.0	3.04	49.97	55.0
SQ 156C	2.1200	16.960	174.6	8.4	2.1	14.5	2.55E-05	4508.01	135.6	45.84	16.52	131.6	2.32	49.98	91.2
SQ 156D	2.6698	21.358	186.8	8.4	2.1	15.3	3.40E-05	4472.16	137.9	45.65	16.58	133.9	2.47	50.00	67.9
SQ 156E	1.7883	3.577	137.5	8.4	2.1	12.0	4.47E-06	4626.36	128.3	46.47	16.32	124.3	1.91	50.00	534.5
SQ 156F	4.7738	9.548	154.0	8.4	2.1	13.1	1.30E-05	4574.03	131.6	46.20	16.41	127.6	2.08	49.99	181.7
SQ 156G	1.8367	18.367	178.5	8.4	2.1	14.7	2.82E-05	8597.62	136.3	45.78	16.54	132.3	2.37	49.99	157.7
SQ 156H	1.8214	10.928	157.9	8.4	2.1	13.4	1.52E-05	4561.45	132.3	46.13	16.43	128.3	2.13	49.99	155.3

This page intentionally left blank.

6.12.7 Payload Assembly

The payload assembly requirements specified by Section 6.1 of the CH-TRAMPAC apply to Content Code LA 154, SQ 154, and SQ 156 payloads. The allowed methods of compliance for these requirements are the same as those described in Section 6.2 of the CH-TRAMPAC. Because the specific methodology described in this appendix for flammable gas generation rate and decay heat limits is applicable only to payload containers belonging to Content Codes LA 154, SQ 154, and SQ 156, the applicable content code shall be entered as the shipping category on the Payload Container Transportation Certification Document (PCTCD) (Section 6.2.1 of the CH-TRAMPAC) and the Payload Assembly Transportation Certification Document (PATCD) (Section 6.2.2 of the CH-TRAMPAC). The applicable Content Code LA 154, SQ 154, and SQ 156 designation (e.g., LA 154A, etc.) will direct the evaluation of the payload container for compliance with the applicable decay heat limits.

The implementation of the controls specified in Section 6.12.8.2 of this appendix for ensuring compliance with the applicable maximum shipping period also ensure compliance with the requirements of Section 6.2.3 of the CH-TRAMPAC for shipments designated as controlled shipments. A payload container's assignment to Content Code LA 154, SQ 154, or SQ 156 effectively designates the container for controlled shipment, and the implementation of Section 6.12.8.2 of this appendix takes the place of the implementation of Section 6.2.3 of the CH-TRAMPAC. Therefore, entries of "Yes" shall be included on the PCTCD and the PATCD in response to the question "Container/Payload Assembly Designated for Controlled Shipment?" for containers and payloads belonging to Content Codes LA 154, SQ 154, or SQ 156, but Table 6.12-9 shall be substituted for the documentation required for controlled shipments.

Content Code LA 154, SQ 154, and SQ 156 payload containers may be assembled into payload configurations mixing containers belonging to the same content code or dunnage containers as described in Section 6.12.9.4 of this appendix.

6.12.8 Operating Controls and Conditions for Shipments of Content Codes LA 154, SQ 154, and SQ 156

6.12.8.1 Procedures for Loading the Package

Loading the TRUPACT-II for transport involves (1) qualification and approval of each of the payload containers and the payload assembly assigned to Content Code LA 154, SQ 154, or SQ 156 in accordance with this appendix, (2) loading the prepared Content Code LA 154, SQ 154, or SQ 156 payload containers into the TRUPACT-II, (3) applying a vacuum as specified in this appendix and backfilling with a backfill gas, and (4) leakage rate testing of the TRUPACT-II ICV and outer container vessel seals. The process of loading the TRUPACT-II is detailed in Section 7.1 of the TRUPACT-II SAR. The implementation of the vacuum application and the introduction of a backfill gas into the ICV for shipments of Content Codes LA 154, SQ 154, and SQ 156 are controlled using the procedures delineated in Section 7.1 of the TRUPACT-II SAR with the following modifications.

6.12.8.1.1 Perform loading sequence detailed in Section 7.1 of the TRUPACT-II SAR through Section 7.1.5, Step 5 (i.e., Rig an overhead crane, or equivalent, with an appropriate

lift fixture capable of handling the ICV lid. Engage the lift fixture and install the ICV lid onto the ICV body. Remove the lift fixture.).

6.12.8.1.2   Perform Section 7.1.5, Step 6 with a vacuum pump that meets the following minimum specifications: (a) minimum flow rate (at ambient pressure) of 11.9 scfm, and (b) an ultimate vacuum pump pressure of less than or equal to 50 mtorr. Note: Do not disconnect the vacuum system and equalize pressure in the ICV cavity as directed in Section 7.1.5, Step 6.

6.12.8.1.3   Continue to run the vacuum pump for a minimum of 12 hours until the ICV internal vacuum pressure is less than or equal to 2 torr.

6.12.8.1.4   Backfill the ICV with an inert gas (e.g., nitrogen or argon) while equalizing pressure (0 psig) +/- 0.5 psig in the ICV cavity, install the ICV inner vent port plug and torque to 55 – 65 in-lbs, and remove the vacuum pump.

6.12.8.1.5   Perform Section 7.1.5, Step 7 [i.e., Install the three 1/2 inch lock bolts (socket head cap screws) through the cutouts in the ICV locking ring to secure the ICV locking ring in the locked position. Tighten the lock bolts to 28 - 32 lb-ft torque, lubricated.].

6.12.8.1.6   Complete loading sequence detailed in Section 7.1.5, Step 8 through the remainder of Section 7.1 of the TRUPACT-II SAR.

6.12.8.2 Procedures for Required Shipping Period

Compliance with the 5-day (LA 154) or 10-day (SQ 154 and SQ 156) shipping period is administratively controlled through the following steps. The steps must be completed by the Site Transportation Certification Official, or designee, and the designated WIPP operations personnel, as applicable.

Loading Time

The loading time begins with the completion of Step 6.12.8.1.3 (Section 6.12.8.1 of this appendix) of the TRUPACT-II loading process and ends with the departure of the shipment from the site. The loading time is limited to a maximum of 24 hours. The following steps must be completed to ensure compliance with the 24-hour loading time:

6.12.8.2.1   Note date and time that Step 6.12.8.1.3 of the TRUPACT-II loading process is completed (i.e., date and time vacuum process is completed). Record date and time on the Site Control Checklist for High-Wattage CH-TRU Waste Shipments shown in Table 6.12-9. Table 6.12-9 may be reformatted for site use provided that the same information is recorded.

6.12.8.2.2   Note date and time that the loaded TRUPACT-II is ready to depart the site destined for WIPP. Record date and time on the Site Control Checklist for High-Wattage CH-TRU Waste Shipments.

6.12.8.2.3   Review dates and times recorded in Steps 6.12.8.2.1 and 6.12.8.2.2 to calculate total loading time. If total loading time is less than or equal to 24 hours, proceed to Step 6.12.8.2.4. If total Loading Time exceeds 24 hours, the vacuum application portion of the TRUPACT-II loading process must be repeated by returning to Step 6.12.8.1.2 of Section 6.12.8.1 above.

6.12.8.2.4 Indicate compliance with the 24-hour loading time by signature on the Site Control Checklist for High-Wattage CH-TRU Waste Shipments.

Transport Time

The transport time begins with the departure of the shipment from the site and ends with the arrival of the shipment at WIPP. The transport time is controlled as described in Section 6.12.6.1 of this appendix.

Unloading Time

The unloading time begins with the arrival of the shipment at WIPP and ends with the venting of the ICV. The maximum unloading time is 24 hours. The following steps must be completed to document compliance:

6.12.8.2.5 Note date and time that the TRUPACT-II arrives at WIPP. Record date and time on the WIPP Control Checklist for High-Wattage CH-TRU Waste Shipments shown in Table 6.12-10. Table 6.12-10 may be reformatted for WIPP use provided that the same information is recorded.

6.12.8.2.6 Using the date and time recorded in Step 6.12.8.2.5, ensure that the ICV is vented within 24 hours of the arrival of the shipment at WIPP by implementing the WIPP unloading procedures specific to Content Codes LA 154, SQ 154, and SQ 156 shipments. Record date and time to show compliance.

6.12.8.2.7 Indicate compliance with the 24-hour unloading time by signature on the WIPP Control Checklist for High-Wattage CH-TRU Waste Shipments.

Table 6.12-9 – Site Control Checklist for High-Wattage CH-TRU Waste Shipments[①]

Shipment No. _____   Packaging No._____

Content Code[②]: _____

To be completed by the site Transportation Certification Officer, or designee, for each TRUPACT-II:

Appendix 6.12 Section No.	Activity	Recorded Date	Recorded Time	Completion of Activity (Indicate by checkmark [√])
6.12.8.2.1	Record date and time of completion of Appendix 6.12, Step 6.12.8.1.3 (i.e., completion of vacuum process)			
6.12.8.2.2	Record date and time the loaded TRUPACT-II is ready to depart from site			
6.12.8.2.3	Calculate and record total **Loading Time** [Limit = 24 hours]	■		
	Total Loading Time ≤1 day, proceed to Step 6.12.8.2.4. *Total Loading Time > 1 day,* ***STOP****. Repeat vacuum application per Appendix 6.12, Step 6.12.8.1.2.*			
6.12.8.2.4	I certify that the above data is accurate and compliant with the Loading Time limit of 24 hours, as specified in Appendix 6.12 of the CH-TRU Payload Appendices. _____ / _____ TRANSPORTATION CERTIFICATION OFFICIAL DATE (OR DESIGNEE)			

Notes:

①   Table may be reformatted for site use provided that the same information is recorded.

②   Content code must be included in Section 6.12.10 of Appendix 6.12 of the CH-TRU Payload Appendices.

Table 6.12-10 – WIPP Control Checklist for High-Wattage CH-TRU Waste Shipments$^\text{①}$

Shipment No. _____   Packaging No._____

Content Code$^\text{②}$: _____

To be completed by designated WIPP Operations Personnel for each TRUPACT-II:

Appendix 6.12 Section No.	Activity	Recorded Date	Recorded Time	Completion of Activity (Indicate by checkmark [√])
6.12.8.2.5	Record date and time that the TRUPACT-II arrives at WIPP			
6.12.8.2.6	Vent ICV within 24 hours of date and time recorded above and record vent date and time			
6.12.8.2.7	I certify that the above data is accurate and compliant with the Unloading Time limit of 24 hours, as specified in Appendix 6.12 of the CH-TRU Payload Appendices. _____ / _____ WIPP OPERATIONS PERSONNEL DATE			

Notes:

①   Table may be reformatted for WIPP use provided that the same information is recorded.

②   Content code must be included in Section 6.12.10 of Appendix 6.12 of the CH-TRU Payload Appendices.

6.12.9 Derivation of Gas Generation Limits for Content Codes LA 154, SQ 154, and SQ 156

This section describes the methodology and mathematical analysis used for deriving the flammable gas generation rate and decay heat limits for payload containers belonging to Content Codes LA 154, SQ 154, and SQ 156. The limits are defined such that all containers comply with the 5 percent limit (by volume) on hydrogen concentration in all layers of confinement during a shipping period that is administratively controlled.

Containers of Content Codes LA 154, SQ 154, and SQ 156 undergo the following process prior to shipment and receipt at the WIPP:

- Reduction of hydrogen generated during storage by the application of a vacuum to the TRUPACT-II ICV after payload assembly, and backfilling with an inert gas (e.g., nitrogen or argon).

- Evacuation and backfill at the site, shipment from the site to WIPP, and venting at WIPP within a maximum 5-day (LA 154) or 10-day (SQ 154 and SQ 156) period after evacuation at the site.

Using an extension of the methodology in Section 5.0 of the CH-TRAMPAC, decay heat limits are derived using the initial conditions after the vacuum application and a 5- or 10-day shipping period as described below.

6.12.9.1 Gas Evacuation Methodology and Transport Modeling

The application of a vacuum on the loaded ICV is designed to remove hydrogen gas that may have accumulated during storage in containers of Content Codes LA 154, SQ 154, and SQ 156. Subsequent introduction of a backfill gas into the evacuated ICV dilutes the remaining gases. A methodology based on the existing TRUPACT-II gas generation analysis has been developed that describes gas movement between void volumes during the application of a vacuum and the introduction of a backfill gas, and also accounts for hydrogen gas generation from the waste in the innermost layer of confinement.

6.12.9.1.1 Mathematical Analysis of Evacuation and Backfill of Gas in ICV

A system of differential equations defines the rate of accumulation of species i in each void volume in an ICV containing M consecutive void volumes, where the Mth void volume is that of the ICV. There are potentially three primary means of gas transport across each volume boundary:

- Diffusion

- Permeation (bag only)

- Convection.

As a conservative estimate, only gas transport by pressure-induced gas flow, or convection, is considered. The rate of change in species i within the innermost layer of confinement where radiolytic gas generation occurs is defined as:

Equation 1

$$\frac{d(n_{i,1})}{dt} = n_{g,i} - r_{c,i,1}$$

where,

$n_{i,1}$	=	Moles (mol) of species i in innermost void volume
$n_{g,i}$	=	Generation rate of species i, mol/second (s)
$r_{c,i,1}$	=	Rate of convection of species i across the innermost volume boundary (mol/s).

The rate of accumulation of species i in the kth void volume (excluding the ICV void volume) is defined as:

Equation 2

$$\frac{d(n_{i,k})}{dt} = r_{c,i,k-1} - r_{c,i,k}$$

The rate of change of species i in the ICV void volume is defined as:

Equation 3

$$\frac{d(n_{i,M})}{dt} = r_{c,i,M-1} - n_{v,i}$$

where,

$n_{v,i}$	=	Rate in which species i exits the Mth volume.

A negative value for $n_{v,i}$ indicates that gas enters the ICV (as during pressure equilibration after removal of the vacuum).

The rate of convection of all gases, r_c, across a volume boundary in an isothermal system is defined in terms of the pressure gradient across the volume boundary:

Equation 4

$$r_c = K_c \Delta P$$

where,

K_c	=	Flow coefficient across volume boundary, mol/s-atmosphere (atm)
ΔP	=	Pressure difference across volume boundary, atm.

The convection rate for species i across a volume boundary in an isothermal system is defined as:

Equation 5

$$r_{c,i} = K_c y_i^* \Delta P$$

where,

y_i^* =   Mole fraction of species i in the void volume from which the gas flows due to a pressure gradient across the volume boundary.

In order to solve the system of equations, the rate equations are expressed in terms of the quantity of each species in each void volume. In a two-component system, the mole fraction of species i is defined as:

Equation 6

$$y_i = \frac{n_i}{n_1 + n_2}$$

Because there are no species-component terms (permeability or diffusion coefficients) in the rate equations, the first component is hydrogen and the second component is defined as all other gases. All other gases behave the same in a convective environment and are assumed not to be generated in significant quantities within the innermost volume.

The pressure in the kth void volume can be defined in terms of the moles of gas in the volume:

Equation 7

$$P_k = \frac{(n_1 + n_2)_k RT}{V_k}$$

where,

R   =   Gas constant, liters (L) atm/mol Kelvin (K)

T   =   Absolute gas temperature, K

V_k =   Volume of kth void volume, L.

Substituting the equations above into the rate equations yields the following for species i in the kth void volume:

Equation 8

$$r_{c,i,k} = K_c RT y_i^* \Delta_k \left(\frac{n_1 + n_2}{V} \right)$$

where,

$$\Delta_k \left(\frac{n_1 + n_2}{V} \right) = \left(\frac{n_1 + n_2}{V} \right)_k - \left(\frac{n_1 + n_2}{V} \right)_{k+1}$$

$$y^*_i \;\; = \;\; \left(\frac{n_i}{n_1 + n_2} \right)_k \qquad\qquad \text{when } \Delta_k \left(\frac{n_1 + n_2}{V} \right) > 0$$

$$y^*_i \;\; = \;\; \left(\frac{n_i}{n_1 + n_2} \right)_{k+1} \qquad\qquad \text{when } \Delta_k \left(\frac{n_1 + n_2}{V} \right) < 0$$

6.12.9.2 Model Parameters

The determination of vacuum system parameter limits (ultimate vacuum pump pressure, gas flow rate, vacuum duration, ICV internal vacuum pressure, and allowable decay heat) is an iterative process that reflects parameter interactions as well as physical limits. As applicable, the values for the parameters discussed in the following subsections are the same as those used in the gas generation analysis in Section 5.0 of the CH-TRAMPAC.

6.12.9.2.1 Waste Packaging Configuration

The waste packaging configurations in Content Code LA 154, SQ 154, and SQ 156 payload containers are a subset of those approved in Section 5.0 of the CH-TRAMPAC and are as defined in Section 6.12.10 of this appendix. The internal packaging configurations consist of a series of layers of confinement each of which contains a volume of gas. For example, for Content Code LA 154A, waste may be placed within the innermost bag and closed by the twist-and-tape method. Each of the subsequent inner bags is placed around the waste and is closed in a similar manner. These four bag layers are then collectively placed within the first of two liner bags, each closed by the twist-and-tape method, in a 55-gallon drum.

6.12.9.2.2 Void Volumes

Estimates of the void volumes in a 55-gallon drum containing Waste Material Type III.1 (solid organic waste) are the same as those used in Appendix 6.10 of the CH-TRU Payload Appendices. The volume inside the bags is distributed within the different layers of confinement.

As specified in Appendix 2.3 of the CH-TRU Payload Appendices, the void volume in an ICV containing 14 55-gallon drums is 2,450 L. As specified in Appendix 6.10 of the CH-TRU Payload Appendices, the void volume in an ICV containing two SWBs is 1,750 L. The combined void volume in an ICV with one TDOP and in a TDOP with ten 55-gallon drums is 3,346 L. The void volume in a TDOP containing six 85-gallon drums was calculated from the information presented in Appendix 6.10 of the CH-TRU Payload Appendices to be 2,210 L.

Each bag expands during the application of a vacuum (positive pressure differential across bag) and contracts during vent conditions to ambient pressure (negative pressure differential across bag). It is assumed that each bag does not expand more than 20 percent of its original volume nor contract to a volume less than 50 percent of the original volume due to the presence of the waste. When the volume limits are reached, the bag becomes a constant-volume layer of confinement. It is assumed that bags are not breached by expansion or contraction inside the payload container.

6.12.9.2.3 Flow Coefficients

All gases are assumed to be ideal. Gas flow across a filter vent has been measured and determined to be proportional to the pressure drop across the filter vent.[2] The sites use filter vents with the minimum diffusion characteristics specified in Section 6.12.10 of this appendix on 55-gallon drums, 85-gallon drums, TDOPs, and SWBs and inner confinement layers (e.g., the inner containers of Content Code SQ 156H). The lowest filter hydrogen diffusion coefficient for all containers described by Content Codes LA 154, SQ 154, and SQ 156 is 3.7E-6 mol/s/mol fraction.

The minimum flow coefficient across filter vents with an average hydrogen diffusion coefficient of 3.7E-6 mol/s/mol fraction is 2.8E-2 mol/s/atm:

Equation 9

$$K_{c,vent(3.7E-6)} = \{(27-4)\,\text{slpm}\,/\,[(10-1)\,\text{psi}]\}\,\{14.7\,\text{psi}\,/\,(22.4\,\text{L/mol} * 60\,\text{s/min})\}$$
$$= 2.8E\text{-}2\,\text{mol/s/atm}$$

where,

psi	=	Pounds per square inch
slpm	=	Standard liters per minute
min	=	Minute.

The flow coefficient across twist-and-tape closure of polymer bags is estimated by assuming that it is proportional to the hydrogen diffusivity:

Equation 10

$$K_{c,bag} = K_{c,vent}\left(K_{d,bag}/K_{d,vent}\right)$$

where,

K_d = Hydrogen diffusion coefficient, mol/s/mol fraction

therefore,

$K_{c,sb}$	=	2.8E-2 (5.6E-7/3.7E-6) = 4.2E-3 mol/s atm
$K_{c,lb}$	=	2.8E-2 (1.0E-6/3.7E-6) = 7.6E-3 mol/s atm
$K_{c,SWBlb}$	=	2.8E-2 (8.0E-6/3.7E-6) = 6.0E-2 mol/s atm

where,

sb	=	Inner bag
lb	=	Drum liner bag

---

[2] S. H. Peterson, July 1988, *Determination of Hydrogen Flow and Diffusion Properties of Selected Graphite Filters*, Westinghouse R&D Center, Pittsburgh, Pennsylvania.

SWBlb =   SWB liner bag.

The twist-and-tape closure diffusion coefficients are based on the values in Appendix 6.8 of the CH-TRU Payload Appendices.

6.12.9.2.4 Gas Flow Rate Across ICV

For a given amount of decay heat in the payload container, the required vacuum duration and ICV internal vacuum pressure to achieve an initial hydrogen concentration in the innermost void volume (resulting in a final concentration of less than or equal to 5 percent by the end of the shipping period) was evaluated as a function of the ultimate vacuum pressure and gas flow rate. A minimum flow rate (at ambient pressure) of 11.9 scfm was used in the evaluation based on the flow rating of the Swagelok® Quick-Connect QC-8 fitting currently used during TRUPACT-II unloading/loading procedures. This fitting is considered the most restrictive point to gas flow between the pump and the ICV. The double-end shut-off fitting is rated for air at a flow rate of 81 scfm at a pressure differential of 100 psi. Assuming a linear relationship between air flow and pressure differential, at a pressure differential of 14.7 psi (assuming initial system pressure of 1 atm), the initial air flow rate at zero vacuum in the ICV, F_0, is:

Equation 11

$$F_0 = 81\,\text{scfm}\,(14.7\,\text{psi} / 100\,\text{psi}) = 11.9\,\text{scfm}$$

A flow coefficient across the fitting, $K_{c,fit}$, is defined in terms of the gas flow rate, F, at a particular pressure differential, ΔP:

Equation 12

$$K_{c,fit} = F / \Delta P$$

At standard temperature and pressure, 1 mole of gas occupies 22.4 L. The minimum flow coefficient for any fitting is defined in terms of the Swagelok® Quick-Connect QC-8 fitting:

Equation 13

$$K_{c,fit} = (81\,\text{scfm} / 100\,\text{psi})(14.7\,\text{psi} / \text{atm})(10^3\,\text{L} / 35.3145\,\text{ft}^3)(\text{mol} / 22.4\,\text{L})(\text{min} / 60\,\text{s})$$
$$= 0.25\,\text{mol/s atm}$$

where,

ft^3 =   Cubic feet.

6.12.9.2.5 Gas Generation Rate

The rate of hydrogen generation is calculated from Appendix 2.3 of the CH-TRU Payload Appendices as follows:

Equation 14

$$n_{g,H} = CG_{eff}(DH)$$

where,

C   =   Conversion constant = 1.0365E-7 mol (100 electron volts [eV] / molecule watt [W] s)

G_{eff} =   Effective G value, molecules/100 eV emitted energy

DH   =   Decay heat energy, W.

It is assumed that the maximum allowable decay heat is present in each payload container and that the initial ICV pressure equals 1 atm.

6.12.9.2.6 Shipping Period

As determined in Section 6.12.6.1 of this appendix, a maximum shipping period of 5 days is applicable to Content Code LA 154; a maximum shipping period of 10 days is applicable to Content Codes SQ 154 and SQ 156.

6.12.9.2.7 Iterative Procedure to Determine Maximum Allowable Hydrogen Generation Rate

For a given amount of decay heat in the payload container and specified minimum vacuum duration and ICV internal vacuum pressure, the model can determine the hydrogen concentration within the innermost volume at the beginning of the shipping period. The initial hydrogen concentration is that which would result in a final concentration of less than or equal to 5 percent (by volume) by the end of the shipping period.

Using the system of equations defined in this section, the minimum duration of vacuum application to the loaded ICV containing payload containers with up to six confinement layers is 12 hours to reach an ICV internal vacuum pressure of 2 torr. This specification is based on the assumptions of a gas flow rate (at ambient pressure) of 11.9 scfm across the Swagelok® Quick-Connect QC-8 fitting currently used during TRUPACT-II unloading/loading procedures, a vacuum pump with a minimum flow rate (at ambient pressure) of 11.9 scfm, an ultimate vacuum pump pressure of less than or equal to 50 millitorr, and no off-gassing of the waste contents during the vacuum process.

6.12.9.3 Derivation of Limits

Once the ICV has undergone vacuum application, concentrations of hydrogen in the different layers increase due to the generation of hydrogen during the shipping period. Some of the hydrogen generated during the shipping period would accumulate in the payload containers with the remainder being released into the cavity. For the purpose of establishing decay heat limits, the mole fraction of hydrogen within the innermost confinement layer is evaluated using a transient methodology to simulate the generation, accumulation, and transport processes. The ICV cavity (and/or TDOP void volume for packaging configurations using a TDOP) mole fraction of hydrogen is obtained by conservatively assuming that all of the hydrogen generated is released into the ICV cavity (and/or TDOP void volume for packaging configurations using a

TDOP) at the start of the shipping period. The maximum hydrogen concentration in the innermost layer is then limited to less than or equal to 5 percent (by volume) at the end of the shipping period by suitably choosing the gas generation rate and decay heat limits. The temperature dependence of decay heat limits is discussed in Appendix 6.9 of the CH-TRU Payload Appendices. As shown in Appendix 6.9 of the CH-TRU Payload Appendices, for Waste Material Type III.1, minimum values for decay heat limits are obtained by using the hydrogen generation and release rates at an ambient temperature of 70 degrees Fahrenheit.

The mass balance on flammable gas in a container after application of the vacuum during transport is described by the following equation:

Equation 15

$$\frac{dn_d}{dt} = C_g - \frac{y_d - y_{ICV}}{r_{eff}}$$

where,

n_d	=	Moles of flammable gas in the container, mol
t	=	Time, s
C_g	=	Flammable gas generation rate in the container, mol/s
y_d	=	Mole fraction of flammable gas within innermost confinement layer of container, dimensionless
y_{ICV}	=	Mole fraction of flammable gas in the ICV and/or TDOP (for packaging configurations using a TDOP), dimensionless
r_{eff}	=	Total effective resistance of the confinement layers to the release of flammable gas, s/mol.

From the Ideal Gas Law:

Equation 16

$$n_d = \frac{y_d P V_d}{R\ T}$$

where,

P	=	Pressure, atm
V_d	=	Void volume within innermost confinement layer of container, L
R	=	Gas constant, 0.082056 atm L/mol K
T	=	Temperature, K.

It is assumed that all voids (within each container and in the ICV) are isothermal and isobaric, thus, the pressure and temperature may be considered constant. Substituting the Ideal Gas Law relation in the mass balance equation and rearranging terms yields:

Equation 17

$$\frac{dy_d}{dt} = \frac{C_g\ R\ T}{P\ V_d} - \frac{R\ T}{P\ V_d\ r_{eff}}(y_d - y_{ICV})$$

Let,

Equation 18

$$\alpha = \frac{C_g\ R\ T}{P\ V_d}$$

and

Equation 19

$$\beta = \frac{R\ T}{P\ V_d\ r_{eff}}$$

Then, the mass balance for flammable gas within a single container during transport is given by the following equation:

Equation 20

$$\frac{dy_d}{dt} = \alpha - \beta\ (y_d - y_{ICV})$$

The concentration of flammable gas in the ICV is assumed to be constant instead of solving a separate equation for the buildup of flammable gas in the ICV. The maximum mole fraction of flammable gas in the ICV is set equal to the moles of flammable gas generated by all containers during shipment divided by the initial moles of gas in the ICV. Thus, it is assumed that a constant and maximum concentration of flammable gas exists in the ICV after vacuum application at the start of the shipping period. For a given shipping period, the allowable flammable gas generation rate to attain 5 percent (by volume) hydrogen concentration at the end of the shipping period will be a minimum. The actual allowable gas generation rate would be higher if the mass balance equation of flammable gas in the ICV is solved simultaneously with the mass balance equation for flammable gas within the container. The same conservative assumptions regarding the ICV hydrogen concentration are used in the analysis in Section 5.0 of the CH-TRAMPAC.

Let,

Equation 21

$$\gamma = \beta\ y_{ICV}$$

and

Equation 22

$$\lambda = \alpha + \gamma$$

Substituting the definitions of α, β, and λ into the mass balance equation yields:

Equation 23

$$\frac{dy_d}{dt} = \lambda - \beta\, y_d$$

Taking the Laplace Transform yields:

Equation 24

$$s\, \widetilde{y}_d - y_d(0) = \frac{\lambda}{s} - \beta\, \widetilde{y}_d$$

Letting $y_d(0) = y_{d0}$ (i.e., the initial concentration within the innermost confinement layer after vacuum application) and rearranging terms yields:

Equation 25

$$\widetilde{y}_d = \frac{\dfrac{\lambda}{s} + y_{d0}}{s + \beta}$$

Taking the inverse Laplace Transform yields:

Equation 26

$$y_d(t) = \frac{\lambda}{\beta} + (y_{d0} - \frac{\lambda}{\beta})e^{-\beta\, t_t}$$

Replacing λ with $\alpha + \gamma$ gives:

Equation 27

$$y_d(t) = \frac{\alpha + \gamma}{\beta} + (y_{d0} - \frac{\alpha + \gamma}{\beta})e^{-\beta\, t_t}$$

and y_{ICV} in the γ term is given by the relation:

Equation 28

$$y_{ICV} = \frac{n_{gen}\ C_g\ t_t}{N_{tg}}$$

where,

n_{gen} =   Number of flammable gas generators per payload

t_t =   Shipping period duration, s

N_{tg} =   Total moles of gas in the ICV and/or TDOP (for packaging configurations using a TDOP) void volume calculated using the Ideal Gas Law as:

Equation 29

$$N_{tg} = \frac{P\ V_{ICV}}{R\ T}$$

where,

V_{ICV} =   Void volume within the ICV and/or TDOP (for packaging configurations using a TDOP).

Substitution of terms in Equation 27 and simplification results in the following equation for the concentration of flammable gas within the innermost confinement layer of a container at the end of the shipping period (t_t):

Equation 30

$$y_d(t_t) = C_g\left(r_{eff} + \frac{n_{gen}t_t}{N_{tg}}\right) + \left[y_{d0} - C_g\left(r_{eff} + \frac{n_{gen}t_t}{N_{tg}}\right)\right]\exp\{-R\ T\ t_t/(P\ V_d\ r_{eff})\}$$

Rearranging terms to solve for the flammable gas generation rate limit yields:

Equation 31

$$C_g = \frac{y_d - y_{d0}\exp\{-R\ T\ t_t/(P\ V_d\ r_{eff})\}}{\left(r_{eff} + \dfrac{n_{gen}t_t}{N_{tg}}\right)[1 - \exp\{-R\ T\ t_t/(P\ V_d\ r_{eff})\}]}$$

For an initial concentration within the innermost confinement layer after vacuum application, y_{d0}, the limit for flammable gas generation rate, C_g, is calculated with the concentration (in mole fraction units) within the innermost confinement layer of a container at the end of the shipping period, e.g., for the 5-day shipping period, $y_d(t = t_t = 5$ days) set equal to 0.05.

The decay heat limit corresponding to the flammable gas generation rate limit is then calculated through Equation (5) of Appendix 2.3 of the CH-TRU Payload Appendices as:

Equation 32

$$Q = [(C_g \ N_A)/(G \ molecules/100 \ eV)] \ [1.602E-19 \ W \ s/eV]$$

where,

Q   =   Decay heat limit per container, W

N_A =   Avogadro's number, 6.023E+23 molecules/mol

G   = G_{eff}(flam gas) = Effective G value for flammable gas.

The mathematical model of the vacuum evacuation process described earlier shows that the final concentration within the innermost confinement layer at the end of the process is a function of the flammable gas generation rate. For example, if all 14 drums in a payload are assumed to be Content Code LA 154A (4 inner bags and 2 liner bags) and each drum has a decay heat of 1.8219 watts (corresponding to a maximum flammable gas generation rate of 2.0581E-7 mol/s), the ICV vacuum evacuation model shows that the final concentration of flammable gas within the innermost confinement layer is 1.0353 volume percent. The solution of Equation 31 with $y_d(t_t = 5 \ day)$ set equal to 0.05 mole fraction and y_{d0} set equal to 0.010353 yields a flammable gas generation rate limit of 2.0581E-7 mol/s. The corresponding decay heat limit is 1.8219 watts.

Parameter values used to establish flammable gas generation rate and decay heat limits are listed in Table 6.12-12 for Content Codes LA 154, SQ 154, and SQ 156 and are the same values used in the gas generation analysis in the CH-TRAMPAC except for the effective flammable gas G value assigned to Content Code SQ 156 (see Section 6.12.6.2.3 of this appendix). Flammable gas generation rate and decay heat limits for Content Codes LA 154, SQ 154, and SQ 156 are shown in Table 6.12-3, Table 6.12-4, and Table 6.12-5 of this appendix, respectively.

Table 6.12-12– Parameter Values

Parameter	Symbol	Value	Reference
Pressure	P	1 atm	Appendix 2.3, Equation 2 of the CH-TRU Payload Appendices
Temperature	T	294 K	Appendix 2.3, Equation 2 of the CH-TRU Payload Appendices
Void volume within innermost confinement layer of container (i.e., multiple bag void volume)	V_d	53.5 L	Appendix 3.7 of the CH-TRU Payload Appendices, with assumption of 50 percent void volume reduction
Resistance of inner bag	—	1,792,115 s/mol	Appendix 6.10, Table 6.10-1 of the CH-TRU Payload Appendices
Resistance of drum liner bag	—	214,133 s/mol	Appendix 6.10, Table 6.10-1 of the CH-TRU Payload Appendices
Resistance of SWB liner bag	—	125,660 s/mol	Appendix 6.10, Table 6.10-1 of the CH-TRU Payload Appendices
Resistance of punctured rigid drum liner	—	19,646 s/mol	Appendix 6.10, Table 6.10-1 of the CH-TRU Payload Appendices
Resistance of 3.7E-6 mole/sec/mole fraction diffusivity filter	—	270,270 s/mol	Appendix 6.10, Table 6.10-1 of the CH-TRU Payload Appendices
Resistance of 1.85E-5 mole/sec/mole fraction diffusivity filter (5X filter)	—	54,100 s/mol	Calculated from Section 2.5, Table 2.5-1 of CH-TRAMPAC
Total effective resistance of the confinement layers to the release of flammable gas for content code packaging configurations	r_{eff}	As calculated	Calculated by summing the products of the number of layers of each type and the resistance of each layer

Parameter	Symbol	Value	Reference
Void volume within the ICV with fourteen 55-gallon drums/TRUPACT-II	V_{ICV}	2,450 L	Appendix 2.3 of the CH-TRU Payload Appendices
Void volume within a TDOP with six 85-gallon drums	V_{ICV}	2,210 L	Calculated based on values specified in Section 6.10.3.2 of Appendix 6.10 of the CH-TRU Payload Appendices
Void volume within the ICV with two SWBs/ TRUPACT-II	V_{ICV}	1,750 L	Appendix 6.10, Section 6.10.3.2 of the CH-TRU Payload Appendices
Void volume within the ICV and within the TDOP with ten 55-gallon drums/TRUPACT-II	V_{ICV}	3,346 L	Appendix 6.10, Section 6.10.3.2 of the CH-TRU Payload Appendices
Total moles of gas in the ICV with fourteen 55-gallon drums/TRUPACT-II	N_{tg}	101.56 mol	Calculated through Ideal Gas Law
Total moles of gas in a TDOP with six 85-gallon drums/TRUPACT-II	N_{tg}	91.608 mol	Calculated through Ideal Gas Law
Total moles of gas in the ICV with two SWBs/ TRUPACT-II	N_{tg}	72.54 mol	Calculated through Ideal Gas Law
Total moles of gas in the ICV and in the TDOP with ten 55-gallon drums/ TRUPACT-II	N_{tg}	138.70 mol	Calculated through Ideal Gas Law
Number of flammable gas generators per payload	n_{gen}	14 6 8 2 10	14 55-gallon drums/ TRUPACT-II 6 85-gallon drum overpacks/TDOP 8 55-gallon drums in 2 SWBs/TRUPACT-II 2 SWBs/TRUPACT-II 10 55-gallon drums/TDOP
Shipping period duration	t_t	432,000 s 864,000 s	5-day shipping period 10-day shipping period

Parameter	Symbol	Value	Reference
Effective G value for flammable gas (molecules of hydrogen formed/100 eV) for Content Codes LA 154 and SQ 154	G	1.09 molecules/100 eV	Appendix 3.2, Table 3.2-1 of the CH-TRU Payload Appendices for Waste Material Type III.1 (watt*year > 0.012)
Effective G value for flammable gas (molecules of hydrogen formed/100 eV) for Content Code SQ 156	G	0.53 molecules/100 eV	Shaw Environmental, Inc., February 2005, "High-Dose Criterion for Flammable Gas G Values and Dose-Dependent Net Gas G Values for Contact-Handled Transuranic Wastes"

6.12.9.4 Mixing of Containers of Content Codes LA 154, SQ 154, or SQ 156 for Payload Assembly

This section provides the logic and mathematical analysis for assembling a payload of containers belonging to different packaging configurations under Content Code LA 154, SQ 154, or SQ 156. As shown in Section 6.0 of the CH-TRAMPAC, an assembly of payload containers is approved by ensuring that each payload container does not contain a flammable mixture of gases, while accounting for the properties of each of the other payload containers in the assembly, which may include dunnage containers. Each payload container is assessed through the calculation of the flammability index (FI) for the container, which accounts for the properties of each container in the assembly. For each payload container, the FI is calculated as the ratio of the actual flammable gas generation rate to the allowable flammable gas generation rate limit multiplied by 50,000. Thus, the FI must be a non-negative number less than or equal to 50,000 for each payload container. The determination of allowable flammable gas generation rates takes into account the concentrations of flammable VOCs within the innermost layer of confinement, if present, and the void volume of dunnage containers.

The derivation of allowable flammable gas generation rates is based on the methodology established in Section 6.12.9.3 of this appendix. The following definitions are made for container *i*:

Equation 33

$$\alpha_i = \frac{C_{g,i}\ R\ T}{P\ V_d}$$

and

Equation 34

$$\beta_i = \frac{R\ T}{P\ V_d\ r_{eff,i}}$$

where,

P	=	Pressure, atm
V_d	=	Void volume within innermost confinement layer of container, L
R	=	Gas constant, 0.082056 atm L/mol K
T	=	Temperature, K

$r_{eff,i}$ = Effective resistance to the release of flammable gas of payload container i, s/mol

$C_{g,i}$ = Allowable flammable gas generation rate limit per innermost confinement layer of payload container i, mol/s.

The following equation is an extension of the equation for the mole fraction within the innermost layer of confinement (Equation 27) and provides an expression for the allowable flammable gas concentration (AFGC) within the innermost confinement layer of container, i, at the end of the shipping period. The AFGC$_i$ is equivalent to 0.05 if the concentration of flammable VOCs in the headspace of the container is less than or equal to 500 parts per million volume. Otherwise, the AFGC value is calculated as the difference between the container mixture lower explosive limit and the sum of the flammable VOC concentrations within the innermost confinement layer.

Equation 35

$$AFGC_i(t) = \frac{\alpha_i + \beta_i \, y_{ICV}}{\beta_i} + (y_{d0,i} - \frac{\alpha_i + \beta_i \, y_{ICV}}{\beta_i})e^{-\beta_i \, t}$$

where,

AFGC$_i$ = Allowable flammable gas concentration in the innermost confinement layer of payload container i, dimensionless

t = Shipping period duration, 5 days or 432,000 s, or 10 days or 864,000 s.

and

Equation 36

$$y_{ICV} = \frac{\sum\limits_{i=1}^{nc} C_{g,i} \, t}{N_{tg}}$$

where,

nc = Number of containers in the payload, dimensionless

N_{tg} = Total moles of gas in the ICV and/or TDOP void volume calculated using the Ideal Gas Law as:

Equation 37

$$N_{tg} = \frac{P \, V_{ICV}}{R \, T}$$

where,

$$V_{ICV} \quad = \quad \text{Void volume inside the ICV cavity and/or inside the TDOP.}$$

Substitution of terms in Equation 35 and simplification results in the following system of equations that must be solved to obtain the allowable flammable gas generation rate limit for each container $(C_{g,i})$:

Equation 38

$$y_{d0,1}\ e^{-\beta_1 t} + \left[\left(r_{eff,1} + \frac{t}{N_{tg}}\right)C_{g,1} + \frac{t}{N_{tg}}C_{g,2} + \ldots + \frac{t}{N_{tg}}C_{g,nc}\right](1 - e^{-\beta_1 t}) = AFGC_1$$

$$y_{d0,2}\ e^{-\beta_2 t} + \left[\frac{t}{N_{tg}}C_{g,1} + \left(r_{eff,2} + \frac{t}{N_{tg}}\right)C_{g,2} + \ldots + \frac{t}{N_{tg}}C_{g,nc}\right](1 - e^{-\beta_2 t}) = AFGC_2$$

$$\cdot\ \cdot\ \cdot$$
$$\cdot\ \cdot\ \cdot$$
$$\cdot\ \cdot\ \cdot$$

$$y_{d0,nc}\ e^{-\beta_{nc} t} + \left[\frac{t}{N_{tg}}C_{g,1} + \frac{t}{N_{tg}}C_{g,2} + \ldots + \left(r_{eff,nc} + \frac{t}{N_{tg}}\right)C_{g,nc}\right](1 - e^{-\beta_{nc} t}) = AFGC_{nc}\ .$$

The above system of equations may be written in matrix form as:

Equation 39

$$[A]\ \{CG\} = \{b\}$$

where,

$$A \quad = \quad \text{Matrix of gas generation rate coefficients and initial drum concentrations}$$

$$CG \quad = \quad \text{Column vector of allowable gas generation rates}$$

$$b \quad = \quad \text{Column vector of adjusted individual AFGC values within the innermost confinement layers. The elements are:}$$

$$\left(\frac{AFGC_i - y_{d0,i}\ e^{-\beta_i t}}{1 - e^{-\beta_i t}}\right)$$

The solution for the unknown allowable flammable gas generation rate for each drum is given as:

Equation 40

$$\{CG\} = [A]^{-1}\{b\}$$

where,

$[A]^{-1}$ = Inverse of matrix A.

Dunnage containers are excluded from the system of linear equations.

The FI of each drum is then calculated as:

Equation 41

$$FI_i = \frac{C_{g,i,actual}}{C_{g,i,allowable}} \times 50{,}000$$

where,

FI_i = Flammability index of payload container, i

$C_{g,i,actual}$ = Actual flammable gas generation of payload container i, mol/s

$C_{g,i,allowable}$ = Allowable flammable gas generation rate of payload container i, mol/s.

For analytical category payload containers, the actual flammable gas generation rate is calculated as:

Equation 42

$$C_{g,i,actual} = \frac{Q_i \left(G \text{ molecules} / 100 \text{ eV}\right)}{N_A \left(1.602E - 19 \text{ W s} / eV\right)}$$

where,

Q_i = Decay heat of payload container, W

N_A = Avogadro's number, 6.023E+23 molecules/mol

G = G_{eff} (flam gas) = Effective G value for flammable gas.

For test category containers, the actual gas generation rate is obtained either through measurement of the flammable gas concentration in the drum or liner headspace and calculation of the rate, or through container testing pursuant to Section 5.2.5 of the CH-TRAMPAC. A payload is qualified for shipment only if the FI of each payload container is a non-negative number less than or equal to 50,000. If one or more containers fail the FI requirement, the payload shall be reconfigured until all containers satisfy this requirement. The FI determination can be performed either manually or by the use of a validated software package.

6.12.10 Content Codes

Content Codes LA 154, SQ 154, and SQ 156 are provided on the following pages.

This page intentionally left blank.

CONTENT CODE: LA 154 (See Waste Packaging Description Table)

CONTENT DESCRIPTION: Mixed Combustible/Noncombustible Waste

GENERATING SITE: Los Alamos National Laboratory (LANL)

WASTE DESCRIPTION: 55-gallon drums, some of which are overpacked in 85-gallon drums, of mixed combustible/noncombustible waste generated from plutonium processing activities at LANL. The shipment of Content Code LA 154 waste is subject to the requirements and operating controls specified in Appendix 6.12 of the CH-TRU Payload Appendices.

GENERATING SOURCES: The waste originates from plutonium processing activities at LANL.

WASTE FORM: Mixtures of combustible and noncombustible waste consist of paper, rags, plastic, rubber, absorbed organic liquids, leaded glovebox gloves, glass, motors, pumps, tools, and miscellaneous metal waste. The waste is contaminated primarily with Pu-238 and/or Pu-239.

WASTE PACKAGING: Details of the waste packaging for each code are presented in the following table:

WASTE PACKAGING DESCRIPTION TABLE

Code	Description
LA 154A	The waste is packaged in a maximum of four layers of inner plastic bags. Bagged out items are placed in a 55-gallon drum lined with a maximum of two plastic liner bags. All bag closures are by the twist and tape method, or the twist, tie, and tape method.
LA 154B	The waste is placed in a 55-gallon drum lined with a maximum of one plastic liner bag. The bag liner is closed by the twist and tape method, or the twist, tie, and tape method.
LA 154C	The waste is packaged in a maximum of four layers of inner plastic bags. Bagged out items are placed in a 55-gallon drum lined with a maximum of two plastic liner bags. All bag closures are by the twist and tape method, or the twist, tie, and tape method. The 55-gallon drum is overpacked in an 85-gallon drum. For shipment, six 85-gallon drums are overpacked in a ten-drum overpack (TDOP). No additional bags are used in the 85-gallon drum or TDOP.
LA 154D	The waste is packaged in a maximum of four layers of inner plastic bags. Bagged out items are placed in a 55-gallon drum lined with a maximum of two plastic liner bags. All bag closures are by the twist and tape method, or the twist, tie, and tape method. Four 55-gallon drums are overpacked in a standard waste box (SWB). No additional bags are used in the SWB.

ASSAY: Each drum is assayed by means of a neutron or gamma counter according to written procedures. Which instrument is used depends on the matrix and nuclide content of the drum. The results of the assay are expressed in terms of grams of each radionuclide present. Assay results are used to calculate Pu-239 fissile gram equivalent (plus 2 times the error), decay heat,

and plutonium equivalent curies (plus error) (required to ensure compliance with the waste acceptance criteria for disposal at the Waste Isolation Pilot Plant [WIPP]).

FREE LIQUIDS: Each drum is examined by radiography in accordance with written procedures to ensure the absence of free liquids. A subset of the waste assigned to Content Code LA 154 is also subjected to visual examination for the purpose of verifying the compliance determinations made by radiography. Special emphasis during these examinations is applied to internal containers (e.g., bottles and cans) and motors and pumps to ensure the absence of free liquids. Any drum containing free liquids will be set aside for mitigation activities to remove the free liquids (e.g., absorption or solidification activities) in accordance with written procedures.

EXPLOSIVES/COMPRESSED GASES: Explosives are prohibited in the LANL plutonium processing areas. Each drum is examined by radiography in accordance with written procedures to ensure the absence of explosives or compressed gases. Special emphasis during these examinations is applied to ensure the absence of any pressure vessels or spray cans that could potentially contain gases under pressure. Any drum containing explosives or compressed gases will be set aside for mitigation activities to remove the prohibited item (e.g., blocking open, puncturing, flattening, or cutting a pressurized container) in accordance with written procedures.

PYROPHORICS: No pyrophoric materials will be present as determined by radiography. Drums containing pyrophoric materials as identified during the examinations are set aside for mitigation activities in accordance with written procedures.

CORROSIVES: No corrosive materials will be present as determined by radiography in accordance with written procedures. Drums containing corrosive materials as identified during the examinations are set aside for mitigation activities (e.g., neutralization) in accordance with written procedures.

CHEMICAL COMPATIBILITY: Because the LA 154 CH-TRU waste containers belong to an approved waste material type (Waste Material Type III.1), the chemical compatibility analysis described in Appendix 6.1 of the CH-TRU Payload Appendices bounds Content Code LA 154. All waste is chemically compatible for materials in greater than trace (>1% weight) quantities. The chemicals found in this content code are restricted to the table of allowable materials for Waste Material Type III.1 in Section 4.0 of the CH-TRAMPAC.

PAYLOAD CONTAINER VENTING AND ASPIRATION: Payload containers in this content code that have been stored in an unvented condition will be vented and aspirated to comply with the requirements of Section 5.3 of the CH-TRAMPAC or through the vacuum application process described in Appendix 6.12 of the CH-TRU Payload Appendices.

ADDITIONAL CRITERIA: In accordance with Section 2.9 of the CH-TRAMPAC, for 55-gallon drums, the rigid liner (if present) contains a 0.3-inch minimum diameter hole, or filter with a hydrogen release rate equivalent to or greater than the 0.3-inch minimum diameter hole.

(LA 154A) The 55-gallon drum is fitted with a minimum of one filter with a diffusivity of 3.70E-6 moles per second per mole fraction.

(LA 154B)   The 55-gallon drum is fitted with a minimum of one filter with a diffusivity of 1.85E-5 moles per second per mole fraction.

(LA 154C)   The 55-gallon drum is fitted with a minimum of one filter with a diffusivity of 3.70E-6 moles per second per mole fraction. Each 85-gallon drum used to overpack a 55-gallon drum (85-gallon drum overpack) is fitted with a single filter with a diffusivity of 3.7E-6 moles per second per mole fraction. Each TDOP used to overpack 85-gallon drum overpacks is fitted with a minimum of nine filters, each with a diffusivity of 3.7E-6 moles per second per mole fraction.

(LA 154D)   The 55-gallon drum is fitted with a minimum of one filter with a diffusivity of 3.7E-6 moles per second per mole fraction. Each SWB used to overpack four 55-gallon drums is fitted with a minimum of four filters, each with a diffusivity of 3.7E-6 moles per second per mole fraction.

All waste shipped under Content Code LA 154 must comply with the additional conditions and controls specified in Appendix 6.12 of the CH-TRU Payload Appendices. Compliance with these additional conditions and controls is documented per Appendix 6.12 of the CH-TRU Payload Appendices.

SHIPPING CATEGORY: For Content Code LA 154 payload containers, "LA 154A," "LA 154B," "LA 154C," or "LA 154D," as applicable, shall be used as the shipping category to direct the evaluation of the payload container for compliance with the applicable decay heat or flammable gas generation rate limit. Applicable decay heat limits for the packaging configurations under Content Code LA 154 are specified in Appendix 6.12 of the CH-TRU Payload Appendices.

MAXIMUM ALLOWABLE WATTAGE: The maximum allowable wattages for this waste are calculated according to the methodology specified in Appendix 6.12 of the CH-TRU Payload Appendices and are listed in Appendix 6.12 of the CH-TRU Payload Appendices.

This page intentionally left blank.

CONTENT CODE: SQ 154 (See Waste Packaging Description Table)

CONTENT DESCRIPTION: Mixed Combustible/Noncombustible Waste

GENERATING/STORAGE SITE: Various

WASTE DESCRIPTION: Containers of mixed combustible/noncombustible waste generated from plutonium processing activities. The shipment of Content Code SQ 154 waste is subject to the requirements and operating controls specified in Appendix 6.12 of the CH-TRU Payload Appendices.

GENERATING SOURCES: The waste originates from plutonium processing activities at the DOE sites.

WASTE FORM: Mixtures of combustible and noncombustible waste consist of paper, rags, plastic, rubber, absorbed organic liquids, leaded glovebox gloves, glass, motors, pumps, tools, and miscellaneous metal waste.

WASTE PACKAGING: Details of the waste packaging for each code are presented in the following table:

WASTE PACKAGING DESCRIPTION TABLE

Code	Description
SQ 154A	The waste is packaged in a maximum of four layers of inner plastic bags. Bagged out items are placed in a 55-gallon drum lined with a maximum of two plastic liner bags. All bag closures are by the twist and tape method.
SQ 154B	The waste is placed in a 55-gallon drum lined with a maximum of one plastic liner bag. The bag liner is closed by the twist and tape method.
SQ 154C	The waste is packaged in a maximum of four layers of inner plastic bags. Bagged out items are placed in a 55-gallon drum lined with a maximum of two plastic liner bags. All bag closures are by the twist and tape method. The 55-gallon drum is overpacked in an SWB with four filters. No additional bags are used in the SWB.
SQ 154D	The waste is placed in a 55-gallon drum lined with a maximum of one plastic liner bag. All bag closures are by the twist and tape method. The 55-gallon drum is overpacked in an SWB with four filters. No additional bags are used in the SWB.
SQ 154E	The waste is packaged in a maximum of five layers of inner plastic bags. Five or more such bagged out items are placed directly in an SWB lined with a maximum of one plastic SWB liner bag. All bag closures are by the twist and tape method. The SWB is fitted with four filters.
SQ 154F	The waste is placed directly in an SWB lined with a maximum of one plastic SWB liner bag. All bag closures are by the twist and tape method. The SWB is fitted with four filters.
SQ 154G	The waste is packaged in a maximum of four layers of inner plastic bags. Bagged out items are placed in a 55-gallon drum lined with a maximum of two plastic liner bags. All bag closures are by the twist and tape method. The 55-gallon drum is overpacked in a TDOP. No additional bags are used in the TDOP.

ASSAY: Assay for all payload containers shall be performed in accordance with the CH-TRAMPAC. The isotopic composition of the waste is determined from measurements taken on the product material during the processing at the site. The processing organizations transmit the isotopic composition information to the site waste certification organization.   Therefore, the isotopic composition of the waste need not be determined by direct analysis or measurement of the waste unless process information is not available. The results of the assay are expressed in terms of grams of each radionuclide present. Assay results are used to calculate Pu-239 fissile gram equivalent (plus 2 times the error), decay heat, and plutonium equivalent curies (plus error) (required to ensure compliance with the waste acceptance criteria for disposal at the Waste Isolation Pilot Plant).

FREE LIQUIDS: Liquid waste is prohibited in the payload containers except for residual amounts in well-drained containers. The total volume of residual liquid in a payload container shall be less than 1 volume percent of the payload container. Waste packaging procedures ensure that free liquids are less than 1 volume percent of the payload container.

EXPLOSIVES/COMPRESSED GASES: Explosives and compressed gases in the payload containers are prohibited by waste packaging procedures.

PYROPHORICS: Nonradioactive pyrophorics in the payload containers are prohibited by waste packaging procedures. Waste packaging procedures shall ensure that all pyrophoric radioactive materials are present only in small residual amounts (less than 1 weight percent) in payload containers.

CORROSIVES: Corrosives are prohibited in the payload containers. Acids and bases that are potentially corrosive shall be neutralized and rendered noncorrosive prior to being a part of the waste. The physical form of the waste and the waste generating procedures ensure that the waste is in a nonreactive form.

CHEMICAL COMPATIBILITY: Because the SQ 154 CH-TRU waste containers belong to an approved waste material type (Waste Material Type III.1), the chemical compatibility analysis described in Appendix 6.1 of the CH-TRU Payload Appendices bounds Content Code SQ 154. All waste is chemically compatible for materials in greater than trace (>1% weight) quantities. The chemicals found in this content code are restricted to the table of allowable materials for Waste Material Type III.1 in Section 4.0 of the CH-TRAMPAC.

PAYLOAD CONTAINER VENTING AND ASPIRATION: Payload containers in this content code that have been stored in an unvented condition will be vented and aspirated to comply with the requirements of Section 5.3 of the CH-TRAMPAC or through the vacuum application process described in Appendix 6.12 of the CH-TRU Payload Appendices.

ADDITIONAL CRITERIA: In accordance with Section 2.9 of the CH-TRAMPAC, for 55-gallon drums, the rigid liner (if present) contains a 0.3-inch minimum diameter hole, or filter with a hydrogen release rate equivalent to or greater than the 0.3-inch minimum diameter hole.

(SQ 154A) The 55-gallon drum is fitted with a minimum of one filter with a diffusivity of 3.70E-6 moles per second per mole fraction.

(SQ 154B) The 55-gallon drum is fitted with a minimum of one filter with a diffusivity of 1.85E-5 moles per second per mole fraction.

(SQ 154C) The 55-gallon drum is fitted with a minimum of one filter with a diffusivity of 3.70E-6 moles per second per mole fraction. The SWB used to overpack up to four 55-gallon drums (SWB overpack) is fitted a minimum of four filters with a diffusivity of 3.7E-6 moles per second per mole fraction.

(SQ 154D) The 55-gallon drum is fitted with a minimum of one filter with a diffusivity of 1.85E-5 moles per second per mole fraction. The SWB used to overpack up to four 55-gallon drums (SWB overpack) is fitted a minimum of four filters with a diffusivity of 3.7E-6 moles per second per mole fraction.

(SQ 154E, SQ 154F) The SWB is fitted with a minimum of four filters, each with a diffusivity of 3.7E-6 moles per second per mole fraction.

(SQ 154G) The 55-gallon drum is fitted with a minimum of one filter with a diffusivity of 3.70E-6 moles per second per mole fraction. The TDOP used to overpack 55-gallon drums is fitted with a minimum of nine filters, each with a diffusivity of 3.7E-6 moles per second per mole fraction.

All waste shipped under Content Code SQ 154 must comply with the additional conditions and controls specified in Appendix 6.12 of the CH-TRU Payload Appendices. Compliance with these additional conditions and controls is documented per Appendix 6.12 of the CH-TRU Payload Appendices.

SHIPPING CATEGORY: For Content Code SQ 154 payload containers, the content code (e.g., "SQ 154A") shall be used as the shipping category to direct the evaluation of the payload container for compliance with the applicable decay heat or flammable gas generation rate limit. Applicable decay heat limits for the packaging configurations under Content Code SQ 154 are specified in Appendix 6.12 of the CH-TRU Payload Appendices.

MAXIMUM ALLOWABLE WATTAGE: The maximum allowable wattages for this waste are calculated according to the methodology specified in Appendix 6.12 of the CH-TRU Payload Appendices and are listed in Appendix 6.12 of the CH-TRU Payload Appendices.

This page intentionally left blank.

CONTENT CODE: SQ 156 (See Waste Packaging Description Table)

CONTENT DESCRIPTION: Mixed Combustible/Noncombustible Waste

GENERATING/STORAGE SITE: Various

WASTE DESCRIPTION: Containers of mixed combustible/noncombustible waste generated from plutonium processing activities. Each payload container assigned to SQ 156 meets the high-dose criterion of >1.2 watt*year and is part of a waste population that has been approved in accordance with Section 6.12.6.2.3 of Appendix 6.12 of the CH-TRU Payload Appendices. The shipment of Content Code SQ 156 waste is subject to the requirements and operating controls specified in Appendix 6.12 of the CH-TRU Payload Appendices.

GENERATING SOURCES: The waste originates from plutonium processing activities at the DOE sites.

WASTE FORM: Mixtures of combustible and noncombustible waste consist of paper, rags, plastic, rubber, absorbed organic liquids, leaded glovebox gloves, glass, motors, pumps, tools, and miscellaneous metal waste.

WASTE PACKAGING: Details of the waste packaging for each code are presented in the following table:

WASTE PACKAGING DESCRIPTION TABLE

Code	Description
SQ 156A	The waste is packaged in a maximum of four layers of inner plastic bags. Bagged out items are placed in a 55-gallon drum lined with a maximum of two plastic liner bags. All bag closures are by the twist and tape method.
SQ 156B	The waste is placed in a 55-gallon drum lined with a maximum of one plastic liner bag. The bag liner is closed by the twist and tape method.
SQ 156C	The waste is packaged in a maximum of four layers of inner plastic bags. Bagged out items are placed in a 55-gallon drum lined with a maximum of two plastic liner bags. All bag closures are by the twist and tape method. The 55-gallon drum is overpacked in an SWB with four filters. No additional bags are used in the SWB.
SQ 156D	The waste is placed in a 55-gallon drum lined with a maximum of one plastic liner bag. All bag closures are by the twist and tape method. The 55-gallon drum is overpacked in an SWB with four filters. No additional bags are used in the SWB.
SQ 156E	The waste is packaged in a maximum of five layers of inner plastic bags. Five or more such bagged out items are placed directly in an SWB lined with a maximum of one plastic SWB liner bag. All bag closures are by the twist and tape method. The SWB is fitted with four filters.
SQ 156F	The waste is placed directly in an SWB lined with a maximum of one plastic SWB liner bag. All bag closures are by the twist and tape method. The SWB is fitted with four filters.

Code	Description
SQ 156G	The waste is packaged in a maximum of four layers of inner plastic bags. Bagged out items are placed in a 55-gallon drum lined with a maximum of two plastic liner bags. All bag closures are by the twist and tape method. The 55-gallon drum is overpacked in a TDOP. No additional bags are used in the TDOP.
SQ 156H	The waste is packaged in a maximum of four layers of inner plastic bags. Bagged out items are placed into a filtered container. Three filtered containers are placed into an SWB lined with a maximum of one plastic SWB liner bag. All bag closures are by the twist and tape method. The SWB is fitted with four filters.

ASSAY: Assay for all payload containers shall be performed in accordance with the CH-TRAMPAC. The isotopic composition of the waste is determined from measurements taken on the product material during the processing at the site. The processing organizations transmit the isotopic composition information to the site waste certification organization. Therefore, the isotopic composition of the waste need not be determined by direct analysis or measurement of the waste unless process information is not available. The results of the assay are expressed in terms of grams of each radionuclide present. Assay results are used to calculate Pu-239 fissile gram equivalent (plus 2 times the error), decay heat, and plutonium equivalent curies (plus error) (required to ensure compliance with the waste acceptance criteria for disposal at the Waste Isolation Pilot Plant).

FREE LIQUIDS: Liquid waste is prohibited in the payload containers except for residual amounts in well-drained containers. The total volume of residual liquid in a payload container shall be less than 1 volume percent of the payload container. Waste packaging procedures ensure that free liquids are less than 1 volume percent of the payload container.

EXPLOSIVES/COMPRESSED GASES: Explosives and compressed gases in the payload containers are prohibited by waste packaging procedures.

PYROPHORICS: Nonradioactive pyrophorics in the payload containers are prohibited by waste packaging procedures. Waste packaging procedures shall ensure that all pyrophoric radioactive materials are present only in small residual amounts (less than 1 weight percent) in payload containers.

CORROSIVES: Corrosives are prohibited in the payload containers. Acids and bases that are potentially corrosive shall be neutralized and rendered noncorrosive prior to being a part of the waste. The physical form of the waste and the waste generating procedures ensure that the waste is in a nonreactive form.

CHEMICAL COMPATIBILITY: Because the SQ 156 CH-TRU waste containers belong to an approved waste material type (Waste Material Type III.1), the chemical compatibility analysis described in Appendix 6.1 of the CH-TRU Payload Appendices bounds Content Code SQ 156. All waste is chemically compatible for materials in greater than trace (>1% weight) quantities. The chemicals found in this content code are restricted to the table of allowable materials for Waste Material Type III.1 in Section 4.0 of the CH-TRAMPAC.

PAYLOAD CONTAINER VENTING AND ASPIRATION: Payload containers in this content code that have been stored in an unvented condition will be vented and aspirated to comply with the requirements of Section 5.3 of the CH-TRAMPAC or through vacuum application process described in Appendix 6.12 of the CH-TRU Payload Appendices.

ADDITIONAL CRITERIA: In accordance with Section 2.9 of the CH-TRAMPAC, for 55-gallon drums, the rigid liner (if present) containers a 0.3-inch minimum diameter hole, or filter with a hydrogen release rate equivalent to or greater than the 0.3-inch minimum diameter hole.

(SQ 156A) The 55-gallon drum is fitted with a minimum of one filter with a diffusivity of 3.70E-6 moles per second per mole fraction.

(SQ 156B) The 55-gallon drum is fitted with a minimum of one filter with a diffusivity of 1.85E-5 moles per second per mole fraction.

(SQ 156C) The 55-gallon drum is fitted with a minimum of one filter with a diffusivity of 3.70E-6 moles per second per mole fraction. The SWB used to overpack up to four 55-gallon drums (SWB overpack) is fitted a minimum of four filters with a diffusivity of 3.7E-6 moles per second per mole fraction.

(SQ 156D) The 55-gallon drum is fitted with a minimum of one filter with a diffusivity of 1.85E-5 moles per second per mole fraction. The SWB used to overpack up to four 55-gallon drums (SWB overpack) is fitted a minimum of four filters with a diffusivity of 3.7E-6 moles per second per mole fraction.

(SQ 156E, SQ 156F) The SWB is fitted with a minimum of four filters, each with a diffusivity of 3.7E-6 moles per second per mole fraction.

(SQ 156G) The 55-gallon drum is fitted with a minimum of one filter with a diffusivity of 3.70E-6 moles per second per mole fraction. The TDOP used to overpack 55-gallon drums is fitted with a minimum of nine filters, each with a diffusivity of 3.7E-6 moles per second per mole fraction.

(SQ 156H) The SWB is fitted with a minimum of four filters, each with a diffusivity of 3.7E-6 moles per second per mole fraction. Each inner container is fitted with a minimum of one filter with a diffusivity of 3.7E-6 moles per second per mole fraction.

All waste shipped under Content Code SQ 156 must comply with the additional conditions and controls specified in Appendix 6.12 of the CH-TRU Payload Appendices, specifically Section 6.12.6.2.3. Compliance with these additional conditions and controls is documented per Appendix 6.12 of the CH-TRU Payload Appendices.

SHIPPING CATEGORY: For Content Code SQ 156 payload containers, the content code (e.g., "SQ 156A") shall be used as the shipping category to direct the evaluation of the payload container for compliance with the applicable decay heat or flammable gas generation rate limit. Applicable decay heat limits for the packaging configurations under Content Code SQ 156 are specified in Appendix 6.12 of the CH-TRU Payload Appendices.

MAXIMUM ALLOWABLE WATTAGE: The maximum allowable wattages for this waste are calculated according to the methodology specified in Appendix 6.12 of the CH-TRU Payload Appendices and are listed in Appendix 6.12 of the CH-TRU Payload Appendices.

APPENDIX 6.13

**SHIPMENT OF CH-TRU WASTE PACKAGING CONFIGURATIONS
WITH AN UNVENTED HEAT-SEALED BAG LAYER**

This page intentionally left blank.

6.13 Shipment of CH-TRU Waste Packaging Configurations with an Unvented Heat-Sealed Bag Layer

6.13.1 Introduction

The purpose of this appendix is to describe the shipment of contact-handled transuranic (CH-TRU) waste packaging configurations with a single unvented heat-sealed bag layer, in addition to other layers of confinement, as authorized contents in the TRUPACT-II or HalfPACT. This appendix includes analyses demonstrating compliance with gas generation and all other applicable requirements, and establishes limits and conditions of compliance for this CH-TRU waste inventory. The key elements of this appendix are as follows:

- Quantifying the hydrogen release by permeation through the heat-sealed bag layer and establishing the resistance factor for this confinement layer using the same methodology described in Section 5.0 of the Contact-Handled Transuranic Waste Authorized Methods for Payload Control (CH-TRAMPAC) for other authorized confinement layers.

- Defining shipping categories for the waste forms expected to have a heat-sealed bag layer as a confinement layer and establishing gas generation limits using the same methodology outlined in Section 5.0 of the CH-TRAMPAC.

- Authorizing contents with unvented heat-sealed bag configurations using the same methodology as for other content codes in the CH-TRU Waste Content Codes (CH-TRUCON) document.

6.13.2 Scope

This appendix applies to CH-TRU waste containers with an unvented heat-sealed bag as a layer of confinement. Specific content codes, describing the waste attributes, shall be developed and approved as described in Section 1.5 of the CH-TRAMPAC prior to transport of these wastes.

6.13.3 Container and Physical Properties

The container and physical properties requirements and the associated methods of compliance are the same as those described in Section 2.0 of the CH-TRAMPAC.

6.13.4 Nuclear Properties

The nuclear properties requirements and the associated methods of compliance are the same as those described in Section 3.0 of the CH-TRAMPAC.

6.13.5 Chemical Properties

The chemical properties requirements and the associated methods of compliance are the same as those described in Section 4.0 of the CH-TRAMPAC.

6.13.6 Gas Generation Properties

The gas generation requirements and the associated methods of compliance are the same as those described in Section 5.0 of the CH-TRAMPAC. The quantification of the hydrogen release rate

and resistance factor for the unvented heat-sealed bag layer is described below. This release rate and the associated resistance factor shall be used for the heat-sealed bag layer in determining decay heat and other gas generation related limits using the methodology defined in Section 5.0 of the CH-TRAMPAC. Determination of limits and assignment of shipping categories for specific configurations with an unvented heat-sealed bag layer are also provided in this section.

6.13.6.1 Quantification of Hydrogen Release Rate for Unvented Heat-sealed Bags

Hydrogen release rates for an unvented heat-sealed bag layer meeting the requirements of Appendix 3.8 of the CH-TRU Payload Appendices are as follows.

For an unvented heat-sealed bag, the mechanism for hydrogen release is by permeation across the available surface area of the confinement layer. As specified in Appendix 3.8, unvented heat-sealed bags shall have a minimum surface area of approximately 390 square inches (2,516 square centimeters [cm^2]).

The release rate from an unvented heat-sealed bag meeting the specifications of Appendix 3.8 can be calculated as:

$$RR = \Pi * \frac{SA}{\delta} * \frac{mole}{22.4x10^3 \ cm^3 \ (STP)} * \frac{76 \ cm \ Hg}{1 \ mole \ fraction} \tag{1}$$

where,

RR = Release rate of hydrogen [mole/second/mole fraction (m/s/mf)]

Π = Permeability of bag to hydrogen ([cm^3 at standard temperature and pressure (STP) cm]/[cm^2 s cm Hg])

SA = Surface area of the bag (cm^2)

δ = Thickness of bag (cm).

While the thickness of an unvented heat-sealed bag is typically at the low end of a range from 5-mil (0.0127 cm) to 14-mil (0.03556 cm), a maximum thickness of 14-mil has been used to calculate the hydrogen release rate from unvented heat-sealed bags.

The unvented heat-sealed bags may be made of polyethylene (PE) or polyvinyl chloride (PVC). Since the permeability of hydrogen in PVC is lower than in PE (3.6×10^{-10} [cm^3 (STP) cm] / [cm^2 s cm Hg] for PVC versus 8.6×10^{-10} [cm^3 (STP) cm] / [cm^2 s cm Hg] for PE), the more conservative value for PVC at ambient temperature (Reference 6.13.8.1) is used to calculate the release rate, similar to the release rates for other configurations of Waste Type III in Appendix 6.9 of the CH-TRU Payload Appendices. Substitution of the values for the bag surface area, bag thickness, and permeability into Equation (1) yields a hydrogen release rate of 8.64×10^{-8} m/s/mf.

As described in Appendix 2.3 of the CH-TRU Payload Appendices, the resistance of the unvented heat-sealed bag to the release of hydrogen is the reciprocal of the release rate or 11,574,074 seconds/mole. Division of the resistance by 100 yields a resistance factor for the unvented heat-sealed bag of 115,741, which can then be added to the resistance factors from Table 2.2-1 of Appendix 2.2 of the CH-TRU Payload Appendices for the other confinement layers that may be present in the drum.

6.13.6.2 Determination of Limits

The allowable flammable gas generation rate and decay heat limits are calculated in this section for two different packaging configurations with an unvented heat-sealed bag using the methodology described in Section 5.0 of the CH-TRAMPAC. The packaging configurations have waste packaged in an unvented heat-sealed bag. The waste is then placed in up to four inner bags with twist-and-tape or fold-and-tape closures. The bagged waste is then placed either in a liner bag with a twist-and-tape or fold-and-tape closure (Packaging Configuration 1) or in a rigid liner that is filtered or punctured (Packaging Configuration 2) inside a 55-gallon (208-liter) metal drum. The drum is fitted with a filter with a minimum hydrogen diffusivity of 3.7×10^{-6} m/s/mf. The waste is classified as debris waste (i.e., Waste Material Type III.1, Solid Organic Waste). As discussed in Section 5.0 of the CH-TRAMPAC, the flammable gas effective G values are 3.40 if the dose criteria is not satisfied (i.e., watt*year $\leq$ 0.012) and 1.09 if the dose criteria is satisfied (i.e., watt*year > 0.012).

Based on the two different packaging configurations, the shipping categories are determined as per Appendix 2.2 of the CH-TRU Payload Appendices using Table 2.2-1 for the resistance terms and a resistance factor for the unvented heat-sealed bag as derived above. The individual contributions to the total resistance factor are summarized in Table 6.13-1.

Table 6.13-1 —Resistance Factors for Each Configuration with an Unvented Heat-Sealed Bag Layer

Resistance Contribution Type	Packaging Configuration 1 Total Resistance Factor	Packaging Configuration 2 Total Resistance Factor
1 Unvented Heat-Sealed Bag	115,741	115,741
4 Twist-and-Tape Inner Bag Layers	71,688	71,688
1 Twist-and-Tape Drum Liner Bag	2,142	—
Rigid Drum Liner With 0.3-inch Diameter Hole	—	197
55-Gallon Drum with 3.7×10^{-6} m/s/mf Filter	2,703	2,703
Load Type (14 55-Gallon Drums)	7,147	7,147
Total Resistance Factor Sum	199,421	197,476

As per Appendix 2.2 of the CH-TRU Payload Appendices, dividing the total resistance factor sum for each packaging configuration by 100 and rounding up to a whole number results in the four-digit Total Resistance Notation (ZZZZ) values of 1995 for Packaging Configuration 1 and 1975 for Packaging Configuration 2.

Combining the two digit Waste Type Notation (XX) value of 30 from Table 2.1-1 of Appendix 2.1 of the CH-TRU Payload Appendices with the two possible values of the four-digit G Value Notation (YYYY) of 0340 and 0109 and the ZZZZ values results in the following four distinct shipping categories:

Packaging Configuration 1	30 0340 1995	Watt*year ≤0.012
	30 0109 1995	Watt*year >0.012
Packaging Configuration 2	30 0340 1975	Watt*year ≤0.012
	30 0109 1975	Watt*year >0.012

The maximum allowable flammable gas generation rate per drum is calculated for each shipping category using Equation (8) of Appendix 2.3 of the CH-TRU Payload Appendices as:

$$CG = \frac{0.05}{(ZZZZ * 10,000 \; s/mole)} \tag{2}$$

where,

CG   =   Maximum allowable flammable gas generation rate per drum (mole/second)

ZZZZ =   Four-digit total resistance notation term from the numeric payload shipping category notation form, XX YYYY ZZZZ.

The maximum allowable decay heat per drum is calculated for each shipping category using Equation (9) of Appendix 2.3 of the CH-TRU Payload Appendices as:

$$Q = \frac{4824.42 \; molecules/mole * watt-s/eV}{(ZZZZ * YYYY) \; s-molecules/mole-eV)} \tag{3}$$

where,

Q   =   Maximum allowable decay heat limit (watt)

YYYY =   Four digit G value notation term from the numeric payload shipping category notation form, XX YYYY ZZZZ.

The limits for these shipping categories are as shown in Table 6.13-2.

Table 6.13-2 —Example Flammable Gas Generation Rate and Decay Heat Limits

Shipping Category	Allowable Flammable Gas Generation Rate Limit per Drum (moles/second)	Decay Heat Limit per Drum (watts)
30 0340 1995	2.506×10^{-9}	0.0071
30 0109 1995	2.506×10^{-9}	0.0222
30 0340 1975	2.532×10^{-9}	0.0072
30 0109 1975	2.532×10^{-9}	0.0224

Shipments of drums of these shipping categories under the test category (exceeding 500 parts per million flammable volatile organic compounds [VOC] or the decay heat limits [Table 6.13-2]) are as described in Section 5.2.5 of the CH-TRAMPAC, with headspace gas measurement and testing as options. The requirements of Section 5.2.4 of the CH-TRAMPAC apply with respect to determining steady-state (90%) VOC concentrations from drum age criteria and prediction factors. In addition, mixing of shipping categories is subject to the requirements described in Appendix 2.4 of the CH-TRU Payload Appendices and Section 6.2.4 of the CH-TRAMPAC.

Payload containers that have been stored in an unvented condition (i.e., no filter and/or unpunctured liner) shall be aspirated for the specific length of time to ensure equilibration of any gases that may have accumulated in the closed container. The derivation of aspiration times for packaging configurations with an unvented heat-sealed bag layer is as outlined in Appendix 3.7 of the CH-TRU Payload Appendices. Release rates for the confinement layers are as specified in Table 3.7-1 of Appendix 3.7 of the CH-TRU Payload Appendices, with a release rate of 8.64×10^{-8} m/s/mf to be used for an unvented heat-sealed bag as derived in Section 6.13.6.1.

In summary, this section derives the release rate and resistance factor to be used for an unvented heat-sealed bag layer meeting the requirements of Appendix 3.8 of the CH-TRU Payload Appendices. The methodology for determining compliance with gas generation limits with this confinement layer is identical to that used for other confinement layers.

6.13.7 Payload Assembly

The payload assembly requirements and compliance methods for these wastes are the same as those specified in Section 6.0 of the CH-TRAMPAC.

6.13.8 References

6.13.8.1   Perry, R.H., D.W. Green, and J.O. Maloney, 1984, *Perry's Chemical Engineers' Handbook*, Sixth Edition, McGraw-Hill Book Company, New York, New York.

This page intentionally left blank.